Volume

1

A Continuing Study of
CWF Fuels and Atomizers
With Development of
Numerical Analysis of
Atomization and Spray
Formation and a Statement
on Experimental Research
Work Required

Final Report

by

Ralph Grossman

Consultant

Work on this Project was conducted under the auspices of the Canada Centre for Mineral and Energy Technology, Energy Mines and Resources Canada.

DSS FILE NUMBER: 14 sq. 23440-4-9170
DSS CONTRACT SERIAL NUMBER: OSQ 84-00233
CANMET PROJECT NUMBER: 506801
CANMET SCIENTIFIC AUTHORITY: Dr. Horace Whaley

44 pp

MICROMEDIA

INTRODUCTION

1. The initial directive of this work was entitled "An Assessment of Potential Coal-Water Slurry Atomizers and Burners," and was intended, essentially, as a continuation of a previous study under DSS Contract 0SQ 82-00040. In the first study data on numerous atomizers was tabled and a hierarchy of atomizers having the most probable degree of success was established.

2. It was found in this prior work that only a limited number of atomizers had a significant degree of experience (at that time) with coal-water fuel.

As part of this work, contact was to be established to determine the quality of performance improvement of the earlier CWF producers and atomizer designs, and to determine what further atomizers had entered the field and had obtained a degree of significant results with coal-water fuel.

A prior requirement was the careful reading of the papers in Sympia 5 and 6, and to summarize those papers covering CWF types and atomizer designs that could be correlated and lead to a fundamental knowledge of fuel and atomizer characteristics that could yield an ability to predict quality of performance from the combination use of various fuels and atomizers.

---

3. This symposia study yielded reports X.1 to X.16 and W.1 to W.22 for the 5th and 6th Symposia respectively.

4. From these reports was extracted the data expressing the empirical relationship of viscosity to CWF characteristics and to this end Agendas 1-10 were developed.

5. However, it was found that in the Symposia data there was no correlation between fuel and atomizer design, and that atomizer design was a trial and error process of extrapolations from previous design and/or field results. (Chiefly to wed a particular atomizer to a particular CWF.)

6. From the paucity of fundamental physics knowledge of the CWF and atomizing functions, available in the literature and from the field, it was concluded that a numerical analysis of CWF flow mode, viscosity and the atomizing function,be developed to throw light on the research required to develop predictive equations for efficient atomization of a CWF together with a high efficiency of burn-out. To this end papers G.1 to G.16 were prepared. These are discussed in the following Summation, followed by a statement of Experimental Research required.

SUMMATION

The framework around which the "numerical analysis" was made was:

1. CWF - Factors affecting viscosity and flow mode, viz:

1.1 Parent Coal.

1.2 Grind size range.

1.3 Size consist.

1.4 Surface Chemistry and ionic state.

1.4.1 Ph.

1.5 Crystal Structure.

1.6 Additive chemistry.

1.7 Degree of Wetting.

1.8 Water/additive adsorption on coal.

1.9 Film thickness.

1.10 Degrading effect of pumping.

1.11 Coherence - in storage.

1.12 Coherence - in supply pipe.

1.13 Shear rate.

1.14 Effect of heat.

1.15 Fundamental flow mode
viz.: pseudoplastic or dilatant.

2. VISCOSITY

2.1 Generally, all factors given in 1 above have an effect on the CWF Viscosity.

2.2 With high ionic charge i.e. high electrophoretic mobility the repulsive force between particles will cause the flow mode to be pseudoplastic.

2.3 Some additives provide a negative charge and are termed anionic (anode seeking) and wil not break down if heated by atomizing steam.

2.4 Other additives are non-ionic (of polymer structure) and will break down if heated, causing agglomeration and large increase in viscosity.

2.5 Some flow modes are dilatant (which can lead to catastrophic increase in viscosity.)

2.5.1 In this regard see (X.12)
Figs. 6, 7 and 8, and note the dilatant effect as a function of Time 1, and in Figs. 9 and 11 as a function of shear rate.

2.5.2 The concept of high shear rate creating a "crowding" seems rational. But why should time create dilatancy? In Figs. 6 and 7 the time period is approx. .5 hrs. and in Fig. 8, graph A, (8 hrs. at 100 sec.$^{-1}$) then shear rate increased to 1000 sec.$^{-1}$ with sharp asymptotic) viscosity increase. Of interest is graph B of Fig. 12

---

which shows that after 65 hrs. of shut-down that the viscosity level started low (about 1200 Cp) then shot up as shear rate increased.

Question:

a) What happened to the CWF while in storage?

b) What caused dilatancy?

2.6 These questions are not addressed by the authors (X.12) Only the empirical (test) evidence is stated.

2.7 The questions are most valid if one considers that the shear rate in an atomizer can be as high as 400,000 sec.^{-1}

2.8 Obviously, at present, only the empirical evidence can determine which CWF should not be used.

2.9 Most of the rheograms shown in the Symposia, indicate a "working" viscosity range of 800 to 1500 Cp with an average at 900 - 1000 Cp at shear rates well under $1000^{\text{sec.}-1}$ (though the max. recommended (X.12) is 150 sec.^{-1})

2.10 The foregoing data on viscosity then led to the need of determining the viscosity of the CWF plus atomizing fluid, in order to know if a given CWF having some dilatant tendency, could be expected to block up in the atomizer. This led to the analysis of viscosity under the ϕ / ϕ max. concept as discussed in Appendix 1.

---

3. VISCOSITY DETERMINATION USING THE Ø/Ø max. CONCEPT (Appendix 1)

3.1 Using the basic equation

$\mu = (1- Ø/Ø \text{ max.})^{-3.54}$ of (X.2 - App.1);
good correlation was found with Ø concept
equations of (X.2) and X.15) viz.
977 CP - 883 Cp and of Viscosity plot
Fig. 3.X.15 and
Eq. 9 (X.15) & Viscosity plot 2.X.15,
Viz. 1242 Cp - 1096 Cp
realistic Ø max. value established (X.15) was .70.

3.2 In this regard Funk-Dinger -Funk (B .1) experimented with a filter press from which a Ø max. of .925 was obtained. With a Ø value (% coal Vol.) of .64 (corresponding to 70 % wt. coal concentration, gave an out of general statistic value of 63.2 Cp.
Paper (B.1) however, contained an anomalous value of 806 Cp from a Viscometer test.
This viscosity value would require a Ø max. of .807 (in conjunction with a Ø of .685 for a 75 Wt. % coal concentration.)

3.3 This was brought to the attention of Dr. Dinger at Alfred University, who could not give an explanation, but said that further work would be done on the viscosity implication of the filter press results.
(See correspondence dated Aug. 20, 1985).

3.4 The concept of ϕ/ϕ max. technique of viscosity determination, was essential to a numerical determination of the viscosity of a CWF/steam emulsion.

3.5 See appendices 4.R and 5 R. for calculations made which showed an emulsion viscosity of ≤ 1.4 Cp.

3.6 Appendix 7 calculations show laminar flow for CWF only and turbulent flow for the CWF/ steam emulsion. The atomizer design implications will be discussed later.

3.7 Effect of atomizing steam condensation in the CWF was calculated in Appendices 7 & 8, showing that emulsion viscosities were held well below the limit of 4 Cp for turbulent flow.

4. ATOMIZATION OF A HOMOGENEOUS EMULSION

4.1 Atomization is the "art" of causing the break down of a CWF/atomizing fluid emulsion into the smallest possible drops.

4.2 The fact that the viscosity of a homogeneous emulsion was < 4 Cp - led to the establishment of the basic fact that the flow of an emulsion would have a Re number well in the turbulent range (see item 3.6 above)

4.3 For turbulent flow of a CWF/steam emulsion (i.e. CWF and steam fully intermixed) the governing equations are: (See Appendix 7)

4.4 $$\Delta P = \frac{0.000\ 336\ fW^2}{d^5 \rho}$$ Eq. 1

ΔP (friction) plus Velocity head pressures equals total P present at entry points, so that

$P - \Delta P =$ Velocity head pressure
(outlet press. assumed Opsig.)

4.5.1 Velocity in fps of exit points is:

$$V = \frac{\text{Vol. flow (cu. ft./sec.)}}{\text{area of exit ports}}$$ Eq. 2

4.5.2 P & V are related by the equation:

$$\frac{C\ V^2}{2\,g} = h_{\lambda} = \frac{P \times 144}{\rho}$$ (See G.16 Add. 3 Eq. 1)

(c = orifice coefficient)

4.6 The interrelations between P, ρ, V, and d and flow requirements were calculated, for a postulated flow condition in paper G.16 with Addenda G.16.1, G.16.2 and G.16.3.

4.7 In the case of a homogeneous emulsion a basic fact I obtained from discussion with Geo. Farthing of B & W and Dr. Ken Olen of Florida Power and Light Co. was that adequate velocity in the effluent jet stream was essentialto good atomization.

4.8 In G.16 Add.3, the calculations show a velocity of 966 fps capable of a turndown to 242 fps for a 4:1 load turn down.

4.9 This presumes very efficient atomization (small drop formation) and a reasonable atomizing efficiency at the 1/4 load point, in Section 18 below, of this summation.

4.10 An arithmetical technique to predict degree of breakdown of a homogeneous emulsion jet, for any velocity,could be based on that fully developed for a 2-phase system as detailed in Section 6.

4.11 Recourse however, must be taken to an experimental test determination of drop formation in a cold chamber with air flows around the jet stimulating combustion air flow.

Preferably, if technically feasible, the test should be done in a hot test chamber (i.e. a test furnace) with multiple viewing ports.

4.12 Pressure values must be accurately measured from which the velocity at which the observations were made can be determined.

4.13 Need of suitable lighting and photographic techniques, which I understand the current state of this technology can provide.

4.14 It is presumed that if the drop size resolution is poor that recourse can be had to special techniques.

4.15 I understand that there are advanced techniques of drop size resolution, including stroboscopes, laser lighting, magnification; and also the use of X-rays to produce a diffraction pattern, or neutron bombardment to create gamma ray dispersion from impact on droplets with a suitable sensor and recorder. My sense of memory from past reading indicates the possibility of the use of computer techniques to create a magnified image.

4.16 The foregoing discussion (Section 4) on atomization, considers CWF and atomizing steam to have formed a homogeneous emulsion. However, this seemingly simple situation was upset by a discussion with Dr. N. Chigier of Carnegie-Mellon University who stated that experiments conducted in 1974 with an associate

4.16 P. J. Mullinger, using a Y-Jet atomizer mode of a transparent material. They found that the flow was not a homogeneous emulsion but was a 2-phase flow system with a centre steam core and an annular CWF film. Under this situation I could not use turbulent flow and velocity headequations which would leave only the need of experimental verification of CWF drop breakdown under high velocity flow. It was necessary to "invent" techniques of determining drop formation from rational hypotheses, in order to develop a concept of drop formation by numerical analysis. This was developed in papers G.1 to G.16 which is the substance of the next Section (5)

4.17 (In this section it will be shown that some of the numerical analysis concepts developed to obtain numbers for a two-phase flow can be applied to obtain drop numbers for a homogeneous flow (treated as a uniform liquid). In the end, however, experimental work is still required to confirm or modify the "numbers".

5. A NUMERICAL ANALYSIS OF DROP FORMATION IN A TWO-PHASE FLOW OF CWF AND ATOMIZING STEAM

5.1 In Paper TP.1 by Mullinger-Chigier - (see Technical Paper Section Book III). Fig 4 shows an idealized model of the 2-phase flow.

5.2 To establish a means of developing numbers for drop size and spray formation, and drop interaction within the spray development, it was necessary to establish some working hypotheses and which were. (See G.1)

5.2.1 Steam expansion in a divergent nozzle to yield zero exit pressure - or by suitable divergent nozzle dimensioning - a pre-determined pressure at nozzle exit.

5.2.2 The pressure causing CWF flow creates a stress throughout the flow mass (in the annular films).

5.2.3 The expanding atomizing steam in the core of the two-phase flow will create a breakdown of the film in the divergent nozzle such that the ratio of area of the number of drops formed versus the film surface will be a multiple that will reduce drop stress to zero psig.

5.2.4 That the drops issuing from the divergent nozzle will come under the divisive force of the Weber Number

Number $\frac{Pa, \; V^2, \; r}{\gamma} \geq 10$ (G.1. item 18.4)

The γ value (surface tension) to be modified by a factor to account for the CWF viscosity (See G.1 .2 R and G.1 item 46)

5.2.5 That the drop break-up (due to 5.2.4) would be mitotic.

5.2.6 That the ultimate drop diameter would be determined by the r (radius) factor in the Weber formula.

5.2.7 That the initial drops would contain coal particles in accordance with the Funk distribution, ranging from 1 um to 400 um.

5.2.8 That the time element of drop formation in the divergent nozzle will be that of the time rate of atomizing steam flow through the divergent nozzle.

5.3 A divergent nozzle design dimension was calculated so that exit pressure would be zero psig.

5.3.1 For a 15° nozzle the length calculated was 2.25 cm. (later rounded to 2.5 cm.) with a diameter at exit of .70 cm.

5.4 From the dimensional and operating data of the Chatham C.E. atomiser (made known to me by C.E. Canada) it was found that:

5.4.1 The time rate of drop formation was calculated to be 2.10^5 drops/sec. (G.1 - 60)

5.4.2 The limit number of drops that could be formed in 1 sec. was determined by the input rate of 102 $cm.^3$/sec. for a drop forming actual capability rate of 3000 drops/sec. (G.1 Item 61).

5.4.3 Drop diameter formed in the divergent nozzle was 4000 um. (G.1 item 34.1)

5.4.4 Hence under the postulated hypotheses the system was calculated (first calculation) to exit in waves of 3000 drops per .015 sec., with a drop separation of 1080 um. (G.1 item 40)

5.4.5 It was seen, however, that the restriction of divergent nozzle end diameter could restrict rate of drop formation by 1/3 or 1000 drops per .005 sec. (G.1 Item 42.7)

This is developed in G.1 Addendum 2.

5.6 The value of drop rate of 3000 per .015 sec. yields a flame front axial distance from nozzle of 272 cm. (approx. 9 ft, which in turn fields a burno[illegible]istance of 12.25 ft. to 16 ft. for a 375 u.m. diameter drop (assumed "normal" max. diameter), for a spray angle spread of 45° (total) from the G. M. (geometrical mean) point. This value of 9 ft. to flame front is obviously excessive.

5.7 A rationalization is attempted in G.1 Addendum 1 and in G.1 Addendum 2.

5.8 In G.1 Addendum 1 - Items 5- 6.1 a spray angle of 45° (total) starting at nozzle exit, with an assumed combustion wave velocity of 140 cm./sec. (very conservative) yields a flame front axial distance of approximately 4 cm. (which, presumably, could cause overheating of the nozzle, and further, as will be seen, will not allow adequate CWF emulsion jet break-up.

5.9 In G.1 Addendum 2, calculations based on a drop emulsion rate of 1000 per .005 sec. (Item 6.4 above) with 45° spray angle from G.M. point, yielded a flame front and distance of 53 cm. (G.1 Addendum 2 Item 9) and a burn-out distance for a 375 um drop of 8.35 ft. to 12 ft.

5.10 The 53 cm. dimension compares to a distance of 35 cm. for a 50 um drop spray in MIT experiments (10).

5.11 The considerations of:
a 15° divergent nozzle; a 45° spray angle from G.M. point; and a burning velocity of 140 cm. sec. we then adopted as a standard for burn-out lengths, based on a .1 sec. to .2 sec. time for a 44 um. particle determined experimentally in (9) (W.19). The results are shown in Tables G.9.1 and G.9.2.

5.12 The viscosity factor modification for the Weber was calculated in G.2.R. and shows an addition to the denominator value (76 for water) of $.01154\mu$.

6. EFFICIENCY OF CARBON CONVERSION

6.1 The ultimate aim of CWF quality atomizer performance, and combustion air supply, is to secure a maximum carbon conversion (> 98%), with a min. of atomizing fluid per lb. CWF., and a minimum of excess air.

6.2 Carbon conversion efficiency depends largely on drop size and max. coal particle diameter.

6.3 Drop size is affected by coherence of coal particles before entering atomizer, and coalescence of drops by collision within the spray.

7. Coherence is attributed (by Geo. Farthing of B & W) to the use of a polymer additive as a stabilizer in the storage tank. This type of additive can cause "coagulation" of coal particles which may or may not be broken up by the transfer and supply pumps.

7.1 It is then, logically, the principal reason that atomizer orifices are sized 5 to 10 times the max. (normal) diameter in the CWF, thus limiting the vital factor of velocity (kinetic energy) as a drop breaking medium. (See G-16 and Fig. 16.1 for a design concept to break up coherent ("globs"). The addition of a "Cuno" motorized self-cleaning strainer should also be considered.

7.2 In a homogeneous emulsion system, temperature of the emulsion will rise above 300°F (very fast condensation rate assumed) If the additive is non-ionic (i.e. a polymer type) there is significant probability of trouble unless additive breakdown has a time factor in excess of the emulsion flow time after mixing, and just prior to exiting from the mixing chamber orifices.

7.3 The above thought is detailed in G.5 with elaboration of possible CWF consist modification to permit the use of a non-ionic (polymer type) additive. (What is the imperative that impels a decision to use a non-ionic type additive?)

COALESCENCE

8.1 Coalescence occurs in a CWF spray due to collision between drops.

8.2 The relationship between total drop area at a flame front and the virtual area of the flame front is developed in G.11.

8.3 For a flame front 4 cm. from nozzle at a spray angle of 45° at the nozzle exit, the flame front area is 14.4 cm.^{2} versus a drop area of 50 cm.^{2}. (The flame front is less than 1 mitotic dimension from nozzle and the drops have not divided and the 400 drops appearing at the flame front has an area of 50 cm.^{2} (G. 11 Item 7)

8.4 There is "overcrowding" at the flame front as the jet is essentially a stream of 4000 um dia. drops at the initial issue state from the nozzle (See Tables G.1 and G.9.1)

The effect of the "overcrowding" on carbon conversion efficiency (for a "normal" furnace length) would be bad.

8.5 To provide the minimum area requirement of 50 cm^2 it would be necessary that the spray total angle be 90° (for a flame front distance of 4 cm.)

8.6 Allowing a 20% safety factor or a flame front area requirement of 60 cm.^2, the total angle of spray required for a 4 cm. axial distance is: 95°

8.7 Such angles would require to be "guided" by a jet attachment surface (the "Coanda" effect) (see Drg. G.1.2)

8.8 Reverting to a more probable total spray angle of 45°, the axial distance is 10.6 cm. (See G.11drg. P.4.) and the drop velocity needed to attain this distance to flame front is 5300 cm./sec.

8.9 To attain a drop velocity of 5300 cm/sec. (173 fps.) instead of the assumed velocity of 60 fps at nozzle exit, it would be necessary to redesign the atomizer (Y-Jet) to decrease diameter and/or to increase atomizing steam velocity.

8.10 The resulting combustion (i.e. flame) velocity is: 87 cm/sec. – well within the postulated maximum of 140 cm./sec.

8.11 The drops would be well dispersed.

8.12 With the "standard" design postulate of a 15° divergent nozzle and a total spray angle of 45° at the G.M. point, with a flame front distance of 53 cm., we obtain a total drop area of 80 cm.^{2} versus flame front area of 804 cm.^{2} - a well dispersed condition.

8.13 Fig.G.11.4 shows the spray geometry for a total spray angle of 60°.

8.14 The data of G.11 Addendum 1 shows ratio of end of spray area versus total drop area as 5882 (or 16129) and concern is expressed as to whether this might destabilize (extinguish) the flame, and the possible answer may lie in the products of combustion flow, or a redesign of the divergent nozzle to give a narrower spray beam.

---

9. INTERACTION AT INTERSECTION POINTS OF SPRAY FORMATION FROM A SINGLE ANNULUS

9.1 The spread of a spray from a circular annular flow of 45^{o} from G.M. point, will create intersection points where collision could cause coalescence. The degree of coalescence will, to a large extent, depend on the drop separation in the intersection zone. This is explained in (G. 12) and the data expressed in Figs. G.12.1 and G.12.2 (attached to G.12)

9.2 The calculations showed dro separation in the intersection zone X^{i} OX – (Figs. G.12.1 – G.12.2) as being :

Transverse	.2775 cm. (G. 12– Item 9)
Lineal ...	.032 cm. (G. 12 – Item 9.1)

9.3 The collision zone (for a single annulus) occurs well behind the flame front, allowing significant opportunity for drop break down by Weber "Force" before drops enter the flame front.

9.4 The collision probability is explored in (G.13).

---

10. COLLISION PROBABILITY in a 45° spray from a single Annulus.

10.1 In G.13 sketch showing /free zone" and drop diameter at intersection zone O for the spray formation of cases 3000 drops/.015 sec., and 1000 drops/.005 sec. (Cases 1 and 11).

10.2 The collision probability is calculated which is 2% for Case 1 and 10% for Case 11.

10.3 The coalescence effect is:

Case 1 - 500 um.dia. with the good possibility of a dia. of 250 um entering the flame front maintaining the burn-out distance at 12 to 15 ft. from nozzle, (approx.)

Case II - 2000 um, with a breakdown before flame front estimated at 500 um, when the burnout distance is 10.34 to 16.1 ft.

N.B. Burn-out distance for various drop diameters are shown in Table G.9.1 and G.9.2
(Located in flap of Vol.11)

11. THE EFFECT OF INTERSECTIONS OF SPRAYS FROM NEIGHBORING ANNULI

11.1 In G.14 the figures 14.1 and 14.2 show the G.M. Zones (annular) from which the spray is postulated to spread at 45° (for the 2 cases of 3000 drops/.015 sec. and 1000 drops/.005 sec.

11.2 Figures 14.3 and 14.4 indicate that the major point of insection will be at the points 0^1 and 0^2 with further coalescence at points O^3.

11.3 The drop size formations are:

Case 1 - 1000 to 2000 um with a breakdown to 125 and 250 um at the flame front with the axial burn-out distance 8.5 to 12 ft. (Table G.9.1).

Case 11 - The same degree of intersection coalescence will take place as for Case 1.

11.4 The collision rate probability is estimated to be double the values calculated in G.13 or a probability of 4% (Case 1) or 20% (case 11).

11.5 It appears that in the worst case, with the Weber effect causing mitotic breakdown, that the flame front will receive 100-1000 drops of 500 um. dia.

11.6 This represents a volume of $\frac{4}{3} \Pi r^3$ volumes are:

$$\frac{4}{3} \Pi (.02)^3 \times 400 = .0134 \text{ cm.}^3$$

$$\frac{4}{3} \Pi (.05)^3 \times 1000 = .52 \text{ cm.}^3$$

11.7 The initial input is 102 cm.^{3}, therefore the worst case (.52 cm.^{3}) represents a potential carbon loss of $\frac{.52}{102} = .5\%$

or with a safety factor of 2a loss of 1%.

11.8 (N.B. The burn-out length for a 500 um drop is: 10.5 to 16 ft.)

It is important to note that the burn-out lengths are derived from values of .1 to .2 sec. for a 44 um. (9)

12. BURN-OUT TIMES AND AXIAL DISTANCES

12.1 Burn-out time is based on experimental values given in (9) of .1 to .2 sec. for a 44 um drop.

12.2 From this base G.8 develops a time formula of: .00226 D - min.

and

.0044 D - max.

12.3 The burn-out length is then a function of drop dia. and drop velocity.

12.4 Drop velocities (and break down) are given in Tables G.1, G.9.1, and G.9.2.
G.1 for the case of 3000 drops / .015 sec., and G.9.1 from 1000 drop per / .005 sec.

12.5 This concept is developed in G.9 from velocities taken from Fg. G.9.1 which shows a decelerating steam velocity from 166 to 4.45 fps, and an acceleration / deceleration mode for the drops of 60-105 fps accelerating, and 105-40 fps decelerating.

12.6 The deceleration of the atomizing steam jet stream is developed in G.7.

12.7 Burn-out data and burn-out lengths for drop sizes 720 to 40 um for the 2 cases of drop rate formation, and for several cases of spray angle and points of angle formation are given in Tables G.9.1 and G.9.2., where the numbered rows are co-related.

12.8 A detailed discussion of the arguments developed in G.9, and the derivative background for the data of Tables G.9.1 and G.9.2 is given in G.10.

13. CHAR FORMATION

13.1 Before the drop has entered the flame front, all or nearly all water has been evaporated. Volatiles will first volatilize and burn leaving all the coal particles behind as char particles. With some coals these particles will remain as individuals, and with other coals they will cohere, and perhaps the char particle will swell.

13.2 A combination of coheredchar plus some swelling is bad news for high carbon conversion in a given furnace length.

13.3 There is then the evident need of: Securing sufficient

13.3.1 mitotic breakdown before the flame - i.e. the flame front must be at least 4 mitotic divisions from the nozzle. (4 divisions will give a dia. of 250 um - commensurate with the "standard" of Table G.9.2 based on 375 um for a burnout distance of 8.5 to 12 ft.). At an average velocity of 2400 cm. /sec. (approx.) the axial distance to flame front is 4 x .005 x 2400 = 48 cm. (Table G.9.1 gives 53 cm.).

13.3.2 With a lesser distance,analysis indicates the need of a sharp breakup at the nozzle exit (See G.16 re thin film as in Fig. G.1.3)or a high velocity emulsion jet as in Fig. G.16.1.

13.3.3 A sound technique would be to reduce the particle top size in the CWF to 200 um.

13.3.4 An extension of the distance to flame front could, presumably, be achieved by increasing fluid jet velocity but this could be limited by considerations of flame stability, and possibly negated by a high combustion velocity of a particular coal in the CWF.

14. COMBUSTION PROCESS AND OVERALL EFFICIENCY

14.1 Overall high thermal efficiency is more than % carbon conversion.

14.2 The further basic needs (of course) are:

14.2.1 Sufficient combustion air temperature to ensure flame stability.

14.2.2 Sufficient swirl and suitable velocity profile of the combustion air and hot products of combustion flow to ensure adequate recirculation for stable ignition and combustion.

14.2.3 Suitable coal burning characteristics to meet the flame temperatures of various boilers and processes.

In this regard J. Pinta of Gulf Research (W. 18) discusses various coal qualities which have varying degrees of ignition temperature, rate of volatilization; char reactivity, ash structure and fusion temperature. The terms used to identify these coal qualities are: fusain; durain; vitrain; vitrinites; exinites.

15. CORRELATION WITH MIT (10)

15.1 It was considered desirable to see what correlations existed between the numerical data established by this work, and the experimental work of MIT (10) even though the data they gave was largely based on a 40 um - 50 um drop stream under laboratory test conditions.

15.2 Interestingly, the ratios of CRL versus MIT data averaged a value of approx. 5 for burn-out distance and burning velocity, and a ratio of nearly 1 for differential velocity of drop and atomizing fluid flow.

15.3 One significant non-correlation was the fact of an MIT burning velocity of 924 cm./sec. versus the postulated 140 cm./sec. A further investigation found that a value of 400 cm./sec. was tenable resulting in a reduction in burn-out distance of .524 ft. for the 1000 drop./ .005 sec. hypothesis or 2.2. ft. for the 3000 drop/ .015 sec. hypothesis.

16. TWO PHASE VERSUS HOMOGENEOUS FLOW OF CWF/ATOMIZING STEAM

16.1 Two-phase flow study in a Y-Jet atomizer was developed because the Mullinger Chigier experiments in 1974 so indicated.

16.2 The previously developed study based on a homogeneous emulsion ("proven" to be turbulent) leading to relatively simple equations useable in atomizer design which required only experimental verifications of drop break-up versus emulsion velocity.

16.3 With 2-phase flow a series of rational hypotheses were developed to provide a basis for numerical analysis. The end result is pictured in Fig. G.1.3., which shows fluid film thicknesses of 156 and 184 um in the end of the divergent nozzle. These dimensions compare favorably with those of a mechanical atomizing system, and the significance is:

16.4.1 Drop formation could occur by stress of pressure, surface tension and kinetic energy in the CWF jet stream.

16.4.2 The effect of atomizing steam flow is augmented.

16.4.3 With the divergent nozzle designed to provide a low pressure at the exit, the thin fluid should readily be blown apart, with diminished or no need of the Weber "effect".

16.5 However, I have not heard of a confirming experiment proving the two phase flow. In the absence of such confirmation the fact of homogeneous or mixed phase flow must be considered.(e.g., Geo. Farthing of B & W has stated that there was a separated film on the wall of the mixing chamber of the T-Jet atomizer, entering the exit orifices along with the emulsion.) This would be a very complex situation difficult to analyse in terms of spray formation predictability.

17. SINGLE PHASE HOMOGENEOUS EMULSION FLOW

17.1 The possibility of condition 16.5 led to the concept that a homogeneous emulsion could be established by "forcing" the CWF into the atomizing steam. (Based on the thermodynamic fact that the molecular free path of steam was under greater than that of water.)

17.2 This led to the design of Fig. G.16.1 which is dubbed the "Whaley-Grossman Homogenizer". It is examined in detail in G.16 Add. 2 and with requirements for turn-down in G.16 Add. 3.

18. CWF TOLERANCE FOR TEMPERATURE

18.1 In a fully homogeneous emulsion there will be a temperature rise due to atomizing steam condensation to a limit level of the temperature of saturated steam at the CWF pressure. This is discussed in G.5.

18.2 Because of lack of field data on annuli pressures and temperatures for CWF and steam, it was necessary to consider the calculated condensation taking place in the interval between the point of start of mixing and the point of exit.

18.3 With such data the amount and rate of heat transfer can readily be calculated and the "actual" temperatures of the emulsion determined which may well be some significant degree below the saturation temperature (.e.g. 350° F.)

18.4 This would be an important factor in determining the effect on the type of additive used. For example if the additive were of the non-ionic (polymer) type the effect could be a degradation leading to a "coagulant" effect and possibly causing blockage of the atomizer.

18.5 The temperature rise of CWF in the "mixing system" is limited (also) to the amount of atomizing steam present to transfer heat.

18.6 In the CWF gun barrell passing through a windbox 15" - 24" deep, with combustion air temperature up to 500°F, there is no BTU content heat transfer constraint, and it has been found that the CWF can dry, i.e. all water turned into steam.

18.7 In such case the burner gun design must be provided with insulation or contained in a sealed carrier tube with an insulating air space.

13.1 EXPERIMENTAL RESEARCH REQUIRED

DROP SIZE DETERMINATION

In developing a numerical analysis for a homogeneous emulsion flow in a Y-Jet atomizer, it was found that a basic turbulent flow equation could be applied to the flow in the annulus and a basic velocity head equation for the exit velocities.

13.2 The unknown was the drop sizing and spray formation created by one (or more) exit velocities.

13.3 Dr. N. Chigier and P.L. Meyer (11) attempted to do this but their photographs, figures 8.W.22 to 12.W.22 showed solid jet emission with no resolution of drop sizes.

13.4 This was thought to be due to such fine atomization as to create an opacity to the strobe light used.

13.5 They concluded that further experimental research was necessary and their intended continuing work would use laser light to illuminate the jet stream from within.

13.6 A technique of photomicrography or X-ray crystallography (or other " advanced" techniques) may be found necessary to secure adequate resolution of drop formation in the effluent emulsion jet.

13.7 The need is essential to determine:

13.7.1 Emulsion velocity required for a requisite spray formation.

13.7.2 Drop size breakdown at flame front.

13.7.3 Minimum distance of flame front that will allow time for drop breakdown to avoidance formation of large char particles.

14. Two other techniques described in the physics literature (which may or may not be applicable) are mentioned here on the chance of relevancy to the problem of drop size resolution.

14.1 There are:
CAT - Computerized axial tomography.
PET - Positron - emission - tomography.

14.2 With the availability of the foregoing drop size identification technique, reasonably accurate use of turbulent flow and velocity head equations (See items 4.4 and 4.4.2) can be obtained.

14.3 If such drop size data in the spray formation cannot (or cannot readily) be available, then recourse must be had to % carbon conversion, and flame length, from standard field test technology with the use of Schlieren photography.

15. DROP FORMATION IN A 2-PHASE Y-JET ATOMIZER WITH AN ADDED DIVERGENT NOZZLE

15.1 Paper G.1 develops a basis for numerical analysis of two-phase flow in a Y-Jet plus Divergent Nozzle atomizer, based on the hypothesis detailed in items 6.2.1 to 6.2.8.

15.2 The total development of spray formation from Paper G.1 - G.16 produced a rational value, the ultimate aim, of 100% carbon conversion in a calculated distance of 8.5 ft. min. to 12 ft. max. for a CWF with top particle size of 400 um (for CWF Funk process base).

15.3 It is worthwhile then, to do the experimental work to prove that the hypotheses are rational and the results therefrom realistic (to within a reasonable margin of error.)

15.4 The experimental requirements are:

15.4.1 An atomizer constructed of transparent material.

15.4.2 A (Schlieren) photographic technique to prove 2-phase flow and the thickness of the CWF film at the entrance and exit of the cylindrical annulus and the divergent nozzle, to give reasonably accurate film thickness dimensions.

15.4.5 It would be very desirable to prove the film thickness of Divergent Nozzle exit as shown in Fig. G.1.3).

15.4.6 Should density difference photographic techniques not prove to give sufficiently accurate determination of film thickness then possibly foreign material can be introduced into the CWF whose movement can be measured by strobe or laser lighting with suitable type of camera.

15.5 The formation of drops within the divergent nozzle as per Section 5 in G.1 may prove difficult to resolve.

15.6 In that case recourse must be had to the techniques discussed in item 13.5 and following, which would achieve essentially the required data information.

16. COALESCENCE

16.1 Because coalescence is an adverse factor for efficient carbon conversion, proof of mitotic division, before the flame front, the hypothesis of the Weber "effect" is highly desirable.

16.2 Such observation must be made in a test furnace with sufficient observation ports, and again with lighting and photographic techniques that will resolve the development from nozzle exit to flame front.

16.3 The position of the flame front would, presumably, be established by Schlieren photography.

16.4 It will be interesting to know if photographic techniques for spray development can establish the collision concentration points as calculated in G.11 - G.14.

17. CHAR BURNING

17.1 The size of char particles and their reactivity should readily be observable because the char is burning and radiating both optical and infra-red light, and so would be a high energy source for an optical or I.R. detector.

17.2 The most important data required here is the time rate of size degradations of the char particles and the possibility of extinction of burning before the end of the firing zone is reached.

17.2.1 The time rate of char burning would determine whether the complete char particle had burned at the end of visible flame.

17.2.2 This can be checked by determining the carbon content in the ash.

17.3 Consideration of coal maceral quality would be a factor in the char burn-out time and completeness. (Pinto-Gulf Research (W.18))

18. CWF RHEOLOGY

18.1 The actual assumed viscosities of CWFs, in commercial practice, ranges from (generally) 800-1500 Cp. for a coal loading of 70% wt.

18.2 There are some cases where the viscosity is significantly lower, or higher.

18.3 Such commercial viscosities have particular bearing on pressure drop flow characteristics. in supply lines.

18.4 Most CWFs have a pseudoplastic flow mode where viscosity decreases with increase in shear rate,
though, of course, unit stress increases with increase in shear rate.

18.5 The literature shows that some of the factors affecting viscosity in pseudoplastic flow are: size range; size consist; particle structure, Ph and elephoretic mobility (ionic charge) additive type, tendency to floculate. These factors are discussed in (X.15) and see Figures 3-9(.X-15.)

18.6 From the considerations of contributing factors to viscosity and following Viscometer Tests the authors (X.15) have developed a viscosity determining formula:

$$\eta = \eta_{o} (1 - \varnothing/\varnothing \text{ max.})^{-[\eta]\varnothing \text{ max.}}$$

(See Fig. 1.X.2 of part X.2 of Appendix 1.) where the desired value n is determined from experimentally determined values for $\varnothing$ & $\varnothing$ max.

18.7 There is no mathematical model linking all the variables in 18.5 to flow mode or viscosity.

18.8 Two basic facts given are:

18.8.1 Surface Chemistry can create attractive forces.

18.8.7 Additives are thus required to ensure repulsive ionic charge on coal particles.

18.9 It is reasonable then to deduce from the foregoing that:

18.9.1 Pseudoplasticity is a function of ionic charge on the coalparticles, and that velocity increase decreases viscosity.

18.10 Conversely with attractive forces caused possibly by inadequate quantity or quality of additives, dilatancy may result.

18.11 Viscosity as such within normal bounds (i.e. 800 - 1500 Cp) will cause no problem in the atomizer because the addition of the atomizing steam volume reduces the viscosity to $<$ 1.4 Cp.

18.2 But the possibility of a dilatant mode due to one of the factors in 18.5 is most important, as dilatancy can create blockage.

18.3 Experimental work is needed to determine the cause of dilatancy.

18.14 Observation of particles in flow is needed.

18.14.1 A test loop could be set up containing transparent sections sized to provide normal shear rates for CWF supply (say 1" - 2" dia. pipe) at shear rates up to 1000 sec.$^{-1}$, and also a transparent loop section to simulate the condition of flow in an annulus

e.g. - consider the dia. of .487 cm. for the C.E. Chatham atomizer where shear rate is in excess of 400,000 sec.$^{-1}$

18.15 It will be necessary of course to use the lighting and magnification techniques discussed in items 13.3 and following.

18.16 Of course, it should be noted that this discussion of items is to obtain knowledge of flow of CWF only in a pipe system to enable some correlations to be obtained between coal factors of item 18.5 in relation to a Viscometer established foot of a dilatant mode.

18.17 The work of Dr. Dooher et al (Adelphi University) establishes the fact of dilatancy but with no relation actual or indicated, to possible fundamental cause.

19. COHERENCE

19.1 This term is analogous to coalescence but its occurrence is in the storage tank.

19.2 Coherence is caused by the gelling effect of a polymer type additive (non-ionic) required by the size range and size distribution consist of the CWF to secure stability (i.e. minimum settling rate.)

1 .3 If the gel "blobs"/ flow through the pump without adequate breakup, they will appear in the atomizer and can cause trouble (blockage).

1 .4 So called gel "blobs" can be likened to an amoeba like concentration of additive cum CWF.

19.5 If in a flow test to determine mode characteristics (pseudoplastic or dilatant) polymer gel coagulation should show up then presumably tests of varying CWF/additive characteristics for storage stability should be made to determine:

19.5.1 Change of CWF consist to require a minimum of polymer type additive.

19.5.2 Change of CWF consist to enable the use of a non-polymer (i.e. ionizing type additive.)

19.5.3 N.B. It may be that the effect of 19.5.2 might be destabilizing (for storage stability consideration) then requiring a minimum amount of additive or the use of mechanical or hydraulic means of maintaining coal dispersion.

19.6 If the use of a polymer type additive is necessary (as it may be in the case of Carbojel, or other similar CWF), then a test on the use of a Cuno strainer plus an atomizer design as shown in Fig. G.16.1 could provide rewarding.

19.7 As a final thought, the use by C.E. of a safety factor of 12 in their annular dimension might be due to the need of preventing blockage due to the presence of gel formations originating in the storage tank.

Volume

2

VOLUME II

DSS OSQ 84-00233

CLM STUDY

PHASE II

FIGURES AND TABLES IN FLAP

G.1.1

G.9.1

G.9.2

1.A.6.R

2.A.6.R

TABLE G.9.1

SPRAY FORMATION & BURNOUT LENGTHS BASED ON TIME DATA
VELOCITY IN A DECELERATION MODE AND CWF in an ACCEL

1	2	3	4	5	6	7	8		9	10
DROP GENERATION & SEPARATION						BURNOUT LENGTHS FROM NOZZLE EXIT (				
						Average Velocities				
Row & Mitotic Division No.	No. of Drops	Drop Dia. um	Drop Velocity fps	cm./sec.	Separa- tion CM 4)	6)Division spread per fig. a)	fps	cm/sec.	Time from flame front sec.	Ax. Dist from Nozz cm
Initial	1000	4000	60	1829	1.4	0 - 4 flame front	87.5	2438	000	53
1	2000	2000	80	2438	1.2	4-7	82.5	2514	.015	35
2	4000	1000	90	2743	.58	7-9	52.5	1585	.010	16
3	8000	500	105 110	3200 3359	.35	9-10	22	690	.070	46
4	16000	250	110	3200	.175				.095	153 (5 f
5	32000	125	90	2743	.072	Min. Vel.	4.45			
6	64000	62	80	2435	.03					
7	128000	32	70	2133	.013					
1)7.1	Weighted Average	40	4)e.75	2290	.0137					
7.2	MIT-Cor.	50	e.78	2352	.0136					
8	256000	16	60	1829	.0054	Row 8.A Table G.9.2	(3000 drops - 60°)			
9	512000	8	40	1219	.0016	0 - 9		2000	.135	270
10 5)	Min.	Velocity	4.45	136		9-10		670	.070	46
2)11	Coales- cence	720	105	3207	.33				.205	316
3)12	Coales- cence	110	70	2133	.022					(10.3
						Row 8.1A Table G.9.2	(1000 drops - 60°)			
						0 - 9		2000	.045	90
a) G.9.2						9-10		670	.07	46
									.115	136
										(4.5

TABLE G.9.1

S BASED ON TIME DATA OF G.8 WITH ATOMIZING STEAM
E AND CWF in anACCELERATION/DECELERATION MODE

	9	10	11	12		13		14		15	
S FROM NOZZLE EXIT (Ft.)											
es cm/sec.	Time from flame front sec.	Ax. Dist. from Nozzle cm.	Drop Dia. um	Total burnout Time. (Sec.) Min.	Max.	Net burnout time at 4.45 fps Min.	Max.	Burnout Dist. (ft.) at 4.45 fps Min.	Max.	7) Total burnout DDist. (ft.) from Nozzle Exit Min.	Max.
2438	000	53									
2514	.015	35									
1585	.010	16									
690	.070	46 See Fig. G.9.2 ($\frac{46}{670}$ = .07 sec.)									
	.095	153 (5 ft.)									
			720	1.63	3.26	1.535	3.165	6.83	14	11.83	19
			500	1.3	2.6	1.2	2.5	5.34	11.1	10.34	16.1
			375	.8475	1.7	.7525	1.60	3.35	7	8.35	12
			110	.2485	.497	.1535	.40	.68	1.8	5.68	6.8
			50	.113	.226	.018	.13	.08	.58	5.08	5.58
rops - 60°)			40	.09	.180	000	.085	000	.38	5.00	5.38
2000	.135	270									
670	.070	46									
	.205	316									
		(10.35 ft.)									
			720	1.63	3.26	1.43	3.055	6.36	14.5	16.7	24.8
			375	.8475	1.70	0.64	1.495	2.85	6.65	13.2	17.0
			110	.2485	.497	0.385	0.292	0.17	1.3	10.5	10.6
			50	.1130	.226	0.000	0.021	0.00	0.1	10.35	10.5
rops - 60°)			40	.09	.180	0.000	0.00	0.00	0.00	10.35	10.35
2000	.045	90									
670	.07	46	720	1.63	3.26	1.50	3.145	6.7	14.0	11.2	18.5
	.115	136	375	.8475	1.70	0.732	1.585	3.3	7.05	7.8	11.6
		(4.5 ft)	110	.2485	.497	0.135	0.382	0.6	1.7	5.1	9.6
			50	.1130	.226	0.00	0.111	0.00	0.5	4.5	9.0
			40	.09	.180	0.00	0.065	0.00	0.3	4.5	9.0

TABLE 1-A.6.R

SUMMARY OF APPENDIX CALCULATIONS TO DETERMINE CONST
AT CWF VISCOSITY OF (a) EMULSION VELOCITY AND (b) OF CWF

			SHEAR RATE FUNCTION				
						(8V/D) CWF at emu	
CASE	ATOM. STEAM PRESS. PSI	ANNULUS ΔP PSI	Tw DYNES/CM^2	POISE	$\frac{Tw}{\mu}$	VELOCITY fps	8V/D cm./sec.
A	175	350	$1.85.10^6$	8.95	$(2.067)10^5$	500	$(2.50)10^5$
B	82	350	$1.85.10^6$	8.95	$(2.067)10^5$	930	$(4.65)10^5$
C	175	350	$1.85.10^6$	0.63	$(2.94)10^6$	500	$(2.50)10^5$
D	82	350	$1.85.10^6$	0.63	$(2.94)10^6$	930	$(4.65)10^5$
E	125	150	794550	0.63	$(1.26)10^6$	663	$(3.3)10^5$

TABLE 2-A.6 .R

SUMMARY OF APPENDIX 6 CALCULATIONS TO DETERMINE CONST
VALUES WHEN VISCOSITY IN EMULSION VISCOSITY IS .01 POISE

			SHEAR RATE FUNCTION				
						(8V/D) Emulsion Rate	
CASE	ATOM. STEAM PRESS. PSI	ANNULUS ΔP PSI	Tw DYNES/CM^2	POISE	$\frac{T_w}{\mu}$	VELOCITY fps	8V/D cm./sec.
A	175	350	$1.85.10^6$	.01	$(1.85)10^8$	500	$(2.723)10^5$
B	82	350	$1.85.10^6$	.01	$(1.85)10^8$	930	$(4.65)10^5$
C	175	350	$1.85.10^6$	.01	$(2.85)10^8$	500	$(2.723)10^5$
D	82	350	$1.85.10^6$	.01	$(1.85)10^8$	930	$(4.65)10^5$
E	125	150	794550	.01	$(7.94)10^7$	663	$(3.3)10^5$

TABLE 1-A.6.R

ALCULATIONS TO DETERMINE CONSTANTS N & K
) EMULSION VELOCITY AND (b) OF CWF ONLY VELOCITY

E FUNCTION

w	(8V/D) CWF at emulsion vel.			(8V/D) (CWF ONLY VEL.)			CWF 70/30 MIX. REF. X.2 APP. 1				CWF 75/25 MIX. REF. X.2 APP. 1						CWF ONLY
u	VELOCITY fps	8V/D cm./sec.	n_1	VELOCITY fps	8V/D cm./sec.	n_2	ϕ	ϕ_∞	$\frac{\phi}{\phi_\infty}$	Viscosity, Cp $\left(1-\frac{\phi}{\phi_\infty}\right)^{-3.54}$	ϕ	ϕ_∞	$\frac{\phi}{\phi_\infty}$	Vis. for $\phi = .75$ $\left(1-\frac{\phi}{\phi_\infty}\right)^{-3.54}$	K_1	K_2	τ_w/μ
.067)10^5	500	$(2.50)10^5$	.79	18	9.10^3	.995	.64	.75	.853	895	.685	.75	.913	5677	10.83	9	$(8.9)10^4$
.067)10^5	930	$(4.65)10^5$	.47	18	9.10^3	.905	.64	.75	.853	855	.685	.75	.913	5677	11.13	9	$(8.9)10^4$
94)10^6	500	$(2.50)10^5$	1.17	18	9.10^3	.106	.64	.925	.69	63	.685	.925	.740	118	.506	1.016	$(1.262)10^4$
94)10^6	930	$(4.65)10^5$	.702	18	9.10^3	.106	.64	.925	.69	63	.685	.925	.740	118	.782	1.016	$(1.262)10^4$
26)10^6	663	$(3.3)10^5$	.193	18	9.10^3	.1045	.64	.925	.69	63	.685	.925	.740	118	.446	1.016	$(1.262)10^4$

TABLE 2-A.6.R

6 CALCULATIONS TO DETERMINE CONSTANTS N & K
EMULSION VISCOSITY IS .01 POISE

EMULSION DATA

E FUNCTION

w	(8V/D) Emulsion Rate			CWF 70/30 MIX. REF. X.2 APP. 1					CWF 75/25 MIX. REF. X.2 APP. 1				
	VELOCITY fps	8V/D cm./sec.	n_3	ϕ	ϕ_∞	$\frac{\phi}{\phi_\infty}$	Viscosity, Cp $\left(1-\frac{\phi}{\phi_\infty}\right)^{-3.54}$	n_4	ϕ	ϕ_∞	$\frac{\phi}{\phi_\infty}$	Vis. for $\phi = .75$ $\left(1-\frac{\phi}{\phi_\infty}\right)^{-3.54}$	K_3
85)10^8	500	$(2.723)10^5$	.67	.024	.75	.032	1.12		.026	.75	.035	1.13	.013
85)10^8	930	$(4.65)10^5$	.40	.012	.75	.016	1.06		.0113	.75	.015	1.0555	.0117
85)10^8	500	$(2.723)10^5$	.67	.024	.925	.026	1.10		.026	.925	.028	1.106	.013
85)10^8	930	$(4.65)10^5$	.400	.012	.925	.013	1.05		.0113	.925	.0122	1.04	.0117
94)10^7	663	$(3.3)10^5$	.515	.017	.925	.018	1.07		.0187	.925	.02	1.07	.0127

$K_4 = K_3$

$n_4 = n_3$

TABLE G.1-1

DROP FORMATION DATA

Division No.	No. of Drops	Cumulative No. of Drops	Radius um	Droplet Velocity, fps	Droplet Velocity, cm.sec.	Separation cm	Separation um
Initial	3000	3000	2000	60	1829	.21	2100
1	6000	9000	1000	66	2012	.135	1350
2	12000	21000	500	73	2225	.085	850
3	24000	45000	250	82	2470	.054	540
4	48000	93000	125	90	2743	.032	320
5	96000	189000	62	100	3048	.0193	193
6	192000	381000	31	110	3353	.0113	113
7	384000	765000	16	182	3718	.0065	65
8	768000	1533000	8	135	4115	.0037	37
9	1536000	30069000	4	150	4572	.0022	22

G.1.1

TABLE OF CONTENTS

Item No.	Description	Page	Section Indexed	Vol.
1	List of Reports 5th Symposium	ii	Reports X 5th	ii
2	List of Reports - 6th Symposium	v	Reports W 6th	ii
3	List of Papers (G)	viii	Papers	ii
4	References	xi		
5	List of Tables 5th Symposium	xiv	Tables X - 5th	iii
6	List of Figures 5th Symposium	xv	Figures - 5th	iii
7	List of Tables 6th Symposium	xx	Tables 6th	iii
8	List of Figures 6th Symposium	xxiii	Figures	iii
9	List of Appendices	xxviii	Appendices	iii
10	List of Reports on Telephone discussions	xxx	Reports - Tel.	iii
11	List of Reports Meetings	xxxi	Reports (M)	iii
12	List of Engineering Drawings	xxxii	Eng. Drgs.	iii
13	List of Technical Papers	xxxiv	Tech. Papers	iii

383 pp

MICROMEDIA

LIST OF REPORTS - 5TH SYMPOSIUM

Report Code No.	Location	Title of Paper
X1	5th-79	Rheological Characteristics of Coal-Water Mixture With High Coal Content Li Xing-Chang, etal
X2	5th-151	Effects of Coal Type, Surfactant, and Coal Cleaning on the Rhiological Properties of Coal Water Mixture R. Kaji, etal Hitachi Research Laboratory, Hitachi, Ltd., Japan T. Kawamura Hitachi, Ltd., Japan M. Murata Babcock-Hitachi, Japan Y. Takahashi Kure Works, Babcock-Hitachi,d Japan Y. Arikawa, H. Kikkawa Kure Research Laboratory, Babcock-Hitachi, Japan T. Igarashi, H. Higuchi Nippon Oils & Fats Co., Ltd., Japan
X3	5th-238	The Availability of Very Low Ash Coal for Coal-Based Fuels Dr. Peter J. Bethell A.T. Massey Coal Company, Richmond, Virginia Mr. Frederick R. Sell COMCO, Pittsburgh, Pennsylvania
X4	5th-318	Com Burner Development Paul L. Bartown Unit 1 William E. Dudley, etal Florida Power Corporation
X5	5th-323	Operation and Testing of the Paul L. Bartow Unit 1 on Coal-Oil Mixture Gary L. Petersen, David T. Buell Florida Power Corporation Stephen A. Scavuzzo, John Neidert, Jr. Babcock & Wilcox Company

LIST OF REPORTS - 5TH SYMPOSIUM

Report Code No.	Location	Title of Paper
X6	5th-625	A New Burner Design for CWS Combustion (Lezzon) Sushil K. Batra Gimret International, Inc., Shrewsbury William A. Walsh, Jr. The Lezzon Group, Manchester
X7	5th-873	Coal Slurry Fuels: Moving Towards Commercial Utilization Gary A. Mailer Florida Power & Light Company Richard E. Barrett, etal Battelle's Columbus Laboratories
X8	5th-897	Comparison of Coal Conversion Alternatives E. Kimel Burns & Roe, Inc. R. Kurtzrock Doe Pittsburgh Energy Technology Center
X9	5th-1023	Combustion & Fuel Characterization of Coal-Water Mixtures M.J. Hargrove, A.A. Levasseur Combusion Engineering, Inc. B.E. Davis Gulf Research & Development Co.
X10	5th-1053	Large Scale CWS Firing Tests at the S. Barbara Power Station G. DeMichele, etal Enel-Crtn Pisa Snamprogetti
X11	5th-1119	Rheology and Pumping Characteristics of Coal-Water Slurry Fuels Prepared in a Columbia Chase Intergrator Sushil K. Batra, Etal Gimret International, Inc. Austin O'Toole Columbia Chase Corporation

LIST OF REPORTS - 5TH SYMPOSIUM

Report Code No.	Location	Title of Paper
X12	5th-1142	Handling Properties of Coal-Water Slurries John Dooher, etal Adelphi Center for Energy Studies, Adelphi University Martin Mullarkey Long Island Lighting Company
X13	5th-1158	Rheological Characteristics of Coal Water Mixture Yasuhiro Kiyonaga Lion Corp. Shin-Ichi Watanabe Kao Corp.
X14	5th-1182	Coal/Water Slurry Rotating Cup Atomization Ronald J. Marnicio, Holger T. Sommer Carnegie-Mellon University, Pittsburgh
X15	5th-1205	Rheology of Coal/Water Slurries E.Z. Casassa, Etal Department of Chemical Engineering, Carnegie-Mellon University
X16	5th-1229	Some Rheological Data and Atomization Behavior of CWM's Containing 68 to 83% Coal Lars Gillberg, Etal AB Carbogel, Helsingborg, Sweden

LIST OF REPORTS -6 TH SYMPOSIUM

Report Code No.	Location	Title of Paper
W1	6th-109	Combustion Histories of Various Coal-Water Fuels K.J. Mattews and P.J. Street Marchwood Engineering Laboratories, U.K.
W2	6th-127	Combusion Characterization of Coal-Water Mixtures M.J. Hargove, Etal Combustion Engineering, Inc., Windsor, Conn., USA
W3	6th-143	Space Resolved Coal-Water Mixture Combustion & Pollutant Formation Studies in a Laboratory Scale Furnace Geoffrey J. Germane, Etal Combustion Laboratory, Brigham Young Univ., USA
W4	6th-165	No$_x$ and Carbon Emission Control in Coal-Water Slurry Combustion W.F. Farmayan, Etal Massachusetts Institute of Technology, USA
W5	6th-234	Research on CWM Preparation Technique with Chinese Coals Zheng Rong-Zeng, Etal Beijing Coal Mine Administration, China
W6	6th-251	The Effects of Surface Active Agents on Coal/Water Slurry Stability N.Z. Casassa, Etal Carnegie-Mellon University, USA
W7	6th-266	A Direct Rheological Characterization of Highly Loaded Coal-Water Slurries Through Pipes G. Antonini, Etal Universite de Technologie de Compiegne P. Girard Centre de Recherches, Elf - Solaize, France
W8	6th-283	Effects of Weathering of Coals on Slurriabilities T. Igarashi, Etal Institute of Photographic Chemistry, Academia, Sinica

LIST OF REPORTS - 6TH SYMPOSIUM

Report Code No.	Location	Title of Paper
W9	6th-304	Effect of the Interaction Between Particles on the Viscosity of Coal-Water Slurries Gregory D. Botsaris Department of Chemical Engineering, Tufts Univ., USA Kenneth H. Astill Dept. of Mechanical Engineering, Tufts Univ., USA
W10	6th-313	Relationship Between Properties of Adsorption Layer on Coal Surfaces and Rheological Characteristics of Coal Water Slurry Tiefeng Chen, Etal Institute of Photographic Chemistry, Academia, Sinica
W11	6th-325	Coal-Water Methanol Slurries: Viscometric Properties and the Effects of Coal Type Amy C. Ekman and James Ekman United States Department of Energy, Pittsburgh Energy Technology Center, USA
W12	6th-404	Conversion Study of an Oil-Designed Commercial Boiler with SRC - Water Slurry M. Reza Chassemzadeh Utility Power Generation Division, Babcock & Wilcox Ray Holtzapple International Coal Refining Co., USA
W13	6th-481	EPRI Industrial Coal-Water Slurry Demonstration Rowan P. Perkins E.I. DuPont de Namours & Co, Inc. Rolf K. Manfred Electric Power Research Institute Brian E. Taylor Babcock & Wilcox Company, USA
W14	6th-499	Design and Test Firing of a 125 Million BTU/Hr Combined Coal Water Mixture and Oil Burner Dr. J. W. Allen NEI International Combustion, Derby, England
W15	6th-548	EPRI Coal- Water Demonstration Using Co-AL® Richard C. Furman, Consulting Engineer USA

LIST OF REPORTS - 6TH SYMPOSIUM

Report	Location	Title of Paper
W16	6th-557	Status Report on Co-Al Fuel E.G. Atkins Babcock Power Ltd., England
W17	6th-571	Selective Flocculation Coal CLeaning for Coal Slurry Preparation Yusry, A. et al Battelle's Columbia Laboratories, USA
W18	6th-649	Refining Solid Coal to Enhance Characteristics of Coal-Water Slurry Fuels J. Pinta, Jr. Gulf Research & Development Company
W19	6th-667	Ash Deposition from the Combustion of Clean Coal-Water Slurries Arthur A. Boni, et al Morgantown Energy Technology Centre, USA.
W20	6th-710	A Study of the Combustion Characteristics of a Number of Coal-Water Slurries S. Bortz et al International Flame Research Foundation, The Netherlands
W21	6th-791	Densecoal - An ALternative to Gas and Oil Reinhard B. Klose Salzgitter, F.R.G.
W22	6th-827	Atomization of Coal-Water Slurries N. Chigier, P.L. Meyer Mechanical Engineering Department, Carnegie-Mellon University, USA.

LIST OF PAPERS

NO.	DESCRIPTION
1) G.1	An Analysis of the C.E. Y-Jet Function Based on the Mullinger-Chigier Separated Phase Observation.
G.1. Add. 1	Spray Development based on a 45° total angle starting at Nozzle.
G.1 Add. 2	Revised Spray Formulated based on Production of 1000 drops per .005 sec.
G.2.R	Hypothetical Determination of Effect of Viscosity on the Weber Number. Revision of G.2 - based on Clearer Numerical Analysis and Correction of error in one of the cgs transformations.
G.3	A Discussion on Coalescence.
G.4	Discussion on Research Requirements for a Y-Jet and other Atomizer Design for CWF use.
G.4 Add. 1	Continued Research Discussion.
G.5	Discussion on Temperature Tolerance of a CWF.
G.6	Discussion on Atomizing Efficiency.
G.7	Velocity changes in Atomizing Steam and Spray Droplet Flows due to Energy Exchange, with comparison to "Turbulent Free Jet Velocity Characteristics". (12)

1) G.1 - Erratum
G.1 - Erratum - Addendum 1.

LIST OF PAPERS

NO	DESCRIPTION
G.8	Droplet Burn-Out time.
G.9	Burn Out Axial Distances.
G.9 Add. 1	Derivation of weighted average droplet
G.9.Add. 2	Logic of Item 19 (G.9)
G.10	Discussion of Tables G.9.1 and 2, showing Data Source, Data Development, Spray Formation, and Lengths to Flame Front and Burn-out.
G.11	Relationship between the Areas of the Number of Drops and the areas of the Flame Front zones
G.11 Add.l	Further considerations from Paper G.11.
G. 12	**Interaction** at intersection points of an Annular 45° spray Dispersion under cases of: 3000 Drops per .015 Sec. and 1000 Drops per .005 sec.
G.13	Cohesion Probability in transverse flow at intersections of 45° fuel spray streams.
G.14	Interaction of 45° Fuel Spray Streams from neighboring Annuli of a C.E.Y. Jet (Chatham) Burner Gun.

G. 15 Discussion M.I.T. Paper

G.16 Discussion as Atomizer Design

G.16 Addendum 1 - Further Discussion on atomizer design

G.16 Addendum 2 Calculation of atomizer Design of Fig. G.16.1.

G.16 Addendum 3 - Turn Down of Burner Design of Fig. 16.1

REFERENCES

---

1. P.J. Mullinger and N.A. Chigier
"The Design and Performance of
Internal Mixing
Twin Fluid Atomisers"
Journal of the Institute of Fuel (251)
December 1974

2. Giffen and Muraszew
"The Atomization of Liquid Fuels"
Wiley, 1953

3. "Control Parameters for 75 wt. %
Coal-Water Slurry: Co-Al "
J.E. Funk Jr., D.R. Dinger, J.E. Funk, Sr.
(Binder Section - Tech. Report - B.1)

4. R.G. Report Appendix 5-R.

REFERENCES

5. "Combustion, Flames and Explosions of Gases"
Bernard Lewis and Guenther Von Elbe
2nd Edition, Academic Press Inc.
New York, 1961 (p. 239)

6. "Flow of Fluids Through Valves, Fittings and Pipe"
Crane Technical Paper, No. 410.

7. "Technical Data on Fuel", Edited by H.M. Spiers,
Published by British National Committee, World
Power Conference, London, England (p. 409)

8. "Theoretical and Experimental Investigation on Attached Jet Entrainment"
R. Medeot
Riello Bruciatori - Research Centre,
Padova, Italy.

REFERENCES (continued)

9. "Ash Deposition from the Combustion of Clean Coal-Water Slurries" (See P. 672 - 6th Symposium for Discussion on Burn-Out and Residence Times)

10. "Ignition and Combustion of Utility Grind Coal-Water Slurry in a lean confined Turbulent Diffusion Flame", P.M. Walsh, J.M. Beer et al, MIT Energy Laboratory Paper No. MIT-EL-84-004WP, Nov. 1984

11. "Combustion Aerodynamics, J.M. Beer and N.A. Chigier, Halstead Press Division, John Wiley & Sons, Inc., New York 1972.

12. "Chemical Engineers Handbook", See Table 5-6 P5-20 re "Free Turbulent Jet Velocity Characteristics", Perry and Chilton - 5th Edition, McGraw Hill, 1973

LIST OF TABLES - 5th Symposium

Table No	Report Code	Description
2	X.2	Viscosities at solid concentration of 65 wt%.
3	X.2	Viscosities at solid concentration of 70 wt%.
4	X.2	Properties of coals.
1	X.7	Analyses of slurry fuels.
2	X.7	Combustion conditions and emissions for slurry tests.
4	X.8	Performance of major modified boiler - oil firing.
5	X.8	Performance of modified boiler - coal-water mixture firing.
6	X.12	Capital cost estimates.
1	X.12	Rheological Properties - Viscometer Measurement.
1	X.16	Viscosity at various shear rates, density and moisture content of the master batch and slurries diluted therefrom.
2	X.16	Viscosity, density and moisture content of slurries containing stabilizer.
3	X.16	Viscosity of slurries numbers 1 to 7 measured at constant shear rates for a period of 60 minutes.

LIST OF FIGURES - 5th Symposium

Fig. No	Report Code	Description
2	X.2	Relationship between O/C atomic ratio and inherent moisture.
4	X.2	Effect of O/C atomic ratio on the viscosity of coal water mixtures.
5	X.2	Relationship between O/C atomic ratio and water absorption.
6	X.2	Effect of water absorption on the viscosity of coal water mixtures.
7	X.2	Plot of viscosity vs. $\left(1-\frac{\phi}{\phi_\infty}\right)$
11	X.2	Ash content vs. particle size.
I	X.6	Prior experimental work.
II	X.6	Early experimental work.
III	X.6	Application to lezzon nozzle.
IV	X.6	Enlarged view of test nozzle tip.
4	X.10	Schematic section of Y-mixing atomizer.
1	X.11	Schematic of CWS Pilot Plant
2	X.11	Particle Size Analysis "A" Coal.
3	X.11	Effect of blending on coal Particle Size Distribution.
4	X.11	Particle Size Distribution of Nominal 62 Weight % CWS

List of Figures - 5th Symposium

Fig. No	Report Code	Description
5	X.11	Particle Size Distribution of Nominal 65 Weight % CWS.
6	X.11	Particle Size Distribution of Nominal 70 Weight % CWS.
7	X.11	Effect of Chemical Additives on the Viscosity Characteristics of Nominal 62 Weight % CWS Fuels.
8	X.11	Effect of Chemical Additives on the Viscosity Characteristics of Nominal 65 Weight % CWS Fuels.
9	X.11	Effect of Chemical Additives on the Viscosity Characteristics of Nominal 70 Weight % CWS Fuels.
10	X.11	Schematic of CWS Pumping Test Loop.
11	X.11	Effect of Pumping on Viscosity of Nominal 65 Weight % CWS Fuel.
12	X.11	Effect of Pumping on Viscosity of Nominal 68 Weight % CWS Fuel.
13	X.11	Effect of Pumping on Coal Particle Attrition of Nominal 65 Weight % CWS Fuel.
14	X.11	Effect of Pumping on Coal Particle Attrition of Nominal 68 Weight % CWS Fuel.

List of Figures - 5th Symposium

Fig. No	Report Code	Description
15	X.11	Variation of Pressure Gradient with Flow Velocity in the Pumping Test Loop.
16	X.11	Particle Size Distribution of Micronized Coal.
17	X.11	Viscosity Characteristics of 68 Weight % MCWS Fuel.
18	X.11	Viscosity Characteristics of 70 Weight % MCWS Fuel.
Table 1	X.11	Proximate Analysis of Various Coals.
Table 3	X.11	Stability Characteristics of Typical CWS Fuels.
6	X.12	Apparent Viscosity Versus Time, Sample A-1.
7	X.12	Apparent Viscosity Versus Time, Sample B-1.
8	X.12	Apparent Viscosity Versus Time, Sample D-1.
9	X.12	Apparent Viscosity Versus Shear Rate, Sample B-2.
10	X.12	Apparent Viscosity Versus Shear Rate, Sample B-3.
11	X.12	Apparent Viscosity Versus Shear Rate, Sample D-4.
3	X.13	Viscosity of CWM.

List of Figures - 5th Symposium

Fig. No	Report Code	Description
5	X.13	Effect of amount of ACC-700.
6	X.13	Effect by combined use of stabilizer.
1	X.15	Viscosity of coal/water slurries.
2	X.15	Viscosity of coal/water slurries.
3	X.15	Plot of Dougherty and Krieger equation with [illegible] = 0.70.
5	X.15	Viscosity of 50% (wt) coal/water slurries.
6	X.15	Rheological data (Herschel-Bulkley Equation) for 50% (wt) Coal/Water Slurries.
7	X.15	Electrophoretic mobility of 50% (wt) coal/water slurries.
8	X.15	(a) Electrophoretic mobility, (b) viscosity of 50% (wt) Pittsburgh #8 coal/water slurries, one week after preparation.
9	X.15	(a) Electrophoretic mobility, (b) viscosity of 50% (wt) washed Pittsburgh #8 coal/water slurries.
1	X.16	Viscosity (Pas) vs. shear rate (s-1) for slurries number 1, 4 and 6.
2	X.16	Atomization test facility.

List of Figures - 5th Symposium

Fig. No	Report Code	Description
3	X.16	Feed pressure vs. moisture content.
4	X.16	Mass Median Diameter (pm) vs. moisture content.
5	X.16	Mass Median Diameter vs. air to slurry ratio for six slurries.
6	X.16	Initial viscosity - Lowest viscosity at 450 s^{-1} (Pas) vs. moisture content (% w/w).
G.1.X.12	B.1	Constant Low Shear - Rheopectic Mode
G.2.X.12	B.1	Constant Low Shear - Thixotropic Mode

LIST OF TABLES

6th SYMPOSIUM (CODE W)

Table No.	Report Code	Description
1	W.1	Coal water mixtures Properties.
2	W.1	0.5 M W, combustion facility
3	W.1	Burnout and mean particle Size after 0.85 seconds - Slurry B.
4	W.1	Burnout and mean particle Size after 2.5 seconds - Slurry B.
5	W.1	Effect of coal loading on burnout and mean particle size - Slurry B.
6	W.1	Effect of slurry composition on burnout and mean particle size
7	W.1	Particle size variation with time
8	W.1	Typical drop histories
5	W.2	Typical FPTF operating conditions during lower Kittanning tests
6	W.2	Typical FPTF operating conditions during splash dam tests
7	W.2	FPTF test results coal, atomizer droplet size and fly ash size
8	W.2	Lower Kittanning relative slagging characteristics
9	W.2	Splash dam CWM tests relative slagging characteristics
1	W.3	Coal-water mixtures used in combustion characterization, and mapping tests
2	W.4	MIT Coal-water slurry trials summary of input and operating conditions of selected fames.

Table No.	Report Code	Description
2	W.2	Lower Kittanning FPTF test fuel analysis.
3	W.2	Splash dam FPTF test fuel analysis.
5	W.2	Typical FPTF operating conditions during lower Kittanning tests.
6	W.2	Typical FPTF operating conditions during splash dam tests.
3	W.4	Analytical data on the Occidental Research Corp. experimental coal - water slurry fuels.
1	W.6	Coal Analysis
2	W.6	Soluble Inorganic IONS in slurry superstant.
5	W.6	Surface tension of slurry supernatants - as a function of time.
1	W.9	Viscosities of coal -water slurries (Pocahontas Coal)
2	W.9	Maximum coal volume fraction, O m.
1	W.10	The thickness of adsorption films formed on coal surface by different additives.
2	W.10	Density of adsorption layer on coal surface.
1	W.12	Fuel analysis.
2	W.12	Combustion test data.
4	W.10	Effect of different additives on the viscosity of CWS at constant concentration of CWS. (concentration of CWS is 65%).
1-A	W.13	Raw Coal Analysis.
1-B	W.13	Slurry Analysis(1).
11-B	W.13	Arc-Coal Field Measures (1) (2)
11-C	W.13	Co-Al Sampling.

Table No.	Report Code	Description
3	W.13	Boiler predicted performance by Babcock and Wilcox.
5	W.13	EPRI COAL - WATER slurry Demonstration burn Test data summary and boiler efficiencies.
1	W.14	Coal water mixture properties.
4	W.14	Diagram of coal water mixture burner nozzle.
1	W.15	Co-Al provided for EPRI-sponsored demonstration.
4	W.15	EPRI coal-water slurry demonstration burn[1] Test data summary and boiler efficiencies.
1	W.17	Results of selective flocculation of bituminous coal from National Coal Board (U.K.)
2	W.17	Results of selective flocculation of selective U.S. coals.
3	W.17	Results of selective flocculation tests on selective coals by Dai-Ichi Kogyo Sei Yaku Company, Ltd., Japan.(4)
2	W.20	Coal water slurries for the NEOM/CANMET trials (CNM - NOT Measured).
4	W.20	Summary of the slurries combustion performance (NA - NO attempted).

LIST OF FIGURES

6th SYMPOSIUM - (CODE W.)

Figure No.	Report code	Description
3		Coal - Methanol - water mixture burner.
4		Coal - Methanol - water mixture burner. Atomizer assembly.
5	3	Viscosity of hvC B CMW Mixtures (51% coal) as a function of methanol concentration in the liquid phase.
6	5	Variation of carbon conversion and boiler efficiencies with methanol content in hv AB and hvCb CMW Mixtures (full load, 500°F combustion air).
8	5	Effect of methanol content on particulate emissions - hvAb GMW mixtures (Full load, 500° F. combustion air).
2	W.1	0.5 MW, combustion facility.
3	W.1	Burnout and mean particle size after 0.85 seconds - slurry B.
4	W.1	Burnout and mean particle size after 2.5 seconds - slurry B.
5	W.1	Effect of coal loading on burnout and mean particle size - slurry B.
6	W.1	Effect of slurry composition on burnout and mean particle size.
7	W.1	Particle size variation with time.
1	W.3	Utah Coal - Water Rheogram with no additives, inherent moisture before pulverization was 2.4 mass %.
7	W.3	Effect of swirl number and stoichiometric ratio on burnout of coal in CWM.
9	W.3	Photograms of CWM flames showing the effect of slight variations in the OR-KVB atomizer internal dimensions on the position of the flame front with corresponding no. emission.

6th Symposium - (code W.)

Figure	Report Code	Description
11	W.4	Photographs of CWS flames showing the effect of combustion air swirl on the axial position of the flame front with corresponding no. emission.
15	W.4	Photograph of the run 3106 or fine grind CWS flame O_2 injection.
20-23	W.4	Photographs of char particles in flame.
24-25	W.5	SEM closeup of several char particles from figure 23. SEM view of the surface of one of the char particles in Figure 24.
26	W.4	SEM of Char particules captured from the run 306 CWS at 1.07 m from the burner (or standard grind CWS).
27	W.4	SEM of char particules captured from the run 309 CWS flame at 1.37 m from the burner (or fine grind CWS).
1	W.5	Volume content of solid vs modulus n according to Alfred equation at = 1.3 and D_1 = 300 um.
2	W.5	Models of monosphere packing.
3	W.5	Volume content of solid vs modulus n according to R-R equation at s = 1.3 and D_1 = 300 um
4	W.5	Size distribution according to R-R and Alfred Equations at CWT = 70% and s = 1.3.

Figure	Report Code	Description
2	W.8	Equilibrium moisture V.5 slurry viscosity.
1	W.9	Interaction between particles.
3	W.9	Coal water slurries without additives.
4	W.9	CWS without additive (points from curve in Fig. 3) Frankel and Acrivos Method (1).
5	W.9	CWS without additive (points from curve in Fig. 3) Heath and Tadros Method (8).
6	W.9	Testing of correlations.
1	W.10	Relationship between the thicknesses of adsorption films and the additive concentrations (additives A, B, C)
2	W.10	Adsorption isotherms of three additives (A, B, C) on coal powder.
3	W.10	Effect of different additives on the viscosity of CWS at constant concentration of CWS (concentration of CWS is 65%).
5	W.10	Effect of different additives (A, B, C) on the viscosity of CWS at constant concentration of additives (concentration of additives is 1.0% to dry coal).
2	W.11	Viscosity vs. percent methanol in water - methanol and 47.5% Montana Rosebud coal-water - methanol mixtures.
3	W.11	Viscosity vs. percent methanol in water-methanol and 56% Canadian coal-water - methanol mixtures.
4	W.11	Viscosity vs. percent methanol in water-methanol and 50% lignite coal-water mixtures.

Figure	Report Code	Description
10	W.11	Ciscosity vs. percent methanol in water - methanol and 50% petroleum coke-water - methanol mixtures.
8	W.13	T-Jet atomizer.
2	W.16	Babcock Power CWM burner.
1	W.17	Conceptual representation of the selective flocculation process.
5	W.17	Separation of pyrite from coal by the use of a polyxanthate dispersant.
4	W.18	Figure 4.
8	W.18	Figure 8.
2	W.21	Figure
3	W.21	Figure
2	W.21	Figure 2.
3	W.21	Figure 3.
5	W.20	Figure 5: Particle size distributions wet sieve technique.
6	W.20	Figure 6: Maximum CWS burnout recorded for the 7 slurries as a function of atomizing air rate.
7	W.20	Air/steam atomization.
8	W.20	Figure 8: Minimum secondary air temperature required for unsupported combustion.
6	W.21	Viscosity vs. shear rate with additive K154.
8	W.21	R = n (additive(ONC) for additive B11.
4	W.22	Parker - Hannifin atomizer.
3	W.22	Coen # 1MV Atomizer.

Figure	Report Code	Description
8	W.22	Slurry spray produced by the Parker-Hannifin atomizer at the nozzle exit slurry: 500 lb./hr.; atomizing air: 175 psig.
9	W.22	Slurry spray produced by the Parker-Hannifin atomizer 1 inch down stream from the nozzle exit slurry; 500 lb./nR atomizing air; 175 psig.
10	W.22	Water spray produced by the Parker-Hannifin atomizer water: 500 lb. lb./nR, 12 psig: atomizing air 41 psig.
11	W.22	Water spray produced by the Parker-Hannifin atomizer wrater: 500 lb./nR 26 psig: atomizing air 153 psig.
12	W.22	Slurry spray produced by the Coen atomizer water: 500 lb./hr.: atomizing air: 175 psig.

LIST OF APPENDICES

Sources: X – 5th Symp.; W – 6th Symp.; See List of Reports

App. No.	Sources	Description
1	X.2	Equations for the determination of
	X.12	
	X.15	Viscosity, Shear Rate, and Shear Stress.
	W.7	
	W.9	For Newtonian and Non-Newton Modes of fluid flow
	1) B.1	Control Parameters for a 75 lot. % Coal-water slurry: Co-AL
2	2) G.	Calculation of Volume Equivalent of a 70/30 wt. mix in CWF.
2.1	G.	Calculation of Volume Equivalent of a 75/25 wt. mix in CWF.
2.1. Add.1	G.	Conversion of Coal Vol. fraction to Wt. Fraction
3	G.	Derivation of Symbols on Ordinate and Abscissa on Graph Plots Showing Shear Rate versus ΔP with conditions for Atomizer Design.
4.R	G.	Function Data on Operation of Mark 3 C.E. Atomizer (EPR1)
4.R, Add.1	G.	CWF Requirements for the 22.5 Meg.$_e$ Boiler at Chatham

---

1) B.1 – Section: Tech. Papers, Vol. 1.
2) G. – Calculation by R.G.

App. No.	Sources	Description
5.R	G.	Viscosity Determination from Φ and Φ max. Values of Average CWF and of Co-Al.
6.R	G	Determination of Constants n and K by Application of the Rabinowitsch-Mooney modification of the Newtonian Flow Basic Equation to the Dimensional and Operating Data of the Mark 3 C.E., Atomiser (EPRI) (Chatham).
6.R, Add.1	G	Calculation of the Rabinowitsch-Mooney Constants n & K if based on: a) Velocity of the CWF at its volume rate; b) Viscosity of the CWF/atom-steam emulsion at the emulsion velocity.
7	G	Application of Equations derived from the Basic D'Arcy and Poiseville formulae (from Crane Tech Paper 410) to the C.E. Mark III (EPRI) Atomizer design and the Chatham Operating Parameters (See Appendix 4.R, page 1)
8	G	Potential for Total Drying.
9	G from X.2 X.15 W.9	Determination of Cp Viscosity Values from Various Equations of Appendix 1.
10	G	Specific Volume of Air at 175 psig and Resulting Viscosity of the Emulsion.

LIST OF REPORTS OF TELEPHONE DISCUSSIONS

Report Code	Description
T.1	Florida Light & Power Corp.
T.2	Hauck Manufacturing Co.
T.3	Coal Liquid Co.
T.4	Process Combustion Corp.
T.5	Florida Power Co.
T.6	Peabody Engineering Corp.
T.7	North American Mfg. Co.
T.8	John Zink Co.
T.9	Arco Petroleum Products Co. (Harvey Ill.)
T.10	National Research Council
T.11	Atlantic Research Corp.
T.12	Conamara Ltd. (Vorto Metric)
T.13	Carnegie - Mellon University Chemical Engineering Dept.
T.14	Babcock - Wilcox Co. Research Development Division
T.15	New Brunswick Electric Power Commission
T.16	Chatham Plant of the N.B.E.P.C.
T.16 Add.1	Further discussion with Keith Keoughan (N.B.E.P.C.)
T.17	M.B.B. Mechanical Co., Halifax, N.S.

LIST OF REPORTS OF MEETINGS

Report Code No.	Description
M.1	Geo. Farthing - B & W. at Alliance, Ohio.
M.1 Add. 1	Further Discussions with Geo. Farthing - Telephonic.
M.2	Dr. N. Chigier and Miss Pat. Meyer - Carnegie-Mellon University, Pittsburgh, Pa.

LIST OF ENGINEERING DRAWINGS

(Drawings Located Section Eng. Drgs. - Vol. III)

Report Code	Figure	Description
A.4.	1	Mark 3 (EPRI) CE. Atomizer.
A.4.1	3	Critical Dimensions "Y" jet atomizer design, cross section view.
A.4.2	1	Atomizer alternatives.
G.1	1	Schematic of Y-Jet, atomizer with added divergent nozzle.
G.1	2R	Spray formations.
G.1	2 ×	Use of attached jet (Coanda surface) to develop specific spray angle.
G.1	3	C.E. Annulus with divergent nozzle.
G.1	4	Distance to zone where velocities reduced from
G.1	1.5	Modes of Fluid mixing.
G.9	1 ×	Steam velocities - deceleration from point 6 cm. from nozzle.
G.9	2 ×	Axial distance from Div. 9, Fig. G.9.1 to Min. velocity point of 4.45 FPS.
G.10	1	Dimension data for Eq. 1 - G.10.
G.11	1	× Spray Geometrics
G.11	2	
G.11	3	
G.11	4	
G.11	5	

List of Engineering Drawings (continued)

Report Code	Figure	Description
G.12	1 ×	Spray Intersections.
G.12	2 ×	Spray intersections.
G.12	14.1 ×	Determination of the G.M. Zone for a spray rate of 3000 drops/.015 sec.
G.12	2 ×	Determination of the G.M. zone for a spray rate of 1000 drops/.005 sec.
G.14	3 ×	Intersections of spray flows from adjoining annuli. Case 1 - 1-3000 drops/.013 sec. Scale: 1/4" - 6 cms.
G.14	14.4 ×	Intersections of spray flows from adjoining annuli Case II - 1000 drops/.005 sec. Scale: 1/4" = 1 cm.
G.15	5	× Drawings from MIT Report (10)
G.15	3	
G.15	7	
G.15	10	
G.15	11	
G.1	5 (10) ×	Idealized disintegration of Fuel issuing from an Internal Mixing Twin Fluid Atomizer.
G.16	1 ×	Whaley-Grossman Homogenizer.
G.16	2 ×	Division point of 50% Flow.

× = Drawings located with Report (as Coded) as well as in Eng. Drgs. Section.

LIST OF TECHNICAL PAPERS

Paper Code No.	Description
T.P. 1	The design and performance of internal mixing multijet fluid atomizers by: P.J. Mullinger and N. Chigier
T.P.2	Coanda effect Theoretical and experimental investigation on attached - jet entrainment. By: R. Medeot
T.P. 3	Applications of the Coanda effect By: Imants Reba.
T.P. 4	Control parameters for a 75 WT% coal-water slurry: Co-Al By: Alfred University
T.P. 5	C.E. Canada CWM nozzle development and firing experience.

An Analysis of the C.E. Y Jet Function Based on the Mullinger-Chigier Separated Phase Observation

---

1. In a 1974 paper (1) Mullinger and Chigier found that the flow through a Y-Jet train fluid atomizer observed through a transparent annulus showed that the fuel flow and atomising flow were separate phases.

2. The type of "fuel" used in the experiments was not named nor its viscosity. However, from the air/fuel mass ratios shown in their Fig. 5, giving values from 0.02 to 0.12, it seems logical to assume that the "fuel" in the experiments was water, or possibly a very light fuel oil or diesel oil.

3. A basic assumption for this analysis is that a similar two-phase behavior would exist with a CWF fuel at a commercial average standard viscosity of 800 to 900 centipoise.

3.1 Geo. Farthing of the B & W Research Division at Alliance, Ohio, has stated to me that he considered that their CWF ((a Co-al type) had a fuel component flowing as a film across the outer face of their T-jet mixing chamber - towards the exit ports.

4. Assuming that the ideal sketch of the Mullinger-Chigier experiment (Fig. 4 attached) was drawn reasonably to actual dimensions. An average scaling of the annulus flow channels and the inner atomizing steam core was made to establish ratio of annulus areas and core

4. (continued)

areas, averaged over cross-sections A-A' and B-B' (See Fig. 4)

4.1 The area ratios for the fuel annuli and the steam core were respectively .76 and .24 or a ratio of fuel to steam area of approx. 3.1 (See Work Sheets 1 attached). This is a Number 1 seem to recall having being given to me by Dr. Chigier.

5. Applying the scaled fractions to the actual dia. of the C.E. atomizer (Chatham) gave the following areas:

a) Fuel annulus area .1416 cm^2
b) Steam core Area .045 cm^2
Total area .186 cm^2

5.1 The actual I.D. of the C.E. atomiser
is .487 & $\pi \times \left(\frac{.487}{2}\right)^2 = .1863, cm^2$
which is suitably close to the values of item 5

6. The equipment and operational data of the CE (Chatham) **atomiser** are given in the following:

6.1 Length of annulus -0521 ft.
= 1.6 cm,

6.2 Dia. of C.E. annulus (each of 7 per burner) .192 in.
= .016 ft.
= .487 cm.

6.3 I.D. area of the C.E. atomizer annulus (each) .0002 ft^2
= .1863 cm^2

7. Dimensions based on the M.C.[1] (1) 2 phase system and the area ratios determined as in item 5 are:

7.1 Core radius:

$\pi r^2 = .045 \text{ cm}^2$, hence

$r = \left(\frac{.045}{\pi}\right)^{1/2}$, $= .1197$ cm

$= .2354$ cm.dia.

7.2 Width of fluid annulus is then:

$\frac{.487 - .2384}{2} = .124$

8. Operating Data

8.1 Max. CWF Volume Flow rate = .0036 cfs

= 102 cm^3

8.2 Max. CWF weight flow rate = .267 lbs./sec.

= .121 kg./sec.

9. C.W.F. Velocity flow rate C.E. annulus:

$\frac{.0036}{.0002} = 18$ fps

= 5.5 m./sec.

10. Check now for CWF Re. No.

$Re = 6.31 \frac{W}{d\mu}$; W = w lbs./hr

d = dia. ins.

(Crane(6) p.311) μ = viscosity, centipoise

---

[1] M.C.= Mullinger - Chigier

10. (continued)

$$\text{Re: } \frac{6.31 \times .267 \times 3600}{.192 \times 900} = 35$$

Flow is Laminar

11. Atomizing Steam Flow

Atom, Steam Press entering core (estimate) = 175 psig

11.1 Atom, steam rate **is:** .15 lb/lb fuel

$= .15 \times .267 = .04$ lb./sec.

$= 144$ lbs./hr

11.2 $\overline{V}$ for 175 psig is 2.404 cf /lb.

11.3 normally for pipe flow in a .2" dia. tube fully turbulent flow would be assumed with an f value of .0365

11.3 But because steam flow is within water walls it is assumed that the f factor would be reduced by 1/2 or .0183 rounded to .02

11.4 The Crane (1) equation for Turbulent Flow is:

$$\underline{\Delta P_{100}{}^1} = \frac{.00036 \, f \, W^2}{d^5 \rho} \qquad (1)$$

Substitute:

$f = .0183$

$W = 144$

$d = .192$

$$\rho = \frac{1}{\overline{V}} = \frac{1}{2.404} = .416$$

11.4 (continued)

Then ΔP 100^1 $= \dfrac{.00036 \times .183 \times (144)^2}{66 \quad (.192)^5 \times .416}$ = 1242 psi

11.5 Then ΔP for annulus length of .0521 ft.

is $\dfrac{1242}{100} \times .0521$ = .65 psig

negligible

11.6 Check Re number (Steam vis. =.018 (p[1]

$\mathrm{Re} = \dfrac{6.31 \times (144)^2}{.192 \times .018} = 38.10^6$

Fully Turbulent Flow

12. Then conditions are correct for full sonic flow

ΔP req'd at annulus exit is: $\dfrac{14.7}{.545}$ = 27 psia

12.1 Hence affective sonic press. at end of cylindrical annulur is 27 - 14.7 =

13.3 psig - rounded to 15 psig

12.2 Therefore steam pressure at exit point - (entrance to divergent nozzle - is 175 - 15 = 160 psig

13. The formula for Sonic Velocity is

1) $Vs = (kg\ 144\ P^1\ \overline{V})\ 1/2 =$ where

k = specific heat ratio = $C_p / C_v = 1.3$

g = gravity acceleration = 32 ft./sec.$^{-2}$

P = absolute pressure = 160 + 14.7= 174.7 psia

$\overline{V}$ = specific volume of steam at 1 7 4.7 psia = 2.616

then $Vs = (1.3 \times 32.2 \times 144 \times 174.7 \times 2.616)^{1/2}$

$= \left((2.755)\ .10^6\right)^{1/2}$ = 1660 fps

---

1) Crane p.A. 2.

14. The velocity number based on the steam rate of .04 lbs/sec. and an annulus area of (.24 1) x .0002) is

$$\frac{.04 \times 2.616}{.24 \times .0002} = 2180 \text{ fps}$$

15. But the velocity limit is the sonic value of

1660 fps

15.1 Therefore the steam core dia. formed by the separated phases is calculated

from the equation $1660\ \pi r^2 = (.04 \times 2.616) = .10464 \text{ ft.}^3$

(where .04 is steam flow wt.rate/sec. & $\overline{V} = 2.616$

Then $\pi r^2 = \frac{.10464}{1660} = .000063 \text{ ft}^2$

$.0585 \text{ cm}^2$

and $r = \left(\frac{.000063}{\pi}\right)^{1/2} =$

$= .0045 \text{ ft}$

$= .137 \text{ cm}$

The core dia. is $2r = 2 \times .137 = .274$

15.2 The fluid annulus width is then

$$\frac{.487 - .274}{2} = .106 \text{ cm}$$

16. The fluid annulus area is: =

$(.1866 - .0585)$ $.131 \text{ cm}^2$

$= .02 \text{ in.}^2$

16.1 The ratio of fluid annulus area to $= 00014 \text{ ft}^2$

Steam core area is now:

$$\frac{.131}{.0585} = 2.24:1 \quad 1)$$

---

1) .240 area fraction for the M.C. mode as per item 4.1.

16.2 The revised fluid film velocity (unaccelerated) is:

$$\frac{.0036}{.00014} \quad = \quad 26 \text{ fps}$$

17. Consideration must now be given to a hypothesis of jet break-up, droplet and spray formation to establish an algorithm for numerical analysis.

18. Considerations are:

18.1 Steam expansion will be guided to a point where the pressure is zero psig via a divergent nozzle having a total angle of 15 °(accepted practice in "Thermo dynamics" by Faires)

18.2 The pressure of the CWF flow is a linear function of its viscosity

18.3 The jet annular flow will be broken by the atomizing steam into N equivalent spheres such that the pressure within each fuel drop is zero psig.

18.4 That droplet breaking beyond the divergent nozzle is a function of the Weber No.[1)] $\frac{\rho_a . V^2 . r}{\dot{\gamma}} \geq 10$ (1)

[1)] Weber Number to be modified by the addition of a factor in the denominator to account for viscosity (See item 46 and paper G.2.R)

18.4 where:

ρ_a = density of steam

V = differential velocity between CWF drops and atomizing steam

r = radius of CWF droplets.

$\dot{\gamma}$ = Surface tension - dyne. c m.

18.5 That droplet break up will be mitotic and that it will continue until final droplet size is approx. 2 um diameter (corresponding to assumed min.diameter of coal droplets in the CWF coal size distribution.

18.6 That the droplet sizing will contain max. coal sizing in accordance with the Funk Distribution (see Fig. 2. Tech. paper, B.1 in Binder) ranging from 1 um to 400 um

18.7 That the time element between droplet break up shall be based on the time number for the formations of droplets as the time for steam flow through the length of the divergent nozzle.

19. A numerical analysis based on the hypotheses of item 18 follows:

19.1 Dimension D_2 (Fig. G. 1) at 0 psig is a

function of the ratio $^{1)}\left(\dfrac{\overline{V}_2}{\overline{V}_1}\right)^{1/2} = \left(\dfrac{26.8}{2.61}\right)^{1/2} = 3.2$

Then $D_2 = 3.2 \times .274 = .876\text{cm}$

19.1.1 Velocity of steam at divergent nozzle exit is inversely proportional to the ratio $\dfrac{\overline{V}_2}{\overline{V}_1} = 1/10 \times 1660 = 166$ fps

19.2 Now find length L of divergent nozzle as follows:

$$\frac{AB}{CB} = \tan \left(\frac{15}{2}\right)^{\circ} = .1316, \text{ then}$$

$$AB = \frac{D_2 - .274}{2} = \frac{.866 - .274}{2} = .296$$

19.2.2 Now $\dfrac{AB}{CB} = .1316$

Subt. A B = .296, to obtain $\dfrac{.296}{CB} = .1316$

so that $CB = \dfrac{2.96}{.1316} = 2.25$ i.e. Length L of divergent nozzle = 2.25 cm.

19.3 Now determine press. of fluid film at point C.

19.3.1 Initial pressure (estimated - Chatham) 150 psig

19.3.2 Item 9 shows velocity of liquid film to be 18 fps

19.3.3 This velocity (unaccelerated by the steam core flow) is revised (item 16.2) to 26 fps. The velocity head is then obtained from the equation $V^2 = 2\,ghl$. (Eq.2)

---

1) $\dfrac{\overline{V}_2}{\overline{V}_1} = f\ (\text{area})$

19.3.3 (cont'd) where h_l = head in feet of fluid

now $h_l = \frac{P}{\rho}$, and ρ = density = 1.19 × 62.4

= 74.26 lbs/cf.

P = psi × 144 = psf

Then subst. values of V, P & p in Eq.2, we find

$$V^2 = \frac{2 \times 32.2 \times 144\ P}{74.26} = 125\ P$$

$$V = 26, \text{ then } P = \frac{(26)^2}{125} = 5.4 \text{ psig.} = \Delta P \text{ due to velocity head}$$

19.4 The friction head due to internal fluid friction due to its viscosity (standard commercial value of about 900 centipoise is then (150 – 5.4) = 144.6 psi.

20. Note that the viscosity of 900 cp is equivalent to an SSU value of 3505.

Atomization of a fuel of this viscosity by mechanical or steam assisted atomizers is not known (at least to me) in engineering practice. The max. viscosity normally consistent for a steam atomization burner is 300 SSU

21. Item 10 shows an Re no. of 35 which is at the low end of the laminar flow scale)

22. Even if the value of 63 Cp. is obtained for Co-Al from the Funk-Dinger-Funk porosity data were possible, the Re No. would be $\frac{900 \times 35}{63} = 500$ which is still well within the Re limits for laminar flow (N.B. The anomaly between the use of the Funk-Dinger-Funk (3) porosity values in establishing a low Φ max. value versus the 806 Cp value established by them from viscometer readings,has not been resolved by Dr. Dinger as per my recent telephone conversation)

23. We now come to the question of the breaking of the annular fluid jet within the confines of the divergent nozzle (hypothesis 18.3)

24. It has been shown that the friction pressure stress within the annular jets is 144.6 psig.

25. It is hypothecated that this stress will be broken by the atomizing steam core so that the terminal stress is O psig.

---

26. To accomplish this the jet stream must be broken into equivalent spheres such that $N \times 4\pi r^2 = \left(P_1^1 - P_2^1\right)$ $= \left(159.3 \text{ psia} - 14.7 \text{ psia}\right)$

27. The ratio of surface increase is then

$$\frac{159.3}{14.7} = 11$$

28. The inner surface of the jet from entrance to exit of the divergent nozzle is:

mean dia. x vector length x π

29. Refer to Fig. G.1 and find the vector

length $\dfrac{CB}{EA} = \text{Cos } 7.5^\circ = .9914$

so that $EA = \dfrac{CB}{.9914} = \dfrac{2.5}{.9914} = 2.52 \text{ cm}$

30. The mean dia. of the divergent nozzle

is: $\dfrac{.909 + .274}{2} + .106 = .70 \text{ cm.}$ (rounded)

31. The liquid jet surface area in the divergent nozzle is then

$\pi dL = \pi \times .70 \times 2.52 = 5.54 \text{ cm}^2$

32. The volume of the liquid jet in the divergent nozzle

is $5.54 \times .106 = .587 \text{ cm}^3$

33. It is hypothesized that the atomizing steam will cause breakup of the volume, such that the surface of the number of pieces expressed as equivalent spheres will be increased by a factor

---

33. (continued)

of 11 to bring the residual friction stress pressure in the drops to O psig.

34. We then have:

$$\left(11 \times 4\pi r^2\right) = 5.54$$

$$1^2 = \frac{5.54}{11 \times 4 \times \pi} = .04$$

34.1 Then $r = (.04)^{1/2}$ = .20 cm

= 2000 um radius

= 4000 um dia.

35. The volume of these spheres is:

$$\frac{4}{3}\pi r^3 = \left(\frac{4}{3} \times \pi \times \left(.20\right)^3\right) = .0335\ \text{cm}^3$$

35.1 The number of drops formed in the divergent nozzle is $\frac{.587\ \text{(item 32)}}{.0335\ \text{(item 35)}}$ = 18 per wave

36. Flow rate of CWF (Chatham) (item 8.1) 102 cm^3/sec.

37. No. of drops formed per sec. is $\frac{102}{.0335}$ = 3044 rounded to 3000

37.1 Time rate for steam flow through divergent nozzle is calculated:

Av. Velocity $\frac{1660 + 166}{2}$ = 913 fps

= 27829 cm /sec.

37.2 Time rate $= \frac{2.5}{27829}$ (item 19.2.2) rounded = 9.10^{-5} sec. (basic "wave" time)

38. The average velocity in spray formed in the divergent nozzle (see item 44).

is: $\frac{40 + 60}{2}$ = 50 fps

= 1524 cm./sec.

---

39. Drop radius (item 34.1) = 0.20 cm

40. Separation between drops from

Eq.2 (item 43) is

$$Sd = \left((2 \times .2) + X\right) \times 3000 = 1524$$

$$.4 + x = \frac{1524}{3000} = .508$$

$\therefore$ S d = X = .108 cm

= 1080 um.

(within divergent nozzle)

41. Hence the above means that the passage of atomizing steam through the divergent nozzle will create the discharge of 3000 drops per sec. having a (mean equivalent) radius of 2000 um at a mean separation of .108 cm.

42. Consider drop distribution in divergent nozzle

42.1 Surface area of liquid in divergent nozzle (item 31) 5.54 cm^2

42.2 Drop diameter 2 x .2 (item 34) .4 cm

42.3 No. of drops formed (item 35.1 18

42.4 Drop Distribution in divergent nozzle is:

$$\frac{18 \times .4}{5.54} = 1.3/cm^2$$

$$= 1/.77\ cm^2$$

42.5 Spatial need of drops at divergent nozzle

exit = drop diameter .40

plus "separation"(item 40) .108 = .508 cm

42.6 Oce. of divergent nozzle exit = π × .909 (item 19.1)= 2.85 cm

42.7 Hence drops exit in waves of

2.85/.508 = 6 drops per wave

or approx. $\frac{18}{6}$ = 3 waves per steam

passage time through through divergent nozzle

or a wave time rate of $\frac{9.10^{-5}}{3}$ = 3.10^{-5} **sec.**

43. The formulae for the foregoing are

$$N_D = \frac{.238 \text{ Vol.}}{r^3} \qquad (1)$$

$$S_D = X = (2r + X) \times N_D = V_D \qquad (2)$$

where

Nd = No. of drops

Vol. = Vol. of liquid flow (CWF) cm^3/sec.

r = radius of particle, cm

S_D = separation distance, cm

V_D = Differential velocity between particles and atomizing fluid

44. It is assumed that the liquid in the straight annulus will be accelerated from 26 fps (item 16.2) to 40 fps

44.1 It is further assumed that the transformation of the liquid jet into droplets in the divergent nozzle will be accelerated from 40 fps to 60 fps

SPRAY FORMATION BEYOND DIVERGENT NOZZLE

45. As the spray initiated in the divergent nozzle exits, it will come under the influence of the Weber number (to be called Weber Force) - corrected for the factor of viscosity.

46. The Weber number modified for the viscosity factor is

$$\frac{P_a V^2 \quad r}{\dot{Y} + (.01154\,\mu)} \geq 10$$

Where P_a = atomizing fluid density grams /cc

V = differential velocity between particles and atomizing fluid, cm./sec.

$\dot{Y}$ = Surface tension, dyne. cm

μ = viscosity, centipoise

r = droplet radius

---

47. The Weber no. at the exit of the divergent nozzle. (for this Chatham exercise) is calculated as follows:

47.1 Substitute:

$P_a = \frac{1}{V}$ (V = 26.8 for steam at zero psig) $= \frac{1}{26.8}$ = .0373 lb.

= 17 grams

r = .20 cm.

V = 166-60 = 106 fps

= 3231 cm/sec.

$\dot{\gamma}$ = 76 dyne.cm.

μ = 900 Centipoise

Weber No. is $\frac{17 \times (3231)^2 \times .183}{76 + (.01154 \times 900)}$

$\frac{35.5.10^6}{86.38}$ = $3.76 \cdot 10^5$

= $\gg 10$

48. Hence the Weber "Force" will cause disintegrations of the drops until a value of V & r is formed so that Weber No. is $\geq$ 10

49. Assume an ultimate particle velocity in the developing spray as 90 % of the steam velocity or a velocity of 166 x .90 = 149.4 fps say 150 fps

and so a differential velocity of

166-150 = 16 fps

= 488 cm/sec

50. The dia. of the particle at this end point is calculated as follows:

$$\text{Weber No.}: \frac{17 \times (488)^2 \times r}{86.38} = 10$$

$$\text{Whence } r = \frac{10 \times 86.38}{4.05.10^6} = 2.13^{-6} \text{ cm.}$$

= 2.13um radius

= min. theoretical radius

50.1 (N.B. The value of **2**.13 radius appears to be a rational value for the smallest drop formed) It **compares** to the value of 4 um noted in Table G.1 - following the 9th "mitotic" division.

51. The problem now is to determine the spray formation velocity versus the ignition rate and mass burning rate.

52. The basic time rate will be taken as (for 18 drops) as: 4.10^{-5} sec.

53. First determine:

a) mean radius of particle, um

b) mean velocity - cm.sec.

54. Total no. of particles per sec. exiting from nozzle (item 37 rounded) = 3000

---

55. The number of mitotic divisions (See Table G.1) is : 9

55.1 The G.M. division point is $(1 \times 9)^{1/2} = 3$

56. Particle velocities postulated are:

56.1 At exit divergent nozzle 60 fps

56.2 At end of 9 mitotic divisions:

(90% of steam velocity = (90 x 166) = 150 fps

= 4572 cm/sec.

57. The particle velocity for each division will change in geometric ratio as per the series:

$$a, \quad ar, \quad ar^2 \qquad - \quad ar^9$$

57.1 From postulates

$$60\, r^9 = 150$$

$$r^9 = 2.5$$

$$r = (2.5)^{1/9} = 1.106$$

58. From the particle velocity and the number of drops at each division the separation between drops is calculated. (Eq. 2 item 43)

58.1 Table G.1 shows all this data.

59. 18 drops are formed within the divergent annulus in 9.10^{-5} (See Item 37.2)

60. The rate of formation per sec. is:

$$\frac{18}{9.10^{-5}} = 2.10^{5}$$

61. The actual no. of drops formed from the input rate of 102 cm^3/sec. (item 37) = 3000 (rounded)

62. Time rate of "wave" formation is:

$$\frac{3000}{2.10^{5}} = \frac{3.10^{3} \times 10^{-5}}{2} = 1.5.10^{-2}$$

= .015 sec. (rounded)

63. No. of waves formed i e .

No. of mitotic divisions is: 9

64. Hence, the time required to form 9 divisions (waves) is (9 x .015) = .135 sec.

65. Geometric mean velocity is:

$$(60 \times 150)^{1/2} = 94.87 \text{ fps}$$

66. Hence the distance from the exit of the divergent nozzle to the end of the spray formation (division 9) is:

---

66. (continued)

(94.87 x .135) - 12' 9"

Plus starting wave length 11"

Total distance to division 9 13' 8" 13' 8"

= 417 cm.

67. Distance to the geometric mean section of spray formation (point G. in drg. G.2, G.9 is calculated as follows:

67.1 Mean velocity for total spray (item 65) 94.87 fps

67.2 Mean velocity from nozzle exit to point G (mitotic division 3)is:

$(60 \times 94.87)^{1/2}$ = 75 fps

= 2286 cm/sec.

67.3 Time factor is (3 x .015) = .045 sec

67.4 Hence distance from nozzle exit to division Section 3 is: (.045 x 75) = 3' 5"

add initial distance of starting wave (.015 x 60) 11"

total distance 4' 4" 4' 4"

= 132 cms

68. Consideration must now be given to flame formation

68.1 From geometric mean droplet radius of 250 um - spray will be subject to influence from:

a) Combustion air

b) Drag

c) Heat from Flame Front

d) Exchange of energy between steam and liquid

e) Other annuli in the atomizer

f) Recirculation of hot combustion gases

68.2 The exchange of energy between atomizing steam and CWF fuel will be calculated and reported in an Addendum. The effect on originating steam velocities and the need, if any, of altering the divergent nozzle design (or supply pressure) to provide necessary differential velocity to effect drop separations shall be determined.

68.3 It is estimated that these factors will tend to slow down theoretical spray speed and the spray will tend to broaden due to these factors, from the geometrical mean point of 250 um radius. (Point G. Fig. G2.)

---

69. Development of flame geometry.

69.1 Theoretical steam/liquid flow relations as developed to this point shall be considered as in effect to down to the geometric mean point of division 3 Point G (Fig. G.1.2-R)

70. From point G it is considered that divergence from the 15° total angle, will occur and that the liquid drop flow velocity will be reduced in proportion to the new areas, as required to meet the needs of:

a) ignition speed

b) combustion wave speed

71. From Lewis and Von Elbe (5) and from "Technical Data on Fuel" (8), I believe that the following values can be used for this numerical assessment of CWF burning and ignition rates

a)	Combustion rate	=	140 cm/Sec.
b)	Ignition rate (50% estima ted)	=	70 cm/Sec.

72. Refer to Fig. G.2

$$\frac{FN}{DN} = \text{Tan } 7.5^{\circ} = .1316$$

72.1 Value of DN is 132 cms. (item 67.4)

plus nozzle length 2.5 cm, then DN = 134.5 cm.

FN = (134.5 x .1316) then FN = 17.7 cm.

72.2 Diameter FH (at geometric mean spray development point G) is then

$\underline{FH} = (2 \times 17.7) + .274$, then $\underline{FH}$ = 36.5 cm

= 1' - 2"

73. The particle velocity at geometric mean vertical section G (Table G.1) is = 82 fps

(This is approx. 1/2 terminal spray velocity based on 90% steam velocity at the 15° total angle expansion rate.) = 2500 cm/Sec.

72. It has been postulated (item 71) - that a value (for this numerical analysis) of ignition rate is 70 cm.sec.

73. Now consider that at vertical plane G that the half angle of the spray is increased to: 22.5°

= 45° total angle

Then the ignition point section will have a diameter D_3 such that

$$\frac{(FH)^2}{(D_3)^2} \times 2500 = 70$$

74.1 Then $(D_3)^2 = (FH)^2 \times 2500/70$

$= (36)^2 \times 2500/70$

$= 324000. /70$

$= 46286$

Then $D_3 = P_Q = (46886)^{1/2}$ $= 215$ cm.

$=$ 7' 0"

75. Now find length D'R'

$2\ PR + RS = PQ = 215$

$2\ PR = 215 - .274 = 214.1$

$PR = \frac{214.8}{2}$ $= 107.4$

76. $PT = PR - FN = (107.4 - 17.7)$

PT $= 89.7$

---

77. $PT = \tan\ (15^\circ + 7.5^\circ) = \tan 22.5^\circ = .414$

$FT = \frac{PT}{.414} = \frac{89.7}{.414}$ then FT $= 217$ cm

$= 7'\ 1''$

78. ∴ Total distance

$D'\ R' = (132 + 2.5 + 217) = 351.5$ cm.

79. This calculated length from entrance to divergent nozzle to point of ignition results from estimated velocities of the particles as accelerated by the atomizing steam.

79.1 The interaction of the spray from the other annuli in the atomizer, plus the effect of combustion gas recirculation may well decrease this calculated length of 11' 6" from nozzle to ignition plane.

80. The spray angle may well spread over the full 22.5° (half angle) as soon as the spray leaves the divergent nozzle.

80.1 This will be numerically examined in an addendum to this paper.

81. Much calculating time would be gained if field observations could be made on the approx. angle of the spray leaving the divergent nozzle.

82. N.B. There is also the factor of interaction between the numbers of nozzles on a burner gun which could reinforce the ignition energy phenomenon.

83. A more accurate picture of flame pattern using the same postulates as in this analysis may result by considering the combustion wave of velocity estimated from the noted sources, i.e. 140 cm/sec.

84. Let D_4 be diameter of combustion wave

84.1 Then item 74 becomes

$$D_4^2 = \frac{2500 \times (36)^2}{140}$$

$$= 23143$$

and $\underline{D_4} = (23143)^{1/2}$, then $D_4 =$ $\underline{152 \text{ cm}}$

for 140 cm/sec.
velocity
combustion
wave

85. Now calculate the distance and dia. of the combustion wave, (D_4)

86. Refer to Fig. G.2 and note that

$$D_4 = AJ = 152 \text{ cm. (See item 84.1)}$$

87. From the drawing it will be seen that:

$$2\,AV + VV^1 = AJ = 152 \text{ cm.}$$

$$VV^1 = FH = 36$$

$$\therefore \quad AV = \frac{152 - 36}{2} = \frac{116}{2} = 58 \text{ cm.}$$

88. $\frac{AV}{FV} = \tan 22.5^\circ = .414$

$$\text{Hence} \quad FV = \frac{AV}{.414} = \frac{58}{.414} = 140 \text{ cms}$$

88.1 Then Distance D V = (134.5 + 140) = 274.5 cms
= 9' 0"

89. This dimension seems excessive for the equilibrium front of a flame carrying approx. 10.10^6 BTU (per each of 7 annuli.)

90. The original thought in considering a 15° total angle divergent was to conserve the expansion energy of the atomizing steam, - to prevent "wild" turbulence resulting in heat generation and loss of momentum and decrease in differential velocity required for CWF drop break-up.

---

91. Experiment could determine whether the use of a jet-attachment curved surface (Coanda effect.), instead of the divergent nozzle as shown in Fig. G.2, might efficiently affect the development of an equivalent included angle of 45° (22.5°half-angle) as indicated in Fig. G.1.2.R.

91.1 The combustion wave plane is shown stabilized at the plane $\dot{Y}$ P running through G the geometric mean plane for spray formation.

92. The distance for the combustion wave is then 132 cms. (4' 4") from nozzle exit.

93. Combustion gas recirculation and eddy effects could shorten even this distance to a point possibly only 12" x 18" from nozzle exit.

94. An important "finding" of the numerical analysis of this paper is the "Separation of the drops" which possibly can lead to a solution of the coalescence problem.

95. Should the use of a widened divergent nozzle, (or even the suggested jet - attachment surface) cause violent disruption of the CWF liquid, into large "chunks" then possibly the provision of a high velocity air atomizing stream directed to a suitable downstream point, could re-establish the Weber "Force" based on differential velocity.

95.1 With drop separation developed into a fact, the use of a "micronized" CWF (reference Dr. Ken Olen, Florida Power & Light Co.) could prove advantageous.

96. A further paper will attempt to analyse flame length from the data of Report W19 (6th Symposium).

TABLE G.1.1

DROP FORMATION DATA BASED ON GENERATION OF 3000 DROPS PER .015 sec. and DROPLET ACCELERATION FROM 60 - 150 fps.

Division No.	No. of Drops	Diameter u m	Droplet Velocity, fps	Droplet Velocity, cm.sec.	Separation cm.	Separation um
Initial	3000	4000	60	1829	.21	2100
1	6000	2000	66	2012	.135	1350
2	12000	1000	73	2225	.085	850
3	24000	500	82	2470	.054	540
4	48000	250	90	2743	.032	320
5	96000	125	100	3048	.0193	193
6	192000	62	110	3353	.0113	113
7	384000	32	122	3718	.0065	65
8	768000	16	135	4115	.0037	37
9	1536000	8	150	4572	.0022	22

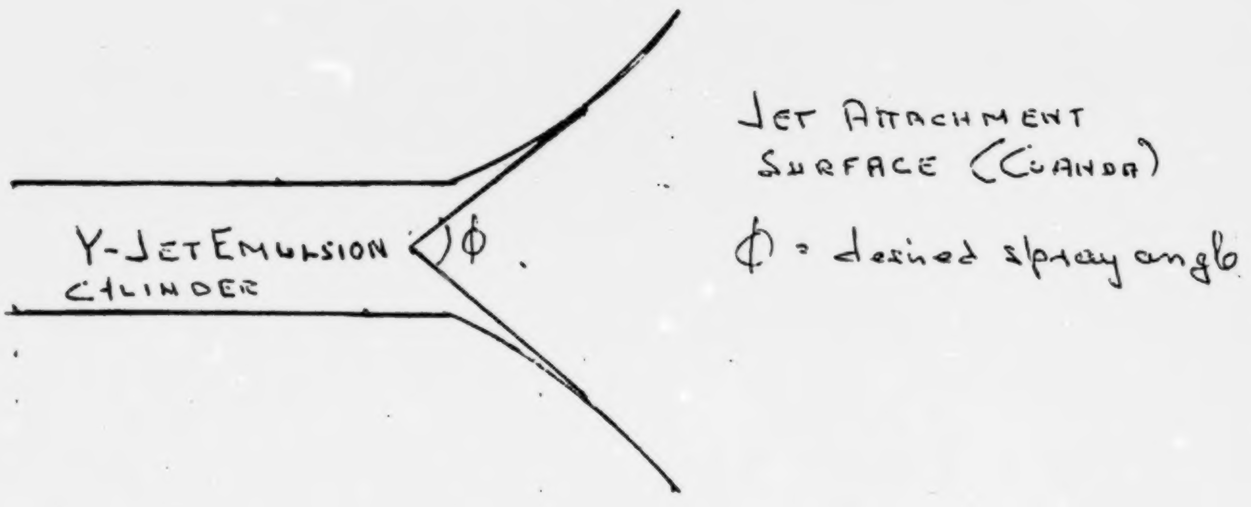
Y-JET EMULSION
CYLINDER
ϕ
JET ATTACHMENT
SURFACE (COANDA)
ϕ = desired spray angle

FIG. G.1.2

SCHEMATIC of the
ATTACHMENT of a COANADA SURFACE
to
A Y-JET ATOMIZER

FIG. G·1·2·R

SPRAY FORMATIONS

NOT TO SCALE

REF. TABLES G·1·1 ; G·9·1 ; G·9·2

FIGS. G·9·2 - G·9·3

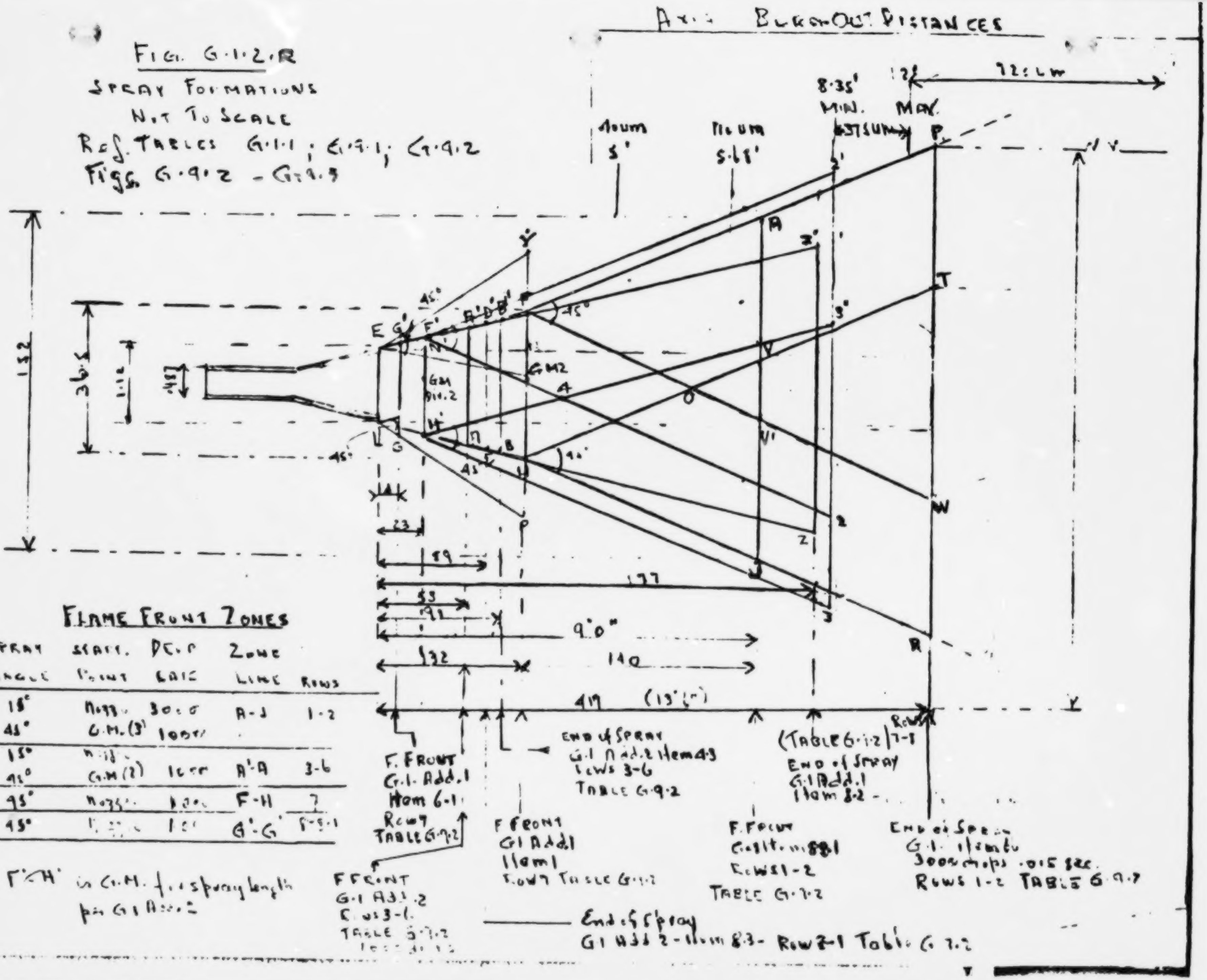
AXIAL BURN-OUT DISTANCES
4 dum 5'
11 dum 5.18'
8.35' MIN.
MAX.
72: LW
P
A
Z'
3'
T
S'
Y'
45°
E
G'
F'
A'
D'
B'
F
N'
GM2
GM DIA.2
A
O
V
H'
N
B
45°
L
G
45°
W
2
Z
J
3
R
Y
P
1:1
36.5
1.5
132
23
59
53
91
177
9'0"
132
140
419
(13' 9")
ROWS 7-8

F. FRONT
G.1. Add.1
Item 6.1
Row 7
TABLE G.9.2

F FRONT
G.1 Add.1
Item 1
Row 7 TABLE G.9.2

END of SPRAY
G.1 Add.2 Item 4.3
Rows 3-6
TABLE G.9.2

F. FRONT
G.1 Item 8.1
Rows 1-2
TABLE G.9.2

(TABLE G.1.2)

END of SPRAY
G.1 Add.1
Item 8.2

END of SPRAY
G.1. Item 6
3000 mops .015 sec.
ROWS 1-2 TABLE G.9.2

F FRONT
G.1 Add.2
Row 8-1
TABLE G.9.2

End of Spray
G1 Add 2 - Item 8.3 - Row 8-1 Table G.9.2

FLAME FRONT ZONES

SPRAY ANGLE	START. POINT	DRIP RATE	ZONE LINE	ROWS
15° 45°	Nozzle G.M.(3)	30.0 100%	A-J	1-2
15° 45°	Nozzle G.M.(2)	100%	A'-A	3-6
45°	Nozzle	100%	F-H	7
45°	Nozzle	100%	G'-G	8-8.1

N.B. F'-H' in G.M. for spray length per G1 Add.2

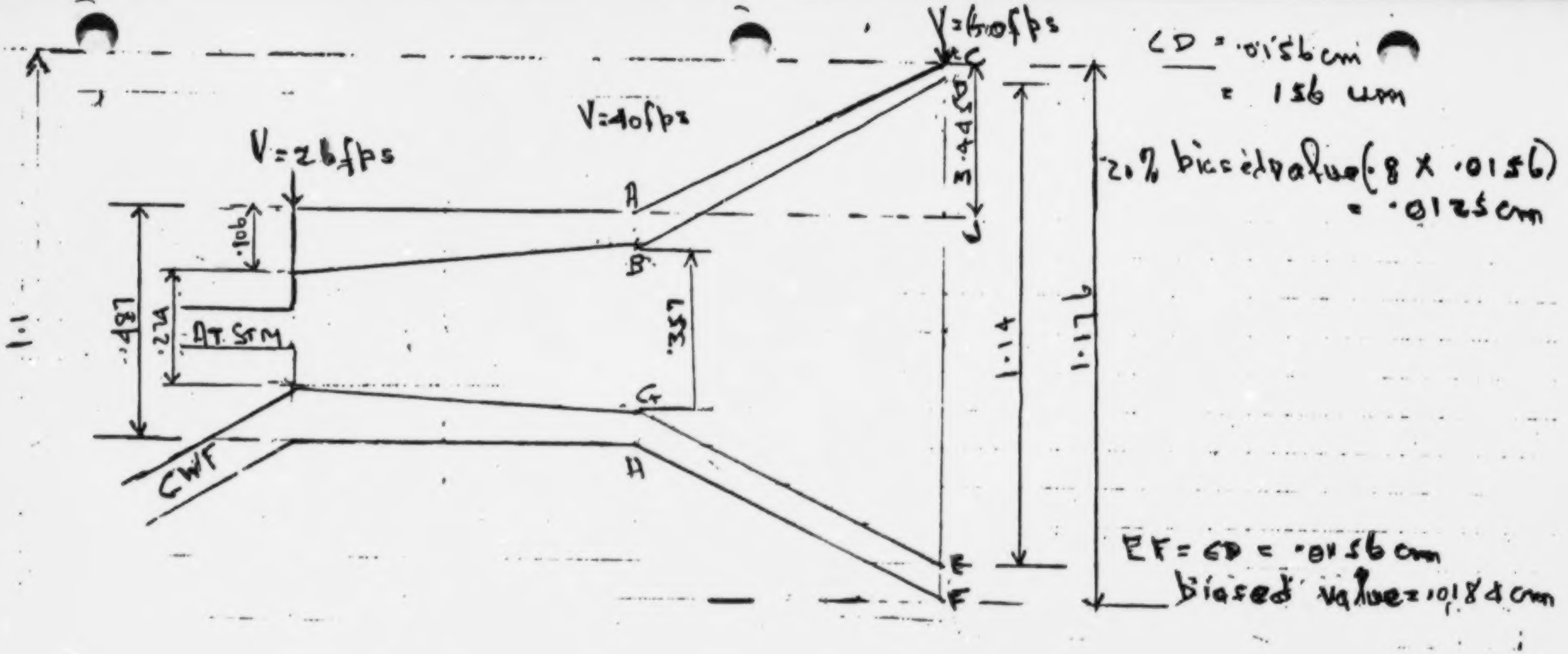
V=60fps
V=40fps
V=26fps
A
B
C
D
E
F
G
H
J
.106
.274
.487
AT.STM
.357
3.445
1.14
1.176
1.1
CWF
CD = .0156cm
= 156 um
20% biasedvalue(.8 x .0156)
= .0125cm
EF = CD = .0156 cm
biased value=.0184 cm

FIG. G.1.3 (N.T.S. - all dim. cm.)

C.E. ANNULUS WITH DIVERGENT NOZZLE
FLOW ASSUMED UNIFORM WITHIN OCE. OF
ANNULUS AND OF DIVERGENT NOZZLE

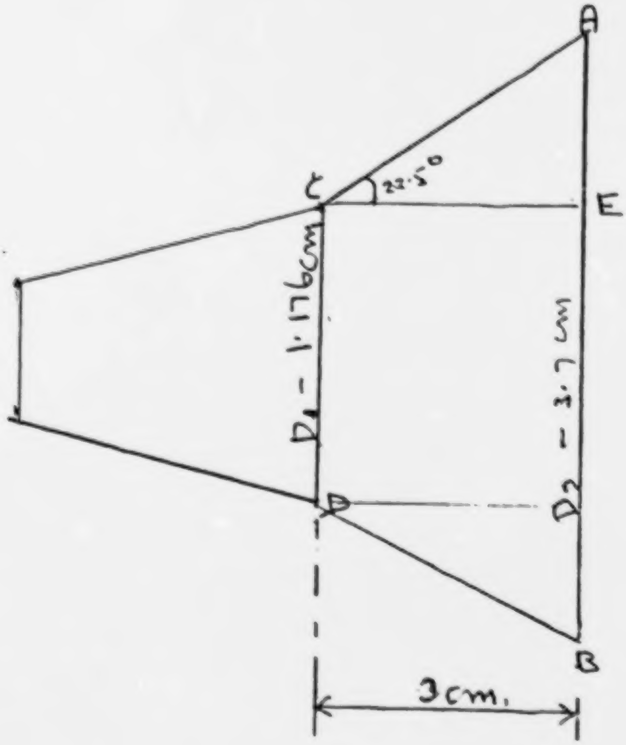
A
C
22.5°
E
D1 - 1.176cm
D2 - 3.7 cm
D
B
3cm.

FIG. G. 1.4

DISTANCE TO ZONE WHERE VELOCITIES

REDUCED FROM 1660 fps to 166 fps

(NOTE: CD is Divergent Nozzle Exit)

FIG G.1.5.
MODES OF FLUID MIXIN

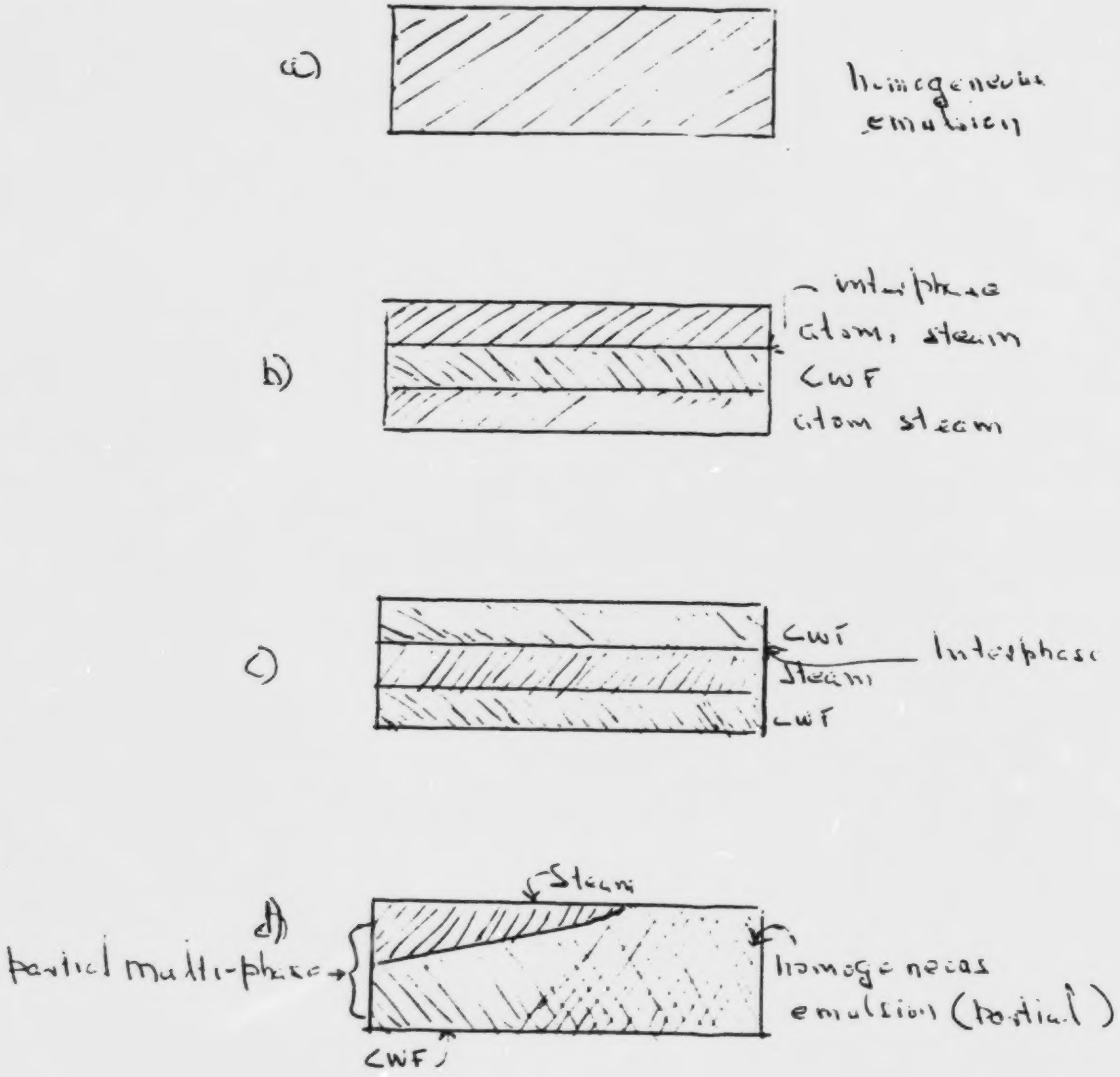
a)
homogeneous emulsion
b)
interphase
atom. steam
CWF
atom steam
c)
CWF
Interphase
Steam
CWF
d)
Steam
partial multi-phase
homogeneous emulsion (partial)
CWF

Determine Modes by:

1.- Use transparent annulus material

2.- Use Laser lighting plus electron microscopi
for modes a or b or c

3. Use Schlieren technique for mode d)

4.(10)G.1

FIG. 3 The disintegration of the fuel jet issuing from the atomizer (magnification 3.5 × full size).

(iii) the effect of axial and radial distance from the atomizer on the drop size distribution.

4.2.3. Pressure distribution within the atomizer

A second single jet atomizer was manufactured to the standard dimensions but with pressure tappings in the walls of the atomizing fluid port, fuel port and mixing chamber. The pressures within the atomizer were measured over the operating range of fuel and air flow rates.

4.2.4. The effect of atomizer geometry on the drop size distribution

Each geometrical dimension was changed independently and its effect on the drop size distribution measured under the same air/fuel mass ratio and fuel flow rate. In order to do this a series of atomizers had to be manufactured.

5. The experimental results

5.1. Fuel and air mixing and the disintegration of the liquid fuel

The disintegration of the liquid fuel remained fundamentally the same over the wide range (20:1) of fuel and air flow rates studied. A typical photograph of the break-up region is shown in Fig. 3. Increasing the air/fuel mass ratio reduced the break-up length. A similar break-up mechanism was observed in the jet issuing from the large-scale model. The break-up mechanism bears a similarity to that previously described for swirl spray pressure jet atomizers.[1] Fig. 4 shows an idealized model of the mixing between the atomizing air and the fuel with the subsequent disintegration of the fuel.

5.2. The effect of operational conditions on the performance of the atomizer

Fig. 5 shows that an increase in the air/fuel mass ratio

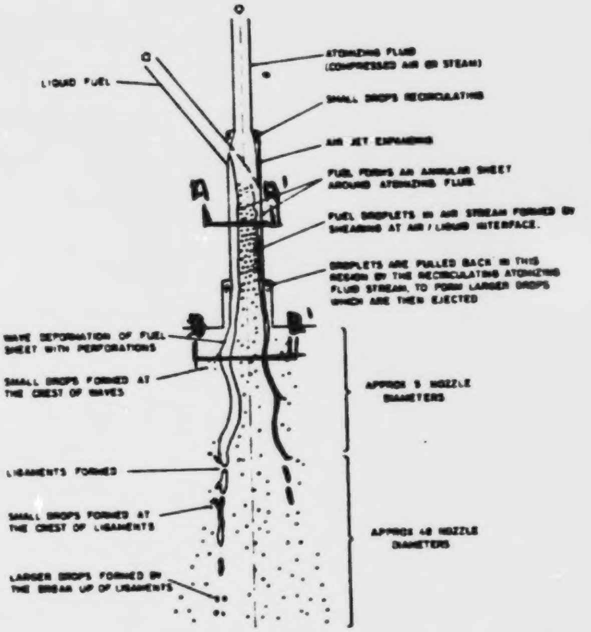
LIQUID FUEL
ATOMIZING FLUID (COMPRESSED AIR OR STEAM)
SMALL DROPS RECIRCULATING
AIR JET EXPANDING
FUEL FORMS AN ANNULAR SHEET AROUND ATOMIZING FLUID
A
A'
FUEL DROPLETS IN AIR STREAM FORMED BY SHEARING AT AIR / LIQUID INTERFACE.
DROPLETS ARE PULLED BACK IN THIS REGION BY THE RECIRCULATING ATOMIZING FLUID STREAM, TO FORM LARGER DROPS WHICH ARE THEN EJECTED
B
B'
WAVE DEFORMATION OF FUEL SHEET WITH PERFORATIONS
SMALL DROPS FORMED AT THE CREST OF WAVES
APPROX 5 NOZZLE DIAMETERS
LIGAMENTS FORMED
SMALL DROPS FORMED AT THE CREST OF LIGAMENTS
APPROX 40 NOZZLE DIAMETERS
LARGER DROPS FORMED BY THE BREAK UP OF LIGAMENTS

FIG. 4 Idealized disintegration of fuel issuing from an internal mixing twin fluid atomizer.

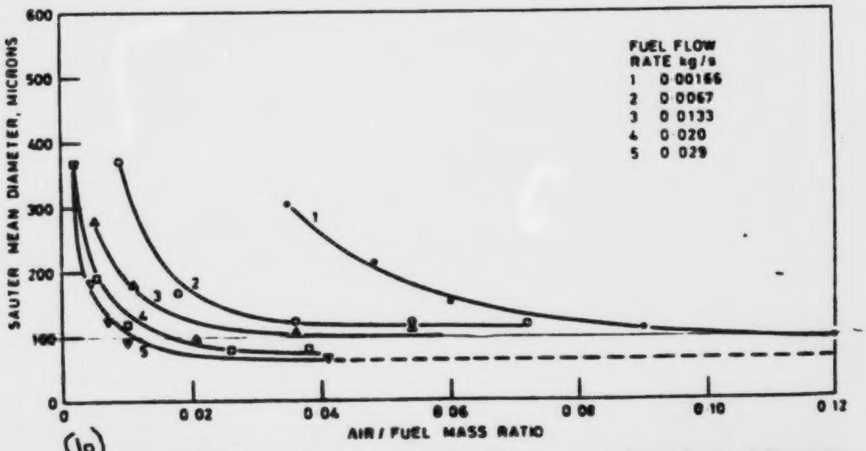

(10)

FIG. 5 The effect of air/fuel mass ratio on the Sauter mean diameter for various fuel flow rates.

ERRATUM (See Erratum Addendum for Modified Calculation)

19.1.1 The expansion ratio 3.2 based on $\overline{V}$ for 174.7 and 14.7 psia provides for the increased area necessary to reduce the steam pressure to 14.7 psia.

But, since both $\overline{V}$ and areas expand by a ratio of 3.2, then the initial velocity does not change. That is the exit velocity remains at (approx.) the sonic value of 1660 fps

19.1.2 Fig. G.1.2.R has been maintained.

19.1.3 The essential change with respect to drop break-up (assumed mitotic) has been an increase in the differential velocity between atomizing steam and CWF drops (See G. 15.) This would only increase the effect of the Weber Number and create possibly one or more drop divisions, especially in the cases where drop coalescence has occurred. With a minimum of (say) 2 - 4 um dia. (See G.1 page 18)

19.1.4 It will be seen in Fig. G.1.2.R that the initial velocity has been reduced to a min. of 4.45 fps (not to zero in order to conform to the data of Tables G.9.1 and (G1.9.2).
This is in conformity with the data shown in Fig. 5 of the MIT paper (10) where the atomizing air velocity drops to zero value at the burn-out point

G.1. ERRATUM - ADDENDUM 1

REVISION

---

1. From Fig. G.1.4 determine

1.1 Length AB

Distance CE

So that velocity of 1660 fps of zone C-D is reduced to 166 fps at zone AB

1.2 Hypothesis: The velocities of zero psig will vary inversely as the areas of zones C D and A B, i.e.

Velocity in zone AB will be

$$\frac{D_1}{D_2}^{2} \times 1660$$

1.3 From Fig. G.1.3, CD = D_1 = 1.176

Then $\frac{1.176}{D_2}^{2} \times 1660 = 166$

$$\frac{1.176}{D_2}^{2} = \frac{166}{1660} = \frac{1}{10}$$

$$\frac{1.176}{D_2}^{2} = \frac{166}{1660} = \frac{1}{10}$$

$$D_2 = 13.8 =$$

$$= 3.7 \text{ cm.}$$

1.4 $AE = \frac{3.7 - 1.176}{2} = 1.262$ cm.

1.5 Hypothesis: Steam will expand over a half angle of 22.5°, then

$$\frac{AE}{CE} = \tan 22.5^{\circ} = .414$$

$$CE = \frac{AE}{.414} = \frac{1.262}{.414} = 3 \text{ cm.}$$

1.6 Hence, on foregoing position of 166 fps drop velocity, the effect on burn-out length is insignificant.

2. Hence, as a steam velocity of 166 fps at zero psig can be considered as in effect at a zone only 3 cms. from nozzle exit, with a zone radius 4 cm. the relationships of Fig. G.9.1 are maintained, which allows the use of Fig. G.9.1 and the calculations from these to be valid.

PAPER G. 1

ADDENDUM NO. 1

Ref. Drg. G.1.2.

Spray Development Based on a 45° Total Angle at Nozzle Exit (with spray expansion starting at nozzle exit).

---

1. Mean velocity div. nozzle to a plane through point G. (i.e. a plane through mean geometric spray length) (See item 67.2 – G.1) 2286 cm sec.

2. Velocity at exit of div. nozzle is 60 fps = 1829 cm./sec.

3. Mean velocity E ⟷ G is:

$(1829 \times 2286)^{1/2}$ = 2045 cm/sec.

4.* Velocity drop from plane E L to plane (through point G) (132 cm. from nozzle tip)

is $\left(\frac{EL}{\acute{Y}P}\right)^2 \times 2045$

4.1 First calculate dimension $\acute{Y}P$ and resulting vel. at flame front

From Fig. G.1.2 $\frac{\acute{Y}N}{^{1)}\,132} = \tan \angle EN^{1)}$

$= \tan \underline{22.5^\circ} = .414$

$\acute{Y}N = 132 \times .414 = 54.7$

Then $\acute{Y}P$ = 2 x 54.7 (+ inlet dia. of div. nozzle

= (109.4 + .274) then $\acute{Y}P$ = 109.6 cm.

* Then item 4 becomes $\frac{1.12^2}{109.6^2} \times 2045$ = .2045 cm./sec.

4.2 Obviously this is an excessively small value for a spray velocity.

---

1) For dim. 132 cm. see G.1, Item 67.4.

5. Hence calculate the dia. and dist. from div. nozzle exit to equal a combusion wave velocity of 140 cm./sec.

5.1 Let D_1 = required dia.

and we have $\left(\frac{1.12}{D_1}\right)^2 \times 2045 = 140$ cm/sec.

$$140 (D_1)^2 = 2565$$

$$(D_1)^2 = 18.3$$

D_1 = F' H' = 4.28 cm | F' H' = 4.28 cm.

6. Segment F' N' = $\frac{4.28 - 1.12}{2}$ = 1.6 cms

6.1 $\frac{F'N'}{EN'} = \tan 22.5^\circ = .414$

$$\frac{1.6}{EN'} = .414$$

$EN' = \frac{1.6}{.414} = 3.865$ cm | EN' = 3.865 cm.

Distance of combustion plane from nozzle exit

7. NB – If a combustion wave front approx. only 4 cms from nozzle can overheat the nozzle, then the half angle must be reduced to provide a required distance dimension (to protect the nozzle).

8. Length of spray for 5 mitotic divisions (postulated) at 3000 drops per .015 sec. is calculated as follows:

8.1 From Table G.1.1, geometric mean velocity over 5 mitotic divisions is:

$(60 \times 100)^{1/2}$ = 77.45 fps

8.2 Length of spray (for rows 7 & 8 – Table G.9.2) is then:

$(.015 \times 5) \times 77.45$ = 5.81 fpi

= 177 cm.

= Line Z^1-Z
Fig. G.1.2

8.3 Length of spray for row 8.1 Table G.9.2

$(.005 \times 5) \times 77.45$ fps = 1.936 ft.

= 59 cm.

PAPER G.1 - ADDENDUM 2

REVISED SPRAY FORMATION CALCULATION

(See Table G.9.1)

Drop Rate - 1000 drops/.005 sec.

---

1. From the hypotheses set up for Paper G.1, it was shown:

1.1 Drops will exit in 3 waves of 1000 drops each (Item 42.7) for a total of 3000 drops in a time period of: .015 sec.

& Table G.9.1 was constructed accordingly. Item 62-G.1

1.2 Now, item 40 shows a separation between drops exiting from nozzle of .108 cm (within the nozzle)

1.2.1 Therefore, it would be logical to assume that the separation between "waves" is also .108 cm.

1.3 Hence a new appraisal of spray formation can be established based on the considerations of the exit from the nozzle of 1000 drops in a time period of $\frac{.015}{3}$ = .005 sec.

1.4 Table G.9.1 has been constructed accordingly together with the factors of atomizing steam

1.4 (continued)

deceleration (from Paper G.7) and from a process of acceleration - deceleration of the CWF droplets - as shown in Fig. G.9.1.

2. Now determine min. droplet size based on corrected viscosity coefficient of .01154 u and min. differential velocity of 10 fps = 305 cm./sec. (Fig. 4).

Weber No. is $\frac{Pa \times (305)^2 \times r}{76 + (.01154 \times 900)} = 10$

$$\frac{P\ 17 \times 9305 \times r}{76 + 10.38}$$

$$r = \frac{86.38}{9305 \times 17} = \frac{86.38}{158.85}$$

r = .00055

= .0006 (rounded)

= 6 um radius

= .12 um dia.

2.1 Table G.9.1 shows a drop dia. of 16 um at the 8th mitotic division (which is too close to the ultimate "Weber" division of 12 um dia.) Therefore, as a safety factor, 7 only mitotic divisions were considered (dia. = 32 um) with a G.M. of 2.6 (rounded to the nearest integer 3).

2.1 (continued)

Therefore the Geometric Mean can be assumed to be at the 2nd division.

3. Calculation of spray lengths will be obtained from the following mean velocities (See Fig. G.9.1)

3.1 Nozzle to div. 2 $= \frac{60 + 90}{2} =$ 75 fps 1st 2 div.

3.1.1 Div. 2 to beg. of deceleration at division 4

$$\frac{80 + 110}{2} + \frac{110 + 100}{2} = \frac{95 + 105}{2} = 100 \text{ fps}$$ 2nd to 4th div.

3.1.2 Final 3 divisions

$$\frac{100 + 65}{2} = 82.5 \text{ fps}$$ 5th–7th div.

4. Then spray length to div. 7, based on a time factor of .005 sec. (per division) is:

4.1 $(2 \times .005) \times 75 =$ .75 ft. = 23 cms

4.2 $(2 \times .005) \times 100 =$ 1 ft. = 30 cms

4.3 $(3 \times .005) \times 82.5 =$ 1.24 ft. = 38 cms

Total spray length = 91 cms
= 3 ft.

...

3·1

G. 1 ADDENDUM 2

4.4 Obtain distance div. 7–9, at average velocity of $\frac{65 + 40}{2}$ 52 fps (rounded)

4.5 Distance is (2 x .005) x 52 = = 16 cm.

= .5 ft.

5. Now calculate axial distance to flame front (See Fig. G.1.2.R for letter identification)

5.1 Dist. Nozzle exit to G.M.Pt. Div. 2 (item 4.1) 23 cms

i.e. $EN^1 = 23$ cm.

5.2

$$\frac{F^1N^1}{EN^1} = \tan 7.5^\circ = .1316$$

$$F^1N^1 = 23 \times .1316 = 3.027$$

$$F^1H^1 = 2\,F^1N^1 + 1.12 = 6.054 + 1.12 \text{ i.e. } F^1H^1 = 7.2 \text{ cm.}$$

6. Determine axial distance of plane where velocity = combustion wave value of 140 cm

7. The dia. of this plane will be the line $A^1 - A$

$$\left(\frac{F^1H^1}{A^1-A}\right)^2 \times \frac{100 + 82.5}{2} \times 30.48 = 140$$

$$\left(\frac{7.2}{A^1-A}\right)^2 \times 91.25 \times 30.48 = 140$$

$$140\,(A^1-A)^2 = 144182$$

$$(A^1-A) - \left(\frac{144182}{140}\right)^{1/2} = \underline{32 \text{ cm.}}$$

---

8. $A^1V^1 = \frac{(A^1A - F^1H^1)}{2} = \frac{32-7.2}{2}$ = 12.4 cm.

$\frac{A^1V^1}{N^1V^1} = \tan 22.5^o$

$\frac{12.4}{N^1V^1} = .414$ and $N^1V^1 = \frac{12.4}{.414}$; N^1V^1 = 30 cm.

9. Now Axial Distance to flame front is

$EN^1 + N^1V^1 = (23 + 30)$ = 53 cm.

= 1.74 ft.

(Line A^1=A
Fig. G.1.2 R)

10. This dimension of 53 cms to flame front can be compared to data from Fig. 3 of ref. 10 as follows:

M.I.T. Fig. shows:

Axial distance centre line 35 cm.

Axial distance at radial position
Approx. .05 m.
(or 5 cm.) is: 25 cm.

N.B. The size range of the droplets providing the above M.I.T. data is 10 to 100 um.

G.2·R

HYPOTHETICAL DETERMINATION OF EFFECT OF VISCOSITY ON THE WEBER NUMBER

---

1. Consider the Crane Eq. for Δ P = (stress) (Crane p. 31-3)

3) due to Viscosity of a laminar flow fluid

$$\Delta P_{100'} = \frac{.0668 \quad \mu \quad V}{2} \qquad (1)$$

Where P = P si, V = fps and d = in.

Conversion factors into C.G.S.

$$\frac{P \times 68964}{100 \times 30.98} = \text{dynes / cm}^2$$

$$V \times 30.48 = \text{cm/sec.}$$

$$d \times \frac{1}{2.54} = .3937 \qquad = \qquad 100 \times 30.48$$

$$d \times .3937 = \text{cm}\cdot$$

2. Therefore converting Eq 1 into cgs units we obtain (where initial values are English)

$$\Delta P \times 68964/3048 \text{ cm}$$

$$= \frac{.0668 \, \mu V}{d^2}$$

3. Hence P × 22.6 = $\dfrac{.0668 \, \mu \, V \times 30.48}{d^2}$

4. $$= 2.6P = \frac{.0668 \times 30.48}{(.3937)^2 \ d^2} \ .\mu V$$

$$= \frac{2.036 \ \mu V}{.155d^2}$$

$$= \frac{13.135 \ \mu V}{d^2}$$

$$P = \frac{.58 \ \mu V}{d^2}$$

5. From G.1

d = film thickness = .106 cm

$$= \frac{.106}{2.54} = .0417 \text{ in.}$$

$P = 144.6$

μ = CentipOise

$V = \frac{40 + 60}{2} =$ 50 fps (AV. velocity in Div. Nozzle)

d = .0417 in.

Weber modification for numerical analysis of G.1 is:

$$P = \frac{.58 \times 50}{(.0417)^2} \times \mu$$

---

6. Hence

$$P = 16677\ \mu \text{ dynes/cm}^2/\text{Cm.L.}$$

7. Data (operational) from G.1 shows that P has a value of 144.5

(Note that the English value of the variables are used in the cgs transformed equation.

7.1 Hence $16677\ \mu = 144.5\ P$

$\therefore \mu$ per unit of P is:

$$\mu = \frac{16677}{144.5} = 115.4 \text{ dyne/cm}^2/\text{cm L.}$$

i.e. The stress per unit of μ per unit/ of P is 115 dynes/cm^2 / cmL.

8. It is postulated that the "action distance" for the stress when mitosis occurs is 1 um (1 cm = 10^4 um)

Continued

9. Therefore for L of 1 um the coefficient of μ

is $\frac{115.4}{10^4}$

$= .01154$

N.B. (1 cm = 10^4 um)

10. Then the modified Weber No. is

$$\frac{Pa \quad V^2 r}{76 + .01154 \mu}$$

G.3

A DISCUSSION ON COALESCENCE

1. Does coalescence of CWF particles occur due to the tank storage stability polymer additives forming a gel-like structure which is not fully broken up as it passes (once) through the transfer pump?(1)

2. Would re-circulation of a portion of pump-out put back into suction, help in breaking up such "gel" structures ?

2.1 Of course care would need to be taken to control the re-circulation, so that CWF size consist degradation would not occur.

3. IBM, in developing a "jet printer", found it possible to keep drop separation, by "disturbing" the atomiser flow by means of a piezo-electric crystal, and (or) a vibrating diaphragm.

4. Consider a double walled concentric annulus design with the fuel flowing into a closed end annulus at a higher pressure than the atomizing steam, and entering into the steam core through suitably sized ports.

---

1) See G.4 Addendum 1, item 10.1.

5. See Appendix 7 and note that in the case of Item 4 (Page 1 and the design, noted, that the temperature of the CWF will reach an equilibrium point with the saturation temperature of the atomizing steam, after which heat transfer will cease.

5.1 The remaining steam will then:

a) form an "emulsion" with the CWF, or

b) flow in a central core, in accordance with the findings of the Mullinger-Chigier experiments with a transparent annulus.

6. A major benefit from elimination (or significant reduction) of coalescence, will result in finer atomization in a standard Y-Jet by the reduction of the ratio of the annulus diameter versus maximum coal particle size, giving increased velocity of the CWF.

6.1 A higher percent carbon burn-out could then be anticipated.

7. In regard to item 6, consider the use of a motorized self-cleaning "Cuno" strainer of suitable blade separation, and manufactured with suitable wear resistance alloy.

8. Consider the Y-Jet atomizer design function developed in paper G.1 together with the summary results in Table G.1.

G·4

DISCUSSION ON RESEARCH REQUIREMENTS FOR A Y-JET AND OTHER ATOMIZER DESIGNS FOR CWF USE

14-7-85

ITEM NUMBER	DESCRIPTION
1	Pressures at inlet to mixing annulus a) atom. steam b) CWF
2	Pressure at mid point of annulus.
3	Nature of emulsion flow. a) According to Dr. Chigier in his recent book, "Energy, Combustion and the Environment", McGraw-Hill/1981, and in a paper by 1) Mullinger & Chigier - Journal of the Institute of Fuel, 1974, the two phases in an annulus are separated, with the CWF flowing in an annular section around a core of atom. steam flow.
4	Dr. Chigier stated that the area volumes for CWF and atom. steam are of the order of 3:1.
4.1	A calculation of the respective velocities is required and also the values of friction and velocity heads under such two phase flow. These calculations will be made by me.
5	If flows are separated - there would be a need of considering an annulus atomizer that would force a mixing process, e.g. a) a converging design of annulus b) a converging-diverging design of annulus. c) an annulus plus a mixing chanber.

1) See attached copy of paper by Mullinger & Chigier, Journal of the Institute of Fuel, 1974.
2) See also Figs. 1.6.R.A, sketches a - d for other possible modes of 2 phase flow in an annulus.

ITEM NUMBER	DESCRIPTION
6	From field experience there would seem to be a need of emphasising a design technique that would effect the filament break up at the nozzle or as near to it as possible.
7	To that end IBM in developing their "jet printer" have employed the technique of imparting impulses to the jet stream within the nozzle at frequencies up to sonic value, using an electronically controlled piezoelectric crystal to develop a "fixed ultrasonic" frequency.
7.1	Another form of "velocity disturbance" impressed on the jet is the use of a "metal bellows that is vibrated vertically by means of a voice-coil actuatator".
7.2	The drop dia. developed by IBM was in the order of 25 to 30 microns and the viscosity of the water-glycerol mixture used in scale modelling was between 5 and 20 Centipoise (compared to 1 Cp calculated for a homogeneous CWF/steam mix).
8	One of the problems noted in field operations of a CWF/steam atomizer was coherence of the droplets with the formation of a "large" coal particle coherent core.
9	From the IBM data, consideration could be given to the use of a charge electrode to impart a charge to the droplets creating an enhanced repulsive effect (assuming the electrophoretic effect of the additive was insufficient).

ITEM NUMBER	DESCRIPTION
10	There is a further need of determining whether the acceleration of the annular CWF flow (if actually annular) by the steam core could cause a turbulent effect that would cause the coal particles to collide and cohere.
10.1	The above thought is induced by the fact that present atomizer designs (C.E., B&W, Coen, e.g.) use a ratio of diameter/coal particle size, to provide a safety factor of 5 - 12.
10.2	In the case of the C.E. Y-jet atomizer, (as used at Chatham) a ratio of 12 provides for a coal agglomerate size of nearly .2 in. or 5000 microns versus a max. particle size of 400 um (Carbojel).
10.3	The literature has shown particle size spikes up to 850 microns so that an agglomeration of , say 5 - 6 max. size particles would be required to justify (seemingly) a safety ratio of 12, or a 3 - 4 particle agglomerate to justify a 5:1 safety ratio.
11	The reason for the foregoing discussion on annular dia. is that B&W (and the literature) confirm that a max. of energy in the jet stream enhances the early breakup of the filament and the production of min. droplet sizes.
12	I have suggested (to B&W) that a hybrid design of atomizer utilizing both internal emulsion and external atomization might produce interestsing results.
13	Dr. Chigier of Carnegie-Mellon has stated that in coming research that he will use a transparent annulus with suitable lighting and

ITEM NUMBER	DESCRIPTION
	photographic techniques to obtain advanced data on the questions developed in this report.
14	In this regard, Hauck do introduce some of their atomizing air into the nozzle to create an emulsion effect and the "emulsified" jet is then impacted by the momentum of the external atomizing fluid.
15	B&W Researtch of Alliance Ohio intend to carry out pressure tests at the various points in their T-jet atomizer, with the objective of obtaining a max. pressure in the mixing chamber, primarily (presumably) to maximize exit velocity, and also, (perhaps) to maximize the CWF/steam emulsification.
16	Remarks made to me by Dr. Mchale of Atlantic Research, and an experience which B&W had when testing a Parker-Hannifen atomizer about 2 year ago, suggests the necesity of the thinnest possible film in the jet.
17	From literature reading, it would seem that jet instability due to both kinetic energy and surface tension play important roles in filament break-up.
17.1	I will study this with particular reference to the NRC Flo-Sonics design and do some number analyses to compare with the NRC (and ARC) empirical (?) design experiences.

ITEM NUMBER DESCRIPTION

18 A complete investigation would require knowledge of the relationship between the forces of:

a) emulsification
b) kinetic energy of CWF and atomizing fluid
c) momentum of the internal atomizing fluid
d) effect of a mixing chamber, added to an internal mixing annulus
e) momentum of the external atomizing fluid
f) surface tension of the CWF droplets
  1) with additive
  2) without additive
g) thermal energy in the CWF
h) electrophoretic value due to additive(s)
i) entering viscosity of the CWF
j) particle size range and size distribution in the CWF
k) structural and chemical and electrical characteristics of the CWF's source coal, or coals, with respect to the coal substances and its surface chemistry and ionic state, all before and after the grinding process

ITEM NUMBER	DESCRIPTION
18 cont'd	And the resulting effects on: 1) break-up starting point of the jet filament 2) droplet size 3) distribution of droplet sizes both axially and radially 4) droplet velocities on both the X and Y axes 5) coherence between droplets 6) point(s) at which coherence occurs
19	Geo. Farthing stated that he would try to have the B&W test data on pressures made known to me.
19.1	This data could be highly proprietary and might require reciprocity on atomizer design work done in Canada.
20	Given: mid-annulus pressure; total pressure drop; and acceptable ratio annulus dia. versus max. coal particle size, a tentative predictive equation is possible based on the Crane turbulent equation.

DISCUSSION ON RESEARCH REQUIREMENTS FOR A Y-JET AND OTHER ATOMIZER DESIGNS FOR CWF USE

ITEM NUMBER	DESCRIPTION
21	From the C.E. data from the Chatham test and assuming 2 mid-annulus pressure values (to obtain $\overline{V}$), and with the further assumptions of say two (2) annulus dia./max. coal particle size ratios, a series of four distinctice equations can be developed based on current CWF burning experience.
21.1	This could not guarantee the % carbon conversion or the flame containment with the combustion chamber geometry, but should give design progress indications that would minimize straight trial and error efforts.
22.	The discussion in this section G.4 assumes a homogeneous CWF/steam emulsion.

G.4

Discussion on Research Requirements for an Optimum Design of a T-Jet and Y-Jet and other Atomizer Designs for CWF

ADDENDUM I

1. Following my report dated July 14, 1985, I developed a numerical analysis for a 2 phase flow (Mullinger-Chigier observation).

2. One of the essential needs of the analysis was to find some technique of "numericalizing" the drop formation phenomenon.

3. To this end I set up hypothetical considerations as detailed in Item 18, of paper G.1

4. I found a further need for the analysis of the operational function of the atomizing process, of the addition of a venturi section to the standard cylindrical T-Jet atomizer.

4.1 This was necessary (in my opinion) to establish "controlled" expansion of the atomizing steam which left the horizontal annulus at sonic velocity, so that the exit steam velocity would be constant (at an assumed exit pressure of 0 psig.)

4.2 In this way a calculable differential velocity between atomizing steam and the CWF could be established.

5. With this differential velocity, the "Weber Number",1) modified by the addition of a factor to cover viscosity,2) could be used to determine ultimate drop size of 8 um dia.

6. A further hypothesis (Item 24 of paper G.1) covering breakup of the CWF film in the divergent nozzle section was required to provide a) a starting number of drops, and b) a time factor to determine spray length (theoretical).

6.1 The theoretical length of a spray calculated on the postulated conditions was 13'8 "(which seems high.)

6.2 But, the data does show that there was separation between drops throughout the spray development, i.e. there was no (numerical) indication of coalescence. (See Fig. G.2 and Table G.1).

7. Theory and practice can differ greatly, but because of the promise of the technique used, it is essential that, at least, a cold chamber test be made to establish the actual spray formation, using variations of design of the divergent nozzle.

8. Using the principle of "differential velocity" and the application of the Weber "Force", the importance of the velocity of the CWF itself is (seemingly) much reduced, allowing consideration of variation in annalus diameter versus cold particle size safety factor.

---

1) See Reference 2 Paper G.1.
2) Paper G.2.

9. The "technique" (paper G.1) shows no coalescence in the spray formation (cold).

10. However, as shown in paper G.3 coalescence can occur in the storage tank and transferred through pump suction and discharge lines to the burner.

10.1 It would seem that the prevention of this effect is by a)testing of alternative additives which can provide stability without gel coalescence (or minimal amount) and the testing of controlled recirculation to pump suction, to break down storage tank gel structures, without degradation of the size and consist of the CWF.

11. There is now the ultimate question:
Will the combustion be complete (to at least 98%) with a flame geometry controlled to the dimensions of its furnace ?

12. First required is a combustion furnace test of the atomizer performance. If good cold chamber testing for non-coalescence has been achieved then it must be known how the aerodynamics of actual combustion will affect the spray pattern.

13. For optimum combustion efficiency and control of flame pattern, quantitative data are required, and a correlation between the data developed, on the following points:

13.1 Parent coal:
  a) qualitative analysis
  b) crystal structure
  c) Ignitibility

13.2 Particle size range and size distribution of the CWF manufactured.

13.3 Additive efficiency in a) lowering viscosity b) providing electrophonetic quality to maintain coal particle separation in the CWF flow to the burner.

13.4 A viscosity of CWF in the supply system not to exceed (say) 1000 centipoise and to have viscosity thinning properties under shear stress.

13.5 Efficiency of the atomizer to produce a fine well-distributed spray.

13.6 Atomizing fluid/fuel radio needed to effect a good spray (item 13.5).

13.7 Combustion/fuel stoichiometric ratio.

13.8 Combustion air temperature.

13.9 Combustion air swirl number.

13.10 Aerodynamics of hot combustion gas re-circulation.

14. Test for possible coalesced coal particles in the storage and supply system of the CWF by the following experiment.

    a) Install transparent sections in the piping to the transfer pump; in the piping to burner pump section, and in the piping from burner pump discharge to the CWF burner manifold; and also in the return line from burner manifold to burner pump section - or to storage tank.

    b) Use lighting (I.R., visible, U.V., X-Ray laser with magnification and stop action photographic techniques, that will resolve the coal particles for size, distribution, and coalescence.

G.5

Discussion on Temperature Tolerance of a CWF

---

1. Many, (if not most) CWF formulations require an additive to:

   a) Maintain storage stability.

   b) Provide reasonable viscosity (say 1000 centipoise at a shear rate of, say, 100 secs.)

2. From information received it seems that if the temperature tolerance of the additive is exceeded that the result is a breakdown of the additive chemistry resulting in a potential for blockage or flow reduction in the atomiser due to:

   a) Change of rheology to high dilatancy

   b) Formation of a gel (from the additive)

   c) Formation of a gel encapsulating coal particles in the CWF

3. In the case of Carbojel (Canadian) B & W Research, Alliance, Ohio, have stated that the temperature tolerance is 175°F versus atomising steam temperatures of:

   a) 338°F at 100 psi

   b) 377°F at 175 psi

   c) (212°F at 0 psig.)

3.1 B & W have stated that they were advised by the Carbojel manufacturer at Cape Breton that "a temperature of 50° C (122°F) for 'extended' periods of time is not advisable".

4. From the literature, the quantity and type of additive required is (presumably) a function of:

   a) Surface chemistry of the parent coal

   b) Surface charge

   c) "Normal" pH in a water solution

   d) Actual pH

   e) Electrophonetic mobility

   f) Topography

   g) Flocculation propensity

   h) General structural type involving the concepts of: "fusain, vitrain, vitrinites and exinites"

   (See paper by J. Pinta, Gulf Research and Development Co., Proceedings of the Sixth International Symposium - June, 1984)

   i) Grind size range

   j) Size distribution

   k) Method of slurry manufacture.

5. B & W are working on a solution to the temperature tolerance problem (in particular reference to Carbojel - Canada) by separating the atomizing steam and CWF by providing separate conduits in the burner gun.

6. In the B & W T-Jet atomiser there is a zone from the T entrance of the CWF to the mixing chamber and through the exit ports where the atomizing steam and the CWF are in intimate contact.

7. From my work, as reported in Appendices 7 & 8, (which assumes a homogeneous emulsion of steam and water), the CWF temperature will rise to the temperature of saturated steam at the CWF pressure.

8. It is my opinion that there would be a significant degree of steam/water emulsification, in the B & W T-Jet atomiser, giving high probability of a temperature rise greater than 175°F.

9. To avoid harmful effects of additive breakdowns for a given parent coal there is the (apparent) need of research on:

   a) an additive, where quantity reduction, or chemical quality, would significantly raise the temperature tolerance, or where the effect of breakdown due to temperatures greater than the CWF tolerance level, could be minimal as to potential for blockage, or the impairment of atomisation efficiency.

b) Change of size range and size consist, possibly resulting in elimination (or sharp reduction) of the need of an additive, or

b) 1 Permitting the use of an additive of sufficiently high temperature tolerance

b)2 In this regard I understand that there are CWFs which do not use additives.

10. Should a temperature sensitive additive prove to be an essential addition for a given parent coal and for an existing (or revised) CWF consist, then it would seem that recourse must be had to air atomization.

11. Further (drastic) considerations for assurance of successful operation could be:

11.1 Change of parent coal.

11.2 and/or change of CWF manufacturing process.

11.3 Use of a (successful) design of a fully external type of atomizer.

Discussion of Atomizing Efficiency

26-6-85

1 Combustion efficiency requires that carbon burnout be completed within the combustion chambers of commercial, industrial and utility boilers to a point of at least 98.5% to 99% completion.

2 The evidence of investigations points to agglomerations of droplets to form larger droplets containing numbers of coal particles which could cohere as one coal unit of relatively larger size and so require relatively long residence time to burn out.

2.1 A factor in the residence time is the time required to evaporate the CWF water, dry the coal agglomerate and bring it to ignition temperatures.

3 It is possible, in the case of atomizers with internal atomization that such agglomeration can occur within the annulus or in passage through the exit orifice at a "tip emulsion" design of atomizer.

4 Experimental efforts to examine this possibile phenomenon through the use of a quartz atomizer viewed by Schlieren; pulsed laser, and electron microscopy magnifications photography techniques, have been mentioned in the discussion of Appendix 3.

5 Should coherence be found in the annulus then the effect of pressure can be determined.

6 Coherence, if found in the annulus, could be the result of incomplete shearing of the agglomeration effect of a polymer additive added in the CWF holding tank to keep the coal particles from settling.

7 In heavy oil atomizations, the greater the pressure the finer the atomization post exit orifices.

7.1 If the internal emulsion be homogeneous and essentially a fluid, then conceivably pressure and atomization could be related - but limited by the possible coherence inside the annulus or at the exit orifice.

8 Carnegie - Mellon have stated in their paper in the 6th Symposium ("Atomization of Coal-Water Slurries" by N. Chigier and P.L. Meyer) that they intend to research a technique to introduce laser light into the emulsion jet right at the point of exit from the atomizer, with the required photographic (and magnification - ?) techniques.

9 If a transparent quartz atomizer is not practical, then the information obtained at the atomizer orifice exit, should be comparable to the conditions developed within the annulus.

9.1 Should droplet agglomeration prove inevitable, then techniques of combustion air preheat and high swirl may be the development that has to be advanced.

10 Swirl would increase residence time but too much swirl, conceivably could cause flame stability problems.

11 This brings out the thought of attacking the issuing CWF emulsion jet with a stream of high pressure heated air or steam.

12 Item 11 is not new - it is of course the atomization technique of external atomizers such as Parker Hanniffen, Flo-Sonics, Urquhart, Hauck, Atlantic Research, and North American.

13 The design of the Parker Hanniffen external atomizer design appears intriguing, but the Chigier-Meyer paper did not give data on size range and size distribution of the droplets, nor the degree of coherence.

1) A transparent atomizer has been used in experiments on a Y-jet deisgn on heavy oil using steam atomization by Mullinger & Chigier (Journal of the Institute of Fuels - 1974).

in the droplets, nor the % carbon burn-out.
(2)

14 Should flow condition c), sketch G.1.5 prevail then the streams must be made to mix at the exit, or if the separation continues through the exit, a significant fraction of the atom. effect of the steam will be lost.

15 If research shows that the mean atomizing steam pressure is 175 PSI (or nearly) then the combined emulsion velocity will be 500 fps for a velocity head of 124 PSI (Item 18.2, App. 7).

15.1 This could be increased to 931 fps. for a velocity head of 240 PSI (if atom. steam were 82 PSI).

15.2 Then, conceivably the annulus could be designed as a converging nozzle with the end dia. designed to provide an exit velocity up to 930 or 1000 fps.

15.3 Calculations show that these would be fully turbulence (See Appendix 7).

15.4 Considering a max. practical velocity head pressure of 500 PSI the end velocity would be

$$\sqrt{\frac{500}{240}} \times 930 = 1340 \text{ fps}$$

16 The foregoing assumes that the emulsion through the exit orifice is essentially a liquid at low viscosity (1 Centipoise). (See Appendix 5.R Item 4)

16.1 Were it essentially a CWF fluid flow, the viscosity limit for significant pressure atomizer effect would be the Centipoise equivalent of 100 SSU or $\frac{100}{4.635}$ centistokes x 1.2 (Sp. G.) = 26 Centipoise

2) The Mulliger-Chigier experiments showed the fuel in annular flow around the centre stream of atomzing steam. (The equivalent viscosity will require to be calculated.)

16.2 The minimum viscosity calculated for a CWF is a Co-Al of 63 Centipoise

16.3 Values up to 800 (or more) Centipoise viscosity must be considered (at low β_{∞}) hence significant mixing with atomizing steam must occur, and the atomizer suitably designed.

17 On further thought to enhance the energy of filament break-up, consideration should perhaps be given to a converging-diverging nozzle.

18 The fundamental physics of the issuing jet of filament should be studied. i.e. the factors that tend to hold the filament together (considering only the water surrounding the coal particle) e.g.

a) molecular cohesion of the liquid substance,
b) the Van der Waal effect (or is this the same as a?)),
c) the surface tension,
d) the electrophoretic quality of the water droplets, i.e. its ionic strength - causing repulsion between droplets.
e) the ionic chemistry of the coal surface causing particle repulsion.

18.1 Surface tension data can be obtained.

18.2 Electrophoretic strength can be measured.

19 It is presumed that different additives operate on conditions 18.1 and 18.2. and 18(e).

19.1 Then measurement of the 18.1 and 18.2 for values and empirical knowledge of additive effect could indicate;

a) optimum additive control in CWF
b) the need of injection of additive at nozzle tip or atomizer entrance.

19.2 The whole purpose of the foregoing is to keep the droplets separated at the point of effluence.

20 Arguments of Items 18 - 19 could, conceivably have a bearing on the CWF filament break-up by an externally applied force, air or steam, as in an external atomizing design of atomizer, or as a hybrid internal/external design.

G.7

Velocity Changes in Atomizing Steam and Spray Droplet Flows due to Energy Exchange, with Comparison to Turbulent Free Jet Velocity Characteristics

---

1. Velocity changes due to energy exchange.

1.1	Rate of CWF flow, lbs /sec.		.267 lbs/sec.
1.2	Initial CWF temperature assumed		100°F
1.3	Temp. of atom. steam at O psig		212°F
1.4	Enthalpy of steam BTU/lb		1150 BTU
1.5	Heat in atomizing steam flow per sec. (.15 × .267) × 1150	=	46 BTU
1.7	Assumed temperature rise of CWT droplets		200°F
1.8	Heat absorbed by droplets using Specific Heat of water: (200 − 100) × .267	=	27 BTU
1.9	Remaining heat in steam (per sec. basis): (46 − 27)	=	19 BTU
1.10	Assume atomizing steam mass flow cross-section (Lbs./Sq. Ft.) remains constant.		

1.10 (continued)

Then steam velocity will be reduced to $\frac{19}{46} \times 166 = 68.6$ fps

1.11 There will doubtless be greater velocity drop due to some radial diffusion, and energy loss due to turbulence.

---

2. Velocity loss due to Turbulent Free Jet Characteristics (12)

2.1 Data from reference 12 is based on air, but(for this exercise) will be assumed to apply to steam.

2.2 All free-jets suffer deceleration according to the equation:

$$\frac{V_c}{V_o} = \frac{K\ D_o}{x} \quad \text{along jet center line} \qquad \text{Eq. (1)}$$

V_o = initial velocity, fps

V_c = decelerated velocity fps

K = Constant having value of 6.2 at a velocity of 170 fps and where

D_o = opening dia., ft.

2.2 (continued) x value limits for Eq. 1 are:

$$7 < \frac{x}{D_o} < 100$$

Where x is axial distance, ft.

2.3 Equivalent D_o for the .106 cm. deep CWF film in the divergent nozzle, is calculated as follows:

2.2.1 The area of the liquid annulus is:

$$.131\ \text{cm}^2 = .02\ \text{in.}^2 = .00014\ \text{ft.}^2$$

$$\text{Whence}\quad r = \left(\frac{.00014}{\pi}\right)^{1/2} = .0067$$

$$\text{and} = .013d\ \text{ft.}$$

2.3 Then X required by Eq. 1 for a max. $\frac{X}{D_o}$ value of 100, we find

$$\frac{X}{.0134} = 100 \text{ where}$$

$$x = 1.34\ \text{ft.}$$

2.3 (Continued)

The dimension 1.34 ft. as an axial distance is too small - The axial distance figure should be at least 5 ft. to cover the "calculated" spray length of 3 ft. with allowance for a safety factor for the calculated dimension plus a small allowance for the need of maintaining velocity differential in case some large droplets or coalesced droplets require "further" spray length to provide max. % burn-out.

3. We then have the need of relating the ratio $\frac{X}{D_o}$ to 100, when $x = 5$, and then to establish an enterpolated value for K .

3.1 With $x = 5$ we have:

$$\frac{5}{.0134} = 373 \text{ which is } > 100$$

instead of $<$ 100 upon which is based the K value of 6.2 (12)

3.2 From (12) we also find:

K = 5 for a max. velocity of 16 fps

3.3 The ratio relationships are

Velocity Ratio $\frac{170}{16} = 10.6$

3.3 (continued)

corresponding K values $\frac{6.2}{5} = 1.24$

3.4 From item 31 we obtained an

$\frac{X}{D_o}$ value of 373 (> 100)

3.5 Then an extropolated K value base

would be: $\frac{373}{16} = 23.3$, so that the

K ratio would become $\frac{23.3}{10.6} \times 1.24$

$= 2.72$

∴ versus a vel. of 16 fps,

K for 373 fps would have a value of

$5 \times 2.72 = 13.63$

3.6 Then from Eq. 1 we find

$$\frac{V_c}{V_o} = 13.63 \times \frac{(0.134)}{5} = .027$$

$$V_c = V_o \times .127 = 166 \times .027 = 4.45 \text{ fps}$$

$$= 1.35 \text{ m/sec.}$$

4. Fig. 5, of reference 11 shows axial velocity at burnout of a 50 um particle close to zero.

4.1 The value of 1.35 m/s calculated from free jet velocity characteristics developed in

---

4.1 (continued)

item 3,then has reasonable correlation with the MIT value (for 50 um droplet) at point of burn-out

4.2 The spray dispersion under this study has a range of droplet dia.
(from point of flame front) of 250 to 30 um

4.3 The exit velocity of 1.35 m/s. may well be needed to carry the burn-out of the larger droplets to completion.

4.4 See Paper G.9 for an analysis of flame lengths for 100% burn-out.

5. However, to establish practical dimensions for the axial distances of the flame front and spray length, use is made of the calculated value for decelerated velocity of 68.6 fps (in Item 1) and a judgement value of 40 fps is used for this study.

5.1 Actually, using the decelerated velocity of 40 fps, in Paper G.1 Addendum 2, results were obtained comparable to reference 11 (The M.I.T. Paper)

G. 8

BURN-OUT TIME

1. The purpose of this paper is to determine the burn-out time for droplets of various sizes and the determination of furnace length (axial distance) required to achieve 100% burn-out (theoretical) assuming that combustion air - CWF mixing is adequately thorough.

2. From reference 9 we find:

(presumably from demonstration trials with a "standard" atomizer)

2.1 Droplet burning time: .1 to .2 sec. for a 44 um diameter droplet

2.2 Burning time is an inverse function

of $$\frac{4\pi r^2}{\frac{4}{3}\pi r^3} = \frac{1}{\frac{r}{3}} = \frac{3}{r} = \frac{3}{\frac{D}{2}} = \frac{6}{D}$$

and the inverse is: $$\frac{D}{6}$$

---

3. The time coefficient in secs. for a droplet diameter D is then

$$\frac{D}{6}$$

for a 44 um droplet, we have

the relationship

$$\frac{D}{6} \times 44 = .1 = t \text{ secs.}$$ that is

$$t = \frac{.1 \times 6}{44} \times \frac{D}{6}$$

$$= .0136 \frac{D}{6} \qquad \text{(min. time)}$$

Proof: Let D = 44, then

$$t = .0136 \times \frac{44}{6} = .1$$

Hence $t = .0136 \times \frac{D}{6}$ G . 9 time

$t = .00226\,D$

t = .00226D min.
Eq. 1

3.1 For the max. value of burning time of .2 sec.

t = .0045 D max.
Eq. 2

---

4. From Ref. 10 we find:

(presumably from laboratory experiments – nature of atomiser and spray formations not given. Fig. 3 however, appears to show that the atomiser is an external atomizing type with atomising and combustion air issuing from the same air nozzle).

4.1 Dry time

40 um – .7 ms

20 um – .26 ms

4.2 Ratios: dia. $\frac{40}{20} = \frac{D_2}{D_1} = 2$

time $\frac{.7}{.26} = 2.7$

$\therefore$ Dry time per unit dia.ratio $= \frac{2.7}{2}$

$= 1.35$

4.3 Then based on 20 um dia. drop at a dry time of .26 ms (Fig. 10 (10))

4.3 continued

$$\frac{D_2}{20} \times 1.35 \times .26 = .35\,t$$

so that

$$t = \frac{.35\ D_2}{20} = .0175\ D_2 \text{ ms}$$

then drying time is : $.0175\ D_2$ ms

Proof: Let D_2 = 40, then t = 40 × .0175

= .7 ms

= value for :

40 um in Fig. 10 (Ref. 10)

(See Fig. G.15.10 in G. 15)

5. Char Burn-out

5.1 40 um - 10 ms

20 um - 2.17 ms

5.2 Then $\frac{D_2}{20} = \frac{10}{2.17} = 4.6$

$\therefore$ Burn-out ratio for unity dia. ratio $= \frac{4.6}{2} = 2.3$

5.3 Then based on 20 um dia. at 2.17 ms, we have

$$\frac{D_2}{20} \times 2.3 \times 2.17 = 5\,t, \text{ so that}$$

$$t = \frac{5\,D_2}{20} = .25\,D_2 \text{ Sec.}$$

5.4 Proof: Let D_2 = 40, then = Char Burn-out time

= 40 × .25 = 10 ms

See Fig. G.15.10 in G.15.

5.4 Continued = Value for 40 um in Fig. 10 (ref. 10)

6. Compare Total Burn-out Time

From References 9 and 10

6.1 Reference 10: .1 to .2 sec. for a 44 um dia. droplet

Reference 9 - For a 40 um dia. droplet

dry time - .7 ms

Char burn-out - 10.0 ms

Total Time (for 40 um) 10.7 ms = .0107 sec.

6.2 The difference between value of Reference 9 versus 10 is a factor of 10 x

7. Therefore Reference 9 values of .1 to .2 sec. for a 44 um dia. droplet and giving

t = .00226 D ms (Min.)

t = .0044 D ms (Max.) for all D values

8. Item 7 values will be used in Tables G.9.1 and G.9.12, and the axial distance for burn-out calculated from the plane of the flame front.

AXIAL DISTANCE FROM NOZZLE EXIT TO BURN-OUT

1.	The data to be developed in this paper and its accompanying Tables, G.9.1 and G.9.2, is based on the time factors, as calculated in Paper G.8, Items 3 and 3.1 (from reference 9).	
2.	100% burn-out is assumed, based on these time factors; with the understanding that fuel/combustion air mix and turbulence will be adequate.	
	TABLE G.9.1	
3.	Rows 1 - 9 of Column 1, Table G.9.1 are "Mitotic" divisions, with a time spacing of .005 sec. (derived from G.1 and as modified in G.1, Addendum 2).	
4.	Row 7.1 is the weighted average of the spray diameters to Division 7.	
5.	Row 10 represents the decelerated steam velocity minimum of 4.45 fps (See Fig. G.9.2).	
6.	Rows 11 and 12 represent effect of assumed possible coalescence of 160 um for end of spray at region 7, and of 720 um for beginning of spray region 3 - 4.	
7.	In Item 2 of paper G.1 Addendum 2, it is shown that the smallest diameter of droplet breakdown due to action of the "Weber Number" at an estimated minimum velocity differential of 10 fps is a diameter of:	12 um
8.	At "Mitotic" division 8, the diameter is:	16 um
8.1	Therefore, as a safety factor, and for this exercise, a maximum mitotic division of 7 was taken where the droplet diameter is:	32 um
9.	Similarly, the minimum droplet size of 16 um was derived by assuming a minimum differential velocity of 10 fps.	
9.1	Examination of the values in Fig. G.9.1 indicated:	
9.1.1	A minimum droplet velocity of 40 fps versus a steam velocity of 50 Fps and an equal velocity of 40 fps for both steam and droplets.	
10.	Axial distances from nozzle exit to selected points are:	
10.1	To flame front (G.1 Add. 2, Item 9) =	53 cm 1.74 Ft.
10.2	To end of spray (G.1 Add. 2, Item 4) at division 7 =	91 cm 3 Ft.
10.3	Division 7 to 9 (minimum droplet velocity) (Row 2.1, clm. 10 Table G.9.1).	16 cm

10.4	Nozzle exit to division 9 (Items 10.2 + 10.3)	107 cm
10.5	Division 9 to min. velocity point 4.45 fps (Fig. G.9.1)	46 cm
10.6	Nozzle to min. velocity point 4.45 fps (Items 10.4 & 10.8)	153 cm = 5 Ft.
11.	Droplets will ignite at flame front and all will pass through to division 9 (5 ft. from nozzle - in a partially burned state), except that drops less than 40 um will be burned out within this 5 Ft. passage - if not coalesced into larger diameter drops.	
12.	Time of passage to division 9 from start of ignition at division 4 is: (5 x .005) plus .07 sec. for transit 9 - 10.	= .095 Sec.
13.	Paper G.8 Item 3 shows that time for total burn-out is:	
	Minimum	.00226D
	Maximum	.0045D
13.1	Therefore the remaining time required for burn-out from clm.13 (Table G.9.1) at flame velocity of 4.45 fps is: (.00226D - .095) Sec. (min.) or (.0045D - .095) Sec. (max.)	
14.	The remaining value times for burn-out are shown in clm.13 of Table G.9.1 for D (drop diameter) values of 720, 375, 110, 50 and 40 um.	
14.1	These D values relate to droplet size range entering the flame front (Table G.9.1) as follows:	
	720 um - Assuming top coal particle sizes of 400 um and 300 um, Table G.9.1, indicates that these particles will be released at division 3 and possibly cohere, with a water film covering assumed at 10 um, for a total droplet dia. of 720 um (estimated).	
	375 um - Average of sizes 500 um and 250 um.	
	110 um - Estimated possibility of coalescence of drops in division 6 - 8 incl. due to small (hypothetical) separation.	
	50 um - For comparison to MIT (10) results.	
	40 um - Weighted average of total size range (see Item)	
15.	N.B. Table G.9.1 indicates total burn-out axial distance of 8.5 to 12 Ft. (Row 6) for the full range of the Funk Distribution.	

15.1 Should the 720 um particle form, as noted in Item 14 above, the axial distance for total burn-out becomes 12 to 19 Ft. (from the time postulates of this analysis) (Row 5)..

16. Then, should the available furnace length be less than 12 Ft. (or 19 Ft.), the carbon loss (assuming no partial burning) will be of the order of .5% as shown by the coordinate lines drawn on Fig. 2 (3) (Funk) (See Paper B.1 in "Technical Papers Section - Book II)

16.1 Should coal particle concentration in the upper sizes (300 um 400 um) be greater than in the Funk distribution, then these could be a carbon loss up to 5% if the furnace length was less than 8.5 - 12 Ft (with no top size coherence), or a loss greater than 5% if top size coal particle coherence occured.

17. The particle separation distances, resulting from the hypothesis established for the development of a numerical analysis, as shown in Table G.9.1, suggests that coherence in the top size of the range should not occur, but may occur in the lower micron sizes where the separation distances are much smaller.

17.1 Coalesence of drops in the bottom sizes up to (110 um) can be burned within a furnace length of 6 - 8 Ft.

18. With the drop separation distances of the top sizes, it seems that smaller top size of coal particles will:

18.1 Allow burn-out in shorter furnace lengths.

18.2 Higher burn-out (carbon conversion) efficiency within the 8.5 to 12 Ft. lengths shown in Table G.9.1.

19. The "prediction" of Item 18, assumes of necessity (due to the hypotheses of initial drop formation within the divergent nozzle (G.1) that the smaller top coal particle size will result in smaller initial diameter of droplets generated in the divergent nozzle.

See Addendum2.

20. It is suggested that a fundamental requirement is to determine by suitable experiment, the degree of validity of the bases of this numerical analysis by high resolution observation of the actual spray formation.

21. In this regard, I refer to my Report W.22 re Dr. Chigier's research "intentions".

22. Referencing back to Item 19, one can conjecture that even if the droplet generation in the divergent nozzle remained the same as developed in G.1, that each initial droplet would contain a coal particle consist of reduced top size. Then the principal burn-out factor involved would be the drying time which is a minor element in the total time factor and axial distance required for complete burn-out (see Fig. G.9.5 and G.9.10 of ref. 10), so that smaller max. size in the CWF coal consist would enhance carbon conversion efficiency.

23. Of essential importance is research experimenting to determine the validity (or degree thereof) of the hypothesis on which I have calculated the initial drop size, separation and time factors.

23.1 The use of a transparent atomizer, as in the Mullinger-Chigier experiments of 1974 , is indicated.

24. From the experimental research, confirmation, or evidence of modification of the hypotheses and numerical models of this analysis can be obtained from which drop formation, spray development and burn-out times can be optimized by the continuing workers in this field.

25. Papers G.1 - G.9 refer to the Mullinger - Chigier two-phase flow in a Y-Jet type atomizer.

26. Previous work dealt with homogeneous CWF flow atomizing steam in a Y-Jet type (or T-Jet) atomizer.

27. Derivation of length BC of Fig. G.9.2

27.1 AC = X = Axial distance length used in EQ. 1 (12) paper G.7 to obtain a value for min. velocity from deceleration from an initial value of 166 fps

27.R Then AC = X = 5 ft.

27.3 AB = Axial distance to dia. 9 = 3.5 ft.

(See Fig. G.9.1 and data of Table G.9.1 obtained from calculations of G.1 addendum 2).

27.4 Then BC = distance to div.10 (See Fig. G.9.1)
is: (5 - 3.5) = 1.5 ft.

Based on G-1 Addendum 2

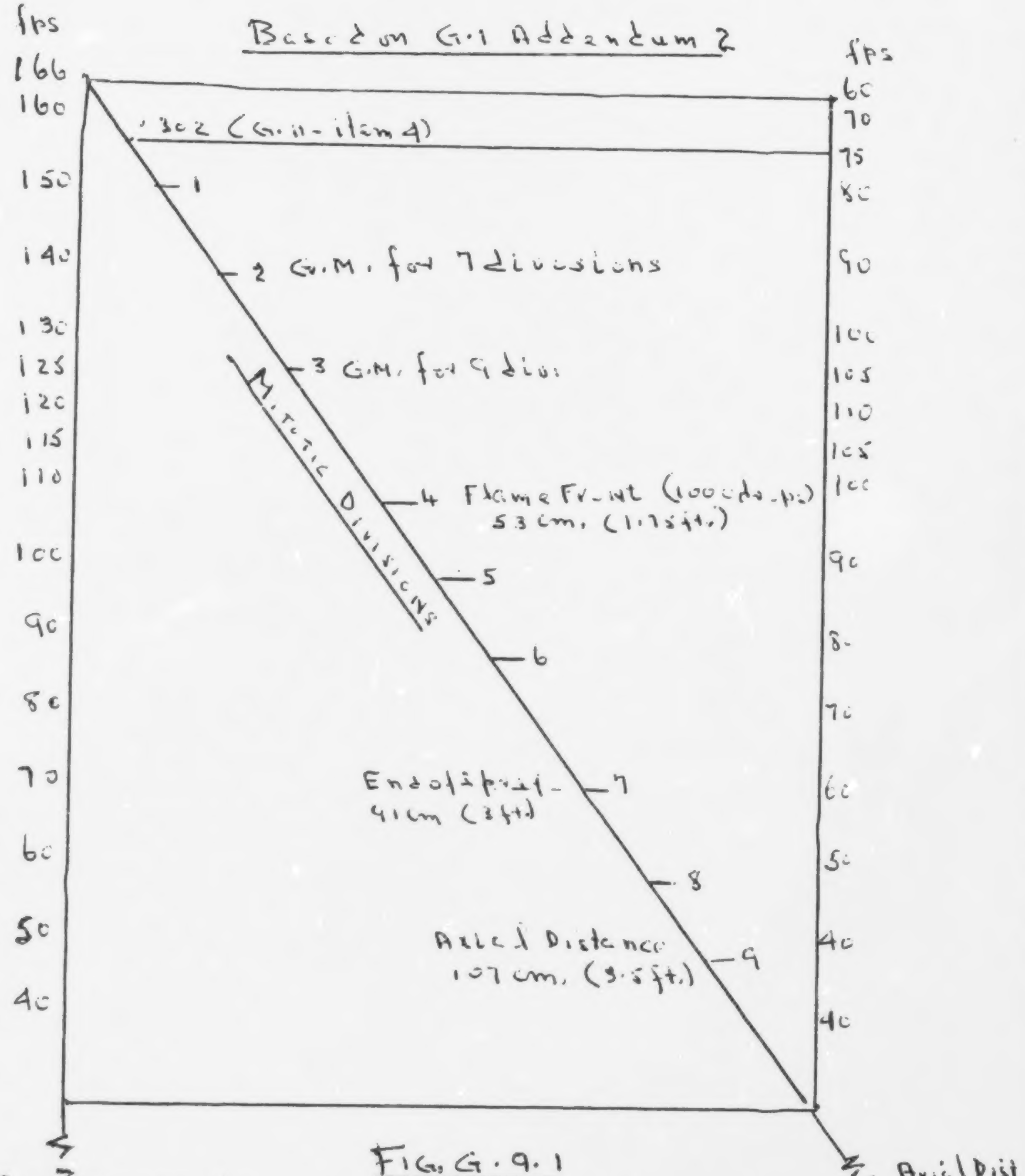

FIG. G.9.1

STEAM VELOCITIES – DECELERATIN from a POINT 3 cm. from NOZZLE (See G-1 Erratum Add. 1)

CWF DROP VELOCITIES – ACCELERATING – DECELERATING from NOZZLE EXIT (at 1000 drops/.005 sec.)

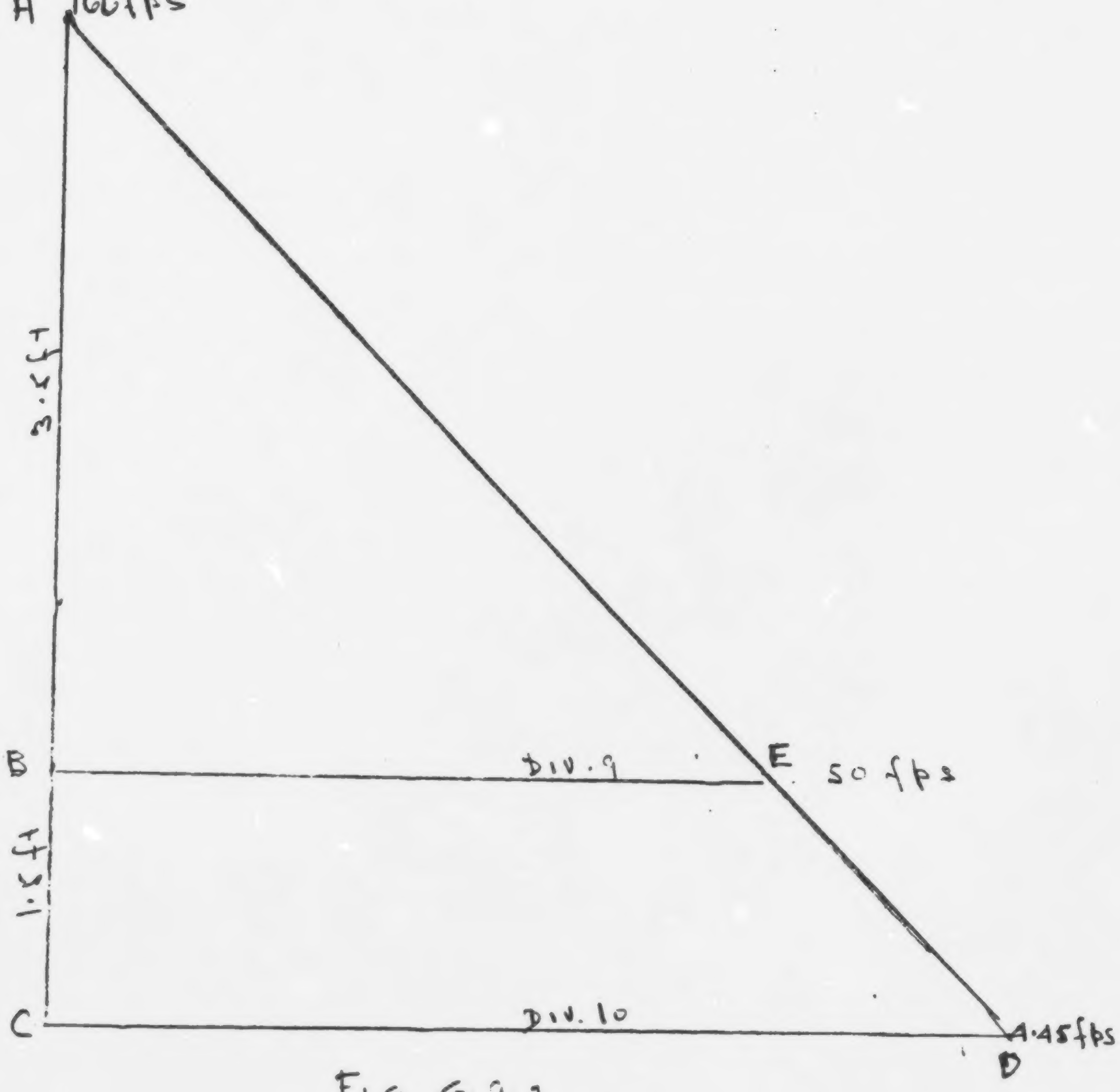
A
166 fps
3.5 ft
B
DIV. 9
E
50 fps
1.5 ft
C
DIV. 10
4.45 fps
D

FIG. G.9.2

AXIAL DISTANCE from DIV. 9, FIG. G.9.1
to MIN. VELOCITY POINT of 4.45 fps.

ADDENDUM NO. 1

	Derivation OF WEIGHTED AVERAGE DROPLET DIAMETER OF A SPRAY	
1.	Initial Drop Diameter	4,000 um
2.	Initial Drop Quantity (per .005 Sec.) (See Row 1 - Table G.9.1)	1,000
3.	Drop Diameter After 7th Mitotic Division	32 um
4.	Drop Quantity (per wave) at the 7th division	128,000
5.	Weighted Average Drop Size: $\frac{(1000 \times 4000) + (128,000 \times 32)}{129,000}$ $+ \quad \frac{(4.10^6) + (4.11.10^6)}{129,000}$ $\frac{8.1.10^6}{129,000}$ rounded to:	= 32 um 40 um

G.9

ADDENDUM 2

LOGIC OF ITEM 19 (G. 9)

---

1. It is presumed that a droplet formed in the divergent nozzle will contain the full range of coal size consist, if the CWF is "fully mixed".

2. Then, if the size consist were (say) 1-200 um instead of 1 - 400 um, a single drop would, conceivably, contain a smaller mass of coal, with a smaller mean cross section diameter of the coal particle consist.

3. Then, it can be considered that, for a given liquidity, the diameter of the water particle would be less.

4. This implies the initial release from the divergent nozzle of a greater number of CWF droplets of smaller diameter.

5. Applying the formula $t = .00266\ D$ to the smaller diameter droplets will then provide a shorter burnout length.

TABLE G.9.1 - Foot Notes

---

1) See G.9 Addendum 1.

2) See G.9 Item 14.1.

3) See G.9 Item 14.1.

4) Separation values calculated from G.1 Item 43 Eq. 2.

5) Division 10 is beyond mitotic divisions and represents point where drop velocity is at the min. value of 4.45 fps (See Fig. G.9.3).

6) Velocity values are not related to rows of mitotic values under clm1, but only for the mitotic division ranges as shown in clm 7.

TABLE G.9.2 FOOTNOTES

1) Weighted average of Funk CWF distribution (See G.9 Add. 1)

2) Spray value for comparison with MIT (and other) data

3) G.M. means Geometric Mean

4) Div. is the mitotic division number at which flame front or end of spray occurs

5) Rev. 7 is purely experimental.

6) See Paper G.11.

7) See MIT Paper (10) Fig. G.15.3 (based on "Utility Grind")

8) See MIT paper (10) Fig. G.15.5.

9) See MIT paper (10) Fig. G.15.5.

10) See MIT paper (10) Fig. G.15.10.

Note: Reference Figs. at end of paper G.15.

G.10

Discussion of Tables G.9.1 and 2, showing Data Source, Data Development, Spray Formation, and Lengths to Flame Front and Burn-out.

---

1. The basic data on atomization and spray formation for a two-phase flow in a Y-Jet type atomiser (Mullinger-Chigier 1974) was developed in paper G.1 and showed a system generating 3000 drops in .015 sec. (based on a set of given hypotheses) with constant accelerating CWF droplet flow. Calculation, therein, for axial distances to flame front and end of spray gave values which intuitively I considered excessive. The data is shown in Fig. G.1.2 and Table G.1.1.

2. In Addendum 1 to Paper G.1, a calculation experiment was carried out resulting in one possibility of a flame front of 4 cm. from nozzle tip.

3. Addendum 2 to Paper G.1 developed the concept (originated in G.1) of cwf droplet generation in "waves" of 1000 drops in .005 sec., which gave an axial distance to flame front of 53 cm. which is comparable to data of, of the MIT paper (10).

3.1 In developing the spray formation data based on this drop generation rate, use was also made of the principal of "Velocity loss due to a Turbulent Free Jet Characteristics"(12) and a velocity acceleration-deceleration mode for the cwf droplets was developed as shown in Fig. G.9.2.

TABLE G.9.1

4. A set of spray formation data, comparable to Table G.1.1, was then developed as shown on the left hand section of Table G.9.1, together with data on droplet burnout time and axial distances. The time data used was from reference 9 (6th symposium.) (The MIT time data (10) was to one tenth less.) This is discussed in Paper G.8).

4.1 The calculated burn-out distances in Table G.9.1 covered droplet diameters from 720 um to 40 um

TABLE G.9.2

5. Table G.9.2 is essentially an extension of Table G.9.1, giving additional information on: spray angles and points of generation; droplet velocities, flame front and burn-out distances; and droplet concentration per cm^2 of flame front and at burnout.

6. Mitotic division points for the flame fronts and burn-out distances are also given.

LENGTH OF SPRAYS - TABLE G.9.2

7. The length of the sprays, based on the postulated mitotic division hypothesis (G.1) and as given in Table G.9.2 are calculated as follows:

7.1 Rows 1 & 2 - Table G.9.2

The number of mitotic divisions, i.e. 9, is obtained by the arguments of G.1 with the data tabulated into Table G.1.1.

7.2 The average speed over the range of the 9 mitotic divisions is 94.87 fps (2897 cm./sec.) as per Item 65 in G.1 and corresponding data in Table G.1.1.

7.3 The time factor between "Waves" of 3000 drops is .015 sec. and the total time to end of spray is (9 x .015) - .135 sec.

7.4 The Length of Spray for rows 1 & 2 of Table G.9.2 is then (.135 x 94.87) = 12.8' plus distance to the start of the first mitotic division (.015 x 60 fps) = 11" for a Total Spray length (rows 1 & 2) of : 13.6 ft.

= 417 cm.

8. Rows 3 - 6 incl. - Table G.9.2.

The initial drop generation rate in the data of rows 3 - 6, is 1000 drops per .005 sec. as developed from G.1 data and extended into full argument in G.1 Addendum 2 and Fig. G.9.2 to give a max. number of mitotic divisions of 7.

8.1 The average speeds over sections making up the seven divisions are given in G.1 Addendum 2. For each of rows 3 - 6 incl. the speeds give:

A total spray length of - - 3 ft. = 91 cm.

9. Rows 7, 8 and 8.1 Table G.9.2

The spray length data are obtained from a purely arithmetical experiment where the spray was assumed to start at nozzle tip at an angle of 45° with end of spray postulated at mitotic division 5 for rows 7 & 8 and division 3 for row 8.1.

9.1 Length of spray for rows 7, 8 & 8.1

As per Item 8.2 of G.1 Addendum 1: rows 7 & 8 = 5.81 ft.
= 177 cm.
row 8.1 = 1.83 ft.
= 58 cm.

AXIAL LENGTHS TO FLAME FRONT

10. Axial lengths to Flame Front are based on a postulated flame velocity of: 140 cm./sec.

10.1 The spray angles for the data of rows 1 - 6 mil are:

15° from nozzle tip to geometric mean division point — See Fig. G.1.2

22.5° (half angle) from geometric mean to 140 cm/sec. flame front plane

10.2. For Length Values shown on Table G.9.2 refer to paper sources as follows:

Rows 1 & 2 - Nozzle Tip to G.M.Pt. (less length of nozzle 2.5 cm.) 132 cm.
G.M. Pt. to flame front 140 cm.
Total Length to flame front 272 cm.

(See G.1 items 67,4 and 88.1 and Fig. G.1.2.

10.3 Rows 3 - 6 incl. - G.1. Adden. 2 - Item 9

Length to flame front 53 cm.

10.a Row 7 - G.1 Addendum 1.

The G.M. plane was deliberately selected as the flame front.

Then the axial distance is: 132 cm.
= 4.32 ft

See item 67.4
G.1.

10.b Row 8 - G.1 Addendum 1 - Item 6.1

Length to flame front 4 cm.

11. The diameters of end of sprays and of flame fronts were calculated. Table G.9.3., p. 6

11.1 The mitotic division points for each calculation of Item 11 was determined.

Rows 1 & 2 - See G.1 item 55

Rows 3 - 7 - See G.1 Add. 2 Item 2.1.

N.B. - Rows 8 & 8.1 - flame fronts are $<$1 mitotic division

11.2 The area of each zone was calculated from diameters.

11.3 The number of drops for each zone was obtained from Tables G.1.1 and G.9.1 to G.9.2, for the mitotic points for the flame fronts and ends of spray from which was calculated the drop concentration per cm^2 for each zone.

TABLE G.9.3

13. Diameter of Areas of Flame Fronts

Rows	Dia. cm.	Area cm^2	Reference
1 & 2	152	18146	G.1. Item 84.1
3 - 6	32	804	G.1. Add. 2 Item 7
7	110	9503	G.1 . Add. 1 Item 4.1
8 & 8.1	4.28	14.4	G.1. Add.1 Item 5.1

13.1 Diameter of End of Spray

From Fig. G.10.1 (attached) it is seen that the dia. of the spray end is:

$D = 2.r^1 + r$, where: EQ. 1

L = Length from G.M. point

$r^1 = L \tan O = L \tan 22.5^\circ = L \times .414$

r = radius of spray at G.M. point

13.2 TABLE G.9.4

Rows	Length from G.M. Point cm.	Value r' cm.	Value r cm.	End Spray Dia. cm.	End Spray area $cm.^2$
1 & 2	285	15.9	36.5	355	98701
3 - 6	68	28	7.2	63.2	3137
7	177	73.3	1.12	148	16286
8	177	73.3	1.12	148	16286
8.1	59	24.4	1.12	50	1963

1)

13.3 L Value References

Rows

1 - 2	L = (417 - 132) = 335 cm from G.M. pt.	
	417 :	See G.10 Item 7.4
	132 :	See G. 1 item 72.1
3-6	L = (91-23) = 68 cm from G.M. pt.	
	91:	See G.1.Add. 2 Item 4.3
	23:	See G.1.Add.2 Item 23
7	L = 177 cm. from nozzle tip, at 3000 per .015 sec. initial drop rate	G.10 Item 9.1
8	L = 177 cm from nozzle tip at 3000 per .015 sec. initial drop rate	G.10 Item 9.1
8-1	L = 59 cm. from nozzle tip at 1000 drop per .005 sec. initial rate	G.1-Add.1 Item 8.3

13.4 r Value References

Rows		
1 - 2	= 36.5 cm.	G.1-Item 72.2
3 - 6	= 7.2 cm.	G.1-Add. 2 Item 5.2
7	= 1.12cm. (O.D. of Divergent Nozzle)	Fig. G.1.1.
8	= 1.12 cm.	Fig. G.1.1.
8.1	= 1.12 cm.	Fig. G.1.1.

14. Derivation of Division Numbers Corresponding to Axial Distance of Flame Front

14.1 Div. No. $\frac{L\ (ff)}{\text{Vel.}\ \times .015}$ - for 3000 drop initial rate Eq. 1

$\frac{L}{\text{Vel.}\ \times .005}$ - for 1000 drop intial rate

14.2 L (FF) = axial distance to flame front from nozzle.

14.3 Velocity values are calculated as follows:

Rows 1 & 2 - 3000 drops / .015 sec.

L (FF) = 272 cm. (9 ft.)

14.3.1 Mean Vel. G.M. pt. to spray is:

$(94.87 \times 150)^{1/2} =$ 119 fps. Item 65 G.1.

Mean Vel. from Nozzle Tip to flame front is:

$(60 \times 119)^{1/2} =$ 84 fps = 2565 cm.

Then No. of Div. (From Eq. 1) is:

$$\frac{272}{2565 \times .015} = 7$$

See clm 14.1 Table G.9.2

14.3.2 Rows 3 - 6 (1000 drops/ .005 sec.

L (FF) = 53 cms. G.1.Add.2 Item 9

Mean Velocity $\frac{(75 + 100)}{(\quad 2 \quad)}$ = 87 fps. G.1.Add 2 Item 4.1 - 4.2

= 2657 cm/sec.

Div. No. is then

$$\frac{53}{2657 \times .005} = 4$$

14.3.3 Row 7 - (3000 drops/.015 sec.)

L (FF) = 132 cm. (plane of G.M.) G.1.Item 67.2

Mean Velocity = $(60 \times 94.87)^{1/2}$ = 75 fps
2290 cm/sec.

Div. No. is then

$$\frac{132}{2290 \times .015} = 4 \quad \text{(no)}$$

But because flame front is
postulated to be at G.M. point.
Therefore Div. No. is: = 3

14.3.4. Row 8 (3000 drops/.015 sec.)

Div. No. 1

L (FF) = 4 cm.

Av. Vel. = $(60 \times 94.87)^{1/2}$

= 76 fps

= 2335 cm/Sec.

Div. No. is then $\frac{4}{2335 \times .015} = < 1$

14.3.5 Row 8.1 (1000 drops/.005 dec.)

Div. No. $\frac{4}{2335 \times .005} = < 1$

15. From data of 4.3.4 and 4.3.5, we find that the drop impact on the flame fronts are the initial generation rates of 3000 and 1000 drops respectively.

See 8.1
Item 37 and
G.1 Add. 2
Item 1.3

16. Similarly for Rows 1 & 2 nozzle design is shown in Fig. G.1.2 .R and relevant Tables are G.9 .1 and G.9.2 and the following data is obtained for flame front

			Reference
17.	Division No.	7	G.9.2
	Axial length to flame front	272 cms	G.9.2
	Droplet Dia.:	32um	G.9.1
	Droplet area:	.000008 cm^2	Calc.
	No. of droplets:	128,000	G.9.1
	Area of flame front:	18146 cm^2	G.9.2

Total Droplet area is:

(128,000 x .000008) = 1.03 cm^2

17.1 Ratio area flame front/ droplets

is $\frac{18146}{1.03}$ = 17617 times

18. The 45° spray angle at the G.M. point is a postulated figure.

19. It should then be possible to increase the angle of the divergent nozzle to create the effect of a greater whole angle of say 60° value to shorten the axial distance to the flame front (for increased ignition stability).

20. Item 19 argument can also apply to nozzle design for rows 3-6 but obviously to a much more limited extent. (Under the given design conditions for rows 3-6 (Fig. G. 1.2 R.)

21.4 However, Sec. G.1 Erratum Addendum and attached Fig. G.1.4 and note the possibility of a reduction of steam velocity within 6 cm. of divergent nozzle Exit.

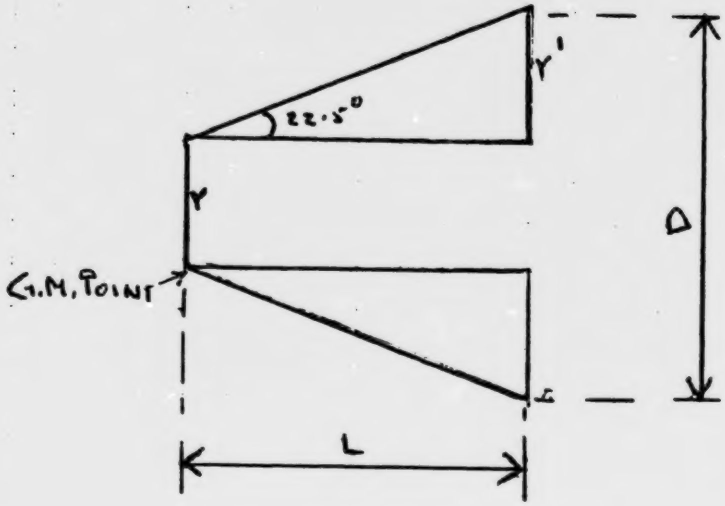

r'
22.5°
r
D
G.M. POINT
L

FIG. G 10.1

DIMENSION DATA for EQ. 1

G.11

RELATIONSHIP BETWEEN THE AREAS OF THE NUMBER OF DROPS AND THE AREAS OF THE FLAME FRONT ZONES IMPACTED

---

1. The experimental conditions of spray formation from nozzle shown in Rows 8 & 8.1 of Table G.9.2, shows that the flame front is established before the first mitotic division.

2. Therefore these flame fronts will receive the unit output from the nozzle

   i.e. Row 8 -- 3000 drops of .4 cm. dia.

   Row 8.1 -- 1000 drops of .4 cm. dia.

G.1/Items 34.1 and 37

G.1 Add. 2 Item 1.3

3. With a flame front distance of 4 cms. (rows 8 and 8.1) versus a flame front distance of 53 cms for rows 3-6 coinciding with division 4, we have that the fractions of one division coinciding with a flame front distance of

   4 cm. is $\dfrac{4}{\frac{53}{4}} = .302$

4. From Fig. G.9.1 the estimated velocity of droplet flow at division .302 is: 75 fps.

4.1 The nozzle exit velocity is 60 fps. we have an average speed to the .302 division point of $\left(\dfrac{60 + 75}{2}\right)$

$= 67.5$ fps

$= 2061$ cm./sec.

$= 2000$ cm./sec. rounded

5. The time to flow 4 cm. is:

$$\frac{4}{2000} = .002 \text{ sec.}$$

6. Then the quantity "impact" on the 4 cm. flame front is

$$\text{Row 8}: \frac{.002}{.015} \times 3000 = .1333 \times 3000 = 400 \text{ drops}$$

$$8.1: \frac{.002}{.005} \times 1000 = 400 \text{ drops}$$

7. The projected area of the quantity of drops reaching the flame front is:

$$400 \times \pi r^2 = 400 \times \pi \times \left(\frac{.4}{2}\right)^2$$

$$= 400 \times .12566 = 50 \text{ cm}^2$$

Versus an acceptance flame front area of : = 8 cm. dia. = 14.4 cm^2

Table G.9.2. rows 8 & 8.1

8. The flame front axial distance and its dia. and area is based on an assumed spray angle of 45° – starting at the nozzle tip.

8. 1 There is then an "overcrowding" at the (given) flame front zone conditions of rows 8 and 8.1

8.2 The evidence from items 8 and 8.1 is that with a spray half angle of 22.5° and a droplet velocity of 2000 cm/s that the spray may well be a solid mass until break-up starts to occur at axial distance of 9.66 cm (1) based on drop emission from nozzle tip of 3000 or even 1000 drops in .015 sec. and .005 sec. respectively.

9.66 cm
For 50 cm^2
(1) See Item 13 re 60 cm^2

9. Conceivably the following events may then take place:

9.1 The drops will coalesce.

9.2 Or, if there is sufficient electrostatic repulsion, the spray angle will increase.

10. As shown in Item 7, the "reception" area required to prevent "crowding" and coalescence is 50 cm^2 or a diameter of 8 cm.

10.1 Given the 4cm flame front distance

G.1. Add.1
Item 6 .1

the half angle required is then:

$\tan^{-1} \frac{4}{4} = \tan^{-1} 1 =$ half angle of : 45°

11. To allow room for droplet spreading assume a required area of 60 cm^2 (See item 14) or a flame front diameter of : **8.75 cm.**

11.1 The half angle is then:

$\tan^{-1} \frac{8.75}{4\times2} = \tan^{-1} 1.084 \quad = \quad 47.5^\circ$

or a whole angle of : 95°

12. To provide a spray angle of 95° it could be necessary to guide the spray by the attachment of a "Coanda" cone tip to the nozzle exit.

13. To attain $60cm^2$ with a whole angle of 45^o, the axial length to flame front would have to be as persketch and calculation shown below:

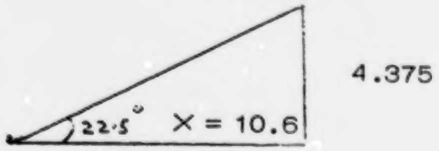

$$\frac{4.375}{X} = \tan 22.5^o = .414$$

$$X = \frac{4.375}{.414} = 10.6$$

13.1 The velocity req'd to flow 10.6 cm in .002 sec. is:

$$\frac{10.6}{.002} \qquad = 5300 \text{ cm/sec.}$$

$$= \underline{173 \text{ fps.}}$$

13. 2 Flame velocity would then be:

$$\left(\frac{1.12}{8.75}\right)^2 \times 5300$$

$$= .0164 \times 5300 \qquad = 87 \text{cm/sec.}$$

13.3 This is less than the postulated flame velocity (in this analysis) of 140 cm./sec.

14. From data of item 13 one can infer that increasing droplet velocity can be effective in maintaining drop separation right from the nozzle tip and at a spray angle of 45^o.

15. Rows 3-6 give the spray angle data of 15^{o} at nozzle tip and an assumed divergence of spray angle to 45^{o} at G.M. point, with a length to flame front of 53cms (burning velocity 140 cm./sec.)

15.1 The flame front (for rows 3-6) at the axial distance of 53 cms. lies at mitotic Division 4

G.10 item 13.3.2

15.2 Then from Table G. 9.1 we find:
Droplet dia.: 250 um.
Whence droplet area: .005 cm^{2}
No. of droplets is: (from initial wave of 1000 droplets) 16000

15.3 From Table G.9.2 we find
Area of flame front: 804 cm^{2}

15.4 Total Droplet area is:
(1600C ×.005) = 80 cm^{2}

15.5 Hence flame front area is 10× droplet area. Drops are well spread and no coalescence will occur due to " crowding " effect.

15.6 There is then adequate droplet velocity and axial length in the nozzle design of rows 3-6 which is shown in Fig. G.1.2 R which also shows Nozzle design for rows 7-8.1.

16.

SPRAY GEOMETRIES

Fig. G.11.1

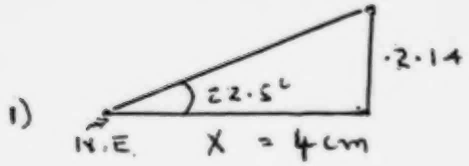
2.14
22.5°
1)
N.E.
X = 4cm

- Area 14.4 cm²

See G.1 addn. 2 to G.11
Item 7

FIG. G.11.2

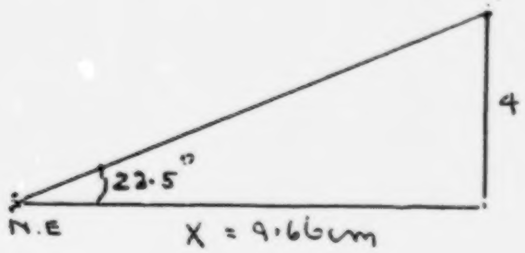
4
22.5°
N.E
X = 9.66cm

- Area 50cm²

See G.11 Item 8.2

FIG. G.11.3

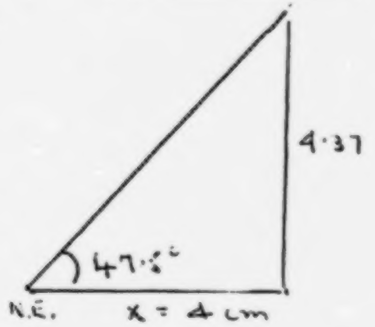
4.37
47.5°
N.E.
X = 4 cm

- Area 60 cm²

See G.11. Items 11 & 11.1

1) N.E = nozzle exit

16. Cont'd.

FIG. G.11.4

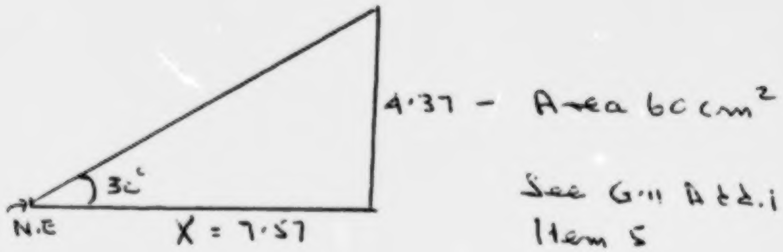
4.37 - Area 60 cm²
30°
N.E
X = 7.57

See G.11 Add.i
Item 5

FIG. G.11.5

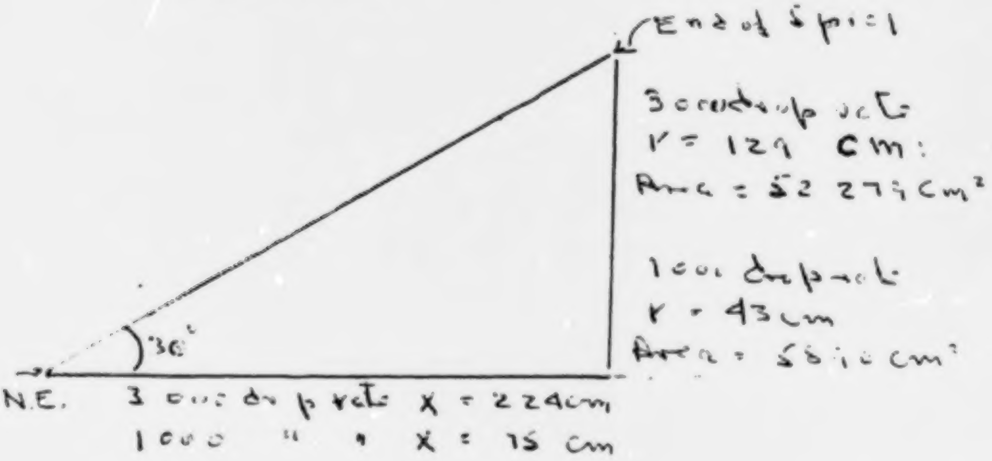
End of Spiral
3000 drop rate
Y = 129 cm:
Area = 52 279 cm²
1000 drop rate
Y = 43 cm
Area = 5810 cm²
30°
N.E.
3000 drop rate X = 224 cm
1000 " " X = 75 cm

G.11

Addendum 1

Further Consideration from paper G.11

---

1. The CWF and atomizing steam velocity at nozzle exit for conditions of item 13 (10.6 cm.) distance to flame front) would be CWF: 175 fps

   Atom. steam: 185 fps

   preferably 195 fps

2. Length of 1 mitotic division

   1000 drops initial rate – (.005 x 5300) = 26 cm.

   3000 drops initial rate – (.015 x 5300) = 79.5 cm.

3. Then flame front occurs before the first mitotic division in a time of $\left(\frac{10.6}{5300}\right)$ = .002 sec.

   (Same time as in item 5) and at rate of 400 drops /.002 sec. or G.11 item 5

   7 drops per 1 cm^2 of front flame area

4. Area of 7 drops of .4 cm. = .88 $cm.^2$

5. Consider spray formation condition at a whole angle of 60^o.

5.1 See Fig. G.11.4 and note:

5.1.1 Radius of Spray (to give 60 cm^2) at .002 sec.: 4.37 cm.

5.1.2 Distance to flame front 7.57 cm.

5.1.3 Drop velocity = 3750 cm/sec.
= 123 fps

5.2 From 15.1.3 it is noted that existing (i.e. for this analysis) steam velocity of 166 fps could be adequate.

5.3 However increased drop velocity will require modifications (of C.E. design) by pressure and/or dimensional change.

5.4 It is further assumed in the case of atomizer conditions, as discussed above, that: (Table G.9.2)

5.4.1 Atomizing steam pressure will decelerate to 4.45 fps (G.7)

5.4.2 Drop velocity will decelerate linearly to a minimum of 60 fps at div. 7 and will further decrease to equal the min. steam velocity at 4.45 fps. See Fig. G.9.2

5.5 The resulting flow averages are closely approximated by the velocity values of Rows 1-6, used for rows 8.A and 8.1 A, in Table G.9.1.

5.6 The G.M. mean velocity through divisions 1-6, for the 60° spray is $(123 \times 40)^{1/2}$ = 70 fps
= 2138 cm/sec.
Rounded to 2000 cm/sec.

5.7 The lengths to end of spray dimensions are based on 7 mitotic divisions giving:

5.7.1 For 3000 drop rate: $7 \times .015 \times 70$ = 7.35 ft.
= 224 cm.

5.7.2 For 1000 drop rate: 7 x .015 x 70 = 2.45 ft.
= 75 cm.

6. The diameters of sprays shown in Fig. G.11.4 and G.11.5 are:

For 3000 drop rate: 258 cm.

For 1000 drop rate: 86 cm.

7. The number of drops division 7 cm.

7.1 For 3000 drops rate: (Table G.1.1) 384,000

7.2 For 1000 drop rate: (Table G.9.1) 128,000

8. Drop diameters at div. 7, are:

8.1 For 3000 drop rate (Table G.1.1.) 32 um

8.2 For 1000 drop rate (Table G.9.1) 32 um

9 drop area at end of spray :

$$\left(\frac{.0032}{2}\right)^2 \times \pi = 8.10^{-6}\ \text{cm.}^2$$

9.1 Total drop area at end of spray

9.1.1 3000 drop initial rate:

9.1.2 $384{,}000 \times 8.10^{-6} = 3\ \text{cm.}^2$

1000 drop initial rate:

$128{,}000 \times 8, 10^{6} = 1.02\ \text{cm}^2$

10. Area of end of spray zones

10.1 3000 drop initial rate:

$$\left(\frac{258}{2}\right)^2 \times \pi = 5.10^4\text{cm.}^2$$

1000 drop initial rate:

$$\left(\frac{86}{2}\right)^2 \times \pi = 6.10^3\text{cm.}^2$$

11. Ratio end of spray areas versus total drop area

11.1 3000 drop initial rate: $\frac{5.10^4}{3.1} = 16129$

1000 drop initial rate: $\frac{6.10}{1.02} = 5882$

12. The data on Item 11 raises the question of combustion stability, and completeness of burnout, due to large drop separation.

12.1 The effect of interaction with neighbouring fuel stream, and the turbulence of the combustion gases, may prove to be the natural answer.

12.2 If not then considerations of increased combustion air swirl, or of modification of atomizer design (to give narrower drop beam) would be required.

G.12

INTERACTION AT INTERSECTION POINTS OF AN ANNULAR 45° SPRAY DISPERSION UNDER CASES OF: 3000 DROPS PER .015 sec. and 1000 DROPS PER .005 Sec.

CASE I - 3000 DROPS / .015 Sec. (45° Spray)

1. Refer to Fig. G.12.1 (end of paper) and note that:

1.1 FH is the G.M. plane for Case I drop generation — See Fig. G.1.2.R

1.2 X^i O X is the plane of intersection from the annular spray having angle of 45°

2. The drop velocity at plane FH (div. 3) is: 82 fps — G.1. Item 73

2.1 The estimated axial velocity at plane

X^i O X is: 100 fps

2.2 The average speed between the two planes is then:

$$\left(\frac{82 + 100}{2}\right) = 91 \text{ fps}$$

$$= 2779 \text{ cm./sec.}$$

3. The mitotic division point at X^i O X

from data of Fig. G. 12.1.

is then: $\left(\dfrac{132 + 27.5}{2779 \times .015}\right) = 3.8$ — See G.1 Item 72.1 for value 132

or the whole integer 4

4. No. of drops at division 4 from initial rate of 3000 drops /.015 sec. = 48000 (Table G.1.1)

5. Dia. of drops at div. 4 is 250 um = .0025 cm

5.1 Area of drops at div. 4 plane (Fig. G.12.1) is:

$$48000 \times \pi \times \left(\frac{.0025}{2}\right)^2 = .235 \text{cm}^2$$

6. Dia. of intersections plane $X^i O X$ (Fig. 12.1) 60 cm

6.1 Area of intersections plane $X^i O X$:

$$\pi \times \left(\frac{60}{2}\right)^2 = 2827 \text{ cm}^2$$

7. Ratio of div. 4 area to drop area is:

$$\left(\frac{2827}{.235}\right) = 12030$$

8. Area of $X^i O X$ available per drop:

$$\left(\frac{2827}{48000}\right) = .06 \text{ cm}^2$$

8.1 Radius at $X^i O X$ available per drop

$$\sqrt{\left(\frac{.06}{\pi}\right)} = .14 \text{ cm.}$$

dia. = .28 cm.

---

9. Drop separation at X^{i} O X with 45° spray angle from G.M. plane is

(.28 — .0025) = .2775 cm.

9.1 N.B. Lineal separation (Table G.1.1) = .032 cm.

9.2 With a lineal drop separation of .2775 cm it would be considered possible to decrease the need of a 45° spray angle and obtain a smaller separation of (say) .15 cm.

9.3 However, the 45° spray angle was an arithmetic requirement to provide a flame front of an area that would limit the flame velocity to 140 cm/sec. at a modest distance from the burner nozzle. In the case of a 3000 drop/.015 sec. condition, the velocity condition was met by a 45° angle, an axial distance of 272 cm. from nozzle and a flame front dia. of 152 cm.

9.4 Experiment may show that the flame velocity is greater than 140 cm/sec. in which case the axial distance to flame front would be less, with a smaller " natural " spray angle, or a change in the assumed need of a 15° divergent nozzle.

(for example - 10° - ?)

9.5 The data of this paper G.12 However, can serve as a guide to for the analysis of the actual absserved spray angle, flame front, drop diameter and carbon burn-out efficiency.

9.6 I am concerned that the arithmetic data in this section showing a drop separation of .2725 cm between drops of .0025 cm.dia., may forbode flame instability.)

9.7 Some "crowding" seems necessary - which may be the functions of the combustion air streams, and/or the effect of neighboring annuli.

CASE II - 1000 DROPS / .005 Sec. (45^{o} spray)

10. Refer to Fig. G.12.2 and note that:

10.1 Intersection flame X" C' X division point is calculated as follows:

10.2 Velocity of $F^{i} H^{i}$ (G.M. point at div. 3 for this 1000 drop spray condition) 73 fps.

10.3 Velocity of $X'' O^{i} X$ estimated (from data of Table G.1.5) to be accelerated to: 82 fps.

10.4 Average velocity is then: $\frac{73 + 82}{2}$ = 77.5 fps. = 2367 fps.

11. The mitotic division point is then:

$$\frac{23 + 5.5}{2367 \times .005} = 2.4,$$

See G.1. Add. 2 for value 23

11.1 Therefore the closest division integer is: 2

12. Diameter of $X'' O^{i} X$ (scaled from Fig. G.9.5) 120 cm.

12.1 Area of $X'' O^{i} X$ is: $II \times \frac{12}{2}^{2}$ = 113 cm.^{2}

13. No. of drops at div. 2 (Table G.9.1 - G.12): 4000

14. Dia. of drops at div. 2: (1000 um) .01 cm.

15. Area of drops at div. 2 - $II \times \frac{.01}{2}^{2}$ = .00008 cm

---

15.1 Total drop area at div. 2 - 4000 x .00008 = .32 cm^2

16. Ratio of div. 2 area to drop area:

$$\frac{113}{.32} = 353$$

17. Area at X" O^i X (Fig. G.12.2 available per drop - $\frac{113}{4000}$ = .0285 $cm.^2$

18. Radius at X" O^i X available per drop

$$\sqrt{\frac{.0285}{\pi}} = .095 \text{ cm.}$$

dia. .19 cm.

19. Transverse separation distance is then:
(.19 - .01 = .18 cm.

19.1 N.B. Item 19 value compares to the 3000 drop condition spray (item G.1) of .2725 (say .28) cm.

19.2 Lineal drop separation at div. 2 (Table G.9.1): .58 cm.

20. There "should" not be any "overcrowding".

FIG. G·12·1

45° Spray Angle from G.M. Point 3
Initial Rate: 3000 Drops/.015 sec

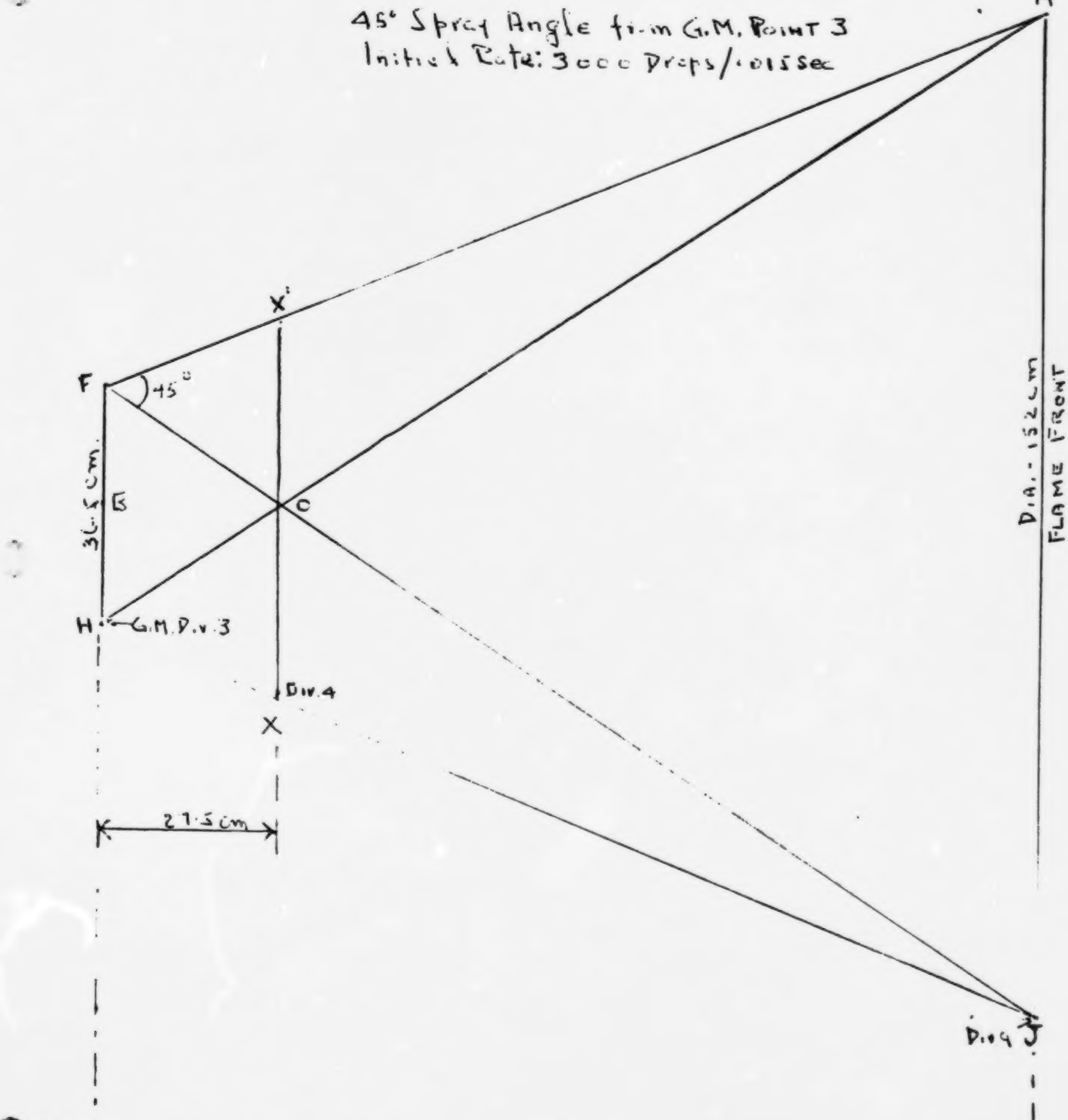
A
X'
F
45°
36.5 cm.
B
C
D.A. - 152 cm
FLAME FRONT
H
G.M. Div. 3
Div. 4
X
27.5 cm
Div. 9
J
32 cm
To Nozzle
140 cm.

Scale: $\frac{1}{4}$" = 5 cm.

FIG. G·12·2

45° Spray Angle from G.M. Point 2
Initial Rate: 1000 Drops/.005 sec.

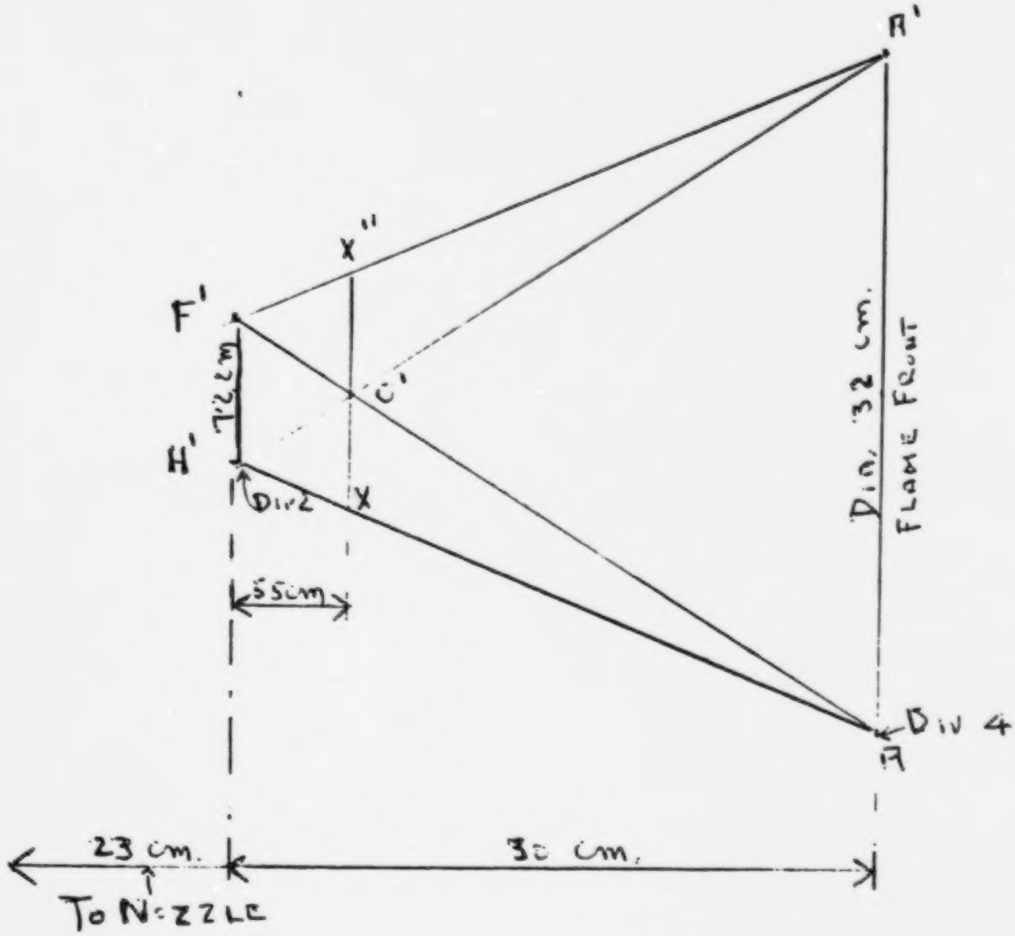
A'
X''
F'
7.2 cm
C'
H'
Div 2
X
5.5 cm
Dia. 32 cm.
FLAME FRONT
Div 4
A
23 cm.
30 cm.
To Nozzle

Scale: $\frac{1}{4}$" = 2 cm.

G. 13

COLLISION PROBABILITY IN TRANSVERSE FLOW AT INTERSECTIONS OF 45° STREAMS

CASE 1

1. 3000 drops /.015 Sec. Fig. G.12.1

Drop dia. and separation at Intersection plane 0

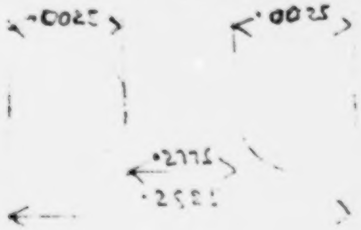

% collision probability is:

2. The probability of a .025 cm droplet entering the "free" .2775 zone will be proportional to the fraction $\frac{.2775}{.2825}$ = 98%

2.1 Therefore the collision probability is (1 - .98) = 2%

3 Hence 2% of the 48,000 or 960 drops et intersection 0 (Fig. G.12.1will coalesce into particles of (2 x 250) = 500 um dia.

4. However between intersection 0 at div. 4 and the flame front at div. 7 there are 3 mitotic possibilities which would reduce drop size by $\frac{1}{2^3} = \frac{1}{8}$ or to a dia. of

$\frac{500}{8}$ = approx. 60 um

---

5. In high probability the Weber "Force" would cause at least 1 mitotic division yielding a drop size of 250 um.

5.1 This would be less than the 375 um value established in G.9 as a top probable size - maintaining the burn-out distance at 8.5 to 12 ft.

CASE II

1000 drops /.005 Sec. - Fig. G.12.2

6. Drop dia. and separation

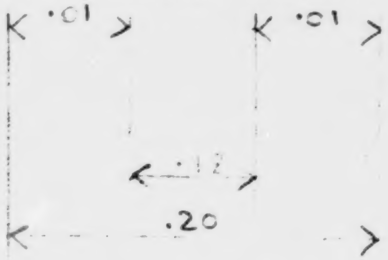

7. % probability of a. 01 cm drop entering the .18 cm zone is:

$$\frac{.18}{.20} = 90\%$$

8. Therefore the % collision probability is

$(1 - .9) = 10\%$

9. Then 10% of the 4000 drops or a quantity of 400 drops appearing at intersection 0 (Fig.G.12.2)will coalesce into (2 × 1000) = 2000 um dia. drops

10. No. of divisions between intersection point (4) at division 2 and the flame front at division 4 (See Fig.G.12.2) is $2^2 = 4$

10.1 Therefore expected drop diameter and quantity at flame front will be =

$$400 \text{ drops at } \frac{2000}{4} = 500 \text{ um}$$

G.14

INTERACTION OF 45° FUEL SPRAY STREAMS FROM NEIGHBOURING ANNULI OF A C.E. Y-JET (CHATHAM) GUN

CASE I - 3000 DROP / .015 SEC.

1. The 45° spray is postulated to start at the G.M. point, i.e. from line FH Fig. G.1.2.

2. This point is 132 cm. from nozzle with a diameter of 36.5 cm. (G.1 items 71.1 and 71.2 and sec. Fig. G.1.2)

2.1 The diameter of FH is: 36.5 cm.

3. There are 7 annuli in the C.E . gun, and it is assumed that the gun is 2" (or 2-1/2") dia. (5 cm.) to accommodate the divergent nozzle design.

4. Fig. G.14.1 shows the Oce. of the G.M. zone in the total spray to be: 351 cm.

5. For seven annuli - available length for each FH zone per annuli: $\frac{351}{7}$ = 50.14cm.

5.1 Therefore separation between FH zones is(50.14- 36.5) = 13.64 cm.

6. Fig. G.14.3 shows the flow lines for 45° spray expansion from the G.M. point (Zone FH).

---

6. It seems reasonable to consider from observations of Fig. G.14.3 that the max. number of collision will occur in the zone F X' X H F H with the collision probability rate doubled to 4% , (See G. 13 item 2.1)

7. The max. drop size in this zone would be (likely) (2 x 500) = 1000 um

8. End of collision areas could be the line Y' Y

9. Further collision could occur at intersection 0^3 creating a few 2000 um particles.

10. However, on the basis of the hypothesis of mitotic breakdown of CWF drops, the interval between Div. 4 and Div. 7, would result in a droplet size of

$$\frac{1000}{8} = 125 \text{ um}$$

With a minor number sized $\frac{2000}{8} = 250$ um

All of which could retain the axial distances for burn-out at 8.5 to 12 ft. as shown in Tables G.9.1 and G.9.2.

CASE II - 1000 DROPS / .005 Sec.

12. From Fig. G.1.2 the distance from nozzle of the G.M. line $F^i H^i$ is: 23 cm.
(G.1. Add. 2, Item 5.1)

13. From Fig. G.14.2 the Oce. of the G.M. line is 73.2 cm.

14. The available length for F^i H^i zones for a 7 annuli borner is $\frac{73.2}{7} = 10.5$ cm.

15. The actual length of F^i H^i (Fig. G.1.2 and G.1. Add. 2, Item 5.2 is: 7.2 cm.

16. The separation between F^i H^i zones is then $10.5 - 7.2 = 3.3$ cm.

17. Comparing Figs. G.14.3 and G.14.4, it will be seen that there are the same degree of intersections, and the same collisions and diameter increase, in this Case II of 1000 drops / .005 sec. as there are in Case I of 3000 drops /.015 sec.

18. Hence, with same drop sizes the burnout lengths for Cases I and II will be the same. This is shown in Tables G.9.1 and G.9.2.

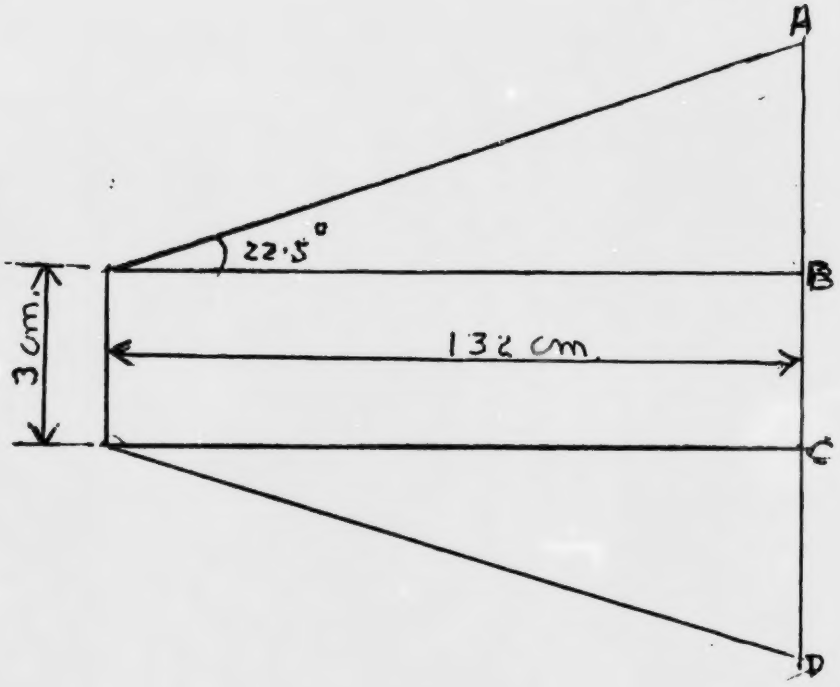

$AB = 132 \tan 22.5^{\circ}$

$= 132 \times .414$

$= 54.5$ cm.

$AD = 2\,AB + BC$

$= 109 + 3 = 112$ cm.

Oce. = $\Pi \times 115 = 351$ cm.

= G.M. Zone of
total spray

FIG. G.14.1

Determination of the G.M. Zone for a Spray Rate of 3000 drops/.015 sec.

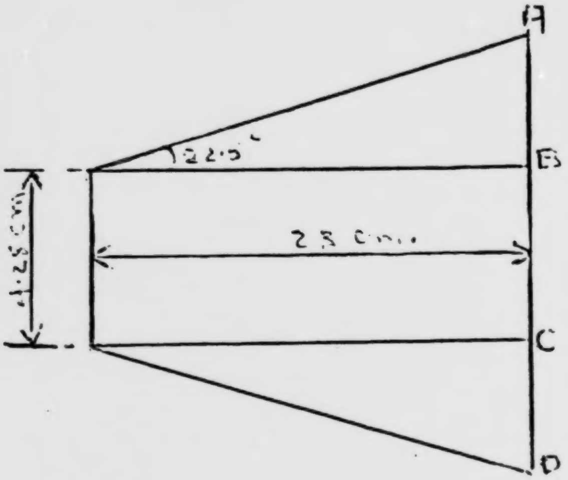
A
22.5°
B
4.28 cm.
23 cm.
C
D

AB = 23 tan 22.5°

= 23 x .414

= 9.5

AD = 2 AB + BC

= 19 + 4.28 = 23.3 cm.

Oce = II x 23.3 = 73.2 cm.

= G.M. zone of total spray

FIG. G. 14.2

Determination of the G.M. Zone
for a Spray Rate of 1000 Drops/.005 sec.

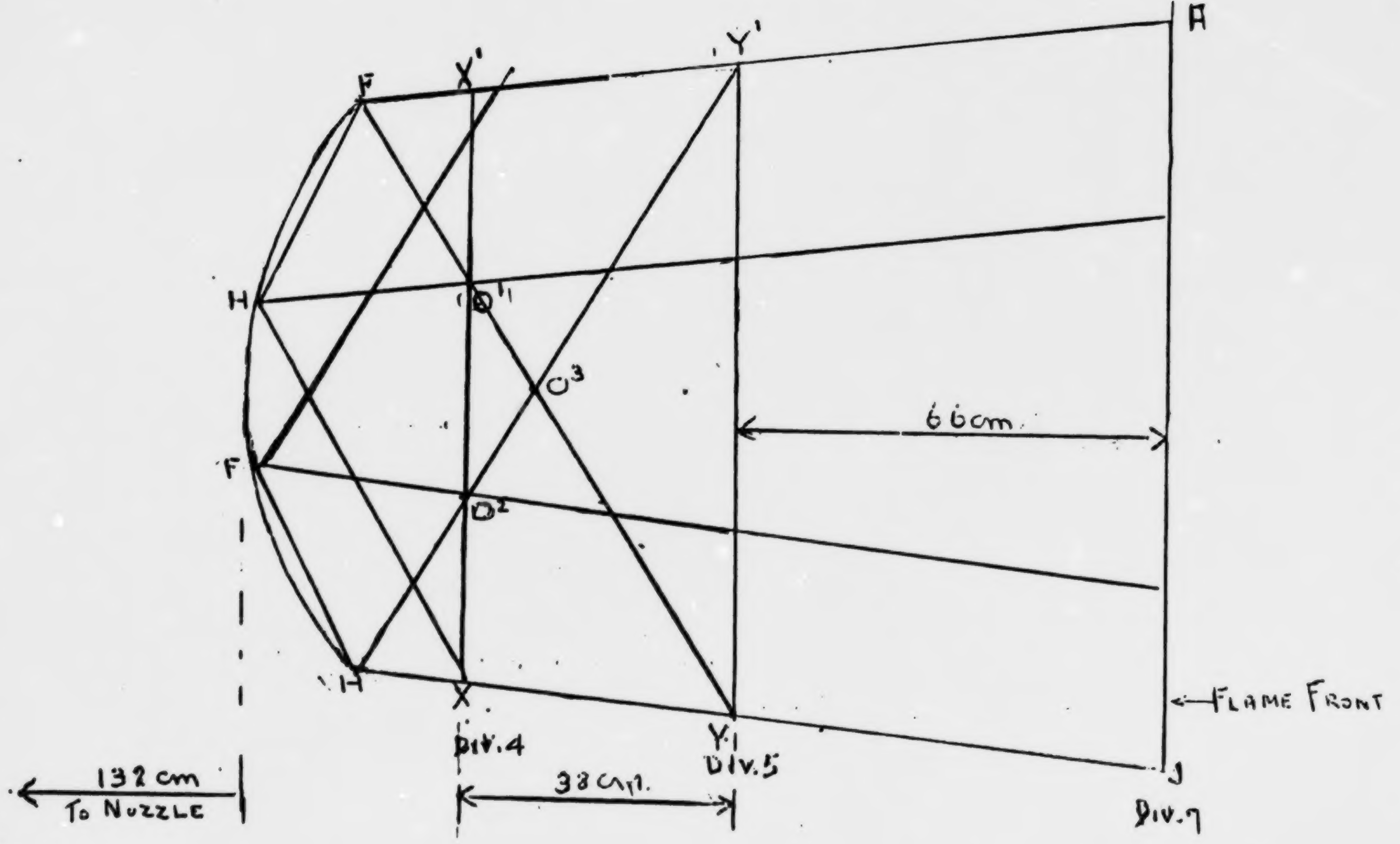

A
F
X'
Y'
H
O^1
O^3
66cm
F
D^2
H
X
Y1
Div.4
Div.5
← FLAME FRONT
J
Div.7
132 cm
To Nozzle
38 cm.

FIG. G. 14.3

Intersections of Spray Flows from adjoining Annuli

CASE I I - 3000 drops/.013 Sec.
Scale: 1/4" - 6 cms.

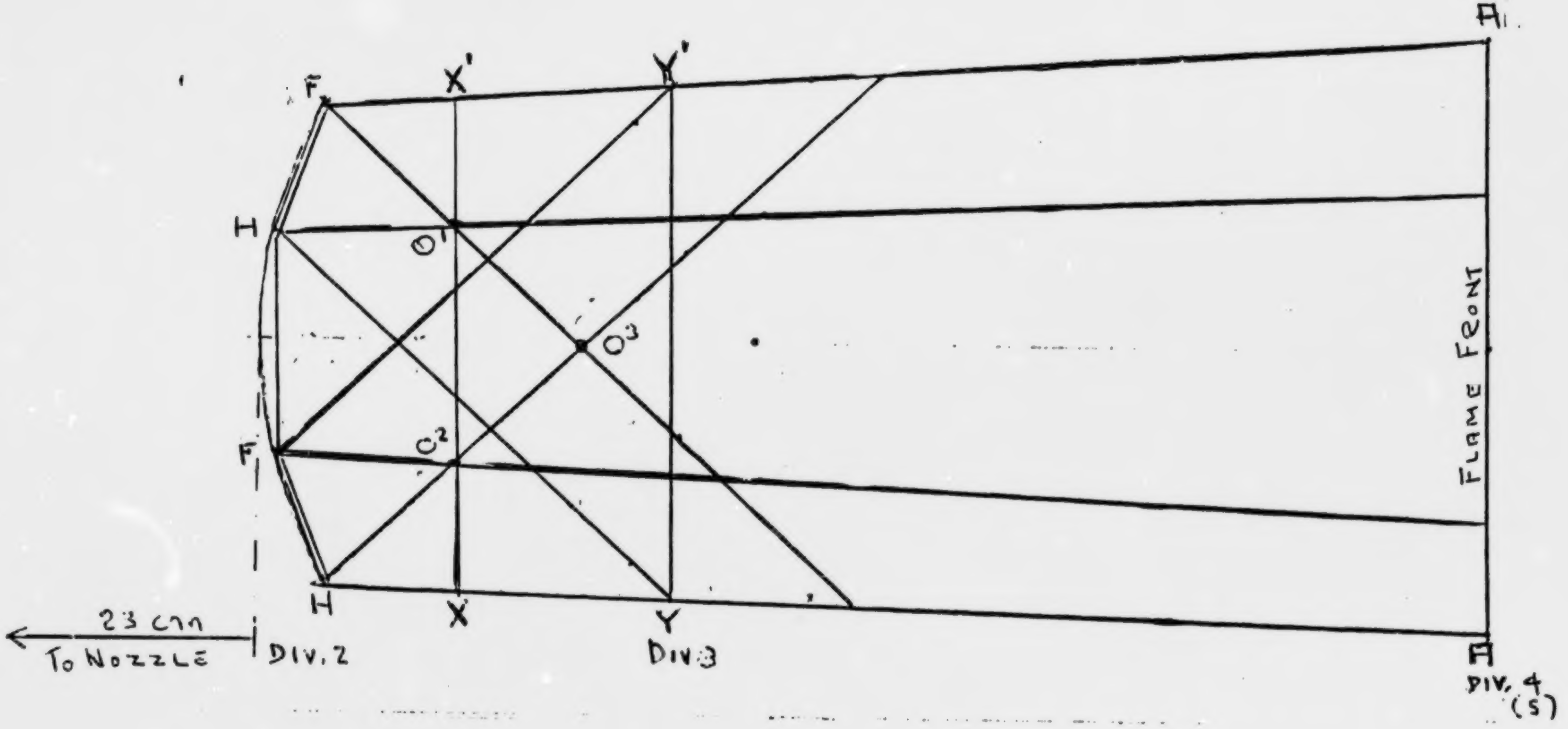

A'
F
X'
Y'
H
O'
O³
F
O²
H
X
Y
FLAME FRONT
23 cm
To NOZZLE
DIV. 2
DIV. 3
A
DIV. 4
(S)

FIG. G. 14.4

Intersections of Spray Flows from Adjoining Annuli

CASE II - 1000 drops/.005 sec.
SCALE: 1/4" = 1 cm.

G.15

DISCUSSION OF MIT PAPER EL-84-004WP - NOVEMBER 1984 "IGNITION AND COMBUSTION OF UTILITY GRIND COAL AND WATER SLURRY IN A LEAN CONFINED DIFFUSION FLAME" by

JANOS M. BÉER et al (10)

---

1. The purpose of this paper is to compare the burn-out timing, and length of burn-out of a 50 um particle as shown in Figs.5 and 10(10) compared to data on a 50 um drop size shown in Table G.9.1 and also to compare the "apparent" burning velocity.

First -

2. It should be remarked that Paper G.8 showed that the time ratios between sources 9 and 10 (G.8 item 6.1) was approx. 10:1.

2.1 The more conservative (ostensibly) time values from reference (9) were used in this analysis work.

3. The burn-out distance shown in Fig. 5 (10) for a 50 um drop, i.e. the distance from axial dimension of ignition at .22 m to the axial burn-out point at .414 m was a distance of (.414 - .22) = .194 metre

= 19.4 cm.

3.1 The time period from Fig. 10 (10) (for a 40 um drop) to char burn-out (from ignition time) is (23 - 2.17) = 9.3 ms.

3.1 Extropolation of char graph with appropriate (well fitting) French curve gave an intercept of char -burn-out at a time value of 23 ms for a 50 um drop (See Fig. G.15.11)

3.2 The start of burning time for a 50 um drop (ignition point) is 2.17 sec. (Fig. 10, ref. 10).

3.3 Therefore the char burn-out time for a 50 um drop is (23 - 2.17) = 20.83 ms.

(rounded = 21 ms.)

3.4 The axial distance for burn-out of a 50 um drop (Fig. 5 ref. (10)) is: .414 m.

= 41.4 cm.

= 1.36 ft.

3.5 The axial position (ignition point) for start of burning is: .22 m.

= 22 cm.

3.6 Therefore burning velocity (10) is:

$$\frac{41.4 - 22}{.021} = 924 \text{ cm/sec.}$$

4. N.B. The value of 924 cm./sec. is to be compared with the postulated value used in this arithmetic analysis of 140 cm./sec.

5. The ratio of time values for a 50 um drop is:

from Table G.9.1 113 ms

÷ = approx. 5

from (10) . 21 ms

---

6. The burn-out distance ratio is:

Table G.9.2 -- (10) $\frac{5.08}{1.36}$ = Approx. 4

7. The burning velocity ratio is:

G.1 - (10) $\frac{140}{924}$ = Approx. .15

7.1 Conversely the burning velocity ratio of (10) versus G.1 is: 6.5

8. Of considerable interest all values are fairly well correlated.

9. The point now is to discover the applicable factors that generate a (approx.) 5 × greater velocity, i.e. 924 cm. sec. versus 140 cm./sec.

10. The data of Fig. 5 (10) shows:

10.1 The 50 um CWF drops enter the burning zone at a velocity of approx. 158 m/s = 15800 cm/sec.

= 590 fps.

10.2 The velocity head pressure required to produce this 590 fps value (CWF assumed to be 1.19,or a density of (62.4 x 1.19) = 74.25 lbs. cu. ft.) is:

10.2 (continued)

calculated as follows:

$$\frac{V^2}{2_g} = h_l$$

$$h_l = \frac{P \times 144}{p}$$

Cohese P = pressure, psi

p = density, lbs. cu. ft.

V = velocity, fps

Then

$$\frac{V^2}{2_g} = \frac{P \times 144}{74.25}$$

$$\frac{(590)^2}{64.4} = P \times 1.94$$

$$P = \frac{(590)^2}{64.4 \times 1.94} \qquad = \qquad 2786 \text{ psi.}$$

10.3 Similarly the atomizing air velocity entering the combustion zone is: 50 m/s

= 5000 cm/s

= 164 fps

10.3.1 Assuming the specific volume of atomizing air to be that at 14.7 psia, then the $\overline{V}$ value is .0753

10.3.2 The velocity pressure head is:

$$\frac{(164)^2}{64.4} = \frac{P \times 144}{.0753} = P \times 1912$$

$$\text{Whence } P \ \frac{(164)^2}{64.4 \times 1912} = \frac{26896}{123133} \qquad = \qquad .22 \text{ psi}$$

Therefore the pressure at inlet to the burner is (likely) = 5.5" H_2O

7" H_2O

---

11. The following question can be asked:

11.1 How is the pressure of 2786 psi obtained in the 50 um drop test?

11.2 How is a "pure" stream of 50 um drops obtained?

11.3 Is it possible that the "apparent" drop entry velocity is an interpretation of the "high speed cine films of (Monroe 1983)" ?

12. We are now concerned with the relative velocities of the drops and the atomizing air.

12. From Fig. 3 (10) we find that in the combustion range, i.e. from ignition to char burn-out that:

12.1.1 For the CWF 50 um drops, the average velocity is:

$$\left(\frac{4500 + 0}{2}\right) = 2250 \text{ cm./sec.} = 74 \text{ fps.}$$

12.1.2 For the atomizing air the average velocity is

$$\left(\frac{3500 + 0}{2}\right) = 1750 \text{ cm./sec.} = 57.3 \text{ fps.}$$

12.2 The average relative and velocity differential is: (74 - 57.3) = 16.7 fps.

13. From Fig. G.9.1 and Table G.9.1 of the analysis, we find:

13.1 An average drop velocity: (acceleration/deceleration) of: $\frac{110 + 40}{2}$ = 75 fps.

13.2 An average atomizing steam velocity of:

$$\frac{110 + 4.45}{2} = 57.2 \text{ fps}$$

13.3 The average differential velocity is then: (75-57.2) = 17.8 fps.

14. We then compare the average differential velocities:

MIT (10)	16.7 fps.
G.9 (CRL)	17.8 fps

15. Now the flame velocity in the MIT (10) situation, of 924 cm./sec. (Item 3.6) versus the 140 cm./sec. established for G.1 may be due tc the fact that:

15.2 The postulated flame velocity value of 140 cm. in this work is too low.

16. In regard to the item 15 comparison, it must be considered that in the case of the CRL work that the time element for burn-out of .1 second (min.) (9) instead of the MIT value of .021 ms was selected as a safety factor.

17. At this point it should be noted that:

ref. (7) (Spiers) (Fig. 76 - P. 409)

does show that for a "coal dust" of 30% V.M., and 5% ash at a combustion air supply of 10 lbs./lb. coal (approx. 118% Stoichiometric) that the flame velocity is approx. 32.5 fps (988 cm./sec.) which is approx. the MIT value (item 3.6).

17.1 The value for a wet CWF droplet could then be possibly taken at 50% of the 988 cm./sec. or say 400 cm./sec.

18. Referring to G.1 Add. 2, and maintaining the assumption of the start of the 45° spray angle at the G.M. point, we would find that Item 7 of G.1 Add.2) could be recalculated to:

$$\frac{7.2^2}{AJ} \times 91.25 \times 30.48 = 400$$

$$AJ = \left(\frac{144182}{400}\right)^{1/2} \text{(See Fig. G.1.2.R)} = 19 \text{ cm.}$$

(instead of 32 cm.)

At a flame velocity of 400 cm./sec.

18.1 The value for NV, item 8, would then be determined:

$$AV = \frac{19 - 2.2}{2} = 5.9$$

$$NV = \frac{5.9}{.414} =$$ Approx. 14 cm.

18.2 The axial distance to the flame front is then
23 (G.1 Add. 2 Item 5.1) + 14 = 37 cm.
which compares to the max. MIT distance of: 35 cm.

19. It should be noted that the value of 35 cm. is taken from Fig. 3 of the MIT paper (10) which is the only Figure that can be presumed to be based on a multimodal CWF "Utility Grind" (prepared by the Occidental Research Corporation).

20. Referring to Table G.9.1, and maintaining the total burn-out time as derived from Ref. (9) (.1 sec. for a 44 um drop) which yields the Equation t (min.) = .0026D (G.8 Items 3 & 3.1)

We find from clm. 10 of Table G.9.1 that the reduction in distance to flame front is 53 - 37 (Item 18.2) = 16 cm.
= .524 ft.

for the CWF atomizing case where the initial drop generation rate is 1000 drops/.005 sec. = reduction in burn-out length.

---

21. For the case of the 3000 / .015 sec. drop·rate we find the axial distance to flame front based on a flame velocity of 400 cm./sec. as follows:

21.1 From G.1 item 8.4.1

$$D_4 = \frac{2500 \times (36)^2}{400} = \sqrt{8100} = 9.0$$

From item 87

$AJ = 90$ cm.

$$AV = \frac{152.90}{2} = \frac{62}{2} = 31 \text{ cm.}$$

$$FV = \frac{31}{.414} = 75 \text{ cm.}$$

DV = (Distance to flame front)

(132 + 75   207 cm.) = 6.8 ft.

21.2 Hence the reduction in burn-out length is

(9.00 − 6.8) = 2.2 ft.

21.3 NOTE: Increase of flame velocity affects only the axial distance to the flame front and the flame front diameter.

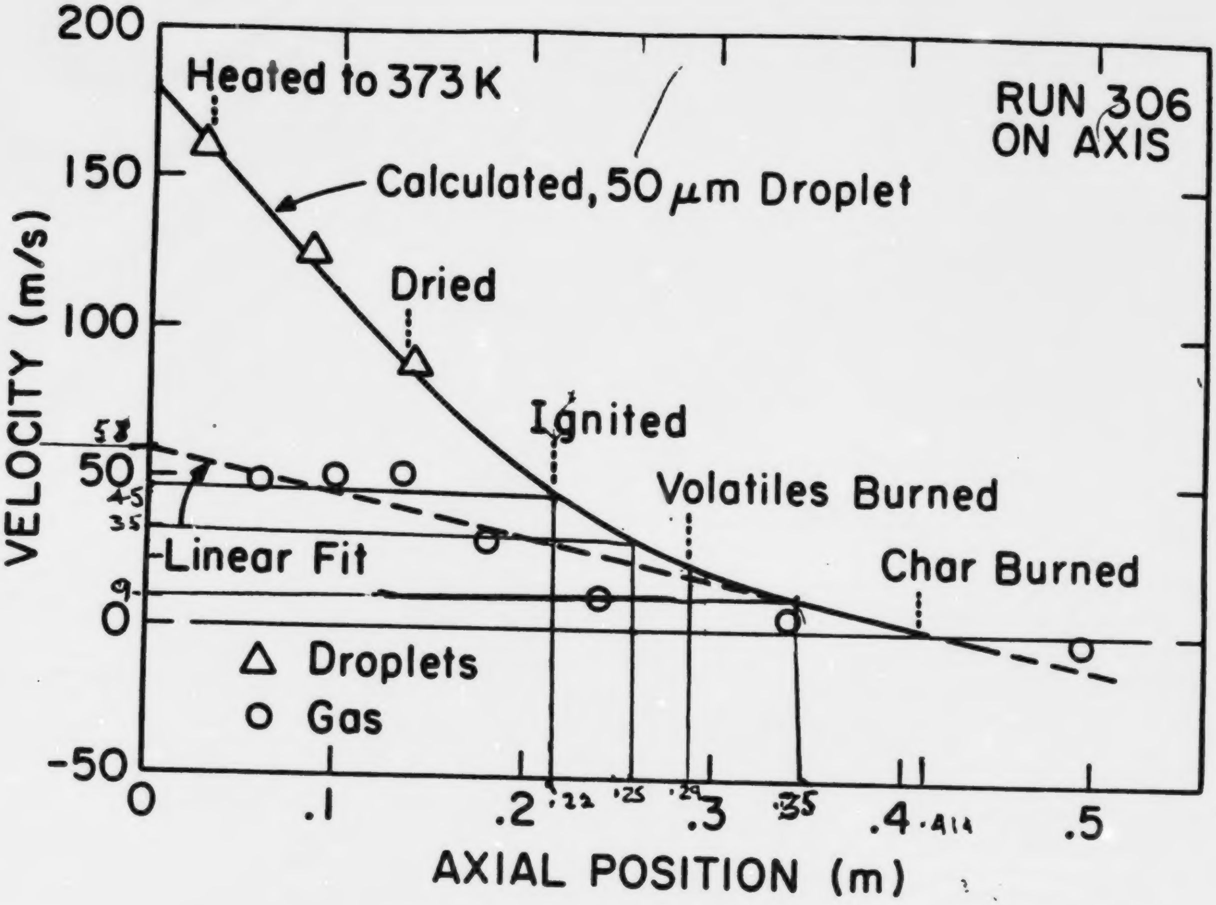

G.15

Figure 5. The dependence of droplet and gas velocities on distance from the burner along the axis. The gas velocity data were taken from Fig. 2; the droplet velocity data from high speed cine films (Monroe, 1983). The positions of the ignition and combustion processes and velocities for a 50 μm droplet were calculated as described in the text.

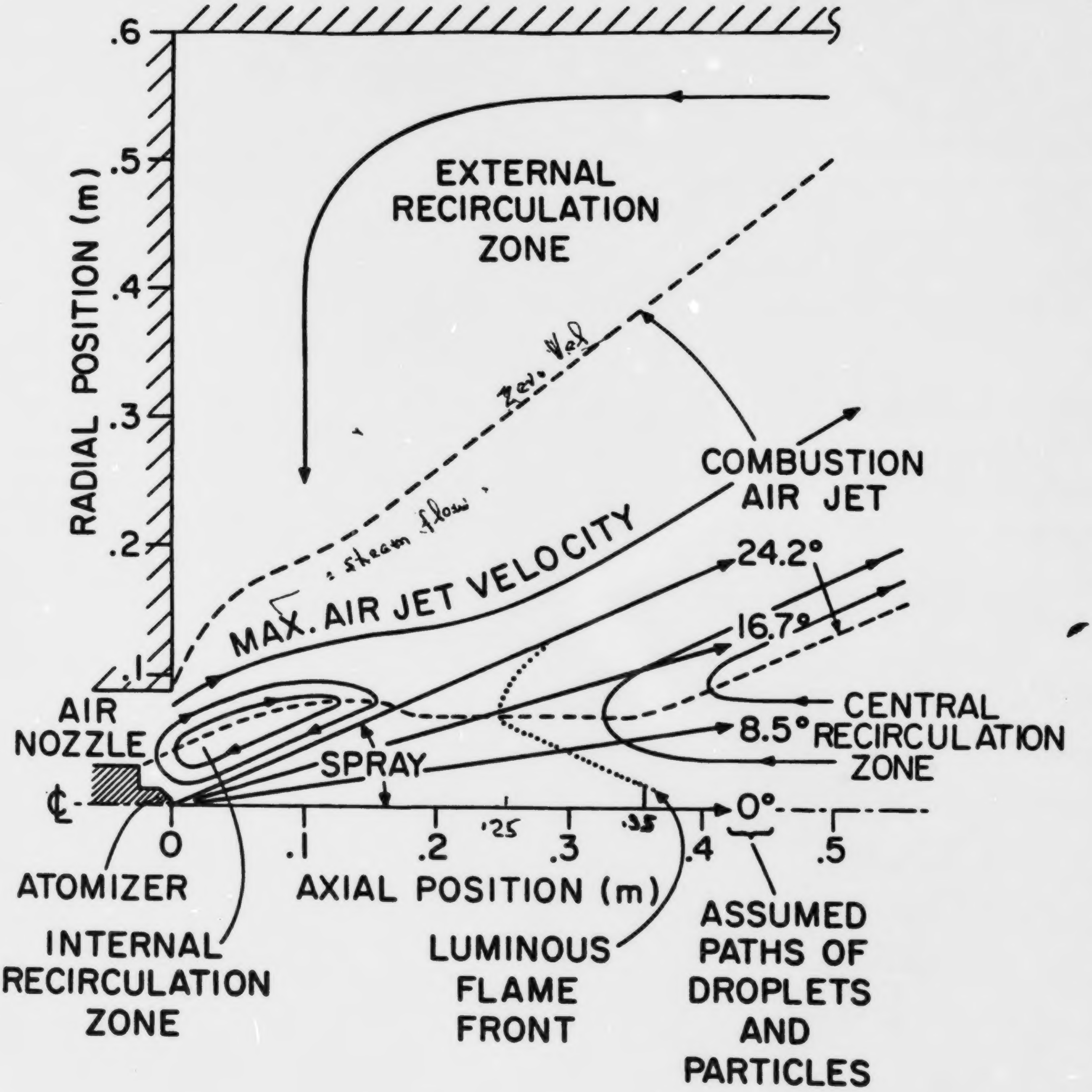
.6
.5
.4
.3
.2
.1
RADIAL POSITION (m)
EXTERNAL RECIRCULATION ZONE
Zero Vel
= stream flow
MAX. AIR JET VELOCITY
COMBUSTION AIR JET
24.2°
16.7°
8.5°
0°
CENTRAL RECIRCULATION ZONE
AIR NOZZLE
SPRAY
℄
0
.1
.2
.25
.3
.35
.4
.5
AXIAL POSITION (m)
ATOMIZER
INTERNAL RECIRCULATION ZONE
LUMINOUS FLAME FRONT
ASSUMED PATHS OF DROPLETS AND PARTICLES

G.15

Figure 3. Gas flow pattern in the region close to the burner.

G.15.7

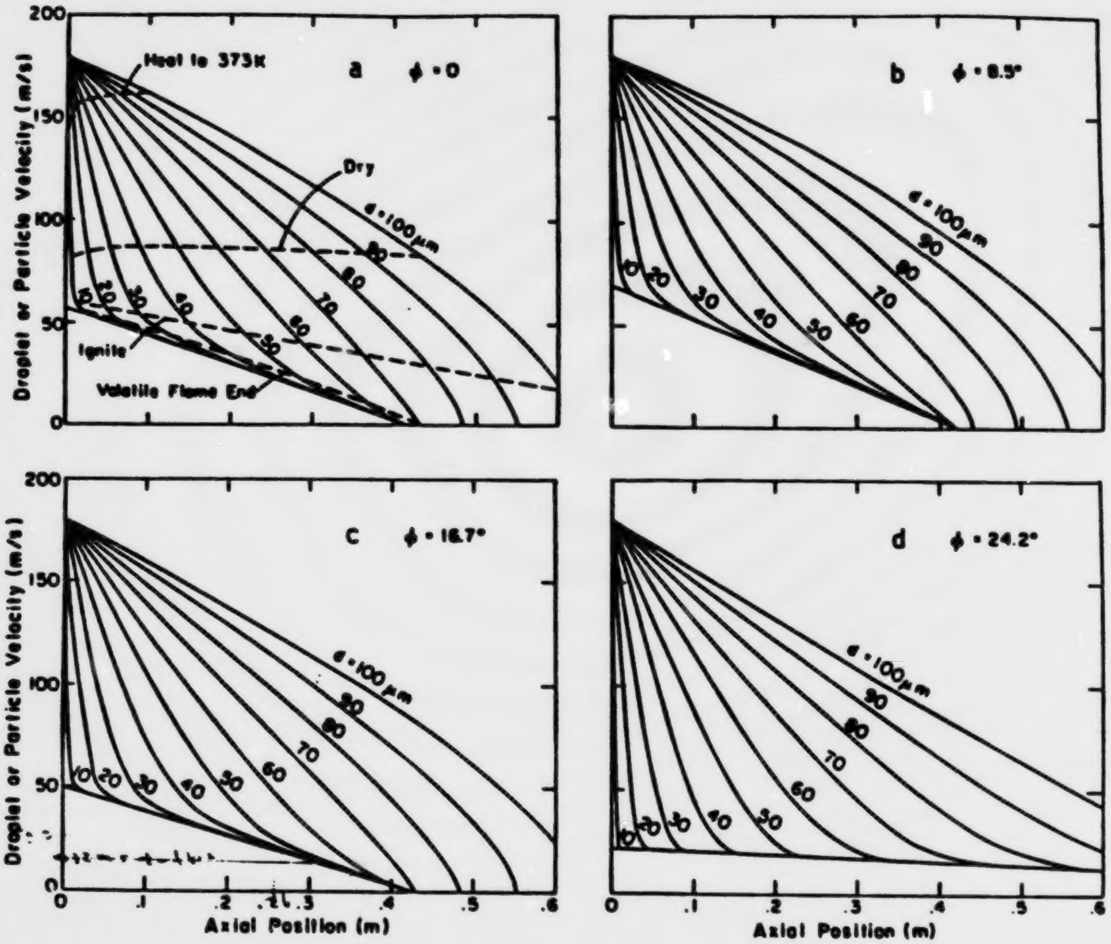

G.15

Figure 7. Calculated velocity decay for droplets/particles of 10 to 100 μm.

a. ϕ = 0
b. ϕ = 8.5°
c. ϕ = 16.7°
d. ϕ = 24.2°

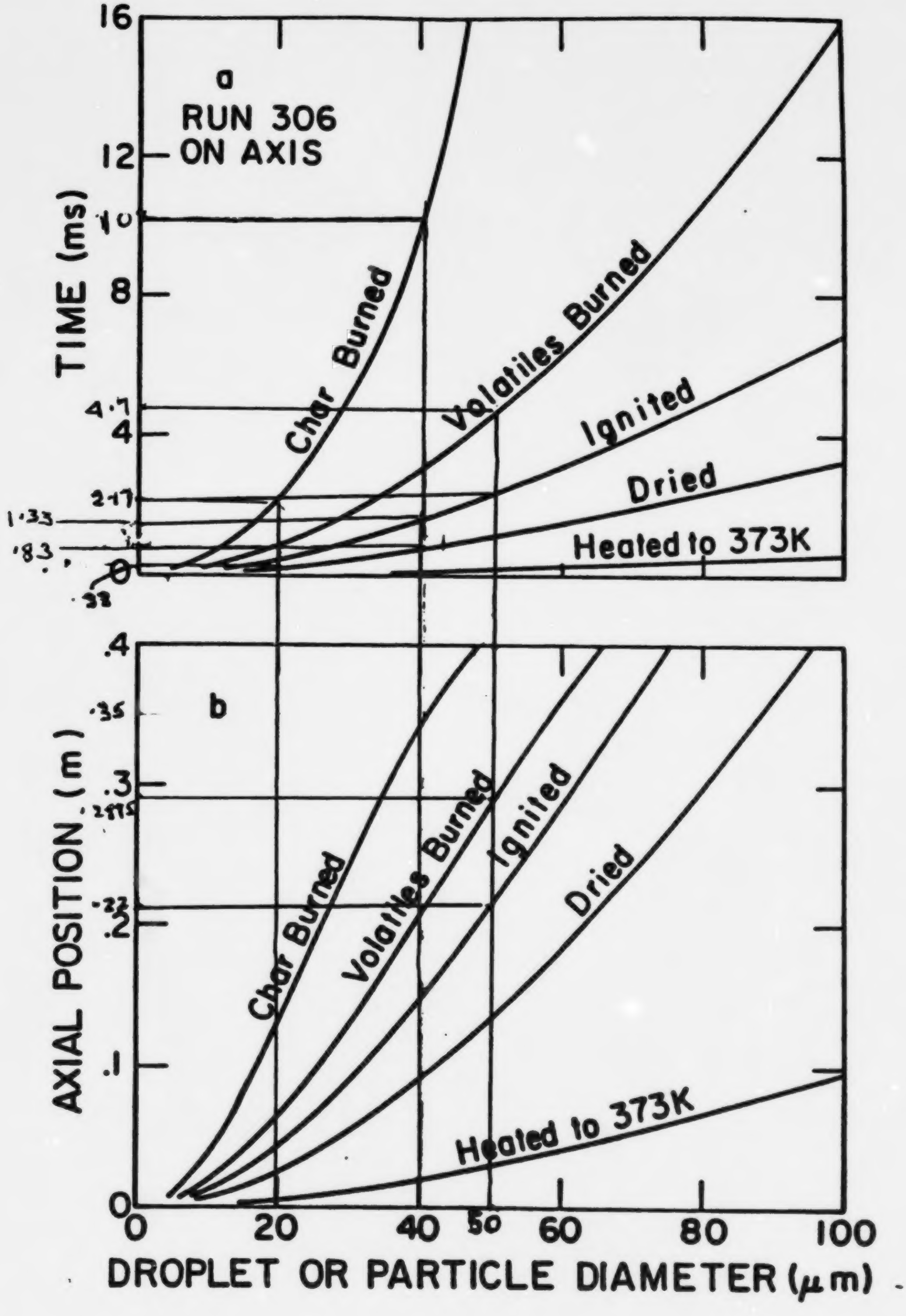

G.15

Figure 10. Dependence on droplet/particle size of: a. cumulative times, and b. Distances required for the ignition and combustion processes.

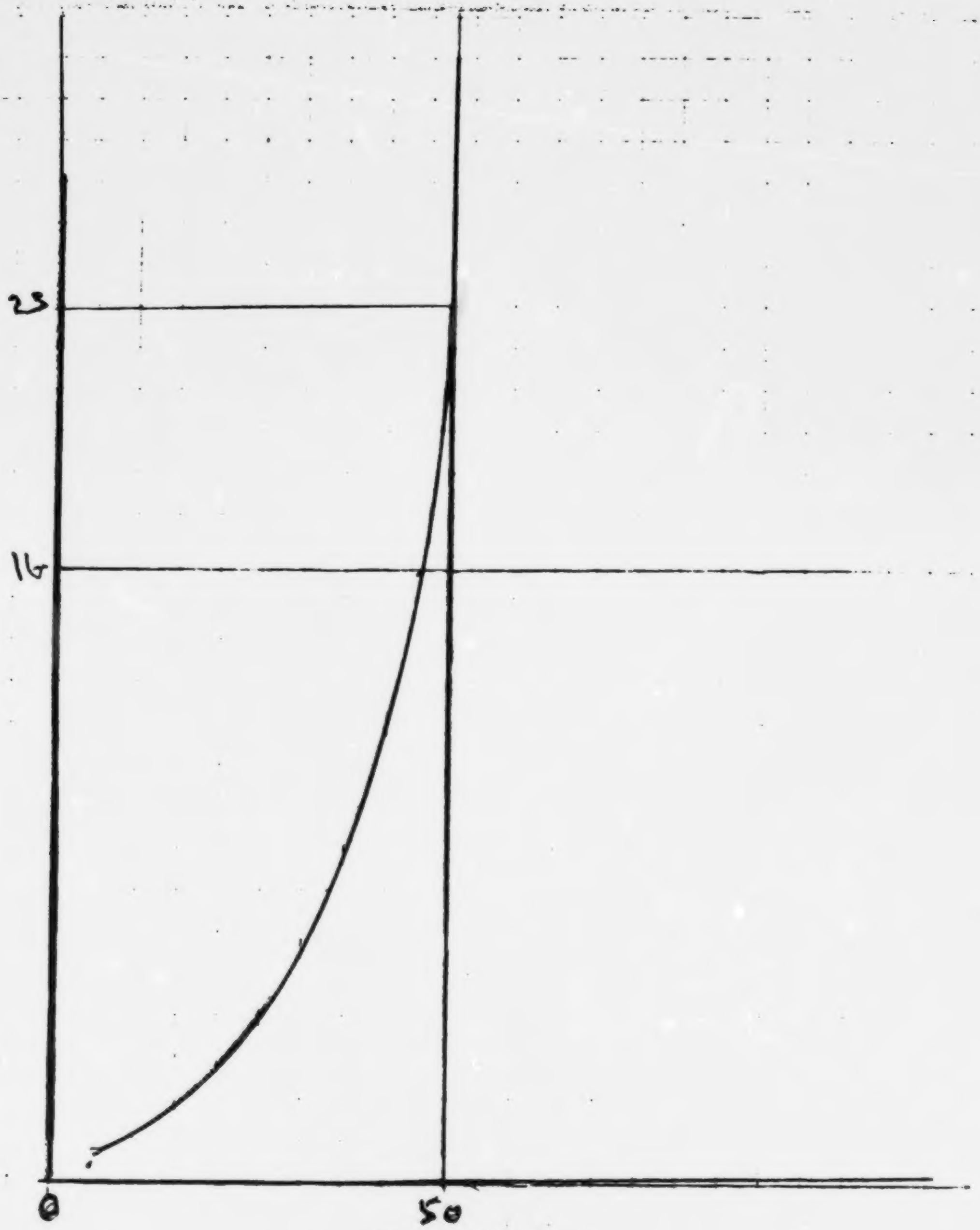

FIG G·15·11
EXTRAPOLATION of CHAR GRAPH
of
Fig. 11 (10)

G. 16

Discussion on Atomizer Design

---

1. Y-Jet - Two Phase Flow

1.1 The Analysis Work on the Y-Jet atomises covered by papers G.1 to G.15, was based on a two-phase flow according to the paper by Mullinger and Chigier (1974). (1)

1.2 It was assumed through the course of the work that the CWF annular flow width was uniform around the circumference of the atomiser including the flow through the divergent nozzle. (This divergent nozzle was an addition to the standard cylindrical C.E. Y-Jet, posited by the writer as a mechanism to develop control of the atomizing steam velocity as a foundation for the hypothesis of initial drop formation and subsequent drop breakdown by the differential velocity between atomizing steam and the CWF drops, according to the Weber formula (2).)

1.3 On a review of Fig. 5 of the Mullinger-Chigier work, I noted that the fluid film was not uniform around the circumference but was thinner on the inner atomizer surface opposite to the CWF inlet.

1.4 I used this observation to determine the actual (or more accurate)film thickness, at the exit of the divergent nozzle.

---

2. First calculated was the effect of the hypothecated increase in velocity from 26 to 40 fps. in the Y-Jet per se. (G.1 item 16.2) and item 44

2.1 The change in annular area would be inversely proportional to the velocities, i.e. the value $\frac{26}{40}$ = .65

2.2 The annulas area for the working condition of a CWF fluid of .0036 cfs (102 cm.^{3}) = .131 cm.^{2} (G.1 item 16)

2.3 Then, the flow area of exit of the horizontal Y-Jet section (and so at the entry to the divergent nozzle is: (.65 x .131) = .085 cm.^{2}

2.4 The cylinder dimensions of the C.E. Y-Jet in question are:
Diameter - .487 cm.
Area - .1865 cm.^{2}

2.5 The fluid annulus width first determined had been: = .106 cm. (G.1 Item 15.2)

2.6 The formula for annulus area is:
(Mean Oce. xX) where X = film thickness
Mean Oce. is: (.487 – X) Π : EQ.1.
Film area is then: (.487 – X) Π x X = .085 cm.^{2}

$$(.487X - X^2) = \frac{.085}{\Pi} = .027 \;; \qquad \text{EQ.2}$$

2.7 EQ. 2 is solved by iteration and X, = .065 is the fluid annular width at the exit of the C.E. cylindrical body, where the velocity is postulated to have increased to 40 fps (from 26 fps)

2.8 Proof:
of EQ. 2 is: $(.487 \times .065) - (.065)^2$ = .027

1) .487 is the I.D. of this particular C.E. annulus.

3. Then the steam core dia. at exit of the cylindrical annulus is: .487 - (2 x .065) = .357 cm.

4. Now steam will expand in the divergent nozzle from an entrance press. of 174 psia when $\overline{V}$ is 2.616, to 14.7 psia when $\overline{V}$ is 26.8

4.1 Expansion ratio is $\left(\frac{V_2}{V_1}\right)^{1/2} = \left(\frac{26.8}{2.61}\right)^{1/2}$ = 3.2

4.2 Then the divergent nozzle diameter is: (.357 x 3.2) + (2 x fluid film width at 60 fps)

4.2.1 Stem core dia. at div. nozzle diameter is (.357 x 3.2) = 1.14 cm.

5. Let X = fluid width at exit of divergent nozzle

5.1 Then from item 4.2.1, we find

$$Oce = (1.14 + X)\ \overline{\Pi}$$

5.2 Fluid film area is then: $(1.14 + X)\ \overline{\Pi} \times X$

5.3 From item 2.3 we find the area of entry to the divergent nozzle is: = .085 cm.^{2}

5.4 Velocity increase from 40 to 60 fps will reduce divergent nozzle fluid exit area to $\frac{40}{60} \times .085$ = .0566 cm^2

5.5 Then from 5.2 we have:

$$(1.14 + X)\pi \times X = .0566$$

$$1.14X + X^2 = \frac{.0566}{\pi} = .018$$

EQ. 3

5.6 By iteration we find X = .0156 cm.

= 156 um

5.7 Proof: Subst. X = .0156 in Eq. 3

$$(1.14 \times \underline{.0156}) + (.0156)^2 = .018$$

Q.E.D.

6. From Fig. 5 (1) we note that the fluid film (in the cylindrical (.C.E) section is thinner in the Oce side opposite the inlet of the CWF.

6.1 Assume a bias of 20% for the thinner section of fluid over an assumed Oce. of 50%.

6.2 The film thickness in the upper semi Oce if then: .8 X .0156 = .0125 cm.

= 125 um

6.3 It is now necessary to determine the film thickness in the fewer semi Oce.

6.4 Because the total CWT flow is fixed at $102\ cm^3$, then the total exit area must remain the same, (i.e. $.0566\ cm^2$) (Item 5.4) despite the bias in the film thickness.

7. From Eq. 3 (item 5.5) and item 6.2, the area of the upper semi Oce is:

$$(1.14 + .0125)\left(\frac{\pi}{2} \times .0125)\right)$$

$$(1.14 \times .02) + (.0125 \times .02)$$

$$.023 + .00025 \qquad = \qquad .023\ cm^2$$

7.1 Let (Y X)= fluid thickness of the lower Oce.

Where X = 'Standard' thickness of .0156 cm based on uniform circumferntial flow.

Y = bias factor deriving from the postulate that the upper Oce. fluid thickness would be 20% less than the uniform value.

7.1.1 Then the exit area of the lower semi Oce is:

$$(1.14 + .0156Y) \ \frac{\pi}{2} \times .0156Y) \qquad \text{Eq. 3}$$

$$(1.14 + .0156Y) \ (.0245 Y)$$

$$(1.14 \times .0245Y) + (.0156 \times .0245) Y^2$$

$$(.028Y) + .0004 Y^2)$$

7.2 Then:

$$.023 + .028 Y + .0004 Y^2 = .0566 \text{ cm.}^2$$

The Y^2 term can be eliminated as insignificant and we have

$$.025 Y = .0566 - .023$$

$$= .033$$

$$\text{Then } Y = \frac{.033}{.028} = 1.78$$

7.3 Then the thickness of the lower semi Oce, film is(Y X)= (1.178 x .0156) = $\underline{.0184}$ cm.

8. Should experimental test prove the values of .0156 cm (or even .0184 cm.), then these film thicknesses would serve as a back up or an alternative to the drop formation hypotheses developed in G.1 .

8.1 These diminished dimensions are small, even for straight mechanical atomizing burners and the annular jet stream "should" be readily atomizable.

8.2 However, it must be considered that the 'actual' min. width will be under the restraint of the top coal size in the CWF (300 - 400 um) standard top size unless micronized coal is used (< 150 um)

8.3 However, the coal particles larger than the diminished film thicknesses calculated in this paper and shown on Fig. G. 1.3. will "simply" protrude into the steam space. (The inner line of the film thickness shown in Fig. G. 1.3 is not a solid body, it is the interface between the steam core and the fluid film.

8.4 It could be expected that the larger coal droplets (or CWF droplets) would be ejected into the CWF spray.

9. It therefore appears desirable to establish atomizing steam conditions where a pressure of (say) 5 psi appears at the divergent nozzle exit, instead of zero psig.

---

10. The divergent nozzle length for zero psig (See Fig. G.1.3) is determined as follows:

10.1 From Fig. G.1.3

dimension $CJ = \frac{(1.176 - .487)}{2} = .3445$ cm.

$\frac{CJ}{AJ} = \tan JAC = \tan 7.5^{\circ} = .1316$

$AJ = \frac{CJ}{.1316} = \frac{.3445}{.1316} = 2.6$ cm.
(length of divergent nozzle for zero psig at exit)

11. The diameter expansion factor for an expansion from 160 psig at point A to 5 psig at point C is:

$$\left(\frac{V\ (5\ \text{psig})}{V\ (160\ \text{psig})}\right)^{1/2} = \left(\frac{20.38}{2.61}\right)^{1/2} = 2.8$$

11.1 Dimension DE is then:

$(2.8 \times .357) = 1.0$ cm.

Then CJ becomes $\left(\frac{1.0 - .487}{2}\right) = .256$ cm.

Then AJ (length of divergent nozzle) becomes: $\frac{.256}{.1316} = \underline{1.945\text{ cm.}}$

11.2 That is: The divergent nozzle is required to be shortened by $(2.6 - 1.94) = \underline{.68\text{ cm.}}$

To provide 5 psig at nozzle exit.

---

12. The expansion of the 5 psig atomizing steam should provide (by itself) effective break-up of the thin fluid steam
(125 um or 184 um)

12.1 Fig. G.1.4 shows that at a half angle expansion of 22.50° the atomizing steam will reach zero psig within 6 cm. of the nozzle tip, when its velocity will become 166 fps due to the area expansion (inverse) :

$$\frac{1.176}{3.7}^{2} = .10$$

$$\text{Then } .10 \times 1660 = 166 \text{ fps.}$$

This velocity of 166 fps is then employed in conjunction with the Weber No. used in this study to obtain "numbers" relating to spray formation and drop size.

12.2 The velocity of 166 fps will decelerate to a min. of 4.45 fps as calculated in paper G.7 and shown in Fig. G.9.2, and Table G.9.1 - as per calculation:

13. From the work of reference (2) (Giffens & **Muraszew,** it would seem that even without an atomizing fluid, that adequate CWF Jet breakup could occur if the velocity and film thickness could be developed in a straight mechanical atomizing design atomizer (for which a special study would be required.)

13.1 But, a mechanical atomizing design could prove to be impractical due to the corrosive effect of the CWF.

14. The NRC atomiser would seem a logical atomiser principle, and it would be interesting to experiment with the atomizer exit annular dimensions of the order shown in Fig. G.1.3 and described in this paper.

15. It seems probable, also, to consider that the atomizing steam expansion principle, for spray formation, could be obtained with a lower inlet pressure to the divergent nozzle with a corresponding change to the nozzle angle and/or reduction of nozzle length.

16. There is the further possibility that the hypothetical fluid film thicknesses, were shown to be realized in practice, that the atomizing fluid/fuel ratio could be reduced below the .15 lb/lb fuel ratio.

16.1 In this regard, Fig. 6 of ref. 1 (Mullinger & Chigier) shows air/fuel mass ratios in the range of .01 to .04 (!)
But of course, the experimental fluid used in their experiments was not stated to be a CWF (but was likely to have been water or a light oil).

---

17. **Important**

In all the work on numerical analysis, consideration has been given only to the CWF spray formations. The consideration of combustion air delivery factors, including swirl, vane design, and excess air control, are essential for control of flame width and will also have an important role in minimizing the flame length determired from the time data of reference (9), as developed in paper G.8,and the effect of possible coalescence on drop diameter, as developed in papers G.11 to G.14 incl.

17.1 Data on diameters of flame front and end of spray are given in Table G.9.2.

17.2 Forsome boiler furnace configurations, atomizer spray angle; fuel and atomizing fluid; pressures; atom. fluid/fuel ratios;and number of atomizers per boiler, together with combustion air register design and combustion air flow control may require careful coordination.

SINGLE PHASE HOMOGENEOUS EMULSION FLOW

---

18. In this generic type of atomizer, the atomizing fluid and CWF mix internally.

19. Three manufactured types illustrate variation in design.

19.1 C.E.Y. Jet - CWF enters a horizontal cylinder at an angle to the atomizing fluid longitudinal inlet
(See Fig. Fig. 1.A.4 - Appendix 4).

19.2 B & W - T-Jet, similar to the Y-Jet except:

CWF enters at a right angle to the steam cylinder and further mixing takes place in a "mixing chamber" equipped with exitports.
(See Fig. 8 - W.22 and also Fig. 1, p. 136, in the Phase 1 Report.

19.3 North American Internal Mix (refer to Phase I report)
See Fig. 13 - Emulsion Tube Type
Fig. 14.1 Tip emulsion type.

20. The first analysis of the C.E. Y-Jet atomizer was made on the basis that the atom. steam/CWF mix was a homogeneous emulsion.

20.1 From the known atomizer dimensional data, and operating conditions of CWF flow (Chatham test) and the atomizing steam and CWF pressures and flow, calculations were made on a 70/30 CWF (by Weight) and a 75/25 CWF (by Weight) resulting in data tabulated in Appendix 4.R, pages 5 & 6.

21. One purpose of this work of Appendix 4.R determine the variations of the function Ø (% coal by vol.) for comparison to Ø max., i.e. max. possible value of Ø (determined experimentally), from which a viscosity in centipoise could be determined, by use of equation in appendix 1 ref. X.2.

22. Now referring to Appendix 2.1, concerning a Co-Al (Shurrytech) CWF, it will be seen that this CWF viscosity was 125 Cp or 149.6 Cp (for a 75/25 CWF) depending on whether a Funk max. value of .94 or .925 was used.

22.1 Actually these viscosity values, based on the Funk Ø max. data did not jibe with the Funk rheogram value of 806 Cp shown in Fig. 3 of the paper B.1 (by J.E. Funk Sr., D.R. Dinger, J.E. Funk, Jr. (See Paper B.1 in Technical papers Section of Vol. II).

23. Of prime importance though is that the Ø values found for the CWF/Steam emulsions, enabled the calculation of viscosity (of a homogeneous emulsion) which led to the fact that at an emulsion viscosity under 4 Cp, the atomizer flow was turbulent,

24. The actual emulsion viscosity for CWF values as calculated in Appendices 6.R (item 4) & 8 (item 17) is <1.4 Cp 1–A.6R Appendix 6 R.

25. In Appendix 7 it is shown (item 5) that for a viscosity of CWF as low as 63 Cp that the CWF flow (under the C.E. atomiser operating conditions) that the CWF (only) flow is laminar.

26. From calculations in Appendix 7, it is shown that :

26.1 An emulsion viscosity up to 4 Cp will maintain flows in turbulent mode.

26.2 To raise the viscosity of the emulsion to 4 Cp (limit for turbulent flow) the atomizing steam volume must be reduced from the original (calculated) value of $.096\ \text{ft.}^3$ (App. 4.R – Item 15.1 to a value of $.0053\ \text{ft.}^3$ (App. 7 item 32.3.)

26.3 The % reduction of atom. steam is:

$$\frac{.096 - .0053}{.096} = \frac{.0907}{.096} = 94.5\%$$

26.4 The "lost" .0907 ft.^{3} is an amount condensed to water and adds to the original water volume of the CWF of .097/2.4 = .038 lb.

26.4.1 The water volume increase is

$$\frac{.038}{62.4} = .0006 \text{ ft}^3$$

27. Hence we see that the turbulent condition of 4 Cp emulsion viscosity is maintained, even with the condensation of 94.5% of the atomizing steam, by virtue of the fact that the condensate is added to the original water volume, so that the resultant emulsion viscosity is $<$ 4 Cp (The turbulence limit of viscosity).

28. However, under the conditions posited in Appendix 7 (i.e. a limit emulsion viscosity of 4(Cp) the CW F temperature will rise to: 345°F

28.1 There is no boil-off of the CWF water

29. The foregoing begs the question: What will be the "emulsion" viscosity if 100% if the atomizing steam is condensed?

---

30. This question is addressed in Appendix 8, in which calculations show that the ultimate "emulsion" viscosity with 100% atomizing steam condensation is: 1.415 Cp
(Add. 8 Item 17.)

30.1 The conclusion reached in comparing steam condensation as per Appendix 7, versus Appendix 8 is that the increase in water volume of the CWF holds the emulsion viscosity < 4 Cp (the turbulent flow limit.)

31. Hence having proven (by calculation) that a CWF/steam emulsion will always be in a turbulent mode we can use the turbulent flow equation of Crane (P 3.10) for atomiser design.

The equation is: $$\Delta P_{100^1} = \frac{.000336\, fW^2}{d^5 p}$$

or $$\Delta P_{100^1} = \frac{.1294\, p f v^2}{d}$$, then:

$$\Delta P \text{ per in.} = \frac{.1294\, p f v^2}{1200\, d}$$

$$= \frac{.000108\, p f v^2}{d} \quad \text{-- Eq. 4}$$

WHERE ΔP = Psi friction head loss

p = density lbs./ cu. ft.

v = velocity, fps.

d = dia. - in.

f = friction factor = .038

31.1 Equation (4) will give friction head in lbs./sq. in. per inch length of annulus.

32. In accordance with the date developed there is only a small (relatively) amount of steam in the emulsion.

33. Therefore the emulsion must be considered as a liquid, subject to the formulae pertaining to the atomization of a liquid.

34. It is known that atomizing effect (i.e. the production of small drops) is a direct function of velocity and so of pressure.

35. Item 18.2 of App. 7 shows that for a head of 21,000 ft. (equal to a velocity of 1162.5 fps) (Cases B & D). that the velocity head pressure is 240 psi.

36. The applicable equation is:

$$\frac{V^2}{2\,g} = h_\varrho = \frac{P \times 144}{p}$$

$$P = \frac{V^2\ p}{64.4 \times 144} = \frac{V^2\ p}{9273.6} \qquad \text{Eq. 2}$$

37. To obtain the p value the mean steam pressure must be known to obtain $\overline{V}$

38. Then $\frac{1}{\overline{V}} = p$ = density, lbs./cu. ft.

39. Velocity is obtained from $\frac{\overline{V} + \text{CWF Vol., ft.}^3}{\text{orifice area (ft.}^2)} = V$

The value of $\overline{V}$ must be determined by experiment to define the velocity that will yield the required fineness of atomization (for a given atomiser design).

Then p , d & P values of Eq.^{2} can be determined (juggled) to provide the experimentally determined velocity requirement.

---

41. The velocity values shown in Appendix 7 are based on a true emulsion volume of steam plus CWF.

42. If condensation of a significant portion of the atomizing steam takes place, as described in Appendices 7 & 8, then the CWF volume is determined as calculated in Appendix 8.

42.1 Item 14 of Appendix 8 shows that for an original given weight of emulsion of .307 lbs., the volume (for an atom. steam press. of 175 psi decreased from .0996 (see Item 15.1 Appendix 4.R) to .0366 (see item 14 Appendix 8).

43. This will then determine (by calculation) the dia. of annulus or orifice to give a velocity of (say) 1000 fps for a given volume of CWF flow.

44. There is fundamental data that must be known to establish the fraction condensation of the atomizing steam in an annulus, viz.:

Atomizing Steam Pressure at:

44.1 Inlet.

44.2 Outlet.

CWF Temperatures at:

44.3 Inlet.

44.4 Outlet.

45. From such date, calculations based on thermodynamic steam tables would allow the calculation of the amount of steam that is condensed.

46. There is left one important consideration: The max. viscosity < 4 Cp assumes the CWF to be in a pseudo-plastic or thixotropic or rheopectic mode.

46.1 Should the CWF have a dilatant mode, then it is conceivable that under the high shear in an annulus that the viscosity might rise to excessive values to the point of blocking (or severely impeding)flow .

46.2 Such dilatant effect would be especially strong in the CWF flow tube, before the CWF meets with the diluting atomizing fluid.

46.3 In App. 1, Ref. X.12,(Dr. Dooher) figures 6. x. 12 to 8.X.12, show dilatancy as a function of time (not applicable to annular flow.) But Graph B of Figure 8.X.12 shows a sharp dilatory effect when the shear rate was increased to 1000 sec.$^{-1}$

46.4 N.B. The shear rate $\frac{8V}{D}$ in the C.E. Annulus, (η assumed ≤ 1) is:

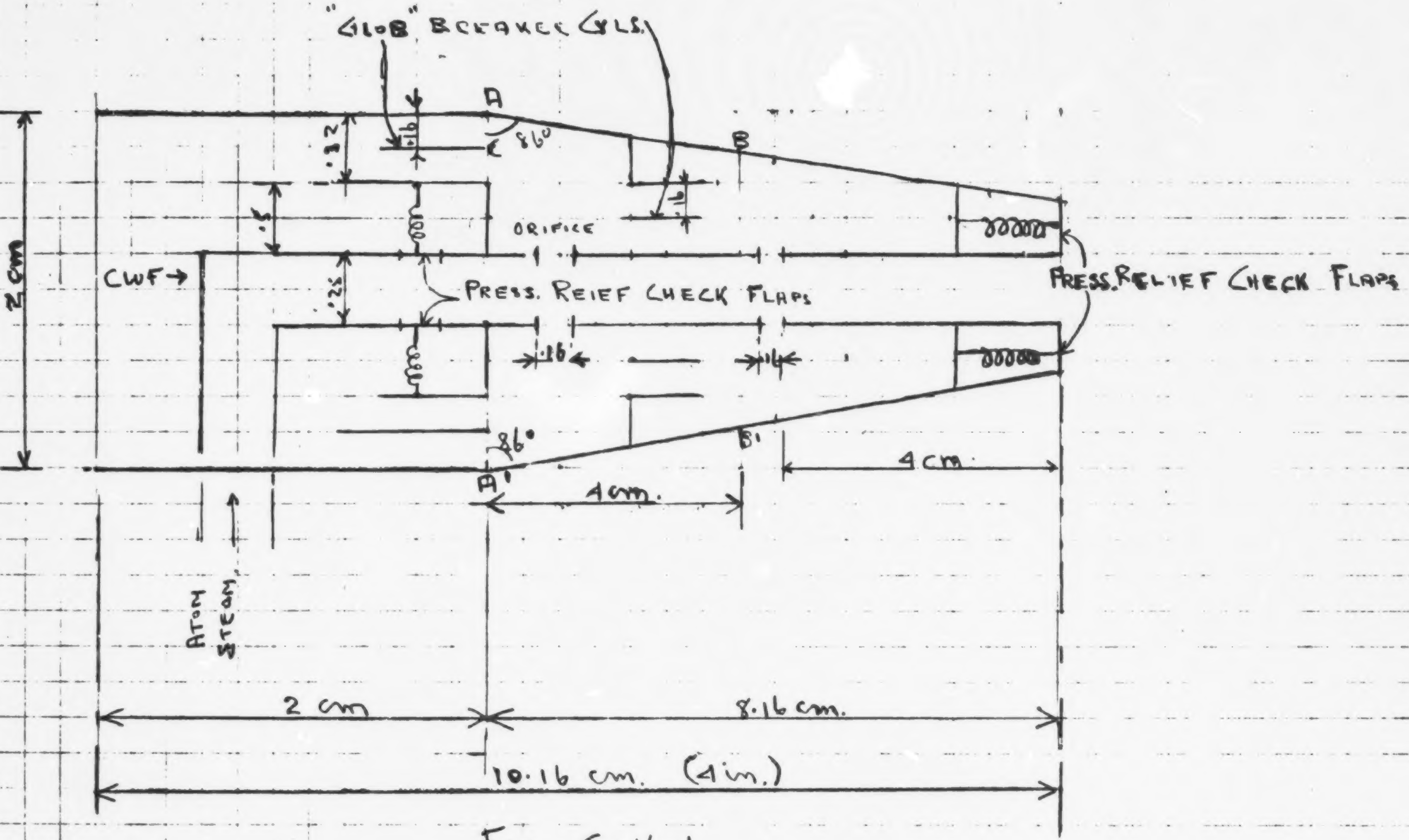
"GLOB" BREAKER CYLS.
A
.16
.32
86°
.5
ORIFICE
B
.16
CWF →
2 cm
.25
PRESS. REIEF CHECK FLAPS
PRESS. RELIEF CHECK FLAPS
.16
.16
86°
B'
A'
4 cm.
4 cm.
ATOM STEAM
2 cm
8.16 cm.
10.16 cm. (4 in.)

FIG. G.16.1

Schematic of a CWF/steam Atomizer Annulu Designed for Optimum Homogeneity of Emulsion (to use base or in conjunction with Divergent Nozzle or with Mixing Chamber).

46.4 (continued)

$$\frac{8 \times (930 \times 30.54)}{(.016 \times 30.54)} = 465000 \text{ sec.}^{-1}$$

47. Also of importance is the heating effect of the CWF by steam energy transfer by condensation to temperatures over 300^{o}F. This may preclude the use of certain CWFs, where additives may suffer breakdown due to temperature (polymerization or depolymerization) - with possible serious effect in viscosity and or coal particle coherence.

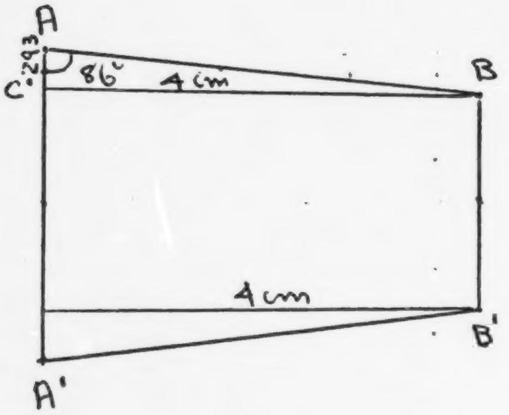

Fig. G.16.2 Division Point of 50% Flow.

Determine angle CAB given

$A\text{-}A^1 = 2$ cm.

$BB^1 = 1.414$ cm.

$$AC = \frac{A A^1 - B B^1}{2} \quad \frac{2 - 1.414}{2} = \quad .293 \text{ cm.}$$

$CB = 4$ cm.

$$\text{Then } \tan \quad CAB = \frac{CB}{AC} = \tan^{-1} \frac{4}{.293}$$

$$= \tan^{-1} 13.65$$

$$= 86^{\circ}$$

G. 16 - ADDENDUM 1

FURTHER DISCUSSION OF ATOMIZER DESIGN FOR TWO-PHASE AND HOMOGENEOUS EMULSION FLOWS

1. Papers G.7 to G.16 have dealt generally with the factors of temperature, pressure, flow, viscosity, burn-out and coalescence.

2. Dimensional data were established in the section on two-phase flow, and potentials for drop collision and possible design means of prevention of collisions, were discussed in papers G.11 to G.15.

3. A means (numerical) of shortening burn-out length was developed in paper G.15, following a comparison between the flame velocity of 140 cm./sec. used in this work and over 900 cm./sec. in the M.I.T. work. It was found from the M.I.T. data, and a comparison with data on coal dust flame velocity (Speirs Fig. 76 p. 408 - ref. (7) that a flame velocity value of 400 cm./sec. could be considered, which would give a modest reduction of burn-out length by decreasing the axial distance to the flame front.

3.1 Whereas preceding papers have dealt with increased burn-out lengths due to drop coalescence in the spray development zone of the furnace, another cause of cohered particles must be considered - that due to additives.

4. It seems, from the literature and my discussions with an atomizer manufacturer, that additives may be of two types.

4.1 Those additives used to maintain stability in the storage tank by forming a gel-type formation which resists precipitation of the coal solids.

4.2 Those additives which serve as an electrophoretic agent, by creating an ionic charge on the atomized, drop and/or the coal particles (or both), which would serve to maintain separation in the flow system to minimize viscosity.

4.3 Now it may be that additives (4.1) may perform both functions.

4.4 But it has been said that cohered[1] particles appearing in the atomizer may be due to inadequate breakup of the gel formations in the tank.

4.5 Such cohered coal particles or gelled drops can (conceivably) cause blockage of an annulus or orifice.

5. Two techniques could be considered to prevent 4.5.

5.1 Use a "Cuno" auto-cleaning strainer with a suitable plate separation.

5.2 Use a cohered particle or gel breaker knife edge in the CWF supply annulus in the atomizer.

5.3 This is shown in Fig. G.16.1, which also shows orifices from the CWF annulus into the atomizing fluid core.

6. The further functions of the design of the G.16.1 atomizer is to secure max. penetration of the CWF into the atom. steam space assumed to be .25 um dia.

---

1) (the term cohered is used to characterize aggregation before the spray formation, and coalescence being the aggregation of drops in the spray system.

---

7. The "glob" breaker passages are sized to .016 in., and the orifices are similarly sized. This provided a safety factor of 4 versus the normal 400 um (max.) sized coal particles, or only twice the (experienced) size of 800 um.

7.1 Accordingly, it will be noted that the closed ends of the CWF passages, and on sections of the steam tube, there are shown spring loaded "flaps". In the event of blockage these flaps will open to rising pump pressure to clear the CWF passages and orifices in the event of a (temporary) blockage. (Pump pressure controlled by a spring-loaded relief valve or a diaphragm operator on a suitable globe, gate or butterfly valve.)

G.16 - ADDENDUM 2

CALCULATIONS FOR ATOMIZER DESIGN OF FIG. G.16.1

1.	Operation and Design Data		
1.1	Max. CWF flow (for this exercise)		.29 lbs./sec.
		=	.004 cfs.
1.2	Atomizing steam press. (initial postulate)		150 psi
1.3	Max. CWF press. (initial postulate) 150 psi + ΔP CWF to steam (see Item 5.1 below)		
2.	Max. coal particle size (standard)		400 um.
2.1	Max. coal particle size observed		800 um.
3.	Orifice dia. for S.F. of two (versus max. experienced particle size)		1600 um
		=	.16 cm. (.063 in.)
3.1	No. of orifices (2 sets of 2 opposed)	=	4.
3.2	Total area of 4 orifices $4 \times \left(\frac{.16}{2}\right)^2$	=	.0804 cm.^{2}
		=	.0125 in.^{2}
		=	.000087 ft.^{2}

---

4. Required velocity flow at an orifice coeff. of(.8 is:

$$(.8\ V \times .000087) = .004$$

$$V = \left(\frac{.004}{.8 \times .000087}\right) = 57.5 \text{ fps.}$$

5. Differential CWF/Steam to velocity head pressure form from EQ.:

$$\frac{V^2}{2g} = \frac{P}{p} \times 144$$

Subst. $V = 57.5$, $g = 32.2$,

$$P = (1.19 \times 62.4) = 74.25,$$

we obtain:

$$\frac{(57.5)^2}{64.4} = \frac{P \times 144}{p}$$

$$\frac{P}{p} = \left(\frac{51.3 \times 74.25}{144}\right) = 26.5 \text{ psi.}$$

5.1 ∴ CWF Press. : (150 + 26.5) = 176.5 psi

Plus estimated friction losses to points of orifices (from atomizer outlet)	12.5	
Plus safety factor	10.0	
CWF inlet pressure to burner		Say
	199.0	200 psi.

---

6. CWF flow rate at Section $B - B^1$ to be one half total flow to maintain constant velocity.

6.1 Hence area at $B - B^1$ is .5 area at $A - A^1$, so that

$$\left(\frac{B - B^1}{A - A^1}\right)^2 = .5$$

$$\left(B - B^1\right)^2 = .5 \quad (A - A^1)^2$$

6.2

$$\left(B - B^1\right) = \sqrt{.5} \times (A-A^1)$$

$$= .707\left(A-A^1\right) = (.707 \times 2) = \left(B - B^1\right)$$

$$= 1.414 \text{ cm.}$$

6.2 From Fig. G.16.2 we find angle

A C B = = 86°

See Fig. G.16.2

7. Now the penetration point of the CWF can be determined from the momentum vectors.

7.1 CWF momentum is M V = (.29 × 57.5) = 16.7 lb. ft.

(Items 1.1 & 4)

17 lb. ft.
(rounded)

7.2 Steam momentum is calculated as follows:

say

Velocity (approx.) - 1500 fps.

Wt. of steam flow per sec. is:

(. 15 × .29) = .0435 lb./sec.

7.3 Steam momentum is: .0435 x 1500 = 65 lb. ft.

7.4 Vector Diagram for CWF and steam MV is:

$$\phi = \tan^{-1} \frac{65}{17} = 75^{\circ}$$

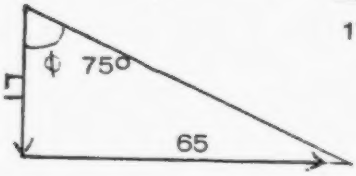

7.5 CWF penetration diagram is:

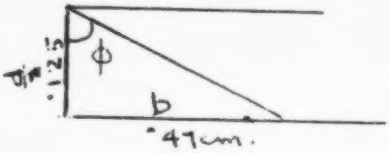

$$\frac{b}{.125} = \tan \phi = \tan 75^{\circ} = 3.73$$

Then $b = 3.73 \times .125 = .47$ cm.

That is CWF will penetrate to half steam core dia. at a point <.5 cm. downstream from orifice.

Then mixing should be thorough.

8. NOTE: The sonic velocity for saturated steam at 150 psig is:

$$V_s = \sqrt{k\,g\,144\,P^1\;\bar{\nabla}}$$

$$= \sqrt{1.3 \times 32.2 \times 144 \times 164.7 \times 2.76}$$

$$= \sqrt{2740087} \qquad = \quad 1655 \text{ fps.}$$

9. Steam vol. is: $(.15 \times .29 \times 2.76) \quad = \quad 0.12$ cu. ft./sec.

$= \quad 34.8$ cm.^{3}/sec.

10. Steam core area = $\pi \times \left(\frac{.25}{2}\right)^2 \quad = \quad .05$ cm.^{2}

$= \quad .0000535$ ft.^{2}

11. Emulsion volume is: .004 + .12 = .124 cfs.
Emulsion velocity in steam core is:

$$\frac{.124}{.0000535} \quad = \quad 2318 \text{ fps.}$$

11.1 N.B. It may be found necessary to increase the diameter of the core to .30 cm. to yield flow velocity of 1655 fps (steam sonic velocity).

G. 16 ADDENDUM 3

TURN-DOWN

---

1. It is assumed that a "homogenizer" developed as per Fig. G.16.1 will be fitted with either a divergent nozzle as per the design of Fig. G.1.3 or with a mixing chamber as shown in the Coen design, Fig. W.22.3 or the B & W T-Jet design as shown in Fig. W.13.8.

2. With a mixing chamber the velocity of the homogeneous emulsion will be a function of the ΔP across the exit orifices.

3. With a furnace pressure of O psig the exit velocities will be derived from the basic equation

$$\frac{V^2}{2g} = \frac{P \times 144}{p} \qquad \text{Eq. 1}$$

4. With an orifice coefficient (assumed) of .8, Eq. 1 becomes

$$\frac{(.8V)^2}{64.4} = \frac{P \times 144}{p}$$

Where: P = psi; p = density of the CWF/steam/emulsion (No condensations of atomizing steam considered here) = 2.7 Lb/cu.ft.

(App.4.R item 12.2.1)

4.1 Then: $\frac{.64}{64.4} (V)^2 = P \times \frac{144}{2.7}$

$$.01 V^2 = 53.3$$

$$V^2 = 5330 P$$

$$V = \sqrt{5330} \sqrt{P}$$

$$V = 73 \times \sqrt{P} \qquad \text{Eq. 2}$$

Conversely: $\left(73 \sqrt{P}\right)^2 = V^2$

$$5330 P = V^2$$

$$P = \frac{V^2}{5330} \qquad \text{Eq. 3}$$

5. A max. CWF pressure of 175 psi is assumed (in the homogeneizer - Fig. G.16.1)

5.1 Then according to the data of G.16. Add. 2 the steam pressure in the "homogenizer" atomizing fluid core must be 26.5 psi lower than the CWF pressure or a value of approx. : 150 psig. (G.16 Add.2 Item 5

to establish flow thru CWF orifices of postulated dimensions. (G.16. Add.2 item 3)

6. From the values derived from Equations 2 & 3 the following table is constructed:

TABLE G.16.1

Load %	Press psi	Velocity fps
100	175	966
75	98	724
50	44	483
25	11	242

7. The total exit orifice area (for max. velocity) in the mixing chamber for a flow condition of .004 cfs (G.16 Add.2 item 1.1) is then 966 x Area = .004 cf.

$$\text{Area} = \frac{.004}{966} = 4.10^{-5}\ \text{ft.}^2$$

$$= 4.10^{-5} \times (30.54)^2 = .037\ \text{cm.}^2$$

7.1 Max. area for 4 ports as per G.16 Add.2 - item 3.2 $.08\ \text{cm.}^2$

7.2 Therefore to secure max. velocity of 966 fps only 2 ports can be considered for a total area of: $.04\ \text{cm.}^2$ to match the calculated value of item 7.

7.3 Given $.037\ \text{cm.}^2$ per 2 orifices or

$.0185\ \text{cm.}^2$ per orifice the diameter is:

$$\text{dia.} = 2r = 2\sqrt{\frac{.0185}{\Pi}} = 2 \times .006 \qquad .012\ \text{cm.}$$

$$= 1200\ \text{um.}$$

7.4 The safety factor versus a possible max. coal particle size of 800 um is then

$$\frac{1200}{800} = 1.5$$

(instead of a SF of 2 as used in G.16 Add.2.

8. If it should be found desirable to have 4 orifices, in order to endure max. homogeneity of the emulsion and to take max. advantage of the CWF particle coherence breaking feature of the "homogenizer" (Fig. G.16.1) then the max. exit flow velocity would have to be decreased by 1/2 or to the value of 483 fps – shown in Table G.16.1 as the velocity for 50% load.

8.1 Then the turn-down would be limited to approx. 2:1.

9. In Appendix 8 it was shown that under the max. condition of atomizing steam condensation that the emulsion density would become 8.4 lbs./cu.ft.

App. 8 item
14.2

9.1 Then Eq. 2 would become

$$\frac{.64}{64.4} V^2 = \frac{P \times 144}{8.4}$$

$$.01 \; V^2 = P \times 17$$

$$V^2 = 1700 \; P$$

$$V = 41 \sqrt{P} \qquad \text{Eq. 2.R}$$

9.2 Conversely $(41 \; \overline{P})^2 = V^2$

$$1681 \; P = V^2$$

$$P = \frac{V^2}{1681} \qquad \text{Eq. 3.R}$$

10. Table G.16.1 then becomes

TABLE G.16.1.P

Load %	Press PSI	Velocity fps
100%	175	542
75%	98	407
50%	44	271
35%	11	135

12. From Table G.16.1 Item 8, we then find a 4-port design (with a S.F. of 1.5) at the 407 fps velocity shown in Table G. 16.1.R for 75% load.

12. Then a turn-down of 3.1 can be anticipated (or close thereto).

REPORTS

Report Code No.	Location	Cross Reference	Item No.	Report
X.1	5th - 79		1	There is an increase in viscosity of approx. 27 to 90μ or a ratio of 3.33 in a 70/30 mix when an additive is added to a straight CWF at a low shear rate.
			2	The additive changed the CWF viscosity/shear mode from pseudoplastic to thixotropic.
			3	The parent coal is from a Chinese mine.
			4.	The final yield value in a CWF storage tank is 500 dynes/cm^2 when convection ceases, and sedimentation rate greatly diminished.

Report Code No.	Location	Cross Reference	Item No.	
X.2	5th‡51		1	A CWF can be considered to be a hydrophobic colloid.
			2	Ionizing charge on coal particle important for particle repulsive forces.
			2.1	Funk has stated a minimum of 50 mv is desirable.
			3	The viscosity of CWF is affected by the O/C ratio of the particle, which affects the degree of particle structural porosity Hence, the greater the O/C ratio, the greater the porosity and the greater the hydrophobic force.
			4	See Appendix 1 for the viscosity determination equations given by the authors (X.2).
			5	Various figures and tables given in this paper are reproduced and attached. In Table 4, the heading "Fuel Ratio" presumably is the ratio C/V.M. I query the reason for the negative sign (-) attached to this ratio and to the column headed O/C.
			6	Note that Table 3 shows a viscosity range of 500 - 3000 Centipoise (=mPa) approx. for various coals and additives combinations. Sources of the coals are given in Table 4.

Report Code No.	Location	Cross Reference	Item No.	
X.3	5th-238		1	This paper deals with the manufacturing procedures for clean coal but provides no rheological or operational data on a CWF.
			2.	Descriptions are given on cleaning technology and benefication and the economics involved.
			3.	There are two paragraphs in this report which I quote verbatim, as follows:
			3.1	"Unfortunately, there is still insufficient data about the performance of very low ash coals in oil/gas boilers to complete this type of analysis, even in generalized terms. In the absence of such data at this time, a 1% to 4% ash level seems to have emerged as a general consensus of how clean the coal should be for reasonable performance in oil/gas boilers."
			3.2	"Timely scale-up within the next five years to viable commercial tonnage remains a significant development hurdle to overcome. A small utility boiler of 100 Mw requires about 175,000 tons of clean coal per year. This requirement is far below the usual capacity of existing coal-cleaning plants, yet represents a large, 50 fold scale-up from a 1 ton per hour pilot unit."

Report Code No.	Location	Cross Reference	Item No.	Report
X.4	5th-318		1.	This paper extends the data in my report, Section 17, of July 1982, in my previous work.
			2.	Many different modifications of the original Peabody atomizer were tried.
			3.	Wear of the atomizer tip has still been their major problem.
			4.	6 modifications were tried and design D.3 gave 40+ days of life with acceptable flame pattern. All tip designs were of steel hardened to "Rex AA".
			5.	The report states that they obtained good atomization, but does not state with which tip design.
			6.	They attempted changes in the atomizing steam jet design in an attempt to reduce atomizing steam consumption. On the average over high and low loads, steam usage was unchanged.
			7.	Since start-up on COM (about May 1982), their igniters gave trouble. They are now trying a Peabody Class 2 and a Cowan Class 2 in an attempt to improve the reliability of the unit to light off on COM or No. 6 oil.

Report Code No.	Location	Cross Reference	Item No.	
X.5	5th-323	X.4	1.	This report covers boiler efficiency testing by F.P.C. and B&W.
			2.	Effects of ash on boiler surfaces with the burning of COM, were reported to be quite acceptable, except with the ash removal system from the ash hoppers, in which problems were encountered. Remedial engineering work was initiated.
			3.	The questions of (a) Unit unavailability due to COM and, (b) Boiler efficiency test results are quoted verbatim from this paper.
			3.1	a) Unit Unavailability Due to COM 1. Fuel pump evaluations and problems 2. Burner tip evaluation and modifications 3. Burner start problems 4. Fly ash transport problems 5. Precipitator sparking
			3.2	b) Boiler Efficiency "Changes in Boiler efficiency are due to fuel type and operation. This is further analyzed in the Boiler Section".
			3.3	The results of these comparisons are shown in Appendix II, attached.
			3.4	"The net heat rate using this comparison method shows a degradation of 168 BTU/KWH or 1.7%, with the largest component being auxiliary steam. Reduction of this component is still being investigated through the reduction of steam-using fuel atomization. More will be said about this in the paper 'COM Burner Development, Paul L. Bartow Unit 1' given at this symposium. This method gives the approximate change in net heat rate from Bunker C fuel to COM fuel. With time, changes in component performance will take place and the need for accurate fuel flow measurement still exists and is being studied.

Report Code No.	Location	Cross Reference	Item No.	Report
X.6	5th-625		1	The R&D on the Lezzon burner included consideration of: a) Exit velocity b) Fuel atomizing fluid swirl c) Recirculation of combustion products d) Turn-down e) Mass flow rates of primary and secondary air f) "Effective" atomization of CWF up to 1000 Centipoise viscosity g) Breakup of particle agglomerate~~r~~s h) Fine atomization by air or steam at minimum pressures i) Turndown capability j) Prevention of coking at burner tip k) Prevention of sedimentation (or separation) in burner passages
			2.	Degree of atomization is a function of relative velocity of fuel and atomizing fluid (thickness of fuel jet or sheet not mentioned at this point, P. 631)
			3.	See Figs. 1.x.6 and 2.x.6, illustrating principles of early experimental work designs. See Fig 4.x.6 for the application of principles of Figs. 1.x.6 and 2.x.6 to create the Lezzon Atomizer tip test nozzle design.
			4.1	It would appear that the fuel and atomizing air combine in circular annular sheets within a converging exit annular space; therefore, the design is generically internal atomization using the exit tip to create emulsion velocity at exit annulus, further accelerated by the atomizing fluid to create formation of CWF droplets.

Report Code No.	Location	Cross Reference	Item No.	Report
X.6	5th-635		5	The authors refer to a paper by Butcher etal, "Atomization of Coal Slurry, etc", Dept. of Energy and Environment -- Brookhaven National Laboratory. It should be interesting to explore this work.
			6	It would seem, that at time of the writing of the Lezzon report, no actual testing of this atomizer had been done.
			6.1	It would be interesting to know if tests have since been made (at this writing Jan., 1985).

Report Code No.	Location	Cross Reference	Item No.	
X.7	5th-873		1	Florida Power & Light Company considers that CWF is moving toward commercial utilization and commissioned Battelle Columbus Laboratories to carry out laboratory scale tests (700,000 BTU/Hr.) on five CWF fuels (See Table 1.x.7 for Analyses of Slurry Fuels).
			2.	On the question of CWM production, there is a delema (say FPL) in that utilities are reluctant to enter into long-term contracts until all technical and economical issues have been resolved by a full scale utility demonstration; and CWF manufacturers are reluctant to build the necessary capacity without the security of a long-term contract.
			3	FPL is associated with M.I.T. on CWF combustion tests and with the Adelphi University loop testing program to obtain pump data and wear with CWF fuel.
			4.	The Battelle work covered: tube metal temperature; combusion data to give values of O_2, CO_2, SO_2, NO/NO_x, air preheat temperature, furnace exit temperature. Also data taken on: air feed rate, fuel feed rate, atomizing air pressure, burner swirl setting; together with assessments of: general flame characteristics; presence or absence of combustion chamber particles; ease of fluid handling; appearance of deposits in furnace walls.
			5	Quantitative results were obtained for fly ash emissions; carbon in fly ash; combustion efficiency; gaseous emissions.
			5.1	See Table 2.X.7 for these quantitative results
			6	A summary of Qualitative assessments used during the tests:
			6.1	Storage Stability: Some settling of all samples within a few days; major settling within a few months with all but one. Best fuel storage time 2 - 3 months with moderate settling, dispersable by stirring.

Report Code No.	Location	Cross Reference	Item No.	Report
X.7	5th-873		6.2	Pumping: A progressive cavity pump with a large stator cavity was successful with each sample.
			6.3	Atomization; An external mix atomizer was designed for these tests with "reasonably good atomization" but a significant number of large agglomerates formed (up to 1/8" dia.) Need of a better atomizer was indicated.
			6.4	Flame Stability: Flame stability was generally good but the distance of the flame front from the burner exit indicated the probability of an ignition delay, which could pose a problem in cold wall units (the lab furnace was refractory lined).
			7.	This paper did not provide any rheological or atomizer function data (i.e., mode, viscosity, pressure, flow).

Report Code No.	Location	Cross Reference	Item No.	Report
X.8	5th-897		1	I quote verbatim the following statement by the authors: "It is hoped that the current extensive research and development work will advance CWM technology to commercial applicability for industrial and utility installations within a few years."
			2	DOE sponsored a study by Pittsburgh Energy Technology Center to assess the technical feasability and economics of converting 3 large utility boilers.
			3	The three boilers selected for study are:
			3.1	AB&W universal pressure boiler, rated 275 Mw, at Jacksonville Electric Authority's (JEA) Northside Unit #1.
			3.2	A C.E. tangential fired boiler, rated 460 Mw at United Illuminating Co.'s New Haven Harbor Unit #1.
			3.3	A. Riley Stoker Box Type boiler, rated 518 Mw at JEA's Northside Unit #3.
			4	This paper is a study of the Riley Stoker Boiler, designed & constructed for oil firing.
			5	Existing 24 oil burners to be replaced with 24 "Controlled Combusion Venturi Low NO_x burners in the same position as the oil fired burners.
			5.1	The existing furnace depth of 40 ft. will be satisfactory for P.C. firing (with the new burners).
			5.2	Other essential boiler dimensions will be suitable for P.C. firing.
			6	"Performance of the existing boiler was evaluated for CWF firing, and again flue gas velocities were found to limit boiler capacity. The boiler was modified to permit

Report Code No.	Location	Cross Reference	Item No.	Report
X.8	5th-897		6	achievement of 100% BMCR steam flows within the parameters established for CWF conversion. The modifications are similar to those required for PC firing, but additional heat transfer surface had to be added to achieve the superheat and reheat design temperatures. Figure 4 presents a tabulation of flue gas temperatures and velocities throughout the boiler. Boiler efficiency on CWF was calculated to be 87.12%. Performance of the retrofited boiler on CWF is summarized on Table 5." "The heat release rates and gas velocities are within acceptable limits for CWF firing."
			7	Tables 4.X.8 and 5.X.8 attached, are reproduced from the test and show the test results from oil firing and from CWF firing and identify the increase in losses due to CWF firing.
			8.	Table 6.X.8 is also reproduced and attached to show the "bottom line" costs of conversion to: P.C., CWF, and a new coal fired boiler.

Report Code No.	Location	Cross Reference	Item No.	Report
X.9	5th-1023	W.2 6th Symp.	1	C.E. & Gulf Research & Development as a team are under contract to PETC for research on the combustion and fuel characteristics of CWF.
			2	Four different CWF's to be tested by C.E. for a) ignition stability, b) carbon burn-out and c) atomization quality as the fuel source, coal source and burner used are varied.
			2.1	Each CWF to be beneficiated to two levels of residual ash.
			2.2	Project time is 3 years, ending in 4th quarter 1985, when a report will be issued.
			3	20 coals from the Eastern USA to be selected and evaluated to the best 4 CWFs.
			4	Bench scale tests will be conducted to determine the factors given in Table 1.X.9 reproduced as in the following: TABLE 1.X.9 BENCH-SCALE TESTS FOR CWM CHARACTERISTICS Total moisture Percent solids Slurry density Particle size distribution Effect of temperature changes Proximate analysis Ultimate analysis Higher heating value Viscosity vs. temperature Viscosity vs. shear rate Settling rate Slurry pH Halogens (C , F) Thermogravimetic analysis Flammability tests Probe surface area (coal and char) True particle density (coal and char) Apparent density (coal and char) Ash composition Ash fusibility temperatures

Report Code No.	Location	Cross Reference	Item No.	
				TABLE 1.X.9 (Cont.) Sulfur forms Gravity fractionation analysis Acetic acid leaching analysis SEM analysis Trace elements (X-ray) Corrosion index Abrasiveness Agglomeration Aging effects
			5	Six burners will be selected for testing on commerciality of design, availability in capacities from 20.10^6 to 50.10^6 BTU/Hr., number of burners in service (? - what service?) and CWF experience.
			5.1	Two burners will be C.E. and four from other suppliers.
			5.2	Test firing rate for each burner will be approximately 25.10^6 BTU/Hr.
			6	First the atomizer will be tested in the C.E. Atomizer Test Facility for cold flow testing and droplet size distribution will be measured by double spark photography technique.
			6.1	Atomization parameters (pressure and supply ratio) will be analyzed to determine optimum values for each CWF mass flow rate.
			6.2	Erosion will be monitored and documented and deviations from original orifice dimension will be recorded.
			6.3	Test duration may allow approximate estimates of atomizer life.
			7	The following paragraph is extracted verbatim from this paper:

Report Code No. | Location | Cross Reference | Item No.

"Based on the pretest results, every burner will be evaluated according to the minimum performance criteria. If a burner fails to meet the minimum requirements, the manufacturer may modify the burner and subject it again to the same pretest procedures."

7.1 Note that no numbers on minimum requirements have been set for these C.E. evaluation tests such as: fuel pressure, atomizing fluid and pressure; atomizing fluid flow versus fuel flow ratio; % carbon burn-out, droplet size range, etc.

7.2 It is not stated either that the burner mfr. will be given rheology data on viscosity or shear stress or plastic mode at varying shear rates - nor CWF coal size distribution.

7.3 Even armed with "normal" rheology data and the results of the test data on his burner, it is doubtful if, in the present state of the art, he can modify his burner design for improved operating results" except by: common sense and intuition governing his trial and error methodology (consider; e.g., C.E.'s experience at Chatham).

7.4 The "rules of the game" allow the mfr. only one extra chance to win acceptance at the C.E. trials.

8. It is questionable if the burner mfr. would have his own test facility or access to an "outside" test facility.

9. It can be hoped that C.E.'s and/or PETC's final report will be published and will give adequate data on the atomizer design and operating data, to allow insight to the design factors for a successful CWF aktomizer; to improve the number of potentially successful "marriages" between CWF and

Report Code No.	Location	Cross Reference	Item No.	
				and burner mfr. for successful wide-scale commercialization in capacities from a minimum of 25.10^6 or 50.10^6 BTU/Hr and upwards.

Report Code No.	Location	Cross Reference	Item No.	Report
X.10	5th-1053		1	The Enel, Snamprogetti group (Italy) tested 68% to 72% loaded CWF in various atomizers to determine primarily, flame ignition and stability.
			2	The boiler used was designed for heavy fuel oil and P.C. firing.
			3	The two existing oil burners were each rated at 1500 kg./hr. or approximately 413 U.S. gh/hr. equivalent to an output at 85% efficiency of approx. 30 mw_t or 13 Mwe.
			4	"Standard" Y jet and an ultrasonic atomizer were tried and proved unsuccessful.
			5	A special atomizer geometry named "Y mixing" proved successful.
			5.1	See reproduced figure 4.X.10, p. 1067, for general design of the "Y-mixing" atomizer.
			6	The actual capacity of the Deutsche B&W boiler is 125 MWe. Therefore, the 2 burners under CWF test represented approx. 10% of boiler rated capacity.
			6.1	The paper does not state whether the boiler's other burners were firing during the CWF test.
			7	Modified vane design to give greater swirl were provided for the two CWF burners.
			8	I quote, verbatim, from the paper, some of the operating results of the CWF trial, in the following: "- CWF temperature: 110°C - atomizing air temperature: 120°C - secondary air temperature: 230°C With this burner, and using always the same fuel CWF 1, both the internal mixing and the Y-jet atomizers did not lead to any satisfactory flame. No appreciable improvement of the burner performance was

Report Code No.	Location	Cross REference	Item No.	Report
				obtained by varying the tip spray angle (in the 50°to 90° range) and the exit port size. "On the contrary, when the newly designed y-mixing atomizing type was used, a flame was immediately established. "Flames of up to 18MW thermal load could be set up even under more difficult operating conditions, i.e.: - CWS temperature: 20°C - atomizing air temperature: 25°C - combusion air temperature: 180°C - support gas burner: off."
			9	Use of steam as atomizing fluid moved the flame front away from the burner quarl and flame stability was impaired.

Report Code No.	Location	Cross Reference	Item No.	Report
X.11	5th-1119		1	The authors tested CWFs, from three types of parent coal, of varying particle size distribution and various additives. Coals were from Pittsburgh seam and West Virginia.
			1.1	The final CWF fuel samples were prepared in a "Columbia Chase Integrator" afater "Standard" pulverization, giving a grind result of 85% through 200 mesh.
			2	Some samples were tested in a pumping test loop to determine the effect of the pumping on the CWF rheology.
			3	Viscosity tests were also made in a Brookfield Viscometer.
			4	CWF based on micronized grind (micronized = < 325 mesh) were tested in addition to the "Standard" grinding ball and race pulverizer.
			4.1	A given arbitrary size dispersion was obtained by lmixing a grind of 85% through 200 mesh, with a grind of plus 100 microns (i.e., less than 200 mesh) in various proportions "as required" (Question: Was the final size distribution in accordance with Funk's equation (Appendix 1) or the Rosin-Rambler equation?)
			5	After thorough mixing with additive, the CWF (item 4) mixing is augmented by circulation through the Columbia Chase integrator, to give an "effective dispersion".
		Funk Appendix 1.	6	Particle size distribution is the most important factor in determining max. loading of the CWF (in agreement with Funk's data) and affects both storage stability and rheology of the CWF.

Report Code No.	Location	Cross Reference	Item No.	Report
			7	In the micronized CWF (of much interest to the utilities), the coal is ground to 95 - 98% of - 44 micron size, using the Columbia Chase Integrator.
			8	Various Tables & Figures of this paper are here reproduced and are as follows:
				Fig. 2.X.11 - Particle Size Analysis Coal "A"
				Fig 3.X.11 - Effect of Blending
				Fig. 4.X.11 - Size Distribution - 62% Wt. CWF
				Fig. 5.X.11 - Size Distribution 65% Wt. CWF
				Fig. 6.X.11 - Size Distribution 70% Wt. CWF
				Fig. 7.X.11, 8.X.11 and 9.X.11 - Effect of Chemical additives on Viscosity of 62%, 65% & 90% Wt. CWFs (Viscosities measured at various spindle speeds of the Brookfield Viscometer)
				It will be noted in Figs. 7 - 9 that the behavior of the CWFs was pseudoplastic.
			8.1	Table 1.X.11 - Proximate Analysis of Coals
				Table 3.X.11 - Stability Characteristics of CWF fuels.
			9	Micronized CWFs B&W tests have shown that micronized CWF (MCWF) i.e., CWF grind to less than 44 microns will:
				a) reduce extent of de-rating b) reduce ash deposition rate c) reduce fly ash particle size and increase ease of removal by soot blowing with air. d) increase rate of burning.

Report Code No.	Location	Cross Reference	Item No.	Report
			9.1	Characteristics of M CWF are shown in various figures reproduced from the text as follows: a) Fig. 16.X.11 - Particle Size Distribution b) Figs. 17 & 18.X.11 - Viscosity Characteristics of 68% and 70% wt. MCWF
			10	Test Loop Pumping Tests were carried out to determine effect of pumping on CWF rheology and to provide data on pressure drop versus flow rate.
			11	The following Figures have been reproduced giving results of the loop test:
			11.1	Figs. 11 and 12.X.11 - effect of Pumping on Viscosity of 65% and 68% wt. CWF.
			11.2	Figs. 13 and 14.X.11 - Effect of Pumping on Coal Particle Attrition of 65% and 68% wt. CWF.
			11.3	Fig 15.X.11 - Variation of Pressure Gradient With Flow Velocity Fig. 16.X.11 - Particle Size Distribution of Micronized Coal
			12	Note from the viscosity figures that the viscosities of M CWF is "much lower" than the CWF fuels at the same concentration and same chemical additive.

Report Code No.	Location	Cross Reference	Item No.	Report
X.12	5th - 1142		1	This paper by Dr. John Dooher, etal, opens with a statement of the Shear Stress/Shear Rate relationship of the CWFs that were tested in his laboratory at Adelphi University.
		SRCE-725	2	The main equations, which I will place in Appendix 1, with definition of terms theorum, I show as follows: $\tau = k\dot{\gamma}^{n}$ (1.X.12) This equation is also used in S.R.C. Technical Report E-725.
			3	Another equation (new to me) is: $\eta(\dot{\gamma}) = k\dot{\gamma}^{n-1} \times 100$ (2.X.12) also in appendix one with definitiojn of terms.
			3.1	I will have, to give some thought to the exponental (η^{-1}) of the right hand term in Item 3.
			4	I have developed curves for the terms thixotropic and rheopectic in accordance with Dr. Dooher's descriptions (you may want to scan these curves with a critical eye, to be sure of the correctness of my interpretations). These curves are designated Figs. G1.X.12 and G2.X.12 (after Dr. Dooher). You will find the curve description at the top of p. 1144 (5th Symposium)
			5	I have reproduced Tables and Figures from this paper as follows: Table 1.X.12 - Rheological Properties. Figs. 6.X.12 and 7.X.12 - Apparent Viscosity Vs. Time, of Samples A.1 and B.1 respec- tively. Both samples were pumped at constant low shear rate. Fig. 8.X.12 - Apparent Viscosity Vs. Time

Report Code No.	Location	Cross REference	Item No.	Report
				SAMPLE D-1
				At point A, $\dot{\gamma}_1$ increased from 100 sec to 1000 Sec.$^{-1}$. Similarly, point B represents start of increase in $\dot{\gamma}$ from 100 Sec.$^{-1}$ to 1000 Sec^{-1} after a storage period of 65 hrs.
			5.1	An apparent dilatancy seems evident from the η values following points A & B on the curves. There is a question (in my mind) as to whether this is due to shear increase, or to time dependency - or both.
			5.2	Fig. 9.X.12 (Sample B.2) and Fig. 10.X.12 (Sample B.3) show viscosity vs. Shear rate in the loop test.
			5.3	Fig 11.X.12 - Viscosity vs. Shear rate for Sample D.4.
				Note CWF test samples, of Figs. 10.X.12 and 11.X.12 were samples that had been subject to variable shear testing before being circulated for any length of time.
			5.4	I conclude this initial report on Paper X.12 with verbatim extract of two paragraphs on Page 1156 (5th Symposium)
				"The rheological behavioer of most of the slurries were evaluated in the loop after eight or more hours of pumping. Some of the slurries behaved as nearly Newtonian fluids, however, others became dilatant or had flow properties which rapidly changed with time. In order to correctly design a fuel forwarding system, both the initial and equilibrium behavior of the slurries must be taken into account.
				"The high shear to which most of the CWFs were subjected in the loop seemed to adversely affect most of the slurries tested. Shear rates should be kept to a minimum, less than 150 s^{-1}, to avoid problems."

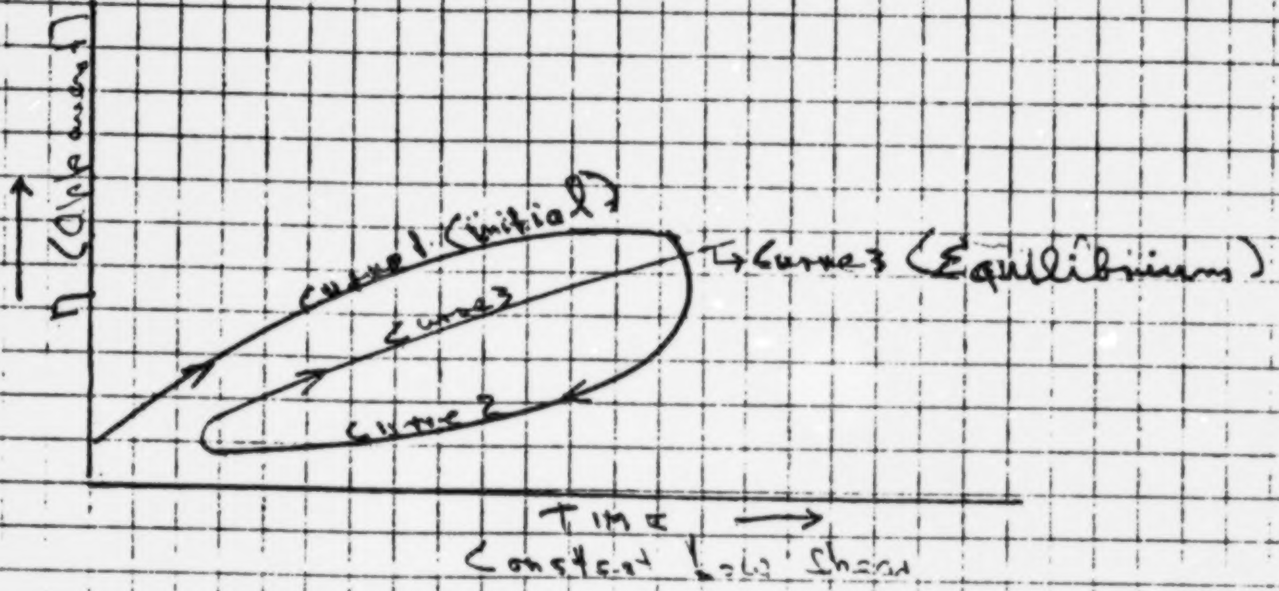

Note: Curve 1 is higher than equilibrium curve 3

Therefore mode is thixotropic

Fig. G-1-X-12 (after Dr. Brooker)

G = Grossman interpretation

X.12

12-1-85

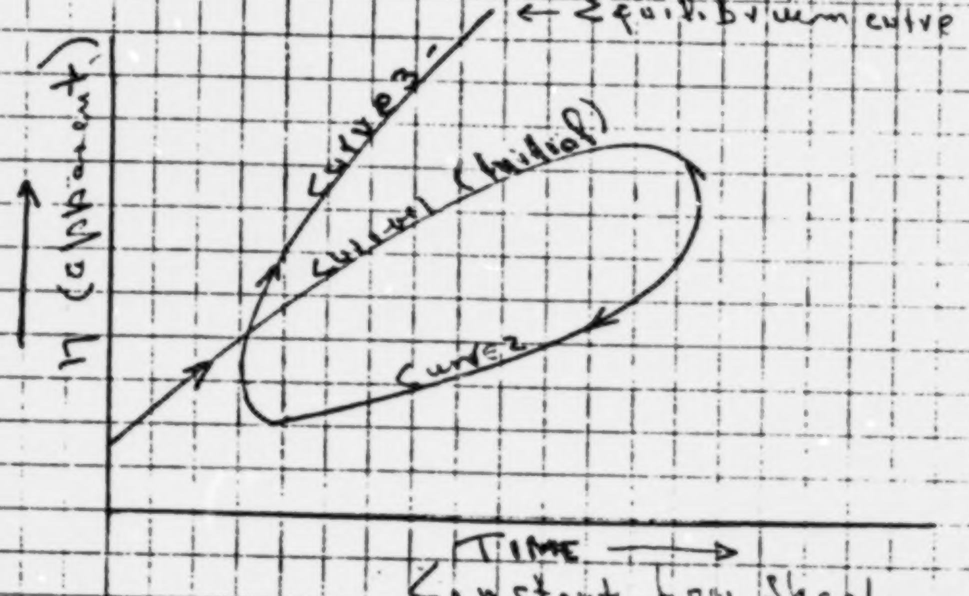

Constant Low Shear

__Note:__ Curve 1 is faster than equilibrium curve 3

Therefore not in thixotropic

Fig G.2. X.12 (after R. Dealy)

G = Grossman

X.12
12-1-85

Report Code No.	Location	Cross Reference	Item No.	Report
X.13	5th-1158		1	This paper deals in large part with the "dispersants" (additives?) of the authors' companies, as they affect CWF, of many coal types.
			2	In a Tatung' coal CWF, a concentration of 65% was difficult to achieve without additive (dispersant).
			2.1	A 65% concentration in the CWF showed a dilatant behavior.
			3	Fig. 3.X.13, attached, shows viscosity range of 1 to 100 Pascals or 1000 to 100,000 MPa, (=1000 to 100,000 centipoise), for % coal concentrations of 68.5% to 72%, with their ACC-700 additive.
			3.1	The thixotropic modes of the Tatung Coal are shown in Figs. 5.X.13 and 6.X.13 (pp. 1170-1171), with various amounts of various additives, over a shear rate range of 0-20 Sec.$^{-1}$. These figures are attached.
			3.2	The shear is not given for Fig. 3.X.13 graph and I have assumed that the letter (P) in the ordinate stands for Pascal.

Report Code No.	Location	Cross Reference	Item No.	Report
X.14	5th-1182		1	This paper deals with rotary cup atomization.
			2	It is basically a theory of rotary performance.
			3	Cup velocity diameter, length and shape are shown to affect the thickness of the CWF circular jet leaving the cup.
			4	The theoretical conditions are shown where coal in the CWF can tend to settle out with consequent de-watering of the CWF.
			5	No numeric of data is given, on atomization fineness nor on pressure or flow ratio of the atomizing air.
			6	Percent coal leading figures for rotary cup burner are not given, nor any data from pilot or commercial testing.

Report ode No.	Location	Cross Reference	Item No.	Report
X.15	5th-1205		1	The intent of the work at Mellon University on CWF derives from the unknown factors in the state of the art of CWF rheology, and to quote the authors: "Although in recent years there have been a number of reports(2) on the rheology of coal/water mixtures, no consistent picture has emerged from the published data on the relationship between slurry rheology and the chemistry of the coals in terms of polydispersity of particle size, the surface chemistry of the coal, the effect of the chemical nature of the suspending fluid, slurry temperature, the effect of added electrolyte, etc. This is the focus of our current studies at Carnegie-Mellon University."
			2	The coals examined were: Pittsburg Seam 8; Illinois #6; San Juan (New Mexico) and Hiawatha (Utah).
			2.1	Grind size was 100% < 100 mesh; 80% < 200 mesh.
			2.2	Size distribution was measured over the range of 7 to 149 um.
			2.3	A Scanning Electron Microscope (S.E.M.) was used to determine particle size, shape, and surface topography.
			2.4	Solubility of surface contaminents was also determined by Atomic Absorption and Volumetric Analyses.
			2.5	The test samples were treated to achieve a range of initial ph of 3-12 (acid to alkaline).
			2.6	The electrophoretic mobility of the coal particles in a 50% wt. CWF was measured, using a Micromeritics Mass Transport Analyser.

Report Code No.	Location	Cross Reference	Item No.	Report
			3.	A Brookfield Viscometer was used to measure viscosities at shear rates of 10-100 $sec.^{-1}$ with necessary corrections to shear rate mode for non-Newtonian fluids.
			3.1	A A Hooke-Rotovise Viscometer was used for shear rates of 100-1000 $sec.^{-1}$ (for some Pittsburgh Seam #8 Cwfs.)
			3.2	Constant CWF temperature was maintained in both types of Viscometers.
			4	The authors then proceed to a theoretical discussion of viscosity (η) and give numbers of equations which are reproduced in Appendix 1.
			5	Table 1 of X.15 (P.1208) is reproduced as follows:

X.15

Table 1. Particle Size Distribution and Coal Density

Diam. (µm)	Pittsburgh #8 Sieve anal. %(wt)	Pittsburgh #8 Coulter Counter %(vol)	Illinois #6 Sieve anal. %(wt)	Illinois #6 Coulter Counter %(vol)	San Juan Sieve anal. %(wt)	San Juan Coulter Counter %(vol)	Hiawatha Sieve anal. %(wt)	Hiawatha Coulter Counter %(vol)
>150	0	0	7	7	8	6	7	8
> 75	13	12	39	40	42	38	42	44
> 37	58	54	67	68	67	66	72	66
> 20	80	75	93	82	88	80	96	81
< 20	20	25	7	18	12	20	4	19
Mean diam. (µm)	43	41	57	57	58	55	65	56
Density	1.37		1.40		1.44		1.35	

Report Code No.	Location	Cross Reference	Item No.	Report
			6	The following paragraph is reproduced verbatim from X.15: "In scanning electron micrographs the particles of Pittsburgh #8 and Illinois #6 resemble small rocks or pebbles, those of Hiawatha coal are plate- or disc-like, and those for San Juan are intermediate between the two. The surfaces of Pittsburgh #8 particles contain sharp edges and cracks, buth the other coals have smooth surfaces."
			7	Item 6 above can be related to Equation 2 and Item 2.1 of X.15 Equations, in Appendix 1.
			8	Removal of surface contaminents (ions) are given in Table 3.X.15, reproduced in the following, verbatim from X.15 (page 1209)

. X.15

Table 3. Water Soluble Surface Contaminants (mg dm^{-3})

	Pittsburgh #8	Illinois #6	San Juan	Hiawatha
Si	4.0	2.0	2.0	5.0
Al	4.6	< 0.1	< 0.1	< 0.1
Fe	50	14.3	< 0.04	0.18
Ca	30	204	187	43.5
Mg	75	4.24	12.7	12.7
K	4.4	2.8	2.5	2.9
Na	8.5	68	50.5	11.5
SO_4	340	540	490	140
Cl	40	60	50	65
NO_3	< 0.3	< 0.5	< 0.5	< 0.5

8.1 "We see that significant amounts of Ca^{2+}, SO_4^{2-}, and Cl^- were dissolved from all the coals, Fe^{2+}/Fe^{3+} dissolved from the Eastern but not the Western Coals, and only small amounts of Si^{4+} and Al^{3+} were removed by washing."

9 The following paragraph, regarding pH, and Table 4.X.15, are reproduced verbatim from X.15, (P. 1209):

Report Code No.	Location	Cross Reference	Item No.	Report
			9.1	When a powdered coal is immersed in pure water a "natural" pH will be observed, a consequence of the acid/base character of the surface. The pH might change with time due to dissolution of surface contaminants and their subsequent oxidation and hydrolysis. pH values of 50% (wt) slurries of the four coals immediately after spreparation and one week later are given in Table 4. Identical values were obtained for the respective supernatant liquids.

Table 4. Slurry pH

	Pittsburgh #8	Illinois #6	San Juan	Hiawath
Initial slurry pH	2.85	4.1	6.3	5.2
After 1 week	2.75	3.9	7.2	5.8

Report Code No.	Location	Cross Reference	Item No.	Report
			10	The following figures have been reproduced and are attached: Fig. 1.X.15 - Viscosities of CWFs Fig. 2.X.15 - Plot of Loge (η/η_o) versus (packing % by vol.) Fig. 3.X.15 - Plot of Loge (η/η_o) versus loge ($1 - \phi/\phi_\infty$) ϕ = % coal by vol. ϕ_∞ = max. packing % vol. of coal = .70 for authors' tests. Fig. 4 - plot of loge ($\tau - \tau_o$) versus loge $\dot{\gamma}$ $\tau - \tau_o$ = shear stress due to viscosity τ_o = field stress $\dot{\gamma}$ = shear rate
			10.1	Obtaining numerical values, i.e., the antilogs for the values given on the ordinate & abscessa of Fig. 4 shows pseudoplastic (small) (or Bingham-plastic) behavior of the CWF (50% wt. Pittsburgh #8.

Report Code No.	Location	Cross Reference	Item No.	Report
			11	Tables 5-6-7 of the paper have been reproduced and located in Appendix 1 - Sect. X.15 - as they relate to viscosity determinations and to the equations in this section.
			12	Electrophoretic mobility and pH are inter-related and both; therefore, are related to viscosity.
			13	Viscosity vs. pH is shown in Fig. 5.X.15.
			13.1	To, η, & K(CP) constants values versus pH are shown in Fig. 6.X.15.
			13.2	Fig. 7 - Electrophoretic mobility versus pH.
			13.3	Fig. 8 - Electrophoretic mobility and viscosity versus pH at 45 sec^{-1}.
			13.4	Fig. 9 - Electrophoretic mobility and viscosity versus pH at 9 sec^{-1}.
			14	Packing of coal particles in CWF is determined by:
			14.1	Size distribution (See Table 1) and coal type.
			14.2	Particle to particle interaction that cause "flocculation"; i.e., structure formation or agglomeration.
			14.3	Attractive and repulsive force and degree of flocculation are related to: a) Size distribution b) Surface chemistry c) Surface Topography
			14.4	There is a definite relationship between viscosity and the ϕ volume fraction of the coal in the CWF.
			14.5	ϕ values in this study have ranged from $\phi = 0.1$ to $\phi = 0.65$ (various coals).
			14.6	Where the viscosity has a shear dependence, Eq. 2 & Fig. 2 do not apply (because the CWF is then non-Newtonian).

Report Code No.	Location	Cross Reference	Item No.	Report
			14.7	For ϕ 0.4 Eq. 3 is applicable and an "intrinsix" viscosity of 9 is derived from tests (physical reasons unknown).
			14.8	Use of Eq. 4 to determine $[\eta]$ involves knowledge of $\phi\infty$ which is difficult to establish precisely. Use of value $\phi\infty = 0.7$ leads to $[\eta]$ values of 6.4 (See Table 6).
			15	Max. viscosity will occur where the electrophoretic mobility is zero (at a related pH for the particular CWF). (See Figs 7 and 8) which is termed the "isoelectric point or IEP"
			15.1	Addition of multivalent ions (in additives) brings about a change from pseudoplastic towards Newtonian behavior.
			15.2	It is stated that "gross floccultion, (high viscosity) occurs at high pH with high La (No_3) concentration". This would be an alkaline effect.
			15.3	With an acidic additive; e.g. KNO_3, there is the opposite effect of increasing pseudoplasticity.
			16	This paper (X.15) will much influence my continuing work on numerical experiments on flow through an atomizer annulus at values of $\phi\infty$ - or greater (when effect may be that of a solid obstruction to flow (?).

Report Code No.	Location	Cross Reference	Item No.	Report
X.16 (Sweden)	1229-5th		1	The slurry used in the Carbojet test is described by the authors as follows: "The coal used was a medium volatile bituminous coal ex United Coal Companies, Virginia (Widow Kennedy seam, 6% mineral matter and 28% volatiles on dry basis). It was milled in a pilot operation at 6 tons/hour in a circuit comprising primary rod mill and secondary ball mill. The size distribution was as follows: 99.9% - 200 u m 90.0% - 132 u m 75.0% - 80 u m 50.0% - 44 u m 24.0% - 15 u m
			2	Rheograms were mode of viscosity versus shear at rates of 0- 450 Sec^{-1} accelerating over 13 mins. plus deceleration over the same time. See Tables 1.X.16 and 2.X.16; and Fig 1.X.16.
			3	Tests were also made at 450 constand shear rates of 31 Sec^{-1} for 60 mins. See Table 3.X.16, showing viscosities and flow behavior mode.
			4	Atomization of the Carbojet CWF was made in a modified Delavan Aero Nozzle Model 30615 - 56; 5gbh; using air as the atomizing fluid.
			5	Their test results are shown in the figures, reproduced as follows: Fig 1.X.16 - Viscosity (Pas) versus Shear rate. NOTE: 1 Pa = 1000 centipoise. Fig 3.X.16 - Feed pressure vs. moisture content. Fig 4.X.16 - Mass Medium Dia. vs. moisture content and air (CWF ratio at 1.6 bar (13-5 Psig) Fig 5.X.16 - MMD vs atomizing air/CWF ration at 32.2% moisture (67.8% coal wt.) at 1.2 Bar Air Press. (13.5 PSIG).

Report Code No.	Location	Cross Reference	Item No.	Report
				N.B. at .15 ratio MMD curve becomes Asymptotic. Therefore, max. particle size at this ratio can be (?). This presumably is a function of the atomizer and atomizing pressure. Fig. 6.X.16 - Initial - Lowest viscosity at 450 sec.$^{-1}$ (in Pas) vs. % moisture content.

Report	Paper Location	Cross Reference	Item No.	Report
W.1	6th-109		1.	Work by Marchwood Engineering Laboratories, England on CWF covered a range of coal types, particle size distributions, additives and ash contents.
			2.	In their test apparatus, coal particles were heated to simulate droplet heating in passing through a flame front.
			2.1	In all cases it was found that the particles agglomerated.
			3.	Combustibility of the droplets was a major effort of the R&D.
			4.	Table 1.W.1, reproduced and attached, shows the ultimate analysis of the various CWFs tested.
			5.	The test combustor was rated at 0.5 MW$_{+}$ (3.5 $.10^{6}$ BTU/W.) and the atomizer type was internal mixing (with swirled atomizing air).
			5.1	Combustion air was preheated.
			5.2	Generally the flame front was close to the burner and ignited stably. In other cases the flame front lifted.
			6.	Test results are given in the following reproduced figures:
				Fig 3.W.1 - Burnout and Mean Particle Size - after .8 sec. - CWF (B)
				Fig. 4.W.1 - Ditto after 2.5 Sec.
				Fig. 5.W.1 - Effect of Coal Loading on Burnout and Mean Particle Size - CWF (B).
				Fig. 6.W.1 - Effect of Slurry Composition on Burnout and Mean Particle Size (? - slurry "composition"?) variable shown is % excess O_2.

Report	Paper Location	Cross Reference	Item No.	
				Fig 7.W.1 - Particle size variation with time.
				Fig 9.W.1 - Typical drop histories
			7.	% carbon burn-out experienced was disappointing and was reported as due to: a) quality of atomization b) little control in matching spray and aerodynamic patterns. c) Initial flame development d) Combustor duct temperature close to burner varying with: 1) windbox temperature 2) atomizing air pressure N.B. d.1 and d.2 improved flame stability and raised combustion temperature.
			8.	Noteworthy is the fact that initial flame temperature is inversely proportional to CWF ash content.
			8.1	As lowest ash content produced max. flame temperature: improved % burn-out and had the highest viscosity, the improved flame temperature was not due to better atomization.
			9.	Single drop experiments can be used for qualitative comparisons of CWF performance under large scale combustion conditions, but it is not advisable to predict flame performance in non-specific cases by extrapolation of the combustion test data.

6th SYMPOSIUM

Report	Paper Location	Cross Reference	Item No.	Report
W.2	6th-127	X.9, P.1023	1.	This paper covers the work of C.E. and Gulf Research & Development Co. (as a team) under contract from D.O.E. (and PETC).
			1.1	The paper covers combustion testing of CWFs.
			2.	Oil fired design boilers have ½ the radiant surfaces and volume of P.C. designed boilers.
			2.1	Therefore, coals used in O.F. units must be low in ash slagging and fouling tendencies and high in combustion reactivity in which coal beneficiation is a major factor.
			3.	This paper is evidently an update of similar R&D goals and work described in Reference X.9, P. 1023 of the Fifth Symposium.
			4.	Six burner types were selected for testing, viz; "- register-type burner refractory chamber burner Combination of register-type and refractory-type - rotary cup atomizer burner - high-swirl, wall-fired burner - tangentially fired burner
			5.	Atomizer performance requirements were: -Mass median drop size less than 200 microns at full flow. -Mass median drop size remains constant or decreases at reduced flow -No atomizer erosion during test period -no atomizer pluggage -Atomizer assist fluid consumption less than .25 lbs. per lb of fufel at full load"
			6.	Preliminary burner performance objectives included:

6th SYMPOSIUM

Report	Paper Location	Cross Reference	Item No.	Report
				o Air preheat requirements less than 500°F o Excess air requirements less than 40% @ 100% load o Turn down without support fuel greater than 4:1 o Ignition requirements less than 20% of full load heat input in a cold boiler for 30 minutes o Carbon conversion efficiency greater than 98% at full load.
			7.	Results of test work on some of the burners were not available at time paper was written.
			8.	The burner tests reported on were of the 20 - 25.10^6 BTU/Hr.capacity class for commercial CWF application.
			9.	The "Critical Burner Evaluation" tests had determined optimized atomizer and burner register parameters, and the selected burners were subject to further testing in the "Sub Scale Burner Facility" (SSBF) to determine as a function of excess air, combustion air temperature, and firing rate -- the following operating data: a) Optimized ignition requirements and turn-down limits. b) % carbon burn-out c) gaseous and particulate emissions d) Stack opacity e) atomization quality f) atomizer life.
			10.	Six CWFs were to be tested at two beneficiation levels for: a) atomization quality b) combusion performance N.B. a) and b) tests on one 50.10^6 BTU/Hr burner.
			10.1	Tests also were to determine effect on burner combustion performance of: c) CWF Rheology d) beneficiation e) CWF manufacturing process

6th SYMPOSIUM

Report	Paper Location	Cross Reference	Item No.	Report
			11.	Proximate and ultimate analyses of 2 parent coals, 4 CWFs, and oil mix of 45% and 55% 02; are shown in Tables 2.W.2 and 3.W.2 reproduced.
			12.	The CWFs used in the FPTF tests had the properties as shown in Table 4.W.2 reproduced.

TABLE 4.W.2

FPTF TEST CWM PROPERTIES

SAMPLE MANUFACTURER COAL	CWM#1 C L. Kittanning	CWM#2 D Splash DAM	CWM#3 E Splash Dam	CWM#4 C Splash Dam
Percent Solids (%WT)	66	69	66	70
pH	8	8	8	9
Screen Analysis				
Plus 60 Mesh	0.1	0.2	0.1	0.1
60 X 100 Mesh	0.7	3.5	0.2	0.9
100 X 200 Mesh	0.5	15.5	0.4	3.8
200 X 325 Mesh	7.6	18.5	11.2	8.9
Minus 325 Mesh	91.1	62.3	88.1	86.3
Mass Mean Particle (1) Diameter (Microns)	15	50	25	15
Viscosity (2) (cp)	1500	840	860	640
Power Law Exponent(3)	0.96	1.5	1.2	1.4

			13.	Further test data are given in Tables reproduced as follows: Table 5.W.2 - Operating Conditions Lower Kittaning Coal Table 6.W.2 - Operating Conditions Splash Dam Coal Table 7.W.2 - Coal, atomizer droplet size and Fly Ash Size. Tables 8.W.2 and 9.W.2 - Relative slagging characteristics of Kittaning and Splash Dam CWFs.

6th SYMPOSIUM

Report	Paper Location	Cross Reference	Item No.	
			14.	Note from Table 7, evidence of good atomization and moderate agglomeration of coal particles, and good % carbon conversion.
			15.	"Combusion tests show that the CWFs from 2 parent coals and from 4 different manufacturers can be efficiently burned under conditions of oil designed commercial furnaces, without severe ash slagging and fouling behavior."
			15.1	"Ash properties of the CWFs appear to be the dominant factor influencing ash deposit characteristics."

6th SYMPOSIUM

Report	Paper Location	Cross Reference	Item No.	Report
W.3	6th-143		1.	The paper describes work done on CWF rheology characterization.
			2.	Fig 1.W.3 reproduced shows an important result for Utah coals: The characteristic delitant curve becomes straighter or more plastic (i.e., less dilatant) with higher coal loading.
			2.1	The max. loading is only 58/42 (in Fig. 1) versus a "standard" loading of 70/30.
			2.2	In final report margin notes will be eliminated from the figures.
			3.	Ordinate units for shear stress: $N/m^2 = \frac{100,000 \text{ dynes}}{10,000 \text{ cm}^2} = 10 \text{ dynes/cm}^2$ To obtain viscosity in Cp multiply ordinates by 1000 & divide by corresponding abcissa value (shear rate).
			4.	The atomizer design is similar to the test atomizer of the Atlantic Research Corp. (See Fig 6, P. 149 of my 1983 report).
			5.	Fig 7.W.3, reproduced, shows % carbon burn-out versus a) stoichiometric ratio and b) Swirl number. Nozzle exit velocity is near sonic value considering extrainment of atomizing air.
			5.1	Average particle velocity in the reactor was 28-30 m/sec. (82-98 fps).
			6.	From conditions of item 5 and 5.1, residence time is very low which decreased % carbon burn-out.

6th SYMPOSIUM

Report	Paper Location	Cross Reference	Item No.	Report
W.4	6th-165		1.	For purposes of this report, various figures have been reproduced, together with verbatim extracts, giving insight into the CWF/Atomizer parameters and their consequent effect on combustion history.
			2.	The following material has been extracted verbatim from the paper:
			2.1	"Atomization quality was found to be the most important variable affecting the carbon burnout characteristics of coal water flames. Figures 20 through 25 show scanning electron micrographs of solids sampled from coal-water slurry flames at a distance of just over one meter from the burner."
			2.2	"The process of atomization is generally characterized by the formation of a liquid jet or sheet which then breaks down into cylinders or ligaments and, finally, into droplets. The char particle shown in Fig. 21 looks very much as if it could have been a ligament from which 3 or 4 drops were in the process of forming. It appears that the water was driven off before the atomization process was complete leaving a more or less intact ligament composed of individual coal particles bonded together by a sticky matrix."
			2.3	"Further investigation is required to determine the causes for the agglomeration observed in the scanning electron micrographs. It is possible that the individual coal particles are held together by surface forces or that during the heat-up process tars are exuded which serve as a bonding agent. The chemical additives, which comprise approximately 1% of the fuel, can also possibly play a role in bonding individual coal particles together during their initial stages of heating."
			2.4	"Runs 306 and 309 consisted of detailed flame structure studies on high swirl

Report	Paper Location	Cross Reference	Item No.	Report
			2.4 (cont.)	unstaged flames obtained with the Occidental Research standard and fine grind slurries respectively. The input conditions for these two flames were identical except for the water content of the slurry. In the case of the fine grind slurry, the viscosity was found to be prohibitively high, and the fuel was consequently diluted to a greater extent than the standard grind fuel so as to maintain comparable pressures at the fuel nozzle for the two slurry types. Examination of the axial burnout profiles for the two flames (Figs. 16 and 18) show the standard grind fuel (Run 306) to have given better results; the burnout in this case was substantially more rapid. The better burnout achieved with the standard grind slurry is again considered to be attributable to better atomization quality. Possibly, in spite of the greater degree of dilution with water, the viscosity of the fine grind fuel at the nozzle tip was greater, causing the atomization to be poorer. "Comparisons of the burnout profiles (Figs. 16 and 18) and also of electron micrographs taken of selected solids samples (Figs. 26 and 27) from the Occidental Research, standard and fine grind flames clearly demonstrate that atomization effects easily dominate those due to particle size in the slurry. This is consequence of the fact that the char particles in the flame take on a size that is closer to the spray doplet sizes than to the original coal particle sizes. It may be said that particle size determines that lower limit in the spray droplet size distribution since it determines the smallest allowable dimensions in the atomizer and consequently the smallest droplet size. However, unless this lower limit of droplet size is actually approached by the atomizer in practice, the benefits to be achieved by use of fine grinds in coal-water slurry are minimal.

6th SYMPOSIUM

Report	Paper Location	Cross Reference	Item No.	Report
			3.	The data in Item 2.3 seems to indicate the probability of agglomeration of coal particles within the atomizer before exiting. This could help establish a value for the constants in the viscosity equations given in Appendix No. 1.
			4.	The data in Item 2.4 seems to indicate that carbon burnout efficiency is more a function of CWF droplet size, rather than the fineness of the coal grind. It will be important, especially in view of the Funk formula to compare these verbatim statements and the Tables and Figures of this paper with data from other papers in the 5th and 6th Symposia to establish relationships that will promote ideals[1] of optimum atomizer design for field discussion with the atomizer manufacturers, including Occidental Research and K.V.B. Inc.
			5.	Tables and Figures of this paper are reproduced as follows:
			5.1	Table 2.W.4 - MIT CWF Trials - Input and Operating Conditions of Flames
				Table 3.W.4 - Analytical Data on Occidental Research with experimental CWF.
				Fig. 9.W.4 - Effect of Small Variations in Atomizer Design, etc., on Flame front.
				Fig 11.W.4 - Effect of Combustion Air Swirl on Flame Front Position.
				Figs 16.W.4 & 17.W.4 - Show % carbon burnout from various test conditions.
			5.2	Figs. 20.W.4 to 27.W.4 - show S.E.M. photographs of coal particles from various test CWFs.

---

[1] The 1983 paper by Knell of Occidental Research & Muzio & Avand of KVB will be obtained (if non-proprietary) and studied.

6th SYMPOSIUM

Report	Paper Location	Cross Reference	Item No.	
			6.	The char particles of item 5.2 are related to droplet size and affect the % carbon burnout.
			7.	It would be of interest if a study of the data of the papers reported on, can show the influence of swirl number as a contributing factor in atomization and droplet size.

Report	Paper Location	Cross Reference	Item No.	Report
W.5	6th-234	X.15	1.	The authors establish an equation linking CWF to Cv which is given in Appendix 1., Item W.5.
			2.	It is stated that the Cv must be greater than 64.22% or 69.77% to formulate a CWF or a P.C. of 70% or 75% Wt loading (See Fig. 4, P. 242 attached). If the CWF has a Cv of 60% - 62%, which is commond practice for industrial grind (say the authors), then a highly loaded CWF cannot be prepared. Check with Report X.15 and Equations in Appendix 1. and Item X.15.
		B.1, App.#1	3.	Reference is made to the Alfred (Dr. Funk) equation, where the value of the exponent "n" has been shown by computer modelling to be .37 for max. packing (see Appendix 1, Item B.1) for the Funk Equation.
			3.1	The value of .37 is based on a max. particle size of 300 um (D_L) for any smaller size (D_s).
			4.	The theoretical array models are shown in Fig. 2.W.5, A-B-C.
			4.1	Packing models A & B will produce a dilatant mode. Model C will diminish this tendency.
			4.2	The Cv value of model C packing (Tetrahedral is about 48%.
			4.3	Note in Table 1 that the Cv values for P.C. grind, range from 48.94% to 52.55%.
			5.	The Funk Equation for particle sizing is then given (See Appendix Item B.1 for the Funk Equation.
			5.1	The authors do not agree that the Funk Equation best fits the max. packing distribution for P.C. and CWFs.
			6.	Tables from the paper are reproduced as folows:

6th SYMPOSIUM

Report	Paper Location	Cross Reference	Item No.	Report
				Table 1.W.5 - Cv's of P.C. Table 2.W.5 - Size Distribution by different equations 1) Alfred (Dr. Funk) 2) Rosin-Rambler Table 3.W.5 - Properties of CWMs from different coals
			6.1	Figures reproduced are as follows: Fig. 1.W.5 - Volume Content of Coal Versus Alfred Modulus n (see Eq. B.1 in Appendix 1). Fig. 2.W.5 - Theoretical Packing Structures Fig. 3.W.5 - Coal Vol. Content from R-R Equation and Modules n at density of 1.3 and D_L of 300 um. Fig. 4.W.5 - Size Distribution Comparisons with given Alfred (Dr. Funk) to Rosin-Rambler values of Modulus n.

6th SYMPOSIUM

Report	Paper Location	Cross Reference	Item No.	Report
W.6	6th-251	X.15, 5th P. 1205	1.	This paper repeats much of the Carnegie-Mellon paper repsorted on in X.15 (5th Symp.)
			2.	Certain sections are new and some are reemphasized and reported on in the following verbatim quotes::
			3.	"Coal particle surfaces are both hydrophobic and heterogeneous. The charge developed on the particle surface depends upon the degree of wetting of the powder. Hydrophobic agglomeration of incompletely wetted coal particles can be an important factor in determining slurry behavior at the time of mixing; it increases viscosity somewhat as well as sedimentation rate. As wetting improves over time, the surface charge may change markedly from the initial value. The two most hydrophobic coals, Pittsburgh Seam #8 and Hiawatha, show considerable change in behavior over time, while the less hydrophobic Illinois #6 and San Juan show only small changes. "For the better wetted particles the surface charge depends both upon the inherent charge of the hydrocarbon portions of the surface with associated functional groups and also upon the presence of soluble inorganic materials in the ash, which can apparently be readsorbed as hydrous oxides, with the result that the particles have a complex dependence of electrophoretic mobility upon pH, reflecting the presence of several types of surface each with its own isoelectric point. Both pyrite oxidation products and calcium salts appear to show such effects with Pittsburgh Seam #8. When soluble inorganic materials are removed from the surface of this coal by repeated washing, the variation of electrophoretic mobility with pH becomes much simpler, exhibiting only one point of zero charge at about pH 3 and an increasingly negative electrophoretic mobility at higher pH values. The behavior of Hiawatha, the coal with the least quantity of soluble

Report	Paper Location	Cross Reference	Item No.	Report
			3. (cont.)	inorganic materials, resembles that of washed Pittsburgh #8 coal. "The pH of the slurries changes with time, shifting toward the natural pH of that coal in water, a pH which is different for each of the four coals. The electrophoretic mobility changes with the pH, and rheology and sedimentation stability also change. The rate at which these pH shifts occur can vary greatly from coal to another. For Pittsburgh Seam #8 the drift toward the natural pH may continue over a period of months, while for San Juan slurries may change by several pH units to the natural pH in about twenty minutes. "Surface charge also affects the maximum achievable concentration of solids. When charge is high particles tend to pack more efficiently, maximizing interparticle distance. Therefore higher solids concentration can be achieved. "Measurements on a series of sieved fractions of Pittsburgh Seam #8 suggest that the maximum achieveable solids concentration decreases with decreasing median particle size. The cause of this unexpected result is unknown. However, as expected, increased particle size distribution width increases the maximum attainable solids concentration. "The relative viscosity of coal slurries was found to be independent of temperature over the range 10° to 50°C. Similarly, changes in sedimentation rate between 10° and 60°C could be accounted for by changes in the density and viscosity of water."
			4.	"From this summary of slurry behavior without additives it can be seen that among the possible functions of additives are the improvement of wetting, the modification of particle surface charge and therefore of slurry behavior, the creation

Report	Paper Location	Cross Reference	Item No.	Report
			4. (cont.)	of three-dimensional structure to prevent sedimentation in a slurry with a high surface charge, or the inducement of weak flocculation to increase median particle size and maximum solids concentration. The four additives used in this study provide illustrations of several of these possible effects."
			5.	Table 1, reproduced, gives analysis of the four coals used in the CWF tests (of this paper).
			6.	It is interesting to note that the medium dia. by Coulter counting and by Sieve sizing are very close.
			7.	It should be noted that the Sauter method of determining mean diameter can give a better appraisal of the "fineness" of atomization.
			7.1	Table 2.W.6 - Soluble Inorganic Ions in Slurry Supernatant Table 3.W.6 - Natural pH and Critical Surface Tension for Wetting of the Coals Table 5.W.6 - Surface Tension of Slurry Supernatants (pp. 255 & 256)
			8.	"A number of processes may occur when dry coal is mixed with surfactant solution. First, the decreased surface tension of the fluid allows better wetting than in water alone. If the solution surface tension is less than the critical surface tension for wetting of the coal, the entire surface will be wetted spontaneously and rapidly and the powder will become well dispersed, whereas in water alone wetting is slow and initially at least only partial, causing a hydrophobic agglomeration of coal particles."
			9.	"As expected, surface charge strongly affects slurry properties, because the degree of flocculation is dependent upon

Report	Paper Location	Cross Reference	Item No.	Report
			9(cont.)	surface charge. The electrophoretic mobility measured in concentrations of surfactants high enough to ensure complete wetting of coal particles may be quite different from that found in water alone. The electrophoretic mobility measured for the well-wetted coal appears to depend strongly upon the quantity and type of inorganic ions dissolved from the coal surface into the slurry, especially hydrous iron oxides. "The additives used all lower the surface tension of the fluid, leading to more complete wetting of the hydrophobic coal particles. The sequential wetting of different regions of the particle surface leads to marked fluctuations in electrophoretic mobility in the flower surfactant concentration range. Only when the surfactant concentration is high enough that the entire surface is wetted does the electrophoretic mobility become constant and reproducible."

6th SYMPOSIUM

Report	Paper Location	Cross Reference	Item No.	Report
W.7	6th-266		1.	Antonini etal give the basic design equations for Newtonian liminar flow as given by McLain, in "Fluid Flow in Pipes". i.e., $\mu = \frac{\pi P r^4 t}{8 L v}$ where V = volume flow
		Sec.E725	1.1	S.R.C. E725
		R.G Appendix C		R.G. - Appendix "C", entitled "Derivation of Ordinate and Absissa Terms as Shown in Fig. 30 S.R.C. E725."
		X.12, App.1 S.R.C.E725	2.	For the authors' Equations covering time - independent non-Newtonian flow, see Appendix 1, Item W.7, item 2.
			2.1	The authors refer to a "slip" factor and show its derivation from test data and fundamental equations.
			2.2	This "slip" factor will require study by me to fully assess the nomenclature and equation modifications to values of Q (flow) (to become Q_L) and $\dot{\gamma}_o$ (to become $\dot{\gamma}_c$ and Beta factor B as the general modifier and expressed in their Fig. 7.
			3.	My first efforts will be with the Rabinowitsch-Mooney modification of the Newtonian equation. $\dot{\gamma}_w = \frac{8V}{D}$ (See Appendix 3)
			3.1	(I have a "hunch" that the Antonini, etal, work is directed towards larger dia. pipes as required for total flow from the CWF pumps to the burners.)
			4.	A precise definition of the term "Slip" will be required. (I will communicate with the author(s).)

6th SYMPOSIUM

Report	Paper Location	Cross Reference	Item No.	Report
W.8	6th-284		1.	It has been noted in other papers that the "slurriability" of coals are correlated to characteristics such as: water absorption; O/C ratio; specific area.
			2.	"Ageing" of coal increases viscosity of CWF which is presumed due to oxidation.
			3.	There "have been" no specifics known regarding oxidation and viscosity.
			3.1	The authors' research is aimed at clarification of this phenomenom.
			4.	Their research confirmed the following:
			4.1	Oxidation increased: water1) absorption "equilibrium" value; specific surface area; COS θ (surface tension factor); viscosity of the slurry.
			4.2	Viscosity of CWF was increased by incresed "equilibrium value" which was in turn increased by oxidation.
			5.	Fig. 2 reproduced, shows the graph of slurry Viscosity vs. Equilibrium Moisture.

---

1) I gathered from the paper that water "equilibrium" values was the max. amount extracted from the fluid by both absorption and adsorption.

6th SYMPOSIUM

Report	Paper Location	Cross Reference	Item No.	Report
W.9	6th-304		1.	The object of the authors' research was "How to achieve a minimum viscosity for a given solids concentration."
			2.	The equations presented by the authors are functions of μ based on volume of fraction ratio $\frac{\phi}{\phi_m}$ (packing ratio).
			2.1	See Appendix 1 - Section W.9 for these equations.
			2.2	The relative viscosity is proportional to the value $\frac{\phi}{\phi_m}$ and lowering the viscosity is achieved by decreasing ϕ or increasing ϕ_m.
			3.	Funk and others have shown that Om is a function of size distribution (See Appendix 1).
			4.	Item 3 (say the authors) neglects (?) an important variable "the interaction between the solid particles".
			4.1	The inter-particle forces are: a) Van der Waals intermolecular force - attractive b) Electric --- repulsive c) Steric --- repulsive d) Solvation.
			5.	The "Solvation effect" is an increase in the effective diameter of the coal particles.
			5.1	The "electric" effect is an electroviscous effect causing viscosity change due to flocculation.
			6.	In cross reference X.15 it was speculated that the "electroviscous" effect on viscosity operated only through an effect on ϕ_m.
			6.1	In addition, and depending on the type of interaction between particles, it was stated that these types of suspensions can be identified.

Report	Paper Location	Cross Reference	Item No.	Report
W.9			6.2	See Fig. 1, reproduced and note that: a) The suspension is aggregatively stable b) & c) The particles aggregate as a result of the weak and strong attractive interactions respectively.
			6.3	A fundamental statement by the authors is reproduced verbatim: "The maximum attainable solids volume fraction ϕ_m, is expected to be different in each type of suspension. For instance, if the interaction is predominantly repulsive, the particles can slip past one another and produce a denser packing (See Fig. 1 (a)) than the dense random packing of dry solid spheres. However, if there is an attraction between the particles, weak or strong, the particles will stick to each other at random points and yield looser packings. "In other words, for a given particle size distribution, all the effects of particle interactions can be lumped together into an effective maximum solids volume fraction ϕ_m which could be determined experimentally for a particular slurry and be used to characterize that slurry.
			6.4	Experimental work is (or has been) conducted to explore the foregoing ideas. (It will be my intention to contact the authors).
			7.	Variations of their fundamental Equation are given and are reproduced in Appendix 1 (Item W.9).
			7.1	From these equations the work of two scientists is given in which plots of $f(\eta_r)$ are made against the values of ϕ and ϕm.
			8.	From the equations and their resulting graphs, ϕm was obtained.

6th SYMPOSIUM

Report	Paper Location	Cross Reference	Item No.	Report
W.9			9.	The Tables and Figures illustrating the foregoing are:
			9.1	Table 1 – Viscosities of Coal Water Slurries (Pocohontas Coal)
			9.2	Table 2 - Max. Coal Volume Fraction
			9.3	Table 3 - Correlation Testing Schemes
			9.4	Fig. 1 - Interaction Between Particles
			9.5	Fig. 2 - TSV, i.e., Terminal Sediment Volumes
			9.6	Fig 3 - Viscosity vs. Coal Vol. Fraction ϕ
			9.7	Fig. 4 - $f(\omega_r)$ vs. % Coal Vol. Frankel & Acrivos Method
			9.8	Fig. 5 - $f(\omega_r)$ vs. Coal Fraction ϕ Heath & Tadros Method.
			10.	From Table 2, I shall use a value of Om = .80 for analysis of atomizers.

6th SYMPOSIUM

Report	Paper Location	Cross Reference	Item No.	Report
W.10	6th - 313		1.	In this paper emphasis on CWF rheology is placed on the thickness of the water film on the coal particle, influenced by the type and quantity of additives.
			2.	The film thickness is determined through the principle of "ellipsometry" using their lab's Model TP-77 Ellipsometer (made in China) together with a TRS-80-1 Microcomputer.
			3.	The thickness of the film, rather than its strength (tension factor?) was the dominant factor in the CWF Rheologyj.
		W.9, Fig. 1 p. 309	3.1	The thicker the adsorption layer, the greater the dispersion factor or the lower the viscosity (3.1 to be checked against data of other papers versus Fig. 4 of this paper W.10.)
			4.	Fig 1.W.10 and Table 1.W.10, reproduced, illustrate the effect of three different additives at % concentrations of 0 - 1.0 and at equilibrium, on film thickness.
			5.	Fig 1.W.10 reproduced: Viscosity in Centipoise vs. Amount of Additive at Shear Rate of 4.76 sec^{-1}.
			6.	Fig 5.W.10: Viscosity vs. % Coal Concentration at Constant % Additive Concentrations of 1% of Dry Coal.
			7.	Table 2.W.10: Density of Adsorption Layer on Coal Surface Where: Γ = amount of adsorbtion (m) vs. weight of coal (W), and ρ = Adsorption mass (m) per volume of surface layer (V_a).
			8.	See authors' Appendix to their paper for detailed description of "ellipsometry" and its measurement (W.10, p. 322)

6th SYMPOSIUM

Report	Paper Location	Cross Reference	Item No.	Report
W.11	6th-320		1.	This paper by A.C. Eckmann etal, of PETC deals with the effect of adding methanol to a CWF.
			2.	The addition of methanol significantly increases viscosity except in the case of petroleum coke which showed a decrease when methanol was added to the petroleum coke water mixture.
			3.	Two benefits of methanol addition are:
			3.1	Possible elimination of combustion air pre- heat.
			3.2	Inhibition of freezing during storage.
			4.	If "low grade methanol", which contains water, is used, the viscosity of the methanol/water addition effect is small.
			5.	I quote verbatim, the following passage of the report: "Physical and electrochemical properties of the coals will play a greater part at high coal loadings, and it might be anticipated that variations in liquid viscosity would not predict all of the resulting variations in slurry viscosity. Because of the importance of controlling viscosity in highly loaded slurry fuels, it is necessary to be able to predict changes with any variation in fuel make-up."
			6.	Dried lignite re-absorbs liquid from the water-methanol carier and; therefore, cannot be as highly loaded as bituminous coal.
			7.	The viscosity predictive equation is: $\eta_r = \eta_s/\eta_m = 1 + 2.5\,\phi + 7.\,\phi^2 + 37.4\,\phi^3$

6th SYMPOSIUM

Report	Paper Location	Cross Reference	Item No.	Report
W.11			7. (cont.)	Where: η_r = "Reduced" viscosity η_s = "Suspension" viscosity η_m = Viscosity of the water-methanol mixture ϕ = Volume fraction of solids
			8.	Viscosity determined by test had poor correlation with the values of the theoretical equation.
			8.1	The answer may lie with the "surface characteristics" of the coal particles (presumably ionic charge and topography) and this will be the subject of continuing research by PETC.
			9.	The following reproduced figures illustrate the viscosity/liquid relationships described above: Figs. 1.W.11, 3.W.11, 4.W.11, 10.W.11.

NOTE: I will obtain definition of terms "suspension viscosity" and "reduced viscosity".

6th SYMPOSIUM

Report	Paper Location	Cross Reference	Item No.	Report
W.12	6th-404		1.	This paper by M. Reza Ghassemzadeh of B & W, etal, deals with the CWF based on very low ash "Solvent Refined Coal".
			2.	The low ash % plus low viscosity makes an (SRC) CWF of particular interest in the case of oil firing designed boilers.
			3.	See Figs 1.W.12 and 2.W.12 for data on Fuel Analysis and Combustion Test, respectively.
			3.1	Regretably, the ash F.T.A. is not given at PETC.
			3.2	Fig 2 data are results of test in a 700 HP boiler.
			4.	The boiler tested was a B&W El Pas Radiant Oil fired design unit - rated at 4 million lbs/hr steam flow at 2600 PSIG at 1005°F.
			5.	Full test results for the large utility boiler are not given, but the authors state an overall boiler efficiency of 86% at MCR, using 70% loaded (SRC) CWF.
			6.	An interesting point made by the authors and boding well for CWF use, is that production of good quality residual #6 oil by the refineries is diminishing (more distallate fuel is being produced).

Report	Paper Location	Cross Reference	Item No.	Report
W.13	6th-481		1.	This paper deals with a 35-day test of CWF at the Memphis Plant of E.I. Dupont by Rolf K. Manfred of EPRI and Brian Taylor of B&W Barberton.
			2.	The boiler was a B&W "Standardized" design rated 60,000 PPH.
			3.	Two CWFs were tested; one at 70% loading, the other at 75% loading and both used a near normal P.C. coal sizing.
			4.	Both CWFs were pretested by B&W, which resulted in a decision to use combustion air at 600°F at 17" H_2O pressure. Compressed air was to be used as the atomizing fluid.
			4.1	This pretest was reported by EPRI in their report RP-1895-3, Volume 3, published in June 1984.
			5.	The CWFs were provided by Atlantic Research (ARC-Coal) and by Slurrytech (Co-Al).
			6.	Fig 1.A.W.13 shows the raw coal analysis Fig 1.B.W.13 shows the slurry analysis
			7.	% coal loadings were: ARC-Coal --- 70% CO-Al --- 75%
			8.	Data on viscosity and settlement are given in Tables 11.B.W.13 and 11.C.W.13.
			9.	Predicted performance by B&W is given in Table 11.W.13.
			10.	The atomizer was a B&W
			11.	It was found necessary to provide tungsten-carbide on all contact surfaces.
			12.	It is interesting that the Moyno pump showed no appreciable wear after about 1500 hours of operation.

Report	Paper Location	Cross Reference	Item No.	Report
W.13			13.	Ignition stability required gas recirculation provided by vane design and a windbox pressure of a "--12" H_2O (see Fig. 9.W.13).
			14.	Table V.W.13 gives detailed report on burner-boiler performance.
			15.	Of particular interest for CWF firing (combustion) were:
			15.1	Atomising air pressure - 200 psig +
			15.2	Atomizing ratio - .25 (reported in text) CWF pressure: ARC Coal - at 93% MCR @ 800 CP - 187 psi Co-Al at 85% MCR @ 500 CP - 154 psi N.B. - The atomizer CWF ΔP is apparently not linear to CP.
			15.3	Excess air of 75% with register system in use was found necessary to provide necessary swirl for flame stability. "This amount of excess air would not be needed for 'new burners'".
			15.4	Viscosities were: ARC - 800 (70% coal) Co-Al - 860/500 75%/74% - coal
			15.5	Preheated combustion air necessary for flame stability.
			15.5.1	Test combustion air temp. - 480°F.
			16.	I quote the following verbatim: "Burner designs have improved as the relationship between slurry properties, atomization behavior, and combustion characteristics have become clearer. A second generation of utility-size burners is required with better performance and reliability."

6th SYMPOSIUM

Report	Paper Location	Cross Reference	Item No.	Report
W.14	6th-499		1.	At last, a paper relating rheology to atomizer design, by Dr. J.W. Allen, NEI Int'l Combustion, Derby, England.
			2.	Their test rig can test a burner rated up to 125.10^6 BTU/Hr., minimizing problems of scale-up in atomizer design.
			3.	However, initial basic combustion test work was done on a 1.5 BTU/Hr testing and atomizer development work was done on a 30.10 BTU/Hr. rig, involving only a 4.1 scale-up for the large testing.
			4.	Fig 4, reproduced, shows the design principle of the ICL (NEI) atomizer, indicating a large CWF tube into which 4 shear holes and 8 swirl holes introduce atomizing air.
			5.	Early designs used steam for atomizing, but problems were encountered due to:
			5.1	Breakdown of the additive
			5.2	Dilatancy created in the CWF caused blockages in the narrow fuel slots and orifices of the "scaled-down version of the steam assisted atomizer.
			6.	These blockage problems were overcome by:
			6.1	Air as the atomizing medium. 1)
			6.2	Change in atomizer design to avoid narrow orifices and sudden changes of direction in the slurry flow stream.
			6.3	The text impliesd that exit of the air/CWF emulsion is via a "fuel tip" (orifice?).
			7.	Of considerable interest is that this early design of atomizer required:
			7.1	Max. coal size 250 microns (NOTE: C.E. Chatham Mark IV design was based on 400 micron max. coal particle size. Also of

---

1) Did steam as the atomizing fluid dry the CWF?

6th SYMPOSIUM

Report	Paper Location	Cross Reference	Item No.	Report
W.14				interest to remark at this point, is that the C.E. Mark 3 had an emulsion exit annulus of .194 in. dia. equal to 4928 Um or an atomizer annulus ratio to max. particle size of 4928/400 = approx. 12:1 - Why? Possibly the reasons were: a) Agglomeration of CWF particles b) Considerations of ΔP for the required flow.)
			7.2	A minimum V.M. of .25% (dry basis) was required for stable flame.
			8.	Design requirements for flame stability were found (by ICL) to be:
			8.1	Preheated combustion air
			8.2	Products of combustion recirculation
			8.3	Refractor blocks around burner exit.
			9.	Hot flame gas recirculation was found to be of primary importance.
			9.1	Of second and third order effects were those of items 8.3 and 8.1, respectively.
			10.	Table 1 gives the properties of the CWFs-tested (P. 503 reproduced).
			11.	Table II gives the CWF combustion performance (p. 505 is reproduced)(various swirlers).
			12.	ICL tested various atomizer designs and the results are shown in Table III (p. 506 is reproduced).
			12.1	Regretably, no data is given on atomizing fluid pressures or on atomizing fluid/CWF ratio.
				There is also a noticeable absence of dimension data on annuli and exit orifices, on which shear rate could be determined for a given CWF flow. (I will try to obtain such information from ICL - or from Ken Olen).

Report	Paper Location	Cross Reference	Item No.	Report
W.14			13.	ICL will be testing (cold test) sonic and external mix types of atomizers.
			13.1	Both types (Item 13) offer potential as low wear atomizers.
			13.2	ICL consider that external mix atomizers are of particular interest for corner fired installations.
			14.	ICL are also considering thermally-assisted atomization.
			14.1	Preheat of CWF under equivalent saturated pressures of 200 - 250 C (392-482°F) could induce flash evaporation of water in CWF at exit of atomizer, thus assisting in promoting ignitibility. Limitations in thermal assist is the type of additive used in the CWF.

6th SYMPOSIUM

Report	Paper Location	Cross Reference	Item No.	Report
W.15	6th-548	X	1.	R.C. Furman, Consultant, describes an EPRI sponsored slurry test produced Co-Al/B&W test.
			2,	The Co-Al provided was a 75% coal concentration, with 5% ash and a viscosity of 1000 CP.
			3.	Tests in a demonstration plant for Co-AL were planned by B&W/Ashland Oil, in South Point, Ohio, June 1984.
			4.	A similar test is planned by B&W in the UK to start in mid-1985.
			5.	Slurrytech are planning for a commercial plant of 1,000,000 tons per year capacity.
			6.	Co-AL was developed at Alfred University and the exclusive license and marketing rights are owned by Slurrytech, Inc.
			7.	Table 1.W.15, reproduced, gives the proximate and ultimate analyses of the parent coal and the Co-AL produced from it.
			8.	Results of test (Item 1) are given in Table 1.W.15.
			9.	Points of major interest for this report are:
			9.1	Efficiency - 800 CP-74.57% 500 CP-75.98% - 1st run 500 CP-75.967% - 2nd run
			9.2	O_2 - 860 CP - 9.3% 500 CP - 8.8% - 1st run 500 CP - 8.5% - 2nd run
			9.2.1	Compare boiler efficiencies & O_2 vs. CP
			9.3	Pressures: CWF - 860 CP - 175 psi 500 CP - 154 psi Atom. Air (to burners) - 860 CP - 203 psi 500 CP - 207 psi

6th SYMPOSIUM

Report	Paper Location	Cross Reference	Item No.	Report
W.15			9.4	It is stated that the excess air of 70% (at a W. Box Press of 11 & 12.7 ins. H_2O), was required to give the necessary swirl (presumably for flame stability).
			9.4.1	It was expected that "new burners" would operate at 25% - 30% excess air.
			9.5	Atomizing air consumption ratio was not given.
			10.	Of interest: At 75% concentration-CP --860 At 74% concentration-CP -800

6th SYMPOSIUM

Report	Paper Location	Cross Reference	Item No.	Report
W.16	6th-557		1.	In reporting on slurry developments in England, the author, E.G. Atkins of Babcock Power Ltd., England, has put forward the Funk equation which has made Co-AL one of the most successful coal-water mixtures.
			2.	The Funk equation is repeated (see Appendix 1), namely; $CPFT = \left[\frac{D^n - Ds^n}{D_1 - Ds^n}\right] \times 100$
			3.	To this fundamental equation values are given for D_1 ---- < 300 um D_s ---- > 0.1 um n --------.33 to .50 with ratio of .37 used for max. packing in Co-AL.
			4.	A modified form of PF burner is described and is shown in Fig 2.
			5.	Fig 2 burner converts the CWF (Co-AL) into a P.F. nozzle of the burner and burns as a straight pulverized coal fuel.
			6.	The author's description of the Fig 2 burner function is quoted verbatim as follows: "Work is also continuing at Babcock Power on the development of another type of burner for Co-AL applications. The normal PF burner tube is too constricted to allow proper atomisation for drying by the preheated primary air with insuffucient residence time in the tube for satisfactory drying. To overcome these problems, a form of 'in line' cyclone drier is incorporated in the design, taking preheated drying air from the bur "One form of this design is shown in Figure 2. The cyclone (1) is of a diameter small enough to pass through the

Report	Paper Location	Cross Reference	Item No.	Report
W.16				windbox opening (2) (i.e. essentially the same diameter as the secondary air swirl type register (3)). The inlet vanes (4) of the cyclone impart a swirl motion to the preheated air entering the windbox. Control of the quantity of air is by means of the sleeve damper (5). Coal water slurry is pumped via the inlet pipe (6) to the annular atomiser (7) from which it emerges in spray form to meet the incoming drying air in Figure 2 to reach the PF burner exit (8) where the conical deflector (9) helps to mix with the incomiong secondary air. Light-up and stabilisation is effected by the oil burner (10) which is ignited by the igniter (11) both housed in the co-axial ,carrier tube which also supports the deflector (9)."

6th SYMPOSIUM

Report	Paper Location	Cross Reference	Item No.	Report
W.17	6th-571		1.	Coal cleaning by "selective flocculation" is discussed in this paper.
			2.	The terms "flocculation" and "froth flotation" are defined as follows:
			2.1	Flocculation: The chemical treatment of finely ground coal to create "flocs" (or aggregates) which sink rapidly to the bottom of the treatment vessel. The ash forming mineral and pyrite remain dispersed
			2.2	Froth Flotation: This method is normally used in the cleaning in commercial practice of 28 mesh coal. This technique is based on the hydrophobic property of coal, and the hydrophilic property of the coal's associated impurities.
			2.2.1	Separation is achieved by passing air bubbles through a dilute coal-water slurry, when the hydrophobic coal and pyrite are floated to the surface and removed as a concentrate.Verbatim discription follows:
			2.2.2	"The hydrophobic coal and pyrite are floated to the surface and removed as a concentrate. Tailings are passed to a thickener for mineral matter removal and water recycle. To enhance the separation, chemicals called collectors are added during a conditioning stage to establish a more hydrophobic surface on the coal. The coal particles when contacted with air bubbles, are captured, and floated to the surface."
			3.	There is difficulty in obtaining efficient separation of coal and mineral matter with very fine grinds. Especial difficulty is encountered with micronized coal.
			4.	"Selective flocculation" is an advanced physico-chemical separation technique where a number of operational steps are used:

Report	Paper Location	Cross Reference	Item No.	Report
W.17			4. (cont.)	"o dispersion of coal suspensions, o flocculant adsorption and floc formation, o floc conditioning, and o floc separation."
			5.	Fig 1.W.17, shows, conceptually, the basic steps in "selective flocculation".
			6.	Tables 1.W.17 to 3.W.17 show ash reduction resulting from "selective flocculation".
			7.	The removal of pyritic sulphur in finely ground coal can be efficiently effected by the selective flocculation technique using a suitable dispersant (see Fig 5.W.17 reproduced).

6th SYMPOSIUM

Report	Paper Location	Cross Reference	Item No.	Report
W.18	6th-649		1.	This paper deals with coal fractions or "structure" and their effect on coal refining to enhance combustion characteristics.
			2.	The major constituents are:
			2.1	Macerals - organic matter of varying crystal structure and combustibility
			2.2	Mineral Matter - non-combustible constituents which determine ash characteristics as to size, fusion temperature and topography.
			3.	Macerals are of several orders; viz: vitrain and fusain (friable) and durain (harder material).
			3.1	Further maceral descriptive characteristics are: Invertinites which produce fly ash with high carbon content (lower combustion efficiency) and require longer residence time; higher proportion of primary air and smaller size particles to improve combustion. Also, invertinites do not fuse below 1000°C and are not reactive at these temperatures. Vitrinites & Exinites Partially fuse at 400°C and combust readily.
			4.	A continuing R&D by Gulf R&D Co. is the refinement of a coal to produce various fractions suitable for a wide variety of applications with the immediate concern of the formulation of apremium coal product of high reactivity for a CWF.
			5.	A goal for CWF is to produce a "fine" processed coal (grind & washing factors) consisting essentially of fusain - with lesser amounts of vitrain and durain.

6th SYMPOSIUM

Report	Paper Location	Cross Reference	Item No.	Report
W.18			5.1	NOTE: If the % reactive macerals are low, the % conversion can drop to 50%.
			6.	See Fig 4.W. for description of a coal process diagram showing yield of separate fractions of fusain vitrain and durain.

5-2-85

REPORT CODE NO.	PAPER LOCATION	CROSS REF.	ITEM NO.	REPORT
W-19	6th 667		1	This is a study of coal and ash composition and particle fineness both in the CWF and the atomization droplet size.
			1.1	Droplets can be large and contain numerous coal particles.
			2.	Size distribution of droplets is a function of atomizer design and operating conditions (?); coal particle size distribution (N.B. "particularly the largest coal particles) irrespective of the distribution, and the apparent viscosity of the CWF (? at what point in the system).
			3.	Ignition starts only at about 500°C and not until 90-95% of the moisture has evaporated.
			4.	Ignition delay due to heat and water evaporation can be estimated: $i_d = \frac{P_d \, (C_v)_d V_d \, \Delta T_d}{A_d T_f^4}$ i_d = ignition delay σ = Boltzman constant A_d = droplet diameter T_f = effective flame temperature P_d = droplet density $(C_v)_d$ = droplet specific heat V_d = droplet volume ΔT_d = temperature rise required to vaporize the moisture.

5-2-85

REPORT CODE NO.	PAPER LOCATION	CROSS REF.	ITEM NO.	REPORT
			4.1	A 10 um droplet heated by a 2000°K flame requires about .35 sec. to dry.
			4.2	The drying time varies inversely with the droplet surface to volume ratio; larger diameter droplets require longer residence time.
			4.3	The additional residence time requirement for ignition and burn-out of the char also depends on particle size.
			4.4	In micronized CWF the top particle size approximates 44 um and the burn-out time is in the range of 0.1 - 0.2 secs.
			4.5	Poor atomization - large droplets (100um) may promote extensive agglomeration of the coal particles, hence inadequate burn-out.
			4.6	? - mechanism of agglomeration in "large droplets"?
			4.7	The authors found no evidence for "micro explosions" under their experimental conditions.
			5.	The mmd for micronized CWF droplets approaches 4 um as the ratio of atomizing air to CWF increases.
			5.1	Large ash particles do not diffuse to a surface, but they penetrate the boundary layer and can be captured by the surface.
			5.2	Inertial impaction depends on particle size, surface configuration; and flow velocity, with a weak dependence on temperature "contributed mainly by the stickiness" of the collision.

5-2-85

REPORT CODE NO.	PAPER LOCATION	CROSS REF.	ITEM NO.	REPORT
			6.	Bulk of coal particles burn at 1600°C ± 200°C for about .3 sec.
			6.1	Estimate time dryburn 100 um particle - .8 sec.

6-2-85

REPORT CODE NO.	PAPER LOCATION	CROSS REF.	ITEM NO.	REPORT
W-20	6- 710		1	This work covers the trial by the International Flame Foundation of 7 CWFs from various coal types and particle sizes.
			2	Many designs of atomizers were tested with 3 types selected as suitable for CWF atomization (What are these atomizers?)
			3	With the "optimum" atomizer, the slurries were tested over a wide range of firing rates and operating conditions and it was found:
			3.1	All slurries could be burned without a support flame.
			3.2	A carbon burn-out of 95-99%
			3.3	However a larger range of atomization air ratio was required to achieve the above results ranging from 14% to 28%.
			3.4	It was found that of the slurries which could be burned at the lower atomizing ratios were also those which could be burned without air preheat and which had the largest turn down.
			3.5	The following is quoted verbatim:
				"From the slurry characteristics which were measured, it was not clear why such a great difference in the slurry atomization process for different slurries was found."

6-2-85

REPORT CODE NO.	PAPER LOCATION	CROSS REF.	ITEM NO.	REPORT
W-20	6- 710		4	The author's report on atomizer evaluation is quoted verbatim as follows:

"During the course of the experiments, the atomizers shown in figure 4 were all tested with air as the atomizing fluid. Atomizers D and E, the internal mix and the single hole atomizers did not perform satisfactorily. The internal mix atomizers had a strong tendency to block. The apparent cause of the blockage was that the slurry would dry in the mixing chamber and form large agglomerates that would not pass through the exit holes. The single hole atomizer would not alow a stable slurry flame to be established without gas support. The reason for this problem did not appear to be a result of poor atomization, but more a result of the slurry spray penetrating completely through the IRZ centered on the burner axis. Consequently hot gases produced from combustion of the CWS would not be efficiently returned to the IRZ, and unless a natural gas support flame was maintained the slurry flame woudl extinguish".

"The performance of the other atomizers, the normal Y-jet, the divergent Y-jet, and the T-jet were relatively satisfactory. It is difficult to select a clearly optimum atomizer from this group, as their performance was dependent on the slurry type. With 300°C air preheat and a 3/4 furnace coverage, a flame stabilized back in the quarl could be achieved without gas support with any of these atomizers. When the slurries were fired under more difficult conditions, such

REPORT CODE NO.	PAPER LOCATION	CROSS REF.	ITEM NO.	REPORT
				as with cold combustion air or without furnace insulation, or when the amount of atomizing air was reduced, then some atomizers had a clear advantage over others. The atomizer that gave the best performance over the widest range of slurry types and over burner parameters was the eight hole T-jet. In the data plotted in figures 6-13, the atomizer used was either type A, B or C; see figure 4. The trends shown in these figures were valid for any of these three atomizers, although the ignition limits or burnout levels might vary slightly for the different atomizers in this group".
				"The optimum spray angle for the Y-jet type atomizers was found to be a 25° half angle. This initially directs the spray into the internal recirculation zone - see figure 4 - and later into the forward air flow. Solid concentration measurements taken at the quarl exit, show the slurry to be reasonably well distributed in the forward flow at this axial distance. All data shown in this report, for the Y-jet or T-jet type atomizers was achieved with a 25° half angle spray".
			5	From the verbatim quote, I query the following: Why were not external atomizing types selected such as: Process Combustion Hauck, I.C.L. Vortometric Flo Sonics.
			5.1	My "hunch" is that these burners (perhaps with some modest modifications), could perform well.

6-2-85

REPORT CODE NO.	PAPER LOCATION	CROSS REF.	ITEM NO.	REPORT
			6	I further quote verbatim from the paper summary as follows: "Good atomization is certainly the first step in achieving a stable CWS slurry flame without gas support and with a high burnout. Both the slurry type and the atomizer design are important in achieving a fine particle size didstribution in the spray. Once a combination of slurry type and atomizer design has been found which produces a suitable spray, then other slurry, burner and furnace parameters, such as coal particle size, type of coal. combustion air temperaturee etc., become important". "In these experiments, Y-jet or T-jet type atomizers were found to produce the best atomization and also allow the spray to be directed into the optimum region of the burner flow pattern", "In general the slurry made with high volatile bituminous coals, and those with the finest particle size distribution gives the most flexibility regarding ignition particularly when operating without air preheat or under high flame extraction rate conditions. The same slurries giving the most flexibility regarding ignition also gave the highest coal burnout levels."
			7	The following Figs. and Tables are reproduced (some with my notations): Table 2: CWFs FURTHER NEOM/CANMET TRIALS. Table 4: SUMMARY OF CWFs COMBUSTION PERFORMANCE. Fig. 4 CWF ATOMIZERS.

6-2-85

REPORT CODE NO.	PAPER LOCATION	CROSS REF.	ITEM NO.	REPORT
			7.1	I am impelled to observe that the T-jet atomizer designs (A) FIG. 4 is dissimilar to the T-jet design shown in FIG. 8 of Report W.13. FIG. 8 W.13 shows a definite "mixing chamber" with an ensuing set of exit portals.
			7.2	The indifferent performance of the single hole design (E) FIG. 4 would infer the problem to reside in the "thicknes" of the jet. (my opinion).
			7.3	Attached hereto are copies of the following: Fig. 5 PARTICLE SIZE DISTRIBUTIONS Fig. 6 CWS BURNOUT AS A FUNCTION OF ATOMIZING AIR RATIO Fig. 7 BURNOUT COMPARISON AIR VERSUS STEAM ATOMIZATION AT VARIOUS STOICHIOMETRIC RATIOS Fig. 8 MIN. VARIOUS SECONDARY (COMBUSTION ?) AIR TEMPERATURE REQUIRED FOR UNSUPPORTED COMBUSTION WITH VARIOUS QUARLS AND WITH VARIOUS FLAME EMISSITIVY VALUES

6-2-85

REPORT CODE NO.	PAPER LOCATION	CROSS REF.	ITEM NO.	REPORT
W-21	6th 791		1	I presume that the word denseral means CWF.
			2	Stability of suspension depends on "zeta " potential to offset the Van der Waals weak and other forces.
			3.	I quote the following verbatim: "Therefore, in order to calculate pressure losses in pipelines and spray nozzles, it is necessary to determine the apparent viscosity for each shear rate. Under no circumstances should this apparent viscosity exceed 1,000 centipoise at 20°C. With regard to the maximum particle size, this 1,000 centipoise means a maximum size consist of 0.3 mm. (300 um).
			3.1	Max. viscosity in pipelines and spray nozzles should be less than 1000 centipoise.
			3.2	How did they derive 1000 CP as a realistic viscosity in the spray nozzle? They provide no data on atomizer design nor any rheology graphs.
			4.	Figure 11 is reproduced.
			4.1	Max. velocity 1 m/sec. (shear rate not given).
			4.2	Max. $\Delta P/m$ 1) at vel. of 1 m/sec. is shown to be 500 Pa (Pascals)/m = .075 psi = $\frac{.075 \times 444822}{6.45}$ = 521 dynes/cm^2/per meter length of tubing at 73% coal wt. loading. 1) /m - judged to mean per meter long tube, - dia. of tubing not given.

8-2-85

REPORT CODE NO.	PAPER LOCATION	CROSS REF.	ITEM NO.	REPORT
W-22	6th 827	X-15	1	This paper by the Carnegie Mellon University is essentially a "practical" extension of the analytical paper on rheology/viscosity which they presented at the 5th Symposium.
			2	I quote verbatim from their introduction: "Early in CWS atomizer development the solution was simply to enlarge the fuel passage of oil burners. This practice reduced blockages, but resulted in a coarser spray and reduced atomization quality. More recently, however, several groups have undertaken the design and evaluation of atomizers specifically made for slurry fuels. A third goal is to understand the relationship between spray characteristics and combustion performance. This is required in order to design atomizers with the proper spray patterns for good combustion. To date coal-water slurry atomizer design has been a trial-and- error process. Experimenters have identified which atomizers will support combustion but they do not know why. Research is required to show how systematic changes in atomizer design affect spray characteristics and combustion performance. Now that the feasibility of coal-water slurry combustion has been demonstrated it is necessary to concentrate on the process involved in atomization and combustion in order to understand and improve atomizer performance and combustion efficiency."

8-2-85

REPORT CODE NO.	PAPER LOCATION	CROSS REF.	ITEM NO.	REPORT
			3	Carnegie-Mellon are:
			3.1	Studying atomizer designs.
			3.2	Evaluating atomizer performance
			3.3	Studying spray characteristics for: droplet size and velocity distribution.
			4	TABLE 1-W-22 (with some notations thereon by me) is reproduced which shows operating test conditions.
			5	Testing rig contains a Y strainer limiting max. oversize to 20 mesh = 841 micron = .033 inch.
			6	Note: Fuel pressure is measured at pump outlet and atomizer inlet. QUES. What are fuel and atomizing air pressures at the atomizer inlet for any given atomizer design?
			6.1	Is pressure within the atomizer measured?
			7	Carnegie-Mellon's experiments to date have been made with a CWF from Atlantic Research Corp. (ARC-Coal), with nominal specified ions reproduced as follows:

Solids loading %	70
Btu/barrel	4.2×10^6
Viscosity, cps	750 - 1000
Volatiles % (dry, basis)	30
Ash Content, % (dry basis)	5.5
Sulfur content, %(dry basis)	0.7
Ash Fusion Temperature, °F	2600
Density, lb/gallon (U.S.)	10
Sp. Gravity	1.2

8-2-85

REPORT CODE NO.	PAPER LOCATION	CROSS REF.	ITEM NO.	REPORT
			8	Table 2.W.22 (reproduced/gives "Analysis of ARC CWF"
			9	The two atomizers studied are:
			9.1	Coen No. 1 MW
			9.2	Parker-Hannifin Counter Swirl
			10	Coen chosen because of PETC experience
			10.1	Parker-Hannifin being evaluated as an atomizer specifically designed for CWF.
			10.2	Design flow rate in both atomizers is 1(US) gpm = 600 lbs./hr. = 6.10^6 btu/hr.
			11	Figs. 3.W.22 and 4.W.22 show design principles of the Coen and Parker-Hannifin atomizers respectively.
			12	CWF atomizing air presure in Coen burner are each 150 psig (required).
			13	Note: The Coen design appears similat to the B&W T-jet.
			14	Ratio of exit holes dia. to max. particle size of ARC CWF = $\frac{0.156}{0.0335} = 4.66$
			14.1	Note: Ratio of mark 3 C.E. versus 400 um top size = $\frac{.192}{.0157} = 12.2$
			15	Pressures are measured by diaphragm steam guages and by pressure transducers.
			15.1	Diaphram is flush with inner surface of pipe wall to minimize possibility of slurry caking.

8-2-85

REPORT CODE NO.	PAPER LOCATION	CROSS REF.	ITEM NO.	REPORT
			16	Dimension and distribution of droplets resulting from atomization, is obtained by still & high speed movies photography. Strobe light source used for still photography and a continuous light source (Pallite and/or Koolbeam lights) for Hycarm high speed camera.
			17 ✓	Recommended condition for both atomizers are ~~500~~ psi CWF and 175 psi atomizating air.
			17.1	Figure 6.W.22 & 7.W.22 Show spray patterns for the Parker-Hannifin atomizer at 48 and 45 psig for the CWF and atomizing air respectively for Fig. 6,and 72 and 162 psig in Fig. 7. (N.B. Compare with item 17!)
			17.2	The increased CWF effluent break at the higher atomizing pressure is evident, as is the smaller size of the droplets at approx. 25 mm from burner tip. (approx one inch)
			17.3	The particle size in Fig. 7 is of the order of 15-20 um and the estsimated value in Fig. 6 is 30-50 um.
			18	Figs. 8.W.22 to 9.W.22 shows the spray conditions at 175 psig atomizing air pressure at nozzle exit and at 1 inch from nozzle, respectively.
			19	I query why the CWF pressure increased from 48 to 72 psig.(from Fig. 6 to 7)
			19.1	Is this due to: a) viscosity variation due to shear rate effect in atomizing annulus which in turn could be, 1- a function of dilation effect in rheology mode 2- variation in consist in the CWF.

8-2-85

REPORT CODE NO.	PAPER LOCATION	CROSS REF.	ITEM NO.	REPORT
			20	Fluctuations (or pulsations) were noted. Presumably there are pulsations of: a) mass flow or b) exit velocity.
			20.1	Variation in "coal particle packing" function due to high shear rate in the atomizers could be a reason.
			20.2	Variation of exit velocity could also be due to variation of the atomizing air pressure and consequent variation in specific volume.
			21	Fig. 12 shows atomization from the Coen atomizer at 175 psig.
			22	Measured velocities (average) of 50 - 100 m/s (164-328 f/s) were observed at 175 psig. (? Coen atomizer - ?) for water.
			22.2	CWF velocities were17 m/s (55 ft/s) and 40 - 50 m/s (131 - 162 ft/sec.) also psig & 175 psig atomizing air respectively.
			23	Flow rate in all tests was held at 500 lbs/hr.
			24	Pulsation rate in CWS varied from 50 Hz at low atomizing pressure to about 71-110 Hz at high atomizing pressure.
			25	Pulsation cause clusters of CWF droplets.
			26	Numbers of coal particles are held together within the CWF droplet. The coal particle could agglomerate (and so require increased residence time.)
			26.1	If agglomeration occurs, "micronized" CWF is not worth the cost.

8-2-85

REPORT CODE NO.	PAPER LOCATION	CROSS REF.	ITEM NO.	REPORT
			27	The investigation of the CWF spray, at and near the nozzle, will be done by laser techniques in which light guides will penetrate the spray.
			28	The relation of droplet and coal particle quantitative data will be related to combustion performance.
			29	The paper concludes with the statement that the effect of preheated air will be studied only of the combustion air - not with the atomizing air, to avoid plugging problems in the nozzle.
			29.1	Ques. What would be the mechanisms of plugging due to heated atomizing air?
			29.2	NOTE: Consider the proven use of steam as the atomizing fluid.

Volume

3

VOLUME III
DSS OSQ 84-00233
CLM STUDY
PHASE II

431 pp

FLORIDA LIGHT & POWER CORP.

JUNO BEACH, FLA.
DR. KEN OLEN

Oct. 28, 1985

1. On enquiring as to progress by FPLC, on CWF application, Ken Olen said the CWF R & D work was (at the time of telephone call a "dead horse".

2. However, as in all meetings and telephone discussions, Ken very kindly (and much appreciated by me) proferred the most recent development news that had come to his attention.

3. The Sanford plant had been on COM for 1 yr. until this was removed and the boiler (s) returned to their original oil burning status.

4. The preferred parent coal for CWF, was considered to be a metallurgical quality:
high BTU; high volatility; high free swelling ;
high free swelling factor.

5. In flame, coal particles (those remaining in drops), will tend to dry, swell and fuse).

5.1 200 um coal particles may survive flame.

5.2 (R.G. note) Assuming flame continues to end of spray, see Tables G.9.1 and G.9.2 to determine expected dropsize and therefore particle content, and relation of fuel spray axial distance to calculated burn-out length for various drop sizes entering flame front.

6. B & W preheat CWF to 150° (then they cannot be worried about additive deterioration. In this regard to B & W have stated they do not use an additive - but obtain stability by grind size limits and % size dispersion through the CWF (e.g. the Funk distribution (B.1).

7. Ken had noticed that the CWF resulting from the ICL atomizers did not form a homogeneous spray with the atomizing air. It was necessary to control velocities to provide "toroidal" recirculation just outside of the spray cone to a distance of 12" from the nozzle.

8. The MIT research paper whose data I have been using for comparison to my numerical analysis was sent me by Ken. (This comparison led to the thought that a flame velocity of 400 cm./sec. could be considered, proving an overall reduction in burn-out length as given in

---

9. Ken is also of the opinion that the dropping of R & D on CWF does sufficiently recognize the potential for harm from dependence on the Persian Gulf.

T-2

HAUCK MANUFACTURING CO.

LEBANON, PA.

Mr. Neal Robertson

Oct. 23, 1985

1. Jack Marino (one time Vice-President) is no longer with the Hauck Manufacturers.

2. The Hauck Mfg. Co. secretary, Mrs. Baumgarten, put me in touch with Mr. Neal Robertson, who is their applications engineer (formerly a Hauck Mfg. Sales Rep.)

3. Neal is not an atomizer designer.

4. He definitely stated that Hauck were not doing any work with CWF.

5. He referred me to Chuck Lauer of Coal Liquid Co., Louisville, Kentucky, with whom they had worked on an Israeli project to burn COM (See my report on Coal-Liquid Co. (T - 3)

6. They had one experience with a Hauck cup burner with CWF, at 20.10^6 BTU/Hr. in a Mississipi project.

6.1 The results were "not conclusive".

---

7. Hauck (i.e. Robertson?) fear that the pressures used in a Hauck would be (or are) inadequate for CWF, and they also fear the erosion problem.

8. Robertson made reference to a CWF manufacturer in Otisca, Syracuse, N.Y.

9. The omens here were definitely negative.

T-3

COAL LIQUID CO.

LOUISVILLE, KENTUCKY

Chuck Lauer

July, 1985

---

1. Coal Liquid first entry into the coal liquid mix business was for a 14,000 pph 3-pass firetube boiler.

2. This was a joint project with an Israeli company, who subsequently bought out Coal Liquid Co.

3. A Hauck burner was selected of the open cup single hole design.

4. The fuel was a 50:40:10 COW, with no additives, and the results were "very satisfactory".

5. The coal was ground then mixed according to a "Patented process".

6. The boiler dimensions were 39" dia. by 18' - 20' long.

7. The process load required a high turn-down and Hauck put forward a 5:1 T.D. ratio.

8. Coal Liquid have no commercial experience with CWF.

---

9. A "lab test" proved inconclusive.

10. They seem involved in producing a beneficiated COM.

11. Chuck stated they were involved at Iron Ore Co. - using a Verloop burner with COM.

12. Verloop have replaced rotary cups and Eclipse in various cases.

13. Chuck commented favorably on the Coen burner and its "2-stage" emulsifying design.

14. It seems Coen has been used, with CWF, in a utility plant in South Carolina.

PROCESS COMBUSTION CORP.

PITTSBURGH, PA.

Peter Nutcher

Oct. 1986

---

1. Process Combustion had converted a 200.10^6 BTU/ Hr phosphate dryer for American Cyanamid, using a 40:60 COM supplied by Comco.

2. Process Combustion had made no guarantees, - their involvement was only the burner equipment and the start-up. American Gyanamid installed their own auxiliaries.

3. Flame appearance was the same as with oil only.

4. The Process Combustion burner was not the Vorter Cup on which I reported in Phase I - but was a "modified" Bloom.

5. Peter had no hard data on A/F ratio or % carbon conversion, or flame dimensions (or was not in a position to give them to me.)

6. There was no data on coal grind consist under 200 mesh.

7. Peter believed that the only market for COM or CWF would be the utility industry where the boilers were oil designed.

7.1 But "Nobody was doing it" (said Peter Nutcher).

8. Industry, generally, had no interest in conversion to CWF Technically, a 100.10^6 B.T.W. boiler could be converted but a big problem was ash deposition and removal.

9. In my report of 1983 (Phase 1) I was enthused with the possibilities for COM/CWF firing with the Urquhart Vortex Cup atomizer (and I so reported).

10. The only "come on" that Process Combustion received was from C.E. - but they would not pay for the equipment,hence "no deal". (Despite EPRI & DOE sponsorship.)

T-5

FLORIDA POWER CO.

Mike Higgins

Oct. 28/1985

1. Florida Power Corp. will not be involved in R & D for CWF application "at present", due to low oil cost economics.

2. When their present COM supply contract runs out, F.P.C. will return the Bartow boilers to straight oil.

3. This decision to use oil, instead of P.F. was influenced by the 2-year period required to convert to P.F.

4. The Bartow boilers were designed for coal-oil-gas.

5. The F.P.C. Crystal River plant is now on coal, and will stay.

6. Their Anchlate Key plant was designed as an oil plant only. There is no space for coal for P.F. Presumably this plant could be a target for CWF, when and as economics and commercially successful CWF atomizers concur.

T-6

PEABODY ENGINEERING CORP.

Stamford, Conn.

Ray Frauenhofer

October 29, 1985

1. Peabody had not done R & D to adopt their atomizers to CWF. (Some R & D had been done by the Paul Bartow plant of the Florida Power Co., Tampa, FLA.

2. Two Peabody tips for CWF use had been provided by the Peabody Boiler Group (Frank Gullo) to MIT and G.E. Research groups.

3. These tips were the "bullet nose" type rated at 3.10^6 BTU/Hr..

4. Hard data from operation were not available. "General" satisfaction had been expressed, except for an erosion problem.

5. Ken Frauenhofer stated that the F.P.C. Bartow plant had returned to original Peabody bullet nose design, with replaceable alloy steel inserts made locally. (Tampa).

5.1 It was found by FPC that even with the more frequent replacement,that use of alloy steel inserts was cheaper than tungsten-carbide. (The fuel was a COM.)

6. Status of CWF R & D at Peabody Engineering - NIL.

T-7

NORTH AMERICAN MFG. CO.

Cleveland, Ohio

Mr. Geisendorfer

Nov. 1, 1985

1. I made contact with Mr. Bruce Geisendorfer who was involved in burner application work.

2. It seems that Mr. Jas. Watson, R & D Chief, had not gone ahead with any new atomizer development for CWF, as he implied in my meeting in Cleveland on October 14, 1982.

3. Mr. Geinsendorfer did refer to some equipment furnished to Canmet (Kelly Thambimuthu.) This was a North American Tip Emulsion burner No. 6526-70-43. He was not sure of type of application or location of test (made in 1983), but had heard of favourable results.

4. A report on the above test was expected in early 1986.

5. North American expect to "do something" in 1986 to fulfill a "promise" to (some) slurry manufacturer.

6. Two North American emulsion tips (in series ?) had been tried in a job in Sept Iles where Atlantic Research were involved).

T-8

JOHN ZINK CO.

Tulsa, Oklahoma

Dr. Richard Waibell

Oct. 29, 1985

1. In Dr. Waibell's letter to me dated August 9, 1983, (included in Phase 1 work) he had stated "John Zink Company is currently engaged in a program to develop an atomizer/burner for petroleum coke/oil mixtures "- These projected designs were considered to be applicable to coal/water mixtures.

2. When I called on October 29, 1985, Dr. Waibell said that they had not proceeded further with this work.

3. He spoke of an application of large COM burners, rated 190, 10^6 BTU/Hr., of internal mix design,using compressed air.

4. The application was on a phosphate dryer 30'-40' long and 12' dia.

5. The tips were fabricated of titanium carbide for which the life expectancy was 6 months.

6. The fuel was supplied by Comco and the size consist was 100 mesh top size (149 um) and bottom size 5 um.

ARCO PETROLEUM PRODUCTS CO. (Harvey, Ill.)
DR. FRANK CHLOPEK
ex Manager Planning and Business Development

Sept. 1985

1. The "ex" in ex manager means that Arco Petroleum Products Co. have closed down their CWF R & D operation completely, due to the oil price situation. Dr. Chlopek did not know when and if they will reopen the CWF program.

2. Since my meeting in October, 1982, (reported in Phase 1, Section 18) there had been, it seems, no substantial progress in the understanding of CWF performance per se (viscosity, characteristic mode) nor in the correlation of CWF rheology and atomiser type or design.

3. However, Dr. Chlopek said that some research would be carried on in a process plant of Atlantic Richfield oil in Los Angeles, CA., and he referred me to a Mr. Tom Clough, who was involved in Corporate R & D,(Tel. No.: 213-986-1980)

4. It seems they are involved in the spray drying of a catalyst named "Katalco"(by Nalco in Chicago).

5. Reference was also made to a company named Engelhard who dealt in noble metals and produced catalysts.

6. Dr. Chlopek thought that our experience in atomizing CWF could be applicable to spray drying.

T-10

NATIONAL RESEARCH COUNCIL

OTTAWA, ONT.

Kevin Jonasson

August 17, 1985

1. I discussed the general progress N.R.C. had in mind for the further development of the Flo-Sonics basic atomizer.

2. At the time of my call Kevin could not give me any specific details of design progress.

3. He did say that N.R.C. were planning a research setup for the fall of 1985 in which basic parameters for atomizer efficiency,(study and experiment) would be undertaken

3. This effort would cover observations on
   1) Drop Size; spray formation and (possibly) combustion conditions (including presumably efficiency of carbon conversion).

4. On fundamental fluid dynamics, he advised that pressures upstream of the nozzle in excess of critical would be carried into the furnace, and expressed as a density values which result in the development of shock waves reflected back into the spray formation.

---

5. An excess of turbulence could result in coalescence of drops. (This thought is in accord with my stratagem of using a 15° divergent nozzle to guide the expansion of the atomizing steam.)

6. An effort would be made to secure an atomizer of transparent material (unless this were to be undertaken by Neil Stover at Nova Scotia Research Institute.)

7. NRC had appointed CLM Technologies of Halifax as a licensed dealer for the N.R.C. atomizer (interested parties are Dave Burnett and Ken Burrell.

8. It seems that CLM Technologies would not have a fuel tie-up.
1) Other NRC "Campus" facilities would probably be in the research program picture, particularly in the realm of fluid dynamics or laser technique for measuring drop size.

T-11

ATLANTIC RESEARCH CORP.

ALEXANDRIA, VA.

Dr. E. McHALE

July 25, 1985

1. In July, 1982, I had met with Dr. McHale and had an extensive and useful discussion on their development of ARC CWF fuel, and a semi-commercial burner to test the combustion characteristics of their CWF product, in their own lab.

2. They did not involve themselves with other atomizer designs to ensure wide scale compatability with numbers of burners.

3. They considered that burner manufacturers would adopt their design to their (ARC) CWF.

4. Dr. McHale stated that in some of the tests made by Dr. Chigier of Carnegie-Mellon with a Parker-Hannifin burner, that ARC CWF was used.

5. Photographs of the sprays were made by Dr. Chigier (and/or his assistants),

   (See "Atomization of Coal-Water Slurries" by N. Chigier and P.L. Meyer - in Proceedings of the Sixth International Symposium on Coal Slurry Combustion and Technology - Orlando, FLA. 1984 (Page 827)

---

6. The spray photographs were chiefly a mass of black blobs with none orlittle resolution of the drop formation.

6.1 The explanation was that the drops formed were so fine that with the photographic techniques used, the "fineness" caused an opacity and so resulted in no drop discrimination.

6.2 It was intended (said the authors) to introduce laser light into the "amorphous" exit CWF jet to secure a means of drop resolution.

7. Dr. McHale said "millions of tons" of CWF had been used (presumably in commercial boilers of utilites - if millions.)

8. Dr. McHale could not (or would not) give me a statement on the Ø max. value of his CWF, on which an estimate of viscosity could be determined from Equations in reference X.2.

9. Dr. McHale said that he would provide ARC CWF of varying viscosities "to suit user requirements".

10. When I queried the reason why a higher viscosity would be selected, instead of a lower viscosity (which would require less pumping power and presumably lead to a better atomization) and higher carbon conversion efficiency) - I was stone-walled.

11. He further stated that "some" large users were considering full conversion based on equipment suppliers "quarantees" (?).

12. My final point of discussion was a request to receive rheograms of the various ARC CWF fuels.

12.1 The answer was yes - if - officially requested by a potential user with intent to place a contract.

13. Did not Canmet have an experience with ARC CWF?

CONAMARA LTD. (Vortometric)

RICHMOND HILL, ONT.

RICHARD FULLELOVE - Chief Engineer

---

1. Conamara have done test work with CWF on cold and hot test chambers.

2. Conamara were involved in an observer/consultant capacity on CWF tests made on a pelletizing furnace for Iron Ore.

3. The two burners tried were NRC (Flo-Sonics) and Keeler External Air Atomizing.

4. Both burners gave reasonable performance but Fullelove stated that the URC burner "appeared" to have a better flame.

5. He had no data on % carbon conversion, nor on actual flame geometry or heat transfer characteristics.

6. % excess air was in the order of 26%.

7. Conamara's R & D will emphasize COM.

8. They expect (hope ?) to have their own burner tried by Iron Ore Co.

T-12

CONAMARA LTD. (Vortometric)

RICHMOND HILL, ONT.

RICHARD FULLELOVE - Chief Engineer

---

1. Conamara have done test work with CWF on cold and hot test chambers.

2. Conamara were involved in an observer/consultant capacity on CWF tests made on a pelletizing furnace for Iron Ore.

3. The two burners tried were NRC (Flo-Sonics) and Keeler External Air Atomizing.

4. Both burners gave reasonable performance but Fullelove stated that the URC burner "appeared" to have a better flame.

5. He had no data on % carbon conversion, nor on actual flame geometry or heat transfer characteristics.

6. % excess air was in the order of 26%.

7. Conamara's R & D will emphasize COM.

8. They expect (hope ?) to have their own burner tried by Iron Ore Co.

CARNEGIE-MELLON UNIVERSITY
CHEMICAL ENGINEERING DEPT.
PITTSBURGH, PA.
MRS. ETHEL CASSASSA

Oct. 9, 1985

1. In the 6th Symposium, 1984, page 251, there is published an article entitled "The Effects of Surface Active Agents on Coal/Water Slurry" by (Mrs.) E.Z. Casassa (N.B. Mr. Edward Casassa, husband, is with the polymer chemistry division of Carnegie-Mellon.)

2. This paper is summarized in my report W.6 and is an extension of work published in the 5th Symposium, summarized in my report X.15.

3. These papers represented, in my opinion, a definite effort to obtain basic (physics) knowledge of the flow viscosity, factors in a CWF.

4. I was thereby intrigued to contact Mrs. Casassa to find out their knowledge status on atomization and spray formation.

5. Regretably, the work of Mrs. Casassa and her group was centered on CWF rheology only, and she was not knowledgeable about atomizers and atomization, and was not actually aware of the work on CWF sprays done by the Mechanical Engineering Dept. of Carnegie-Mellon.

6. I discussed the mode of work in which I was involved and offered to send copies (see copy of my letter to Mrs. Casassa dated Nov. 6th, 1985.

7. She welcomed this and said that evidence that other people (Canada) were working in this field, would give evidence that Carnegie-Mellon "were not alone" in the pursuit of fundamental knowledge, which would help fund raising for C.M.

8. Finally, Mrs. Casassa said she would try and contact Pat Meyer.

9. To date, no communication from Carnegie-Mellon.

BABCOCK-WILCOX CO.

RESEARCH DEVELOPMENT DIVISION

ALLIANCE, OHIO

MR. STAN BECCI

Nov. 1986

1. Stan Becci, of B & W Research, called me to find out if I could, in any way, advise him in the burner selection, thinking for the Charlottetown test.

2. I, of course, replied that I knew nothing (which I didn't) and that such information as available would have to come from you (Horace Whaley .)

3. Stan did bring up one fact though, that be believed that the Carbojel CWF was temperature sensitive and could I have this confirmed.

4. This I confirmed.

5. I phoned you about this and you affirmed, the temperature sensitivity.

6. I must have obtained an O.K. from you (at least I hope I did) to advise Stan Becci about this.

7. This discussion led to the formulation of my paper G.5 entitled, "Discussion on Temperature Tolerance of a CWF".

New Brunswick Electric Power Commission
Fredericton, N.B.
Mr. David Rankin, Manager Tel. (506) 458-4444

9-4-86

1	The last atomizer (latest design) based in the 22 Mege boiler at Chatham was not significantly different from the earlier design.
1.1	The main points of change in atomizer design was in the CWF and steam annulus sizing.
2	However, in the last test -(November 1984) there was significant change in the register design of the combustion air system.
3.	An important cause of the high (too high) carbon loss was the inconsistency in fuel homogeneity due to :
3.1	Grind variations.
3.2	Additive volume variations.
3.3	Ageing.
4.	Atomizing steam pressure was 200 psig - 400°F.
4.1	C.W.F. Temperature ambient.
5.	The CWF fuel does heat up before exiting.
6.	Dave Rankin believed that steam not condensed is retained as bubbles in the C.W.F.

6.1 (In dearators steam and water do not mix fully).

7. This can be harmful, (especially in the case of desuperheaters where the reverse condition of cooling water not being fully evaporated - can be harmful to the turbines).

7.1 The answer to such problems is to increase the water flow velocity.

8. Dilatancy effect can occur at shear rates above 2000 sec.$^{-1}$ (IF) the grind (and presumably the size consist and uniformity of distribution) is not right.

9. An increase in bottom fines and in the top size of the coal grind spectrum, increases the dilatancy effect.

10. A change in proportion of the additive can also be a factor, causing dilatant effect.

11. Pressure and velocity were also factors.

12. With regard to the NRC performance in the No. 1 11 Mege boiler, the apparent need was for improved register vane design for swirl control.

12.1 The NRC atomizer was used in the Forney register.

---

13. The NRC operation was "good and bad", i.e. not constant.

14. The problem could have been in the variation in Carbojel Quality due to: a) inhomogeneity;
b) fluctuations in liquid content;
c) Setting of the coarser coal particles (prior to use).

15. The CWF was known to adhere to the walls of the storage tank.

15.1 They will be installing a mixer in the storage tank at Charlottetown.

16. Dave Rankin's assessmeny of "available" atomizers was: C.E., B. & W., and Coen; with N.R.C. coming up.

T.16

CHATHAM PLANT of the N.B.E. P.C.

Jack Flanagan - Steam Plant Superintendent
Keith Keoughan - Steam Plant Supervisor

Tel. (506) 773-9486

10.4.86

1. Dave Rankin had O.K.'d my request to speak to Don MacDonald of Chatham.

2. Don was not in and I was put in contact with Jack Flanagan, who was most affable but because he had been at the Chatham plant only six months, suggested that I speak to Keith Keoughan, who was very knowledgeable, and he would arrange to have Keith call me the next morning.

3. Keith called and a most useful discussion followed during which I received much valuable information on the Forney and N.R.C. trials.

4. The test conditions were originally 100% load (11 mege) to be obtained at 100 psi air and 80 psi CWF.

5. Under these conditions Forney could only achieve 50% load.

6. By increasing air and CWF pressures to 112-118 psi; and 125-130 psi, respectively and changing the coal/water ratio (weight) from 70/30 to 67/33, Forney were successfully in obtaining 10.7 Mege (the boiler is now rated 10 Mege.)

---

7. The flame appearance was "good", and improved as furnace temperature increased.

8. 100% load was held for 2-3 hours.

9. The flame length approached the rear boiler (approx. 14 ft.)

9.1 It is interesting to compare this flame length with each Forney gun firing at approx. 5.10^6 BTU/hr. compared to a single C.E. Annulus of approx. 10.10^6 BTU/U (app. 4.R. Add.2) - requiring a minimum of 15.8 ft. for a 720 um particle (cohered) or a minimum of 12.25 ft. for a "standard" max. size particle of 375 um. (lengths based on a drop formation rate of 3000 per- .015 sec.
- See G.9 and Tables G.9.1 and G.9.2)

10. Keith mentioned that there were "sparklers" in the flame through the load ranges tested.

10.1 An interprotection of "sparklers" could be large size burning char particles - or char particles that had escaped the main flame body. Both possibilities could result in carbon loss.

11. The viscosity of the Carbojet was 700-850 centipoise.

12. With a 68/32 mix and air and CWF pressures of 90-94 psi, and 80-88 psi, respectively, 100% load was attained.

12.1 The limited compressed air capacity caused an air pressure drop as the firing increased to 100%.

12.2 With oil assist, the carbon carry-over was reduced.

13. (There was an "interesting" experience when Forney experienced a compressed air block because the protective plastic inner film in the pipe had not been cleaned out.)

14. The amount of unburned carbon in ash was 65%-90%.

14.1 The stock effluent "seemed" clean but there was carbon pollution in the stack exhaust as the plant received complaints from neighboring buildings.

15. Keith's (rough) estimate of carbon loss was 10%-12%.

C.E. on Boiler No. 2

16. Keith could not obtain a "feel" for the 'Quality' of the flame - because of the centre fire-ball.

17. The flame could only be "quasi good" because, carbon conversion must have been poor as evidenced by:

17.1 Carbon/ash on furnace floor had to be sluiced off three times per day.

17.2 Dust collectors had to be cleaned daily.

18. In the last trial with "later generation" C.E. equipment there was some improvement but nevertheless:

18.1 Operation could not proceed beyond 9 hours without oil assist.

18.2 Without oil assist: the fire became unstable to the point of causing fear in the operators, and there was unburned fuel.

19. Keith considered an (important) factor in this unsatisfactory performance was the Carbojet quality, (lack of quality control).

9.11 He believed that this may have been occasioned by pressure to push up production rate too rapidly.

N.R.C. on No. 1 Boiler (11 Mege)

20. An admired feature of the N.R.C. atomizer was the ease with which the operation could be switched from Carbojet to oil.

N.R.C. continued

21. The ceramics of the atomizer stood up well.

22. 100% load was attained with the N.R.C. atomiser - but - a bag house was required to contain the carbon/ash efflux. (Prior to bag house installation, the stack exhaust was "black".

22.1 The bag house, however, was suitable for only 30% load operation.

22.2 But even with this bag house plus modification of the Forney combustion air register, air pollution could not be reduced to the point of avoiding complaints from surrounding buildings of the carbon/ash fallout.

23. Need of avoidance of air pollution complaints limited NRC operation to 20% load.

SKI ATOMIZER

1. This(seemingly) is a Lezzon type atomiser.

2. The CWF tube of this burner is water cooled.

3. Nevertheless the burner gun experienced "expansion".

4. Ability to burn CWF was indicated, but in Keith's opinion the design scale-up (to meet field specs.) was too great.

5. More R & D for this unit seems required.

6. (There is a paper on the Lezzon burner available from the authors: Casey, Todd, Thambimuthu and Walsh, of Canmet, and available from TUNS.)

T. 16 Addendum 1

Further Discussion with Keith Keoughan

April 14,1986

1. On the No. 2 22 Mege Boiler C.E. achieved an output of 19.6 Mege with a fuel rate of 31710 lbs./hr. (versus a predicted fuel rate of 24,000 lbs. /Hr.)

2. Much carbon/ash was deposited on floor requiring sluicing 3 times per day.

3. The Venture Cyclone dust collector required clean-out once per day.

4. The carbon content in the ash was:
    Wet floor - 57%
    Dust Collector 79%

5. Fuel/Water ratio of the Carbojel was 68.5/31.5

6. One efficiency test gave an efficiency of 65.7% (heat loss method)

7. Estimated (Keith) top efficiency – 70%

8. Trouble was experienced in the Carbojel fuel handling system (viz.: valves, controllers).

9. The particle loading of the Carbojel had a strong effect on atomizer efficiency.

9.1 Implications of "particle loading" effect were: size range, consist. water ratio.

10. Chatham fuel handling system includes a recirculation to: (tank or pump suction).

10.1 As recirc. progresses original fuel consist breaks down and CWF viscosity drops from 800-900 Cp to 650 Cp.

11. When fines content in Carbojel, increased too much (due to recirc.) the CWF would issue like "shit through a goose".

12. Also when an excess of fines was created the fines/coarse coal ratio disturbance, affected atomization quality.

13. Oil assist L.O. ignition for stable firing was needed on at least one gun for "normal" operation.

13.1 Out of 677 hours of operation only 9 hours (during test)were on CWF ~~only~~ without L.O. assist

14. I gathered that without some L.O. assist the flame could (and did) become unstable with resulting pulsation – causing fear in the operators.

15. The L.O. assist ignition was used in normal operation on only one of the four guns at a rate of 18 gph (presumably U.S. gph) or approx. $2.5.10^6$ BTD./hr.

16. It was not found possible to meet Provincial Standards on stack exhaust gas opacity.

17. When the No. 1 boiler was equipped with a 30% capacity baghouse, the NRC burner nearly met the Provincial opacity regulations.

18. To ameliorlate fallout problems on the No. 1 boiler (with N.R.C. burners) one of the top burners would be put on bunker oil to serve as a carbon burn-out medium.

19. In the initial periods of Carbojel use, the fuel was inconcistent in sizing and size distribution quality causing many operating problems.

20. The Carbojel problem seems to have been one of inadequate quality control.

21. Quality improved and was O.K. following approx. March 1984.

22. Following this improvement in Carbojel quality oil was only used to heatup a cold boiler.

23. Keith made an interesting observation that bacterial action in the additive caused coal particle settlement.

24. I report a final remark by Keith (doubtless known to H.W.) that the No. 2 boiler would be replaced by a Fluidized Bed Boiler to burn Minto Coal and (or?) Oil Shale, with a rating of 210,000 pph.

24.1 It was considered that the calcium in the oil shale would reduce the % SO_2 in the effluent to the necessary low level to meet air pollution standards.

24.2 Limestone would be injected if additional SO_2 reduction was found necessary.

25. The F.B. design would keep the fuel bed temperature down to 1560°F, thereby allowing the use of the low F.P.A. Minto coal. CWF was last used at Chatham about March 5, 1986.

T-17

M.B.B. MECHANICAL CO.
Halifax, N.S.

Mr. David Burnett & Mr. David Lawrence

April 22, 1986

1. The N.R.C. design base burners used by MBB are made by CLM Technologies Co.

2. M.B.B. use a fixed gap design, (whereas N.R.C. has a variable geometry exit gap) for reasons of simplicity and avoidance of problems due to "adjustment" of the gap.

3. Their particular boiler experience was in a B & W package boiler at the Canada Salt Co., Pugwash, N.S.

3.1 The N.R.C. fixed gap unit was rated $10\text{-}15.10^6$ BTU/Hr. (Limit of capacity of this particular atomizer unit)

4. The fuel used was a Carbojel CWT beneficiated to 1.5% ash.

4.1 There was little if any ash deposit within the boiler. The ash exhausted with the stack gases.

4.2 It is presumed from this, that the beneficiation process reduced the ash size to low micron values

5. The test in the package boiler was short, only 7000 gallons of CWF were fired) or approx. 84,000 lbs. (Imp. gals. assumed)

5.1 At a firing rate of 10.10^6 BTU/Hr the test directive is calculated to be:

$$\frac{84{,}000 \times 10{,}000 \times .7 \text{ (eff.)}}{10{,}000{,}000}$$

= approx. 60 hrs.

5.2 The % carbon conversion was not obtained.

6. A problem experienced was the drying of the fuel in the burner gun section passing through the wind box due to the 400°F of combustion air preheat. (There is no limit to steam quantity for heat transfer, as there would be in a CWF/steam emulsion due to saturation pressure equal to CWF pressure attained from the limited amount of atomizing steam.

7. It seems that preheated air was an essential factor for flame stability.

7.1 The problem was solved by providing the gun with a water cooling jacket.

8. There was no evidence of coalescence, provided that CWF and atomizing steam pressures were sufficiently high.

9. Flame stability also required suitable register design with proper relationship of primary and secondary combustion air.

10. With conditions 8 & 9 adjusted to give good gas re-circulation the flame was established close to the burner tip.

11. Dave Burnett did not think that cold test observation of the atomizer only could yield significant data because:

11.1 Effect of primary and secondary combustion air were absent.

11.2 Hot gas recirculation was absent.

12. The M.B.B. (N.R.C.) atomizer was used in a "multiple ash test" of the Carbojel CWT.

12.1 (I had not known that Carbojel had this capability of varying their CWF specification.)

13. Dave Burnett is not planning to proceed with R & D on further commercialization of the N.R.C. burner (his fixed gap design) over an increased range of sizes - at least for the present, due to the stagnant market for CWF applications.

14. (It would be interesting to know if Bill Thayer of N.R.C. has developed a special register system for the N.R.C. atomizer.)

REPORT OF MEETING WITH

GEO. FARTHING
SENIOR RESEARCH ENGINEER
B & W RESEARCH DEVELOPMENT DIVISION
ALLIANCE, OHIO

July 7, 1985

---

1. The main purpose of this meeting was to exchange as much fundamental and technical information as possible for the mutual benefit of Canmet and B & W.

2. When two fluids are applied to a common annulus, chamber, or port the pressures are not additive – the higher pressure will dominate the flow phenomena.

3. In this regard George said that B & W, R & D will be:

3.1 Determining pressures at steam entry, fuel and exit points of their T - Jet atomizer.

3.2 They intend to study the design requirements of increasing pressure in the mixing chamber.

4. Geo. agreed with the generality of my Appendix 8 (Vol. 11) that a CWF could not be dried by saturated steam atomizing fluid, because there would be established a point of temperature/ pressure equilibrium between steam to fluid.

---

5. B & W will be giving consideration to the viscosity equation published in various papers in Symposia 5 & 6. (I had extracted these in my various Appendices and established some correlations in Appendix 9 (Vol.11)

6. It was believed that cohered (agglomerated) coal particles in an annulus originated from the gel action of certain additives added to the CWF to optimize stability in its storage tank.

7. It was considered that the minimum ratio between annulus diameter and max. particle size (agglomerated size) should be 3:1.

8. CWF, as manufactured, is not a "conglomerate" of separate drops but is a true liquid in which the coal particles are suspended and flow with the fluid (but with some tendency to settling).

9. The internal tension in a droplet formed at the exit orifice will be equal to the pressure in the annulus flowing stream. (This supports the hypothesis of drop formation within an expanding (divergent) nozzle in my paper G.1.)

---

10. The nature of a "liquid" is a complex matter involving: Van der Waal attraction forces; ionic forces due to the ovoid structure of an H_2O molecule creating a positive charge at one end. (A more detailed picture is given in "The Fluid Phases of Matter" by J.H. Barker and Douglas Henderson, published in the Scientific American - Nov. 1981).

11. The B & W CWF has a viscosity of 200-250 centipoise.

11.1 This is compared to a value of 63 centipoise using the Funk average Ø max. of 2.5% with a 70 wt. % CWF corresponding to 64% coal by vol.

12. A pressure test will be made to determine min. press. in the mixing chamber.

13. The heat transfer rates for the condensation of steam (items 2 & 2.1 of Appendix 8), should be verified.

14. I put forward the need of making tests to obtain the following data.

14.1 Atomizing steam pressures, and CWF temperatures at the following points:

.1.1 just above CWF inlet.

.1.2 at end of annulus

.1.3 in mixing chamber

15. Data of item 14 will give a precise picture of heat transfer, for the flow time through the atomizer.

16. Even only knowledge of CWF temperature[1] at inlet and at exit of the atomizer can give significant accuracy in the heat transfer rate, and would be very useful for design of length of annulus and design of mixing chambers.

---

[1] For a given flow rate.

M-1 ADDENDUM 1

TELEPHONE DISCUSSION WITH GEO. FARTHING

---

1. This discussion was essentially a continuation of our meeting in Alliance, Ohio.

2. The "gel formation" of the additive used as a storage tank CWF stabilizer was not in their (B & W.) practice.

2.1 B & W used an anionic (non polymer) type additive, in just sufficient quantity to maintain stabilization.

3. The CWF passing through to the atomizer contained only this anionic additive which was not temperature sensitive.

4. B & W use only steam as the atomizing fluid and therefore (my opinion) the CWF must be 300°F or more (50 psi or greater pressure.)

5. Geo. Farthing said a non-Ionic type additive such as the polymer type additive used by Carbojel, had a large molecule structure which " balled up" at temperatures above a relatively low value. (50° C)

---

6. The anionic additive used by B & W created a negative charge on the particles which caused repulsion and so dispersion.

7. Interestingly enough, B & W, said Geo., tried Carbojel in their plant in their standard T-Jet atomizer and it worked well (So, why were they worried re Carbojel use at Charlottetown?)

7.1 Though George did admit that plant trial success did not necessarily guarantee success in the fields. (They have overcome this phenomenon, said George. But how?)

8. Geo. Farthing said I could quote him in the following: "Nova Scotia coal could be used to make a CWF using the B & W proces under licence" and that such CWF would be free from low temperature tolerance.

9. I questioned George about the Dupont Memphis test in September, 1983, where 75% excess air was experienced.

10. The high excess air was due to the fact that only 3 of the boiler's 5 burners were converted to CWF and the inoperative two units could not be made adequately air tight under the 10" plus W.C. pressure required to provide adequate swirl for the CWF burners.

---

11. The atomizing fluid of Memphis was air but B & W now use steam.

12. The A/F ratio at Memphis was .25, but the current B & W standard is .15.

13. The current excess air standard is 20% (The Memphis operation was at 400° F.).

14. I should add that Geo. was not aware of the statement in the 6th Symposium report (page 497) "A second generation of utility-sized burners is required with better performance and reliability."

14.1 It would seem that there has been no radical change in the B & W T-Jet commercial burner.

15. I queried Geo. on the question whether dilatancy could be a result of (high) drag caused by the coal structure and high shear rate. He answered that this could only occur where the CWF flow was under high ΔP i.e. (very) high velocity. In standard pipe sizes and "standard" flow ratio (say a ΔP of 150 psi in a 2" pipe of under 500' (say) length, drag would not be a significant factor.

---

16. The pressure test mentioned in B & W meeting report M.1 was actually based on the need of determining whether the low (relative) pressure of a boiler they wished to convert to CWF firing would allow satisfactory atomizer operation.

16.1 It did.

17. Geo. said there was no correlation (or very little) between surface tension and atomization - but this does not jibe with the Weber theory (G.1 and (2)).

18. Surface tension of B & W CWF .approximates that of water. Carbojel has lower surface tension than water.

M-2

REPORT OF MEETING WITH
DR. N. CHIGIER AND MISS PAT MEYER
CARNEGIE-MELLON UNIVERSITY - Mech. Eng. Dept.
PITTSBURGH, PA.

July 2, 1986

1. Dr. Chigier and Miss Meyer authored a paper on research work done by them at Carnegie-Mellon University and published in the 6th Symposium (page 827) under the title " Atomization of Coal Water Slurries." (See Report W.22)

2. I made contact, first, with Miss Meyer (Dr. Chigier had just returned from Israel and was "diplomatically" unavailable.)

3. On arrival at Carnegie Mellon, Miss Meyer brought me to Dr. Chigier's office.

4. I had hoped to discuss their work in detail to obtain basic information on the nature of CWF drop break-up and spray formation,with relation to CWF consist and rheology, relative to parent coal,and also the effect of the particular atomizing characteristics of the Parker-Hannifin atomizer which they used in obtaining the spray photographs, shown intheir paper. These photos showed little resolution of the drop formation,

---

5. Dr. Chigier stated he could spare me very little time, but I persisted in my questions to the point of being "asked out". (Miss Meyer did not enter into the (hoped for) discussions. Presumably she was only involved in the lab work.

6. Before ejection I did manage to pin Dr. Chigier down to give a statement in answer to my questions " What is the nature of a CWF/ steam emulsion? How do steam elements disparse in the CWF fluid?

7. The answer was a referral to Dr. Chigier's book "Energy, Combustion and Environment", page 254. Fig. 7.2 on this page showed that there was no emulsion - that the flow was two-phase. This was from work done by Mullinger & Chigier in Sheffield, England and published in the Journal of the Institute of Fuel in December 1974 under the title "The Design and Performance of Internal Mixing Multijet Twin Fluid Atomizers".

8. Miss Pat Meyer agreed to receive the work I had done up to that time (July, 1985) covering: my Appendices 1-10 based on the reheology data I had obtained from a reading of Symposia 5 and 6. (With my discussion on each appendix); my correspondence with Dr. Dinger on the Funk

---

8. continued

Dinger - Funk Ø max.determination; and my papers G.4 and G.6 on Research Requirements for a Y-Jet; and Discussion of Atomizer Efficiency, respectively, with the intent to have Miss Meyer read same and offer critical comment.

9. Several telephone calls later I found that Miss Meyer was working on her doctorate to the end of 1985 and could not give the intended time, but would do so in early 1986. To date I have had no communication.

10. My work up to the time of my Carnegie-Mellon visit was based on the concept of a "homogeneous" emulsion of CWF and steam.

11. Following a study of the Mullinger-Chigier two-phase flow concept, I found it necessary to devise a means of numerically analyzing spray formation based on a two-phase flow, which led to my papers G.1 to G.16.

12. In paper G.16, I refined the conceptual basis of 2-stage flow atomization and added a further concept of a "homogenizer" that would ensure a homogeneous emulsion from which an atomizer design basis could be established.

RALPH GROSSMAN

STUDIES AND CONSULTATION IN PROBLEM AREAS OF
FUELS, COMBUSTION AND AIR QUALITY

P.O. BOX NO. 70
TOWN OF MOUNT ROYAL, MONTREAL, QUE. H3P 3B8
TEL. (514) 738-5487

STUDIES

August 20, 1985

Dr. Dennis Dinger,
Alfred University
Alfred, N.Y.
USA 14802

Dear Dr. Dinger,

As we discussed on the telephone a short time ago, I am enclosing:

(1) Paper (B.1) "Control Parameters for a 75 wt. % Coal - Water Slurry - CoAl" by J.E. Funk Sr., D.R. Dinger, J.E. Funk, Jr. This particular paper was in my files and unfortunately without record of source or point of publication.

(2) Appendix 1. "Equations for the Determination of Viscosity, SHear Rate, and Shear Stress for Newtonian and Non-Newtonian Fluid Flows" (from the 5th and 6th Proceedings of the International Symposia on Coal Slurry Combustion and Technology)

(3) Appendix 9 - "Determination of Centipoise Viscosity Values from Various Equations of Appendix 1.

(4) Appendices List with Title and Discussion.

(5) Calculation sheet to determine the value of $\phi\infty$ that will yield a viscosity of 806 Cp as shown on the rheogram of Fig. 3 (Paper B.1 attached) at a shear rate of 44 sec.$^{-1}$, with a CWF of 75% wt. fraction (approx. .685 vol. fraction).
N.B. The viscosity, if based on a $\phi\infty$ of (1 - % porosity)
= (1 - .0725) = .925
is $(1 - \phi/\phi\infty)^{-3.54}$[1]
$= 1 - \frac{.685}{.925}^{-3.54} = (1 - .74)^{-3.54}$
$= (.26)^{-3.54}$ = 118 Centipoise

(6) Report: "Discussion of Atomizing Effeciency", (this is a preliminary assessment).

(7) Report: "Discussion on Research Requirements for an Optimum Design of a T-Jet and Y-Jet and other Atomizer designs for CWF use. (again a preliminary effort.)

1) Kaji et al, Eq. 1 - Ref. X.2; Dougherty-Kriegor, Eq. 4 - Ref. X.15; Cassassa, Eq. 9 - Ref. X.15

... /2

I look forward to meeting with you to discuss:

a) The seeming anomaly between viscosity obtained from the ϕ/ϕ_∞ ratio~~n~~ (where the ϕ_∞ value considered is based on the Dinger-Funk porosity algorithim and actual values obtained from pressure filter tests); and the values obtained by viscosity readings (Haake, Brookfield, e.g.) as per rheogram of Fig. 3. In this regard, my calculation sheet (if correct) shows the need of a ϕ_∞ value of .807 (instead of .925)1) for a 75% wt. slurry, to give the calculated viscosity value of 806 Cp as shown in your Fig. 3, at 44 sec.$^{-1}$ shear rate.

b) A main factor from my search in numerous technical papers is that fineness of atomization is the velocity of the CWF/atomizing fluid (i.e. its kinetic energy) whereas atomizer designs have a safety factor for the ratio (annulus dia./max. particle size) ranging from 5 to 12 - which limits rate of velocity. The inference seems to be that coherence of the CWF coal particles occurs either in the storage tank; the CWF supply line to the burner; or in the atomizer annulus (or exit port).

c) I was advised that Carnegie-Mellon University intend to extend the research of Mullinger and Chigier as in their paper "The Design and Performance of Internal Mixing Multi-Jet Twin Fluid Atomizers" published in the Journal of the Institute of Fuel, England, December 1974. Here an atomizer made with a transparent material was used. Mullinger-Chigier found that the fuel and atomizing fluid flowed in separate phases, with the fuel flowing through an annular space and the atomizing fluid through the centre core, and serving to accelerate the fuel and to capture coal particles from the interface.

Similar research is being considered by the National Research Council, Ottawa, Ontario and (posibly) by B & W Research at Alliance Ohio.

1) Value of .925 obtained from data of porosity values from filter pressure tests. (Paper B.1 - Funk-Dinger-Funk)

By the time we meet, I hope to have completed some numerical analysis of the Mullinger-Chigier phenomenon.

Yours very sincerely,

Ralph Grossman
Consultant

cc. Horace Whaley, CCRL; Canmet, Ottawa
Kevin Jonason, N.R.C., Ottawa
George Farthing, B&W Research, Alliance, Ohio
Pat. Meyer, Carnegie-Mellon University, Pittsburgh, Pa.
Don Dunlop, Slurrytech, Biscayne Bay. Fla.

RALPH GROSSMAN

STUDIES AND CONSULTATION IN PROBLEM AREAS OF
FUELS, COMBUSTION AND AIR QUALITY

P.O. BOX NO. 70
TOWN OF MOUNT ROYAL, MONTREAL, QUE. H3P 3B8
TEL. (514) 738-5487

G STUDIES

August 28, 1985

Miss Pat Meyer,
Carnegie-Mellon University
Dept. of Mechanical Engineering
5283 Northumberland St.
Pittsburgh, PA
USA 15217

Re: Design for an Efficient Atomizer

Dear Miss Meyer,

I regret the delay in sending you the material I referred to in my meeting with you and Dr. Chigier a few weeks ago. I had found a "seeming" anomaly in the data of Drs. Funk and Dinger of Alfred University, which is outlined in my letter to Dr. Dinger of August 20th, copy of which I am pleased to attach.

The material I have made up over the past months has been made for the purpose of (attempting) an assessment, by numerical analysis of the atomizing phenomenon based on atomizer geometry, fuel slurry characteristics, and on the results of field trials, on equipment and operational data actually known to me. The material enclosed is listed as follows:

1- Copy of letter to Dr. Dinger
2- Copy of paper by Funk, DInger & Funk.
3- List of Appendices with title and discussion of each Appendix.
4- Appendices 1 - 10 inclusive.
5- Report: "Discussion of Research Requirements for an Optimum Design of a T-Jet, Y-Jet and other Generic Types of Atomizers".
6- Report: "Discussion of Atomizing Efficiency".

As you will note in Appendices 7 & 8, I have worked out the use of a turbulent flow equation (Crane Tech. Paper No. 410) based on the assumption of two conditions of atomizing steam condensation, and also the assumption that the remaining quantity of atomizing steam formed an emulsion with the coal slurry water.

From the Mullinger & Chigier paper entitled "The Design and Performance of Internal Mixing Multi-Jet Twin Fluid Atomizers" (Journal of the Institute of Fuel, [251] December 1974), in which the slurry fuel and atomizing fluid are shown as separated flows (following experiments with a transparent annulus) and shown in Fig. 4 of their paper, I must now consider the possibility that the assumptions in my Appendices 7 & 8 may be wrong (totally or in some degree). Accordingly I am now studying the work of Given & Maraszek entitled "The Atomization of Liquid Fuels" (Wiley - 1953). This book deals with mechanical atomization of a liquid. From the

... /2

data I will acquire, I shall do a numerical analysis of the following:

1- the annulus jet flow atomization by mechanical pressure (in a 2 phase Y-Jet)
2- the effect of the steam core as it expands from the annulus exit, and impacts the fluid jet stream, using consideration of both kinetic energy and mass momentum ~~#~~1)
3- using temperature and pressure data, in the annulus and mixing chamber of a Y and T-Jet atomizer to determine to what extent (if any) the atomizing steam will:
    a) condense in the fuel water
    b) forms an emulsion with the fuel water.
    b.1) a barrier to the emulsion concept would seem to be the formation of an equilibrium pressure between the atomizing steam and the vapor pressure of the fuel water
    c) a determination of the mass momentum of the fuel and atomizing steam (may) yield the possibility of having a high pressure fuel penetrating into the atomizing steam, using concentric fuel and steam cylinders, with the fuel in the outer cylinder and issuing into the inner atomizing steam cylinder through multiple ports, to achieve some form of emulsion. (I must confess that nothing in the literature I have read so far addresses this question of "steam/water" emulsion.

Should you have knowledge of a source of information on this emulsion concept I would be grateful for your advice.

I gather from the literature and from personal communications, that a main problem remaining in atomizing and combustion efficiency of a coal-water slurry is the coherence (agglomeration or aggregation) of coal particles. Such coherence and its consequences can presumably occur as follows:

1 Through the action of an additive added to the slurry to promote stability in the storage tank. Stability can be obtained by the use of a polymer which creates a "gel" formation in the tank.
1.1 The burner feed pump would (or should) break up this "gel" (or coherent coal particles). If not, it would then create a size problem in the annulus, requiring an adequate and safety factor in diameter sizing (but this safety factor would reduce velocity and so impair jet break up).
1.2 A possible "cure" for such tank gel coherence might be re-circulation of a fraction of pump discharge back to pump suction. Time and/or quantity of such re-circulation would require control to prevent slurry degradation and consequent increase in viscosity.

1) hopefully to be obtained.

... /3

Coherence (continued)

2. Through the effect of pressure and velocity in the flow of the slurry fuel through the annulus.
3. Through "oversize" in droplet formation in which a number of coal particles can be contained in a droplet, cohere therein, and form a large char particle for which there may be inadequate residence time for complete burn-out.
3.1 The literature indicates that high fuel velocity and adequate atomizing fluid pressure will contribute to break up of the jet as close as possible to the exit orifice and so maximize droplet formation - of minimal size in the ensuing spray.

When I had the pleasure of speaking with you and Dr. Chigier at Carnegie-Mellon University some weeks ago, it was mentioned that your continuing research on slurry combustion would involve the use of a transparent atomizer annulus:

May I then ask the following:

Will it be possible to so illuminate and magnify the annulus flow as to determine the nature of the coal particle flow?

If it were found that coherence did occur in the annulus, then I would presume to suggest that further research should be directed to:
the Ph effect of various additives and consequent effect on coal surface ionization - to obtain a maximum inter-particle repulsive force. In this regard I can refer to an article by W.L. Buehner et al in the Vol. 21, No. 1, 1977 issue of the IBM Journal of Research and Development, entitled "Application of ink jet Technology to a Word Processing Output Printer". The general schematic for droplet formation control is shown in their Fig. 1, I quote the following verbatim from the article: (page 3)

> "Conductive ink under pressure is forced through a small nozzle to form a jet. The jet would normally break up into a stream of drops of 'quasi-random size and spacing', but 'drop formation can be controlled' by vibrating the ink within the nozzle cavity at a fixed ultrasonic frequency. The pressure waves cause the jet to break up into a stream of drops 'of uniform size and spacing at a well defined distance from the nozzle'".
> (' ' quotes are mine, R.G.)

It is my intention to follow up on this to see if the IBM technique is applicable to a slurry atomizer.

This letter and attachments cover my past, present and future activities on coal-water-slurry atomization.

... /4

I would greatly appreciate the kindness of your commentary (at your convenience or course).

Much success with your doctoral thesis, and I look forward to a time when I can meet with you again.

Yours very sincerely,

Ralph Grossman
Consultant

✓ cc. Dr. Horace Whaley
Combustion Research Laboratory
E.M.R., Ottawa

RALPH GROSSMAN

STUDIES AND CONSULTATION IN PROBLEM AREAS OF
FUELS, COMBUSTION AND AIR QUALITY

P.O. BOX NO. 70
TOWN OF MOUNT ROYAL, MONTREAL, QUE. H3P 3B8
(514)738-5487

G STUDIES

Nov. 6, 1985

Mrs. Ethel Z. Casassa
Chemical Engineering Dept.
Carnegie - Mellon University
5000 Forbes Ave.
Pittsburgh, Pa. 15213
U.S.A.

Dear Mrs. Casassa:

Again a thousand excuses for the long delay in sending you the material that I've developed for the Canadian Dept. of Energy, Mines and Resources (Canmet - C.C.R.L. Division) but I did think that the material of my paper G.1 should be part of my mailing.

I am pleased to enclose the following:

Papers Nos. G.1., G.1. Addendum, 1, (hand script) G.4., G.4. Addendum 1, (handscript) G.5. and G.6.

I am also enclosing:

1. Copy of correspondence with Dr. Dinger.
2. Appendices List with Title and Discussion.
3. Appendix 1 subsections, X.2, X.12, X.15, Dr. Funk's paper (summary) W.5, W.7, W.9.
4. Appendices: 2,2.1; 3,3.1; 4.R; 6.R; (R.1; 7, 8, 9, 10/
5. Copy of paper, "Control Parameters for 75 wt. % Coal-Water Slurry: "Co-Al" by J.E. Funk, Jr., D.R. Dinger, J.E. Funk, Sr.

Most of the above material has been sent to Miss Pat Meyer of your Mechanical Engineering Dept. New material will be sent shortly to her.

.../2

I hope that in the early Spring of 1986, I may have the pleasure of a meeting with both you and Miss Meyer (and hopefully with Dr. Chigier).

A little early, but my Best Wishes for the Holiday Season.

Yours sincerely,

Ralph Grossman,
Consultant

c.c.

Dr. Horace Whaley,
Canmet - C.C.R.L.
Ottawa

Miss Pat Meyer
Carnegie - Melon University
Mechanical Engineering Dept.

APPENDICES LIST WITH TITLE & DISCUSSION

APPENDIX
NUMBER

1 Equation for the Determination of Viscosity, Shear Rate, and Shear Stress for Newtonian and Non-Newtonian Modes of Fluid Flow

Sect. 1.X.2 R. Kaji et al, Hitachi Research Laboratory
5th Symp.

a) The equation uses the concept of the volume fraction ratio $\emptyset/\emptyset_\infty$ with an experimentally devised exponential to give values of viscosity in Centipoise. (See Fig. 1.2.A)

b) The equation is comparable in concept to those given in Reference X.15 (E.J. Casassa et al - Carnegie-Mellon University) with some viscosity values having high correlation and some with considerable difference, see Fig. 7.X.2 and note limits of validity based on actual experimental data.

Sect. 1.X.12 (Dr. J. Dooher et al. Adelphi Centre for Energy Studies)
5th Symp.

a) The equation is the basic one for Non-Newtonian flow obeying the "Power Law Model" and which is:

$$T = K \dot{\gamma}^n$$

b) Description of thixotropic and rheopectic modes is given to which sketches G.1.X.12 and G.2.X.12, were made.

c) Dilatant effect following periods of pumping are shown in Figs. 6, 7, and 8, but these rheologies are not related to coal sizing and size distribution in the CWFs tested in a test loop.

Figs. 9, 10, & 11 show viscosities versus shear rates of values that would apply in design of CWF supply systems.

APPENDIX
NUMBER
1 (cont'd)

Sect.1.X.15 E.J. Casassa et al, Carnegie-Mellon University
5th Symp.

a) Numbers of equations are given, starting from the fundamental Einstein equation of the viscosity of a very dilute dispersion of uncharged spheres. Equation 2 is a general power series for particle volume fractions where ϕ is $> .01$

b) Values of η for various particle shapes are given, ranging from 2.5 for spheres to 4.0 for rods.

c) This data of (b) can be very useful in confirming (or denying) the validity of the writer's determination of the viscosity of a CWF/atom. steam emulsion (See Appendices 4.R, pages 5 - 7) and Appendix 5.R, pages 2 & 3).

d) Equation 4 is fully comparable to Eq. 1 of Reference X.2

e) Equations 5 - 8 are expressions of the fundamental Power Laws equation $\tau = K\dot{\gamma}^n$.

f) Equation 9 is unique with the K values obtained from tests and shown in Table 5.X.10

g) See Appendix 9 for the calculations of the viscosities from the various equations from References X.2 and X.15 showing a good degree of correlations. (The results from the equations of Reference W.9 are not well correlated to those of References X.2 and X.15).

h) Fig. 5 & 6 show respectively viscosities in relation to Ph and equation 6 is based on a 50% weight coal concentration. There is a question (at least in this writer's mind) why a value of 50% weight concentration was used, whereas the trend is to highly concentrated CWF coal fractions of .70 (to .75).

i) The electrophoretic mobility data of Figs. 7 - 9, will prove valuable in considering the phenomenon of annulus and orifice emulsion flow in an atomizer.

APPENDIX
NUMBER
1 (cont'd)

Sect.1.W.7 G. Andonini et al, Université de Technologie de Compiegne
6th Symp.

a) The equations developed by this group are derived from the basic Newtonian Flow Equation:

$$\mu = \frac{PR^4t}{8LV_0}$$

b) The devised equations for flow design are shown in Appendix 3 as

$$\frac{D\Delta P}{4L} = \mu \times \frac{8V}{D}$$

c) The Rabinowitsch Mooney modification for Non-Newtonian fluids

$$T_w = \frac{D\Delta P}{4L} = \frac{K(1 + 3n)^n}{4n}\left(\frac{8V}{D}\right)^n$$

This equation is the basis of the work done in Appendix 6.R to find the n and K constants.

d) Andonini et al, state that when "slip" occurs, a correction (Jastrezski) must be made to the Rabinowitsch-Mooney modification expressed in item c).

e) This question of "slip" requires to be more precisely defined (in physical terms) and contact with the authors is required for this definition, and the "Jastrezski" function then defined to establish clearly the resulting equation change from the Rabinowitsch-Mooney modification.

Sect.1.W.9 Gregory Botsaris, Dept. of Chemical Engineering, Tufts U.
6th Symp.

a) See Apendix 9 for a numerical value of Equations 4 & 5, and their relation to the figures giving, the plots of the two equations.

APPENDIX
NUMBER
1 (cont'd)

Sect.1.W.9

6th Symp. b) Appendix 9 also includes comparisons of these values with those obtained from Eq. 1 & 2 using the same values of the ϕ/ϕ_∞ ratio.

Sect.1.B.1 Dr. E.J. Funk, Alfred University - Control Parameters for Coal
4th Symp. Size Distribution for Max. Packing at Min. Viscosity

a) This paper giver Dr. Funk's equation for CWF coal sizing and distribution for max. ϕ_∞ and minimum viscosity.

b) The equation is (See Appendix 1 - Sect. 1.B.1)

$$\frac{CP\ Ft}{100} = \frac{D^n - Ds^n}{D_l - D_s}$$

c) See Report B.1 and note recommended value for n is .37

d) Report B.1 is the condensation of Technical Paper B.1 (copy attached).

e) Further basic data by the author is:
   1) Min. particle size .02 to 0.5um
   2) Colloid fraction must be present to give:
   2.1 Min. surface area of > 1.25m^2/cc (to 1.7m^2/cc)
   3) Zeta potential should be 50 mv (electrophoretic value resulting from coal additive chemistry).

f) Minimum porosity attained by algorithm and substantiated by filter press test is < 8%, (ϕ_∞92%)

g) Slurrytech have stated that they have developed a CWF with a porosity of 6% (ϕ_∞ 94%).

h) See Table 1.6.R.A & 2.6.R.A for Cp using ϕ_∞ of 92.5% volume fraction with ϕ of .70 wt. fraction.

APPENDIX
NUMBER

2 Calculation (R.G.) of volume equivalent of a 70/30 wt. mix in CWF

2.1 Calculation (R.G.) of volume equivalent of a 75/25 wt. mix in CWF

3 Derivation of Symbols on ordinate and abscissa on graph plots showing shear rate versus ΔP with Conditions for atomizer design.

a) Basic equation derived from Newton's fundamental realtionship

$$\mu = \frac{s}{\Delta u/\Delta y} \text{ , yielding by final integration} \qquad (1)$$

$$\mu = \frac{PR^4 t}{8LV(\text{vol})} \; 1) \text{ from which is obtained, by converting} \qquad (2)$$

Vo to V, and re-arranging terms $\frac{D\Delta P}{4L} = \mu \times \frac{8V}{D}$ (3) (3)

b) The elements of atomizer design are contained in these equations (2) and (3) provided that the following is known or postulated.

1) Ratio of annulus or orifice dia. versus max. size of agglomerated particles in the annulus or orifice.
2) Velocity of flow to provide energy for disintegration of jet into fine droplets.
3) The viscosity factor μ is important for supply line design, but of min. importance when the atomizing fluid is steam (or air) due to the dilutent effect of the steam (assuming emulsion is homogeneous), (See Appendix 4.R and 4.R Addendum 1) See also sketches a-d of Sketch 1.6.R.A showing homogeneous and separated phase modes of emulsion flow.

(1) C.H. McLain - Industrial Press

APPENDIX
NUMBER

3 (cont'd)

3.1 ΔP due to velocity head loss, will, however set a limit to the max. designed velocity. (See Appendix 7, Items 15 & 19).

3.2 Flow velocities up to 900 fps are seen to be within the scope of system design practice. The velocity volumes were obtained from an atomizer with a ratio of

$$\frac{\text{annulus dia.}}{\text{max. um size of coal particle}} = 12$$

N.B. The Coen burner described in report W.22 1) had a ratio of (approx.) 4.66

3.3 The film thickness of water covering the particle. For a given water volume fraction the greater the number of particles due to designed size consist of the CWF, the thinner the film, and vice versa.

3.3.1 Conceivably film thickness has a roll in determining coherence of droplets in a test or combustion chamber. Conceivably film thickness will have an effect on the electrophoretic value of the particles and coal particle surface chemistry.

c) With a homogeneous emulsion, it would seem that the kinetic energy of the emulsion and the latent energy of the steam (should) produce a fine atomization.

d) However the following factors that can influence fineness of atomization are yet unknown:

(1) Paper by N. Chigier & P.L. Meyer, Carnegie-Mellon 6th Symposium.

APPENDIX
NUMBER
3 (cont'd)

1) Is the emulsion homogeneous or do (or can) the two stream flows follow the possible paths sketched (roughly) in Fig. 1.7.A, conditions a - d.
2) If condition b) existed, then the atomizing steam flow could (conceivably) diverge after passing into the combustion chamber with diminished effect on the CWF jet.
3) Condition c (should) give an atomizing effect comparable to condition b).
4) A similar argument could be made for condition d).

d) There is an apparent need for research to clear these issues by the use of (say) Schlieren photography - to detect phase separation. or pulsed laser CWM electron microscope with the CWF flowing through a quartz tube.

e) There is also a need to know the pressures existing at the points of entry of atom. steam and CWF into their common annulus channel and also to know the pressure at the mid point of the channel.

f) In the case of a Y-jet the points in question are lettered on Fig. 1.A.4 attached, as A, L, Pt.

g) Similar information would be needed in the case of a T-jet with the addition of a pressure reading in its mixing chamber.

h) The pressure data will establish the mean steam pressure and permit an accurate assessment of the $\overline{V}$ value which is the dominant volume factor of the emulsion and determines the $\emptyset$ value of the emulsion and so its viscosity with a known $\emptyset_\infty$

i) In the event that the use of a quartz tube for imaging should not be practical, Carnegie-Mellon have stated in their paper, in the 6th Symposium, by Dr. N. Chigier and P.L. Meyer

APPENDIX
NUMBER
3 (cont'd)

entitled "Atomization of Coal-Water Slurries", that they will experiment with a pulsed laser light brought into the heart of the emulsion issuing jet - to determine details of structure.

j) As a further element of discussion, a calculation was made (See Appendix 10) to determine the Ø values with atomizing air at 175 psig - having a $\overline{V}$ value of 1.033.

k) As shown in Appendix 10, the viscosity values of the emulsion with atom. air are nearly the same as with atom. steam and the conditions for turbulent flow (Re over 36,000) still exists.

l) The friction ΔP values given in Appendix 7, for turbulent flow, can then be substituted for the factor ΔP in the equation (3) viz. $\frac{D\Delta P}{4L} = \frac{8V}{D}$

m) This relationship of $\frac{D\Delta P}{4L}$ versus $\frac{8V}{D}$ as given in (e.g.) S.R.C (Saskatchewan Research Council) Tech. Paper No. E.725 does not include the exponent "n" (as required by the Rabinowitsch-Mooney Modification, but its value, presumably, is implied by the empirical value (ordinate) of

$$\frac{D\Delta P}{4L} \text{ i.e. } = \frac{\frac{D\Delta P}{4L}}{\frac{8V}{D}} \text{ implies } \left(\frac{8V}{D}\right)^n \text{ (?)}$$

n) The n values given in the S.R.C. Report are for CWF flows only and in their Table 5 (Page 18) are shown to vary from a low of .893 to a high of .930 for use in the equation stress in $\text{dynes/cm}^2 = K\gamma^n$, (for a Power Law Mode fluid) so that a μ value resulting from the ratio $\frac{T}{K\dot{\gamma}^n}$ should not be appreciably in error from values of μ obtained from $\frac{T}{K\dot{\gamma}}$

where $\dot{\gamma} = \left(\frac{8V}{D}\right)$

APPENDIX
NUMBER
3 (cont'd

o) Hence, it would appear that the operating condition of $\frac{8V}{D}$ versus $\frac{D\Delta P}{4L}$, can be used to determine line loss (ΔP) in a CWF pipe flow especially as the $\frac{D\Delta P}{4L}$ value is experimentally determined from the $\frac{8V}{D}$ operating condition

p) It is the writer's intention to discuss this reasoning with the Saskatchewan Research Council and to further report thereon.

q) Where it is important to know the apparent viscosity, the values can be obtained by viscometers for shear rates up to (say) 1000 sec.$^{-1}$

r) For high velocities (e.g. of an emulsion) can be obtained from the:

1) ϕ/ϕ_∞ concept.

2) ΔP calculated for turbulent flow from the equation

$$\Delta P = \frac{0.000336\ fw^2}{d^5\rho}$$

by solving for 'f' and by finding the applicable Re number from the charts (Crane) and then using the equation $Re = \frac{6.31W}{d\mu}$ to find μ.

s) N.B. the K constant value is entirely a dependent function of n and relates

$$\frac{T}{\mu} = K\dot{\gamma}^n \quad \text{i.e.} \quad K = \frac{T}{\mu\dot{\gamma}^n}$$

It would seem that the chief value of n is to determine the flow mode - i.e. whether the flow is pseudoplastic or dilatant.

t) It can also be seen from Item 6 Appendix 7 that the viscosity value of a CWF entering an annulus (within reason) has little

APPENDIX
NUMBER
3 (cont'd)

effect on the viscosity of the emulsion due to the dilution by the steam. Note also from items 23 and following, of Appendix 7, that in the worst case of an emulsion viscosity of 4 Cp that the flow is still turbulent for a Ø up to .3 as compared to Ø values ranging from .0118 to .076 as shown in the tables of Appendix 4.R., as the emulsion viscosity.

4.R Function Data on Operation of Mark 3 C.E. Atomizer (EPRI)

a) This appendix covers equipment data and operational values on a test made by C.E. on a 22.5 Meg_e boiler at the New Brunswick Electric Power Commission Station at Chatham N.B.
b) The CWF input per annulus (each of 7) was .0036 cfs.
c) Total ΔP through annulus was considered as the additive values(1) of the atom. steam and CWF pressures for a total of 350 PSI.
d) Two steam pressures and corresponding $\overline{V}$ values were considered; 175 PSI (inlet press.) and 82 PSI (calculated critical pressure if steam flow was subject to expansion).
e) Flow velocities through annulus were:
   @ 175 PSI - 500 fps
   @ 82 PSI - 930 fps
   @ 125 PSI - 663 fps
f) Tabulations were mod. for Ø values for 70/30 mix and 75/252 mix for
   1. CWF only
   2. CWF/atom. steam & emulsion
g) Ø values for CWF only were
   .64 for 70/30 mix
   .685 for 75/25 mix
   Ø values for the emulsion for both 70% and 75% coal concentrations ranged from .012 to .025.

(1) Geo. Farthing of B & W Research observed that this is incorrect and that the max. pressure in the annulus is the max. of either the CWF or the atomizing steam. The 350 PSI value may have some use in determining n & K constants in high pressure drop CWF supply lines.

APPENDIX
NUMBER
4.ADD.1

a) The $\frac{\text{dia.}}{\text{max. coal particle size}}$ ratio with the C.E. unit was approximately 12:1.

b) A numerical experiment was made to determine the velocity possible if the ratio was reduced to 6.

c) The calculations for a ratio of 6 gave velocities of 2000 fps and 3720 fps for the conditions of 175 PSI and 82 PSI steam respectively.

d) It was first thought that this could be considered beneficial for atomizing efficiency BUT the pressure increase was (4^2) (Item 7.1) and relating this to the pressures calculated for turbulent flow (Item 8.2 - Appendix 7) showed the impossibility of such increase in velocity.

e) For "normal" pressures (< 300 PSI) the max. velocity would be about 1000 fps.

5.R Viscosity Determination from ϕ and ϕ_∞ Values of an Average CWF and of Co-Al.

a) This Appendix addresses the concept of viscosity based on the ratio ϕ/ϕ_∞ , e.g. (Ref. X.2) $\mu = (1 - \phi/\phi_\infty)^{-3.54}$ (Centipoise)

b) The effect of a high value of ϕ_∞ is shown as a necessary factor in establishing a low viscosity (and confirms Dr. Funk's statement thereto).

c) Also demonstrated is the fact that the average viscosity of a CWF/atom. steam emulsion (homogeneity assumed) is 1.2 Cp - (approx. av.) which means that the flow will be turbulent (See App. 7).

d) It should be noted that the experimental test data of Ref. X.2 (Appendix 1) gave a max. value of $(1 - \phi/\phi_\infty)$ of .5

e) The value for an emulsion (average) is .985, therefore some correction may prove necessary, but from the ΔP data based on

APPENDIX
NUMBER
5.R (cont'd)

turbulent flow (Appendix 7) which gives values consistent with practice, a variation from the exponent $^{-3.54}$, should not be significant, especially as it is shown in Appendix 7 that the emulsion viscosity could rise to 4 Cp without reducing the Re number below the turbulent range.

f) Items 3.2 & 3.3 show the effect of a lower ϕ_∞ (from .925 to .75) in creating a sharp increase in viscosity from 63 Cp to 895 Cp. This is consistent with statements made by Dr. Funk.

6.R Determination of Constants n & K by Application of the Rabinowitsch-Mooney Modification of the Newton Flow Basic Equation, to the Dimensional and Operating Data of the Mark 3 C.E. Atomizer (EPRI) (Chatham)

a) To solve for n & K, shear stress and viscosity must be known.
b) The shear stress is based on the assumption (in this Appendix) of the addition of th CWF & atom. steam pressure for a value of of 350 PSI or 24.10^6 dynes/cm^2.
c) Two viscosities are used, based on a ϕ value of .64 (coal vol. of 70/30 mix.) and a ϕ_∞ of .75 (assumed a standard case) and a ϕ_∞ of .925 (Co-Al by Slurrytech).
d) The viscosities are respectively 895 CP and 63 Cp.
e) Two velocities are used, derived from atomizing steam pressure of 175 PSI & 82 PSI - the lower pressure based on an assumed expansion of steam and a drop in pressure to the critical pressure value.
f) Values of n & K are then calculated as shown (See Tables 1.6.R.A and 2.6.R.A.
g) The assumption of pressures being additive could be wrong.

APPENDIX
NUMBER
6.R (cont'd)

h) Case E (Item 16) is based on a ΔP of 150 PSI and a viscosity of 63 Centipoise.

i) The change in n values was in number only but the identification of pseudoplasticity remained.

j) Therefore when an actual value for ΔP can be determined by test then the calculations can be repeated and applicable n & K values determined for use in line design. k) N.B. the K values are a dependent function of the constant n.

l) These n & K values determined for the CWF only are not applicable to the emulsion in the annulus.

m) They can be used only in the calculation of suppply line ΔP.

n) For the emulsion a value of 1 Centipoise viscosity can be used for all cases , and related to a ΔP value determined separately. (See Addendum 1 to Appendix 6.R - Item 7 - ff). It will be seen that for an emulsion at ΔP = 350 PSI that n has values of .67 & .40 for atom. steam pressures of 175 & 82 PSI respectively.

o) For a ΔP of 150 PSI the n value is .515. See argument Item 13 re indication of possible dilatancy.

p) Finally, it can be conjectured that a ΔP resulting from the Turbulent ΔP Equation (Appendix 7) based on a measured mean steam pressure in the annulus, can be used in determining the T value (Eq. 1 Page 1).

7 Applications of Equations derived from the Basic D'Arcy and Poiseuille Formulae (from Crane Tech, Paper 410)1) to the C.E. Mark III (EPRI) Atomizer and the Chatham Operating Parameters (See Appendix 4.R - Page 1)

7.1 a) This Appendix uses the Crane equations for Re, Laminar Flow, and Turbulent Flow to determine the appropriate equation for a

---

1) Crane Tech Paper No. 410 "Flow of Fluids through Pipe, Valves and Fittings".

APPENDIX
NUMBER
7 (cont'd)

CWF/steam emulsion.

b) For CWF flow only the Re numbers shows that flow modes, for both μ = 895 Cp and μ = 63 Cp are laminar.

c) All emulsion flows have a Cp < 1.3 and a Re >36,000 and so are turbulent.

d) The ΔP due to friction has a low value of 10.2 PSI and a max. value of 19 PSI.

e) The CWF and atom. steam pressures were each much higher (150 and 175 PSI).

f) Therefore the extra pressure loss, must be due to head loss due to velocity.

g) There were 3 velocities considered, corresponding to atom. steam pressures of 175, 125 and 82 PSI. These were respectively 500, 633 and 930 fps.

h) The calculations found total pressure drops, i.e. friction head and velocity head, for the 3 velocities to be 139, 185 and 259 PSI.

i) All of these are commensurate with general practice capabilities of a system design.

j) In the case of this particular study (Chatham Test), the value of 259 PSI is greater than either the CWF and atom. steam pressures.

k) Note that the $\overline{V}$ calue of 82 PSI, causing the high velocity of 930 fps was derived from the hypothesis that the mean (or critical value) pressure of 82 PSI, was based on a fact of steam expansion in the annulus.

l) Should the atomizing steam be a "driver", then the maximum emulsion pressure would be 175 PSI, for a total friction and velocity head loss of 139 PSI.

APPENDIX
NUMBER
7 (cont'd)

m) In Appendix 8 calculations showed that the ultimate mean pressure in the annulus could be mean of CWF at 135 PSI and atom. steam at 175 PSI or a mean of 155 PSI.
Actually the mean could have been $\frac{190 + 175}{2} = 183$ PSI

n) Therefore the reality could be that the $\overline{V}$ value is that of 175 PSI initially and that of 155 PSI finally (Appendix 8) or say a mean of $\frac{2.4 + 2.675}{2} = 2.54$

o) The CWF emulsion volume, assuming condensation of atom. steam, would then be essentially the value shown on Page 5 - Appendix 8, i.e. .0366 cu. ft. The velocity would then be $\frac{.0366}{.0002} = 183$ fps (with steam condensation) whereas, if there were no condensation the velocity would be that shown in Appendix 4.R Page 2, i.e. 500 fps.

p) The resulting velocity head loss would be

$$\sqrt{\frac{183}{500}} \times 129 = .61 \times 129 = 79 \text{ PSI}$$

plus friction head $\underline{10}$

89 PSI

q) But the actual min. operating pressure found necessary was 150 PSI.

Therefore the truth must lie between the thermodynamics yielding 82 PSI - no steam condensation and that yielding a mean of 155 PSI (Appendix 8, Item 14) - with steam condensation.

APPENDIX
NUMBER
7 (cont'd)

7.2

a) Appendix 7 further addresses the question: What is the max. emulsion viscosity that will give a Re number at the minimum value for turbulent flow of 10,500.

b) The value is calculated as 4 Cp which could occur if 95% of the atom. steam were to condense in the CWF water. Item 4.0 shows that the CWF temp. would have to rise to 345° F compared to a saturation temp. of 366 ° F for its pressure of 150 PSI. The conclusion is drawn that the CWF could not boil off therefore the limit of 4 Cp is practical.

c) Tis is further corroborated by the argument in Appendix 8.

d) Therefore a CWF/steam emulsion is always turbulent.

8 Potential for Total Drying of CWF

a) Appendix 7 only answered the question: What degree of atom. steam condensation could occur and still leave the CWF/steam emulsion at a viscosity <4 Cp and so maintain its status as a turbulent flow fluid?

b) Appendix 8 addresses the question: What is the max. absorption that can occur without consideration of any viscosity limit?

c) Heat transfer from atom. steam to CWF water will exist only up to an equilibrium temp. of both.

d) The equilibrium temp. was taken to be the temp. of the mean saturation pressure of the steam & CWF, viz. the temperature equivalent to 155 PSI cr 368°F.

e) It was found that the max. absorption would be 23.84 BTU versus a heat availability in the steam of 34.26 BTU, versus a heat requirement for 100% evaporation of the water of 92.24 BTU.

f) Therefore the CWF can not go dry.

APPENDIX
NUMBER
8 (cont'd)

g) The fraction of the atom. steam used for condensation is

$$\frac{23.44}{34.26} = 68.5\%$$

h) The remaining amount of steam plus the increase in CWF yields a max. viscosity of 1.415 Cp - well within the turbulent viscosity limit.

i) The atom. steam/CWF ratio is now .0414 (instead of .15).

9 Determination of Cp Viscosity Values from the Various Equations of Appendix 1 (See Appendix 9)

a) The purpose of this Appendix is to calculate the viscosities from the various equations and tables in Appendix 1 and to compare the values obtained and to determine any "maverick" result.

b) From these comparisons, there could be determined the several equations, giving comparable viscosities, that could be used in determining viscosity for line and annulus ΔP values.

c) The only "maverick", i.e. a value out of general consensus, is the result from the Eq. $\eta = \mu_r = \left[\frac{1 + 0.75\phi/\phi_\infty}{1 - \phi/\phi_\infty}\right]^2$ for a ϕ of .583 and a ϕ_∞ of .70, the resultant viscosity is 22 Cp (?).

10 Specific Volume of AIr at 175 psig and Resulting Viscosity of the CWF/Air Emulsion

a) $\overline{V}$ is 1.033 as compared to $\overline{V}$ for 175 PSI steam of 2.4

b) The resulting viscosity is - - - 1.066 Cp which is not significantly greater that the values with steam.

c) The condition for turbulent flow of the emulsion remains unchanged.

Appendices List with Titles and Discussions

10·1 Reference to date of Table 1.A.6.R will show that use of corrected pressure of 200 psi will give some difference in value to constants K and n but the indicated characteristic mode (i.e. pseutoplastic or dilatant) will, generally, remain as shown. (i.e. Modes where n $<$ 1, and where n $>$ 1 will not change).

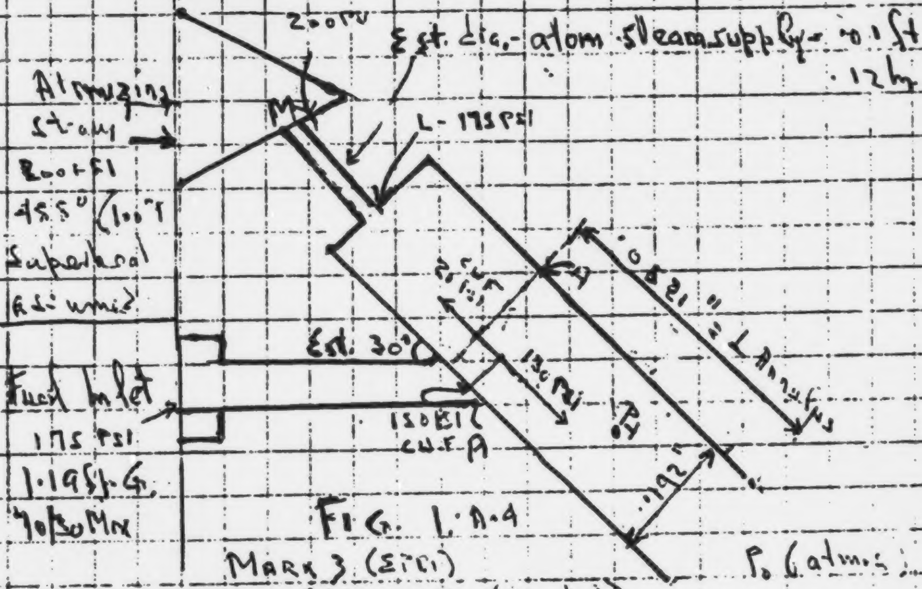
200 psi
Est. dia. - atom steam supply = .01 ft
.12 in
Atomizing Steam
200 psi
45.5° (100°F Superheat)
Estimated
M
L - 175 psi
Fuel Inlet
175 psi
1.195 S.G.
70/30 Mix
Est. 30°
C.W.F. 25 psi
130 psi
150 psi
C.W.F. A
P1
= L Annulus
.192"
P0 (atmos)

FIG. 1 A-4

MARK 3 (S.C.I.)
C.E. ATOMIZER (Y-Jet)

APPENDIX 1

Equations for the Determination of Viscosity, Shear Rate, and Shear Stress for Newtonian and Non-Newtonian Fluid Flows

SOURCE	ITEM	EQUATIONS
X.2	1	$\eta = \eta_o \left(1-\frac{\emptyset}{\emptyset_c}\right)^{-K}$

Where:

η = Viscosity of Coal Water Mixture

η_o = Viscosity of water

$\emptyset$ = Volume of fractional solids

$\emptyset_c$ = Volume packing of solid at maximum random packing

K = Shape factor = (-.354) for values of $(1-\emptyset/\emptyset_c) > .1$ (Experimentally determined)

N.B. K value of -3.54 may not apply due to significant particle to particle participation when $(-\emptyset/\emptyset_c) < .1$

$\emptyset_c = 1-\xi$

where, ξ = solid friction at maximum random packing,

$$\emptyset = \frac{V_s}{V_s + V_a - V_{ab}}$$ where

V_s= Volume of solid

V_w= Volume of water in coal mixture

V_{ab}= Volume of absorbed water.

N.B. See Fig: 7. x. 2 attached.

FIG. 7. x. 2

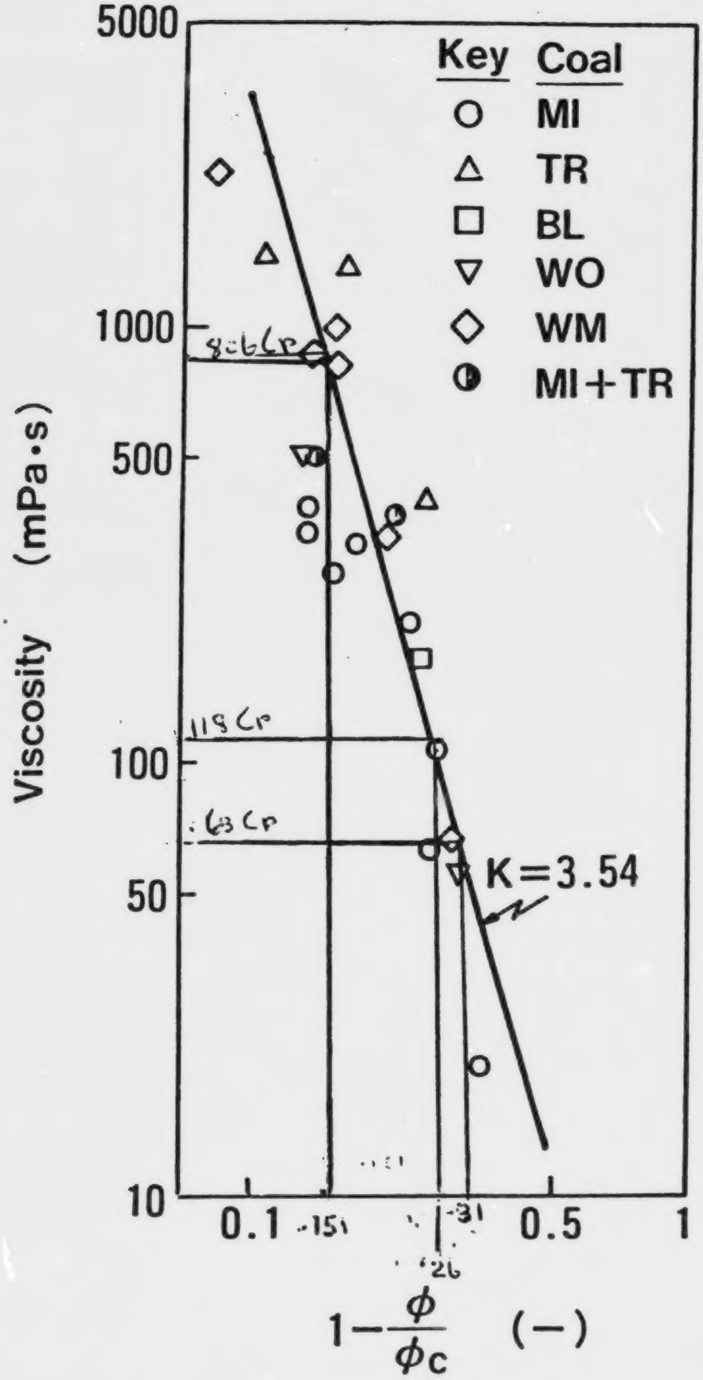

Viscosity from concept of

0 / 0 max. ratio for

Co-HL - 70% wt. fraction

$\frac{0}{0 \text{ max.}} = \frac{.64}{.925} = .692$

$1 - .692^{-3.54}$

$= .41^{-3.54} = 63$ Cp.

Co-AL-75% wt. fraction has

viscosity:

$\frac{0}{0 \text{ max.}} = \frac{.685}{.925} = 74$

$(1- .74)^{-3.54} = 118$ Cp

Figure 7. Plot of viscosity vs. $(1-\frac{\phi}{\phi_c})$

X.2

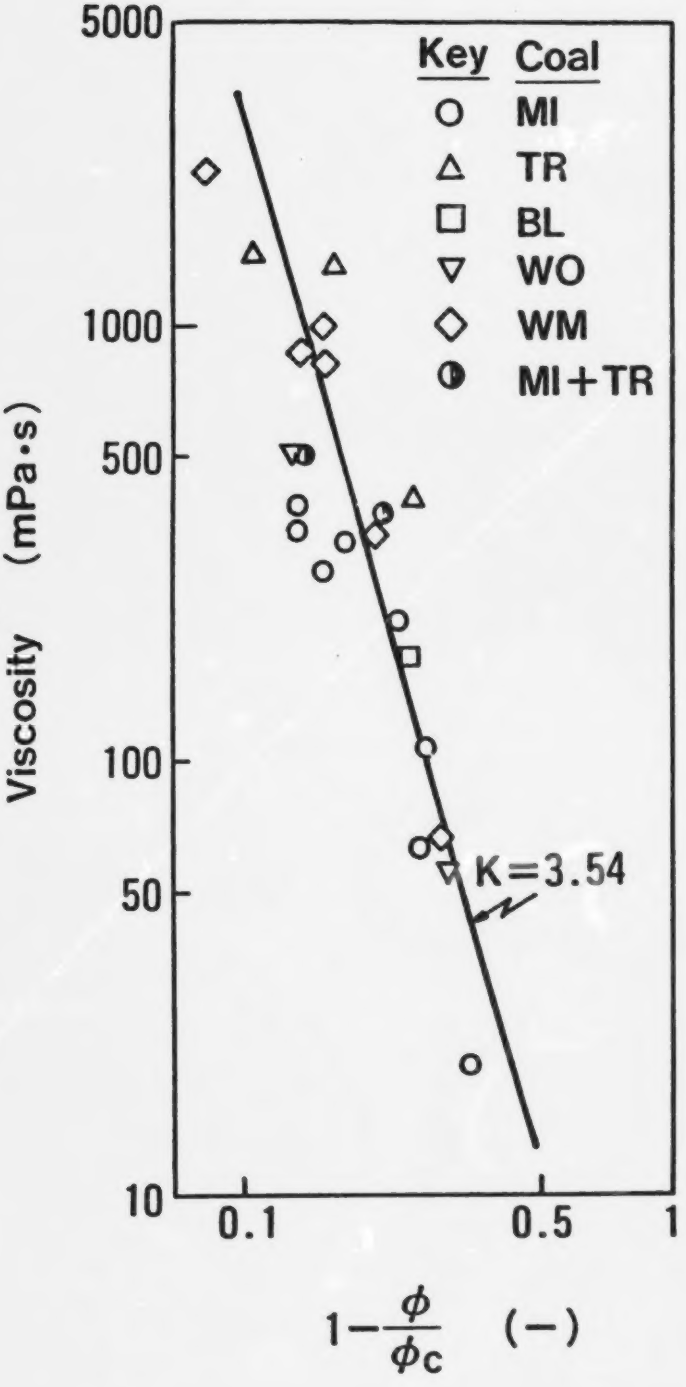

Figure 7. Plot of viscosity vs. $(1-\frac{\phi}{\phi_c})$

X·2.

APENDIX 1

Handling Properties of Coal/Water Slurries"
Dr. John Dooher et al - Adelphi Centre for Energy Studies - Adelphi
University - Garden City, N.Y. 5th Symposium P.1142

SOURCE ITEM EQUATIONS

X.12 1 The shear stress/shear rate (for most samples) relationship were exhibited on the power law model:

$$T = K\gamma^{n} \qquad (1.X.12)$$

which was also used in the S.R.C. Report E725.

Symbols are:

T = Shear stress in dPa(deciPascals)
(a deciPascal = 100 centipoise)
$\dot{\gamma}$ = Shear rate, measured in S^{-1}
K = Flow consistency index, measured in $dPas^{n}$
η = Flow behavior index, dimensionless
$\eta = 1$ - slurry is Newtonian
$\eta = <1$ slurry is thinning
(i.e. pseudoplastic or thixotropic etc.)
$= >1$ slurry is dilatant.

2 The apparent viscosity $\eta(\gamma)$ is

$\eta(\dot{\gamma}) = K\dot{\gamma}^{n-1} \times 100$ mPas = milliPascals = centipoise
(2.X.12)

3 CWF samples were tested at shear rates ranging $0\text{-}250^{-1}$ returning to zero and repeating the cycle.

4 The data from the third flow curve (generated at increasing shear rate) were deemed to be the equilibrium values and represented their behavior often being sheared by pumping action.

4.1 If initial curve values of viscosity > equilibrium value CWF is thixotropic.

APPENDIX 1

SOURCE	ITEM	EQUATIONS
X.12	4.2	If viscosity values are higher than equilibrium CWF is rheopectic.
	5	Figs. 6, 7 show asymptotic rise in viscosity after short 1/2 hour pumping interval.
	6	Figure 8 shows asymptotic after 10 to 15 hours pumping. Pump was a Moyno-progressive cavity.
	6.1	The question that arises here "should" a different type of pump be used (test)? (Would a reciprocating pump do better?)
	7	No tests for coal sizing and distribution were given in the paper to which the pump action on the various CWFs could be related. (To answer the question as to why the asymptotic rise in viscosity shown in Figs. 6, 7, 8 should have occurred in the test CWF.)
	7.1	Also not noted was the number of recirculations that occurred in the test CWF .
	7.2	(N.B. In normal practice a given CWF quantity would be pumped once only to the burners with a minor part recirculated through a return line to storage tank or pump suction.
	8	"The rheological behavior of most of the slurries were evaluated in the loop after eight or more hours of pumping. Some of the slurries behaved as nearly Newtonian fluids, however, others became dilatant or had flow properties which rapidly changed with time. In order to correctly design a fuel forwarding system, both the initial and equilibrium behavior of the slurries must be taken into account."

APPENDIX 1

SOURCE	ITEM	EQUATIONS
X.12		"The high shear to which most of the CWS were subjected in the loop seemed to adversely affect most of the slurries tested. Shear rates should be kept to a minimum, perhaps less than 150 s^{-1}, to avoid problems." (atomizer port or annulus?)

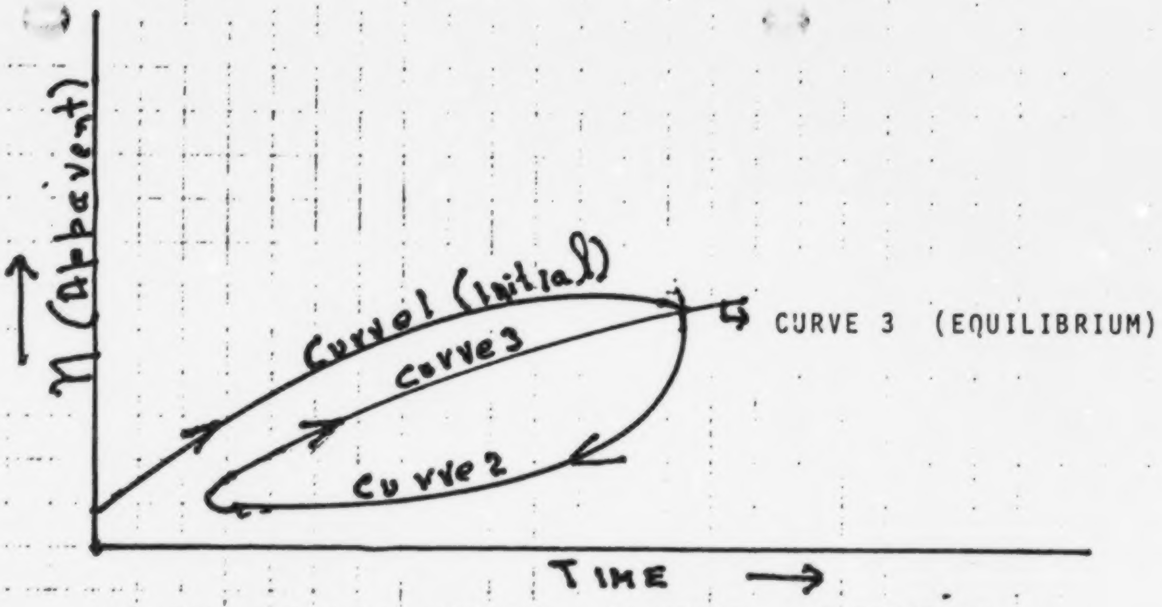

1) FIG. G.1.X.12 CONSTANT LOW SHEAR - THIXOTROPIC

NOTE: CURVE 1 IS HIGHER THAN EQUILIBRIUM CURVE 3
THEREFORE MODE IS THIXOTROPIC

1) After Dr. Dooher

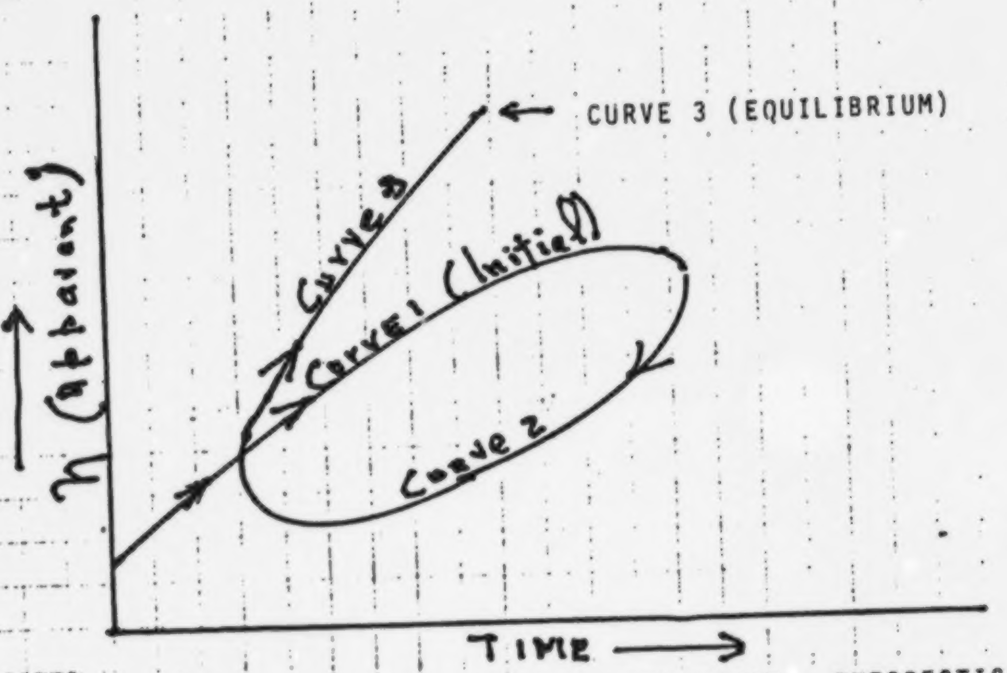

1) FIG. G.2.X.12 CONSTANT LOW SHEAR - RHEOPECTIC MODE

NOTE: CURVE 1 IS LOWER THAN EQUILIBRIUM CURVE 3
THEREFORE MODE IS RHEOPECTIC

1) After Dr. Dooher

APPENDIX 1

SOURCE ITEM EQUATIONS TO DETERMINE VISCOSITY (OR APPARENT VISCOSITY I.E. VISCOSITY AT A GIVEN SHEAR RATE)

X.15 1 Einstein equation for η of a very dilute dispersion of unchanged spheres

$$\eta = \eta_0 (1 + 2.5\phi + 4\phi^2 + \quad) \text{ where} \qquad (1)$$

η_0 = viscosity of the medium

ϕ = volume fraction of the hypothetical spheres

1.1 Eq. 1 assumes no hydrodynamical interaction of the spheres, therefore applying to volume fractions close to zero

See X.2 & X.12 — where $\phi > .01$, η is increased due to formation of temporary doublets, triplets, etc. (which enhance energy of dissipation i.e., shear stress)

1.2 For $\phi > 0.01$ a useful general power series equation is:

$$\eta = \eta_0 = (1 + K_1\phi + K_2\phi^2 + K_3\phi^3 ----) \qquad (2)$$

K_1 is related to intrinsic viscosity [η]

i.e. absolute viscosity in that as
$\phi \rightarrow 0$
$K_1 \rightarrow 1$

2 The magnitude of η can be related to particle shape (Goodwin - "Coilloidal Dispersions" Royal Soc. Chem. Spec. Pub., 43,165 (1982)

2.1 These shapes and the experimental data are

η = 4.0 for rods
= 3.2 for ellipsoids
= 2.9 for discs
= 2.5 for spheres

2.3 Constant K_2 is turbulence of doublets collision

K_3 describes higher order collissions

K_2 lower bound and possible range of 7 - 14

1) From paper on 5th Symposium P. 1025, E.J. Cassassa, et al., Carnegie-Mellon

APPENDIX 1

X.15 2.3 K_3 values not available

2.4 For concentrated dispersions other equations are usually modifications of the Arrhenius equation

$$\eta = \eta_0 = \exp(K_1\phi), \text{ where} \qquad (3)$$

K_1 = constant = 2.5 at infinite dilation

3 The Dougherty & Krieror equation based on "experimental results" is:

See X.2 & X.12

$$\eta = \eta_0 = \left(1-(\phi/\phi_\infty)\right)^{-[\eta]\phi} \qquad (4)$$

ϕ_∞ = max. packing fraction at which flow can occur

Cross Reference
Eq. 1 - (X.2)
3.1 Fig. 2 - X.15

3.2 See Table 5.X.15 for values of K, corresponding to values of Ø. (Eq. 9)

4 Cross Reference
2) Paper X.15 then gives the series of equations as per item 1.X.12 of this Appendix No. 1 and S.R.C. E725
These equations (repeated) are

$$T = \eta\dot{\gamma} = \text{Newtonian} \qquad (5)$$

$$T = K\dot{\gamma}^{n} = \text{non-Newtonian} \qquad (6)$$

$n < 1$ = pseudoplastic
$n > 1$ = dilatant
$n = 1$ = Newtonian

$$T = T_0 + \eta\,pl = \text{plastic/Bingham} \qquad (7)$$

$$T = T_0 + K\dot{\gamma}^{n} \qquad (8)$$

$n <$ = pseudoplastic with yield value
$n >$ = dilatant with yield value

$$\eta = \eta_0 \exp.(K' + K''\phi) \qquad (9)$$

See Table 5.X.15 for values of K, corresponding to values of Ø applicable to Eq. (9).

APPENDIX 1

X.15 4 (cont'd) Constants in Eqs. 5 - 8 are:

K = flow consistency number
n = flow behavior index
T_o = yield stress
η_{pl} = plastic viscosity

5 The values of T_0 & n reflect the magnitude of the deviation from Newtonian flow (Eq. 5) and are dependent upon the "state of dispersion" of the particles

6 Note that Eq. 9 is a modification of Eq. 3 ($\eta = \eta_0$ (Exp.K_1Ø)

7 When $K' = 0$, Eq. 9 becomes the Arrhenius Equation 3

7.1 Values of K' and K'' are given in Table 5.X.15 reproduced as follows

Table 5.X.15 Values of k' and k'' from plots of Equation (9)

	Pittsburgh #8		Illinois #6		San Juan		Hiawatha	
	k'	k''	k'	k''	k'	k''	k'	k''
Ø < 0.4	0	8.7	0	9.7	0	9.2	-1.0	10.0
Ø > 0.4	-2.8	16.8	-3.0	17.1	-3.1	16.8	-2.0	12.9

8 Eq. 4 relates viscosity to coal concentration (by vol.)

8.1 A plot of log e (η / η_0 versus log e (1-Ø/Ø∞) provides a value of "intrinsic" viscosity

8.2 From Table 5 [η] viscosity values are about 9.

9 From Table 6.X.15 reproduced herein the "Intrinsic" Viscosity is about 6.3 to 6.5

10 The Table 6 values are lower than those obtained from Eq. 9 at Ø < 0.4 (reasons not known).

11 The test data showed that a value of Ø∞ of .7 (equivalent to 76-77% wt.) is required.

APPENDIX 1

X.15 11 Table 6. Intrinsic Viscosity from Plots of Equation (4)

Pittsburgh #8 $[\eta] = 6.5$
Illinois #6 $[\eta] = 6.3$
San Juan $[\eta] = 6.5$
Haiwatha $[\eta] = 5.2$

12 The constants for Equation 8 i.e. T_o μ, n & K. (and also pH) are given in Table 7 reproduced in the following (as Table 7.X.15)

"Although in recent years there have been a number of reports(2) on the rheology of coal/water mixtures, no consistent picture has emerged from the published data on the relationship between slurry rheology and the chemistry of the coals in terms of polydispersity of particle size, the surface chemistry of the coal, the effect of the chemical nature of the suspending fluid, slurry temperature, the effect of added electrolyte, etc. This is the focus of our current studies at Carnegie-Mellon University.

Table 7.X.15 - Herschel-Bulkley Constants for Coal/Water Slurries

	T_o (dyne-cm^{-2})	n	K(poise)	Natural pH
Pittsburgh #8	18	0.89	0.74	2.85
Illinois #6	18	0.80	0.75	4.1
San Juan	15	0.78	0.66	6.3
Hiawatha	3.8	0.96	0.24	5.2

APPENDIX 1

SOURCE	ITEM	The equation developed by Dr. J.E. Funk, Jr. of Alfred University (also known as Alfred's Equation) to Determine Coal Size Distribution for Max. Packing at Minimum Viscosity is:
4th Symp B-1	1	$\frac{CPFT}{100} = \frac{D^n - D_S{}^n}{D_L - D_S}$, where (1)
Tech. Papers in Binder		CPFT = cumulative % finer than D = any particle dia. in the distribution D_L = largest particle diameter in the distribution D_S = Smallest particle diameter in the distribution n = exponent the slope at D

N.B. For a highly loaded Coal CWF
n was found to have a value of ·37

The comparable equations given by the authors of W.5. (Zheneg Rong Zeng et al - China Institute of Mining)

for maximum packing are:

$$Cwt = \frac{Ps}{Pw\left(\frac{100}{Cv} - 1\right) + Ps \times 100,\%} \qquad (2)$$

$$Cwv = \frac{Pw}{Ps\left(\frac{100}{Cwt} - 1\right) + Pw \times 100.\%} \qquad (3)$$

where Ps = density of coal = 1.3
Pw = density of water = 1

APPENDIX 1

SOURCE ITEM EQUATIONS

W.5
6th Symp.
p. 236

1 The Rosin-Rambler Equation (in the form developed by "Bennet") is

$$R = 100 \exp. \left(- \frac{D}{D_m} \right)^n \qquad (4)$$

where,

R = cumulative weight % oversize

D = any particle diameter in the distribution

D_m = the particle dia. at $R = 36.7\%$

n = size distribution constant

1.1 The largest dia. D_L in Eq. is undefined

Value of D_L is usually taken at $R = 0.1\%$, then

$$D = D_m \sqrt[n]{\mathrm{In}\ 1000} \qquad (5)$$

1.2 In practice the smallest dia. cannot be zero and Eq. 4 is then revised

$$R = 100 \exp - \frac{(D - D_s)}{D_m} \qquad (6)$$

1.3 See Fig. 3 in report text of W.5

2

Table I1)

Comparison of Measured (Filter Press)
And Calculated Minimum Porosities
For Four Different Grinds Of Upper Freeport Co-Al

Sample	Filter Press	Computer Algorithm
75%	8.1%	7.4%
75% - Diluted to 65%	8.2%	7.4%
75%	8.6%	7.4%
75%	7.0%	6.2%

1) From Tech. Paper (B.1) by Dr. Funk.

APPENDIX 1

W.7 1 For Newtonian Flow the Equation is:

$$T_p = \frac{R}{2}\left(\frac{\Delta P}{L}\right) \qquad (1)$$

$$= \frac{D \, \Delta \, P}{4L} \text{ (as per S.R.C.)}^{1)} \qquad (1.1)$$

1.2 $$\dot{\gamma}_p = \frac{4.Q}{\pi R^3} \text{ , where Q = Vol. flow} \qquad (2)$$

2 For time independent Non-Newtonian Flow "in the absence of 'slip' at the tube wall", wall shear rate is obtained from the Metzner & Reed Modification of the Rabinowitsch-Mooney equation viz.:

$$\dot{\gamma}_p = \frac{3.n^1+1 =}{n'} \quad \frac{Q}{\pi R^3} \qquad (3)$$

where n^1 is the flow index, viz.:

$$n' = \frac{d(\text{Log } T_p)}{d\left(\text{Log } \frac{4.Q}{\pi R^3}\right)} \quad \frac{d(\text{Log } \Delta P)}{d(\text{Log } Q)} \qquad (4)$$

N.B. $$\frac{4\,Q}{\pi R^3} = \frac{4 \times \pi R^2 , V}{\pi R^3} \quad \text{(V = velocity)}$$

$$= \frac{4V}{R} = \frac{4V}{\frac{D}{2}} = \frac{8V}{D} \qquad (4.1)$$

2.1 Apparent viscosity is:

$$T_p / \dot{\gamma}_p \quad \text{, when} \qquad (4.2)$$

T_p = pipe wall stress
$\dot{\gamma}$ = shear rate in pipe flow

3 Where "slips" occur at the wall a Jastrzeski correction to EQ. 3 is required viz.:

$$Qc = Q- \pi R \, T_p = B_c\text{, where} \qquad (5)$$

B^c= 'Corrected' slip factor which varies only with shear rate, but is independent from tube radius R.

---

1) Saskatchewan Research Council Paper E.725

APPENDIX 1

W.7 3.1 Value of B_c obtained by plotting

$$Q/\pi R^3 . \tau_p \quad \text{against} \quad 1/R^2$$

or

$$\frac{2\,V}{D\,\tau_p} \quad \text{against } 1/R^2$$

3.2 τ_p is determined by test and B value is slope of straight lines for selected values of τ_p as parameter

4 EQ. 5 represents value of Q_c as "if no slip was present" (?) (paradoxical)

4.1 The corresponding shear rate at the wall ("true" ?) shear rate is:

$$\dot{\gamma}_c = \frac{3.n^1 + 1}{n'} = \frac{4Q_c}{\pi R^3} \qquad (6)$$

5 From EQ. 5 it can be seen that
Q_c is $<Q$

Therefore,
to obtain required value Q, V must be increased and γ_p must also be increased.

6 Similarly $\dot{\gamma}_c > \dot{\gamma}_p$

7 The B_c factor must be obtained by test, or estimated (guessed) or use mode of P_t (total ΔP values) from regression data (given at top of p. 268 of W.7 paper).

8 For $\dot{\gamma}$ and τ in annulus, P_c values can be neglected.

9 For annulus work consider Beta of .35 corresponding to a shear stress of 250 Pascals
= 2500 poise = 250,000 Centipoise

APPENDIX 1

W.9 1 Einstein Theoretical Viscosity/Packing Equation (theoretical sphere)

See X.2

$$\mu = \mu_o \quad (1 + 2.5\,\phi) \qquad (1)$$

$$\text{or} \quad \mu_r = \frac{\mu}{\mu_o} = 1 + 2.5\phi$$

μ_o = Vis. of suspending liquid = Vis. of water = 1

μ_r = Vis. of mixture as function of ϕ

ϕ = % coal packing volume

μ_r = Ratio : $\frac{\text{Mixt. Vis.}}{\text{Fluid Vis.}}$, μ_o for water = 1, then

$$\mu_r = \underline{\text{Mixt.Vis.}}$$

$$\mu_r = (1 + 2.5\phi) \qquad (2)$$

or for heavy ϕ, $\mu_r = \cap\phi$, i.e. for heavy concentration of coal (3)

1.1 Eq. 2 applies to low ϕ concentration (approaching zero).

2 For high concentrations:
Frankel & Acriyos theoretical equation is:

$$\mu_r = 1 + C' \left[\frac{(\phi/\phi m)^{\frac{1}{3}}}{(1-\phi/\phi m)^{\frac{1}{3}}}\right] \qquad (4)$$

C' = constant =(f)(assumed) geometrical arrangement of the spherical particles. Theoretical value 9/8 obtained from experiments.

3 An empirical equation by Chong, Christiansen & Baer is:

$$\mu_r = \left[1 + 0.75 \left(\frac{\phi/\phi m}{1-\phi/\phi m}\right)\right]^2 \qquad (5)$$

3.1 N.B. Values obtained by use of Eqs. 2 or 3 are not at all comparable to actual viscosities as shown in Table 1 (p. 306 of the 6th Symposium).

3.2 As ϕ approaches $\phi\infty$ so $\frac{\phi}{\phi m} \rightarrow 1$

then for both Eqs. (4) and (5) viscosity value will approach infinity viz

$$\frac{\text{numerator}}{1-1}(X) = \frac{X}{0} = \infty$$

where vol. fraction of particles $\phi \longrightarrow \phi m$

APPENDIX 1

W.9 4 However note that rearrangement of

Eqs. (4) and (5) give, respectively.

$$\frac{C'}{\mu_r - 1} = \left(\frac{\O m}{\O} - 1\right) \qquad (6)$$

N.B. Then if Ø = Øm lefthand term equals zero and if $\frac{C'}{\mu_r - 1}$ is an ordinate value - the curve will pass through zero.

5 Equation (5) is rearranged to the form

$$\frac{0.075}{\mu_r^{\frac{1}{2}} - 1} = \frac{\O m}{\O} - 1 \qquad (7)$$

6 Generally then:

$$\mu_r = 1 + K \ {\frac{1 + \O/\O m}{1 - \O/\O m}}^{2} \qquad (8)$$

where the constant K is different for each slurry

6.1 See Fig. 6c and note that K is the inverse of the slope of a line and its value decreases as the aggregate stability of the slurry increases

This to be further studied.

APPENDIX 2

Conversion of 70/30 wt. mix of CWF from Weight to Volume Ratio

1 Let X = wt. of 1 Imp. gal. CWF.

1.1 Let Sp. G. of coal be 1.3, then

$$\frac{.7\ X}{1.3} = X\cdot 054 \text{ lb/I. gal.}$$

$$\frac{.3\ X}{10} = X\cdot 03 \text{ lb/ I. gal.}$$

$$\overline{\quad X\cdot 084 \text{ lb/ I. gal.}\quad}$$

Then X .084 = wt. of 1 gal.

$$X = \frac{1}{.084} = 11.9 \text{ lbs. per I. gal.}$$

1.2 Sp. G. pf CWF $= \frac{11.9}{10} = \underline{1.19}$

$$\text{Vol. of Coal} = \frac{.7 \times 11.9}{1.3} = .64 \text{ gal.}$$

$$\text{Vol. of water} = \frac{.3 \times 11.9}{10} = .36 \text{ gal.}$$

2 Therefore, vol. ratio = 64/36 for a wt. ratio of 70/30

3 Considering possible variance in Sp. G. of coal

use value of 65/35 for Vol. Ratio CWF.

APPENDIX 2.1

ϕ and ϕ_∞ Values of Co-Al (Slurrytech) CWF

From discusion with Mr. Don Dunlop, Chairman of the Board of Slurrytech, re coal loading and % min. void.

---

1 ϕ = % vol. coal fraction (calculated)

ϕ_∞ @ Void volume - 6% for Co-Al

= 94% max. vol. coal fraction

2 Coal loading = 75% wt. (25% water)

3 From Appendix 2 volume ratio corresponding to 75% wt. coal loading is

$$\frac{.75x}{13} = .0577 \text{ X lb/1. gal.}$$

$$\frac{.25}{10} = \frac{.025 \text{ X lb/1. gal.}}{.0827 \text{ x lb/1. gal.}}$$

$$.0827X = \text{wt. of 1 Imp. gal.}$$

$$\text{Therefore } X = \frac{1}{.0827} = 12.1 \text{ lbs per 1. gal.}$$

4 Sp. G. = 1.21

5 $$\text{Vol. of coal} = \frac{.75 \text{ X } 12.1}{13} = .697 \text{ gal.}$$

$$\text{Vol. of water} = \frac{.25 \text{ x } 12.1}{10} = \frac{.303}{1.000} \text{ gal.}$$

6 Then % vol. ratio corresponding to a
75/25 wt. ratio is: 70/30 vol. ratio (approx.)

7 $$\frac{\emptyset}{\emptyset_\infty} = \frac{.70}{.94} = .7446$$

8 Then from Eq. 1 in Appendix No. 1 (X.2),
we have $\eta = \eta_0 \left(1 - \frac{\emptyset}{\emptyset_\infty}\right)^{-3.54}$ where

η_0 = Vis. of water = 1 centipoise, (approx.)

Subst. .7446 for $\frac{\emptyset}{\emptyset_\infty}$, we find

$$\begin{aligned}\eta &= \eta_0\,(1-.7446)^{-3.54}\\ &= 1\,(.2554)^{-3.54}\\ &= 125 \text{ centipoise}\end{aligned}$$

9 Note: Funk values average 7.5% porosity, in which case,
$$\frac{\emptyset}{\emptyset_\infty} = \frac{.70}{.925} = \underline{.7567}$$

Then,
$$\begin{aligned}\eta &= 1 \times (1-.7567)^{-3.54}\\ &= (.243)^{-3.54}\\ &= 149.6 \text{ centipoise}\end{aligned}$$

N.B. To be checked against actual Rheology Diagram of Co-Al

APPENDIX 2.1

ADDENDUM NO. 1

CONVERSION OF COAL VOL. FRACTION TO WT. FRACTION

---

1 A 70% wt. coal has a vol. fraction of .64

2 Now determine procedure to convert .64 back to .70

3 SPG of CWF = 1.19

4 Wt. of 1 Cu. Ft. = 62.4 x 1.19 = 74.256 lb.

5 Coal Vol. = .64 cu. ft. (by definition)

6 Coal sp. 9 = 1.3

7 Therefore wt. of coal per cu. ft. is 1.3 x 62.4 = 81.12 lbs.

8 Wt. of .64 cu. ft. = .64 x 81.2 = 51.9 lb.

9 Hence fraction wt. of coal is $\frac{51.9}{74.236}$ = .70 (rounded)

10 Arranging algebracally, we have

Sg. CWF = Sgw

Sg. coal = Sgc

V_o = % Vol. coal (expressed as a decimal)

Then wt. CWF per cu. ft. is: 62.4 x Sgw

wt of V_o vol. fraction
of coal is $V_o \times Sg.c \times 62.4$

Then fraction coal wt is:

$$\frac{V_o \times Sgc \times 62.4}{62.4 \times Sg.w}$$

$$= \frac{62.4\, V_o \times Sg.c}{Sg.w}$$

11 Equation for converting from Coal Volume Fraction to Coal Weight Fraction is then

$$CFw = V_o \times \frac{Sgc}{Sgw}$$, where

CFw = Coal fraction wt. in CWF

V_o = Coal fraction volume

Sgc = Sp. G. of Coal

Sgw = Sp. G. of CWF

Proof: Let V_o = .697;[1] Sgc = 1.3; Sgw = 1 , then

$$CFw = \frac{.697 \times 1.3}{1.21} = .75$$ (rounded

Confirmed by data of Appendix 2.1.

Q.E.D.

---

1) .697 = Vol. fraction of Coal in CWF

APPENDIX 3

Derivation of Symbols on Ordinates and Abscissa on Graph Plots Showing Shear Rate Versus ΔP

Reference: Determination of Rheological Properties of Coal/Oil Slurries by R. Gillies

Saskatchewan Research Council
- SRC Publication No. E.725.1.c.81

1 Fundamental Equations for Viscosity under laminar flow (1) (Newtonian)

$$\mu = \frac{\pi P R^{4} t}{8 L V_{o}} \text{ , where} \qquad (1)$$

μ = Viscosity - poise

P = ΔP

R = radius of tubing or pipe

L = length of tubing or pipe

v_{o} = volume flow

t = time of flow = 1 sec.

---

(1) Fluid Flow in Pipes by C.H. McClain - p. 44
The Industrial Press

APPENDIX 3

2 From Equation (1)

$$\mu = \frac{\pi r^2}{V_o} \times \frac{D^2}{4} \times \frac{1}{8L} \times \Delta P \qquad (2)$$

$$\frac{\pi r^2}{V_o} \times \frac{D^{\cancel{2}}}{4} \times \frac{D}{8L} \times \Delta P \qquad (2.1)$$

Now, $V_o = (V \times \pi r^2)$, where V = velocity

Then, $\frac{V_o}{r^2} = \pi V$, and

$\frac{r^2}{V_o} = \frac{1}{\pi V}$, and subst. in Eq. (2.1) we have

$$\mu = \frac{1}{V} \times \frac{D}{8} \times \frac{D}{4} \times \frac{1}{L} \times \Delta P$$

$$= \frac{D}{8V} \times \frac{D \times \Delta P}{4L}, \text{ so that}$$

$$\frac{D \Delta P}{4L} = \mu \times \frac{8V}{D} \qquad (3)$$

$\frac{D \Delta P}{4L}$ = ordinate values in dynes/cm^2 = T_w
= wall stress

and $\frac{8V}{D}$ = abscissa = shear rate number

3 Refer to Figure 30 of the attached reference paper and note the left hand graph which is the rheogram of a slurry of 50.6% coal (in oil) concentration. This graph shows that for a shear number $\frac{8V}{D}$ of 660 that the wall stress is

T_w = 515 dynes/cm^2

Now $\mu = \frac{T_w}{\text{shear rate}} = \frac{515}{660}$ = .78 poise

Figure 30

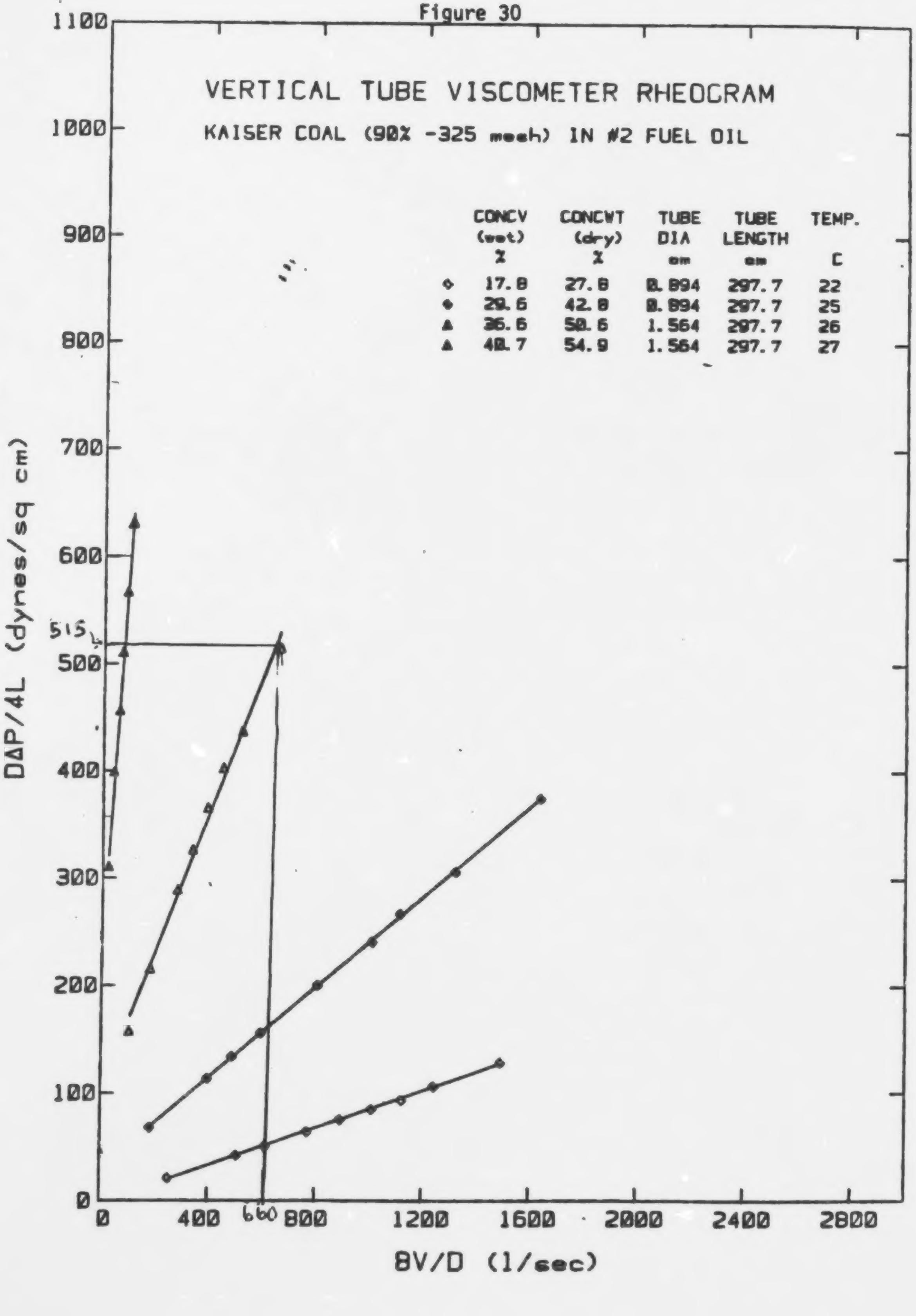
VERTICAL TUBE VISCOMETER RHEOGRAM
KAISER COAL (90% -325 mesh) IN #2 FUEL OIL
CONCV (wet) %
CONCWT (dry) %
TUBE DIA cm
TUBE LENGTH cm
TEMP. C
◇ 17.0 27.0 0.894 297.7 22
◆ 20.6 42.0 0.894 297.7 25
▲ 36.6 50.6 1.564 297.7 26
▲ 40.7 54.9 1.564 297.7 27
DΔP/4L (dynes/sq cm)
8V/D (1/sec)
0
100
200
300
400
500
600
700
800
900
1000
1100
400
800
1200
1600
2000
2400
2800
515
660

5-1-85

APPENDIX 4.R

Function Data on Operation of Mark III C.E. Atomizer (EPRI)

1	Refer to Fig. 1.4.A attached - generalized schematic of a Y-jet atomizer with the dimensions of the C.E. Mark 3 (Chatham).	
2	Atomizer dimensions of Mark 3 used, are as given.	
2.1	L. of annulus ½ - ¾" = (.625" assumed)	.0521 ft.
2.2	Dia. of annulus (ea. of 7)	.192 inch = .016 ft.
2.3	Area of annulus (each)	.0002 sq.ft.
3	Atom. steam pressure in CWF considered on two bases	
3.1	As part of the emulsion at 200 psi inlet to atomizer, less a) ΔP thru steam tube (5 psi est.) b) CWF back pressure (20 psi est.)	175 psi
3.2	As a steam flow subject to expansion to a critical pressure: (175 psi at point L - 20 psi B.P. = 155 psi at Point A,) then pressure at point Pt (critical) in the annulus is 155 x .53 (See Fig. 1.4.A) =	82 psi
4	Total "Systems" ΔP of CWF/steam emulsion assumed additive CWF plus atom. steam pressure	350 psi
5	CWF flow rate (per annulus) for 22 Meg_e (see App. 3.1)	.0036 cfs

6	Wt. of CWF flow/sec at Sp. G. of 1.19 = .0036 x 62.4 x 1.19 =	.267 lbs/sec.
7	Atom steam rate is .15 lb./lb.CWF	
7.1	Wt. of atom steam flow/sec is .15 x .267 =	.04 lb/sec.
8	$\bar{V}$ of atom. steam	
8.1	@ 175 psi	2.4 cf/lb
8.2	@ 82 psi	4.56 cf/lb
8.3	@ 125 psi (experimental value, see Item 14)	3.22 cf/lb
9	Volumes of atom. steam	
9.1	@ 175 psi - .04 x 2.4 =	.096 cfs
9.2	@ 82 psi - .04 x 4.56 =	.183 cfs
10	Volumes of CWF/steam emulsion	
10.1	@ 175 psi - (.0036 + .096) =	.10 cfs
10.2	@ 82 psi - (.0036 + .183) =	.186 cfs
10.3	at 150 psi – (.0136 + .11) =	.1136 cfs
11	Velocities of CWF emulsions	
11.1	@ 175 psi - $\frac{.10}{.0002}$ =	500 fps = 15240 cm/sec.

11.2 @ 82 psi - $\frac{.186}{.0002}$ = 930 fps
= 28346 cm./sec.

12 Density (ρ) of CWF/steam emulsions

12.1 @ 175 psi

Wt. CWF	.267 (item 6)	
Wt. atom steam	.04 (item 7)	
Wt. CWF/steam emulsion	.307 lbs.	
Eq. Volume emulsion	.10 cfs (item 10.1)	
therefore $\frac{.307}{.10}$ =		3.07 lbs/cf

12.2 @ 82 psi

$\frac{.307}{.186}$ (item 10.2) 1.65 lbs/cf

12.2.1 at 150 psi $\frac{307}{.1136}$ 2.7 lbs./cf

13 Sp. G. of CWF/steam emulsions.

13.1 @ 175 psi $\frac{3.07}{62.4}$ = .05

13.2 @ 82 psi $\frac{1.65}{62.4}$ = — .0264

14 Item 17.4 of Appendix 6 develops an experimental condition of atom. steam @ 125 psi and CWF @ 25 psi for a system Δ P (if additional) of 150 psi.

14.1 Calculated velocity of emulsion when steam is 125 psi

$\overline{V}$ (Specific Volume) = 3.220 cf/lb.

14.2 Volume of atom. steam = .04 x 3.220 = .129 cfs
add vol. of CWF .0036 cfs

14.3 Vol. emulsion/sec. .1326 cfs (at 125 psi atom. steam

14.4 Velocity of emulsion = $\frac{.1326}{.0002}$ = 663 fps
= 20,208 cm./sec.

14.5 Density of emulsion with 125 psi atom. steam:
$\frac{.307}{.1326} = \rho = 2.32$ lb./cf

14.6 Sp. G of emulsion with 125 psi atom. steam:
$\frac{2.32}{62.4} =$ .0372

15 Ø = % vol coal fraction (70/30 wt. mix)

Description of factor	175 psi	125 psi	82 psi	150 psi
Wt. of CWF/emulsion/sec	.307 lbs	.307 lbs	.307 lbs	.307 lbs.
Wt. of CWF/sec.	.267	.267	.267	.267
Wt. of 70% coal fraction (in CWF only)	.187	.187	.187	.187
Wt. of 30% water fraction	.08	.08	.08	.08
Wt. of steam component	.04	.04	.04	.04

15.1 Volumes

Volumes	cu.ft.	cu.ft.	cu.ft.	cu. ft.
Coal volume $\frac{.137}{1.3 \times 62.4}$	.0023	.0023	.0023	.0023
Water volume $\frac{.08}{62.4}$	.0013	.0013	.0013	.0013
CWF (only) volumes	.0036	.0036	.0036	.0036
Atom. steam volumes	.096	.129	.183	.1100
Total CWF/atom steam emulsion	.0996	.1326	.1866	.1136

16 Ø based on CWF only

	175 psi	125 psi	82 psi	150 psi
$\frac{.0023}{.0036}$	.64	.64	.64	.64

17 Ø based on CWF/steam emulsion:

175 psi $\frac{.0023}{.0996}$ = .024

125 psi $\frac{.0023}{.1326}$ = .017

82 psi $\frac{.0023}{.1866}$ = .012

150 psi $\frac{.0023}{.1136}$ .020

18 Slurrytech advised that their actual coal fraction is .75 with a max volume loading of .94 (though Funk average of .925 is used herein) i.e. Ø = .925. Ø (i.e. % vol. loading) at various atomizing steam pressures is calculated as follows for .75 coal fraction i.e. a 75/25 wt. mix.

	Description of factor	175 psi	125 psi	82 psi	150 psi
18.1	Wt. of CWF/emulsion/sec	.307 lbs	.307 lbs	.307 lbs	.307 lbs.
18.2	Wt. of CWF/sec.	.267	.267	.267	.267
18.3	Wt. of 75% fraction coal .75 x .267 =	0.20	0.20	0.20	0.20
18.4	Wt. of 25% water fraction .25 x .267	.067	.067	.067	.067
18.5	Wt. of atom steam .15 x .267	.04	.04	.04	.04
19	Coal volume $\frac{0.20}{1.3 \times 62.4}$	.00247	.00247	.00247	.00247
	Water volume $\frac{.067}{62.4}$	.0011	.0011	.0011	.0011
	CWF volume	.0036	.0036	.0036	.0036
20	Atom. steam volume .04 x $\overline{V}$	.096	.129	.182	.1100
21	Total CWF/atom steam vol.	.0996	.1326	.186	.1136
22	Ø based on CWF only $\frac{.00247}{.0036}$	.685	.685	.685	.685

	Description of factor	175 psi	125 psi	82 psi	150 psi
23	**ϕ based on total emulsion volume**				
	175 psi $\frac{.00247}{.0996}$	.0248			
	125 psi $\frac{.00247}{.1326}$		.0187		
	82 psi $\frac{.00247}{.1866}$			.0132	
	150 psi $\frac{.00247}{.1136}$				.022

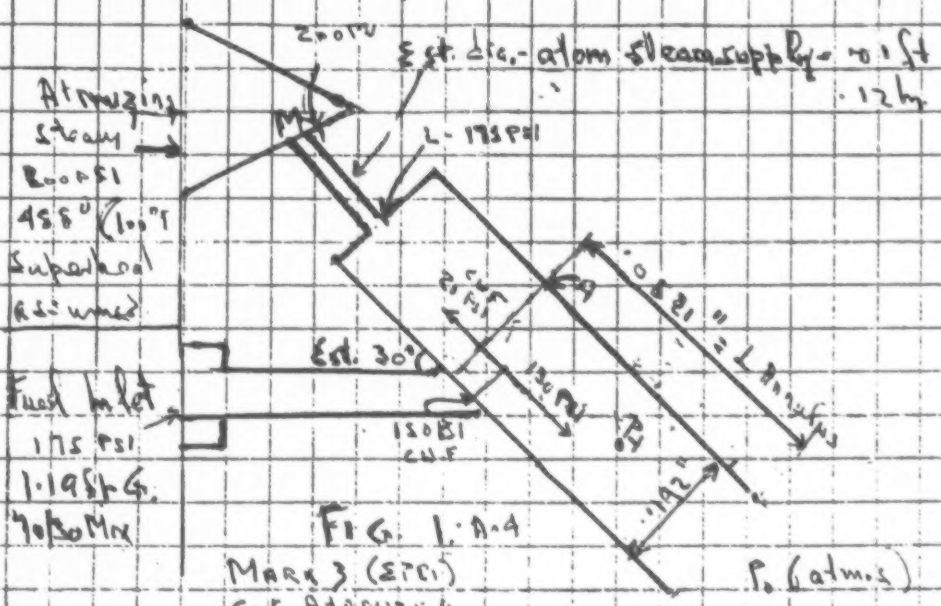
200°F
Est. dia. - atom steam supply = .01 ft
.12 in
L - 175 PSI
Atomizing steam
200 PSI
458°F (100°F
Superheat
assumed)
Est. 30°
Fuel Inlet
175 PSI
1.195 Sp.G.
70/30 Mix
CNF
20 PSI
150 PSI
150 PSI
CNF
.0581" = L Annulus
.192"
P₀ (atmos)

FIG. 1: A-4

MARK 3 (EPRI)
C.E ATOMIZER

APPENDIX 4.R ADDENDUM 1

May 15, 1985

CWF Requirement for the 22-5 Meg_e Boiler at Chatham

1	Estimated Heat Rate - BTU input/hr per Kw output	12,000
2	Calorific value of 70/30 mix CWF (Carbojel), BTU/lb.	10,000
3	BTU input for 22.5 Meg_e output: 22.5 x 1000 x 12,000 $\underline{\text{BTU/hr}}$ =	$270\cdot10^6$
4	No. of burners	4
5	Input per burner, BTU/hr =	$67\cdot5\cdot10^6$
6	Weight of CWF/burner $\frac{67\cdot5\cdot10^6}{10{,}000}$ lbs CWF/hr	$67\cdot5\cdot10^2$
7	No. of orifices per burner	7
8	Weight of CWF per orifice, i.e. annulus, lbs/hr.	$9.643.10^2$
9	Volume of CWF @ Sp. G. of 1.19, per sec., per annulus $\frac{9\cdot643\cdot10^2}{62.4 \times 1.19 \times 3600}$ = cfs	.0036

16-4-85

APPENDIX 5·R.

Viscosity Determination from Ø & $Ø_\infty$ Values of Average CWF and of Co-Al.

---

1 See Report X.2 and note governing equation is:

$$\eta = \eta o\left(1- \frac{Ø}{Ø}\right)^{-3.54} \qquad (1)$$

No = Viscosity of water carrier = 1 Cp

2 $Ø_\infty$ for Co-Al (Slurryjet)

2.1 According to Don Dunlop porosity can be reduced to 6% =.94 Ø
According Dr. Funk data, 7 to 8% porosity,
say 7.5% porosity .925 Ø

2.2 Co-Al % weight coal fraction (assumed here) 70%

2.2.1 (N.B. max % weight fraction Co-Al is 75%)

3 Therefore the computation is:

3.1 $Ø_\infty$ per slurry set - .94; with CWF based on .70 Wt. fraction
At 175 psi (Ø of .64 as per item 1b Appendix 4)

$$\eta = 1\left(1 - \frac{.64}{.94}\right)^{-3.54}$$

$$= .319^{-3.54} = \qquad 57.1Cp$$

At 82 psi Ø = .64 (no change) 57.1Cp

3.2 Viscosity determination on CWF basis (Ø = .64 for coal wt % .70)
$Ø_\infty$ value at average of Dr. Funk of .925
At 175 psi - CWF basis

$$\eta = 1\left(1- \frac{.64}{.925}\right)^{-3.54} = (.31)^{-3.54} = \quad = \quad 63.2Cp$$

At 82 psi η = same as 175 psi = 63.2Cp

3.3 The literature shows that for other than Co-Al, a max $Ø_\infty$ is .70 but a value of .75 is used here i.e. a porosity of 25% (.25), then $Ø_\infty$ = .75 (approx.)
(see Report Code X.15)
Then η (for $Ø_\infty$ of .75 = $1\left(1-\frac{.64}{.75}\right)^{-3.54}$

Then for 175 psi or 82 psi $\eta = (.1466)^{-3.54} =$ 895 Cp (CWF only)

4 Consider viscosity value IF Ø is based on CWF/steam emulsion,
(70/30 wt. mix)
At 175 psi, $Ø = .024$
At 82 psi, $Ø = .012$ (See Appendix 4.R)

4.1 Then for $Ø_\infty$ of .94 for Slurryjet (Co-Al) we have
At 175 psi $\eta = 1\left(1-\frac{.024}{.94}\right)^{-3.54}$

$\eta = (.974)^{-3.54} =$ 1.09 Cp

At 82 psi, $\eta = 1\left(1-\frac{.012}{.94}\right)^{-3.54}$

✓ $\eta = (.987)^{-3.54} =$ 1.044 Cp

4.2 Repeat viscosity determinations of item 4 with $Ø_\infty$ of .925 (Dr. Funk average) for CWF/steam emulsion, we have:

4.3 At 175 psi, $\eta = 1\left(1-\frac{.024}{.925}\right)^{-3.54}$

$\eta = (.967)^{-3.54}$ 1.097 Cp

At 82 psi, $\eta = 1\left(1-\frac{.012}{.925}\right)^{-3.54}$

$\eta = (.987)^{-3.54}$ = 1.047 Cp

4.4 With $Ø_\infty$ of .75, on emulsion basis we have:
At 175 psi $\eta = 1\left(1-\frac{.024}{.75}\right)^{-3.54}$

$\eta = (.976)^{-3.55}$ 1.09 Cp

4.5 At 82 psi, $\eta = 1\left(1 - \frac{.012}{.75}\right)^{-3.54}$

$\eta = (.985)^{-3.54} = 1.055$ Cp

IMPORTANT

5 N.B. Authors, ref. X.2 state that when $\phi < .1$ as in cases 4.1 to 4.5 that the value of $K = -3.54$ may not be applicable because of the effect of electric forces and interparticle interaction in this very high state of fluidity (Could turbulence be a factor?)

6 This brings up the question of the "fluid nature" of a CWF/steam emulsion.

6.1 What is the "real" viscosity of a CWF/steam emulsion at high flow velocities? For example Appendix 4 shows 2 values of possible velocity of 500 fps & 930 fps.

7 See Fig. 7.X.2 in Figures Section and note viscosity range of (approx.) 15 to 4000 mPas (centipoise) for values of $1 - \frac{\phi}{\phi c}$ ranging from 0.5 to 0.1 corresponding to $\frac{\phi}{\phi c}$ values of .5 to .9 ($\phi c = \phi_\infty$).

8 See also Table 3.X.2 (by same authors) and note the viscosity range for a 70% wt. coal CWF of 138 to 2400 centipoise (Chinese coals) with an estimated median value of approx. 500 - 600 centipoise.

APPENDIX 6.R

Determination of Constants n and K by Application of the Rabinowitsch-Mooney modification of the Newtonian Flow Basic Equation to the Dimensional and Operating Data of the Mark 3 C.E. Atomizer (EPRI) (Chatham)

1 In Appendix 3 it was shown that the relationship of Tw, D, ΔP, L, V & μ for the laminar of flow of a Newtonian fluid was expressed by the equation

$$Tw = \frac{D\Delta P}{4L} = \frac{\mu 8V}{D} \tag{1}$$

2 For a non-Newtonian fluid operating under the Power Law relationship of
$Tw = K\dot{\gamma}^n$ in the pseudoplastic mode, the Rabinowitsch-Mooney (R.M.) equation is:

$$Tw = \frac{D\Delta P}{4L} = \frac{K(1+3n)^n}{4n} \left(\frac{8V}{D}\right)^n \tag{2}$$

Then from equation 1, since $Tw = \frac{\mu 8v}{D}$

Therefore the term $\frac{K(1+3n)^n}{4n}$ is the μ value of the equation

2.1 The value of the constant n indicates the flow mode of the CWF, viz.:

$n = 1$ - Newtonian mode
$n > 1$ - dilatant mode
$n < 1$ - pseudoplastic mode

3 There are two unknown constants, K and n.

3.1 Therefore T_w and μ must be known to solve for K and n.

4 For a 70/30 CWF mix it was shown in item 16 of Appendix 4 that $\phi = .64$ and assuming a ϕ_∞ of .75, Item 3.3 of Appendix 5 shows that $\mu =$ 895 Cp

= 8.95 poise

5 The ΔP value is assumed to be 350 psi based on the assumption that atomizing steam and CWF pressures are additive and have values of (Chatham data)

CWF 175 psi
Atom. steam 175 psi i.e. $\Delta P = 350$ psi
350 psi

6 Value (C.E. Mark 3) of D, L, and ΔP expressed in c.g.s. units are:

D = .192" = .488 cm
L = .625" = 1.588 cm
$\Delta P = 350 \times 68948 =$ 24.10^6 dynes/cm^2

7 From the data of item 6 above,

$$T_w = \frac{D\Delta P}{4L} = \frac{.488 \times 24.10^6}{4 \times 1.588} = 1.85.10^6 \text{ dynes/cm}^2$$

8 To solve for n (Eq. 2) we have two velocity values (Emulsion Velocity)
(Item II Appendix 4)

Case A (175 psi atom. steam) V = 500 fps
= 15240 cm./sec.

Case B (82 psi atom. steam) V = 930 fps
= 28346 cm./sec.

APPENDIX 6.R

8.1 From Item 4 above $\mu =$ 8.95 poise

8.2 Fundamentally, $T_w = \mu\dot{\gamma}$

Then for:

8.3 Case A - 500 fps (175 psi) (μ = 8.95 poise)

$$\dot{\gamma} = \left(\frac{8V}{D}\right)^n = \frac{8 \times 15240}{.488}$$
$$= (2.5\cdot10^5)^n$$

9 Now from Item 7 above (Page 2)

$T_w = 1\cdot85\cdot10^6$ = stress, dynes/cm^2, then

$1.85\cdot10^6 = 8.95(2.5\cdot10^5)^n$; then

$$(2.5\cdot10^5)^n = \frac{1.85\cdot10^6}{8.95} = (2.067)10^5$$

Taking logs of both sides, we have

$5n \log(2.5) = 5 \log (2.067)$

$5n(.398) = 5(.316)$

$$n = \frac{.316}{.398} = .79$$

Case A
n = .79 at
500 fps.
8.95 poise
350 psi ΔP

10 Case B - 930 fps (82 psi) (μ = 8.95 poise)

$$\dot{\gamma} = \left(\frac{8V}{D}\right)^n = \left(\frac{8 \times 28346}{.488}\right)^n$$
$$= (4.65 \times 10^5)^n$$

$(4\cdot65\cdot10^5)^n = (2.067)10^5$

$5n \log(4.65) = 5 \log (2.07)$

$n(.667) = (.316)$

$$n = \frac{.316}{.667} = .47$$

Case B
n = .47 at
930 fps.
8.95 poise
350 psi ΔP

APPENDIX 6.R

11 Case C - 500 fps (175 psi) (μ = .63 poise)

$$\left(\frac{8V}{D}\right)^n = (2.5\cdot10^5)^n \text{ (Item 8.3)}$$

$$Tw = \frac{1.85.10^6}{.63} = (2.94).10^6$$

Then, $(2.5.10^5)^n = (2.94).10^6$

$5n \log(2.5) = 6 \log (2.94)$

$5n(.398) = 6(.468)$

$n = \frac{.468}{.398} = 1.17$

Case C
n = 1.17 at
500 fps.
0.63 poise
350 psi ΔP

12 Case D - 930 fps (82 psi) (μ= .63 poise)

$$\left(\frac{8V}{D}\right)^n = (4.65\cdot10^5)^n \text{ (Item 10)}$$

$$Tw = (2.94).10^6 \text{ (Item 11)}$$

Then,

$(4\cdot65\cdot10^5)^n = (2.94).10^6$

$5n \log(4.65) = 6 \log (2.94)$

$5n(.667) = 6(.468)$

$n = \frac{.468}{.667} = .702$

Case D
n = .702 at
930 fps.
0.63 poise
350 psi ΔP

13 It will be seen from Cases A to C inclusive that the value of constant n changes in similar fashion for the two velocities of 500 fps and 930 fps, with the application to each velocity of viscosities 8.95 poise and .63 poise.

13.1 With the 8.95 poise viscosity the n value changes from .79 to .47 with an increase in velocity from 500 fps to 930 fps, indicating a pseudoplastic mode.

13.2 In the case of the lower viscosity of .63 posie the n value changes is from dilatant mode indication number n = 1.17, to a pseudoplastic indication of .702.
(Ques. Is this real?) The normal interpretation of dilatant mode is an increase in viscosity with an increase in velocity. The answer to this "seeming" anomaly is that the viscosity of .63 poise, obtained from the same Ø/Ø∞ ratio, is the same for both velocities. Therefore the anomoly may be that in this type of analysis than an n value >1 is only "apparent" i.e. real for a given singleor several velocity values - but therefore cannot be used to extrapolate for viscosity change over a wide (and high) range of velocities. The plotting of numerous n values for a velocity range, say from 200 to 2000 fps might be quite revealing.

14 At this point the following should perhaps be noted.

a) The annulus ΔP of 350 psi is based on real data from the C.E. Chatham test, (assuming atom. steam & CWF pressures are additive).

b) The concept that viscosity of the CWF (only) is a function of Ø/Ø∞ ratio, with the Ø values being:
Carbojel (at Chatham) 70/30 mix, Ø = .64 (App. 4.R Item 16)
Co-Al (from given data) 75/25 mix, Ø = .685 (App. 4.R Item 22)

c) The $Ø_\infty$ values used are:

.75 (for Carbojel - assumed)

.925 (for Co-Al - given)

d) The $\frac{Ø}{Ø\,\infty}$ ratios are then: (for CWF only)

For a 70/30 mix

$\frac{.64}{.75}$ = .853 (Carbojel assumed value for a viscosity of (Ref. X.2) 8.95 poise

$\frac{.64}{.925}$ = .69 (one value for Co-Al) for a viscosity of (Ref. X.2) .63 poise

For a 75/25 mix (Co-Al), we have

$\frac{Ø}{Ø_\infty} = \frac{.685}{.925} = .74$ for a viscosity of 1.18 poise

14.1 For a 75/25 mix with a CWF having a $Ø_\infty$ of only .75 the ratio of

$\frac{Ø}{Ø_\infty} = \frac{.685}{.75} = .9133$

(for a viscocity of 57.54 poise versus Co-Al CWF of 1.18 poise)

This is proof of Dr. Funk's statement that viscosity will sharply rise if the $Ø_\infty$ value is too low.

15 A viscosity value of .63 poise (used in this work as a Co-Al standard) would be that of a laminar flow fluid and this can be tested from the Reynolds equation for laminar flow.

$$Re = \frac{6.31W}{d\mu} \quad ^{1})$$

Subst. W = lbs./hr - .267 x 3600 = 961 lbs./hr. (.267 from App. 4.R Item 6)

d = .192 inch, = 63 Centipoise

We have $Re = \frac{6.31 \times 961}{.192 \times 63} = 501$(<2000, therefore laminar flow)

---

1) Ref. Crane Tech. Paper No. 410 P.3.8

15.1 The ΔP equation for laminar flow is,

$$\Delta P100 = \frac{.0668v}{d^2}$$ (2), hence, for a given v and d, the ΔP is directly proportional to μ (in centipoise).

In such a case the ΔP component for CWF only would be

$$\frac{63}{895} \times 175 = 12.3 \text{ psi}$$

15.2 As a numerical experiment consider the following pressures of a CWF of 63 Centipoise

CWF	25 psi
Atom. steam	125 psi
Total ΔP	150 psi (through atomizer)

15.3 Then

$$T_w = \frac{D\Delta P}{4L} = \frac{.488 \times 150 \times 68948}{4 \times 1.588}$$

$$= 794{,}550 \text{ dynes/cm}^2$$

16 Case E (663 fps) (App. 4.R Item 14.4) (125 psi) (μ = .63 poise)

$$\left(\frac{8V}{D}\right)^n = \left(\frac{8 \times 20208}{.488}\right)^n = (3.3 \cdot 10^5)^n$$

$$T_w/\mu = \frac{794550}{.63} = (1.26) \cdot 10^6$$

Then $(3.3 \cdot 10^5)^n = (1.26)^6$

$5n \log(3.3) = 6 \log(1.26)$

$5n(.5185) = 6(.16037)$

$$n = \frac{.10037}{.5185} = .194$$

Case E
n = .193 at
663 fps.
.63 poise
150 psi ΔP

16.1 From the fact of an n value of .193 we can surmise that the reduction of the Tw value resulted in a greater degree of pseudoplasticity.

2) Crane Ref. P.3.12

17 Determinations of K values in the Rabinowitsch-Mooney Equation

17.1 The term $K \frac{(1 + 3n)^{n}}{4n}$ is considered to be the μ equivalent, therefore with the substitutions of the calculated n values we obtain:

18 Case A (n = .79)

$$K \frac{(1 + 3 \times .79)^{.79}}{4 \times .79} = 8.95 \quad \text{(Item 4)}$$

$$K \frac{(3.37)^{.79}}{3.16} = 8.95$$

$$K \frac{(2.61)}{3.16} = 8.95$$

$$K = \frac{8.95}{.826} = 10.83$$

Case A

$K = 10.83$

$n = .79$

19 Case B (n = .47)

$$K \frac{(1 + 3 \times .47)^{.47}}{4 \times .47} = 8.95 \quad \text{(Item 4)}$$

$$K \frac{(2.41)^{.47}}{1.88} = 8.95$$

$$K \frac{(1.512)}{1.88} = 8.95$$

$$K = \frac{8.95}{.804} = 11.13$$

Case B

$K = 11.13$

$n = .47$

20 Case C (n = 1.17)

$$K \frac{(1 + 3 \times 1.17)^{1.17}}{4 \times 1.17} = .63$$

$$K \frac{(4.51)^{1.17}}{4.68} = .63$$

$$K \frac{(5.83)}{4.68} = .63$$

$$K = \frac{.63}{1.246} = .506$$

Case C
$K = .506$
$n = 1.17$

21 Case D (n = .702)

$$K \frac{(1 + 3 \times .702)^{.702}}{4 \times .702} = .63$$

$$K \frac{(3.106)^{.702}}{2.808} = .63$$

$$K \frac{(2.26)}{2.808} = .63$$

$$K = \frac{.63}{.806} = .782$$

Case D
$K = .782$
$n = .702$

22 Case E (n = .193)

$$K \frac{(1 + 3 \times .193)^{.193}}{4 \times .193} = .63$$

$$K \frac{(1.58)^{.193}}{.772} = .63$$

$$K \frac{(1.09)}{.772} = .63$$

$$K = \frac{.63}{1.412} = .446$$

Case E
$K = .446$
$n = .193$

23 The values for constant n obtained by calculation based on the Rabinowitsch-Mooney Equation apply only to a CWF with viscosities obtained from the ϕ and $\phi\infty$ values known (or assumed) of a "standard" CWF and a Co-Al.

24 The n values obtained are not basically applicable to the CWF/atom. steam emulsion where a viscosity of approx. one centipoise is indicated (See Appendix 5.R Page 2).

25 The n (and K) constant values obtained are applicable in the calculation of pressure drops in a supply line to a burner at various velocities.

26 The n values for CWF only, may have a use in annulus flow in the event that it is found that atom. steam separation occurs, or that the atom. steam serves as a "driver" of the CWF through the annulus at high velocity, with atomization occuring post annulus exit. The atomizing effect would then be a function of the energy in the CWF and the impact effect of the atomizing steam, as it expands at a probable sonic or supersonic velocity. If the velocity of the atomixing steam were supersonic, then the resultant shock waves could have a significant disrupting effect on the CWF "jet stream" issuing from the nozzle exit.

27 The following Table 1.A.6.R tabulates the results of the calculations for n in Items 8.3 to 13 (Cases A, B, C & D) and in Item 17.6 (Case E).

28 It will be seen that the calculations in this Appendix 6.R are based on viscosity as determined from the ϕ and $\phi\infty$ values of the CWF and on the assumption that CWF and atom. steam pressures are additive in the annulus.

28.1 The value of 350 psi ΔP, used is based on actual field data of CWF and atom. steam pressures in the C.E. Chatham trial.

28.2 It would be very desirable to determine, by test, the actual pressures at the entrance and mid-point of the annulus, i.e. at points L, A and P_t as shown on Fig. 1.A.4 of Appendix 4.

28.3 Such test would prove the additive assumption correct, (or nearly so) or show the need of revision to the values of n and the wall stress Tw, if addition of the pressures are not additive.

APPENDIX 6.R - ADDENDUM 1

Calculation of the Rabinowitsch-Mooney Constants n & K if based on:
a) Velocity of the CWF at its volume rate;
b) Viscosity of the CWF/atom-steam emulsion at the emulsion velocity

1 CWF only Velocity

1.1 Volume Flow .0036 cfs per annulus

1.2 Area of annulus .0002 sq.ft.

1.3 Flow Velocity - CWF only

$$\frac{.0036}{.0002} = 18 \text{ fps} = 549 \text{ cm./sec.}$$

1.4 Estimated ΔP CWF only through annulus = 150 psi

2 $$\left(\frac{8V}{D}\right)^n = \frac{8 \times 549}{.488} = (9000)^n = (9\cdot10^3)^n$$

3 $$T_w = \frac{D\Delta P}{4L}$$

$$T_w = \frac{.488 \times 150 \times 68948}{4 \times 1.588}$$

$$T_w = (7.95)\cdot10^5$$

4 Case A ($\mu = 8.95$ poise)

4.1

$$\frac{Tw}{\mu} = \frac{(7.95)\cdot 10^5}{8.95}$$

$$= (8.9)\cdot 10^4\text{, then}$$

$$(9.10^3)^n = (8.9)\cdot 10^4$$

$$3n \log(9) = 4 \log (8.9)$$

$$3n (.954) = 4(.949)$$

$$n = \frac{.949}{.954} = .995$$

Cases A & B

$n = .995$

$\mu = 8.95$

4.2 Case B - same values as Case A, $n = .995$

5 Case C ($\mu = .63$ poise)

$$\frac{Tw}{\mu} = \frac{(7.95)\cdot 10^5}{.63} = (1.262)10^6$$

$$3n \log(9) = 6 \log (1.262)$$

$$n (.954) = (.10106)$$

$$n = \frac{.10106}{.954} = .106$$

Cases C,D &E

$n = .106$

$\mu = .63$

5.1 Case E = Case D = Case C

6 Cases A to E are pseudoplastic mode

7 CWF/atom. steam Emulsion

7.1 From Appendix 5.R Item 4, it is seen that a value of .01 poise can be used as the viscosity of a CWF/atom. steam emulsion.

7.2 The velocities and total pressure drops for the n calculations, for the emulsion, will be those as used in the calculations of n at viscosities of 8.95 poise and .63 poise.

8 We have then:

8.1 For Cases A - D incl., at ΔP 350 psi.

$$\frac{Tw}{\mu} = \frac{(1.85).10^6}{.01} = (1.85).10^8$$

Then:

Case A (500 fps) (See Item 8.3 Appendix 6.R for $\left(\frac{8V}{D}\right)^n$).

$n(\log 2.5) = \log (1.85)$

$n(.398) = (.267)$

$$n = \frac{.267}{.398} = .67$$

Case A

n = 0.67 at
500 fps
.01 poise
350 psi ΔP

9 Case B (930 fps) (See Item 10 Appendix 6.R for $\left(\frac{8V}{D}\right)^n$).

$n(\log 4.65) = \log (1.85)$

$n(.667) = (.267)$

$$n = \frac{.267}{.667} = .40$$

Case B

n = 0.40 at
930 fps
.01 poise
350 psi ΔP

10 Case C = Case A (Viscosities, fps, and ΔP are the same

Case C

n = 0.67 at
500 fps
.01 poise
350 psi ΔP

11 Case D = Case B (Viscosities, fps, and ΔP are the same

Case D

n = 0.40 at
930 fps
.01 poise
350 psi ΔP

12 **Case E (663 fps, ΔP 150 psi)**

$n(\log 3.3) = \log(1.85)$

$n(.5185) = (.267)$

$$n = \frac{.267}{.5185} = .515$$

Case E

n = .515 at
663 fps
.01 poise
150 psi ΔP

13 Cases A & B (& C & D) show a decline in n values with increase in velocity (i.e. shear rate) - therefore all modes pseudoplastic.

13.1 Comparing A & E, we find n for E at .515 indicative of pseudoplastic mode. However, E at 663 fps is greater than A at 500 fps. - which is a rising trend and conceivably leads to dilatancy at higher shear rates (higher V or smaller D).

Constant K values for conditions a) Velocity of the CWF at its volume rate, and b) Viscosity of the CWF/atom-steam emulsion at the emulsion velocity

14 K values for condition (a), CWF only at the velocity of its volume rate

14.1 Case A $(n = .995)$ $(\mu = 8.95)$

$$\frac{K(1 + 3n)^n}{4n} = 8.95$$

$$\frac{K(3.985)^{.995}}{4 \times .995} = 8.95$$

$$\frac{K(3.96)}{3.98} = 8.95$$

$$K(.995) = 8.95$$

$$K = \frac{8.95}{.998} = 9$$

Case A

$K = 9$

$n = .995$

$\mu = 8.95$

14.2 Case B $(n = .995)$ $(\mu = 8.95)$

K = Case A = 9

Case B

$K = 9$

$n = .995$

$\mu = 8.95$

14.3 Case C $(n = .106)$ $(\mu = .63)$

$$\frac{K(1 + 3n)^n}{4n} = .63$$

$$\frac{K(2.89)^{.106}}{1.7} = .63$$

$$\frac{K(1.06)}{1.7} = .63$$

$$K(.62) = .63$$

$$K = \frac{.63}{.62} = 1.016$$

Case C

$K = 1.016$

$n = .106$

$\mu = .63$

14.4 Case D ($n = .106$) ($\mu = .63$) = Case C

Case D
K = 1.016
n = .106
μ = .63

14.5 Casee E = Case D

Case E
K = 1.016
n = .106
μ = .63

15 K values for Condition (b): Viscosity of .01 poise (emulsion) and with ΔPs and velocities as in Cases A to E in Appendix 6.R, Items 8.3 to 12 and Item 16.

15.1 Case A (500 fps) ($n = .67$) ($\mu = .01$

$$\frac{K(1 + 3n)^{.67}}{4n} = .01$$

$$K \; \frac{2.1}{2.68} = .01$$

$$K(.78) = .01$$

$$= \frac{.01}{.78} = 9$$

Case A
K = .013
n = .67
μ = .01

15.2 Case B (593 fps) ($n = .40$) ($\mu = .01$

$$\frac{K(1 + 3n)^{.40}}{4n} = .01$$

$$K \; \frac{1.37}{1.60} = .01$$

$$K(.856) = .01$$

$$= \frac{.01}{.856} = 9$$

Case B
K = .0117
n = .40
μ = .01

15.3 Case C (500 fps) (n = .67) (μ= .01)

Case C = Case A

Case C

K = .013

n = .67

μ = .01

15.4 Case D (930 fps) (n = .40) (μ= .01)

Case D = Case B

Case D

K = .0117

n = .40

μ = .01

15.5 Case E (663 fps) (n = .515) (μ= .01

$$\frac{K(1 + 3n)^{.515}}{4n} = .01$$

$$K \frac{1.62}{2.06} = .01$$

$$K(.786) = .01$$

$$\underline{K} = \frac{.01}{.78} = .0127$$

Case E

K = .0127

n = .515

μ = .01

APPENDIX 7

Application of Equations derived from the Basic D'Arcy and Poiseuille formulae (from Crane Tech Paper 410) to the C.E. Mark III (EPRI) Atomizer design and the Chatham Operating Parameters (See Appendix 4.R, Page 1)

1 Determine Re number for each flow condition and CWF only characteristics (from $\emptyset/\emptyset_\infty$ values)

2 See Appendix 6.R

3 Equation is: $Re = \frac{6.31W}{d\mu}$ (Crane Page 3.18) (Eq. 1)

3.1 Re number for luminar flow is <2000

W = flow, lbs. hr.

d = annulus dia., inches

μ = viscosity - centipoise

4 $W = 9.643.10^2$

$= 964.3$ lbs./hr. plus atom. steam $(.04 \times 3600)$

$= 144 \times 964$

$= 1108$ lbs. hr.

$d = .192$ inch

5 Case A - μ = 895 centipoise

CWF only

$$Re = \frac{6.31 \times 1108}{.192 \times 895} = 40.7$$

Case A

Re = 40.7

laminar

1) Crane Tech Paper 410 entitled "Flow of Fluids Through Pipe, Valves & Fittings.

APPENDIX 7

5.1 Case B = Case A
CWF only

Case B
Re = 40.7
laminar

5.2 Case C = 63 centipoise
Case D = 63 centipoise
Case E = 63 centipoise

Cases C, D, E
Re = 578
laminar

$$Re = \frac{6.31 \times 1108}{.192 \times 63} = 578$$

6 Check Re no. for CWF/atom. steam emulsion at $\mu = 1$ centipoise for all cases

$$Re = \frac{6.31 \times 1108}{.192 \times 1} = 36414$$

Cases A,B,C,D,E
Re = 36,414
turbulent

7 Equation for turbulent flow (Crane page 3.10)

$$\Delta P_{100} = \frac{0.000336\ fw^2}{d^5 \rho}$$

7.1 Friction factor f for Re 36414 in a .2" dia. pipe is:
(Crane page A.25) f = .038

7.2

ρ for the several cases is:	Density
Case A - 175 psi atom. steam (App. 4.R Item 12)	P = 3.07
Case B - 82 psi atom. steam	P = 1.65
Case C = Case A	P = 3.07
Case D = Case B	P = 1.65
Case E - 125 psi atom. steam (App. 4.R. item 14.5)	P = 2.32

8 Calculations for ΔP through annulus length of .625" = .052 ft.

8.1 **Case A 175 psi, P = 3.07**

$$\Delta P_{100} = \frac{0.000336 \times .038 \times (1108)^2}{(.192^5 \times 3.07}$$

$$= \frac{15.675}{.000261 \times 3.07}$$

$$= \frac{15.675}{.000801}$$

$$\Delta P_{100} = 19.6.10^3 \text{ psi/100 ft.}$$

$$\Delta P_{.052} = \frac{19.6.10^3}{10^2} \times .052$$

$$= 10.2 \text{ psi}$$

Case A

ΔP Friction
Emulsion Flow
10.2 psi

9 Despite an Re of 36,000 with the flow normally in the turbulent zone, an experiment with calculation of ΔP from the use of the laminar flow equation at a vis. of 1 Cp, we find that the laminar flow ΔP is:

$$\Delta P_{100} - \frac{.0668 \times \mu \times v}{d^2} \qquad \text{(Eq. 3)}$$

$$\Delta P_{100} = \frac{.0668 \times 1 \times 500}{(.192)^2} \text{ (emulsion velocity with CWF) (fps)}$$

$$\Delta P_{100} = \frac{33.4}{.037} = 903 \text{ psi}$$

$$\Delta P_{.052} = \frac{903}{100} \times .052 = .47 \text{ psi (not likely)}$$

APPENDIX 7

10 Now apply Case B conditions to Equation 2

Case B (82 psi) $\rho = 1.65$

$$\Delta P_{100} = \frac{0.000336 \times .038 \times (1108)^2}{(.192)^5 \times 1.65}$$

$$= \frac{15.675}{.000261 \times 1.65}$$

$$= \frac{15.675}{.00043}$$

$$\Delta P_{100} = 36.45.10^3$$

$$\Delta P_{.052} = \frac{36.45.10^3}{10^2} \times .052$$

$$= 19 \text{ psi}$$

Case B

ΔP Friction

19 psi

11 Case C = Case A (both 175 psi)

Case C

ΔP friction

10.2 psi

12 Case D = Case B (both 82 psi)

Case D

ΔP Friction

19 psi

13 Case E (125 psi) (P 2.32)

$$\Delta P_{100} = \frac{15.675}{.000261 \times 2.32}$$

$$= \frac{15.675}{.0006}$$

$$\Delta P_{100} = 26.10^3$$

$$\Delta P_{.052} = \frac{26.10^3}{10^2} \times .052$$

Case E

ΔP Friction

13.5 psi

14 From ΔP due to friction calculations, Cases A-E, one can infer that the dominant pressure factor is the velocity head.

15 There are three velocities:

Cases A & C	(175 psi)	500 fps.
Cases B & D	(82 psi)	930 fps.
Case E	(125 psi)	663 fps.

16 The velocity head equation is derived as follows:

$$V \times A = \frac{Q}{.8}\text{, and so } V' = \frac{Q}{.8A} = \frac{V}{.8}$$

V' = velocity, fps
A = area, sq. ft.
Q = volume of flow, cfs.
.8 = orifice coefficient (assumed)

Now:

$$v^2 = 2ah_1 \qquad (2)$$

$$h_1 = \frac{V^2}{2a} = \frac{V^2}{64.4}$$

17 Velocity heads for the various cases are then:

Cases A & C $\dfrac{\left(\dfrac{500}{.8}\right)^2}{2a} = \dfrac{(625)^2}{64.4}$ = 6065 feet of head per sq. ft.

17.1 Cases B & D $\dfrac{\left(\dfrac{930}{.8}\right)^2}{2a} = \dfrac{(1162.5)^2}{64.4}$ = 21,000 feet of head per sq. ft.

17.2 Case E $\dfrac{\left(\dfrac{663}{.8}\right)^2}{2a} = \dfrac{(829)^2}{64.4}$ = 10.670 feet of head per sq. ft.

18 Pressure due to ft. of head, psi is:

$$P = h_1 \times \rho$$

18.1 ρ values are:

Cases A & C	3.07 lbs./cu.ft.
Cases B & D	1.65 lbs./cu.ft.
Case E	2.32 lbs./cu.ft.

18.2 Then P values for velocity head (psi) are:

Cases A & C — PSI

$$\frac{6065 \times 3.07}{144} = 129$$

Cases B & D

$$\frac{21{,}000 \times 1.65}{144} = 240$$

Case E

$$\frac{10{,}670 \times 2.32}{144} = 172$$

19 Total Annulus ΔP = friction head + velocity head

	Total ΔP (psi)
Cases A & C (175 psi) (10.2 + 129)	= 139.2
Cases B & D (82 psi) (19 + 240)	= 259
Case E (13.5 + 172)	= 185.5

20 Remarks

Cases A, C, & E are within operating range 1)

Cases B & D are higher than operating range

20.1 Operating ranges are the individual pressures of the CWF and atom. steam.

1) "Operating ranges" and their values consistent with the operating data of the C.E. Chatham Test. But, should atom. steam and CWF pressures be partially additive, then cases B & D are possible (See App. 4.R).

21 The use of turbulent flow equation (2) is based on a Reynolds number $>$ 2000.

22 It is necessary then to determine the maximum emulsion viscosity that will give $Re > 2000$

23 Assume full turbulence to be at Re 10,500 (Crane Page A.25) then from equation (1) we have

$$\frac{W}{\mu d} = \frac{Re}{6.31} = \frac{10,500}{6.31} = 1664$$

24 Consider ratio $\frac{\text{d (actual)}}{\text{max. particle dia.}} = 10$

Let max. particle dia. be 400 um,
therefore min. d. = 4000 um = .16 inch = 5/32 inch.

25 Let max. W = 1000 lbs./hr., then

$$\frac{1000}{\mu \times .16} = 1664$$

$$\mu(.16 \times 1664) = 1000$$

$$\mu = \frac{1000}{266} = \text{say 4 centipoise}$$

25.1 For C.E. Chatham, dia = .192 whence

$$\mu \times (.192 \times 1664) = 1105,$$

then $\mu = \frac{1105}{.192 \times 1664}$ = 3.5 Cp

26 We must now determine the max $\emptyset$ in a $\frac{\emptyset}{\emptyset_\infty}$ ratio where

$\emptyset_\infty$ is (say) .75, and so the equation $\left(1 - \frac{\emptyset}{\emptyset_\infty}\right)^{-3.54}$[1] = 4 Cp

---

1) Ref. X.2

26.1 Let $\frac{\phi}{\phi_\infty} = X$, and inverting and taking logs, we have

$\log \frac{1}{(1-X)^{3.54}} = \log 4$

$\log 1 - \log(1-X)^{3.54} = .602$

$0 - 3.54 \log(1-X) = .602$

$\log (1-X) = \frac{.602}{-3.54} = -.17$

$= -1 + 1^{(.83)}$

antilog .83 = -1(6.76) = .676

Then 1 - X = .676

X = 1 - .676 = .324

Then, $\frac{\phi}{\phi_\infty} = .324$

Let $\phi_\infty = .75$

Then $\phi = .75 \times .324 = .243$ (when ϕ_∞ is .75)

26.2 (N.B. in a CWF/atom. steam emulsion using. e.g. Co-Al)

Let $\phi_\infty = .925$

then $\frac{\phi}{.925} = .324$

$\phi = .3$ (when ϕ_∞ is .925)

27 Test 26.1

$$\left(1 - \frac{\phi}{\phi_\infty}\right)^{-3.54} = \left(1 - \frac{.243}{.75}\right)^{-3.54}$$

$$(1 - .324)^{-3.54} = (.676)^{-3.54} = 4 \text{ Cp}$$

Test 26.2

$$\left(1 - \frac{\phi}{\phi_\infty}\right)^{-3.54} = \left(1 - \frac{.3}{.925}\right)^{-3.54} = (1 - .324)^{-3.54} =$$

$$(.676)^{-3.54} = 4 \text{ Cp}$$

28 The fixed volumes in a CWF/steam emulsion to give a Ø value of .243 (representing a viscosity of 4 Cp), are:

Coal	.0023 (70/30 mix)
Ø	.243

29 Determine steam volume

29.1 The total emulsion volume must now be

$$\frac{.0023}{X} = .243$$

$$X = \frac{.0023}{.243} = .0095$$

29.2 Revised emulsion volume (Table 1.4.R.A) was .0996

29.3 Therefore reduction in emulsion volume required is:
.0996 - .0095 = .09 cf.

30 This reduction in total emulsion volume must come from reduction in atomizing steam volume by condensation into the water content of the CWF.

30.1 Such condensate absorption will increase the volume of the water content so that more than .09 cf reduction from atomizing steam will be needed.

Let X = the reduction in cf of atomizing steam ($\overline{V} = 2.4$)

31.1 The volume added to the water is X/2.4 lbs. condensate

$$= \frac{X}{2.4 \times 62.4} \text{ cu. ft. water}$$

$= .0067X$, then

$X - .0067X = .0906$

$.993X = .0906$

$X =$ .090 cf. atom. steam reduction

32 The amount added to water volume due to steam condensation (assumed) is .0067X (Item 31.1), and subst. X = .090, we have:

additional amount is .09 x .0067 = .0006

add original water volume (Table 1.4.R.A) .0013

New water volume .0019

32.1 Categorical volumes are then:

Coal	.0023	
Water	.0019	
CWF (only)	.0042	.0042

32.2 Total CWF emulsion volume allowable for a Ø of .243 is .0095

32.3 Then allowable volume for atom. steam is (.0095 - .0042)
= volume of atom. steam = .0053

34 Emulsion volume is then (items 32.2 + 32.3) .0095 cu.ft.

35 Proof: $\frac{.0023}{.0095} = .243$

= Ø for a viscosity of the emulsion of 4 Cp which is the viscosity limit for turbulent flow and use of the turbulent flow equation.

36 The atom. steam/CWF ratio is now
coal weight (Table 1.4.R.A) = .187
water weight (.0019 x 62.4) = .1186
(New) CWF weight .3056 .3056

36.1 (New) atom. steam weight ($\overline{V} = 2.4$) is:

$$\frac{.0053}{2.4} = .0022 \text{ lb}$$

36.2 (New) atom. steam/CWF ratio is:

$$\frac{.0022}{.3056} = .0072$$

37 N.B. the "new" ratio of .0072 compares to a "normal" ratio of .15 or a reduction in ratio of $\frac{(.15 - .0072)}{.15}$

$$= \frac{.1428}{.15} = .952$$
$$= 95.2\%(!)$$

37.1 The increase in water weight is:

$$\frac{.1186 - .08}{.08} = \frac{.0386}{.08} = .4825$$
$$= 48.25\%$$

38 Then fluidity of the emulsion is compatible with the numerically determined vis. of 4 as a limit for a turbulent Re of 10,500, and an annulus dia. of .16 inch at a W of 1000 lbs./hr.

38.1 The dia. of .192 inch and actual W of 1105 lbs./hr. for the C.E. Chatham data yields an emulsion vis. of 3.5 Cp (See Item 25.1)

APPENDIX 7

39 The total weight of the emulsion is unchanged at .307 lbs. (nothing has been added or subtracted) there has only been a hypothetical change of state in fluid viscosity.

39.1 The "new" weight distribution is:

	Weight	
Coal	.187	(unchanged)
Water (.0019 x 62.4)	.1186	(increased)
Atom. steam $\frac{.0053}{2.4}$	.0022	(decreased)
	.3078	

40 The temperature rise in the CWF water due to absorption (or condensation) of atom. steam is determined as follows:

40.1

Original weight of atom. steam (before absorption)	.04 lb.
Weight of atom. steam remaining after absorption	.0022 lb.
Weight of atom. steam absorbed	.0378 lb.

40.2 Latent head of steam at 175 psi is .864 BTU

40.3 Heat released in absorption is:
864 x .0378 = .3266 BTU

40.4 Then temperature rise of CWF water (neglecting heat transferred to coal, is:
$\frac{32.66}{.1186}$ = 275°

40.5 Temperature of CWF is then (275 + 70) = 345°

40.6 Sat. steam temperature for CWF water at (assumed) 150 psi = 366° F

40.7 Therefore CWF will not boil off under conditions as given in the foregoing.

APPENDIX 8

Potential for Total Drying of CWF

1 In Appendix 7 it was demonstrated that the CWF could, conceivably absorb atom. steam and remain a fluid in turbulent flow for an emulsion viscosity up to 4 Cp.

1.1 The amount of heat absorbed to produce this result was 32.66 BTU, from steam at 175 psi which raised the CWF water to a temperature of 345°F with no boil off of the CWF water if its saturation pressure was greater than 345°F or a pressure of 115 psig minimum.

2 The condensation, presumably over the length of .016 ft. of the annulus in a time period of

$$\frac{.016 \text{ (length of annulus)}}{500 \text{ (velocity of flow, fps)}} = 3.2.10^{-5} \text{ sec.}$$

2.1 The ratio of the heat transfer from steam to water "in turbulent flow" would then be

$$\frac{32.66}{3.2.10^{-5}} = 1.02.10^{6} \text{ BTU/sec.}$$

$$= 3670.10^{6} \text{ BTU/hr}$$

3 Appendix 7 has assumed essentially instantaneous heat transfer to have a viscosity of 4 Cp prevail through the whole length of the annulus.

4 If the increase to 4 Cp requiring a change from .04 lbs. atom. steam to .0022 lbs. occurs over the annulus length then the average weight reduction is:

$$\frac{.04 + .0022}{2} = .0211 \text{ lbs}$$

5 The purpose of establishing the top limit value of 4 Cp was to establish the limiting conditions under which turbulent flow would occur.

5.1 Any viscosity less than 4 Cp, indicates turbulent flow.

5.2 That is the atom. steam volume could drop a max. of 95% (See Appendix 7 Item 37) and the CWF emulsion flow would still be turbulent (steam condensate increased water volume by 48%)

6 It is possible of course that the viscosity at the annulus exit could be appreciably below 4 Cp - if the rate of heat transfer was not at the 3.67 billion BTU/hr. rate as shown in Item 2.1 above.

7 However, if the rate of heat transfer in a steam/water turbulent mix was essentially instantaneous, then there would be the possibility of total evaporation of the CWF water as numerically explored in the following.

8 In the course of evaporation, a value of equilibrium pressure would be established between the CWF water evaporation and the heat content of the initial volume of atomizing steam.

9 Assume:

a) Mean CWF pressure 135 psi
b) Mean steam pressure 175 psi.

9.1 Further for simplified calculation assume that the equilibrium pressure is the average of a) and b) or

$$\frac{175 + 135}{2} = \underline{155 \text{ psi}}$$

10 The heat released from .04 lbs. steam from a level of 175 psi condensed at 155 psi would be

Enthalphy of 175 psi	1197.6 BTU
155 psi	1196
	1.6 BTU
Latent heat at 155 psig	855.0 BTU
Total heat available to evaporate CWF water	856.6 BTU per lb. of atom. steam

10.1 Weight of atom. steam is .04 lb., therefore the actual heat available for transfer to CWF water is (.04 x 856.5) = 34.26 BTU

10.2 Heat required to evaporate .08 lb. water at 155 psi at 368°F is:

Hat to raise water to boiling point .08 x (368 - 70)	= 23.84 BTU
Heat required to evaporate 100% of the CWF water is .08 x 855	= 68.4 BTU
Total heat required	92.24 BTU

(Versus total heat available of 34.26 BTU)

11 Hence total CWF water will not be evaporated by .04 lb. atom. steam.

12 Temperature rise of CWF water if the total of .04 lb. of atom. steam condensed is $\frac{34.26}{.08}$ = 428° for a total temp of (428 + 70) = 498°F

12.1 The saturation pressure of steam at a temperature of 498°F is 660 psig.

12.2 Max. pressure in the annulus (even if steam & CWF pressures were additive) is 350 psig.

12.3 Therefore the total of .04 lb. of atom. steam cannot be condensed by the CWF water.

12.4 The max. amount that can condense is calculated as follows:
Let the equilibrium pressure in the annulus be 155 psig (Item 9.1)
Let heat of condensation be 855 BTU per hr. (Item 10)
Let X = lbs. of steam condensed at an equilibrium pressure of 155 psig at the saturation temp. of 368°F.
X will serve to bring CWF water to the boiling point temperature of 368°F, at which point heat transfer will cease.

12.5 Heat to raise CWF water to equilibrium temperature

$$.08(368 - 70) = 23.84 \text{ BTU}$$

Heat remaining in atom. steam is (34.26 - 23.84) = 10.42 BTU
Weight of Atom. steam remaining is then:

$$\frac{10.42}{855} = .0122 \text{ lb.}$$

12.6 Volume of atom. steam remaining when $\overline{V}$ at 155 psig = 2.675, is
X = .0122 x 2.67 = .0326 cf.

13 Increased weight of water in CWF is

$$.08 + (.04 - .0122) = .1078$$

APPENDIX 8

14 The weight and volume relations in the CWF/steam emulsion are now:

Factor	Weight, lbs.	Volume, cf.
Coal	.187	.0023
Water	.1078	.0017
CWF	.2948	
Atom. steam	.0122	.0326
CWF/steam emulsion	.3070	.0366

14.1 SPG. = $\frac{.307}{.0366 \times 62.4}$ = .134

14.2 Density (ρ) = 8.4 lbs./cf.

14.3 V = .0366/.2000 = 183 fps

15 Atom. steam/CWF ration (by weight)

$\frac{.0122}{.2948}$ = .0414

= 4.14%

16 $\phi = \frac{.0023}{.0326} = .07$

17 Determine emulsion viscosity for ϕ_∞ = .75 and ϕ_∞ = .925

17.1 $\frac{\phi}{\phi_\infty} = \frac{.07}{.75} = .0933$

$(1 - .0933)^{-3.54} = (.907)^{-3.54} = 1.415$ Cp

17.2 $\frac{\phi}{\phi_\infty} = \frac{.07}{.925} = .0757$

$(1 - .0757)^{-3.54} = (.924)^{-3.54} = 1.32$ Cp

APPENDIX 8

18 Therefore the reduction in atom. steam by condensation with the CWF water has not materially increased the viscosity which is still < 4 Cp.

19 Hence the emulsion is still in the turbulent range of the Re number at max atom. steam condensation.

APPENDIX 9

Determination of Cp Viscosity Values from Various Equations of Appendix 1

Postulates for Comparison of Various Equations in Appendix 1

Viscosities are based on ϕ and ϕ_∞ values of .60 and .70 so that $\phi/\phi_\infty = .857$ and $(1-\phi/\phi_\infty) = (1.857) = .143$

Section X.2

1.X.2 Eq. 1 from Ref. X.2 - R. Kaji (Hitachi Ltd.) et al (See list of Reports & App. 1

$\eta = \eta_0(1-\phi/\phi_\infty)^{-3.54}$

η = vis. Cp

η_0 = vis. of medium = vis. of water = 1 Cp

Then $= (.143)^{-3.54}$ = 977 Cp

Section X.15

Equations from Ref. X.15 - E.J. Casassa et al - Carnegi~~a~~e Mellon University

1.X.15 Eq. 4 (Dougherty Kriegor)

$\eta = \eta_0(1-\phi/\phi_\infty)^{-[\eta]\phi}$

ϕ = .583 from Fig. 3 X.15

2.X.15 Using $[\eta]$ = 6.5 from Table 6 X.15

$$\eta = 1\left(1 - \frac{.583}{.70}\right)^{-[6.5].583}$$

$$\eta = 1(1 - .833)^{-3.79}$$

$\eta = (.167)^{-3.79}$ = 883 Cp

η Value obtained from Fig. 3 X.15 is * 1242 Cp

X.15 Eq. 9 is: $\eta = \eta_0 \exp (K' \text{ plus } K''\emptyset)$

3.X.15 Let $\eta_0 = 1$ (water) and taking K' and K" from Table 5.X.15 for $\emptyset$ values >.04 we find for $\emptyset = .583$
$\eta = \exp. (-2.8 + (16.8 \times .583))$
$\eta = \exp. (-2.8 + 9.8) = \exp. 7$
$e^7 = 1096$ = 1096 Cp

Fig. 2.X.15 is a Plot of Eq. 9

4.X.15 Co-ordinates (.583; 7) give an ordinate value of 7

$\log_e \eta = 7$
η = antilog 7 = 1096 Cp
(Right on with value obtained from Eq. 9 as in Item 3 above)

5.X.15 Fig. 3.X.15 is a plot of the Dougherty-Kriegor Eq. 4. Co-ordinate lines have been drawn and given their respective $\log_e$ values

5.1 These $\log_e$ values are summarized in Table 1.9.A together with their respective anti-log values.
The anti-log values are:
abscissa - the function $(1-\emptyset/\emptyset_\infty)$
ordinate - viscosity in Centipoise

5.2 The ratio $\emptyset/\emptyset_\infty$ is shown in the table. ($\emptyset_\infty = .70$)

5.3 The $\emptyset$ value is calculated as
$$\frac{\emptyset}{.70} = f(\emptyset/\emptyset_\infty)$$
E.G. where $\emptyset/\emptyset_\infty = .865$
$$\frac{\emptyset}{.70} = .865 \text{ and } \emptyset = .6055$$
$\emptyset$ is shown in Table 1.9.A

* N.B. Test point co-ordinates (1.79, 7.125) are not on curve (but are a test value) (See item 5 and Table 1-9-A)

5.4 The corresponding viscosity = 1808 Cp

5.5 For $\emptyset/\emptyset_\infty = .833$, $\emptyset = .583$ and viscosity = 1242 Cp

G. D. Botsaris et al - Tufts University

Sect W.9

6.W.9 Eq. 5 in ths paper is similar in concept to Eq. 1 of Ref. X.2 and is:

$$\eta = \mu_r \text{ (empirical)}^{1)} \left[1 + 0.75 \frac{(\emptyset/\emptyset_\infty)}{(1-\emptyset/\emptyset_\infty)}\right]^2 \qquad \text{Eq.5}$$

For $\emptyset = .583$ & $\emptyset_\infty = .70$ (as in Eq. 4.X.15)

$\emptyset/\emptyset_\infty = .833$ & $(1 - \emptyset/\emptyset_\infty) = .167$

Then

$$\mu_r = \left[1 + 0.75\left(\frac{.833}{.167}\right)\right]^2$$

$$= (1 + 3.74)^2 \qquad = 22 \text{ Cp}(\underline{?})$$

---

1) Empirical Equation by Chong et al

6.1 Refer back to Eq. 4 (by Frankel & Acrivos) in Section W.9 of Appendix 1.

This equation is:

$$\mu_r = 1 + C'① \left[\frac{(\emptyset/\emptyset_\infty)^{1/3}}{(1-\emptyset/\emptyset_\infty)^{1/3}} \right] \quad \text{........(4)}$$

Then obtaining values of

$\emptyset_\infty$ = .704 from Table 2 (vol. fraction)

$\emptyset$ = .64 wt. fraction from Table 1

= .586 vol. fraction

Then: $\emptyset/\emptyset_\infty = .832$

and $(\emptyset/\emptyset_\infty)^{1/3} = (1 - .94) = .06$

Then μ_r (Eq. 4) $= 1 + C' \dfrac{.94}{.06}$

$= 1 + C'(15.7)$ .....Eq..(5)

Now from Table 1.W.9, we find viscosities for Ø of .63 wt. fraction

Case 1 with no additives	2850 Cp
Case 2 with LIPAL 12A	1140 Cp

Then from Eq. 5 we find

Case 1 $1 + C' \times 15.7 = 2850$

$C' = \dfrac{2849}{15.7} = 181.5$

Case 2 $1 + C' \times 15.7 = 1140$

$C' = \dfrac{1139}{15.7} = 72.5$

① C is termed K in Equation 8.

7.W.9 The viscosity values of Table 1.W.9 are derived from Viscometer Tests and the K values are a function of these test values.

7.1 Hence the value of the theoretical and empirical equations in obtaining viscosities seems questionable.

W.9 Fig. 1

8.W.9 Thought should be given to Fig. 1, 6th Symposium - P.309 which shows interaction between particles, when considering agglomeration potential in an annulus under high pressure and high velocity flow.

9.W.9 The factors affecting possible agglomeration are:

1. Electric Potential (zeta) of 50 Mv1)
   (determined by electrophoretic or electrosmotic analyser)
2. Van der Waal attraction
3. Surface tension
4. Turbulence.
5. Particle size distribution (e.g. (Dr. Funk's equation)
6. Colloid content to give specific surface area $>1.25\ m^2/cc$.
7. Thickness of film. (See report W.10)

---

1) Recommendation of Dr. Funk.

TABLE 1.9.A

Values in Fig. 3.X.15

Ø & η Value Determinations

Determine Values of Abscissa and Ordinates

Abscissa				Ordinates	
Log Number	Antilog[1)] Value	Value of Ø/Ø∞	Value Ø[2)] for Ø∞ =.70	Log no.	Antilog Value = Cp
-2.4	.0907	.91	.637		
-2.37	.0935	.906	.635	7.7	2208
-2.0	.1353	.865	.6055	7.5	1808
-1.79	.167	.833	,583	7.15	1243
-1.6	.202	.80	.560		
-1.2	.3012	.70	.490	5.4	221
-.08	.45	.55	.385	3.75	42.5
-0.4	.67	.33	.231	1.98	7.24
0	1	0	0	0	

1) Antilog value = value of (1 - Ø/Ø∞)

2) Ø = .7 x Ø/Ø∞

X·15

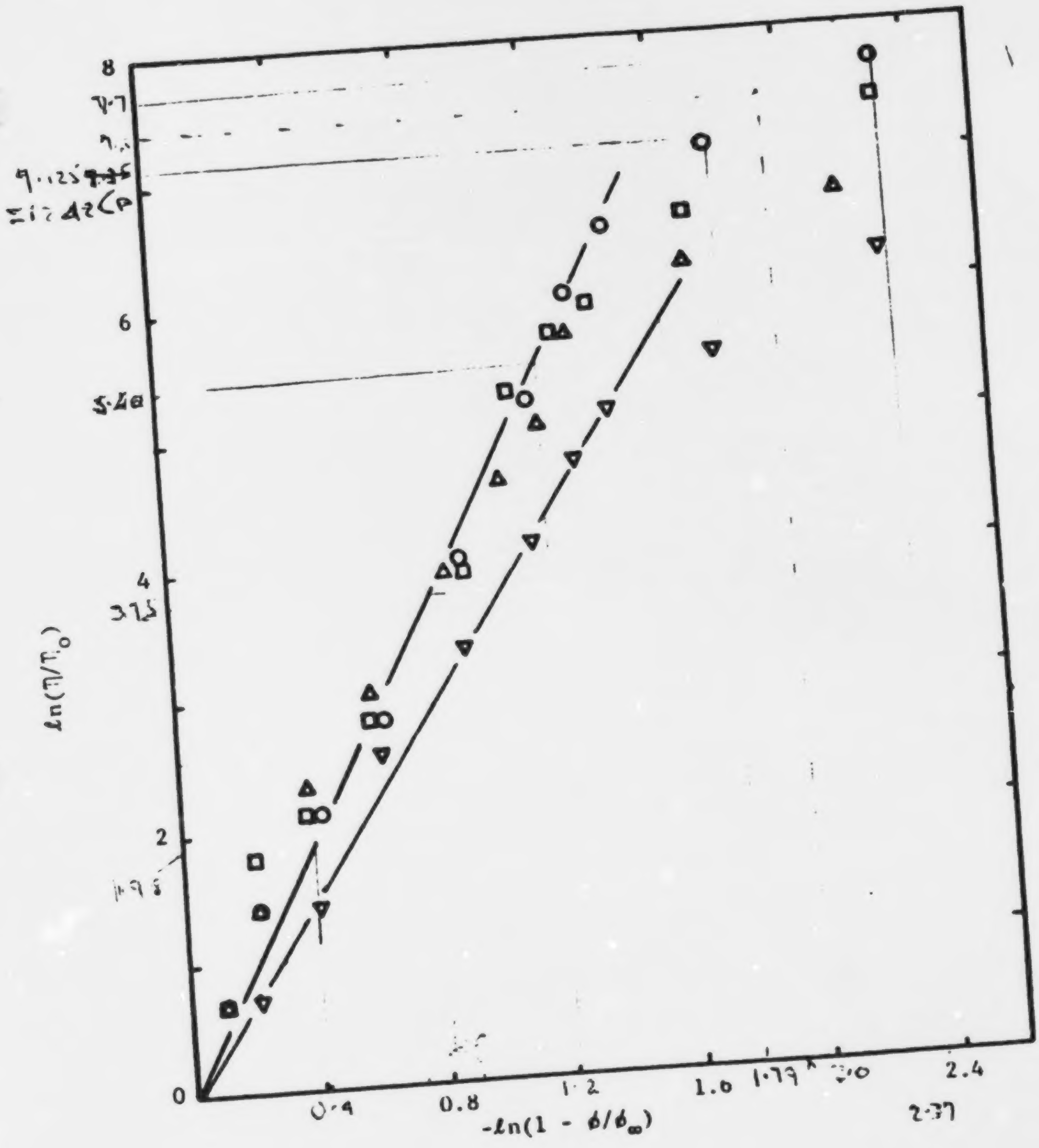

-X.15

Figure 3. Plot of Dougherty and Krieger equation with ϕ_∞ = 0.70. Pittsburgh #8 (○), Illinois #6 (□), San Juan (△), Hiawatha (▽). Shear rate 90 s^{-1}.

x corresponding 1.79 - See Table 1.9.n
= .167 = $\left(1-\frac{\phi}{\phi_\infty}\right)$

X.15

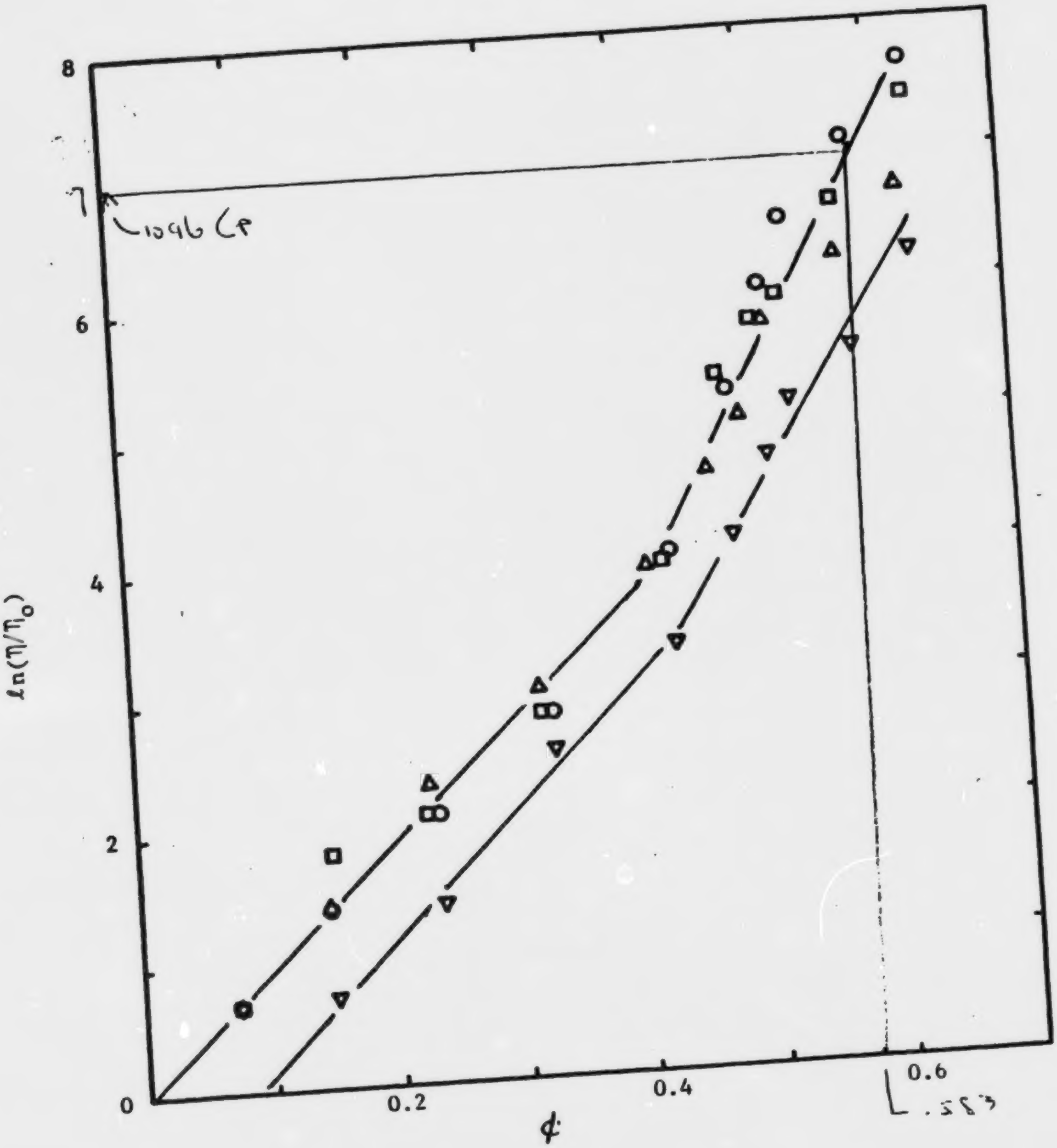

.X.15

Figure 2. Viscosity of coal/water slurries. Pittsburgh #8 (○), Illinois #6 (□), San Juan (△), Hiawatha (▽). Shear rate 90 s^{-1}.

N.B.: Fig. 2 is plot of Eq. 9.X.15

1· W·9

3. RESULTS AND DISCUSSION

3.1 Identification of Suspension Type

Figure 2 shows the Terminal Sediment Volumes for the three types of slurries at various solids concentrations expressed in percent weight. The black areas indicate the terminal sediment formed from settled coal particles, the white areas on top indicate clear liquid and the dotted areas dilute suspensions of non-settled coal particles.

The above clues lead to the following conclusions:

a) The slurries containing LIPAL 12A were aggregatively stable at all concentrations. This is deduced from the fact that the fines did not agglomerate and remained in suspension after the particles which are larger than 1 to 2 μm have settled.

b) On the other hand the slurries with no additives agglomerated at all concentrations. There were no fines to remain in suspension. They agglomerated.

c) The slurries containing AEROSOL OT were aggregatively stable up to concentrations of 55% solids. At higher concentrations, however, they agglomerated.

The above conclusions are confirmed by the TSV values. As is demonstrated in Fig. 1 stable suspensions give low TSV and the TSV increases as the agglomeration becomes more pronounced.

It can be concluded therefore that the three prepared slurries represent three typical suspension types: an aggregatively stable (LIPAL 12A), an agglomerating one (No additive) and an intermediate (AEROSOL OT).

3.2 Viscosity Data and Determination of ϕ_m

The relative viscosity values, obtained by the procedure described in section 2.2, for the three suspensions at various coal concentrations are presented in Table 1.

The data were plotted on a viscosity vs coal concentration graph and a smooth curve was drawn through the experimental points. A typical plot is shown in Fig. 3 for the case of slurries without an additive.

In order to determine the maximum coal concentration ϕ_m in each of the three cases a method employed originally by Frankel and Acrivos (1) was adopted. A plot (η_r-1) vs ϕ was made and the line was extrapolated to zero ordinate to give the value of ϕ_m. Data obtained from the smoothed out curve of Fig. 3 were plotted in this way in Fig. 4. Extrapolation gave a value of $\phi_m = 0.628$.

TABLE 1 · W·9
Viscosities of Coal Water Slurries
(Pocahontas Coal)

Slurries With No Additives		Slurries With LIPAL 12A		Slurries With Aerosol OT	
Weight Concentration	Relative Viscosity cp	Weight Concentration	Relative Viscosity cp	% Weight Concentration	Relative Viscosity cp
35	109	45	19	45	30
40	233	50	43	50	56
45	407	55	69	55	805
50	1251	57.5	114	60	990
55	1697	60	180	61	1404
57.5	1752	61	405	63	1979
60	1975	62	1092	65	2500
63	2850	64	1140		
		65	2300		
		66	3792		
		68.5	4816		

In a recent publication (8) Heath and Tadros used successfully a different plotting method for obtaining ϕ_m values for their polystyrene latex dispersions. In their method $1/\eta^{\frac{1}{2}}$ was plotted against ϕ followed by an extrapolation to zero ordinate. The same data used in Fig. 4 when were replotted according to the Heath and Tadros method gave a value of $\phi_m = 0.725$ (Fig. 5)

Table 2 summarizes the ϕ_m values for the three slurries obtained by both the above methods. It can be seen there that although the two extrapolating methods gave different sets of values, the values within each set follow the expected trend. They increase as the aggregative stability of the suspension increases. In other words, the maximum packing is lower for the agglomerating slurry (without additives) and higher for the stable one (with LIPAL 12A). An intermediate value is found for the slurry with AEROSOL OT, which is stable, but to a lesser degree than the one with LIPAL.

APPENDIX 10

Specific Volume of Air at 175 psig and Resulting Viscosity of the Emulsion

1 Density at 175 psig and 70°F = .968 lbs./cf.

2 $\overline{V} = \dfrac{1}{.968} = 1.033$ cf/lb

3 Consider atom. air/CWF ratio to be same as with steam.
i.e. .15 lb./lb.

4 Then volume of atom. air = .15 x .267 x 1.033 = .04 cf.

5 Subst. .04 for atom. steam vol. of .096 (at 175 psi)
in Table P.8 Appendix 4.R

6 Total CWF/atom. air vol. is then (.0036 + .04) = .044 cf.
(instead of .0946)

7 ϕ then is $\dfrac{.0023}{.044}$ = .0052

8 Let $\phi_\infty = .75$, then $\phi/\phi_\infty = \dfrac{.052}{.75}$ = .07

and $(1 - \phi/\phi_\infty)^{-3.54} = (1 - .07)^{-3.54}$
$= (.93)^{-3.54}$ = 1.29 Cp

8.1 Let $\phi_\infty = .925$(Co-Al) then $\phi/\phi_\infty = \dfrac{.052}{.925}$ = .056

and $(1 - .056)^{-3.54} = (.944)^{-3.54}$ = 1.23 Cp

9 These viscosity values for the emulsion are nearly
the same as those calculated when atom. fluid is steam.

9.1 Therefore, the conditions for turbulent flow still exist
as shown in Appendix 7, Item 6.

X-2

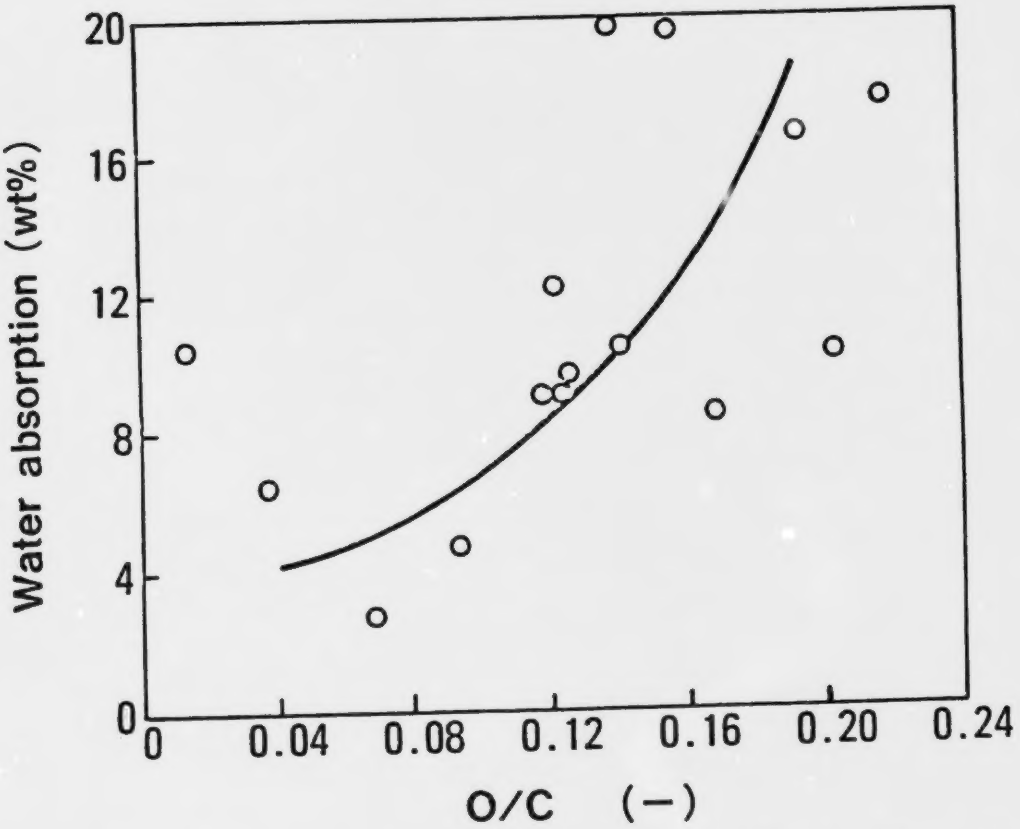

Figure 5. Relationship between O/C atomic ratio
X·2 and water absorption

X·2

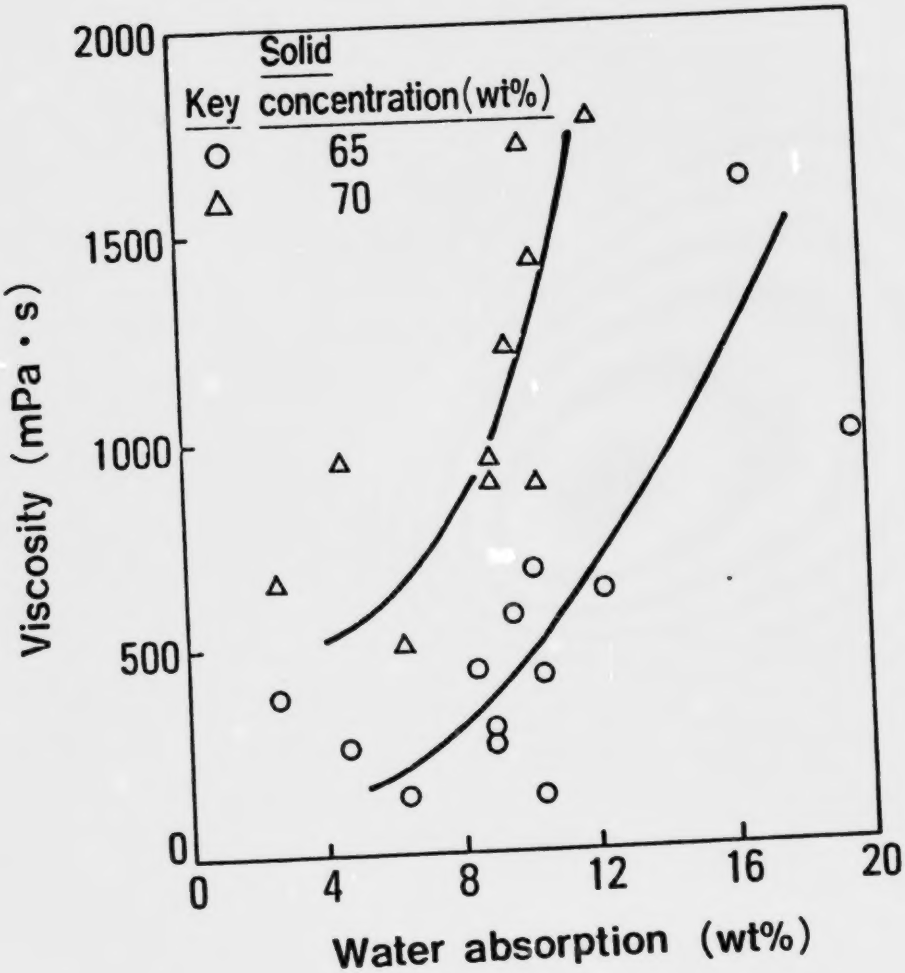

Figure 6. Effect of water absorption on the viscosity of coal water mixtures.

X·2

Surfactant : NOF-1, 0.3wt% on dry coal;
Temperature : 25°C; Shear rate : 126.7s^{-1}

FIG. 7. x. 2

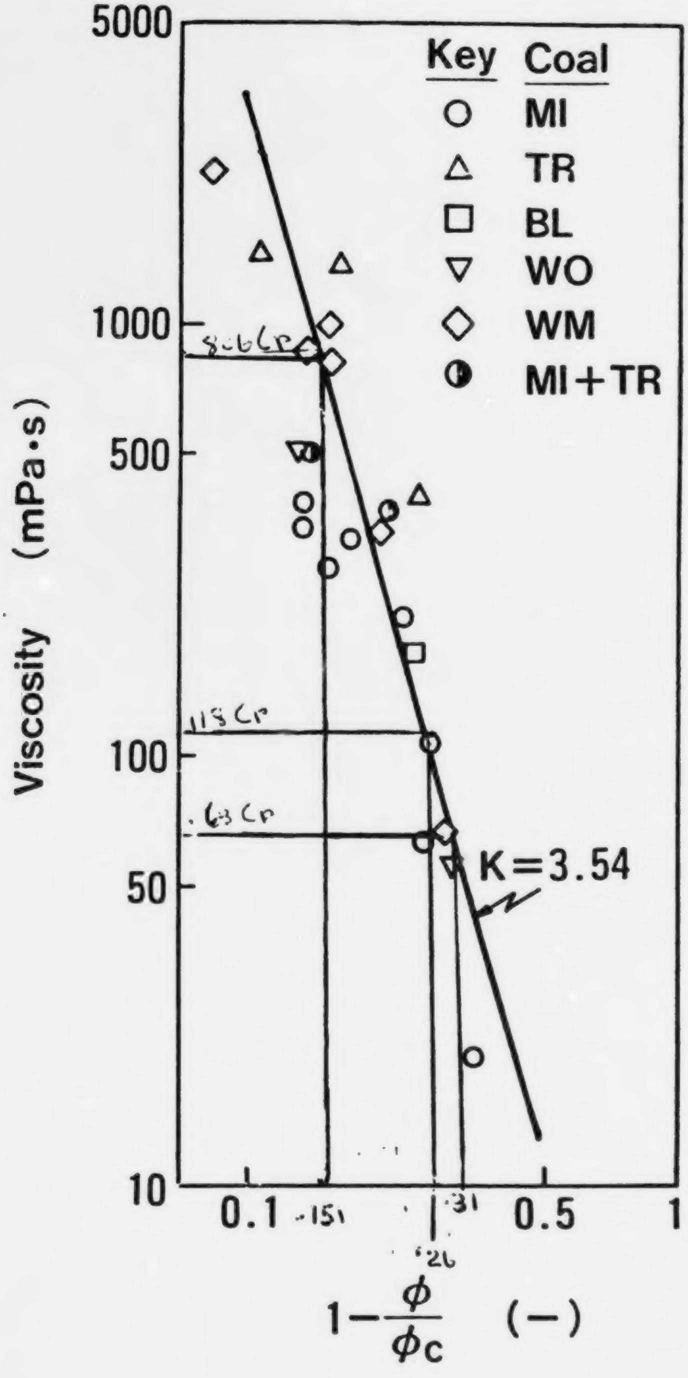

Viscosity from concept of 0 / 0 max. ratio for Co-HL - 70% wt. fraction

$\frac{0}{0\ max.} = \frac{.64}{.925} = .692$

$1 - .692^{-3.54}$

$= .41^{-3.54} = 63$ Cp.

Co-AL-75% wt. fraction has viscosity:

$\frac{0}{0\ max.} = \frac{.685}{.925} = 74$

$(1 - .74)^{-3.54} = 118$ Cp

Figure 7. Plot of viscosity vs. $(1-\frac{\phi}{\phi_c})$

X·2

X-2

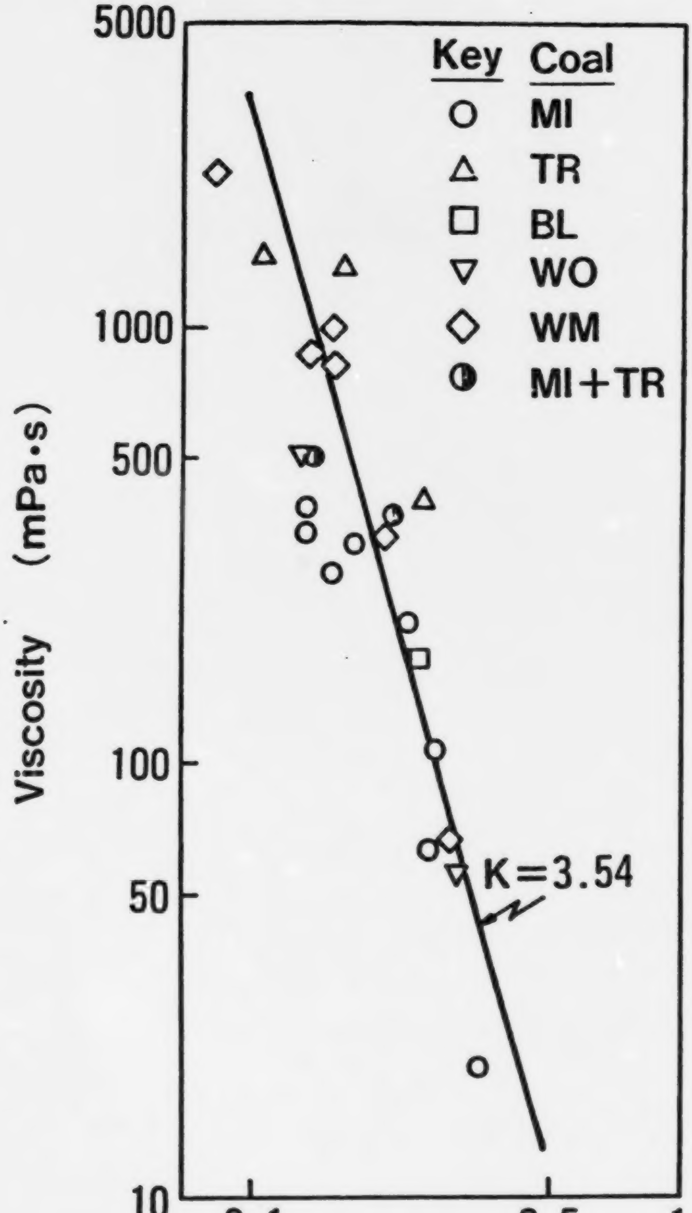

Figure 7. Plot of viscosity vs. $(1-\frac{\phi}{\phi_c})$

X-2.

X-2

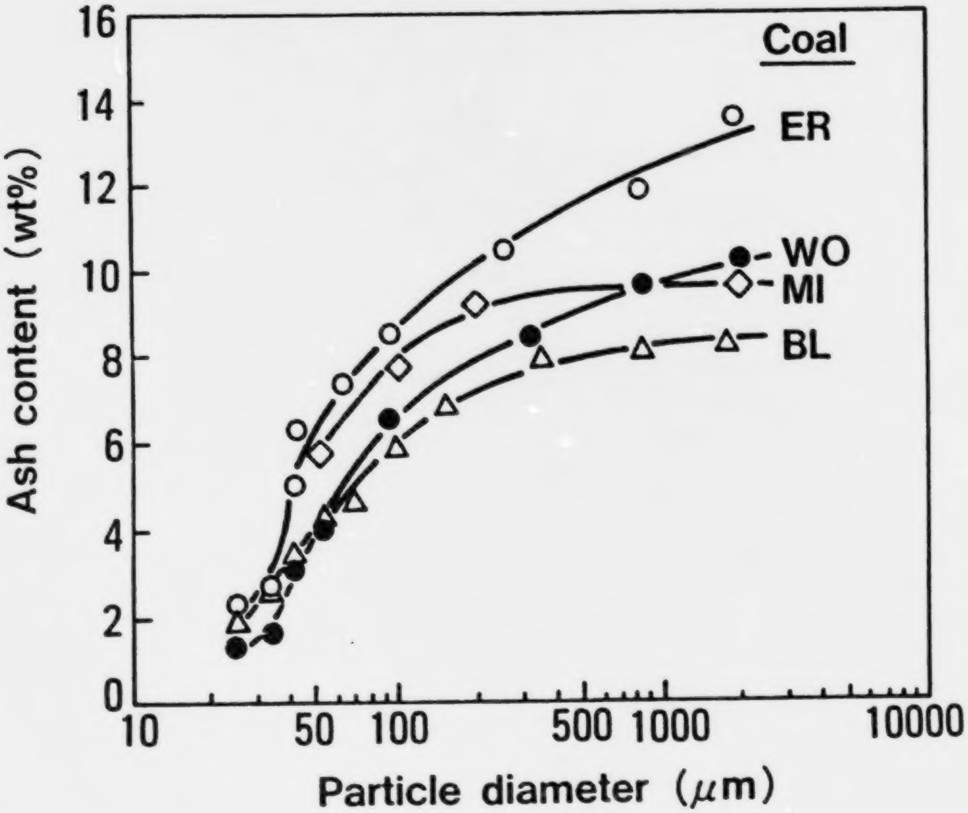

Figure 11. Ash content vs. particle size.

X-2

X6

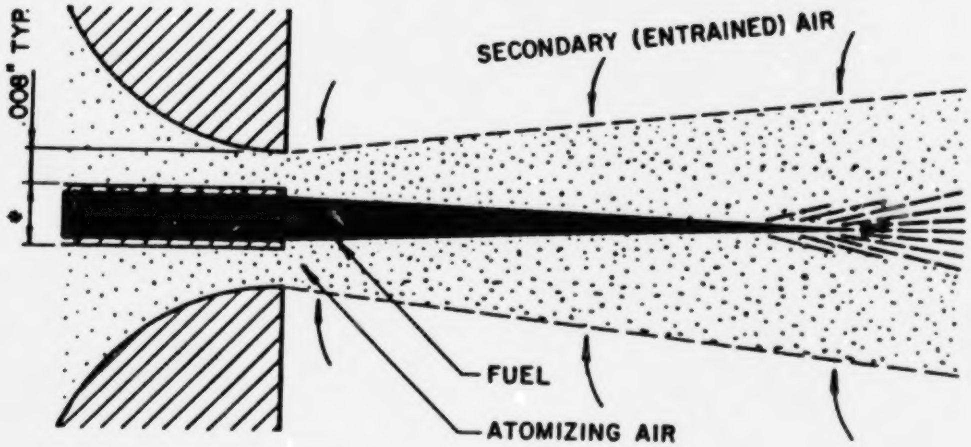
.008" TYP.
*
SECONDARY (ENTRAINED) AIR
FUEL
ATOMIZING AIR

* JET DIAMETER

- ROSEBURY CAPILLARY DIMENSION
- JAPANESE - UP TO 1/16" APPROXIMATELY

DROPLET SIZE INCREASES WITH DIAMETER

PRIOR EXPERIMENTAL WORK

FIGURE I

X·6

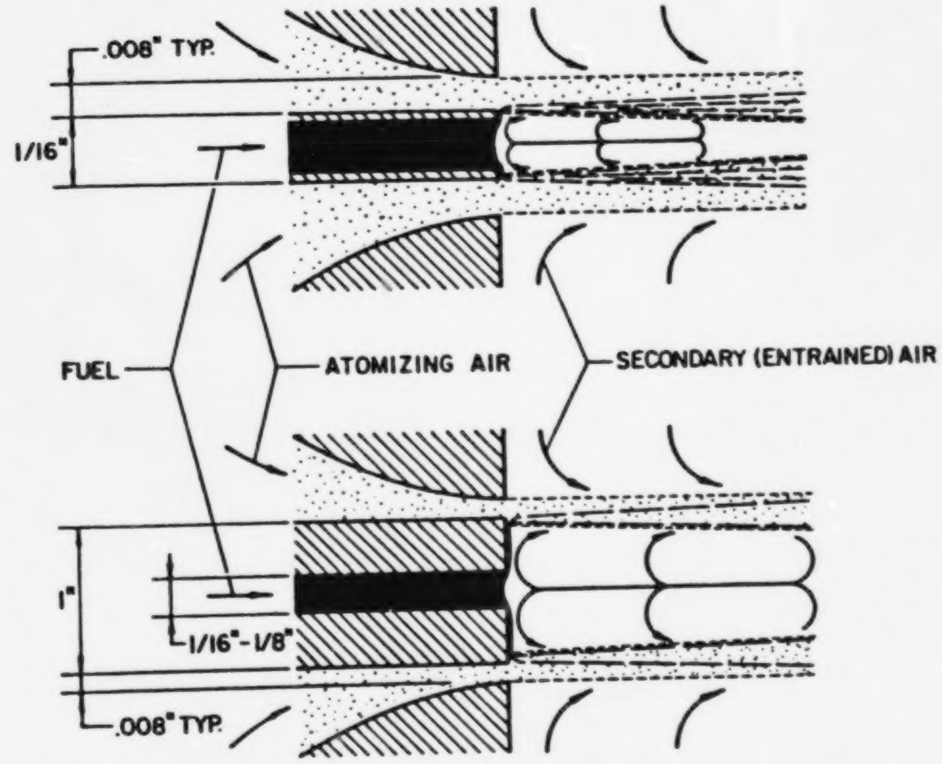
.008" TYP.
1/16"
FUEL
ATOMIZING AIR
SECONDARY (ENTRAINED) AIR
1"
1/16"-1/8"
.008" TYP.

FLOW RATE IS PROPORTIONAL TO DIAMETER
AT ESSENTIALLY CONSTANT MMD

EARLY EXPERIMENTAL WORK

FIGURE II

Y. 6

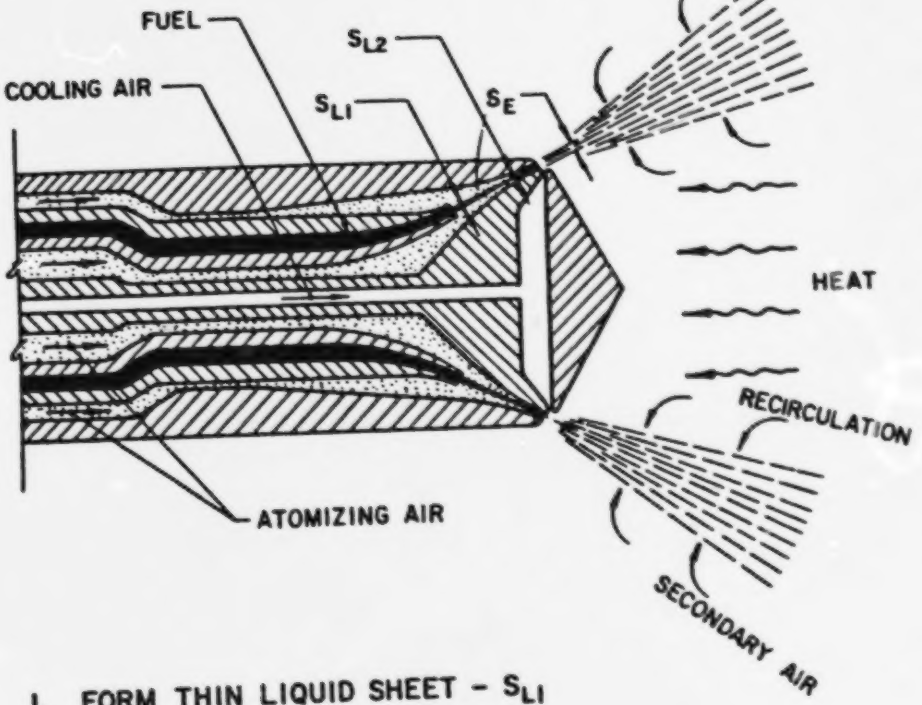
FUEL
S_{L2}
COOLING AIR
S_{L1}
S_E
HEAT
RECIRCULATION
ATOMIZING AIR
SECONDARY AIR

1. FORM THIN LIQUID SHEET - S_{L1}
   THICKNESS 0.1" - .125" MAX.
2. SHEET THINS IN CONICAL FLOW → S_{L2}
3. TWO AIR ANNULI - COMMON FLOW CHANNEL
4. ATOMIZE AT ELONGATED THROAT
5. GAS THROAT WIDTH : $S_T = S_E - S_{L2}$

APPLICATION TO LEZZON NOZZLE

FIGURE III

X.6

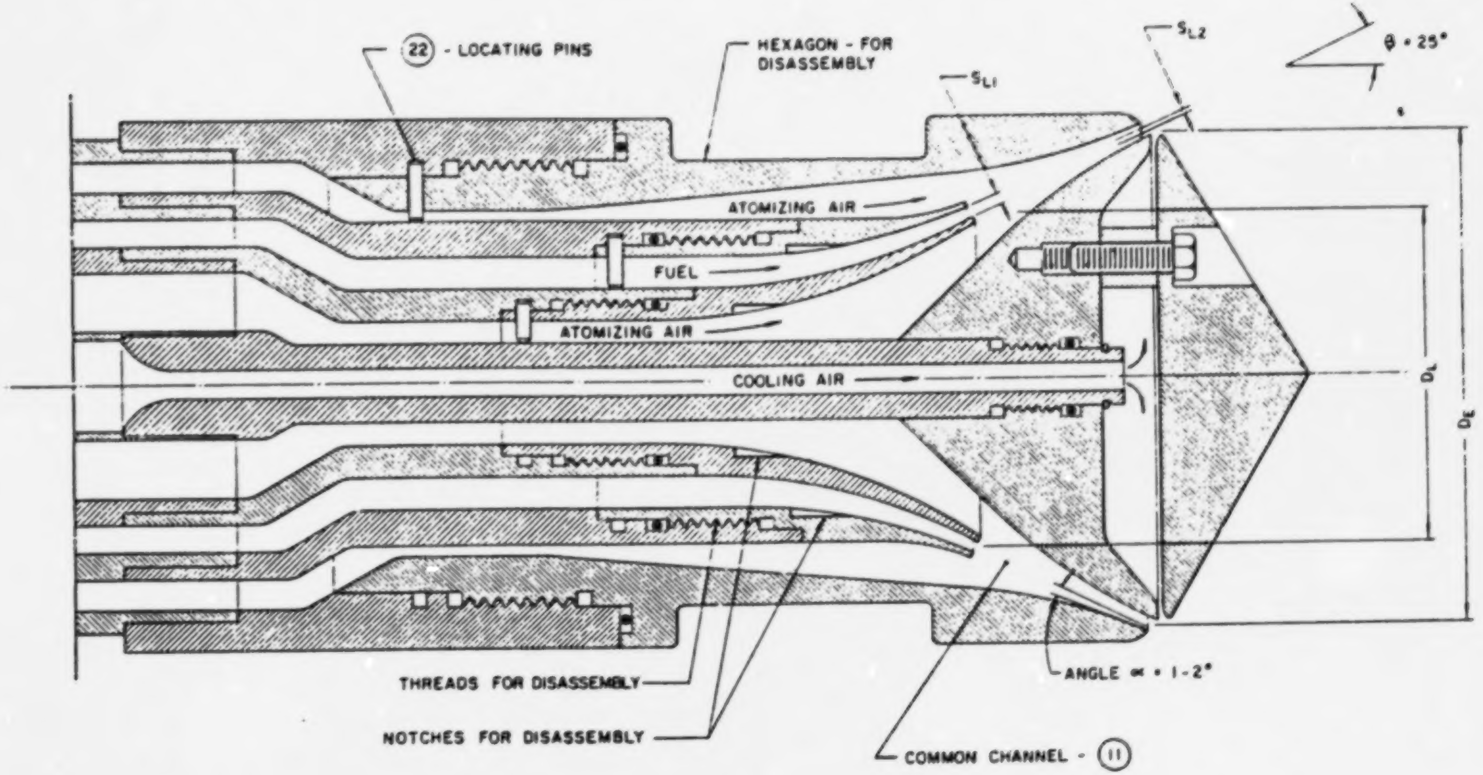
(22) - LOCATING PINS
HEXAGON - FOR DISASSEMBLY
S_{L1}
S_{L2}
$\beta = 25°$
ATOMIZING AIR
FUEL
ATOMIZING AIR
COOLING AIR
D_L
D_E
THREADS FOR DISASSEMBLY
NOTCHES FOR DISASSEMBLY
COMMON CHANNEL - (11)
ANGLE $\alpha = 1\text{-}2°$

ENLARGED VIEW OF TEST NOZZLE TIP
FIGURE IV

X.6

X.6

X·10

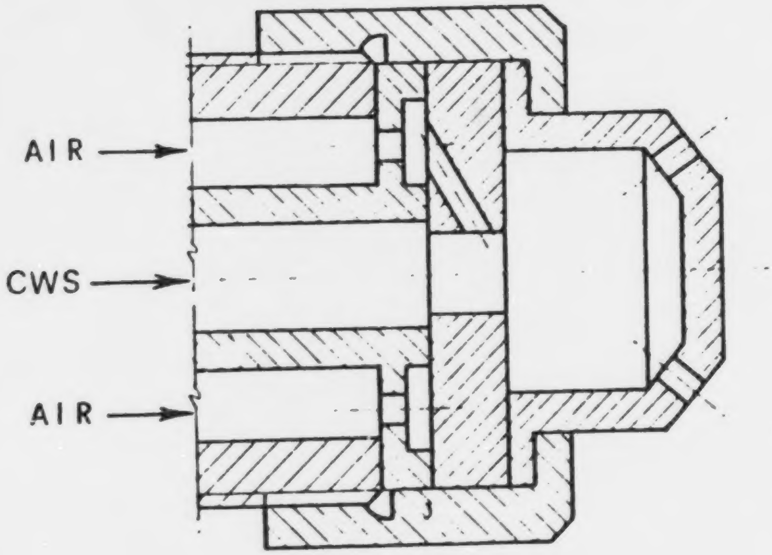

FIG. 4 - SCHEMATIC SECTION OF Y-MIXING ATOMIZER

X·10

X·11

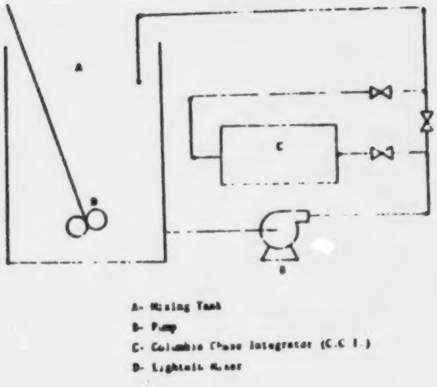
A
B
C
D
A- Mixing Tank
B- Pump
C- Columbia Chase Integrator (C.C.I.)
D- Lightnin Mixer

Figure 1. Schematic of CWS Pilot Plant

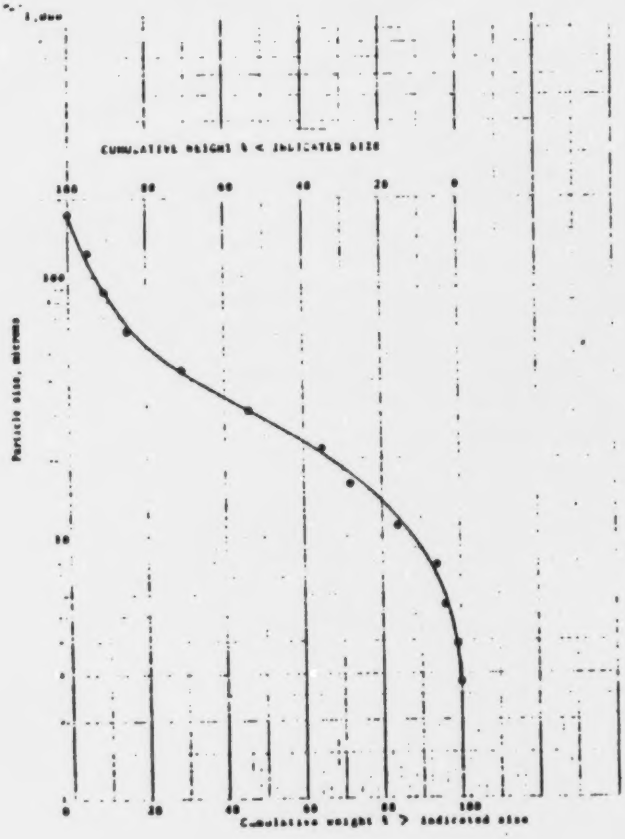

Figure 2. Particle Size Analysis "A" Coal

·X..11

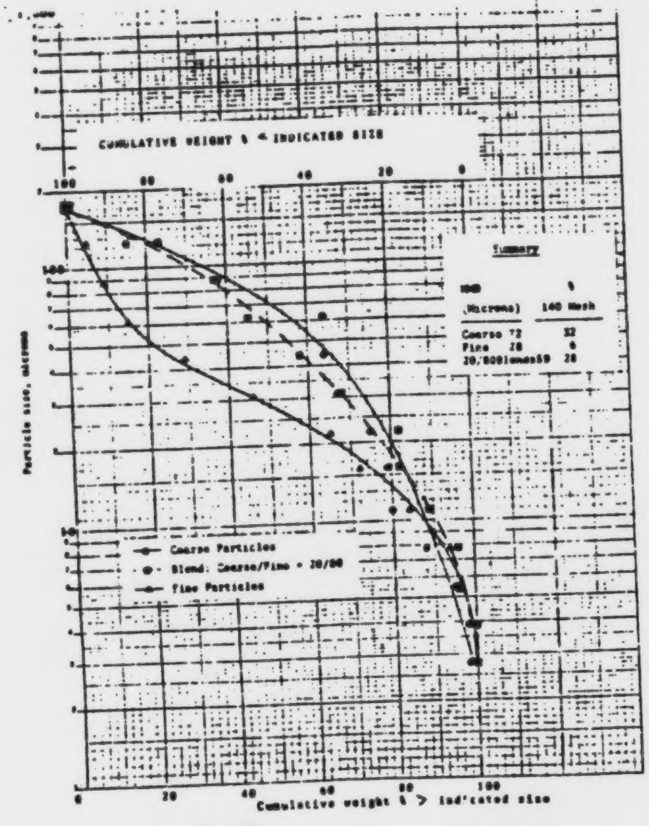

X.11

Figure 3. Effect of blending on coal Particle Size Distribution

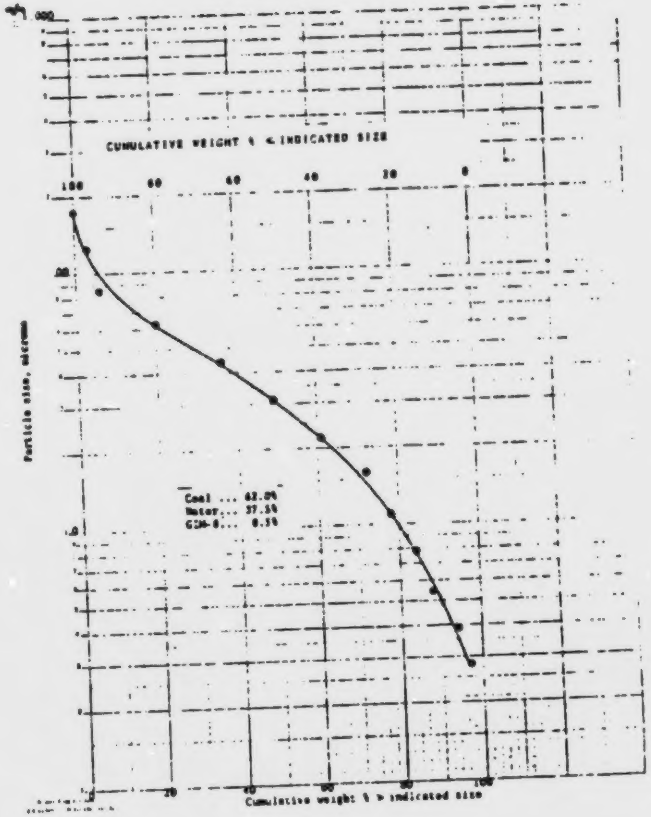

X.11

Figure 4. Particle size Distribution of Nominal 62 Weight % CWS

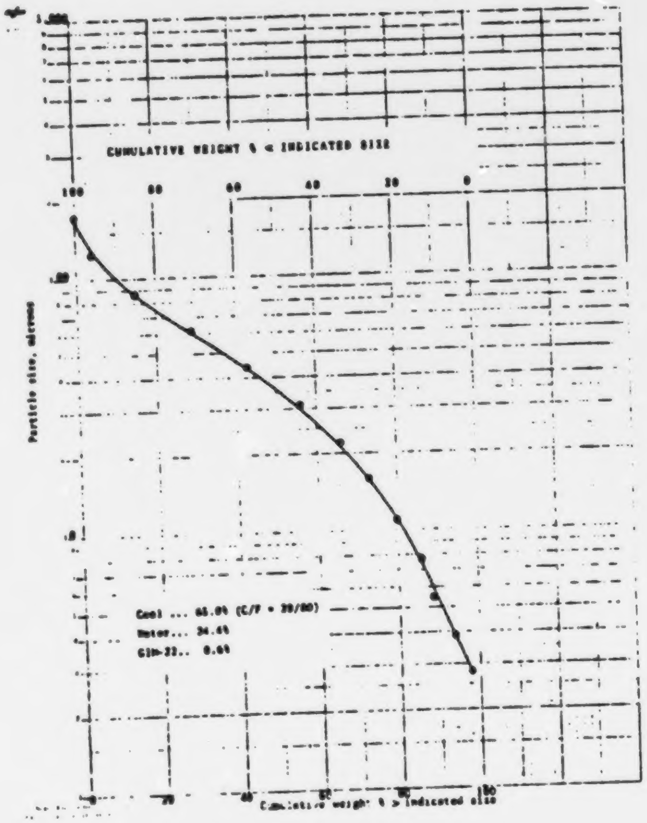

Figure 5. Particle Size Distribution of Nominal 65 Weight % CWS

X-11

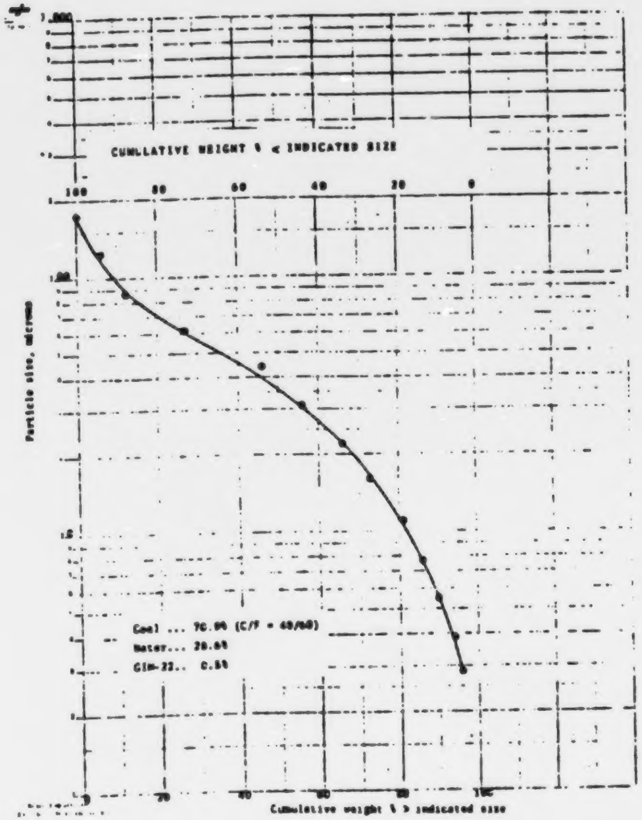

Figure 6. Particle Size Distribution of Nominal 70 Weight % CWS

X-11

X.11

1132

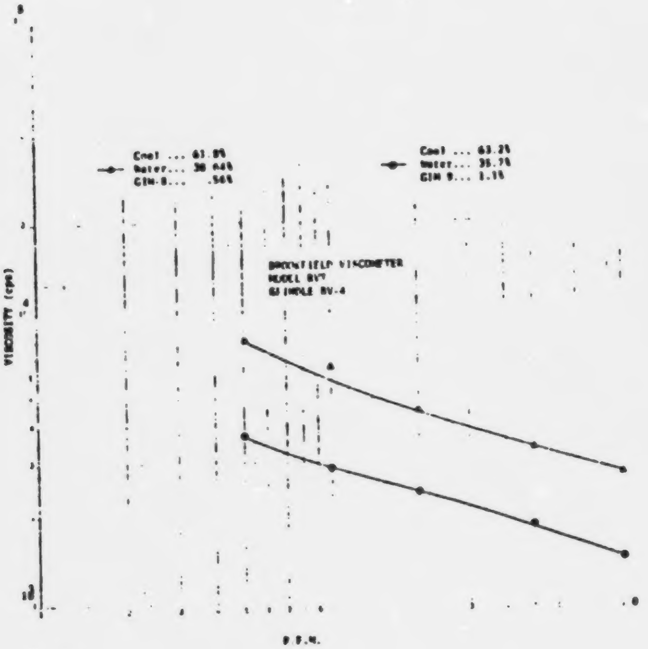

X.11

Figure 7. Effect of Chemical Additives on the Viscosity Characteristics of Nominal 62 Weight % CWS Fuels

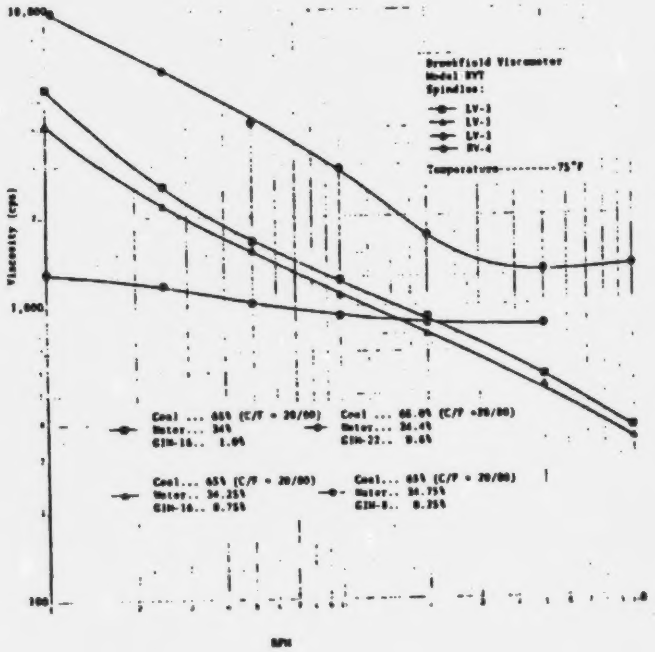

X.11

Figure 8. Effect of Chemical Additives on the Viscosity Characteristics of Nominal 65 Weight % CWS Fuels

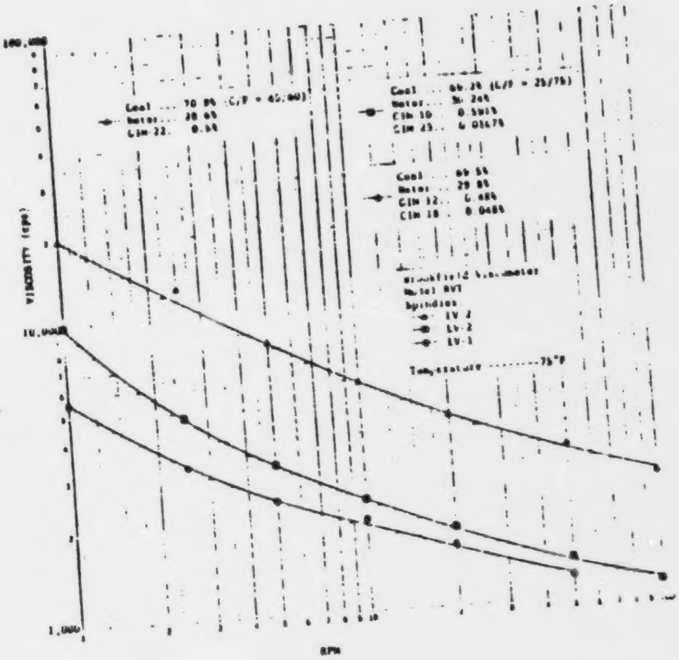

. X.11

Figure 9. Effect of Chemical Additives on the Viscosity Characteristics of Nominal 70 Weight % CWS Fuels

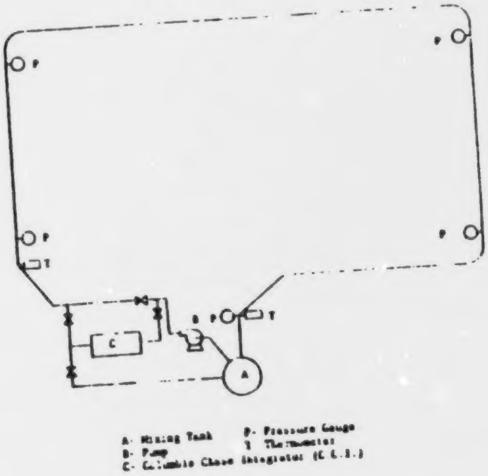
P
P
P
P
T
T
C
B
P
A
A- Mixing Tank
B- Pump
C- Columbia Chase Integrator (C.C.I.)
P- Pressure Gauge
T Thermometer

Figure 10. Schematic of CWS Pumping Test Loop

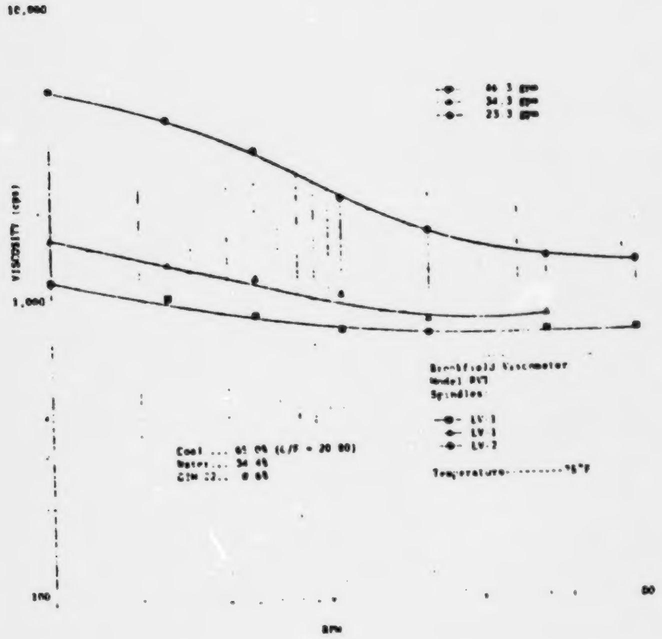

·X.11

Figure 11. Effect of Pumping on Viscosity of Nominal 65 Weight % CWS Fuel

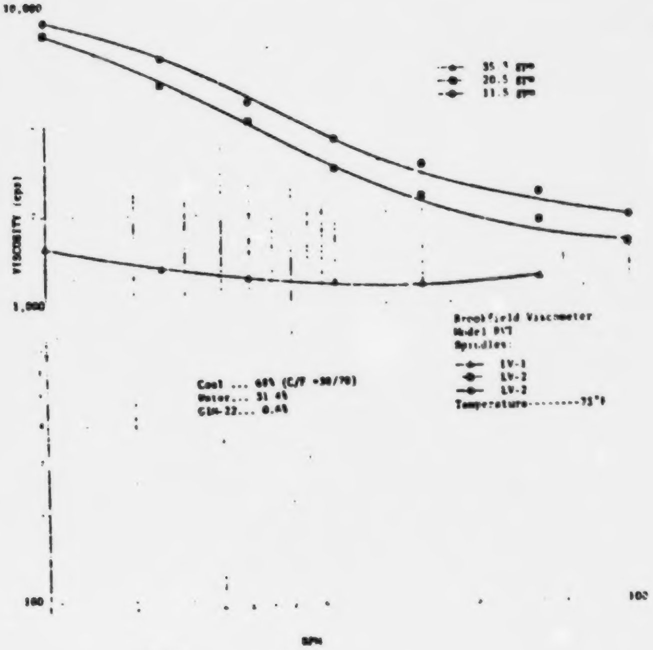

· X.11

Figure 12. Effect of Pumping on Viscosity of Nominal 68 Weight % CWS Fuel

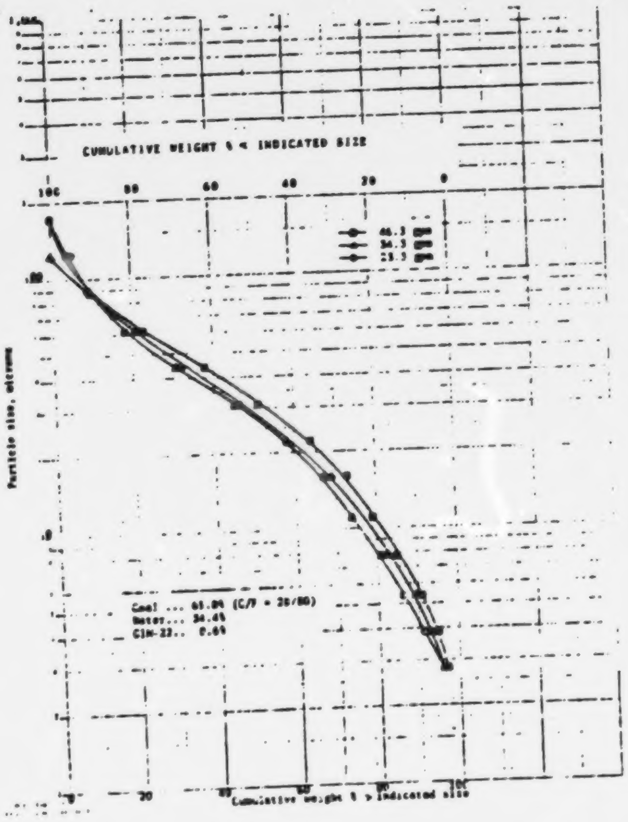

·X·11
Figure 13. Effect of Pumping on Coal Particle Attrition of Nominal 65 Weight % CWS Fuel

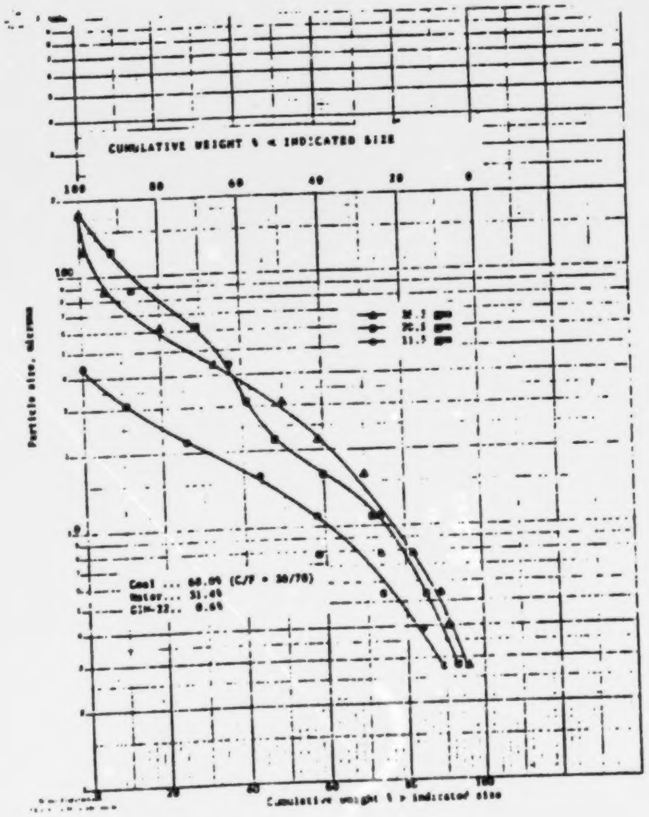

·X.14
Figure 14. Effect of Pumping on Coal Particle Attrition of Nominal 68 Weight % CWS Fuel

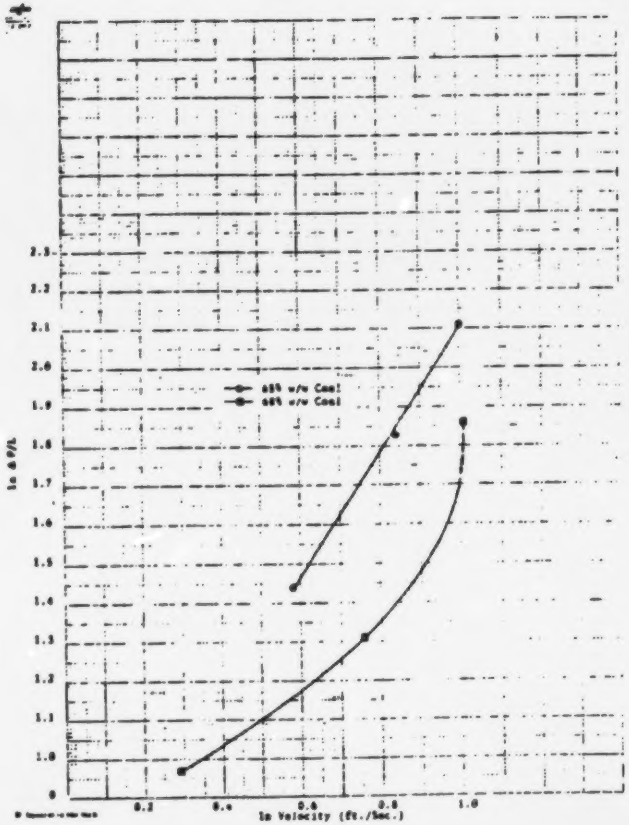

·X-11
Figure 15. Variation of Pressure Gradient with

Flow Velocity in the Pumping Test Loop

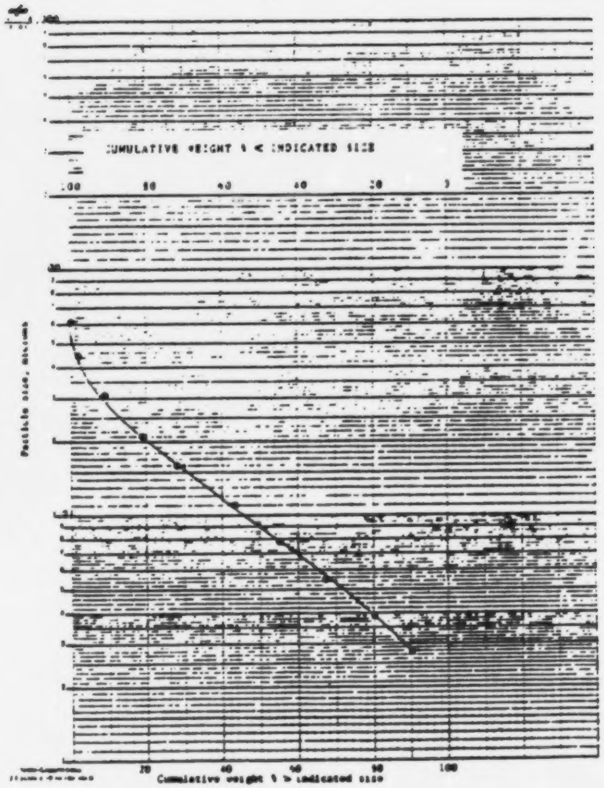

·X-11
Figure 16. Particle Size Distribution

of Micronized Coal

X.11

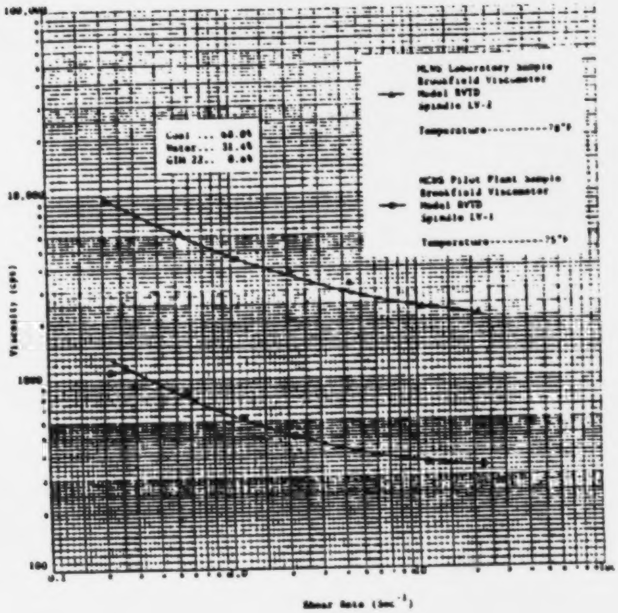

·X·11

Figure 17. Viscosity Characteristics of 68 Weight % MCWS Fuel

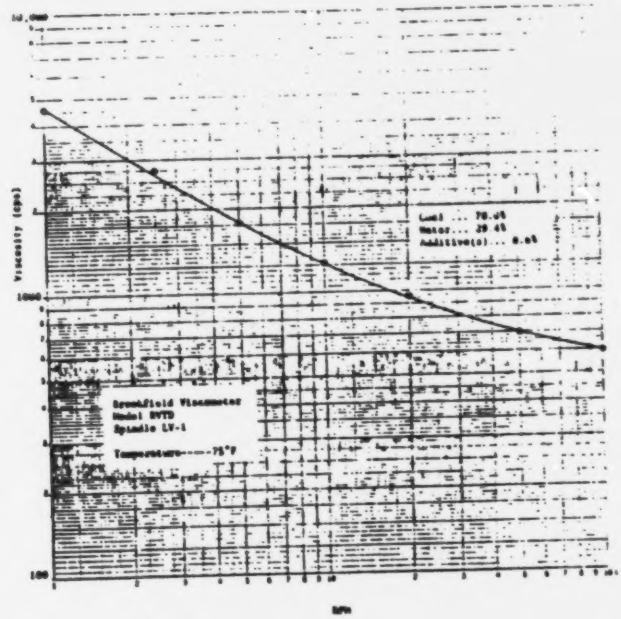

·X·11

Figure 18. Viscosity Characteristics of 70 Weight % MCWS Fuel

	Coal A	Coal B	Coal C
Volatile matter (%)	36.9	36.7	33.44
Fixed carbon (%)	50.5	52.8	55.07
Moisture (%)	1.7	3.3	3.03
Ash (%)	10.9	7.2	8.46
Heating value (Btu/lb)	12,802	13,370	13,811

·X·11

Table 1. Proximate Analysis of Various Coals

- o Nominal 62 % CWS
  - Sample No. 007082-107; Additive - GIM-8
  - No settling in 4 weeks
  - Slight settling in 6 weeks
  - Water Separation in 8 weeks
- o Nominal 65 % CWS
  - Sample No. 010082-2042; Additive - GIM-22
  - Slight settling in 2 weeks
  - Settling in 4 weeks
- o Nominal 79 % CWS
  - Sample No. 010082-2044; Additive - GIM-22
  - Slight settling in 2 weeks
  - Moderate settling in 4 weeks

X·11

Tabel 3. Stability Characteristics of Typical CWS Fuels

X-12

reached an equilibrium viscosity during constant shear testing and were not deleteriously affected by high shear. A slurry from supplier B had been pumped for twenty hours at constant shear before the variable shear testing was begun. Figure 9 shows the results from the four lines in the test loop as well as from the viscometer. There is good agreement among all the measurements. This slurry was Newtonian as received, however, it became slightly dilatant after twenty hours in the loop. This slight dilatancy caused no pumping problems.

Two of the CWS were subjected to variable shear testing before being circulated for any length of time. Figures 10 and 11 show the results for these slurries. The tests were conducted by increasing the flow rate from 0 to 100 gpm (0 to 150 s^{-1}), curve 1, and then decreasing the flow rate back to zero, curve 2. This cycle is repeated three times. The test sequence takes one and a half hours. The slurry from supplier B showed a gradual decrease in viscosity towards an equilibrium value, while the CWS from supplier D still exhibited a strong time dependency. This sample reached equilibrium after two and a half additional hours of pumping.

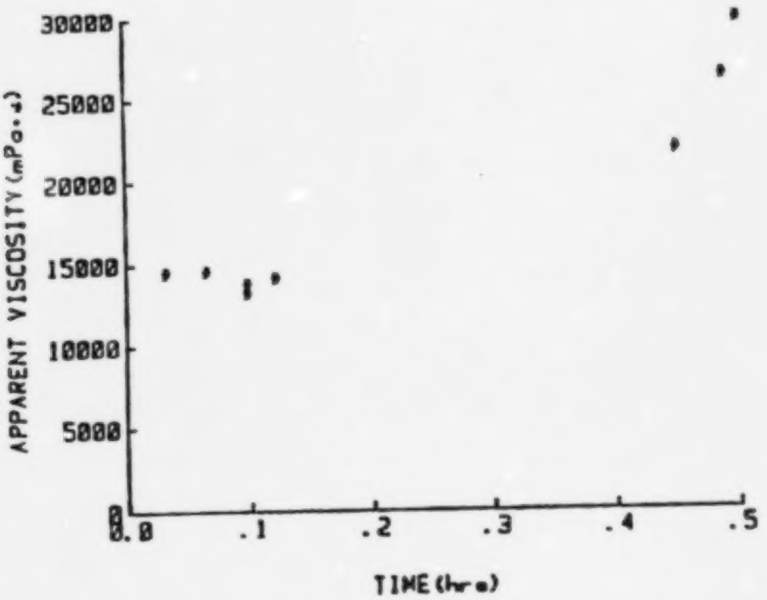

.X.12

Figure 6. Apparent Viscosity Versus Time, Sample A-1.

X.12

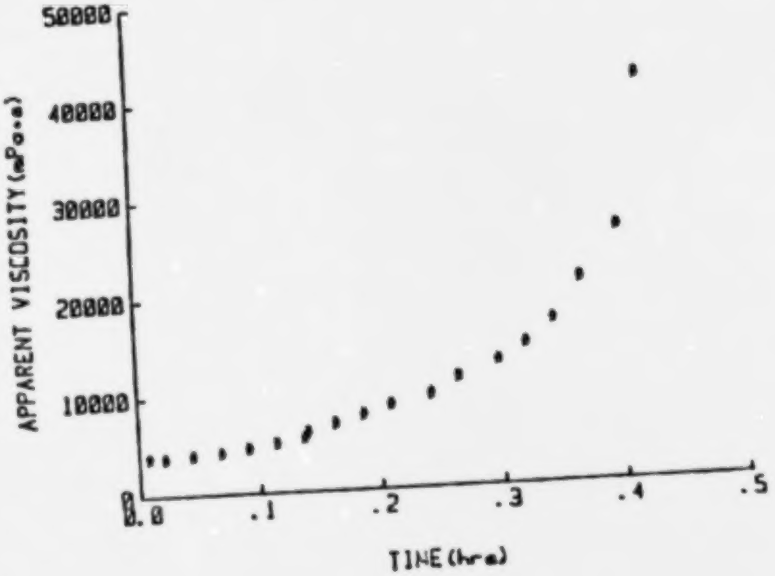

.X.12

Figure 7. Apparent Viscosity Versus Time, Sample B-1.

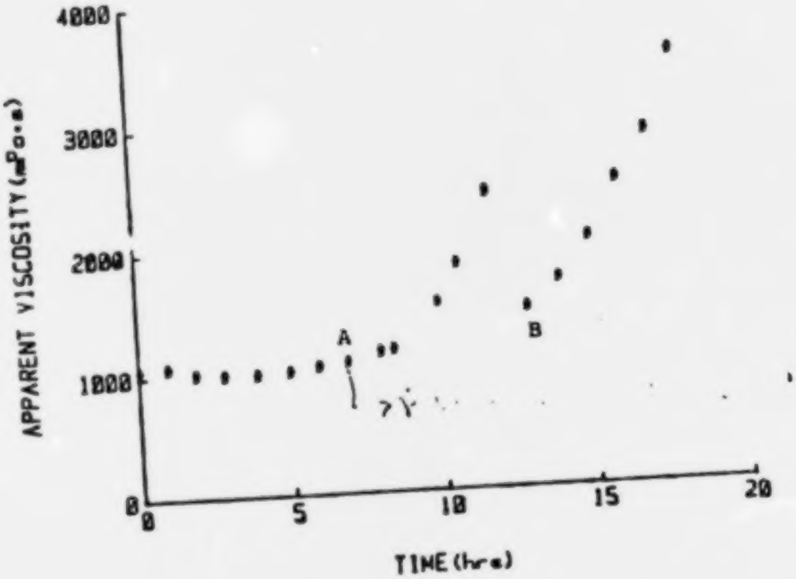

.X.12

Figure 8. Apparent Viscosity Versus Time, Sample D-1.

X.12

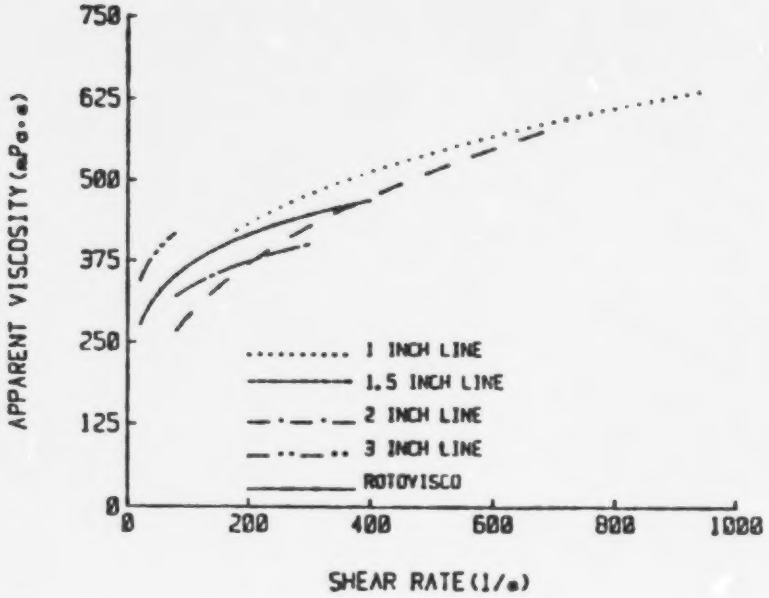

.X.12

Figure 9. Apparent Viscosity Versus Shear Rate, Sample B-2.

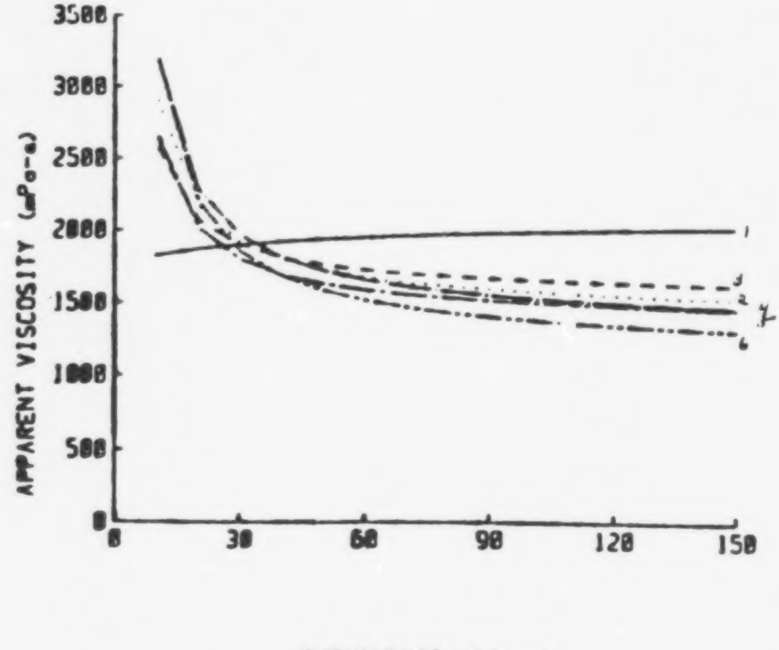

.X.12

Figure 10. Apparent Viscosity Versus Shear Rate, Sample B-3.

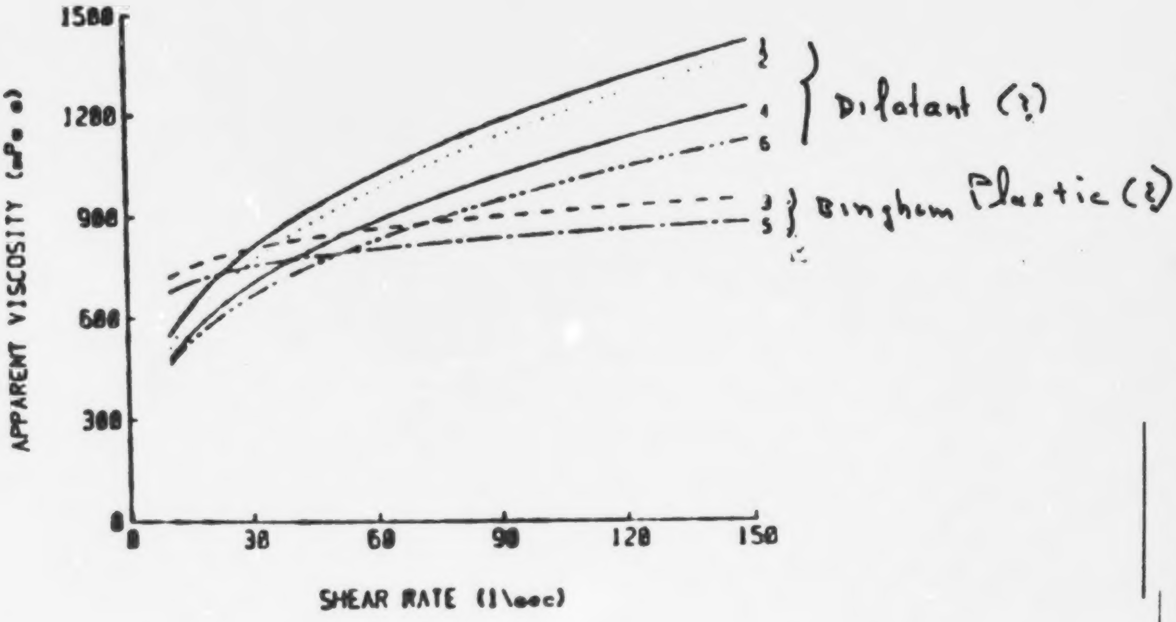

X-12

Figure 11. Apparent Viscosity Versus Shear Rate, Sample D-4.

CONCLUSIONS

From the samples which were examined during this program, some general statements can be made about the handling properties of these fuels. More testing must be performed before coal/water slurries can be successfully used as a fuel in a utility power plant.

- Each of the suppliers has demonstrated that they are capable of producing a technically acceptable utility fuel, however, due to secrecy agreements, it cannot be determined whether or not the specific fuels tested can be produced in large quantities at attractive prices.
- Quality control of the CWS delivered to the plant is critical. Wide variations in slurry properties were seen in the samples tested, some of which were unacceptable for utility use.
- The seventy percent weight coal slurry seems to be, for some suppliers, the borderline level for producing an acceptable slurry. A lowering of the concentration requirement would decrease the viscosity of the CWS and perhaps minimize some of the changes in the slurry after pumping and circulation.

X.13

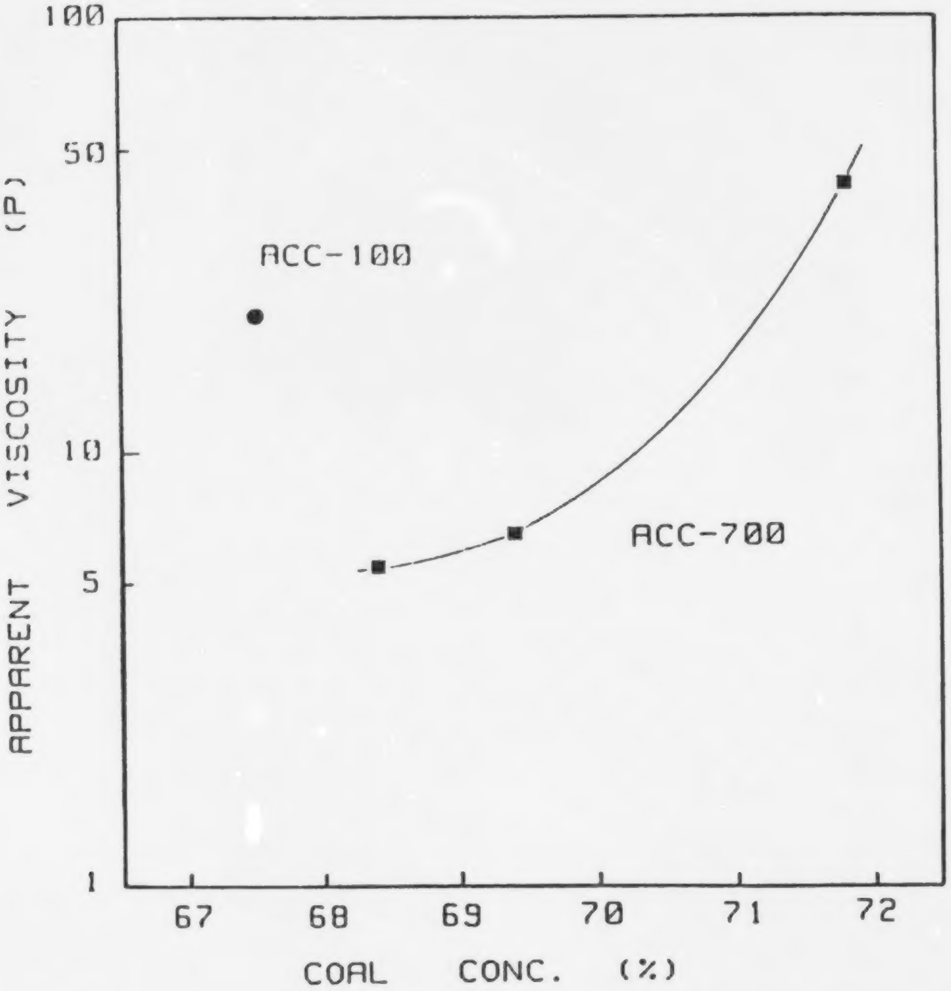

Coal -- Tatung coal (prepared particle size)

X.13

Fig.3 Viscosity of CWM

X.13

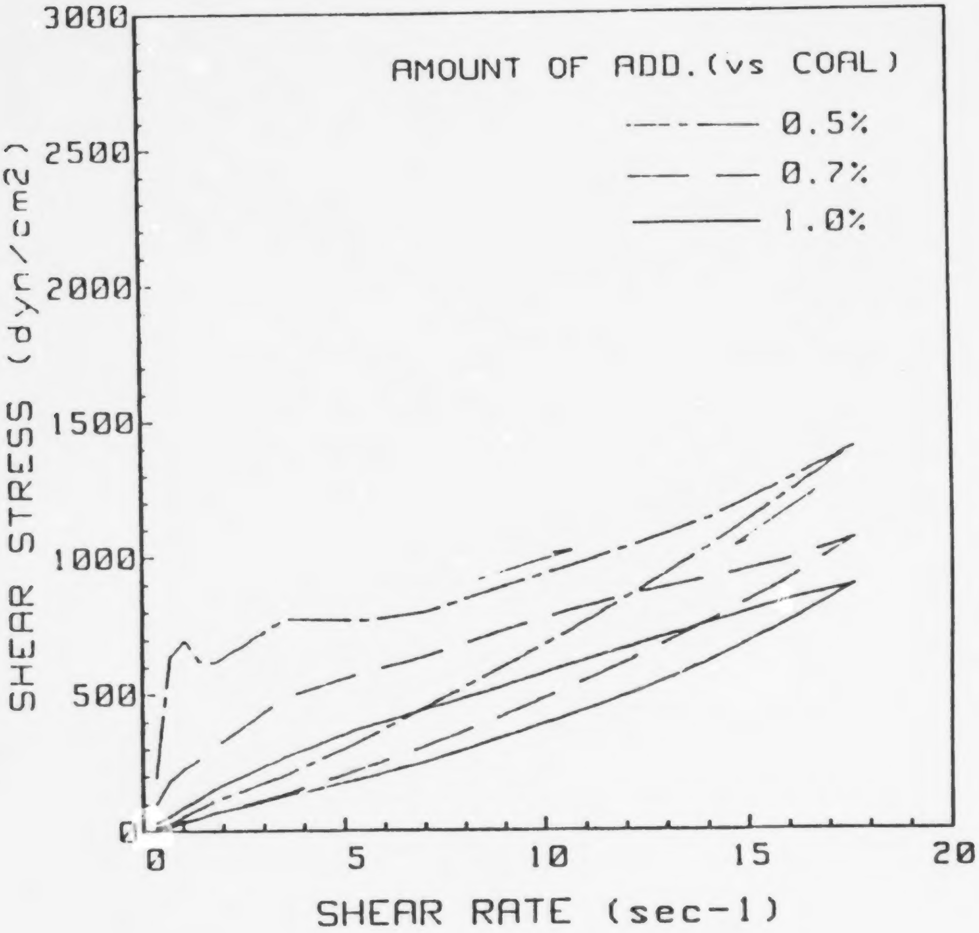

Tatung coal (c.c.66%)

Additive -- ACC-700

Fig.5 Rheogram of CWM

X.13

-- Effect of amount of ACC-700

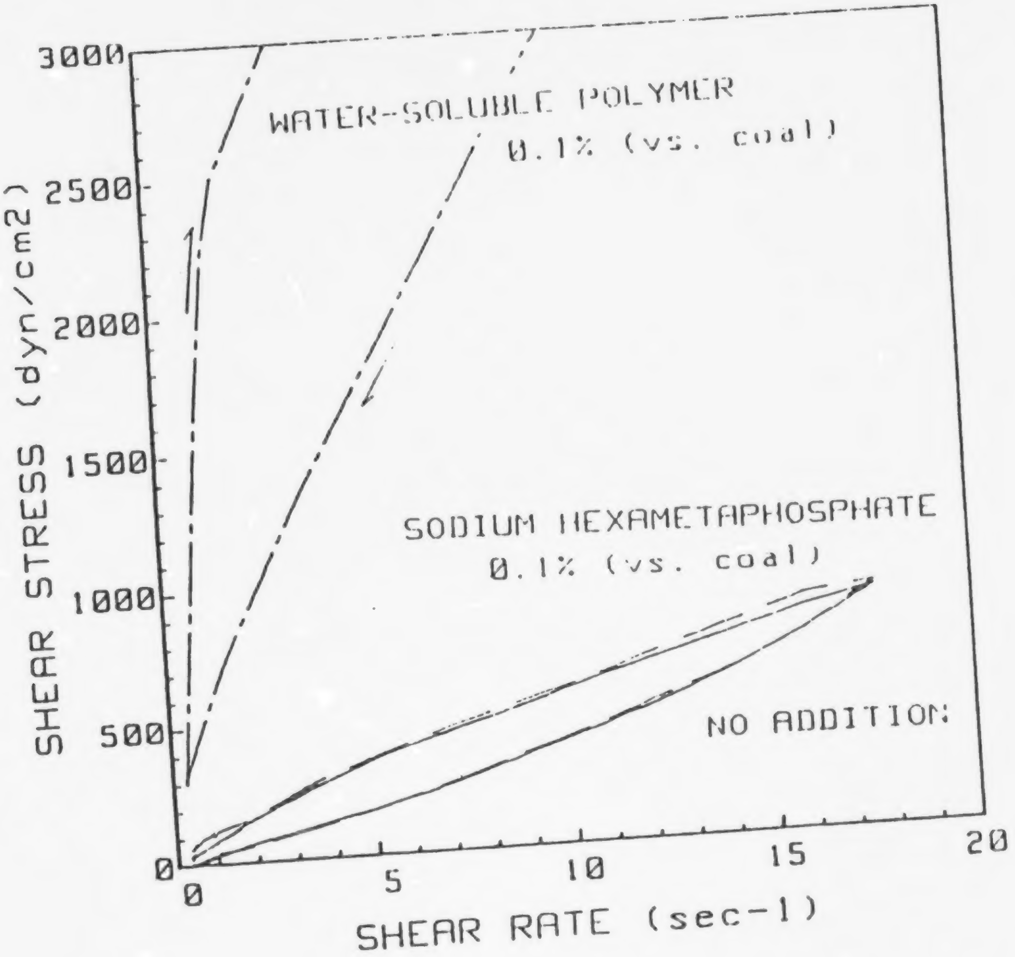

Tatung coal (c.c.66%)

Additive -- ACC-700 1%(vs. coal)

Fig.6 Rheogram of CWM

X.13

-- Effect by combined use of stabilizer

X·15

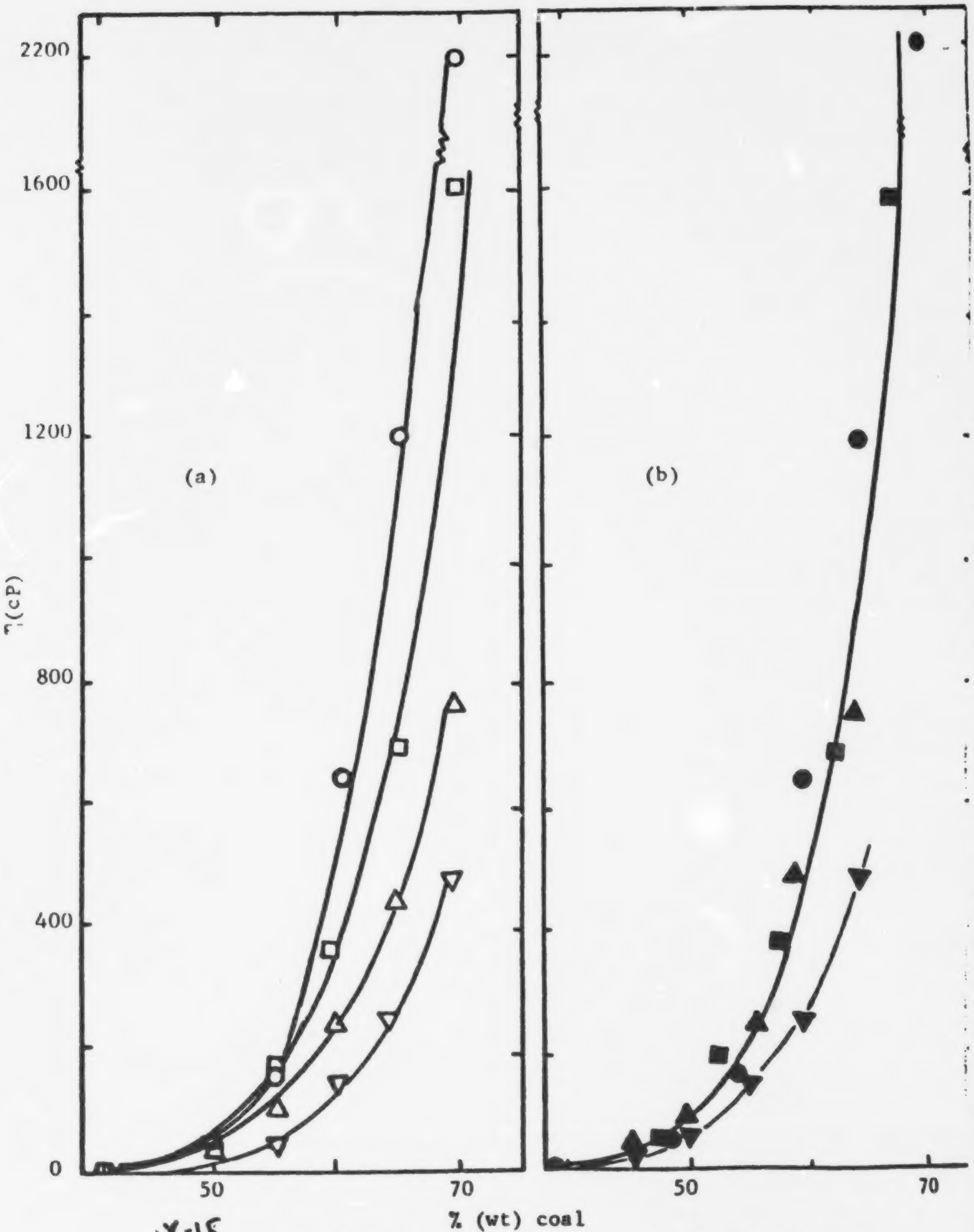

X-15

Figure 1. Viscosity of coal/water slurries. Pittsburgh #8 (○), Illinois #6 (□), San Juan (△), Hiawatha (▽). Shear rate 90 s^{-1}. Concentration based on (a) actual weight of coal, (b) without moisture.

X.15

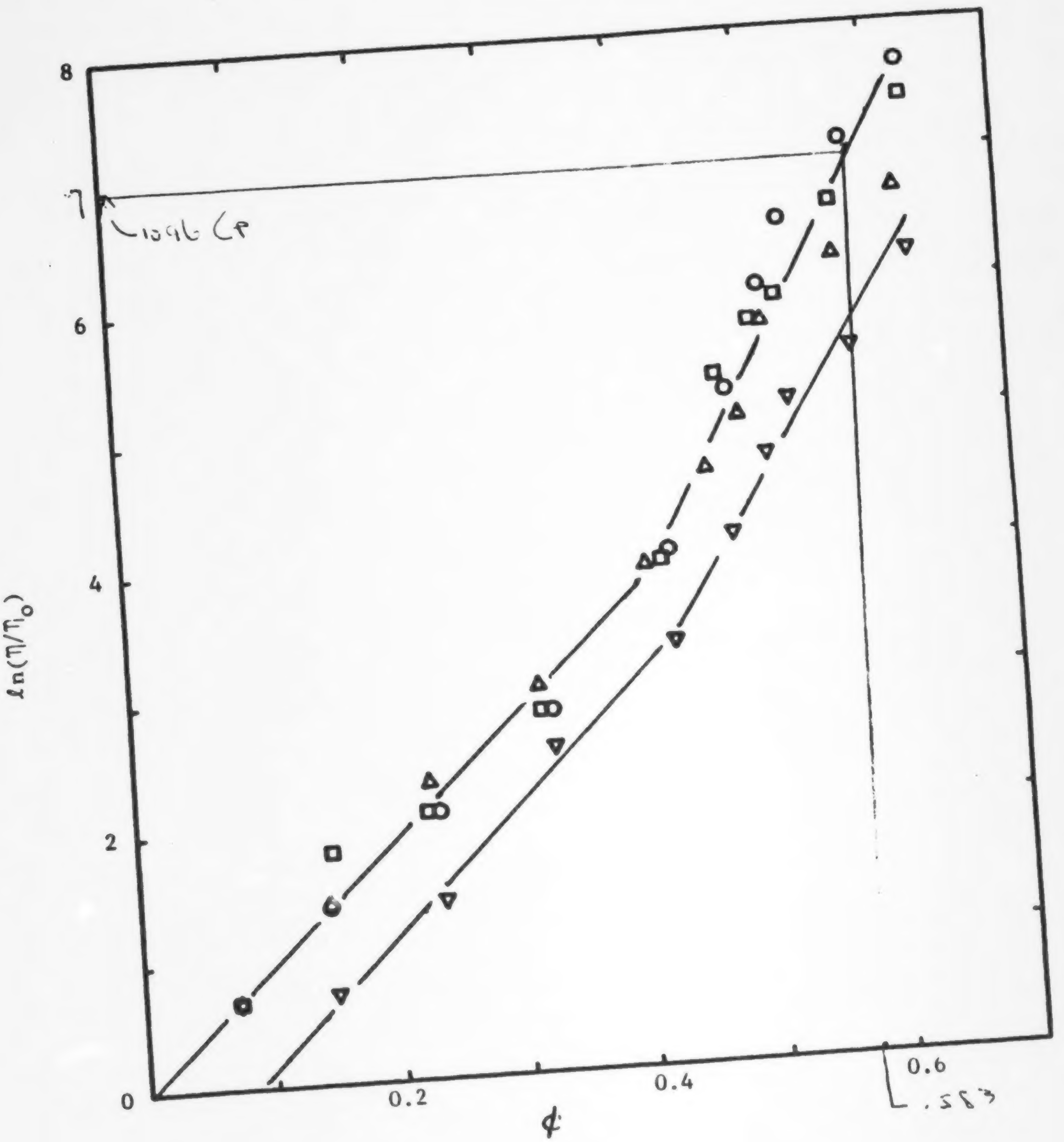

.X.15

Figure 2. Viscosity of coal/water slurries. Pittsburgh #8 (○), Illinois #6 (□), San Juan (△), Hiawatha (▽). Shear rate 90 s^{-1}.

N.B., Fig. 2 is plot of Eq. 9.X.15

X·15

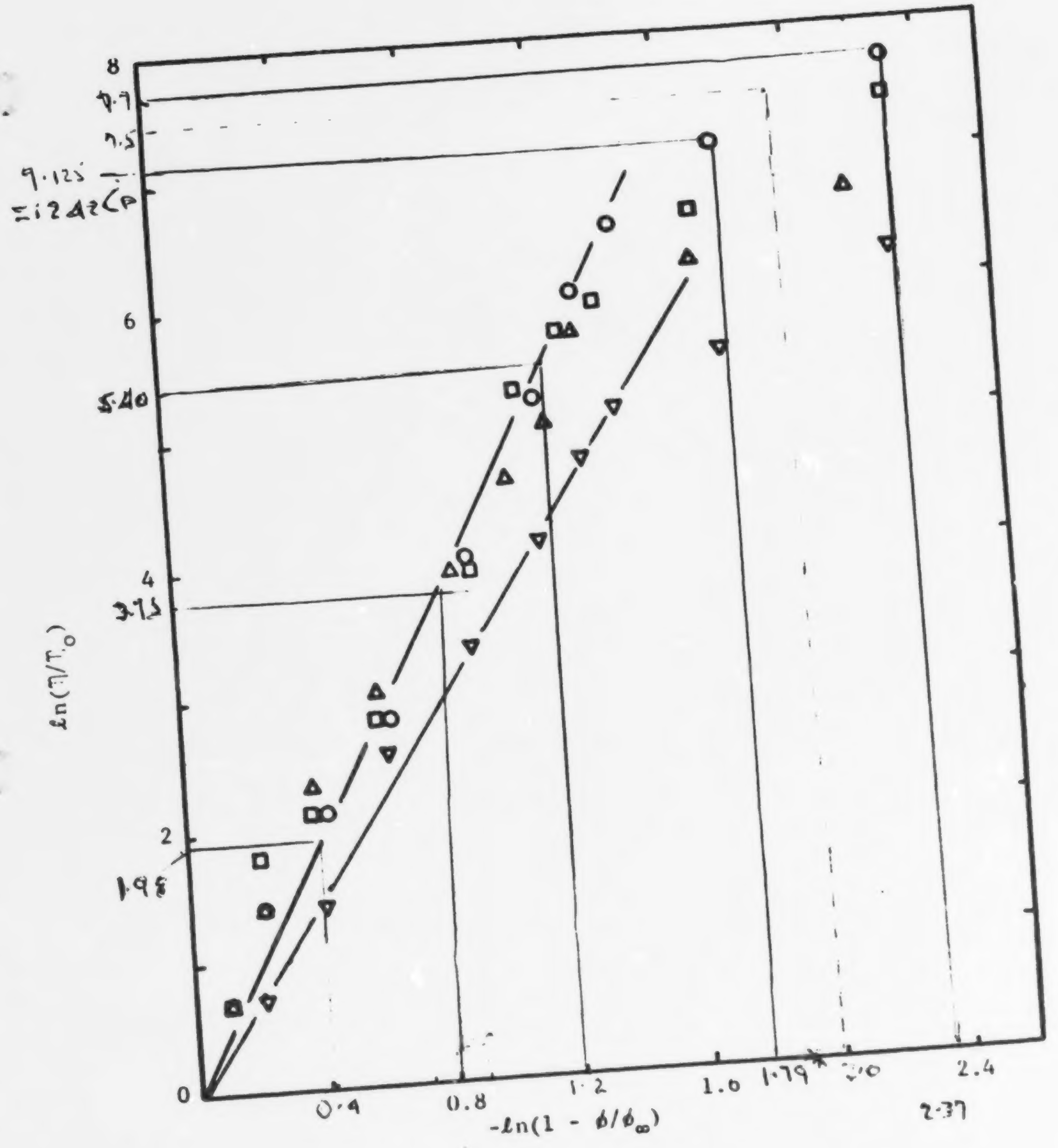

-X.15

Figure 3. Plot of Dougherty and Krieger equation with ϕ_∞ = 0.70. Pittsburgh #8 (○), Illinois #6 (□), San Juan (△), Hiawatha (▽). Shear rate 90 s^{-1}.

$* \text{ antilog} -1.79 = .167 = \left(1 - \frac{\Phi}{\Phi_\infty}\right)$ - S 1.9.A

X.15

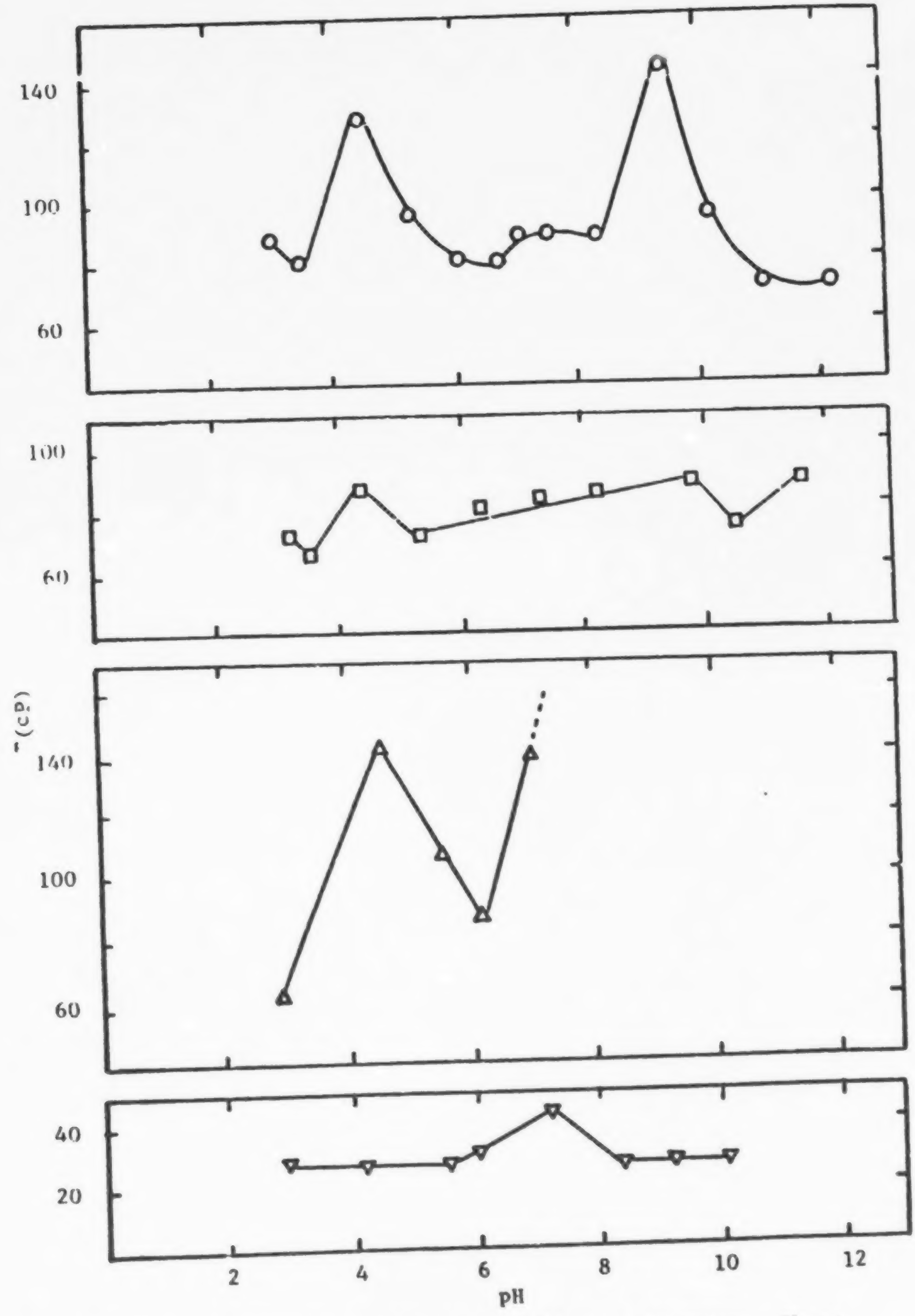

Figure 5. Viscosity of 50% (wt) coal/water slurries. Shear rate 45 s^{-1}. Pittsburgh #8 (○), Illinois #6 (□), San Juan (△), Hiawatha (▽).

X.15

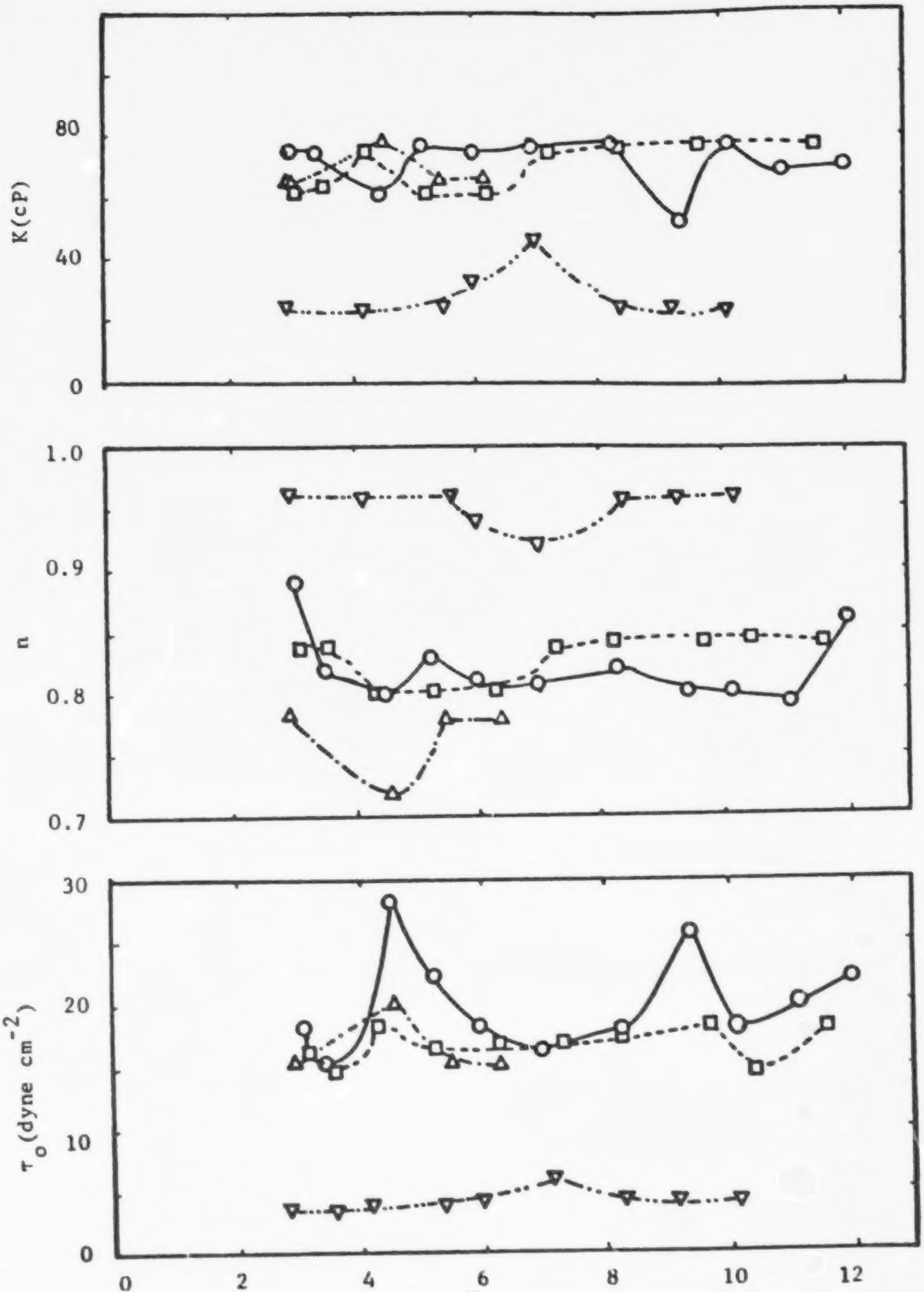

Figure 6. Rheological data (Herschel-Bulkley Equation) for 50% (wt) Coal/Water Slurries. Pittsburgh #8 (○), Illinois #6 (□), San Juan (△), Hiawatha (▽).

X.15

X.15

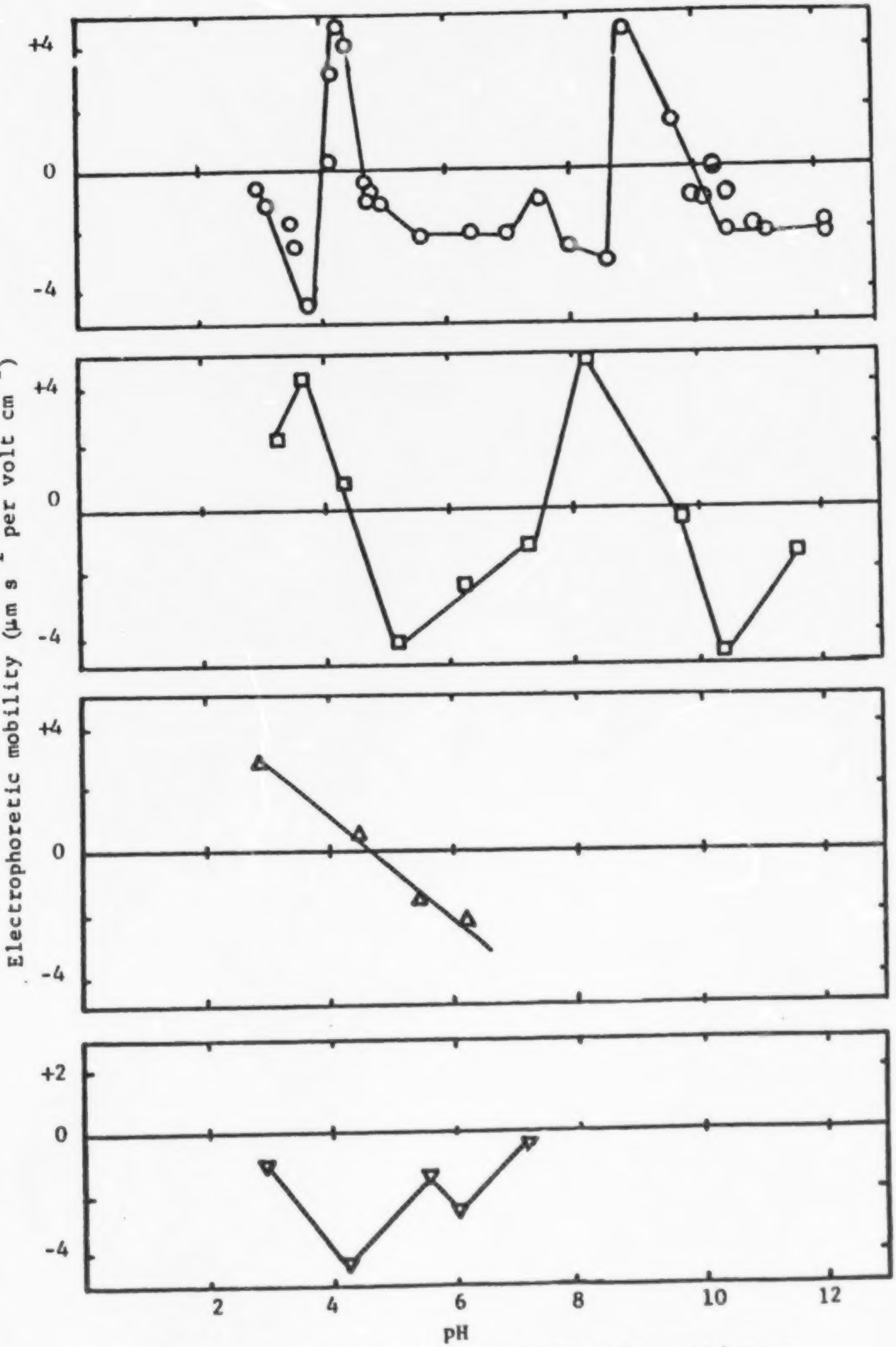

Figure 7. Electrophoretic mobility of 50% (wt) coal/water slurries Pittsburgh #8 (○), Illinois #6 (□), San Juan (△), Hiawatha (▽).

X.15

X.15

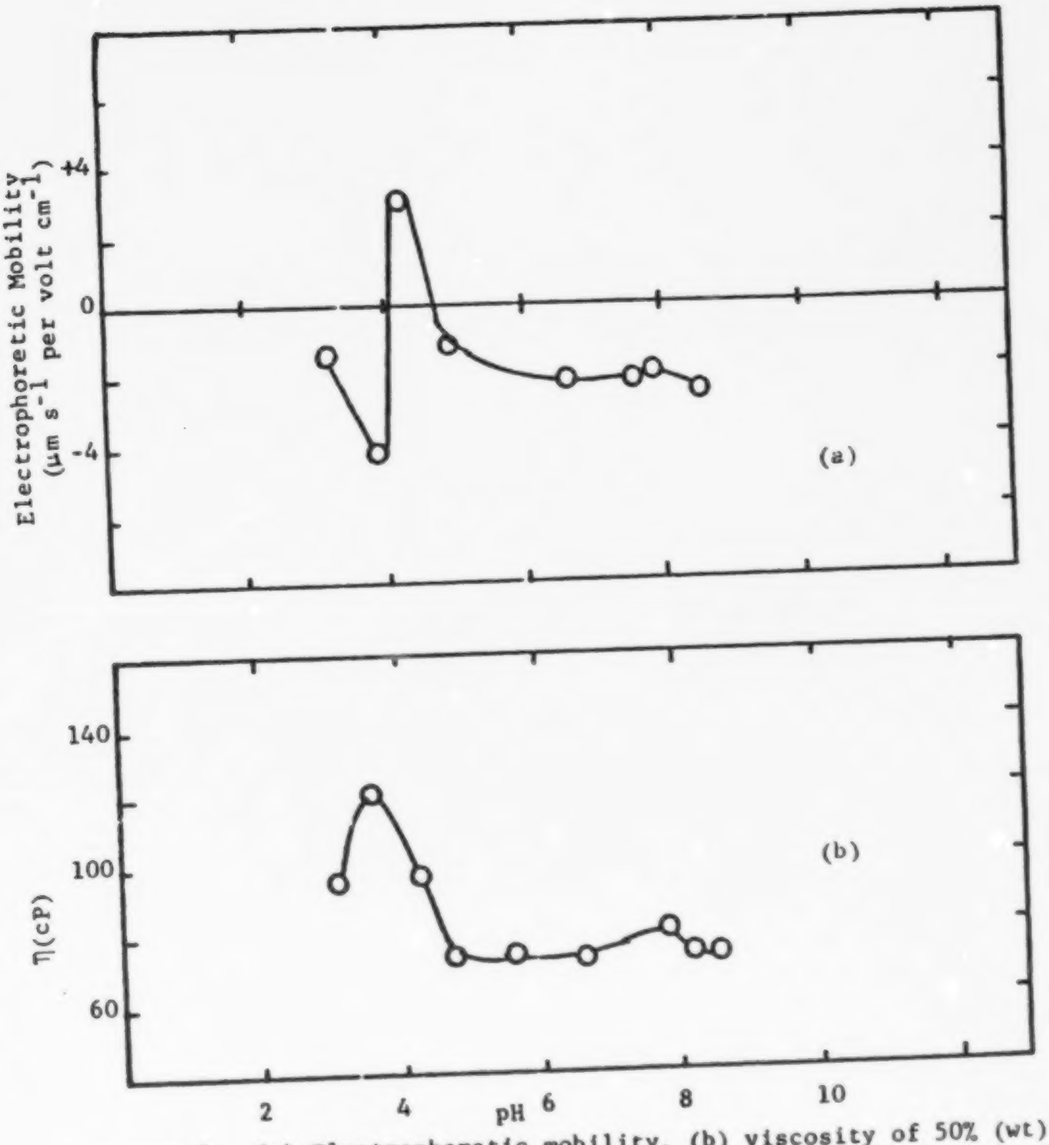

Figure 8. (a) Electrophoretic mobility, (b) viscosity of 50% (wt) Pittsburgh #8 coal/water slurries, one week after preparation. Shear rate 45 s^{-1}.

X.15

X.15

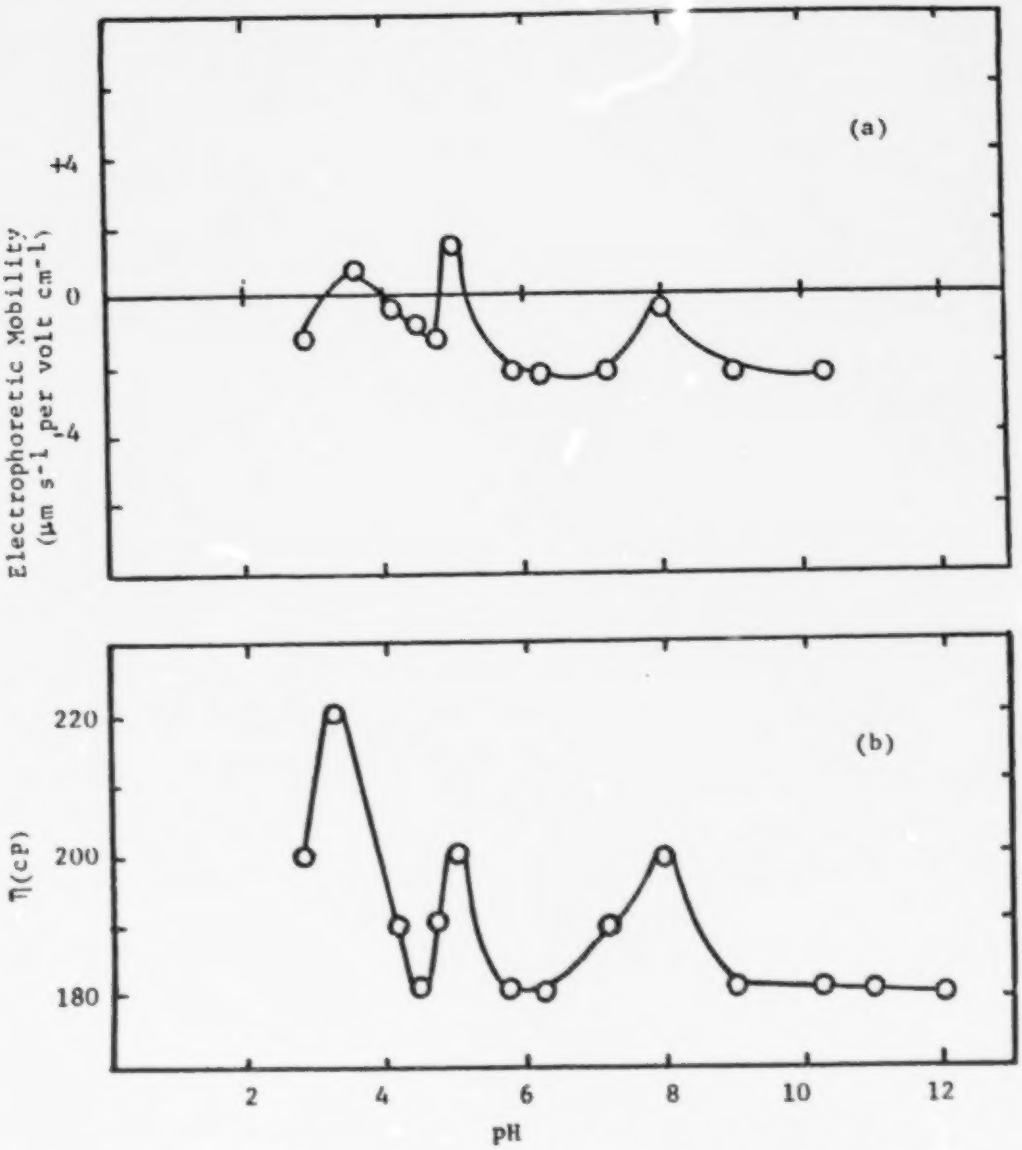

Figure 9. (a) Electrophoretic mobility, (b) viscosity of 50% (wt) washed Pittsburgh #8 coal/water slurries. Shear rate 9 s^{-1}.

X.15

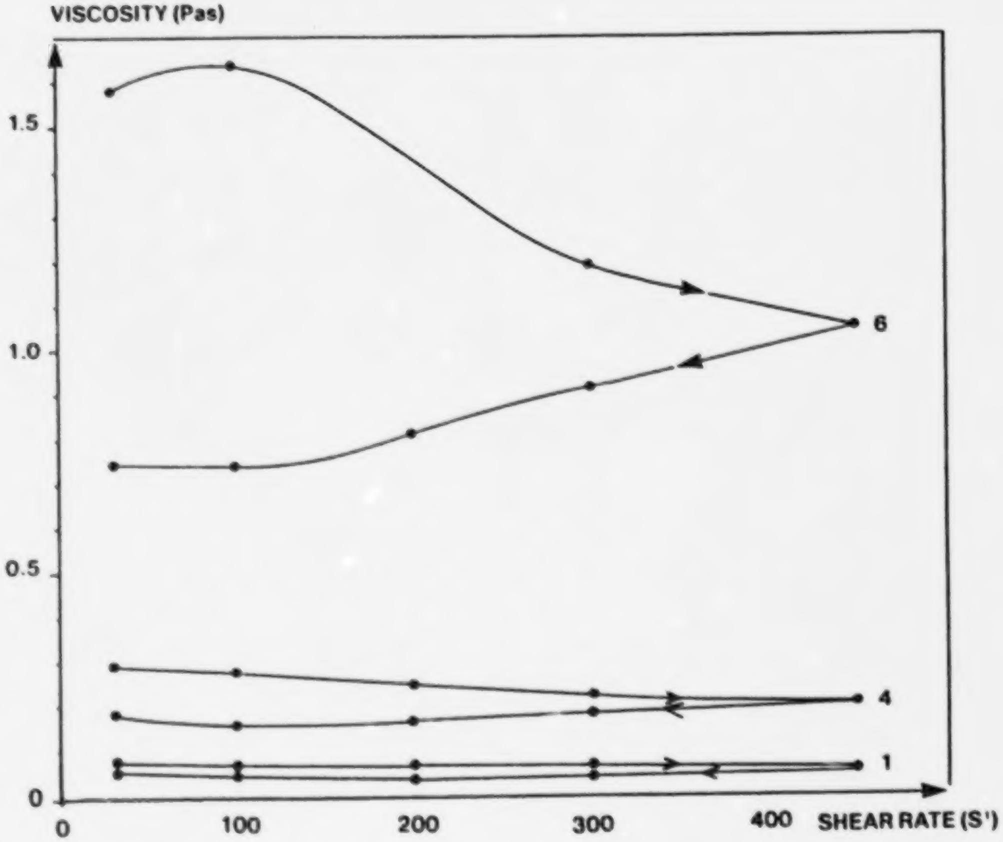

Figure 1. X. 16

Viscosity (Pas) vs. shear rate (s-1) for slurries number 1, 4 and 6.

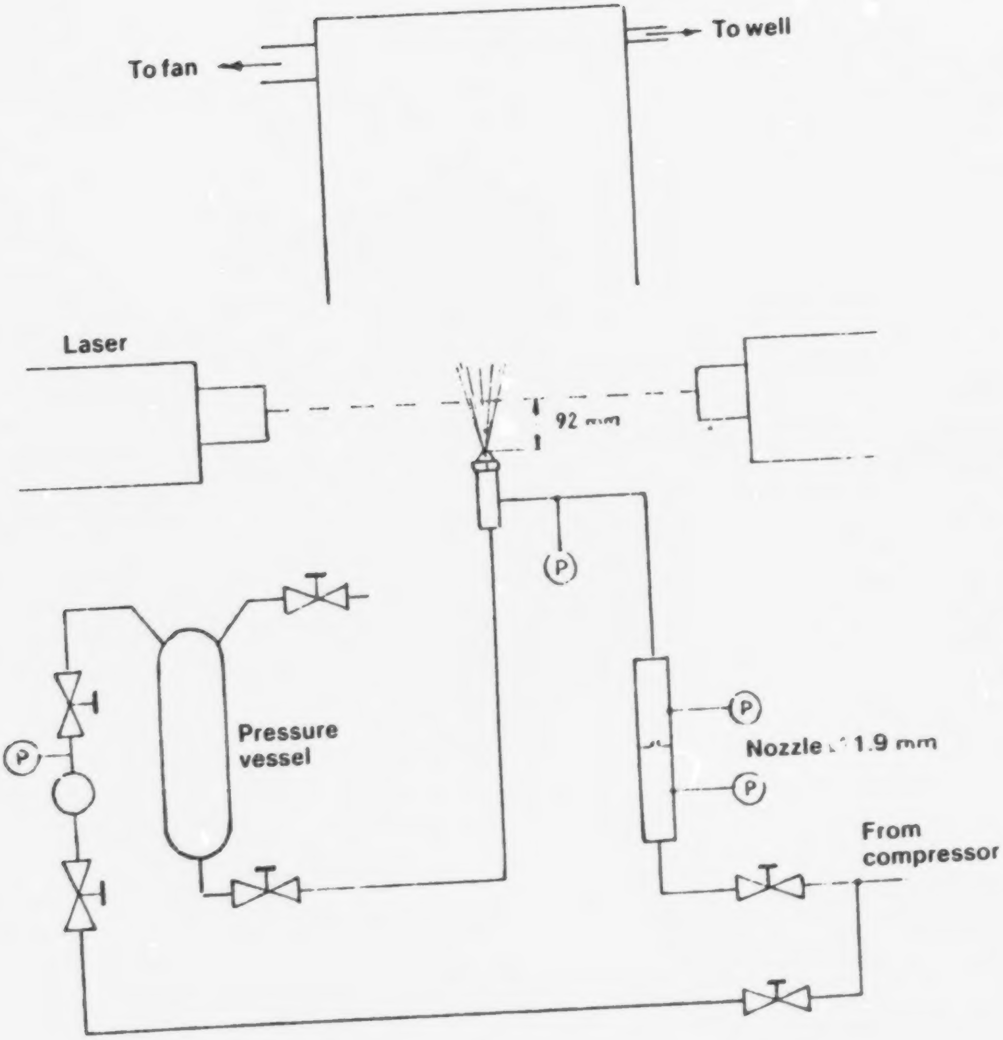
To fan
To well
Laser
92 mm
P
Pressure vessel
P
P
Nozzle ∅ 1.9 mm
P
From compressor

Figure 2. X·16

Atomization test facility.

X·16

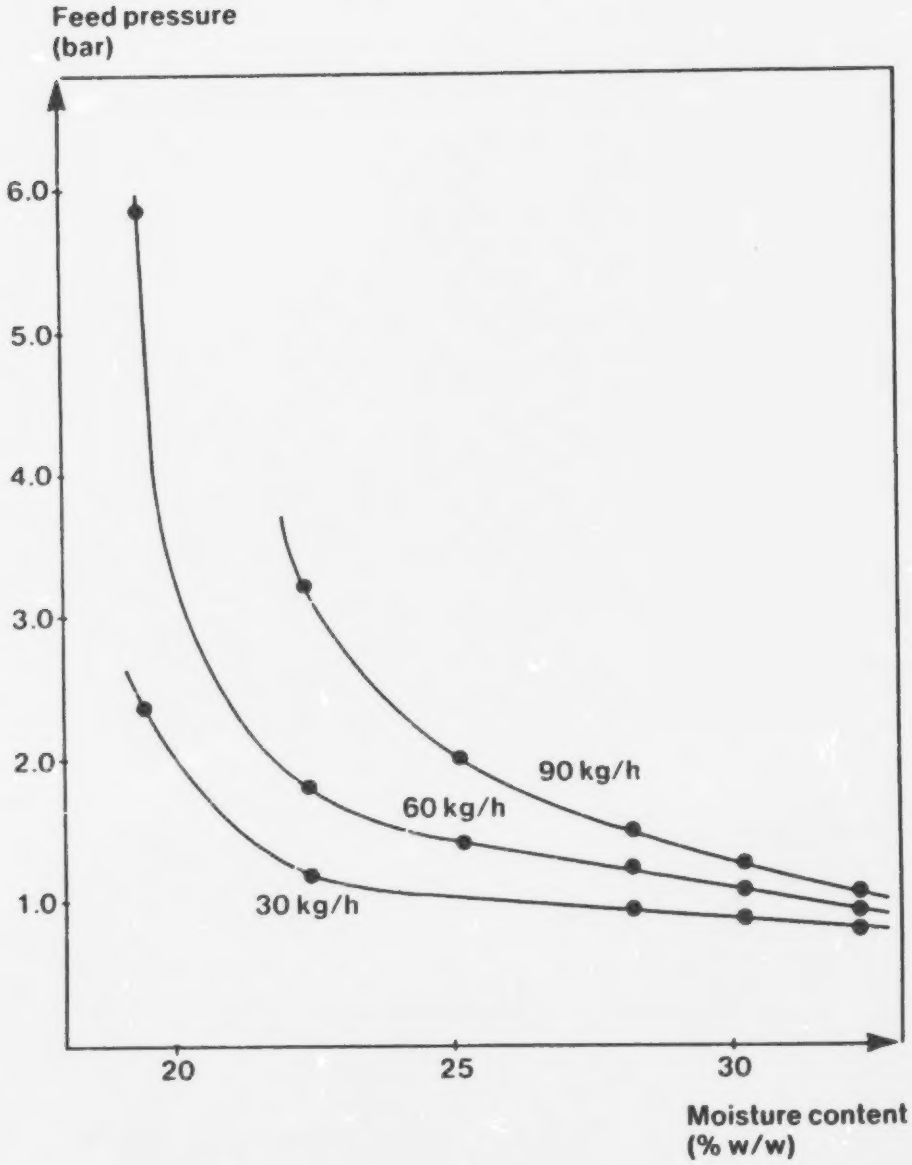

Figure 3. X·16

Feed pressure vs. moisture content at
1.2 bar atomization air pressure and
30, 60 and 90 kg/hr slurry feed respectively.

X.16

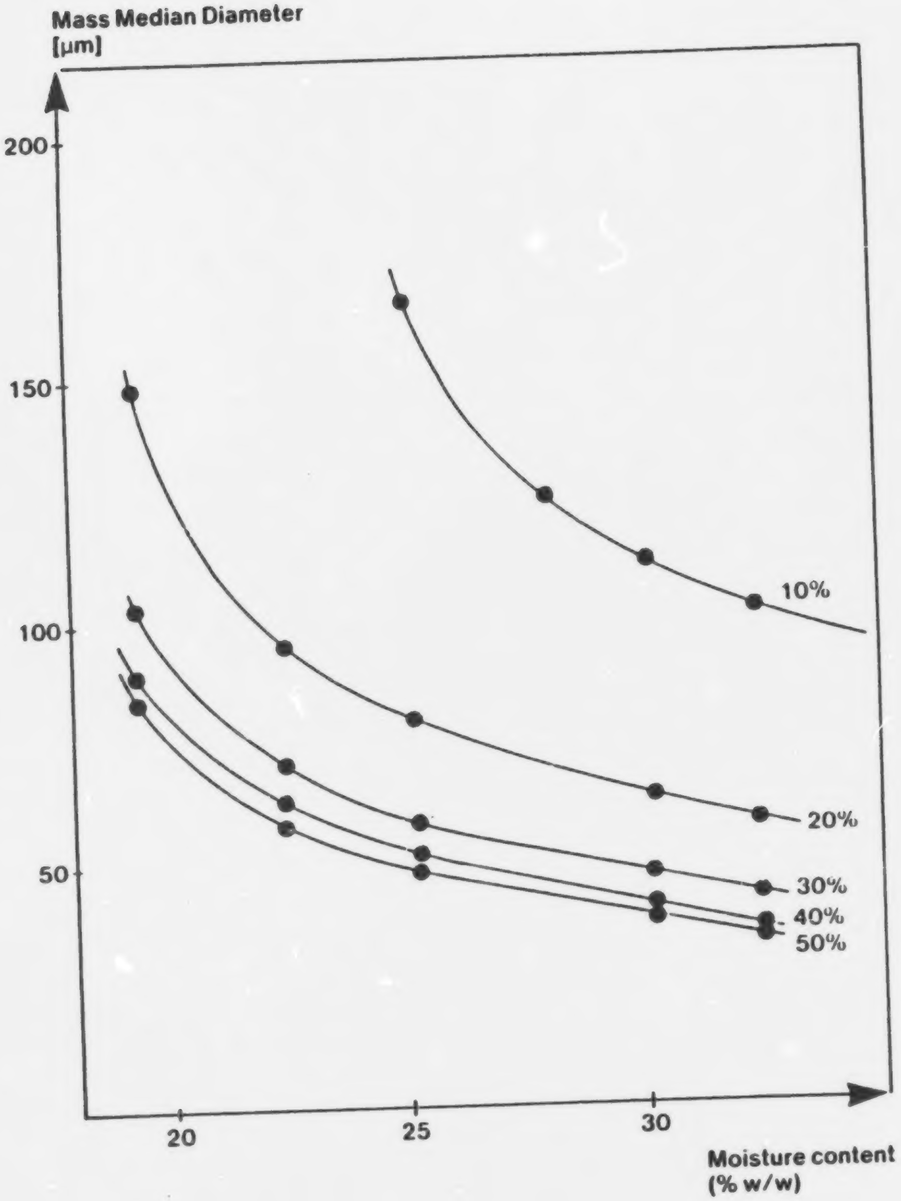

Figure 4. – X.16

Mass Median Diameter (μm) vs. moisture content at 1.2 bar atomization air pressure and 10, 20, 30, 40 and 50 % air to slurry ratios

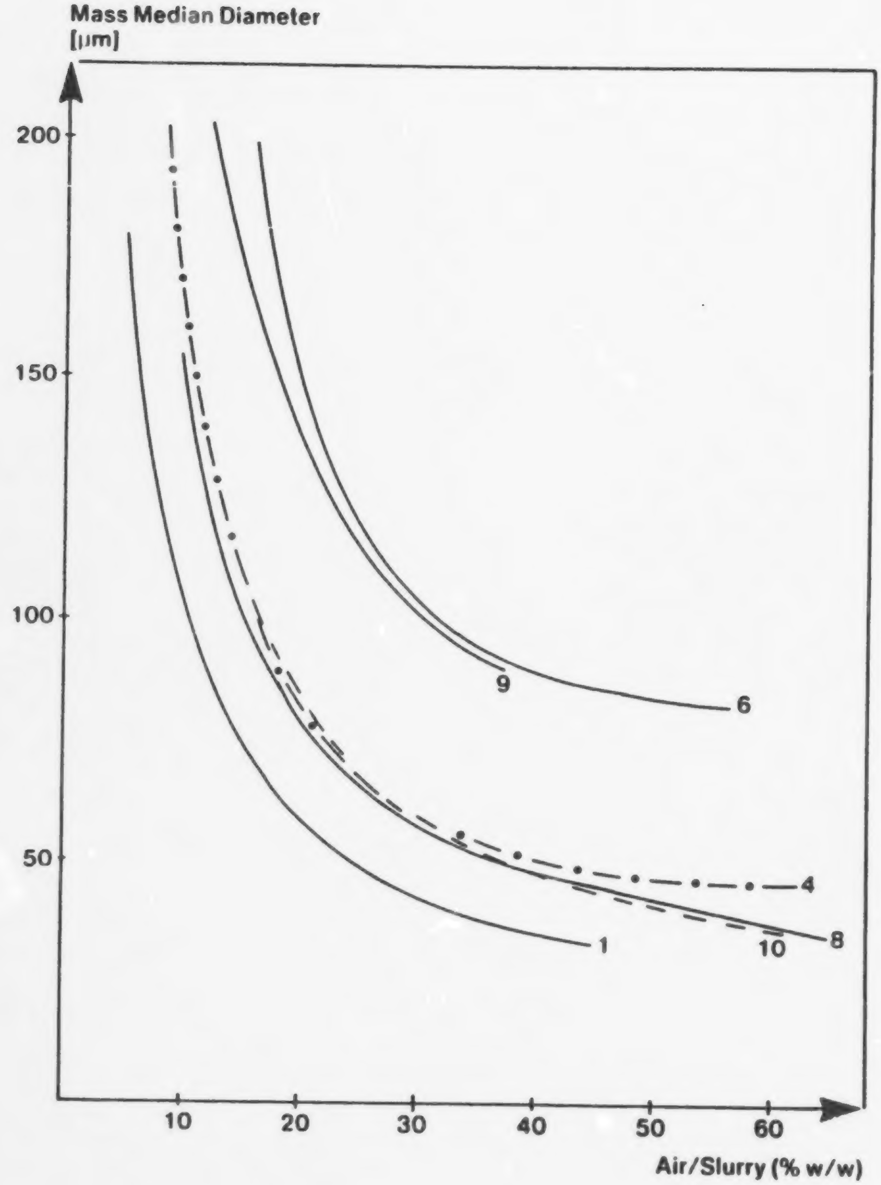

Figure 5. X·16

Mass Median Diameter vs. air to slurry ratio for six slurries, four of which (1, 8, 9 and 10) with a moisture content of 32.2 % and formulated differently. Air pressure at 1.2 bar.

X.16

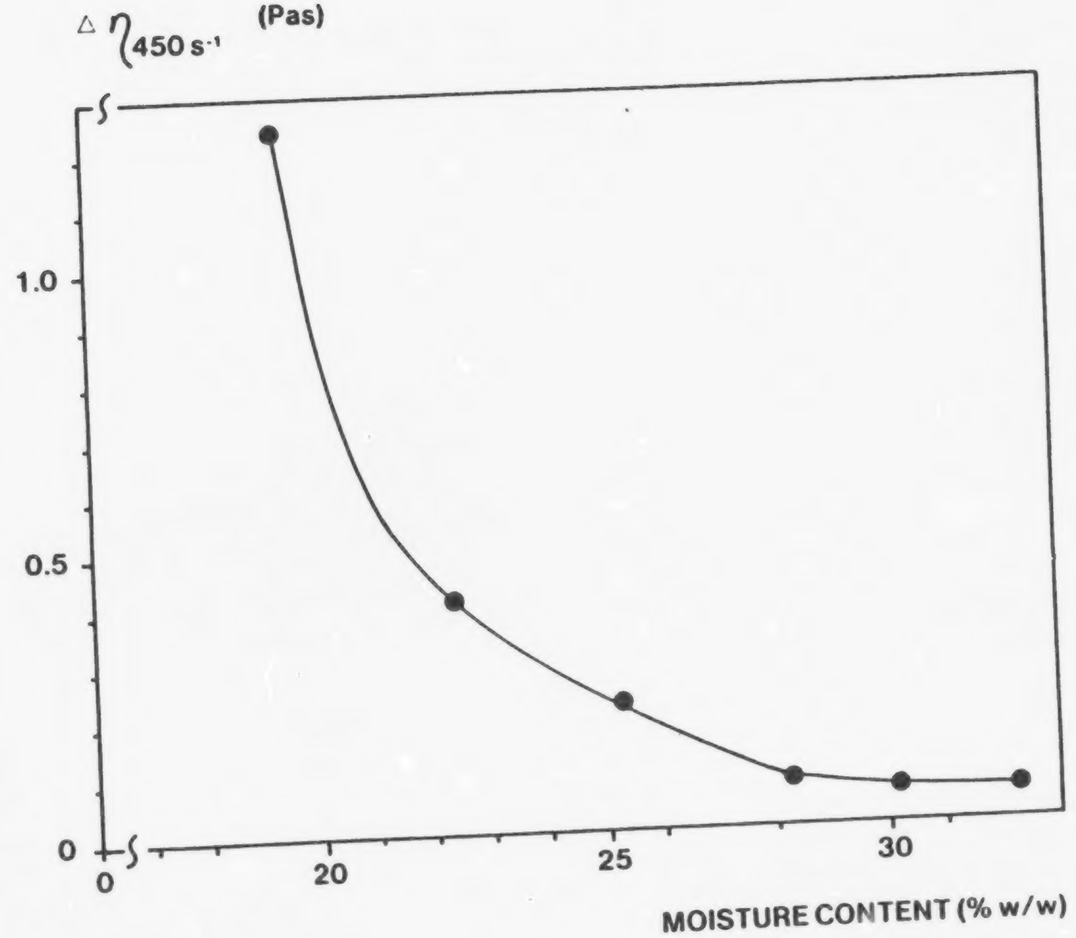

Figure 6. X.. 16

Initial viscosity - Lowest viscosity at 450 s^{-1}
(Pas) vs. moisture content (% w/w)

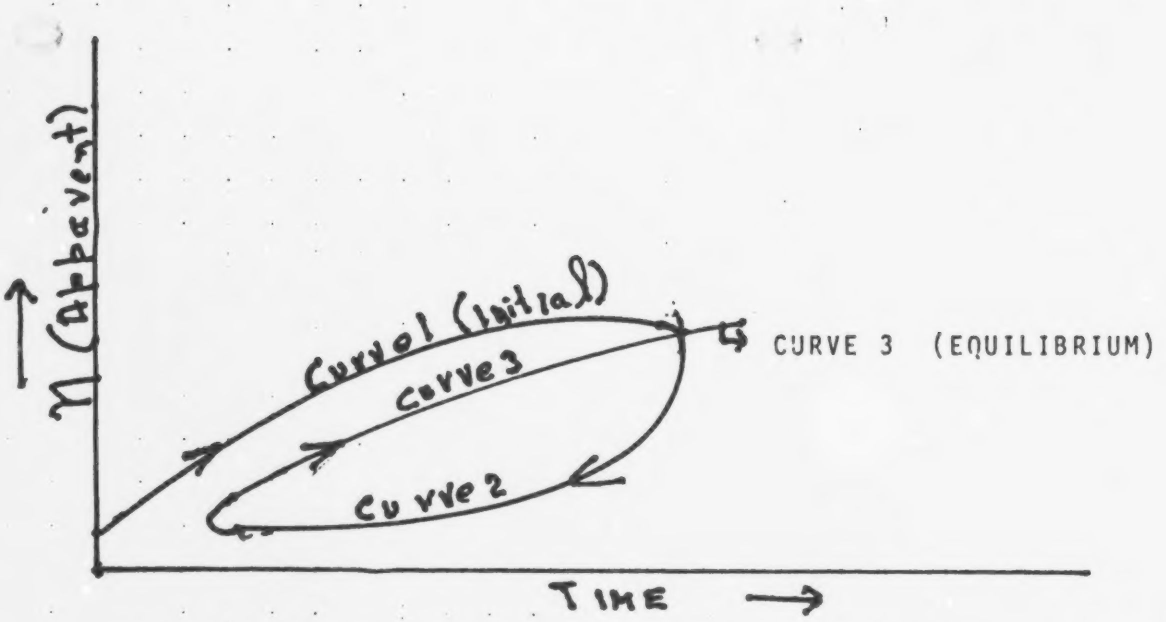

1) FIG. G.1.X.12 CONSTANT LOW SHEAR - THIXOTROPIC

NOTE: CURVE 1 IS HIGHER THAN EQUILIBRIUM CURVE 3
THEREFORE MODE IS THIXOTROPIC

1) After Dr. Dooher

G.1.X.12

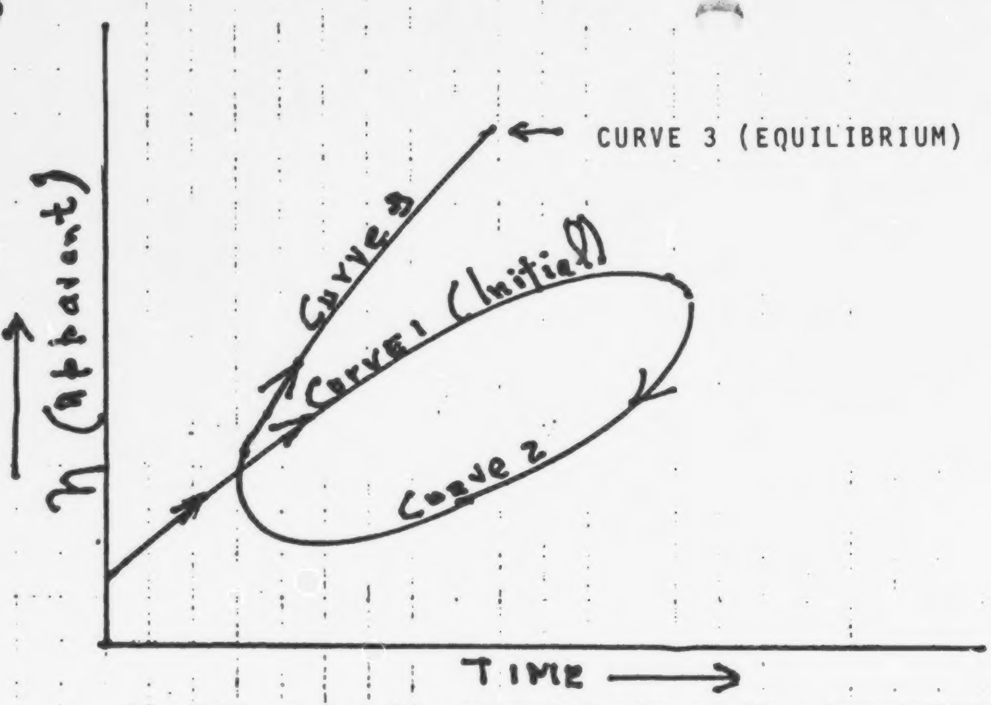

1) FIG. G.2.X.12 CONSTANT LOW SHEAR - RHEOPECTIC MODE

NOTE: CURVE 1 IS LOWER THAN EQUILIBRIUM CURVE 3
THEREFORE MODE IS RHEOPECTIC

1) After Dr. Dooher

X·2

Table 2. Viscosities[a] at solid concentration of 65wt%

X·2

Coal	Additives[b]					
	NOF-1	NOF-2	NOF-3	NOF-4	NOF-5	NOF-6
BA	138	153	198	278	891	308
UF	378	390	430	563	878	1106
MI	256	380	295	417	1011	269
WL	258	300	410	454	948	955
NE	130	140	255	706	548	1706
ER	438	400	502	717	1185	1422
WO	298	325	424	604	1027	1422
TR	420	261	1046	2022	1034	2465
WM	569	592	895	1350	1000	1447
DA	620	635	1095	1453	1090	—
TA	680	408	852	872	458	1517
BL	990	1010	2400	—	—	—
MA	1611	1517	1980	—	1406	—
WN	— [c]	—	—	—	—	—
EM	—	—	—	—	—	—

a) In mPa·s. At 25°C and $126.7 s^{-1}$.

b) 0.3wt% on dry coal

c) No fluidity was observed.

X·2

Table 3. Viscosities[a)] at solid concentration of 70 wt%

X·2

Coal	Additives[b)]					
	NOF-1	NOF-2	NOF-3	NOF-4	NOF-5	NOF-6
BA	497	468	960	1106	—	—
UF	652	682	948	1340	—	—
MI	940	935	1150	—	1675	—
WL	942	896	1210	—	—	—
NE	876	645	2196	—	—	—
ER	2900	2300	3380	—	—	—
WO	885	1147	1400	—	—	—
TR	1420	1517	2980	—	—	—
WM	1210	1420	2420	—	—	—
DA	1760	1790	2150	—	—	—
TA	1700	1720	2450	—	—	—
BL	— c)	—	—	—	—	—
MA	—	—	—	—	—	—
WN	—	—	—	—	—	—
EM	—	—	—	—	—	—

a) In mPa·s. At 25°C and 126.7s^{-1}.

b) 0.3wt% on dry coal

c) No fluidity was observed.

X.2

Table 4 Properties of coals

X-2

Coal	Country	C a) (wt%)	Ash (wt%)	Fuel Ratio (−)	O/C (−)	I.M.b) (wt%)	W.A.c) (wt%)	Contact Angle (deg.)
BA	Australia	88.4	15.3	2.60	0.037	1.17	6.4	
UF	U.S.A.	83.1	11.5	1.83	0.069	1.30	2.7	
MI	Japan	80.2	9.5	1.12	0.094	1.30	4.7	78.1
WL	Australia	69.5	15.6	1.81	0.124	2.07	9.0	
NE	Australia	84.2	12.1	2.23	0.014	2.16	10.4	
ER	South Africa	75.4	13.4	1.75	0.168	2.44	8.5	44.6
WO	Australia	80.4	15.4	1.79	0.118	3.10	9.0	75.1
TR	Australia	79.0	12.4	2.01	0.141	4.10	10.4	
WM	Australia	78.9	6.7	1.77	0.126	4.10	9.6	
DA	China	80.3	6.9	1.94	0.122	4.62	12.2	49.3
TA	Japan	72.5	11.7	0.90	0.203	5.00	10.2	
BL	Australia	76.9	8.0	1.55	0.156	7.70	19.6	28.9
MA	Australia	76.5	14.0	1.00	0.193	7.13	16.6	
WN	Australia	75.8	7.6	0.97	0.218	8.75	17.6	
EM	U.S.A.	60.8	10.5	1.34	0.139	9.04	19.8	

a) Dry ash free basis
b) Inherent Moisture
c) Water Absorption

X.7

TABLE I. ANALYSES OF SLURRY FUELS

X.7

	COM[a]	CWM-A	CWM-B	CWM-C	CWM-D	CWM-E
Proximate Analysis, wt. percent						
Moisture	3.00	29.95	31.46	32.34	30.06	31.01
Ash	3.23	4.64	5.71	1.34	1.46	4.17
Volatile	--	20.54	23.65	26.93	25.43	22.95
Fixed Carbon	--	44.87	39.1	39.38	44.04	41.87
Ultimate Analysis, wt. percent						
Moisture	3.00	29.95	31.46	32.34	30.06	31.01
Carbon	79.86	57.37	51.99	56.21	60.03	56.43
Hydrogen	7.46	3.56	3.58	3.86	3.91	3.64
Nitrogen	1.38	1.09	0.92	1.06	1.13	1.01
Chlorine	0.06[b]	0.05	0.13	0.10	0.10	0.16
Sulfur	1.25	0.53	0.56	0.76	0.67	0.58
Ash	3.23	4.64	5.71	1.35	1.46	4.17
Oxygen	3.82	2.81	5.63	4.30	3.63	3.00
Ash Analysis, wt. percent[c]						
SiO_2	47.30	52.64	58.90	39.49	35.05	47.73
Al_2O_3	31.53	27.14	26.01	26.25	18.32	33.26
TiO_2	1.39	1.40	1.50	1.60	1.41	2.32
Fe_2O_3	8.66	10.04	8.58	20.18	36.47	7.99
CaO	2.70	1.87	1.72	3.92	1.59	3.13
MgO	1.48	1.21	0.84	0.88	0.99	0.86
K_2O	2.28	2.01	2.10	1.25	1.19	1.32
Na_2O	0.83	1.27	0.32	1.19	1.20	0.43
Heating Volume, Btu/lb	16,351	10,203	9,465	10,106	10,820	10,133
Slagging Index	0.25	0.15	0.13	0.46	0.71	0.14
Fouling Index	0.17	0.25	0.05	0.49	0.91	0.06
Free Swelling Index	--	6	3	6.5	8.5	8.0
Fusion Temperature, F						
Oxidizing						
IT	2800+	2420	2635	2300	2070	2700+
ST	2800+	2700+	2700+	2540	2620	2700+
HT	2900+	2700+	2700+	2590	2670	2700+
FT	2800+	2700+	2700+	2700+	2700+	2700+
Reducing						
IT	2660	2270	2592	2250	1910	2700+
ST	2800+	2650	2700+	2400	2150	2700+
HT	2800+	2700	2700+	2440	2200	2700+
FT	2800+	2700+	2700+	2540	2520	2700+

(a) Oil in COM contained 200 ppm vanadium.
(b) Chlorine analysis calculated from coal value (0.14 percent).
(c) Ash analysis for COM is for coal only, not the COM.

TABLE 2. COMBUSTION CONDITIONS AND EMISSIONS FOR SLURRY TESTS

X·7

Fuel	COM[a]	CWM-A	CWM-B	CWM-C	CWM-D	CWM-E
Firing Rate, Btu/hr	624,000	612,000	650,000	698,900	747,000	715,000
Mean Furnace Exit Gas Temperature, F	2150	2150	2140	2070	2070	2030
Flue Gas Conditions,						
O_2, percent	5.3	4.3	4.1	4.8	4.8	4.9
CO_2, percent	12.6	14.8	15.6	14.7	14.9	13.9
Excess Air, percent	32	25	24	29	29	29
Mean Gaseous Emissions, ppm[b]						
CO	34	67	69	245	153	115
SO_2	804	193	511	689	481	487
NO_x	476	501	582	732	620	567
Gaseous Emissions, $lb/10^6$ Btu						
SO_2	0.49	0.45	0.47	0.58	0.53	0.45
NO_x	1.75	--	0.88	1.2	0.89	0.82
Particulate Emissions						
Grains/dscf at 3% O_2	1.0	1.1	0.42	0.47	0.73	1.2
$lb/10^6$ Btu	1.6	1.5	0.54	0.58	0.99	1.5
Carbon Content of Fly Ash, percent	--	23	6	30	37	39

(a) Fired with fuel preheated to 140 F. (b)Corrected to 3 percent O_2.

X·7

X.8

Table 4 X.8

PERFORMANCE OF MAJOR MODIFIED BOILER - OIL FIRING

Percent BMCR	100
Steam Evaporation - lbs/hr	3,548,000
Reheat Steam Flow - lbs/hr	3,139,000
Furnace Exit Gas Temperature - °F	2,110
Excess Air at Economizer Exit - %	15
Temp. of Air Entering Air Heater - °F	122
Temp. of Gas Leaving Air Heater - °F (Uncorr.)	258
Final Superheat Steam Temperature - °F	1,005
Final Reheat Steam Temperature - °F	982
Superheat Steam Pressure - PSIG	2,500
Reheat Outlet Steam Pressure - PSIG	556
Fuel Fired - lbs/hr	248,000
Combustion Air to Furnace - lbs/hr	3,922,600
Total Wet Gas Air Heater Inlet - lbs/hr	4,166,500
Recirculated Gas - lbs/hr	1,000,000
Volumetric Heat Release - Btu/ft^3 hr	21,375
EPRS Heat Release - Btu/ft^2 hr	112,750
Plan Area Heat Release - Btu/ft^2 hr	1,980,000
Burner Zone Heat Release - Btu/ft^2 hr	649,000
Boiler Efficiency - %	90.16
Total Heat to Steam - Btu x 10^6/hr	4105.4
Gross Heat Input - Btu x 10^6/hr	4584.3

Table 5·X·8

PERFORMANCE OF MODIFIED BOILER - COAL-WATER MIXTURE FIRING

Percent BMCR	100
Steam Evaporation - lbs/hr	3,548,000
Reheat Steam Flow - lbs/hr	3,139,000
Furnace Exit Gas Temperature - °F	2,110
Excess Air at Economizer Exit - %	20
Temp. of Air Entering Air Heater - °F	80
Temp. of Gas Leaving Air Heater - °F (Uncorr.)	241
Final Superheat Steam Temperature - °F	1,005
Final Reheat Steam Temperature - °F	1,005
Superheat Steam Pressure - PSIG	2,500
Reheat Outlet Steam Pressure - PSIG	556
Fuel Fired - lbs/hr	473,310
Combustion Air to Furnace - lbs/hr	4,239,900
Total Wet Gas Air Heater Inlet - lbs/hr	4,713,200
Recirculated Gas - lbs/hr	268,200
Volumetric Heat Release - Btu/ft^3 hr	22,235
EPRS Heat Release - Btu/ft^2 hr	112,080
Plan Area Heat Release - Btu/ft^2 hr	1,968,340
Burner Zone Heat Release - Btu/ft^2 hr	645,100
Boiler Efficiency - %	87.12
Total Heat to Steam - Btu x 10^6/hr	4146
Gross Heat Input - Btu x 10^6/hr	4763

X·12

Table 6 • X·12

CAPTAL COST ESTIMATES
(NOMINAL 518 MW)

Item	Description	Conversion to Pulv. Coal	Conversion to CWM	New Coal Fired Boiler
1	Fuel Receiving and Handling	19,769,000	6,858,000	21,646,000
2	Steam Generator and Auxiliaries	36,000,000	27,000,000	80,960,000
3	High Pressure Piping System	-	-	2,161,000
4	Ash Handling and Storage	3,736,000	3,736,000	4,380,000
5	Particulate Controls	13,500,000	13,500,000	15,320,000
6	Flue Gas Desulfurization System	-	-	77,200,000
7	Chimney	-	-	4,500,000
8	Electrical	1,187,000	1,014,000	2,400,000
9	Civil/Structural	6,562,000	2,934,000	12,382,000
10	Instruments and Controls	960,000	1,002,000	3,675,000
11	Misc. Plant Systems	750,000	750,000	1,000,000
12	SUBTOTAL DIRECT COSTS	82,500,000	56,800,000	225,700,000
13	Engineering, Construction Management and Owner's Costs	16,500,000	11,400,000	45,100,000
14	Contingency	14,900,000	10,200,000	40,600,000
15	TOTAL PLANT COST	113,900,000	78,400,000	311,400,000
16	Escalation	24,200,000	16,600,000	96,200,000
17	Interest During Construction	25,600,000	17,600,000	133,700,000
18	TOTAL PLANT INVESTMENT	163,700,000	112,600,000	541,300,000

Table 1 X-17

Rheological Properties - Viscometer Measurement

Sample	n	Viscosity @ 100 s^{-1} (mPa·s)	Time Dependence
A - 1	1.21	2910	moderately thixotropic
A - 2	0.91	1210	moderately thixotropic
B - 1	1.28	1760	slightly thixotropic
B - 2	1.00	2550	negligible
B - 3	0.88	2260	negligible
C - 1	0.93	1420	negligible
C - 2	0.97	1470	negligible
D - 1	0.79	1320	moderately rheopectic
D - 2	1.12	1070	moderately rheopectic
D - 3	1.28	1350	moderately rheopectic
D - 4	1.18	1890	moderately rheopectic

X.16

Slurry number	Total moisture [wt %]	Density [g/cm³]	VISCOSITY [Pas]									
			ACCELERATED					DECELERATED				
			32.3	100	200	300	450	32.3	100	200	300	450
1	32.3	1.208	0.074	0.067	0.063	0.057	0.051	0.057	0.044	0.044	0.046	0.051
2	30.2	1.213	0.099	0.084	0.081	0.076	0.068	0.067	0.058	0.059	0.062	0.068
3	28.2	1.219	0.145	0.137	0.124	0.111	0.101	0.099	0.083	0.086	0.091	0.101
4	25.2	1.231	0.290	0.274	0.245	0.217	0.202	0.177	0.157	0.167	0.180	0.202
5	22.4	1.240	0.593	0.593	0.507	0.440	0.399	0.311	0.310	0.319	0.347	0.399
6	19.4	1.254	1.58	1.64	1.43	1.19	1.05	0.749	0.739	0.819	0.904	1.05
7	16.7	1.264	4.87	5.39	4.78	n.a.	n.a.	2.90	2.77	2.88	n.a.	n.a.

Table 1. X-16

Viscosity at various shear rates, density and moisture content of the master batch and slurries diluted therefrom.
Note: shear rates given in reciprocal seconds.

Slurry number	Total moisture [wt %]	Density [g/cm³]	VISCOSITY [Pas]										Stabilizer [wt %]	Dispersant
			ACCELERATED					DECELERATED						
			32.3	100	200	300	450	32.3	100	200	300	450		
8	32.2	1.203	0.219	0.171	0.143	0.126	0.108	0.117	0.104	0.098	0.099	0.108	0.040	A
9	32.2	1.215	1.41	0.82	0.59	0.48	0.37	1.13	0.62	0.46	0.40	0.37	0.250	A
10	31.9	1.217	1.53	1.05	0.74	0.56	0.45	0.73	0.55	0.46	0.45	0.45	0.060	B

Table 2. X.16

Viscosity, density and moisture content of slurries containing stabilizer.

Table 3. X.16

Viscosity of slurries numbers 1 to 7 measured at constant shear rates for a period of 60 minutes.

Slurry number	Total moisture [wt %]	Shear rate [s⁻¹]	VISCOSITY [Pas] Initial	Lowest	Final	OBSERVATIONS
1	32.3	31	0.08	0.04	0.04	Thixotropy dominates
2	30.2	31	0.12	0.09	0.09	" "
3	28.2	31	0.15	0.11	0.11	" "
4	25.2	31	0.29	0.19	0.19	" "
5	22.4	31	0.64	0.37	0.37	" "
6	19.4	31	1.63	0.95	0.95	" "
7	16.7	31	4.70	2.94	2.94	" "
1	32.3	450	0.10	0.04	0.04	Thixotropic for 20 min
2	30.2	450	0.13	0.07	0.07	" " "
3	28.2	450	0.17	0.09	0.09	" " "
4	25.2	450	0.40	0.17	0.17	Thixotropic for 18 min
5	22.4	450	0.77	0.36	0.37	Faintly rheopectic after 30 min
6	19.4	450	2.25	1.01	1.10	Rheopectic after 16 min
7	16.7	450	n.a.	n.a.	n.a.	

3.5

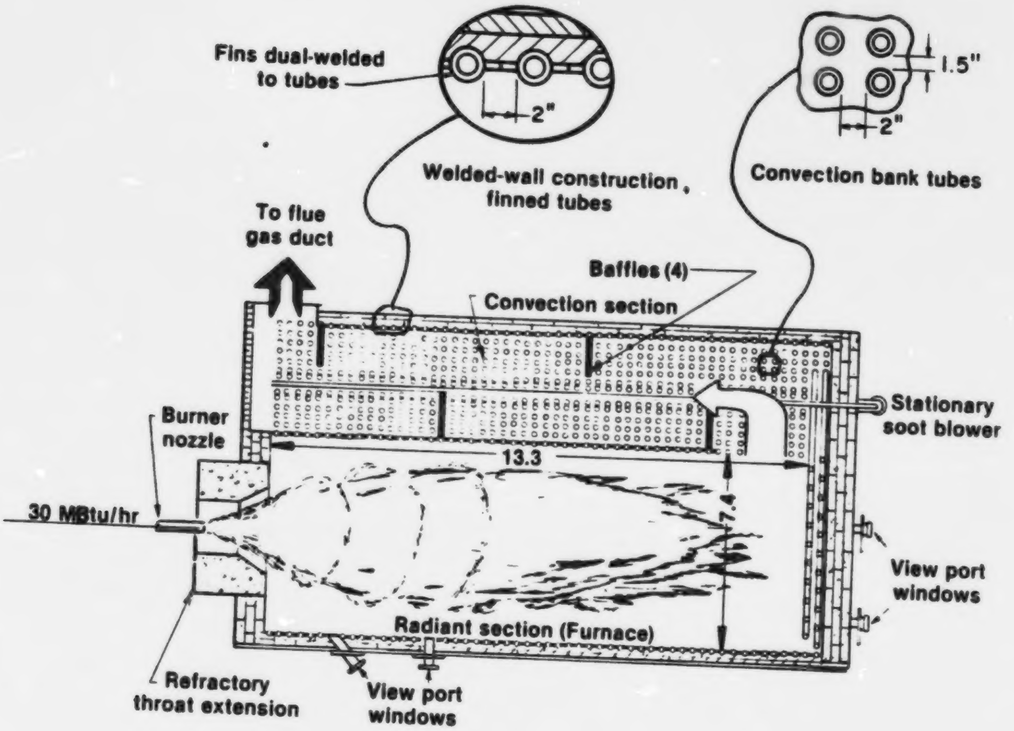
Fins dual-welded to tubes
2"
Welded-wall construction, finned tubes
1.5"
2"
Convection bank tubes
To flue gas duct
Baffles (4)
Convection section
Stationary soot blower
Burner nozzle
13.3
7.4
30 MBtu/hr
View port windows
Radiant section (Furnace)
Refractory throat extension
View port windows

Figure 2. Horizontal Cross-Sectional View of 700-hp Watertube Boiler

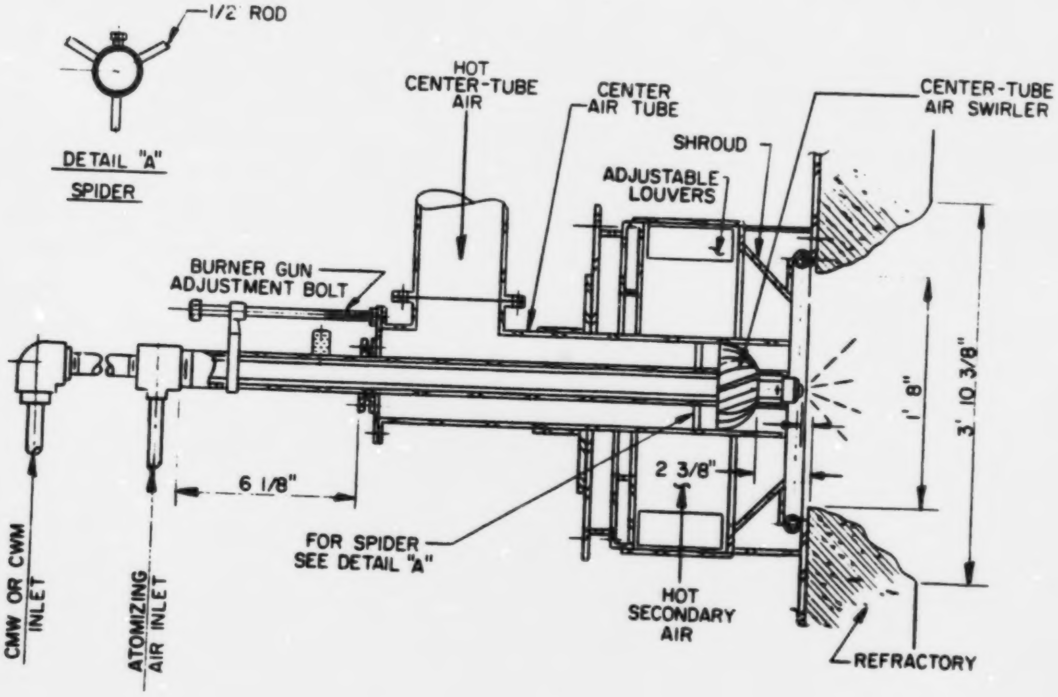
1/2 ROD
DETAIL "A"
SPIDER
HOT CENTER-TUBE AIR
CENTER AIR TUBE
CENTER-TUBE AIR SWIRLER
SHROUD
ADJUSTABLE LOUVERS
BURNER GUN ADJUSTMENT BOLT
1' 8"
3' 10 3/8"
2 3/8"
6 1/8"
FOR SPIDER SEE DETAIL "A"
HOT SECONDARY AIR
CMW OR CWM INLET
ATOMIZING AIR INLET
REFRACTORY

Figure 3. Coal-Methanol-Water Mixture Burner

4.5

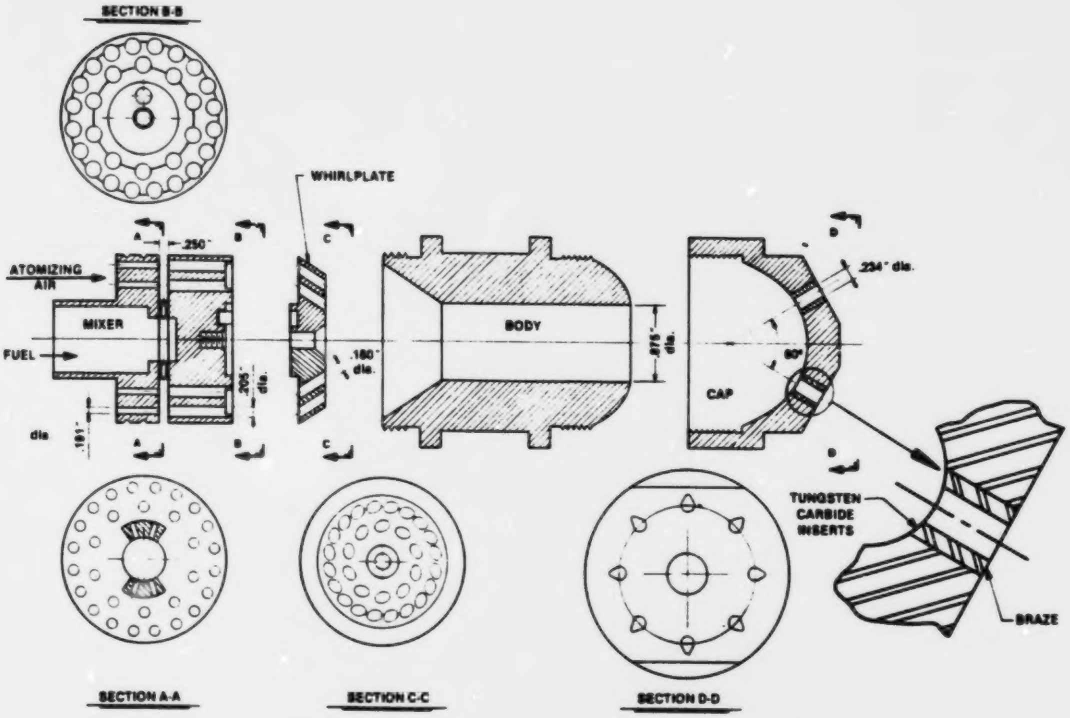
SECTION B-B
WHIRLPLATE
A
.250"
B
C
D
ATOMIZING AIR
MIXER
FUEL
.191" dia
.205" dia.
.160" dia.
BODY
.875" dia.
.234" dia.
90°
CAP
TUNGSTEN CARBIDE INSERTS
BRAZE
SECTION A-A
SECTION C-C
SECTION D-D

.5

Figure 4. Coal-Methanol-Water Mixture Burner Atomizer Assembly

5·5

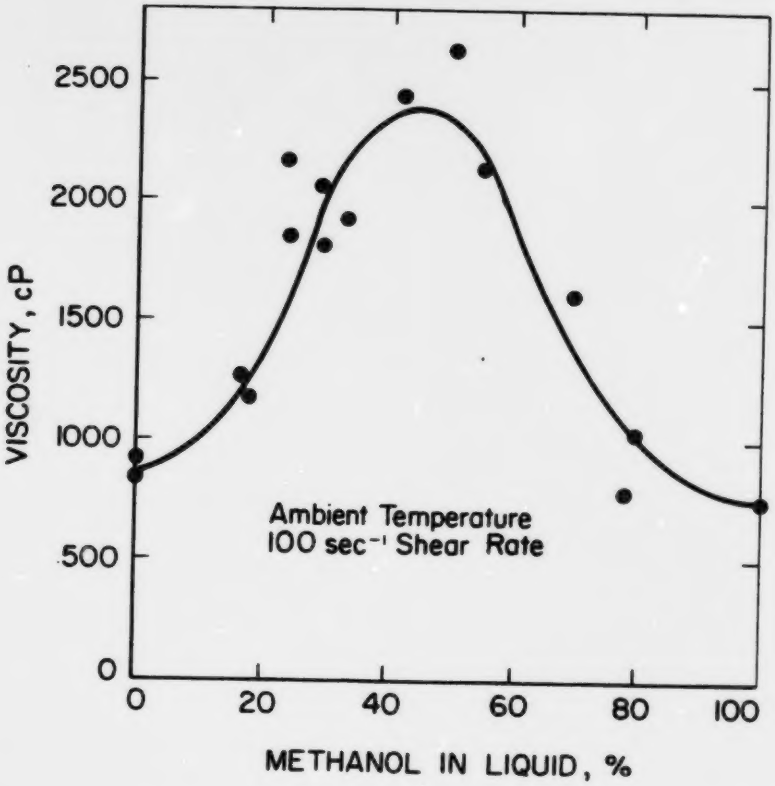

15

Figure 5. **Viscosity of hvCb CMW Mixtures (51% Coal) as a Function of Methanol Concentration in the Liquid Phase**

6.5

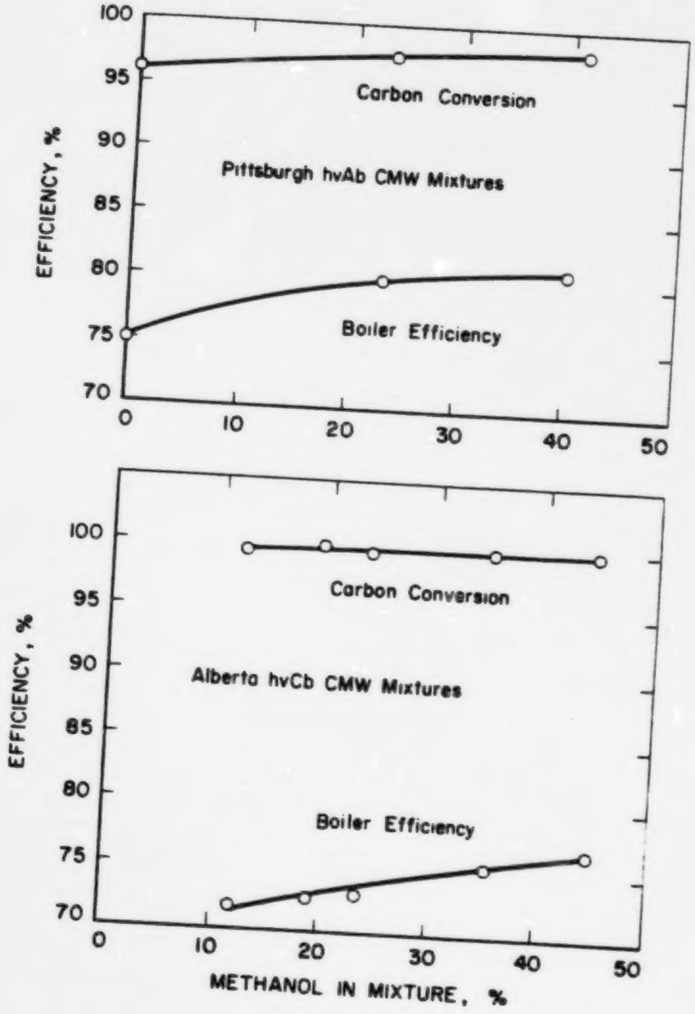

.5

Figure 6. Variation of Carbon Conversion and Boiler Efficiencies with Methanol Content in hvAb and hvCb CMW Mixtures (Full Load, 500°F Combustion Air)

8.5.

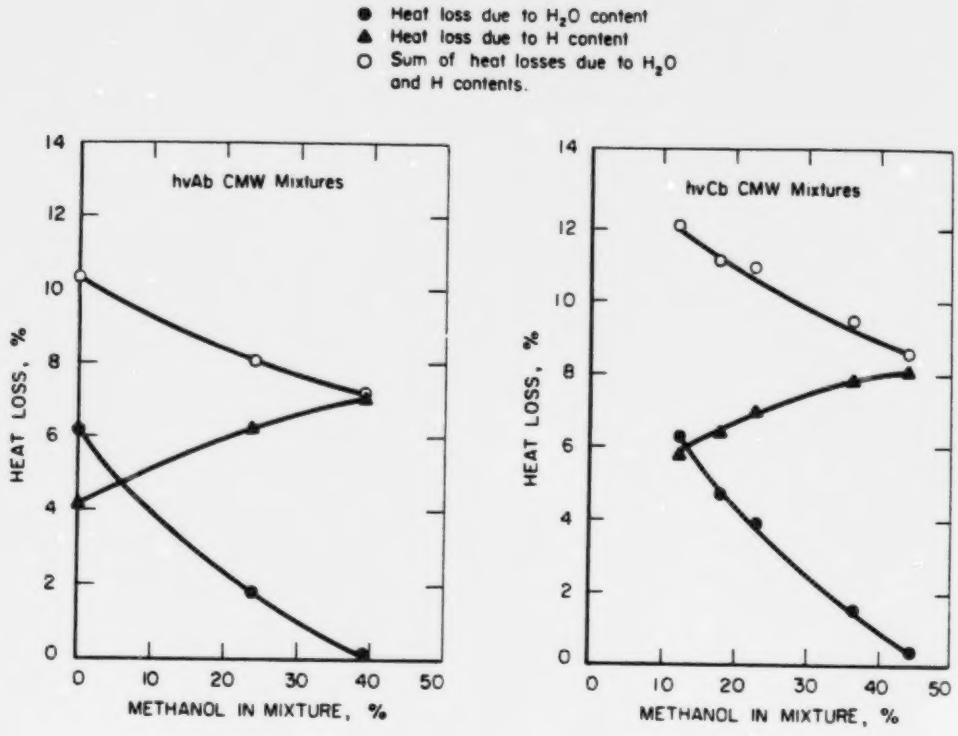

Figure 7. Heat Losses Due to Water and Hydrogen Contents in Fuel (Full Load, 500°F Combustion Air).

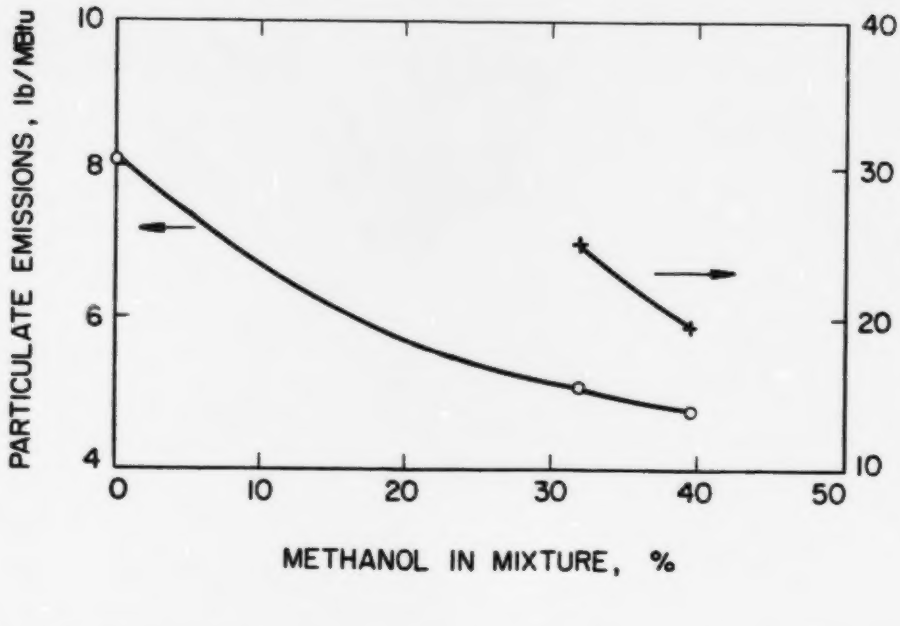

Figure 8. Effect of Methanol Content on Particulate Emissions — hvAb CMW Mixtures (Full Load, 500°F Combustion Air)

2·W·i

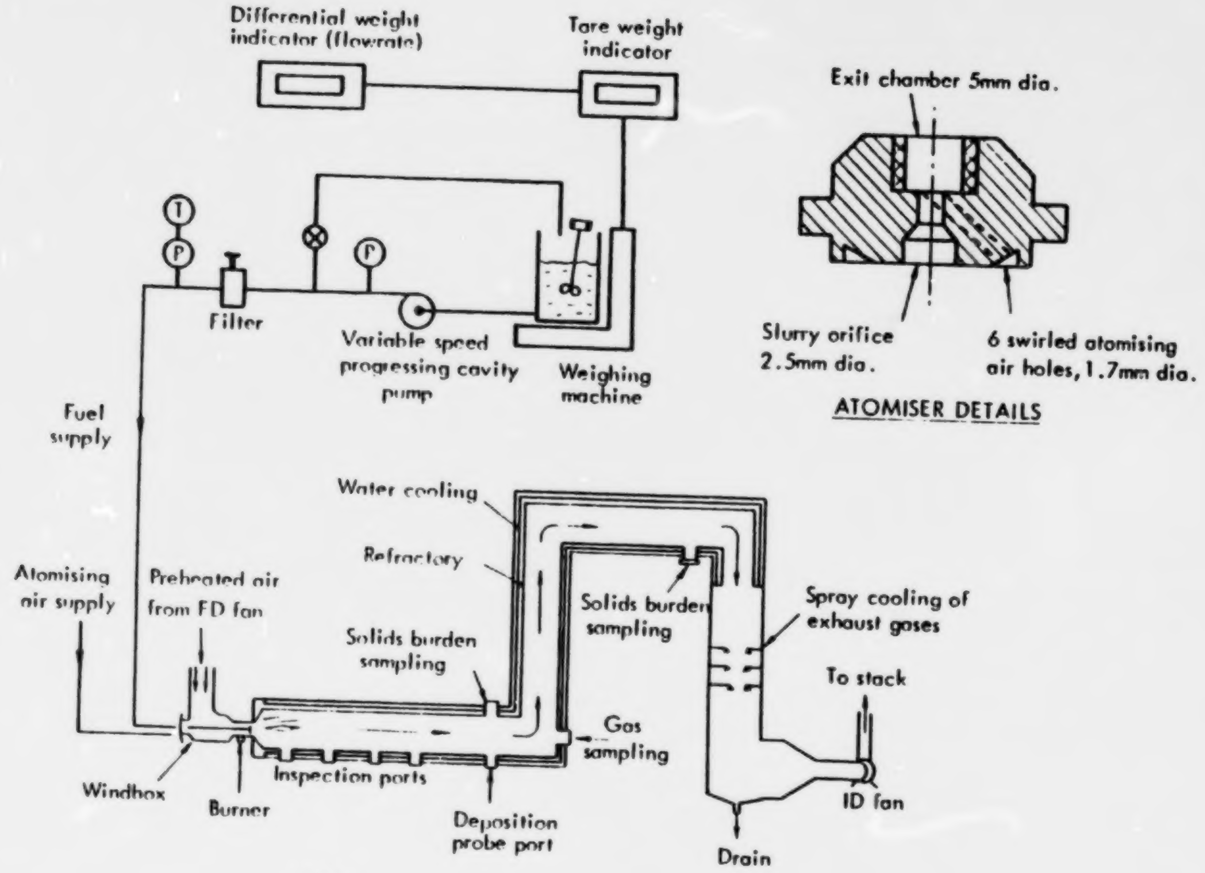
Differential weight indicator (flowrate)
Tare weight indicator
Exit chamber 5mm dia.
T
P
P
Filter
Variable speed progressing cavity pump
Weighing machine
Slurry orifice 2.5mm dia.
6 swirled atomising air holes, 1.7mm dia.
ATOMISER DETAILS
Fuel supply
Water cooling
Refractory
Atomising air supply
Preheated air from FD fan
Solids burden sampling
Solids burden sampling
Spray cooling of exhaust gases
To stack
Gas sampling
Windbox
Burner
Inspection ports
Deposition probe port
ID fan
Drain

·W·I

FIGURE 2. 0.5 MW$_t$ COMBUSTION FACILITY

In the present work, the CWS was pumped from a stirred storage drum by a single-stage,progressing-cavity pump which was capable of producing 10 bar pressure. The drum and its contents stood on a sensitive weighing machine so that a digital output of the rate of change of weight could be monitored as the fuel flowrate. A spill return system was provided, but the main flowrate control was by varying the pump speed. The loop was provided with a number of water purge access points and the fuel was fed to the burner through a 40 mesh (419 µm) filter.

The combustion air supply was preheated to either 300 or 400°C for these experiments. The burner incorporated a 10-bladed,swirl-type stabilizer and the atomiser tip was a single-hole, internal-mix, air blast design similar to that used by Babcock & Wilcox in their early CWS firing experiments (Farthing et al,1982). Initial rapid wearing problems were cured by using a recrystallised alumina insert to form the mixing chamber. The relevant dimensions are given in Figure 2.

Particulates were sampled from the combustion stream at two locations. The first, after about 0.8 seconds mean residence time, was at the end of the horizontal section of the combustion duct where the flame gases had cooled to roughly furnace exit temperature levels (1100–1300°C). The probe used here was oil-cooled to keep the sample gas above its dewpoint and the collecting cyclone and back-up micropore filter were located in an oven kept at 180°C for the same reason.

The second sampling position was after about 2.5 seconds mean residence time,at which point flame gases were generally between 600 and 750°C. The probe used here was uncooled, but lagged to keep the gases above the dewpoint as they passed to a similar collecting system as before.

Solids samples were sieved to determine their particle size distributions. Observations on particle morphology were then made by examining the exterior surfaces of the particles with transmitted and oblique lighting and by mounting them in resin, sectioning and polishing them and examining their interiors by

3. W. 1

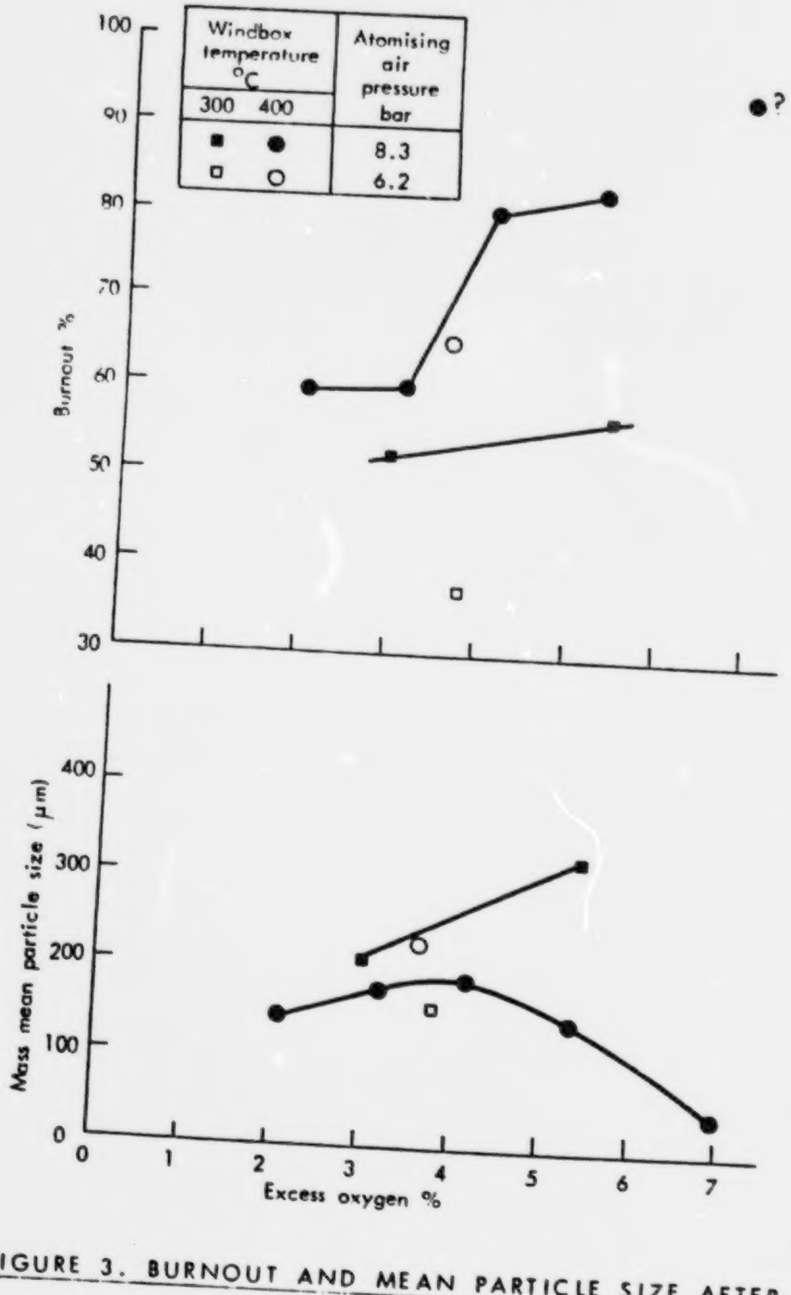

FIGURE 3. BURNOUT AND MEAN PARTICLE SIZE AFTER 0.85 SECONDS - SLURRY B

4.W.1

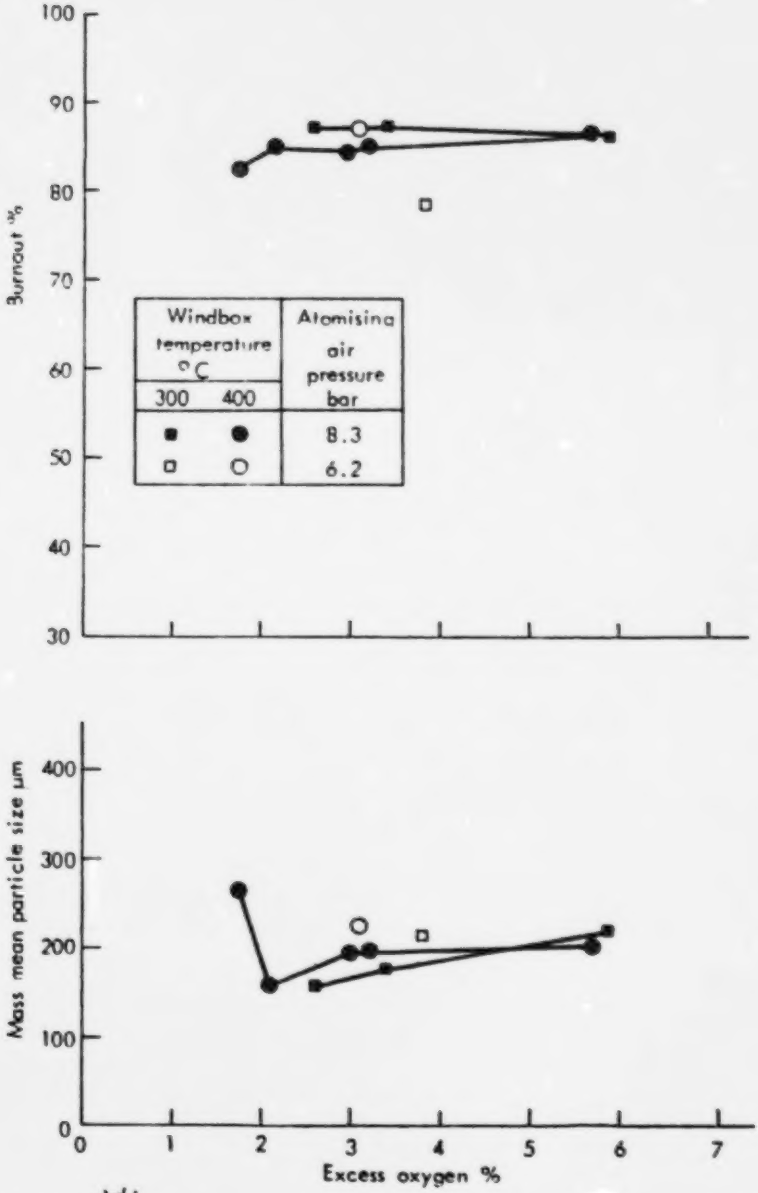

·W·1

FIGURE 4. BURNOUT AND MEAN PARTICLE SIZE AFTER 2.5 SECONDS - SLURRY B

5·W1

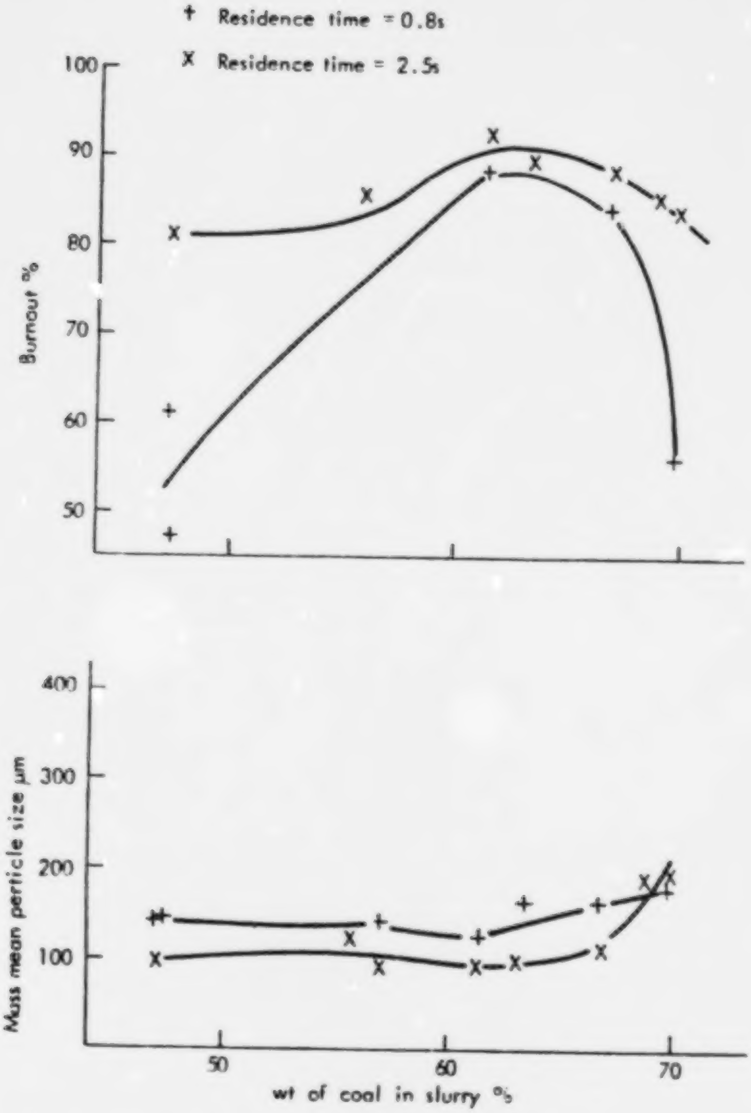

Windbox temp. = 400 $^{+23}_{-0}$ °C

Atomising air pressure = 8.3 bar

Excess oxygen = 3.2 ± 0.2 %

·W1

FIGURE 5. EFFECT OF COAL LOADING ON BURNOUT AND MEAN PARTICLE SIZE - SLURRY B

6. W. 1

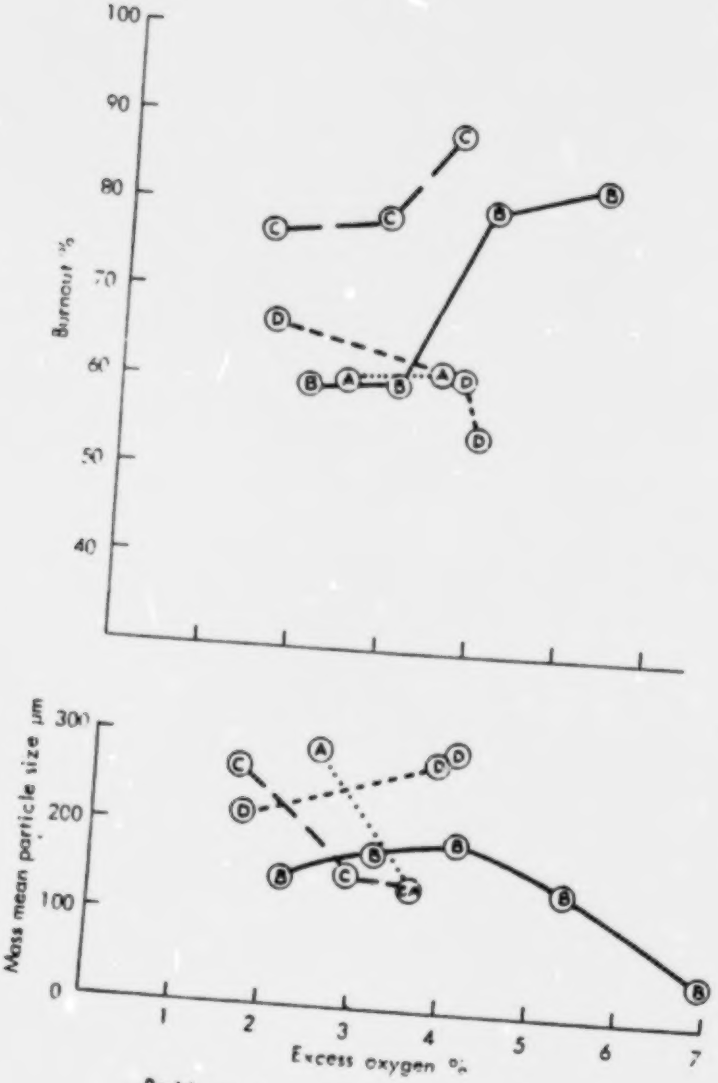

Residence time = 0.8s
Windbox temp = 400°C
Atomising air pressure = 8.3 bar

·W·1

FIGURE 6. EFFECT OF SLURRY COMPOSITION ON BURNOUT AND MEAN PARTICLE SIZE

7·W·1

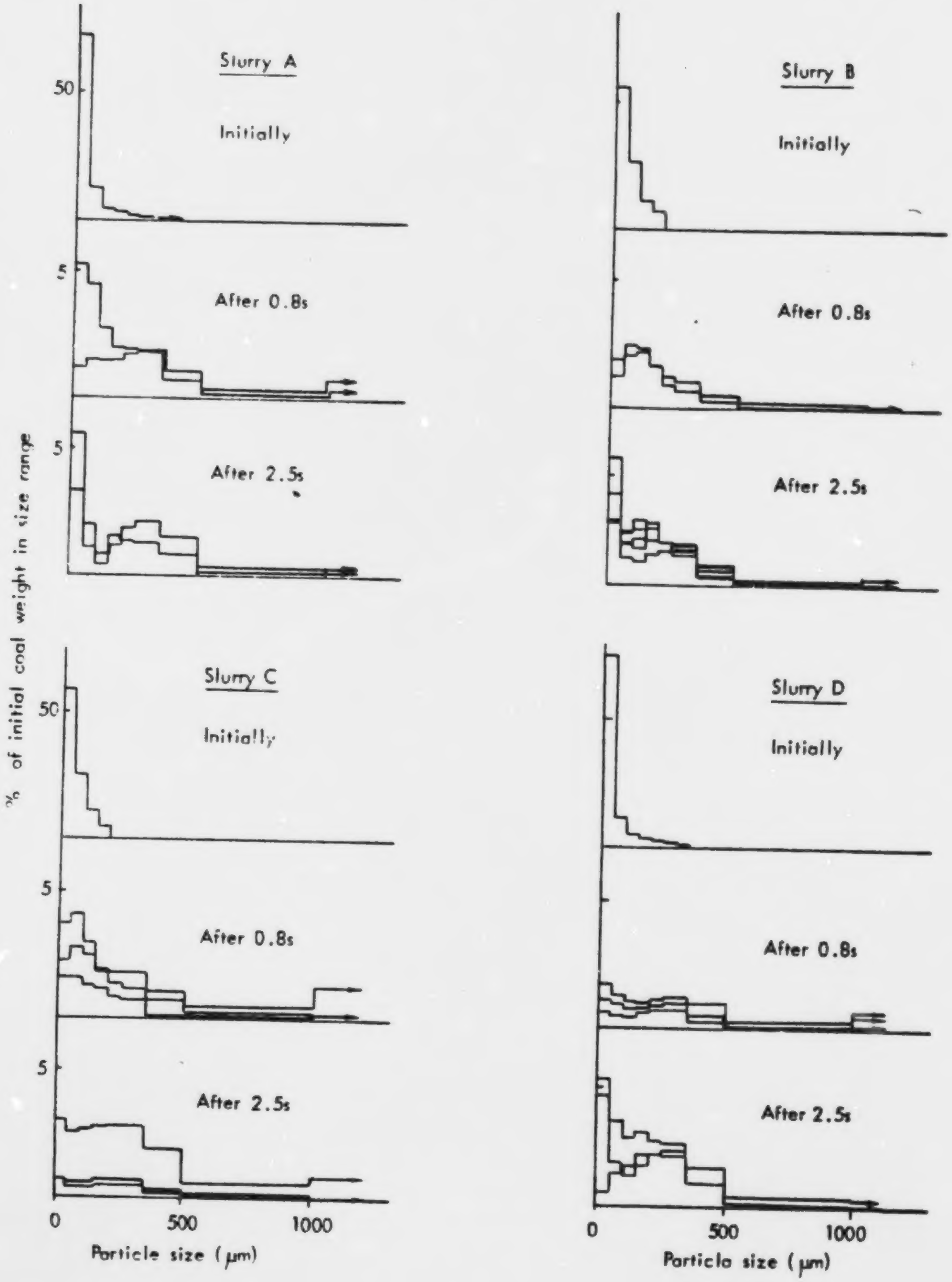

. W·1

FIGURE 7. PARTICLE SIZE VARIATION WITH TIME

9. W.1

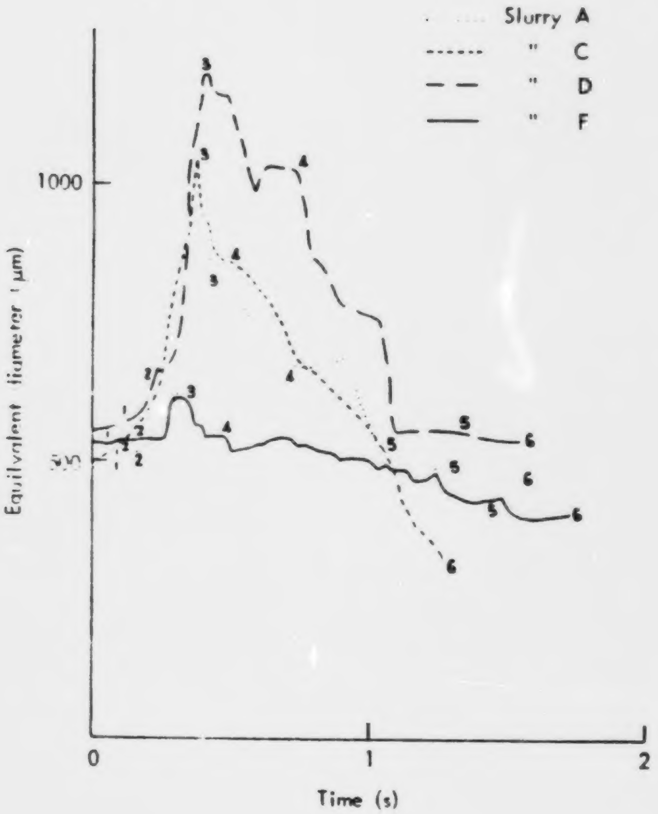

Code
1. Initial volatile release starts
2. Vigorous volatile release starts
3. Volatile release ends
4. First fragment leaves
5. Support fibre visible
6. Oxidation ends

W:1

FIGURE 9. TYPICAL DROP HISTORIES

1·W·3

3

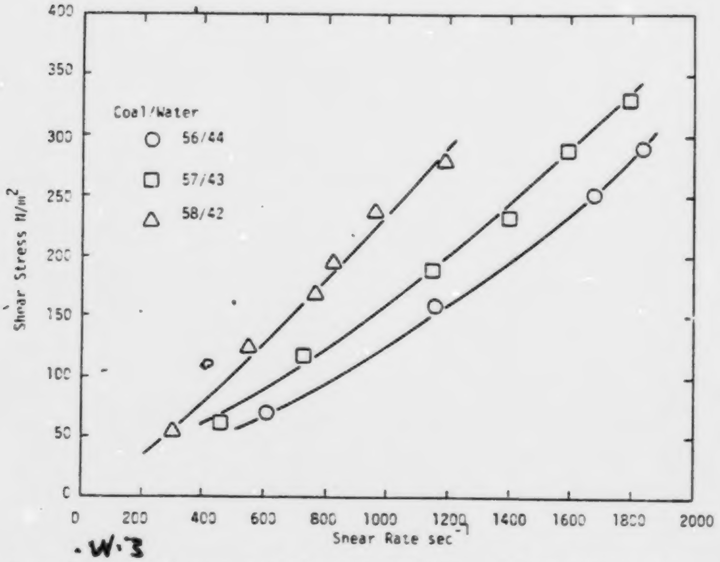

.W.3

Figure 1. Utah coal-water rheogram with no additives. Inherent moisture before pulverization was 2.4 mass %.

CWM Combustor Facility

The CWM reactor is a vertical cylindrical combustor, 2.2 meters long, with slurry and combustion air inlet ports at the top of the reactor (3,6). This configuration eliminates asymmetric buoyancy effects due to particle settling and natural convection, and provides a well defined format for utilizing combustion data in model validation and code evaluations. The reactor was designed and constructed to simulate selected industrial operating conditions in order to provide meaningful results for the computer model.

Reactor Description

The reactor, shown in Figure 2, is designed for combustion profile mapping of coal burnout and pollutant formation from space-resolved measurements within the reactor. Cooling water jackets are attached for wall temperature control under steady-state conditions. Slotted windows are located along the full reactor height for sampling probe and optical access to the combustion chamber. An induced draft fan with a controlled bypass enables slightly sub-atmospheric pressure testing to simulate industrial conditions and to allow removal of the sampling probe and replacement at a different location during tests without interrupting the combustion process.

Combustion air is supplied by a high pressure storage facility located outside the reactor building. The secondary air flow is throttled with an automatic control valve and the rate is measured by a Micro-Motion mass flow transducer. It passes through a Chromalox 75 KW electric heater prior to entering the swirl block plenum on top of the reactor. Atomizing air is supplied by the low pressure building supply with a separate control valve and electric heater, and is measured with a rotameter. Methane is used for reactor preheating, and ignition is achieved using a spark-ignited hydrogen/air jet. The methane flow is measured with a rotameter and enters the reactor through a circumferential burner surrounding the quarl section, to which the swirl block and nozzle are attached. 1)

Coal slurry feed is achieved using a Moyno progressing nine cavity positive displacement pump. The pump is driven hydraulically with capability for infinitely variable speed. A simple low pressure external atomizer, shown in Figure 3, was used for all combustion tests. Feed rate is measured at steady-state using an elapsed timer and an electronic weight scale, with pump speed-slurry flow correlation used as a redundant indicator. Slurry quantities sufficient for combustion tests of several hours duration are contained in a small holding tank on the scale. Typical tests consume about 13 kg coal per hour (18 kg/hr CWM).

High coal burnout values can be achieved by good atomization and mixing as well as sufficient residence time in the combustor, which is related to reactor volume and configuration. A relatively large inside diameter potentially mitigates wall effects such as heat transfer and flow interference in the combustor. Since heat losses also increase with diameter, it is necessary that the diameter not be too large, which is especially important when burning fuels with reduced heating value such as CWM. A detailed description of the analytical design of the test facility is presented in a graduate thesis on the subject (6), and a more general description is given in the proceedings of the Fifth International Symposium on Coal Slurry Combustion and Technology (2).

1) [illegible] [illegible] [illegible] igniter

7·W·3

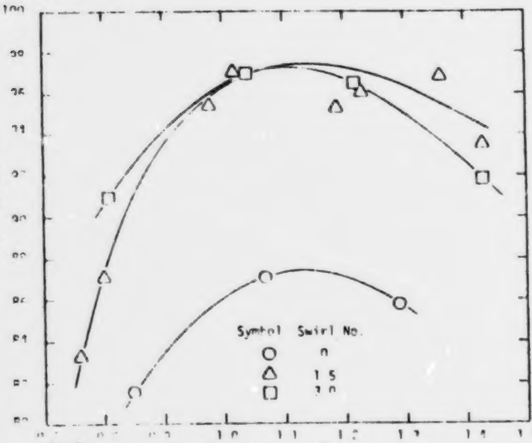

W 3

Figure 7 Effect of swirl number and stoichiometric ratio on burnout of coal [illegible]

The maximum coal burnout was nearly 98% (daf) at a stoichiometric ratio of about 1.15 and a swirl number of 1.5. However, at this swirl number, and within a range in stoichimetric ratio of 1.0 to 1.3, the coal burnout varied by only 1% from its maximum value.

Very low particle residence times in the rector (less than 100 msec) were computed based on slurry and atomizing air flow rates and nozzle orifice diameter. Assuming entrainment in the atomizing air with negligible slip, particle velocities exiting the nozzle approached sonic conditions, with an average velocity in the reactor of about 25-30 m/sec. The slurry momentum was nearly twice that of the secondary air which, when coupled with the slurry spray angle, produced high particle penetration and mixing rates in the secondary air.

Reactor Mapping Tests

Values for SR of 1.28 and SN of 1.5, based on the results of the parametric tests, were selected for a detailed profile map. Char and gas samples were collected from five equally spaced radial locations at each of nine axial reactor positions ranging from 17.8 cm to 207.8 cm from the nozzle tip. After samples were taken from all nine axial positions, two positions (57.8 and 207.8 cm) were repeated to determine reproducibility of the test data. During all tests, the atomizing air was fixed at 21.3 kg/hr, slurry feed rate was maintained at 18.1 kg/hr and the nozzle was located at a fixed depth in the quarl section. To prevent any outside air leakage into the reactor, the reactor pressure was controlled to about 124 Pa (gauge).

Burnout and Temperature

The coal burnout values shown as iso-contours in Figure 8 based on ash analysis, indicate that burnout progressed rapidly as the particles initially moved down the reactor. The shape of the contour lines at the top of the reactor suggests a small recirculation region up near the nozzle section. For locations near the reactor centerline, coal burnout increased from less than 15% at an axial position of 27.8 cm to over 90% at an axial position of 77.8 cm, an increase of over 75% burnout in just 50 cm. Also, 90% of the combustible material in the coal had reacted in the first 40% of the reactor. Most of the particle reaction took place within the first 70 to 80 cm. Beyond this point the rate at which heat was released from the reacting coal particles was presumably less than the rate at which the water in the water jackets removed heat from the combustion chamber, resulting in lower apparent interior reactor temperatures, shown in Figure 9. The heat loss to the cool reactor walls, coupled with the drop in gas temperature, likely impedes further coal burnout of the particles in the aft-sections of the reactor. Low particle residence times also reduced the total average burnout in spite of the vigorous mixing which occurred. Previous tests (2) with lower feed rates and longer residence times produced nearly 100% burnout with the same reactor configuration and volume as for the tests reported here.

9·W·4

5.1.3 Axial Position of the Flame Front; Effects of Atomizer Spray Quality/Geometry, Combustion Air Swirl and Oxygen Enrichment

The axial position of the flame front (relative to the burner) as influenced by combustion air swirl, atomizer spray geometry/quality, and oxygen enrichment was found to be a key factor affecting the emission of NO_x from CWS flames. A change in the position of the flame front away from the burner by ~ 1 1/2 nozzle diameters, as a consequence of slight variations in atomizer dimensions, resulted in an increase in NO_x emission by as much as 100 ppm from ~500 ppm to ~600 ppm (@ 3% O_2) for flames (see photographs, Fig 9) obtained with the OR-standard grind slurry. Strongly lifted relatively unstable low swirl CWS flames yielded NO_x emissions approaching twice the value of the stable high swirl cases. An example of the effect of swirl on NO_x emissions from CWS flames with O_2 enrichment is shown in Fig. 10. Photographs of several of these flames taken at successively lower swirl numbers are shown in Fig. 11; as the flame front recedes from the burner the NO_x emission increases. CWS flames without O_2 enrichment show practically an identical trend.

(a) OR-KVB Atomizer No. 1, NO_x Emission ~517 ppm @ 3% O_2

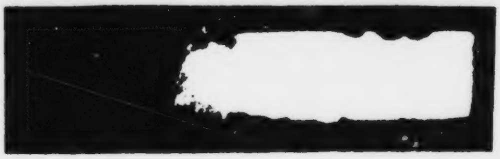

(b) OR-KVB Atomizer No. 2, NO_x Emission ~625 ppm @ 3% O_2

·W·4

Figure 9. Photographs of CWS Flames Showing the Effect of Slight Variations in the OR-KVB Atomizer Internal Dimensions on the Position of the Flame Front with Corresponding NO_x Emission. (Run 306 Flame Conditions)

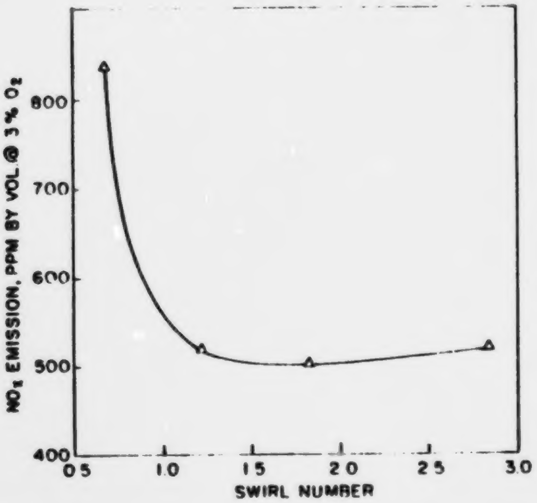

Figure 10 (left). Effect of Combustion Air Swirl on NO_x Emission from CWS Flames (Run 310a, OR-Standard Grind CWS with O_2 Injection, Equivalent O_2 Concentration of Combustion Air ~ 23%).

11.W.4

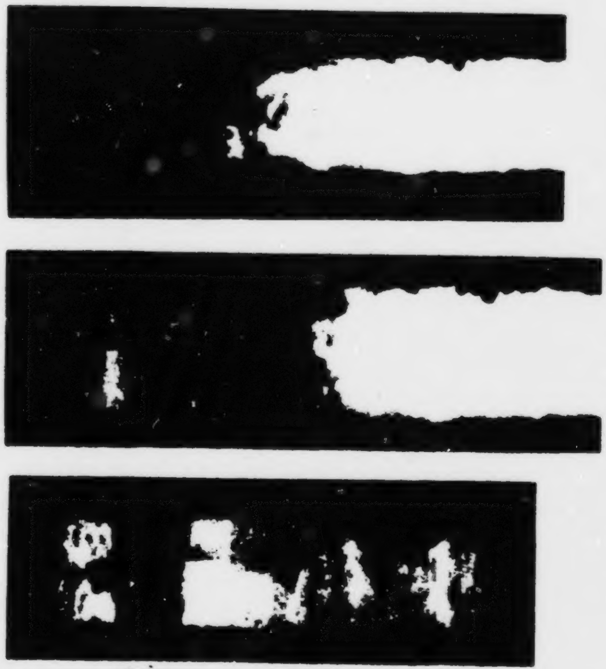

(a) S = 1.8, Main Flame Front 0.20 - 0.25 m from Burner Front Wall, NO_x Emission 504 ppm @ 3% O_2

(b) S = 1.2 , Main Flame Front ~ 0.5 - 0.55 m, NO_x ~ 522 ppm @ 3% O_2

(c) S = 0.68, Except for Few Flamelets the Main Flame Front Has Essentially Blown-off, NO_x ~ 837 ppm @ 3% O_2

W.4

Figure 11. Photographs of CWS Flames Showing the Effect of Combustion Air Swirl on the Axial Position of the Flame Front with Corresponding NO_x Emission (Run 310a OR Unimodal Standard Grind CWS, with O_2 Injection, Equivalent O_2 Concentration of Combustion air ~ 23%):

Figure 12 shows NO_x emissions for a number of oxygen-enriched flames (Run 310a) obtained with OR standard grind slurry. The overall excess O_2 was maintained at 2% and the degree of oxygen enrichment was varied from an equivalent concentration in the combustion air of 21 to 24%. (The O_2 was injected through a separate set of 4 nozzles arranged around the slurry spray nozzle). Surprisingly, practically no adverse impact on NO_x emission was observed with increasing O_2 enrichment, in spite of increases in flame temperature (Fig 13). The result is possibly a consequence of slightly earlier ignition in the O_2-enriched flames. In Fig. 14 axial temperature, O_2, CO_2, CO and NO_x profiles for two flames obtained with the OR fine slurry are shown with (Run 310b) and without (Run 309) O_2 enrichment. In the case of the OR-fine slurry, O_2 enrichment had a significant effect on the position of the flame front, which moved from a position of ~ 0.20 - 0.25 m from the burner directly onto the burner tip (Fig. 15). It is also evident from the NO_x profiles that there was a significant reduction in the emission of this species as the flame front moves in towards the nozzle, again, inspite of increases in local flame temperature (Fig. 14).

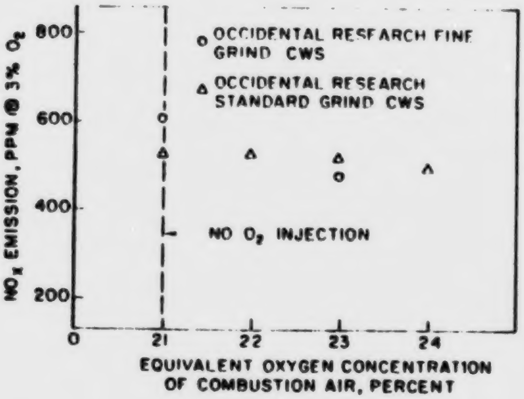

Figure 12. Effect of Oxygen Injection on NO_x Emission from CWS Flames (Run 310)

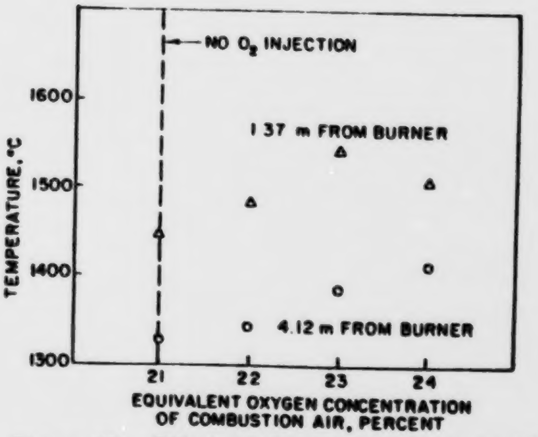

Figure 13. Effect of Oxygen Enrichment on CWS Flame Temperature (Run 310a)

15·WA

W-A

Figure 15 (left). Photograph of the Run 310b OR Fine Grind CWS Flame with O_2 Injection.

The flame front was stabilized at the burner tip with the NO_x emission level at 478 ppm @ 3% O_2. In contrast, the main front for the Run 309 flame was stabilized at 0.20 - 0.25 m from the burner with the NO_x emission at ~ 610 ppm.

The reason why lifted flames result in higher NO_x emission is not fully understood. It is thought that as the flame becomes lifted there is more premixing of oxidant and fuel before ignition. It is likely that under such conditions the fuel nitrogen conversion pathway to NO is much more strongly favored over that to N_2. In cases where the flame front has moved towards the burner the fuel-air mixing is somewhat more delayed, probably having an effect similar to staging on both thermal and fuel-derived NO_x. Similar behavior has also been observed in natural gas and liquid fuel flames at the CRF.

5.2 Effects of Major Input Variables on Carbon Burnout

Axial profiles of total solids concentrations along with the carbon content of the solids are shown in Figures 16 to 19 for several CWS flames (Runs 306, 308 309, and 310b). Towards the experimental furnace exit (3.2 - 4.2 m from the burner) the carbon burnout for all the flames is excellent; based upon the fly ash concentration values and their carbon content, better than 99.5% of the slurry combustibles are calculated as being consumed. At ~2 m from the burner (which corresponds to an average gas residence time of ~2 s) carbon losses as a fraction of the total input are in most instances still in the neighborhood of ~1%.

It should be pointed out, however, that a large fraction of the ash (in the fuel) injected into the combustion chamber drops out of the gas stream (typically of the order of 60 - 70% by the combustion chamber exit); it is likely that this bottom ash initially has a significant carbon content, probably greater than that of the fly ash. Since the CRF furnace walls are in large part refractory lined to maintain thermal similarity with full scale furnaces, much if not most of the carbon contained in the bottom ash is burned on the furnace floor, resulting in unusually high estimates of carbon conversion efficiency. Making a calculation in which the same carbon content is attributed to the bottom ash as the fly ash, values for carbon losses are typically trebled. For example, in the case of Run 309 carbon losses, as estimated from the fly ash alone at 2 m from the burner, are on the order of 1.3%; this value becomes 4.2% if a carbon content similar to the fly ash is assigned to the bottom ash. The higher value for carbon losses is considered to be more realistic. In fact the losses estimated in this manner are still likely to have been under-estimated since the bottom ash carbon content can usually be expected to be higher than that of the fly ash.

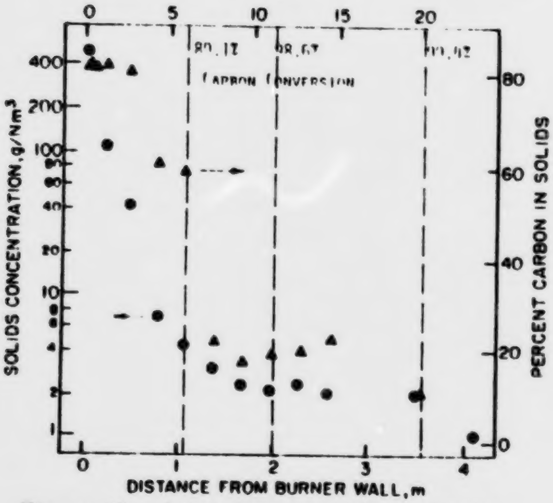

Figure 16. Axial Centerline Total Solids Concentration and Carbon Burnout Profiles; Run 306, OR Unimodal Standard Grind CWS, Unstaged Flame

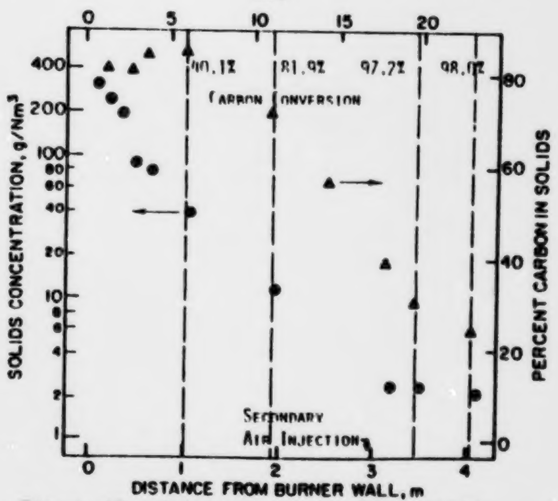

Figure 17. Axial Centerline Total Solids Concentration and Carbon Burnout Profiles, Run 308, OR Unimodal Standard Grind CWS, Staged Flame

22·W·4

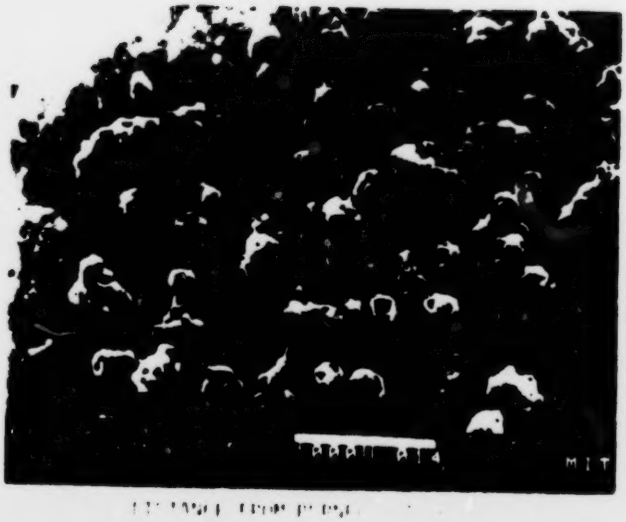
1000U 014
MIT
DISTANCE FROM BURNER

Figure 20. SEM View of Irregularly Shaped Char Particles Captured in CWS Flame the Run 97 (Note Length Scale Shown in Figure for 1000 μm).

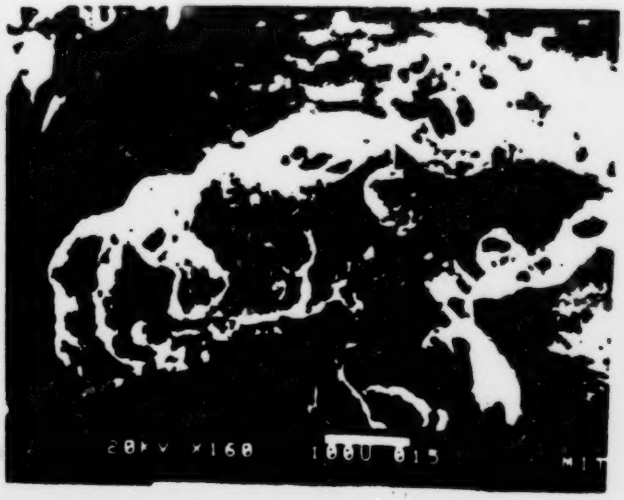
20KV X160
100U 015
MIT

Figure 21. SEM View of One of the Char Particles Shown in Figure 20 (Extreme Right Center)

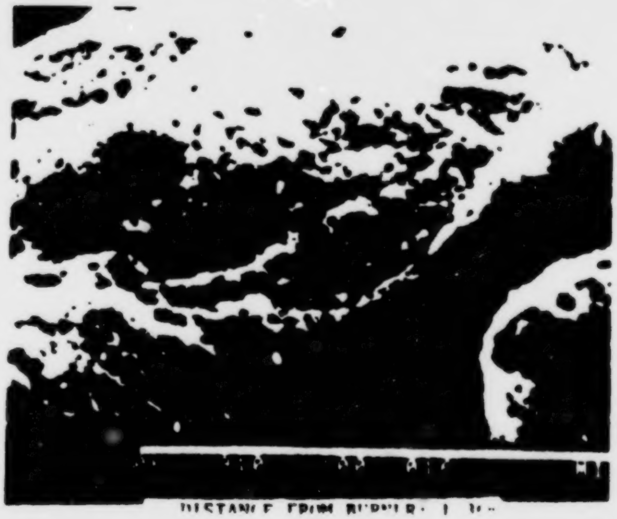
MIT
DISTANCE FROM BURNER: 1.1 m

W·4

Figure 22. SEM View of the Surface of the Char Particle Shown in Figure 21.

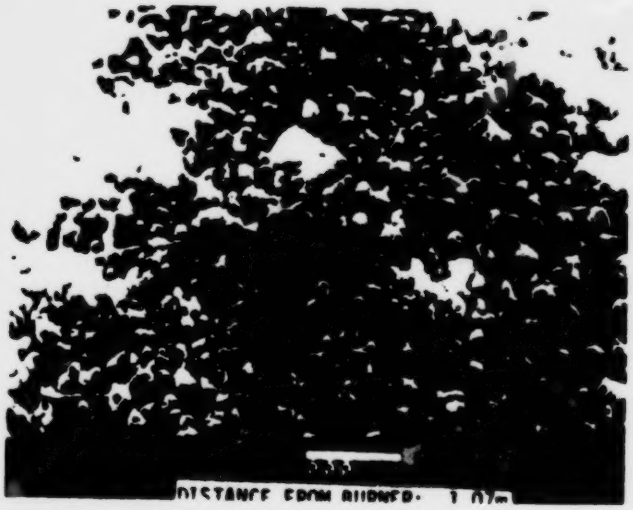
DISTANCE FROM BURNER: 1.07m

·W·4

Figure 23. SEM View of Char Particles Captured in the Run 97 CWS Flame

24-25 W.4

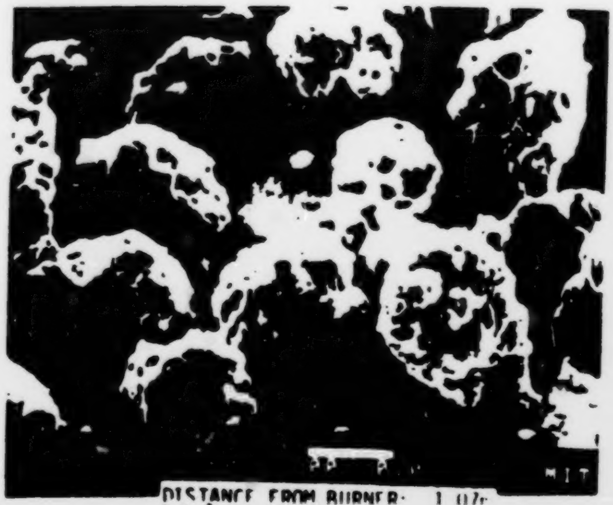

W-A

Figure 24. SEM Closeup of Several Char Particles From Figure 23

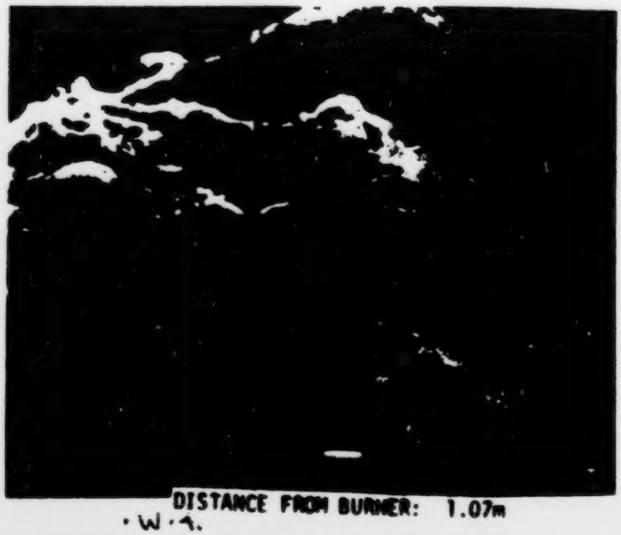

W.4.

Figure 25. SEM View of the Surface of One of the Char Particles Shown in Figure 24.

5.2.2 Coal Particle Fineness versus Atomization Quality

Runs 306 and 309 consisted of detailed flame structure studies on high swirl unstaged flames obtained with the Occidental Research standard and fine grind slurries respectively. The input conditions for these two flames were identical except for the water content of the slurry. In the case of the fine grind slurry, the viscosity was found to be prohibitively high, and the fuel was consequently diluted to a greater extent than the standard grind fuel so as to maintain comparable pressures at the fuel nozzle for the two slurry types. Examination of the axial burnout profiles for the two flames (Figs. 16 and 18) show the standard grind fuel (Run 306) to have given better results; the burnout in this case was substantially more rapid. The better burnout achieved with the standard grind slurry is again considered to be attributable to better atomization quality. Possibly, in spite of the greater degree of dilution with water, the viscosity of the fine grind fuel at the nozzle tip was greater, causing the atomization to be poorer.

Comparisons of the burnout profiles (Figs. 16 and 18) and also of electron micrographs taken of selected solids samples (Figs. 26 and 27) from the Occidental Research, standard and fine grind flames clearly demonstrate that atomization effects easily dominate those due to particle size in the slurry. This is a consequence of the fact that the char particles in the flame take on a size that is closer to the spray droplet sizes than to the original coal particle sizes. It may be said that particle size determines that lower limit in the spray droplet size distribution since it determines the smallest allowable dimensions in the atomizer and consequently the smallest droplet size. However, unless this lower limit of droplet size is actually approached by the atomizer in practice, the benefits to be achieved by use of fine grinds in coal-water-slurries from the point of view of carbon burnout are minimal.

5.2.3 Staged Combustion

The impact of staged combustion on fuel droplet/particle burnout is a major attendant concern in its evaluation as an effective approach towards NO_x emission control. Fig 17 shows the total solids concentration and carbon burnout profiles of the Run 308 staged flame - which may be compared to those in Fig. 16 of the Run 306 flame. As would be expected the carbon content of the solids in the staged flame remains relatively high in the fuel-rich zone.

Once the secondary air has been introduced, the carbon content of the solids rapidly decays to an emission level commensurate with unstaged CWS flames. It is clear, however, that staging of the flame effectively delays the major proportion of the fuel burnout, and could increase the residence time necessary for complete combustion. Previous studies on liquid fuel flames at the CRF (Beér et al. 1982) have shown the mode and rate of secondary admixing to be critical in achieving rapid and effective burnout in the fuel lean stage; perhaps this bears further investigation with CWS.

26-27-W·4

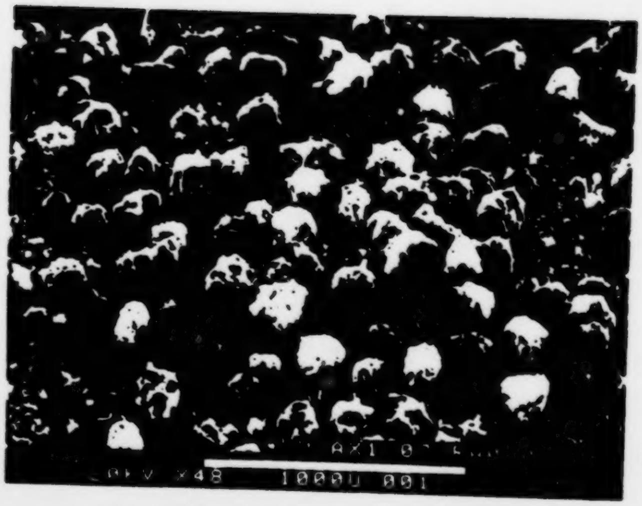

·W·4

Figure 26. SEM of Char Particles Captured from the Run 306 CWS Flame at 1.07 m from the Burner. (OR Standard Grind CWS).

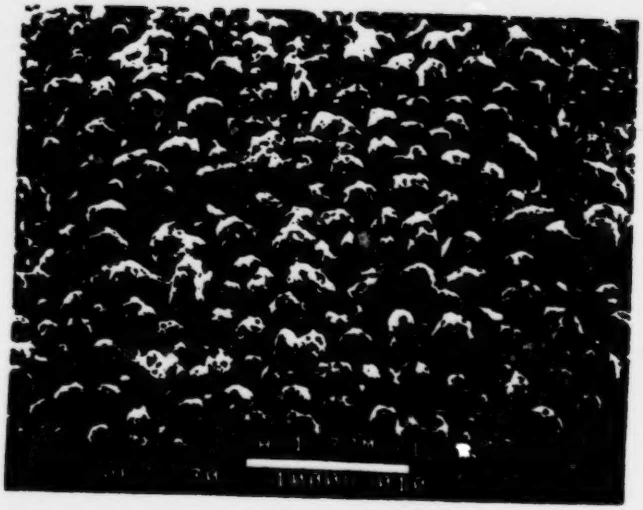

·W·A

Figure 27. SEM of Char Particles Captured from the Run 309 CWS Flame at 1.37 m from the Burner (OR Fine Grind CWS).

The particles are of roughly the same size (200 - 300 μm) as those taken from the Run 306 flame. Note that the length scale is slightly different from that of Fig. 26.

5.2.4 Oxygen Enrichment

Axial centerline profiles of O_2, CO_2 and CO for two Occidental Research fine grind CWS flames one with (Run 310b,) and one without (Run 309) O_2 injection were presented earlier in Figure 14. The overall excess O_2 for both flames was 2%. Examination of the profiles shows that the combustion of the major proportion of the fuel (~95-97%) is completed much more rapidly in the flame with O_2 enrichment (within ~2 m of the burner front wall) than in the flame without O_2 enrichment (3.5 - 4 m from the burner). However, it should be particularly noted that the profiles, specifically that of O_2, indicate that the rates of burnout decay to similar levels at the flame tail end.

Axial centerline solids concentration and carbon burnout profiles for the same flame with O_2 injection are shown in Fig. 19. Comparing these profiles with the fine grind CWS flame without O_2 injection the total solids concentration levels and their carbon content, particularly in the 'near field' region close to the burner, are slightly higher. This somewhat unexpected result is thought to be due to an entrainment effect by the high velocity oxygen jets in the oxygen-enriched flame (Run 310b) which thereby facilitate a higher in-flame solids loading. With less of the bottom ash dropping out of the oxygen-enriched flame, it becomes possible for the in-flame solids samples taken at positions close to the burner to show a carbon content even higher in value than in the case without oxygen enrichment. At positions away from the burner, the carbon burnout profiles of the

1. W.5

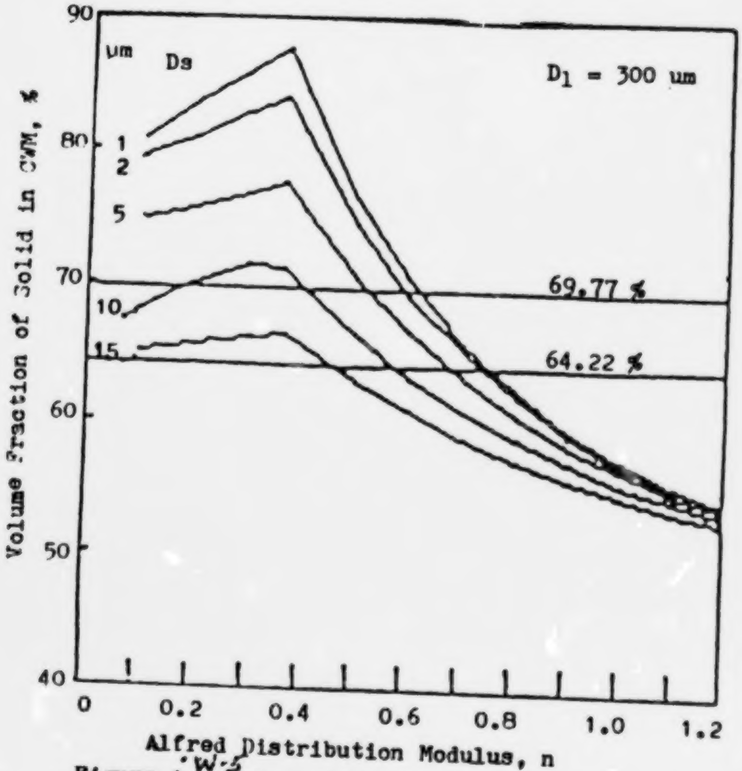

W.5

Figure 1. Volume Content of Solid vs Modulus n according to Alfred Equation at ρ_s= 1.3 and D_1= 300 µm

2·W·5

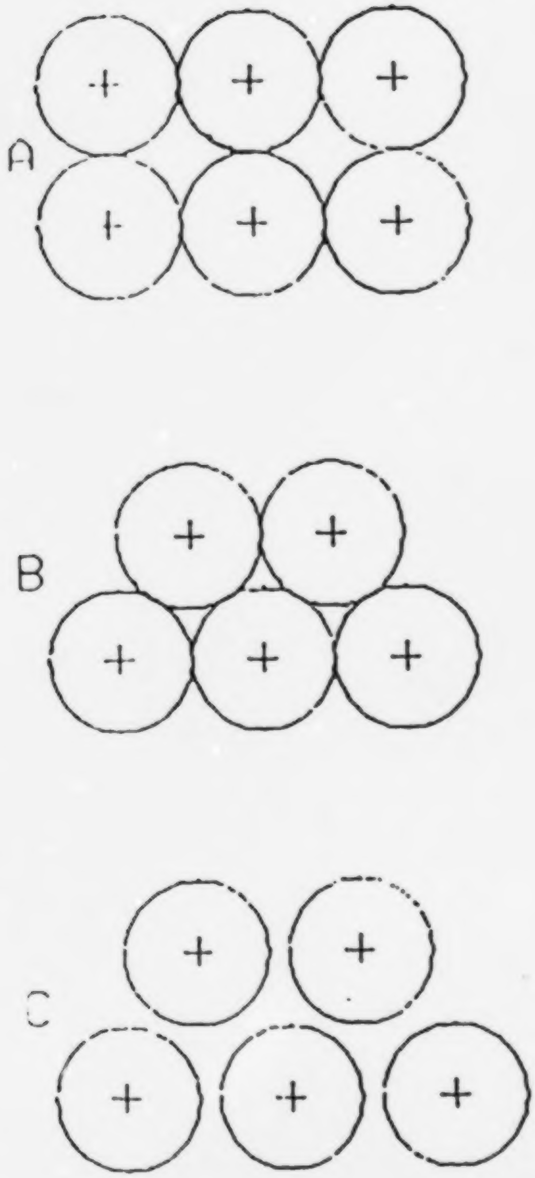

Figure 2. Models of Monosphere Packing

2, W.5

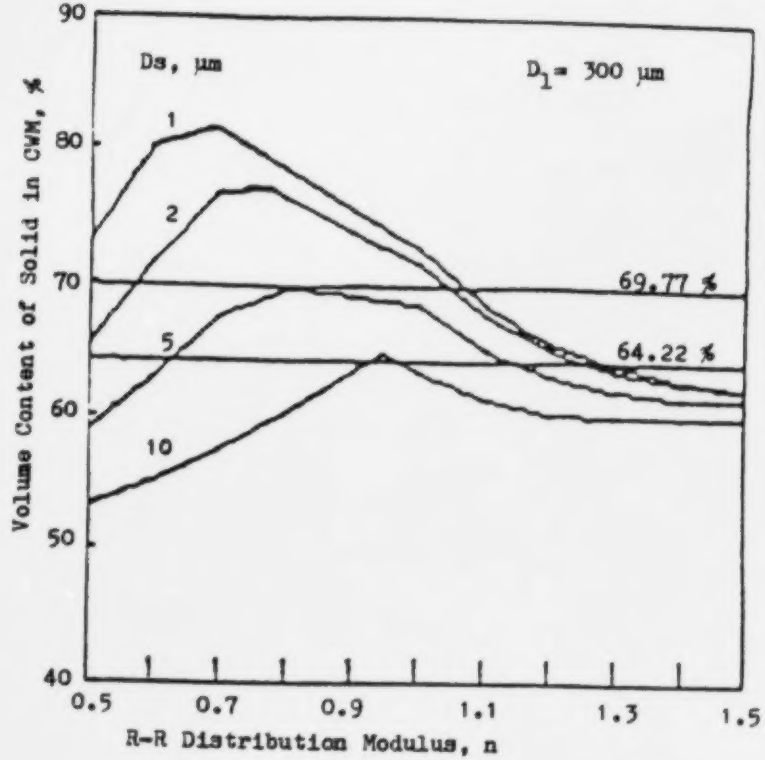

Figure 3. Volume Content of solid vs modulus n according to R-R Equation at ρ_s= 1.3 and D_1= 300 μm

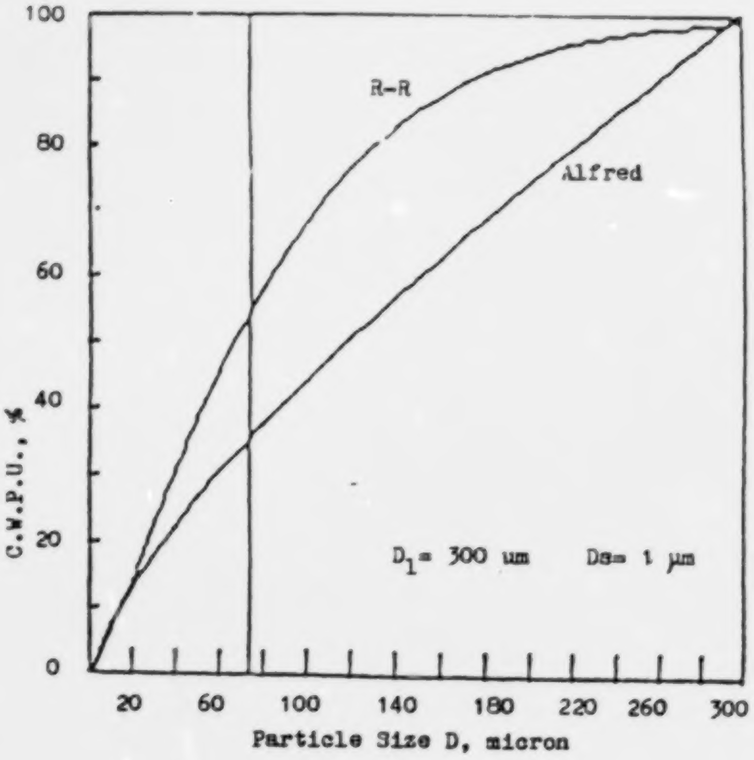

Figure 4. Size Distribution according to R-R and Alfred Equations at C_{wt}= 70 % and γ_s/γ_l =1.3

R-R : n= 1.25
ssa= 2.3145x10 m/cc
Alfred:n= 0.72
ssa= 2.9202x10 m/cc

2· W·8

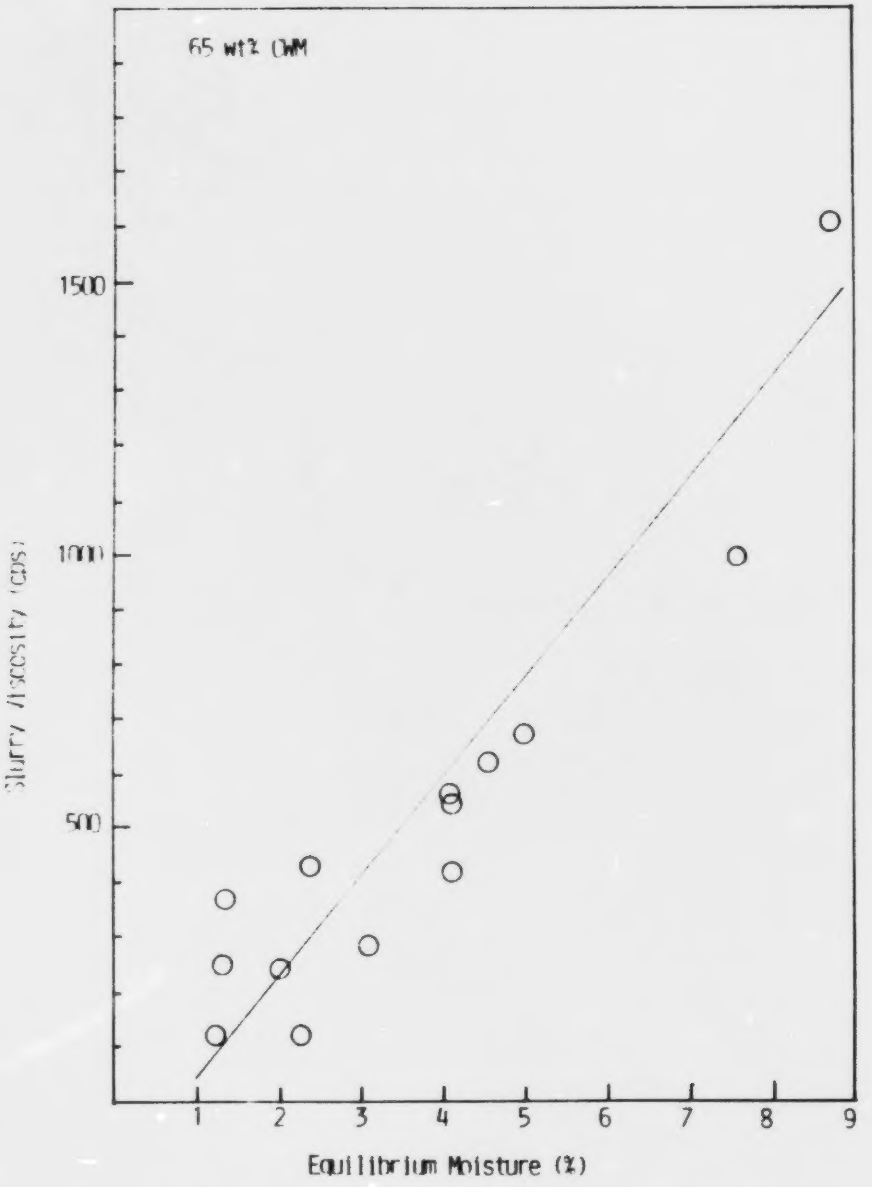

W·8

Figure 2 Equilibrium Moisture v.s. Slurry Viscosity

1·W·9

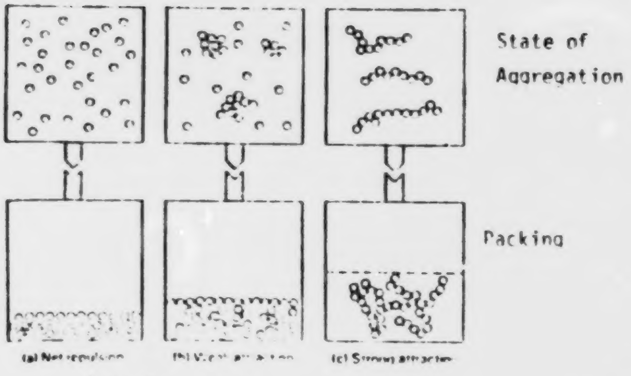
State of Aggregation
Packing
(a) Net repulsion
(b) Weak attraction
(c) Strong attraction

·W 9

Fig. 1. Interaction Between Particles

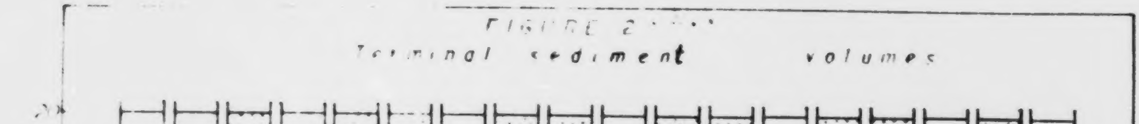
FIGURE 2

Terminal sediment volumes

3 · W 9

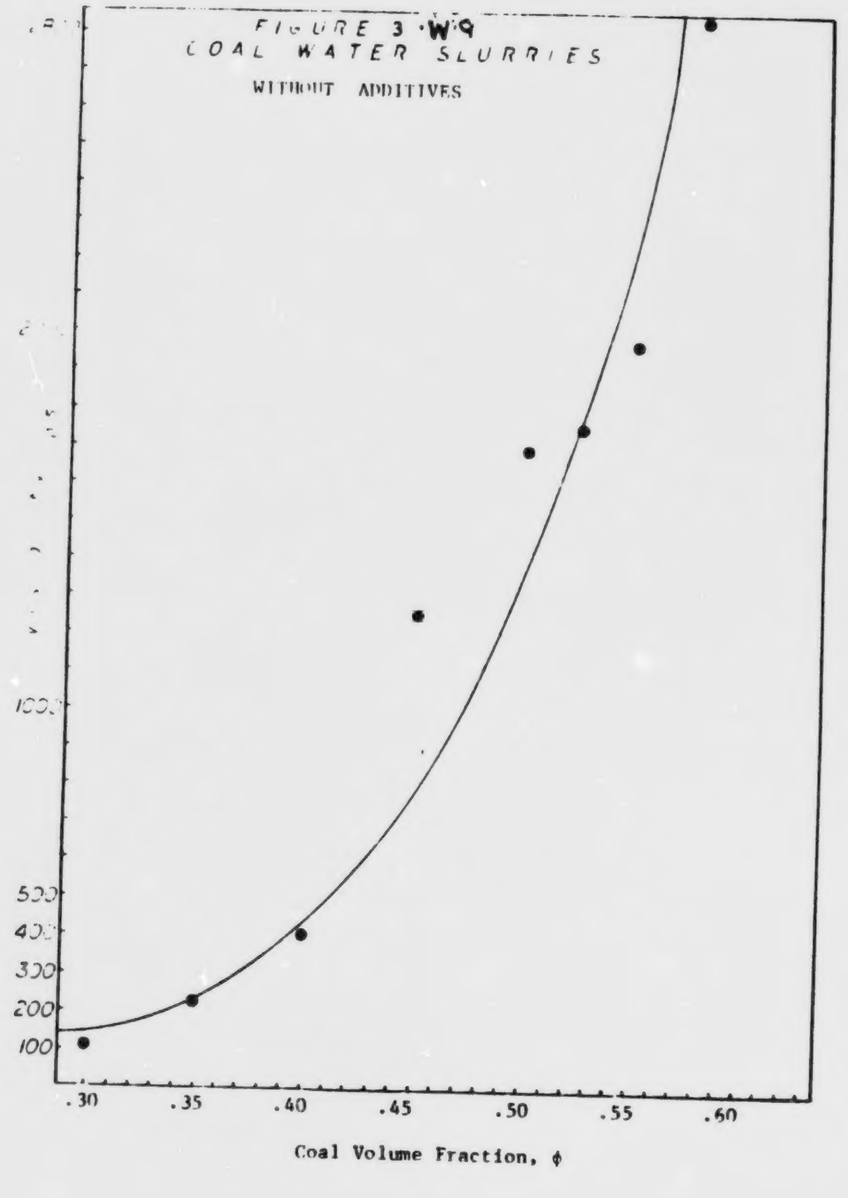
FIGURE 3·W·9
COAL WATER SLURRIES
WITHOUT ADDITIVES

·4-5- W·9

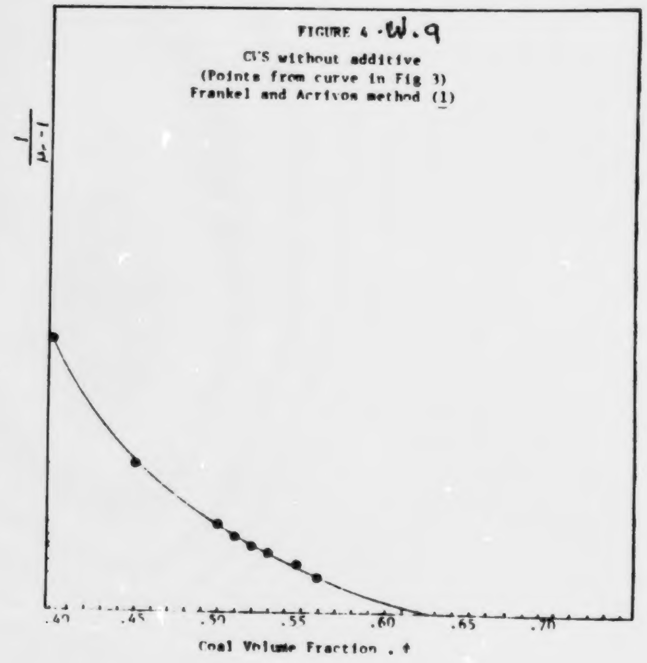
FIGURE 4 ·W.9
CWS without additive
(Points from curve in Fig 3)
Frankel and Acrivos method (1)

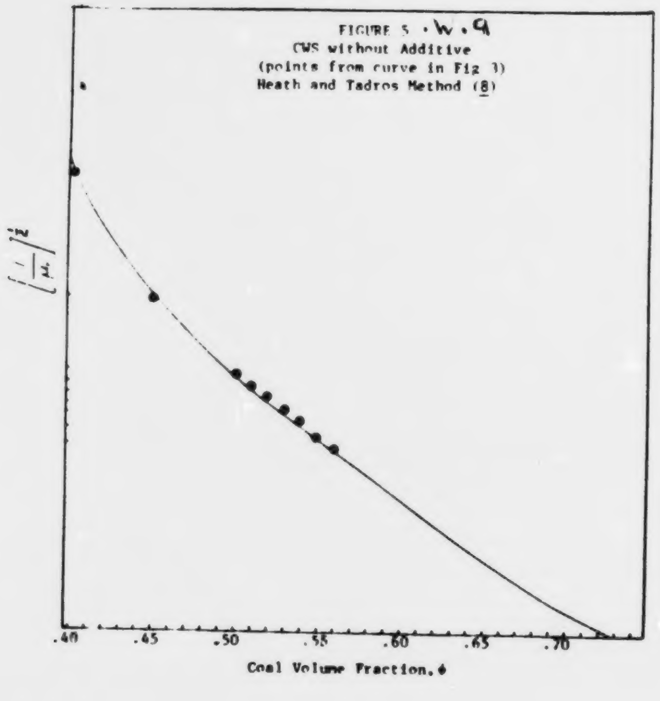
FIGURE 5 · W.9
CWS without Additive
(points from curve in Fig 3)
Heath and Tadros Method (8)

6·w·9

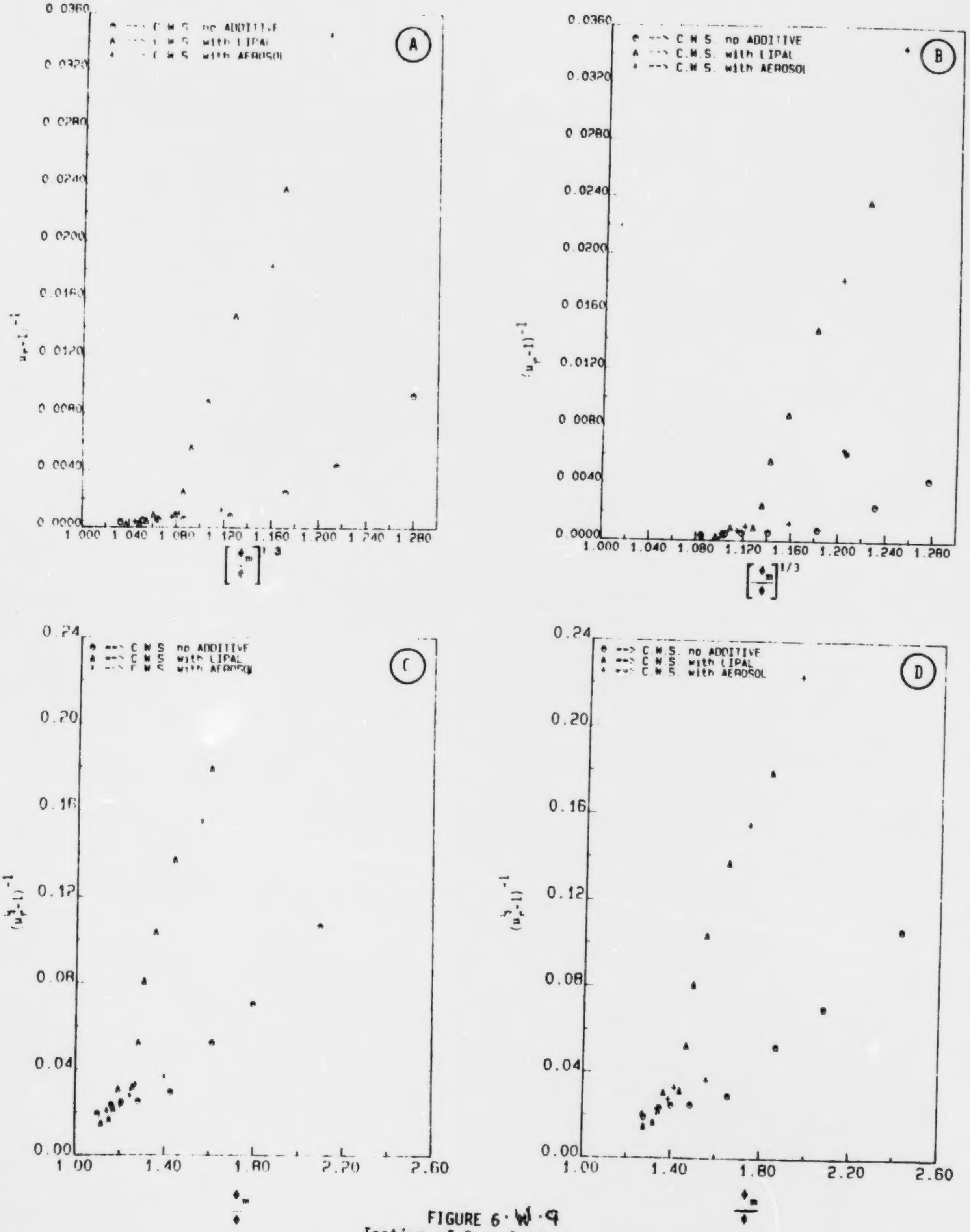

FIGURE 6·W·9
Testing of Correlations

1·W·10

No.C) were used. The results are given in Fig.1 and Table 1.

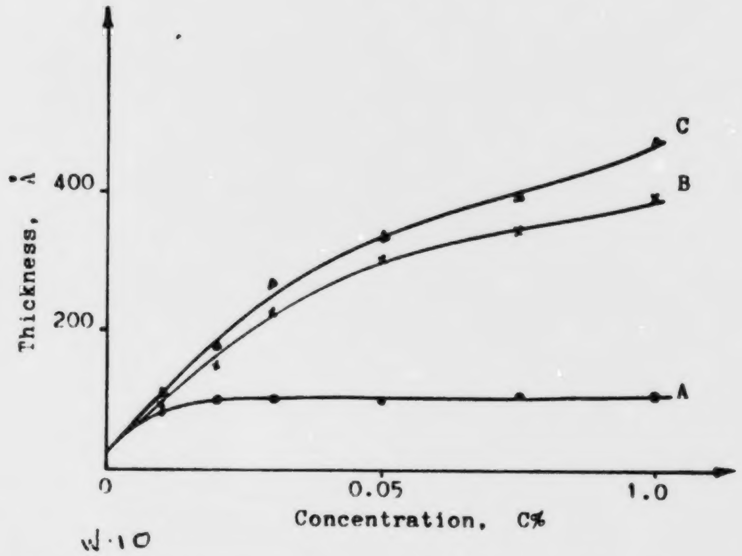

W·10

Fig.1 Relationship between the thicknesses of adsorption films and the additive concentrations(additives A,B,C)

Table 1. The thicknesses of adsorption films formed on coal surface by different additives

Additive No.	The thicknesses of adsorption films(at the equilibrium concentration of 0.05%)
A	100 Å
B	310 Å
C	340 Å

As can be seen from Fig.1, for additive No.A, the thicknesses of the adsorption films do not stop increaseing until the concentration of adsorbate reaches to a certain value, but for additives No.B and No.C, the thicknesses are still increasing continuously. And moreover, the adsorption film formed by additive No.C is thicker than that by additive No.B.

In order to reveal the relationship between the thickness of adsorption films and the adsorption abilities of additives, we have made the experiments of adsorption isotherms and FT-IR spectra as well to acquire a deeper understanding of the nature of the adsorption of additives on the solid surfaces. The results of experiments are shown in Fig.2

2·W·10

and Fig.3.

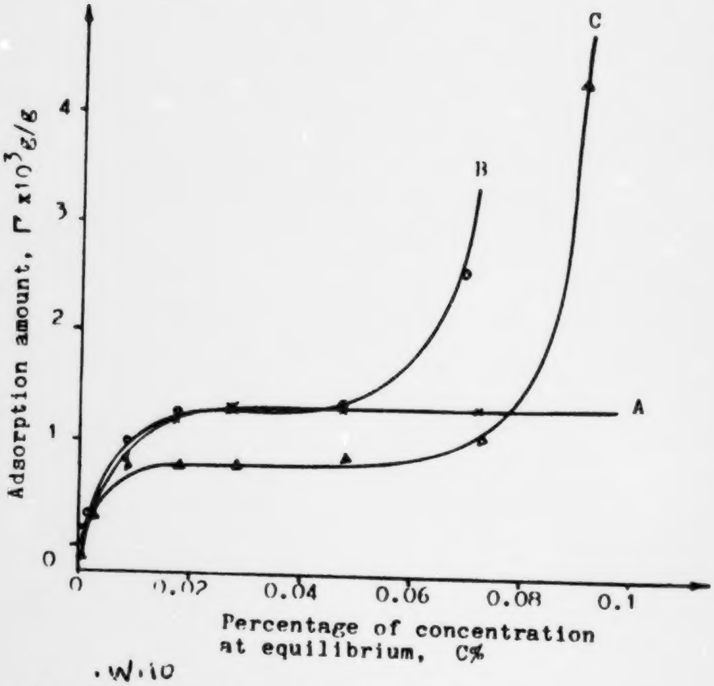

·W·10

Fig.2 Adsorption isotherms of three additives (A, B, C) on coal powder

As shown in Fig.2, the adsorption isotherms of additive A belongs to the type of Langmuir adsorption, whereas multilayer adsorptions are observed in the adsorption isotherms for additives B and C. It is worth noticing that according to Fig.1 the thicknesses of adsorption films for additives A and B are less than that for additive C, although their adsorptions (A and B) are stronger as indicated in Fig.2. As for additive C the adsorption is weak, having negative adsorption at its low concentration, on the contrary, its film formed is the thicknest one.

By means of the subtract spectrum of FT-IR, changes of IR spectra before and after adsorption were examined. The result showed that a new spectral peak appears at the spectrogram of additive A comparing spectrograms befor and after adsorption. This fact may be considered to be that a stronger interaction exists between additive A and coal surfaces. However, for additives B and C there were no changes at their IR spectrograms, thus belonging to the kind of weak interaction. The above results are identical with the results obtained from experiments of adsorption isotherms indicating that the electronic states of additive A have changed, this adsorption is attributed to a specific adsorption (8), nevertheless, the adsorption of additives B and C are attributed to a non-specific adsorption.

According to the results of specific surface area determination, adsorption isotherms and thickness of films, the density of surface layer in terms of g additives per cm^3

3-W.10

can be calculated.

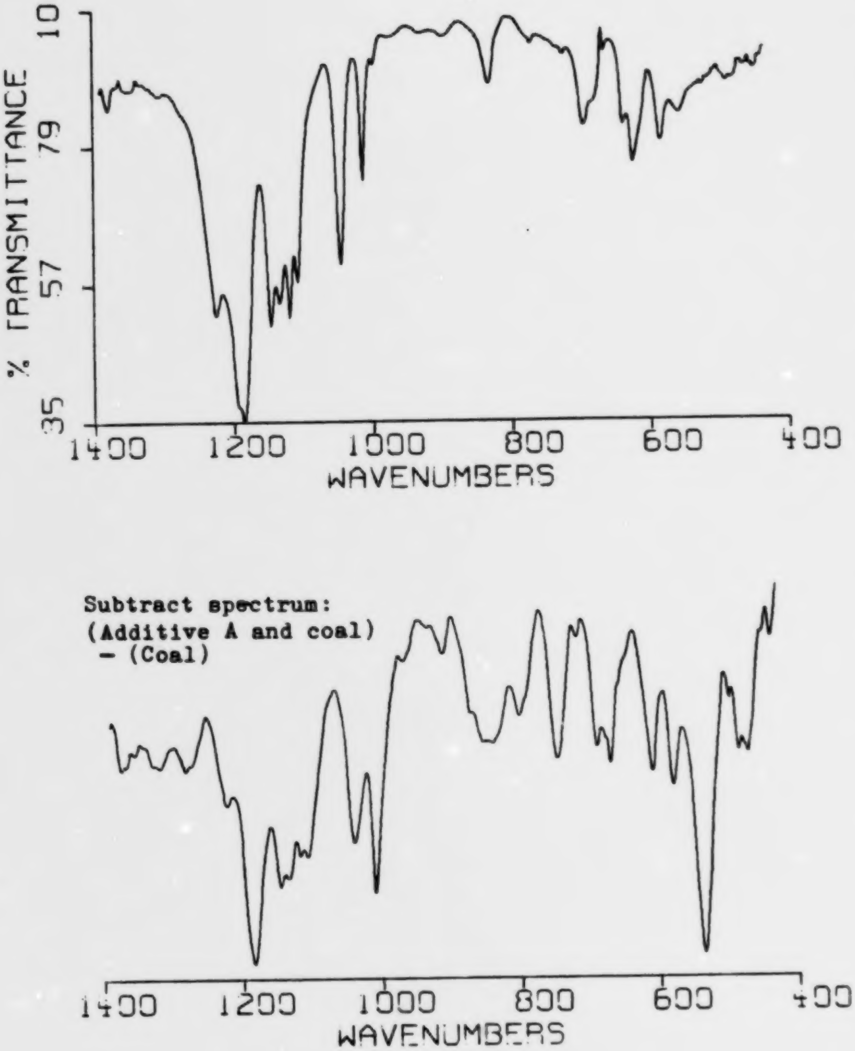

Fig.3 FT-IR spectra of additive A before and after adsorption

W.10

The density of adsorption layer ρ is equal to the adsorption mass(m) per volume of surface layer Va

$$\rho = \frac{m}{Va} = \frac{m}{A\cdot l} = \frac{m/W}{A\cdot l/W} = \frac{\Gamma}{S\cdot l}$$

where W--- coal powder weight; Γ--- adsorption amount m/W; S--- specific surface area A/W ; l--- thickness of adsorption layer; A--- surface area. Take for example, the calculated data at the equilibrium concentration of 0.05% are listed below:

4 · W:10

W:10

Table 2. Density of adsorption layer on coal surface

Additive	Γ (g/g)x10^3	l (Å)	ρ (g/c.c.)x10^3
A	1.25	100	23.3
B	1.25	310	7.71
C	0.80	340	4.38

As indicated by the results, a conclusion can be made that for additive A the adsorption force behaves the strongest, and the adsorption layer is the thinnest and closest; on the contrary, for additive C, the adsorption force behaves the weakest and the adsorption layer is the thickest and loosest. These additives could be arranged in series as following:

Adsorption strength	A > B > C
Thickness	C > B > A

Based upon the investigation mentioned above, experiments to measure rheological characteristics of CWS with these three additives have been carried out respectively. The results are shown in Fig.4 and Fig.5, the shear rate used in the experiment is 4.76sec^{-1}.

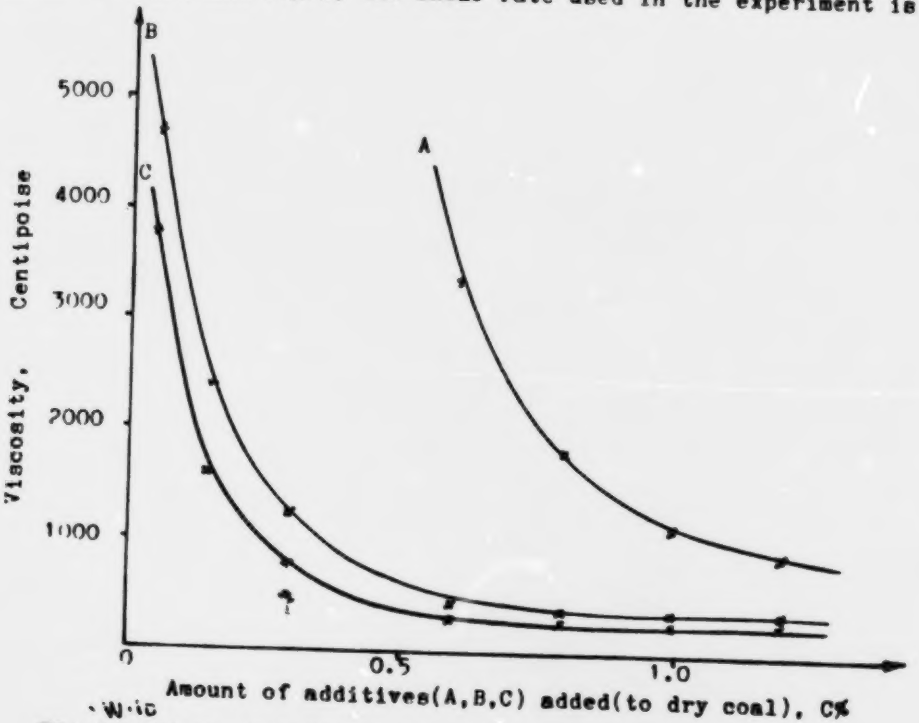

Fig.4 Effect of different additives on the viscosity of CWS at constant concentration of CWS (concentration of CWS is 65%)

S·W·1c

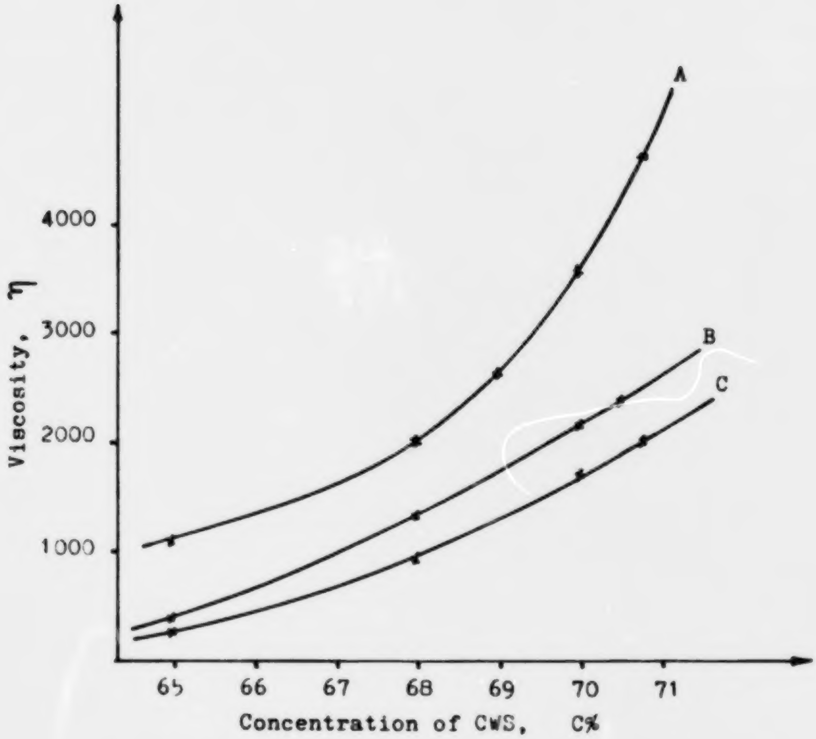

Fig.5 Effect of different additives(A,B,C) on the viscosity of CWS at constant concentration of additives(concentration of additives is 1.0% to dry coal)

W.10

As shown in Fig.4, additive C shown the best effect on reducing the viscosity of CWS as the additive content varies, keeping the coal content constant. Just as that shown in Fig.5, with additive C the highest coal content CWS can be obtained and the viscosity of CWS rises slowest. That is of great significance in preparing of CWS with high content of coal.

In a previous study of the rheological property of CWS(7), we had considered that a structure formation of a high coal content dispersion for CWS was caused by partially losing the stability of the system and some interaction existed among particles. By adding additives which weaken the particle interaction into CWS, it is easy for particles to be dispersed and stabilized, thus reducing the ability of the structure formation and lowering the viscosity for the system. As it is known, there are many factors, such as surface charge, viscosity, surface-active agent and steric stabilization layer, which can stabilize a dispersion system. But which factor will play a major role in a thick dispersion system? If steric stabilization layer is that one, then, what sort of additives can construct an effective steric stabilization layer? And what function does the adsorption phenomena perform in this case? What regularity must be followed in coal suspension? The adsorption processes playing a decisive role in colloidal phenomena has of course

2- W · 11

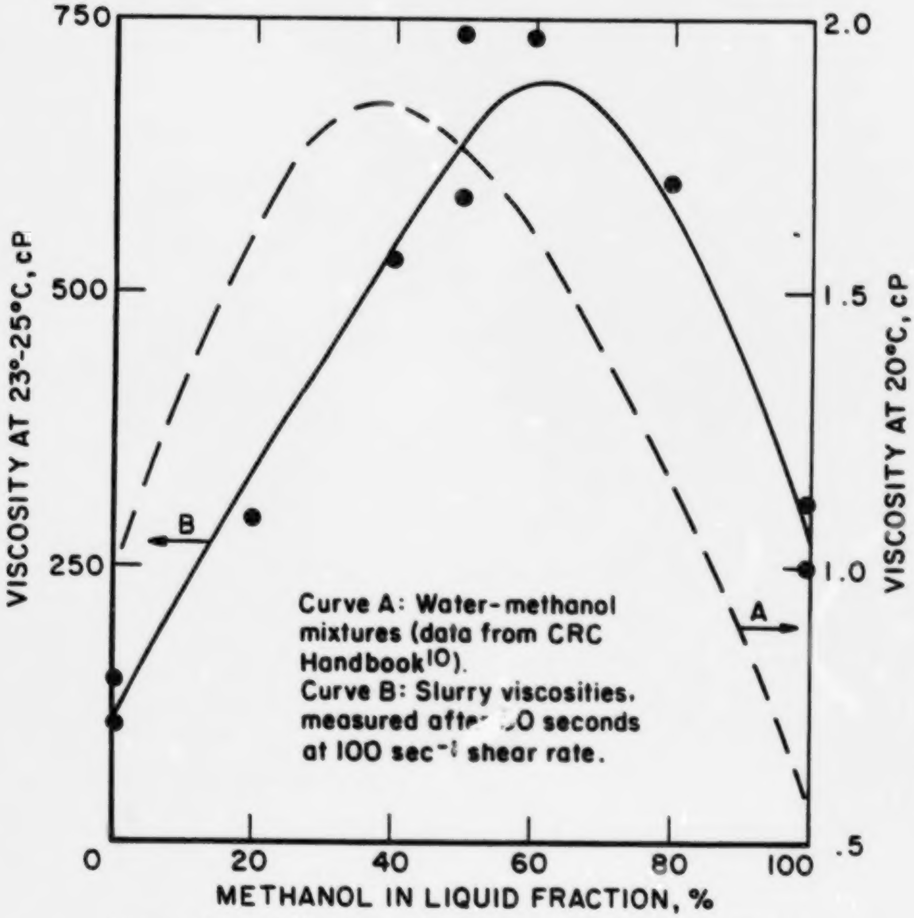

Figure 2. Viscosity vs. percent methanol in water-methanol and 47.5% Montana Rosebud coal-water-methanol mixtures.

W · 11

BSI/3479

3. W. 11

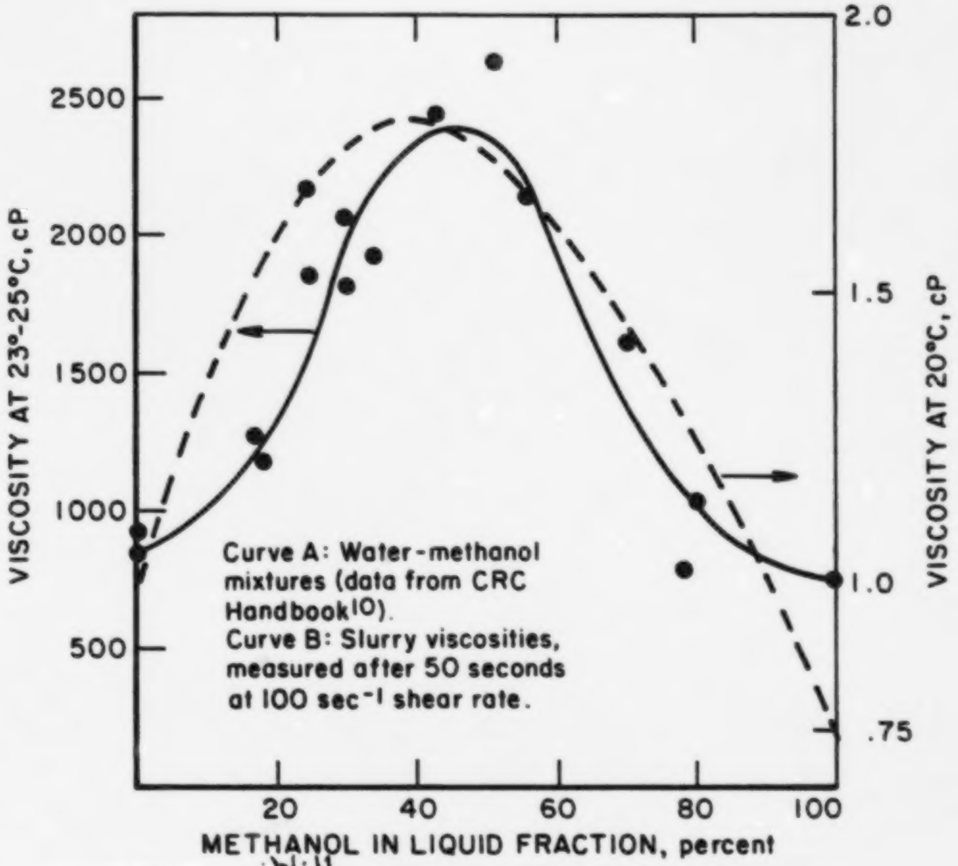

Figure 3. Viscosity vs. percent methanol in water-methanol and 56% Canadian Coal-water-methanol mixtures.

W. 11

BSI/3876

4·W·11

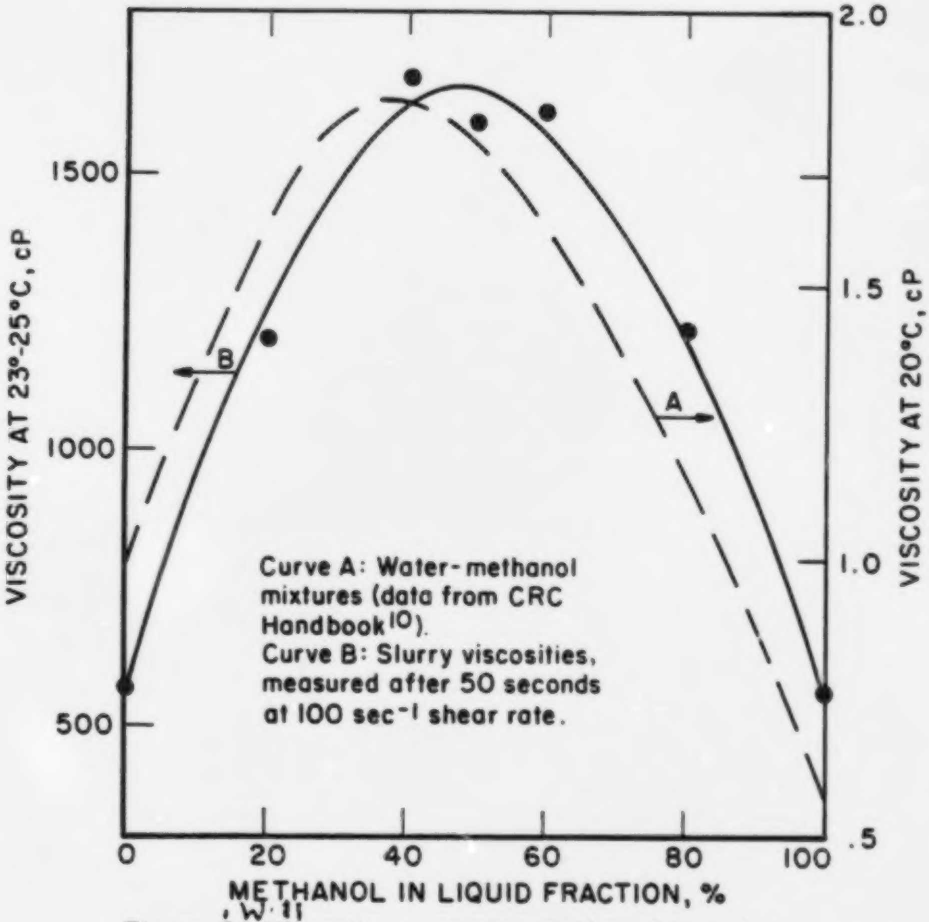

, W·11

Figure 4: Viscosity vs. percent methanol in water-methanol and 50% lignite coal-water-mixtures.

10·W·11

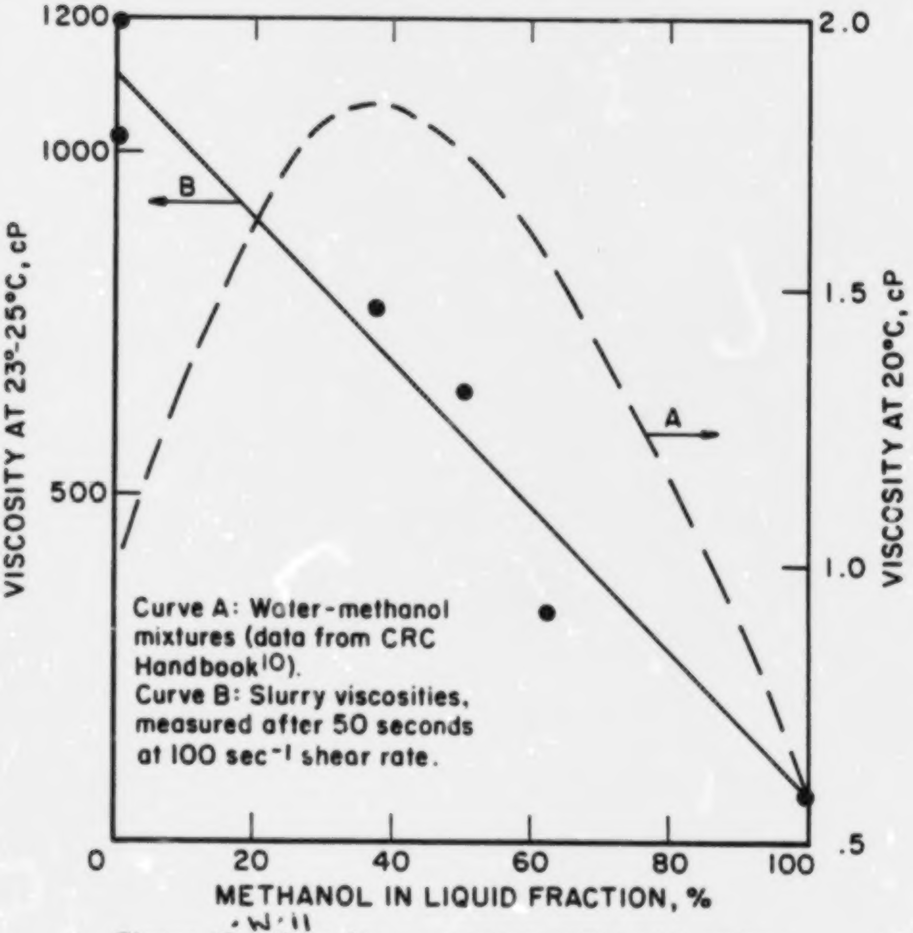

·W·11

Figure 10. Viscosity vs. percent methanol in water-methanol and 50% petroleum coke-water-methanol mixtures.

BSI/3477

V.I.13.8

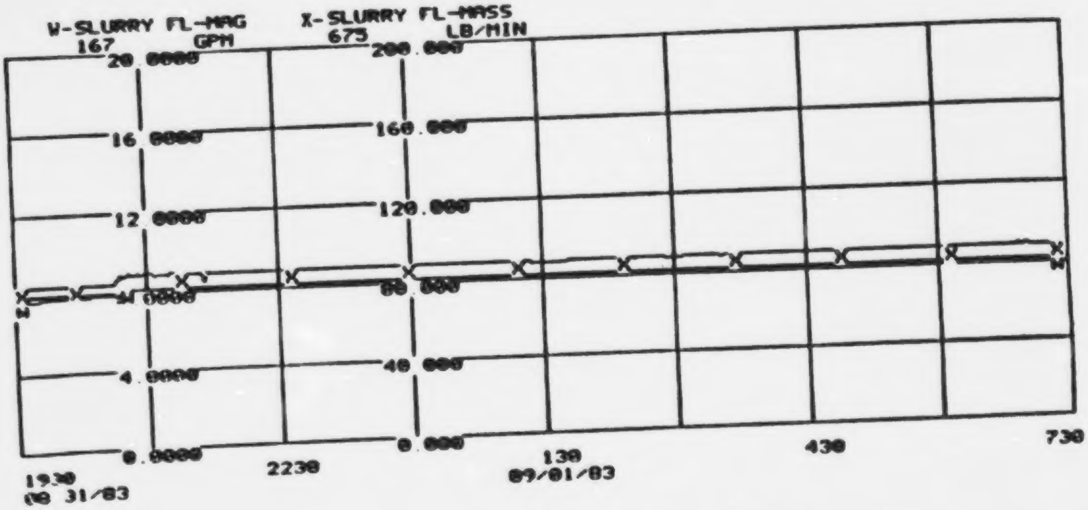

Figure 7. Comparison of Magnetic and Mass Flowmeter

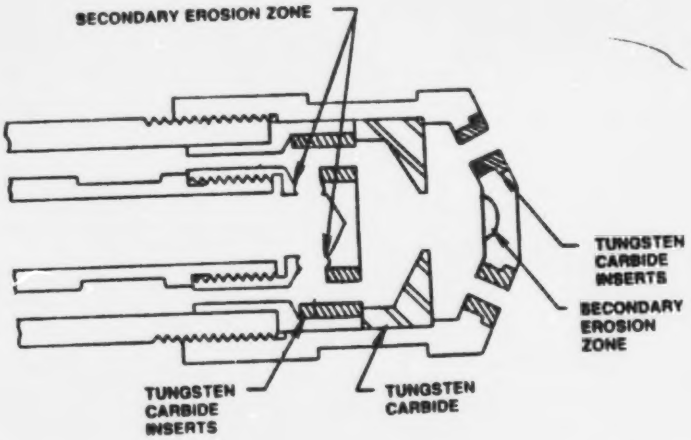
SECONDARY EROSION ZONE
TUNGSTEN CARBIDE INSERTS
SECONDARY EROSION ZONE
TUNGSTEN CARBIDE INSERTS
TUNGSTEN CARBIDE

Figure 8. T-Jet Atomizer

V/.13.8

7. High swirl was required to provide furnace gas recirculation for ignition stabil
This swirl was achieved with 9-12" windbox pressure by operating with burner regi
vanes fully closed. Figure 9 shows a diagram of the burners. This turbul
changed the position of the pilot flame sufficiently that the flame scanners
trouble picking it up. Initial lightoff of intermittent pilot and main gas was
normal 2-3" windbox pressures. After lightoff of CWS, the vanes were grad
closed and air pressure increased to achieve a desirable CWS fire. Main gas f
was removed. The committee action of the two scanners per burner provided accept
reliability during slurry firing.

2.W.16

Babcock Power CWM Burner

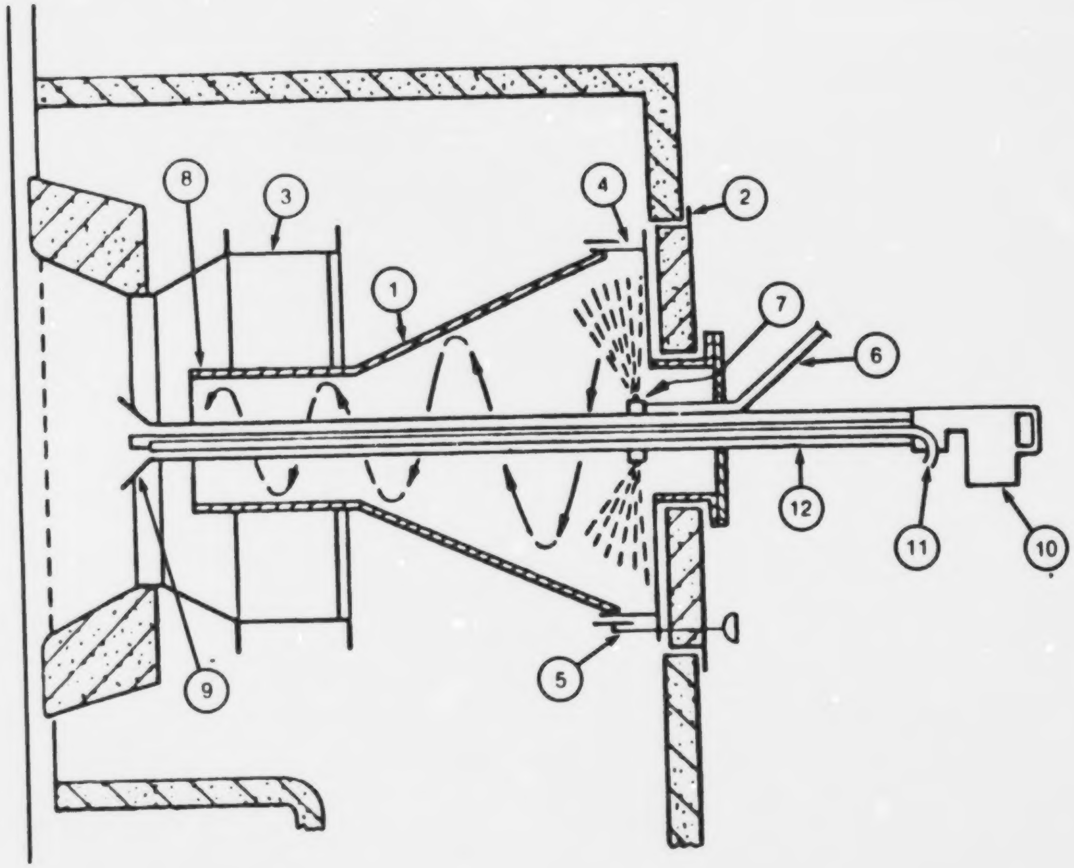
8
3
4
2
1
7
6
12
11
10
5
9

Fig. 2W.16

1· W:17

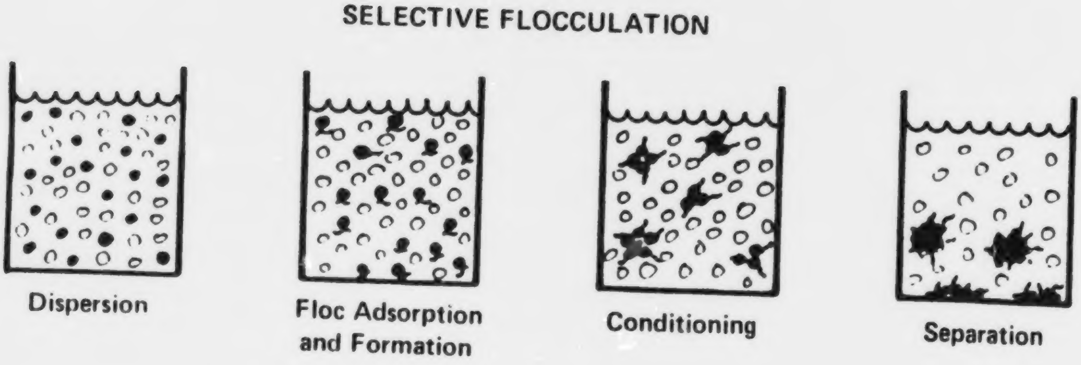
SELECTIVE FLOCCULATION
Dispersion
Floc Adsorption and Formation
Conditioning
Separation

·W·17

FIGURE 1. CONCEPTUAL REPRESENTATION OF THE SELECTIVE FLOCCULATION PROCESS

5·W·17

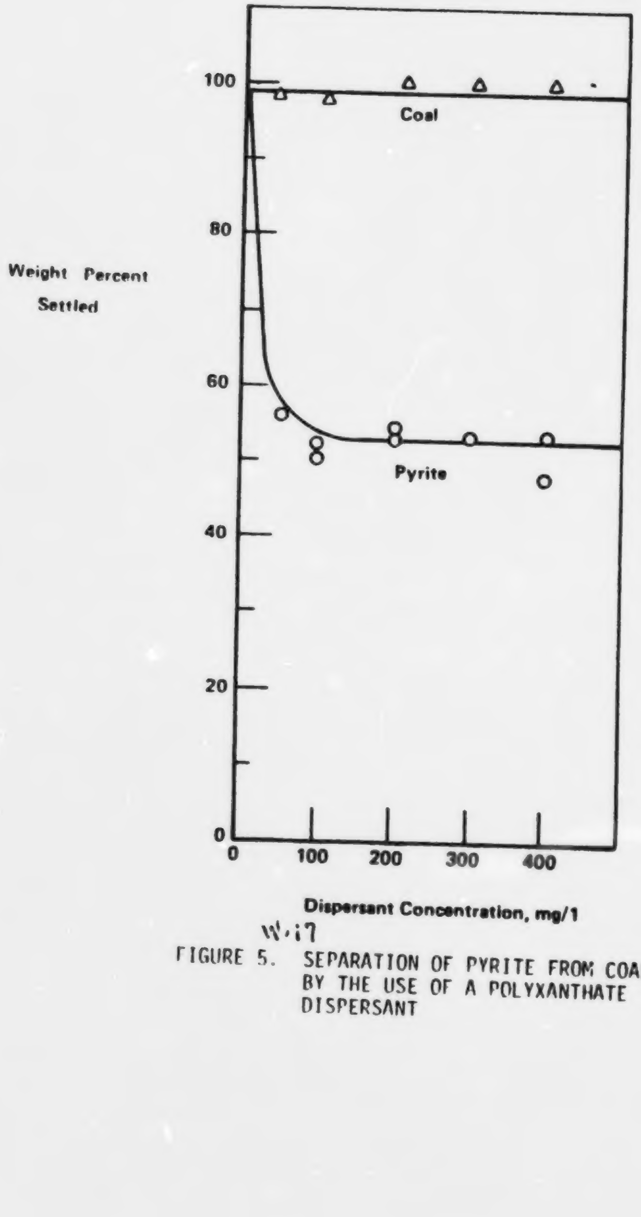

W·17

FIGURE 5. SEPARATION OF PYRITE FROM COAL BY THE USE OF A POLYXANTHATE DISPERSANT

4·W.18

INPUT: Westphalian coal (vitrain 64%, durain 33%, and fusain 3% -maf)

@ 100 tons/hour

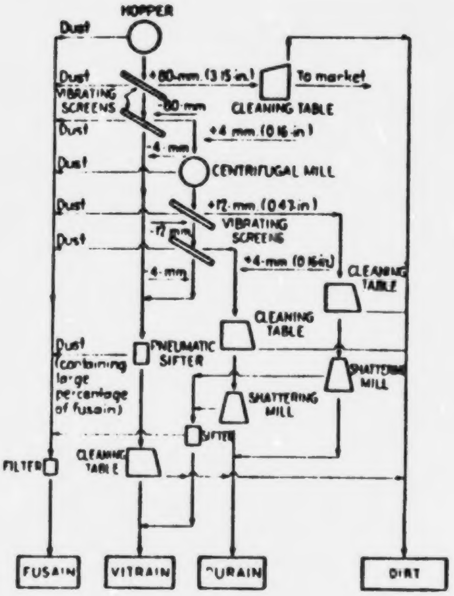
HOPPER
Dust
Dust
+80-mm (3.15 in.)
To market
VIBRATING SCREENS
-80 mm
CLEANING TABLE
Dust
+4 mm (0.16 in.)
-4 mm
Dust
CENTRIFUGAL MILL
Dust
+12-mm (0.47 in.)
VIBRATING SCREENS
Dust
-12 mm
+4-mm (0.16 in.)
-4 mm
CLEANING TABLE
CLEANING TABLE
Dust (containing large percentage of fusain)
PNEUMATIC SIFTER
SHATTERING MILL
SHATTERING MILL
SIFTER
FILTER
CLEANING TABLE
FUSAIN
VITRAIN
DURAIN
DIRT

OUTPUT: 42 tons coal enriched with vitrain (vitrain 80%, durain 20%, fusain 1%)
16 tons coal enriched with durain (durain 60%, vitrain 39%, fusain 1%)
(per hour) 22 tons coarse coal
5 tons dust, mainly fusain and vitrain, with only 10% durain
15 tons shale

Flowsheet for the enrichment of petrographic constituents in various products by utilizing differences in friability of the components - the Lehman Process.

FIGURE 4.W.18

FIGURE 8 · W-18

DROP TUBE COMBUSTION TEST RESULTS FOR SEPARATED COAL FRACTIONS
CONSTANT CONDITIONS 1,000 centigrade
Weight % Reactive Macerals vs. % Carbon Conversion Efficiency

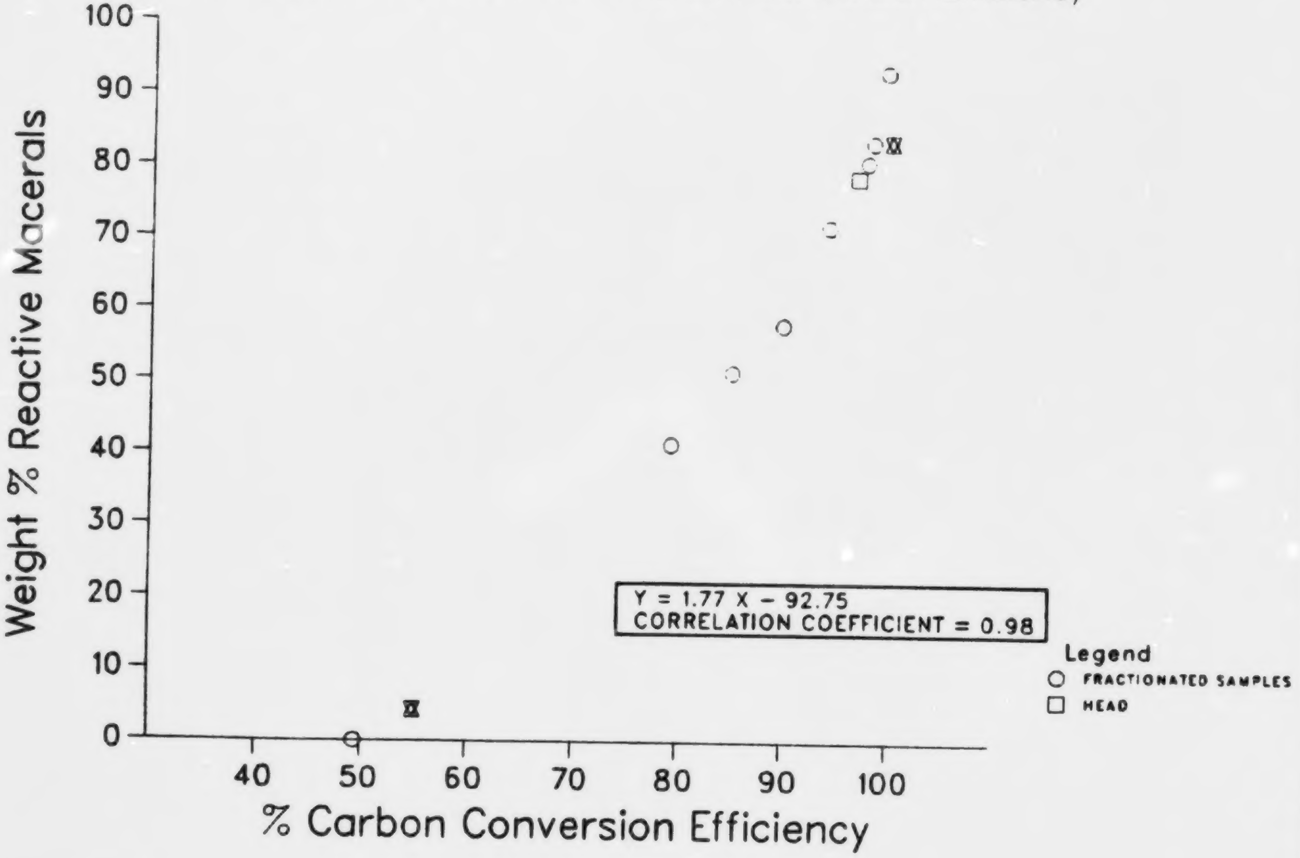

8·W·18

5- W·20

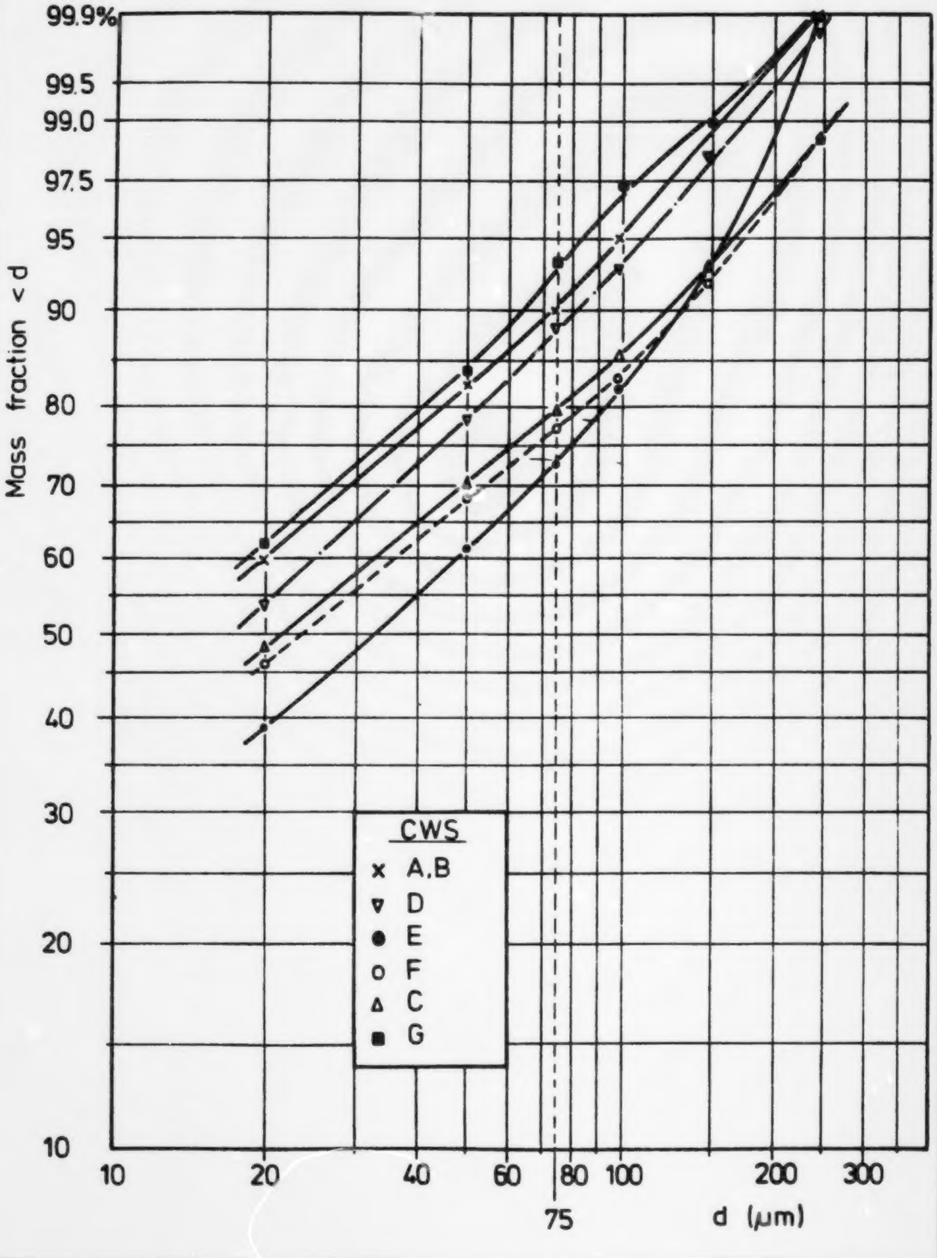

IFRF

84-0014

· W ·20

Fig. 5 : Particle size distributions wet sieve technique

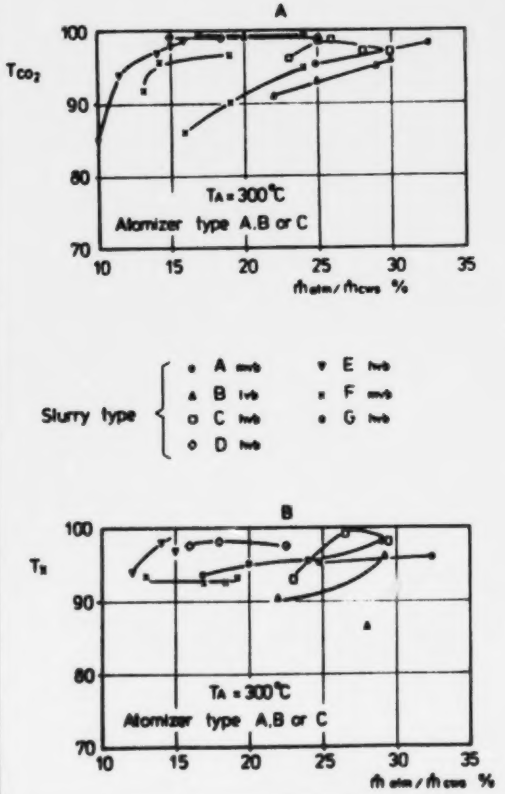

IFRF

Fig. 6: Maximum CWS burnout recorded
W · 2o for the 7 slurries as a function
of atomizing air rate

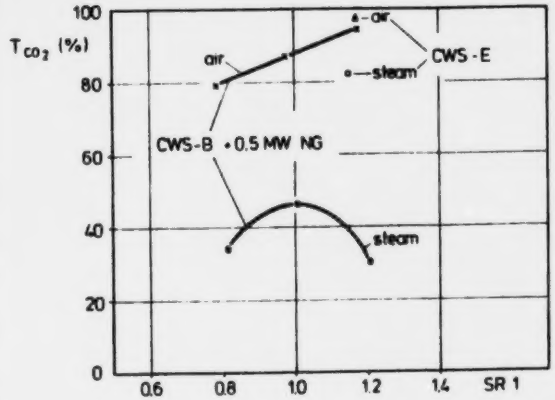

· W · 2o

IFRF

84-0012

Fig. 7 : Air / steam atomization

6-7- W·2:

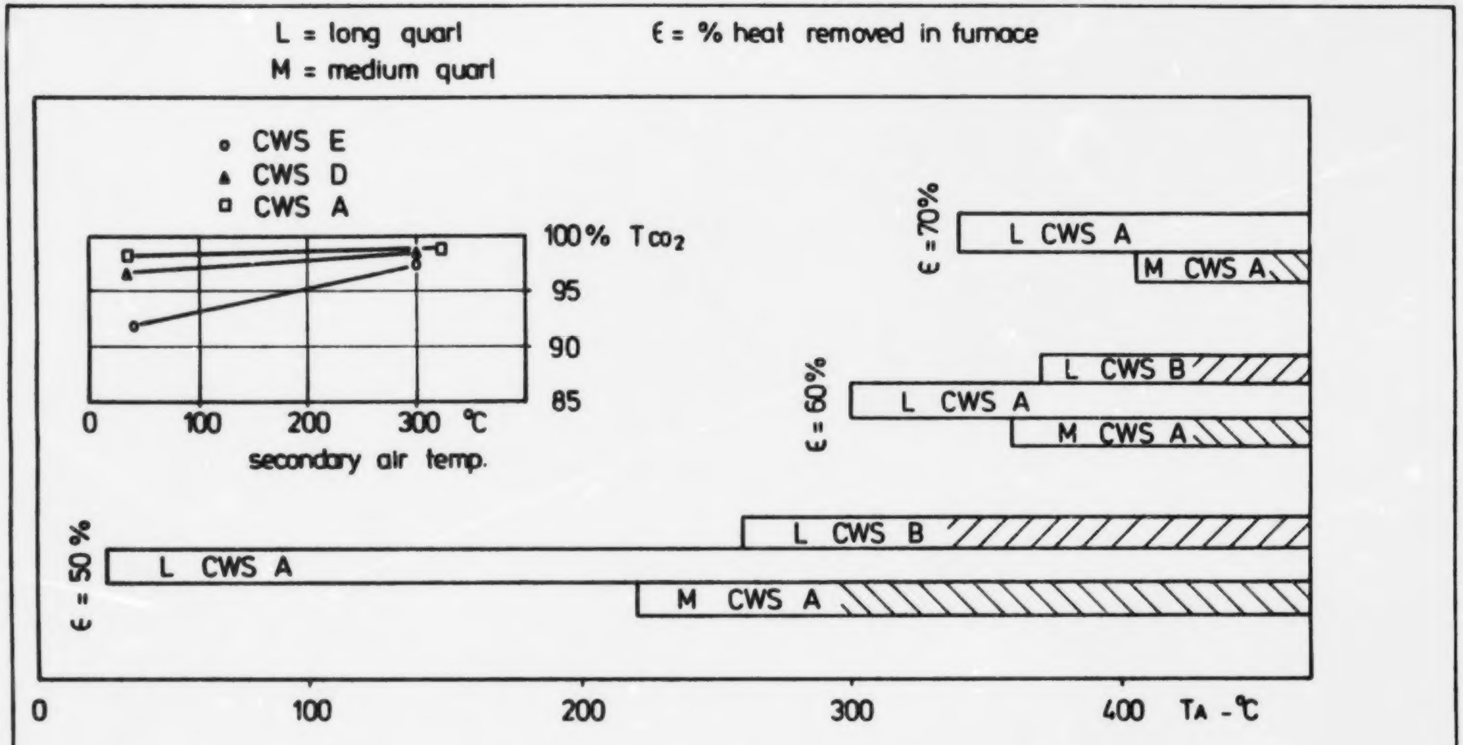

Fig. 8: Minimum secondary air temperature required for unsupported combustion

2-3. W.21

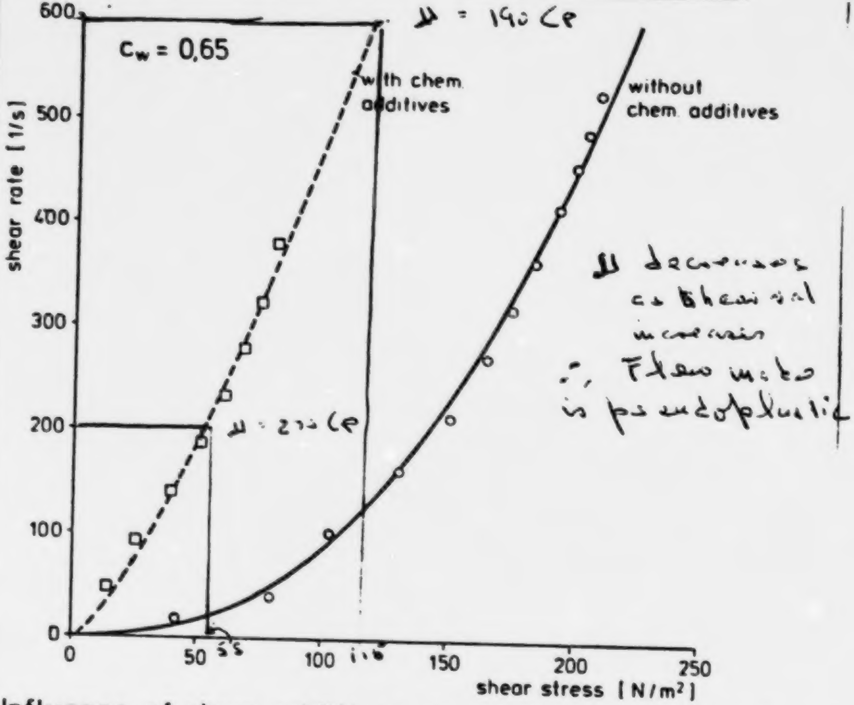

μ decreases as shear rate increases
∴ Flow model is pseudoplastic

Influence of chem. additives on the flow characteristics

Fig. 2 · W 21

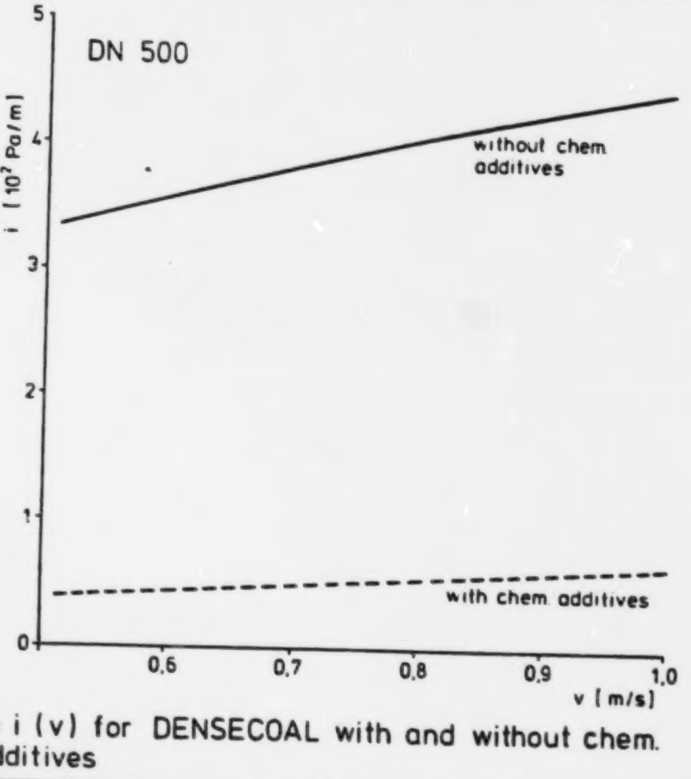

i = i (v) for DENSECOAL with and without chem. additives

Fig. 3 · W · 21

6. W. 21

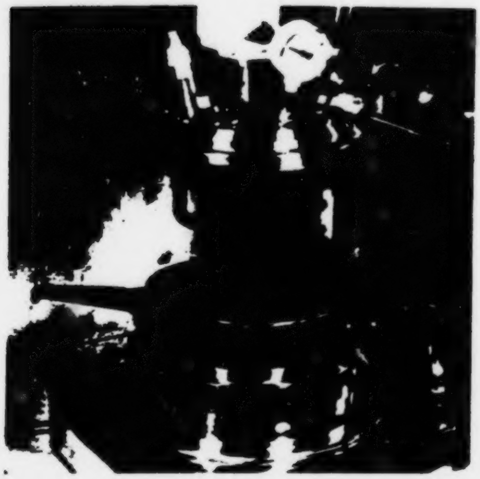

Fig. 4

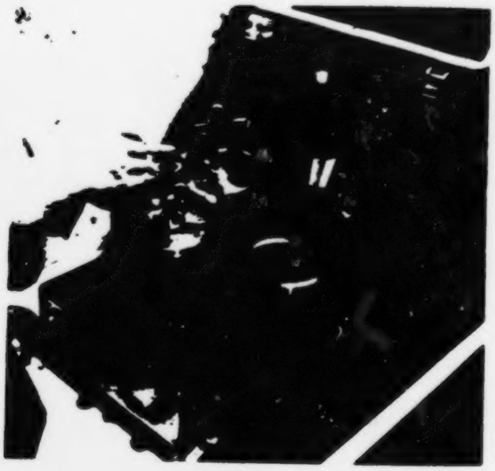

Fig 5

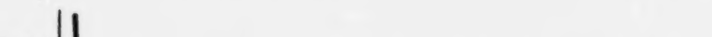

$\eta = \eta\ (c_w)$ for additive K 154

Fig. 6 • W· 21

8 · W 21

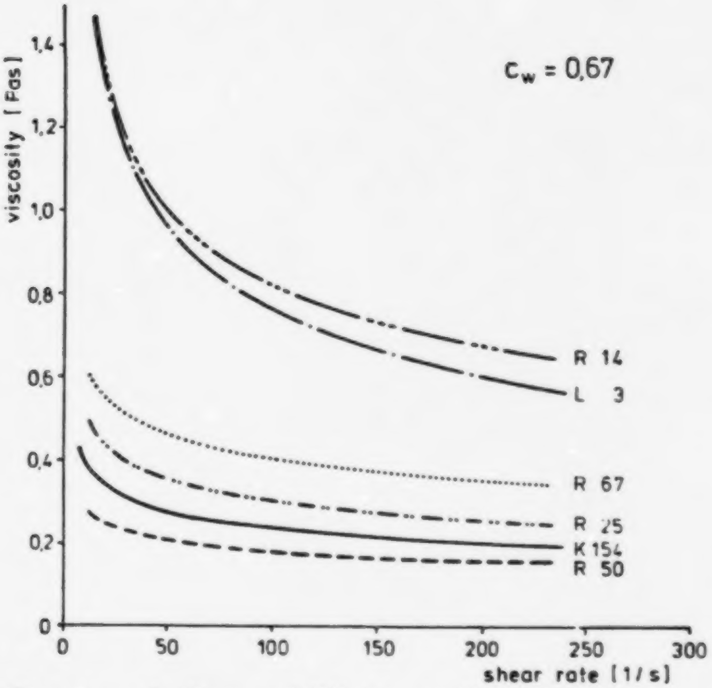

Influence of chem. additives on the viscosity

Fig 7

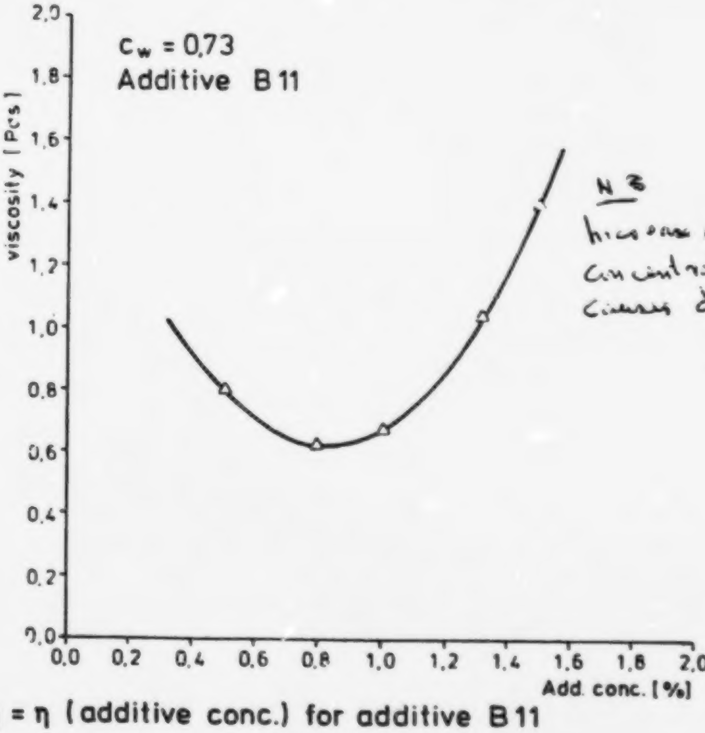

N 3
Increase of the additive concentration over .8%
causes dilatant effect

η = η (additive conc.) for additive B 11

Fig 8 · W · 21

4. W 22

The Parker-Hannifin atomizer (Figure 4) is an external mix design. Coal-water slurry fuel exits the nozzle as a thin swirling sheet which is sandwiched between two air streams. Part of the atomizing air exits the atomizer as an inner core of air swirling in the same direction as the slurry. The bulk of the atomizing air exits the atomizer as a high-velocity counterswirling stream through the outer annulus. The interaction of the slurry film and the outer air stream, which are swirled in opposite directions, generates high shear and results in atomization. The atomizer tip parts are fabricated from 440-C stainless steel. Since slurry velocities are low (maximum 10 ft/sec) erosion is not expected to be a significant problem.

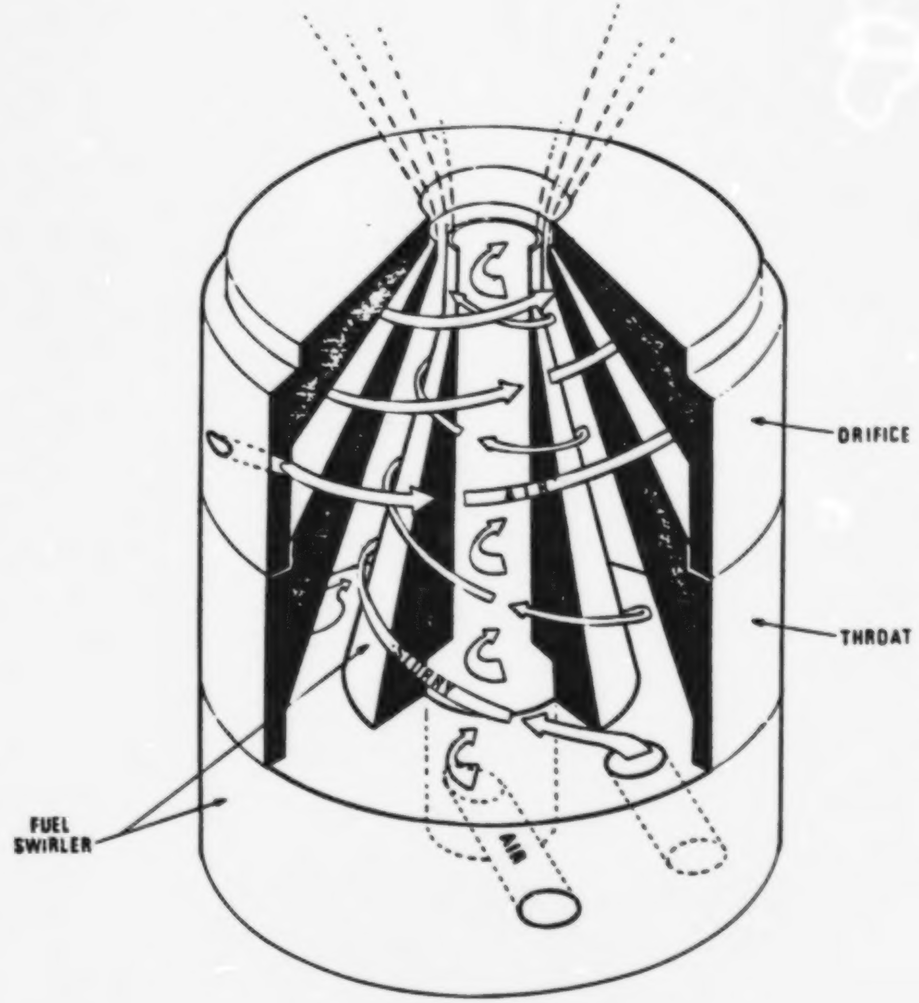

W.22

Figure 4: Parker-Hannifin Atomizer

3·W·22·

mixer the slurry stream spreads radially across a plate. It is broken up at the edges of the plate by twelve concentric atomizing air streams. The air/slurry mixture flows into the mixing chamber and then out through seven 5/32-inch ID holes in the endcap. Since the atomizer parts are fabricated from carbon steel, tungsten carbide sleeve inserts have been placed in the holes of the endcap to reduce wear. The final geometry of the spray from the Coen atomizer is determined by the number, size and location of the holes drilled in the endcap. The atomizer has a total spray angle of 90°. Coen has supplied us with several endcaps so that the spray pattern may be varied.

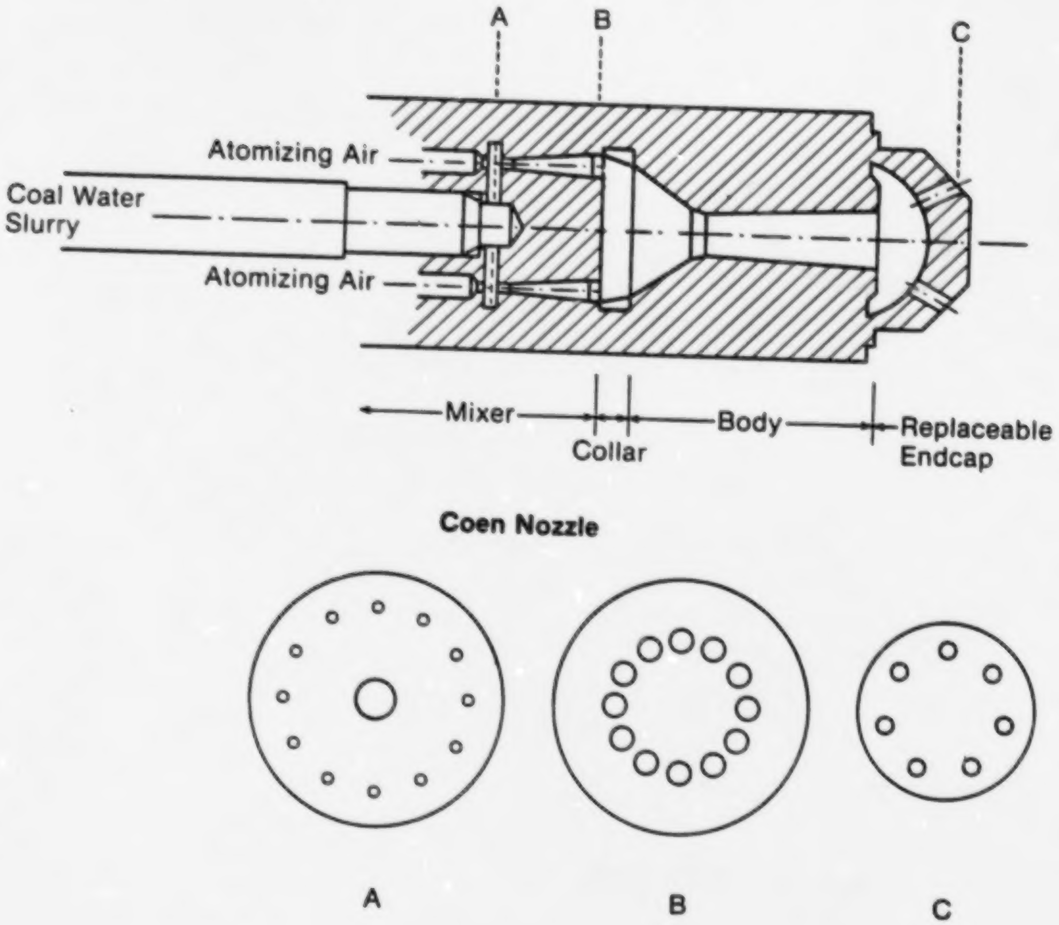
A
B
C
Atomizing Air
Coal Water Slurry
Atomizing Air
Mixer
Collar
Body
Replaceable Endcap
Coen Nozzle
A
B
C

Figure 3: Coen #1MV Atomizer

·W·22·3

8·W·22

.W.22

Figure 8: Slurry Spray Produced by the Parker-Hannifin Atomizer at the Nozzle Exit
Slurry: 500 lb/hr; Atomizing Air: 175 psig

G.W.22

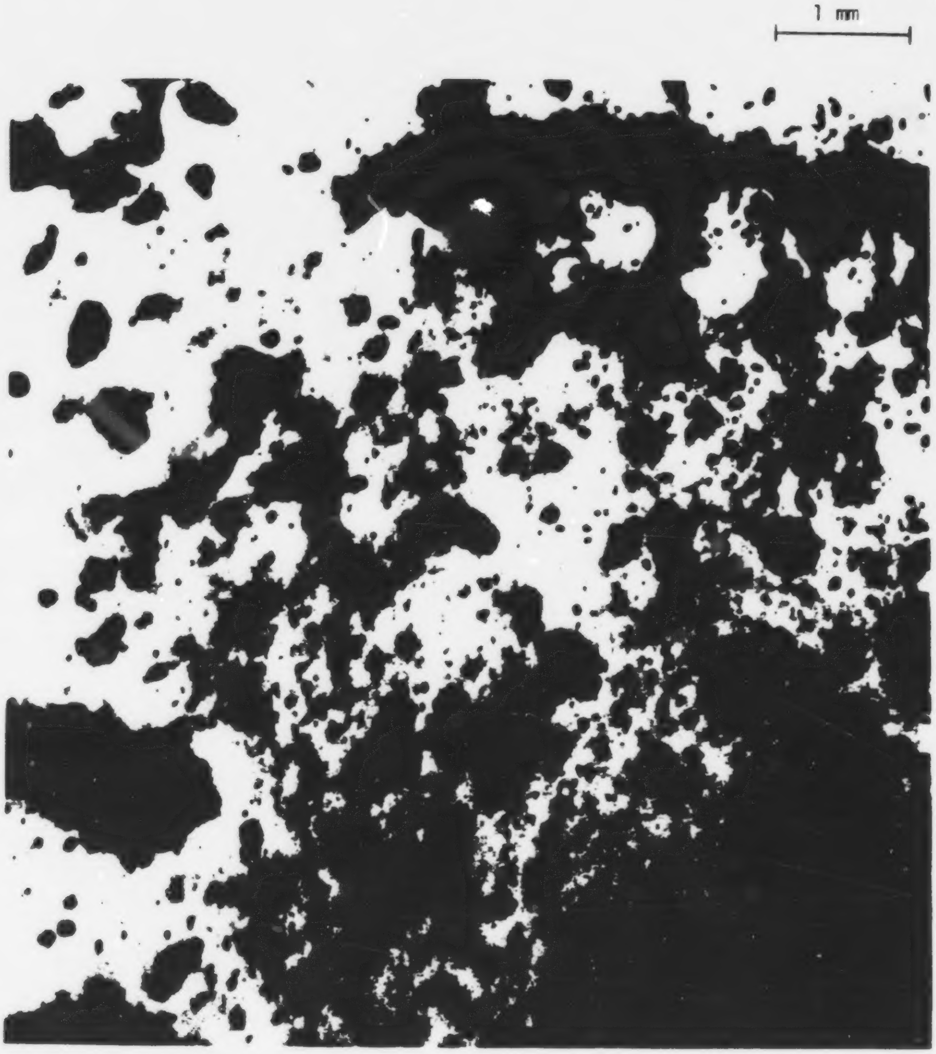

.W.22

Figure 9: Slurry Spray Produced by the Parker-Hannifin Atomizer
1 Inch Downstream from the Nozzle Exit
Slurry: 500 lb/hr; Atomizing Air: 175 psig

10·W·22

In order to compare the atomization of slurry with the atomization of more familiar liquids, tests were run using water as the fuel in the Parker-Hannifin atomizer. Figure 10 shows a 500 lb/hr water spray with an atomizing air pressure of 41 psig and Figure 11 shows a water spray at the same mass flow rate with an atomizing air pressure of 153 psig. One striking difference between water and slurry sprays is the difference in droplet concentrations. A comparison of sprays at similar operating conditions shows that water atomizes more readily and forms a greater number of small drops. As a result the water sprays are optically more dense since there are a greater number of droplets in the light path.

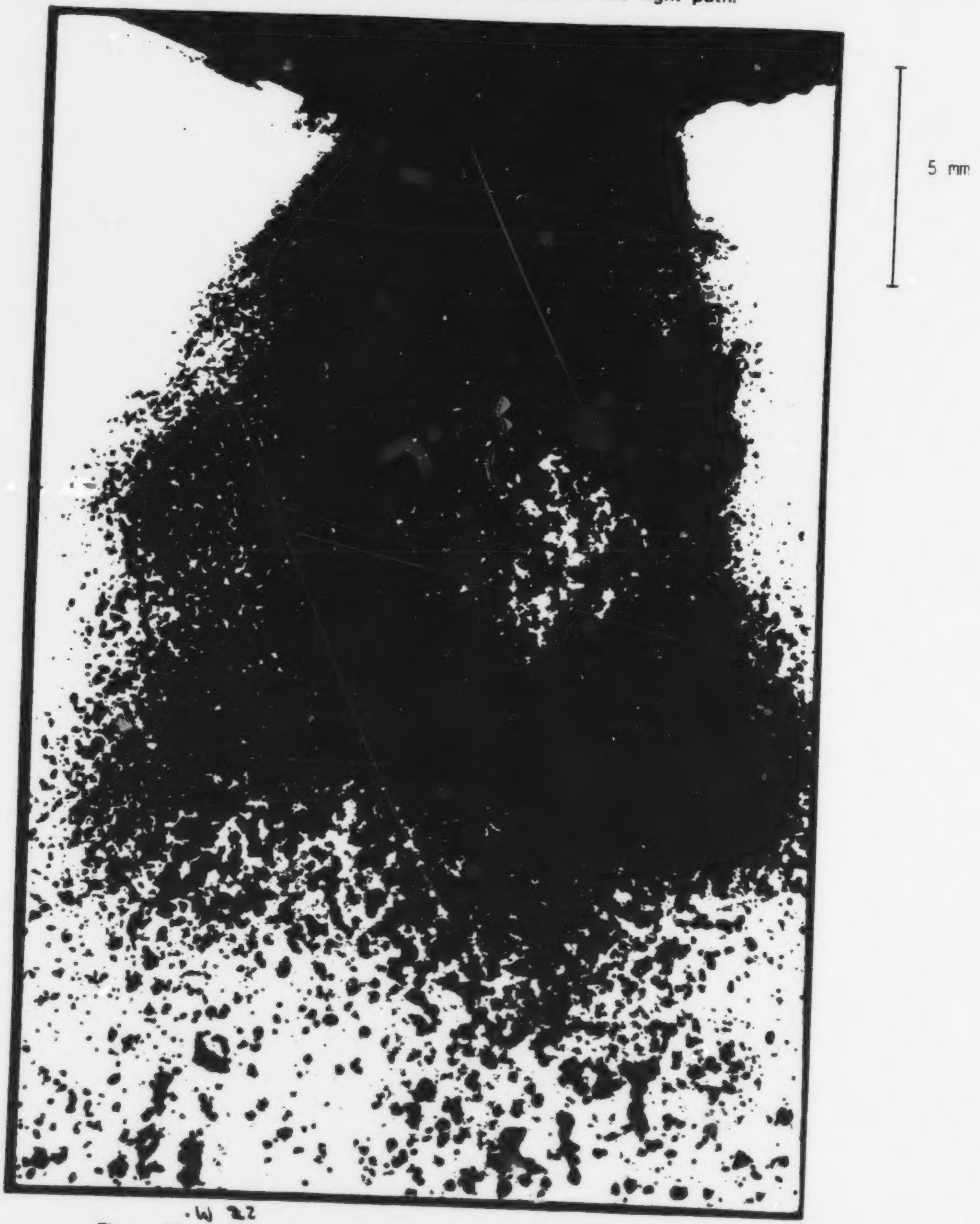

·W 22

Figure 10: Water Spray Produced by the Parker-Hannifin Atomizer
Water: 500 lb/hr, 12 psig; Atomizing Air: 41 psig

11.W.22

·W 22

Figure 11: Water Spray Produced by the Parker-Hannifin Atomizer
Water: 500 lb/hr, 26 psig; Atomizing Air: 153 psig

12.W.22

An analysis of slurry and water sprays from Coen atomizers is also underway. The first photographs were of water sprays from only one of the seven holes in the atomizer endcap. These early photographs determined the light source and film requirements for the later work. Later studies were made of the full spray from the Coen atomizer. Figure 12 shows the Coen atomizer operating at 500 lb/hr slurry flow rate and with an atomizing air pressure of 175 psig. The concentration and direction of the slurry spray by the pattern of holes in the atomizer endcap is clearly evident.

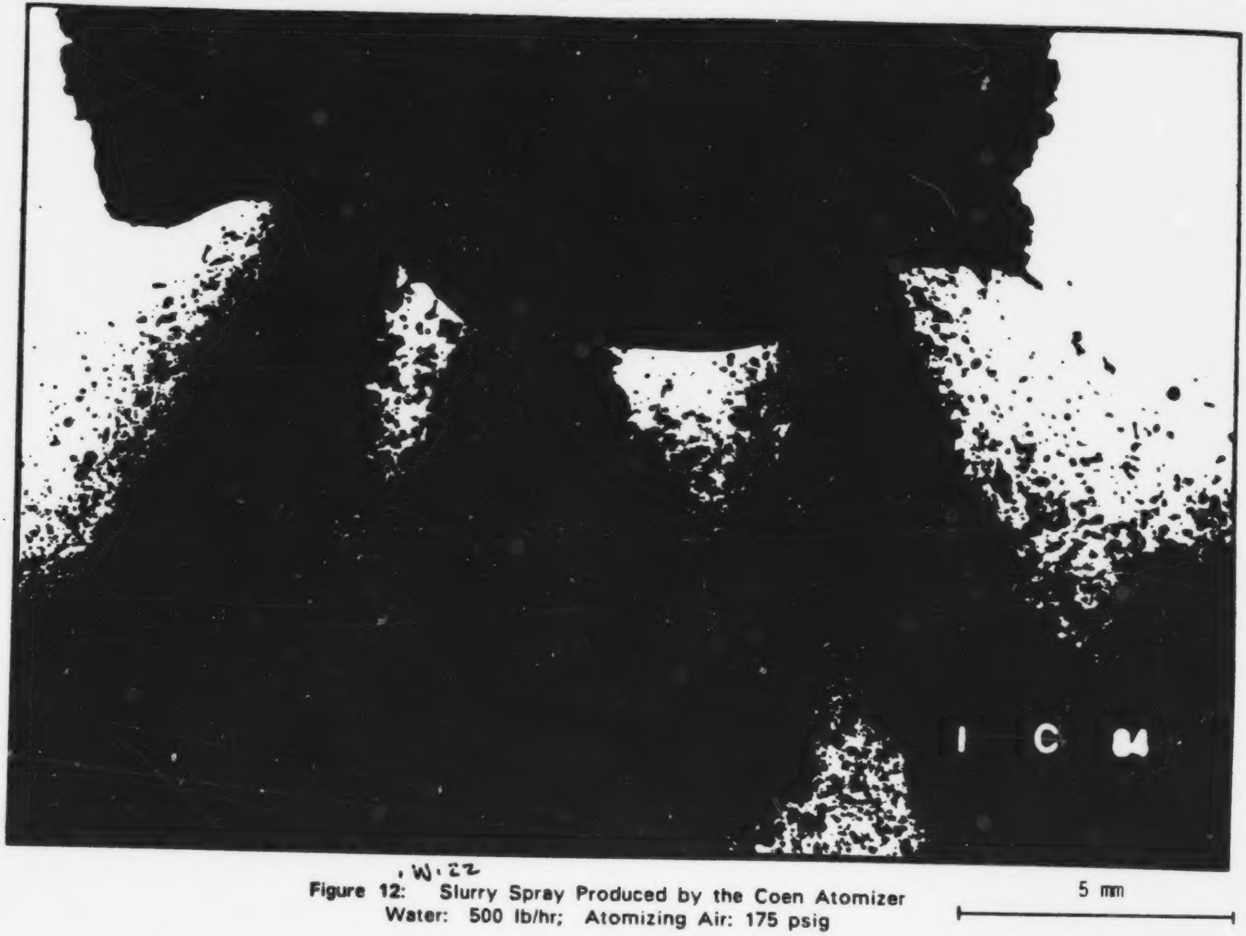

.W.22

Figure 12: Slurry Spray Produced by the Coen Atomizer
Water: 500 lb/hr; Atomizing Air: 175 psig

Motion Pictures

The high-speed movies provide dynamic information about the overall spray structure: the spray angle, spray velocity and the nature of fluctuations or pulsations in the spray. The optical setup is the same as that used for still photography except that continuous light sources (Pallite and/or Koolbeam lights) replace the high-speed flash and the Hycam II movie camera replaces the still camera. Parameters investigated in the photographic work include: film type, camera lens and aperture, lighting, motion picture frame rate, atomizer fuel and air pressures and flow rates.

The Parker-Hannifin counter-swirl atomizer has been studied by high-speed movies at frame rates from 1000 to 10,000 frames/sec. The field of view includes the atomizer tip and the first 13 cm (five in) downstream. Studies of water and slurry sprays were made at two different conditions. The fuel mass flow rate was maintained constant at 500 lb/hr but the atomizing air pressure was varied from 50 psig to 170 psig. The recommended operating conditions for the Parker atomizer are a fuel flow rate of 500 lb/hr and an atomizing air pressure of 175 psig.

1.W.1

The fuels used were supplied by various commercial slurry manufacturers and their properties are recorded in Table 1. Combustion trials and single drop burning experiments are described in the following sections.

Slurry Designation	A	B	C	D	F
COAL					
Ultimate Analysis % wt (dry basis)			*		
Ash	6.17	6.0	3.6	12.35	5.76
C	82.37	80.8	83.48	75.96	?
H	5.20	5.4	5.44	4.68	?
S	0.76	0.87	1.30	1.93	0.58
N	1.38	1.6	1.37	1.35	?
O	4.06	4.8	4.64	3.51	?
Cl	0.06	?	0.17	0.22	0.32
Proximate Analysis % wt (dry basis)					
Ash	6.17	6.5?	1.7	12.35	5.76
V.M.	31.41	32.4	34.0	29.60	38.1
Fixed Carbon	62.42	61.1	64.3	58.05	58.4
Organic Sulphur	?	?	0.65	0.84	?
Pyrite Sulphur	?	?	0.30	1.08	?
Calorific Value MJ/kg	33.69	33.76	34.75	31.66	33.26
B.S. Swelling Index	8	8	9	8½	2
Gray King Coke Type	G6	G9	G8	G8	B
NCB Coal Rank Code	301b	401	501	401	802
SLURRY					
% Solids as delivered	72.8	70.0	72.0	76.1	-
% Solids as fired	70.0	69.8	72.0	72.0	-

* Ultimate analysis before final beneficiation. ? - Analysis not available.

TABLE 1: COAL WATER MIXTURES : PROPERTIES.

Four of the slurries were fired in a 0.5 MW$_t$ combustion facility. They had coal ash contents which varied from over 12 to under 2%. The formulations in terms of particle size distributions and additives were also significantly different from each other. These factors have been taken into account in the analysis of the results.

Various other workers have burnt CWS on similar-throughput combustion facilities (see, for example, Farthing, et al, 1982; Scheffee et al, 1982). Examination of single drop behaviour using various techniques has also been reported (see, for example, Manfred & Ehrlich, 1982; Pourkashanian & Williams, 1983; Yao & Liu, 1983).

The single drop technique is both a rapid and an economical means of assessing fuel behaviour and possesses the considerable merit of enabling drops to be monitored over the whole of their combustion life history. However, its limitations have to be clearly appreciated and care has to be exercised when attempting to use the results obtained and extrapolate them to larger scale conditions.

Our work has enabled us to make comparisons between the single drop data and those obtained from the rig when identical fuels have been fired.

2. EXPERIMENTAL DETAILS.

2.1 Description of the 0.5 MW$_t$ Combustion Facility.

The combustion tests were carried out in a 0.5m diameter, water-cooled, refractory-lined duct fired from one end by a parallel air flow burner, see Figure 2. This facility has been used in the past for investigations into the effect of oil composition and additives on combustion performance (Cunningham & Jackson, 1977) and it was also used to investigate coal-oil dispersion combustion (Conolly & Matthews,1983).

2·W·1

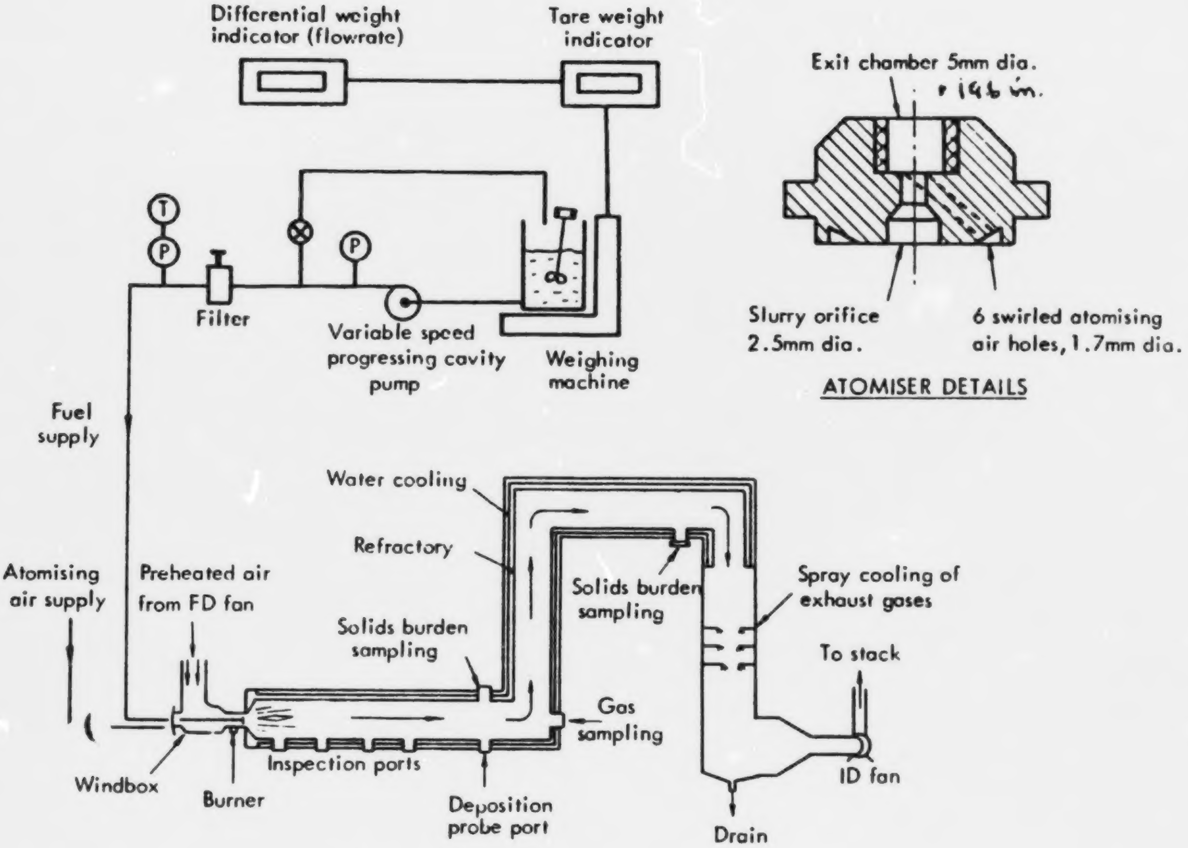
Differential weight indicator (flowrate)
Tare weight indicator
T
P
P
Filter
Variable speed progressing cavity pump
Weighing machine
Fuel supply
Exit chamber 5mm dia.
.196 in.
Slurry orifice 2.5mm dia.
6 swirled atomising air holes, 1.7mm dia.
Water cooling
Refractory
Solids burden sampling
Spray cooling of exhaust gases
To stack
Atomising air supply
Preheated air from FD fan
Solids burden sampling
Gas sampling
Inspection ports
Windbox
Burner
Deposition probe port
ID fan
Drain

ATOMISER DETAILS

W·1

FIGURE 2. 0.5 MW$_t$ COMBUSTION FACILITY

In the present work, the CWS was pumped from a stirred storage drum by a single-stage, progressing-cavity pump which was capable of producing 10 bar pressure. The drum and its contents stood on a sensitive weighing machine so that a digital output of the rate of change of weight could be monitored as the fuel flowrate. A spill return system was provided, but the main flowrate control was by varying the pump speed. The loop was provided with a number of water purge access points and the fuel was fed to the burner through a 40 mesh (419 μm) filter.

The combustion air supply was preheated to either 300 or 400°C for these experiments. The burner incorporated a 10-bladed, swirl-type stabilizer and the atomiser tip was a single-hole, internal-mix, air blast design similar to that used by Babcock & Wilcox in their early CWS firing experiments (Farthing et al, 1982). Initial rapid wearing problems were cured by using a recrystallised alumina insert to form the mixing chamber. The relevant dimensions are given in Figure 2.

Particulates were sampled from the combustion stream at two locations. The first, after about 0.8 seconds mean residence time, was at the end of the horizontal section of the combustion duct where the flame gases had cooled to roughly furnace exit temperature levels (1100-1300°C). The probe used here was oil-cooled to keep the sample gas above its dewpoint and the collecting cyclone and back-up micropore filter were located in an oven kept at 180°C for the same reason.

The second sampling position was after about 2.5 seconds mean residence time, at which point flame gases were generally between 600 and 750°C. The probe used here was uncooled, but lagged to keep the gases above the dewpoint as they passed to a similar collecting system as before.

Solids samples were sieved to determine their particle size distributions. Observations on particle morphology were then made by examining the exterior surfaces of the particles with transmitted and oblique lighting and by mounting them in resin, sectioning and polishing them and examining their interiors by

3 . W . 1

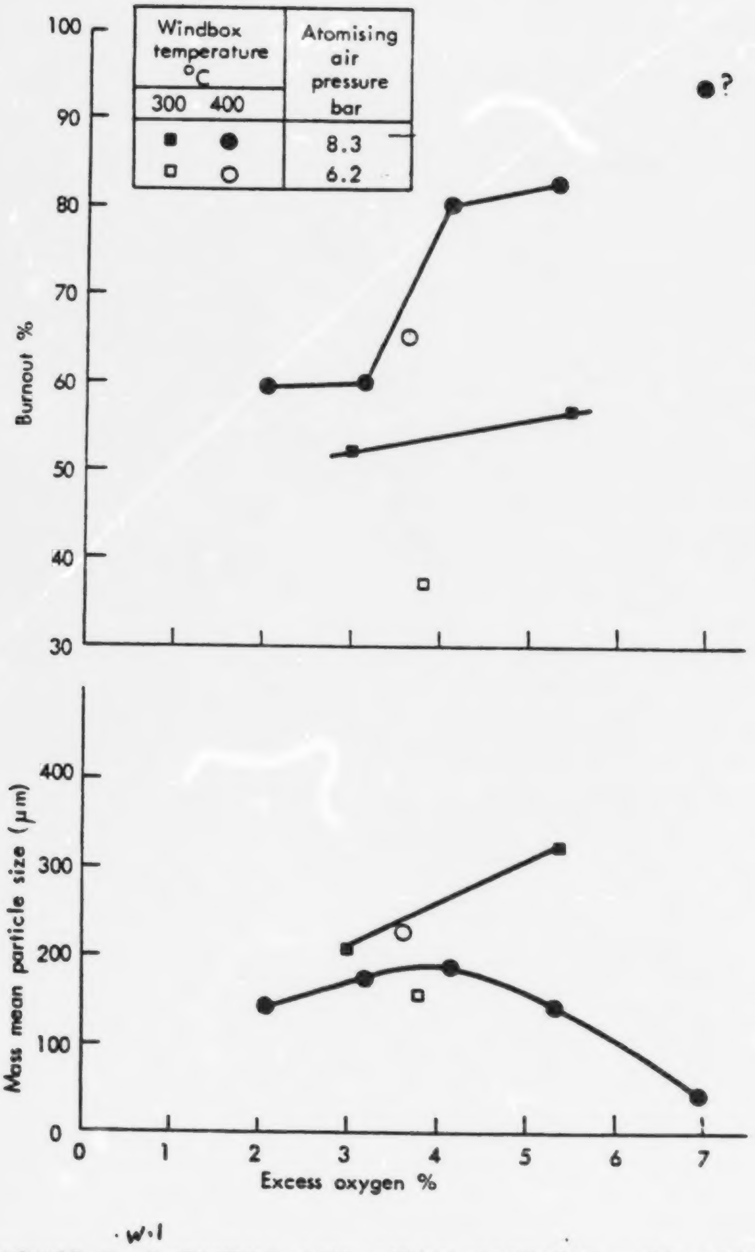

. W . 1

FIGURE 3. BURNOUT AND MEAN PARTICLE SIZE AFTER 0.85 SECONDS - SLURRY B

4·W·1

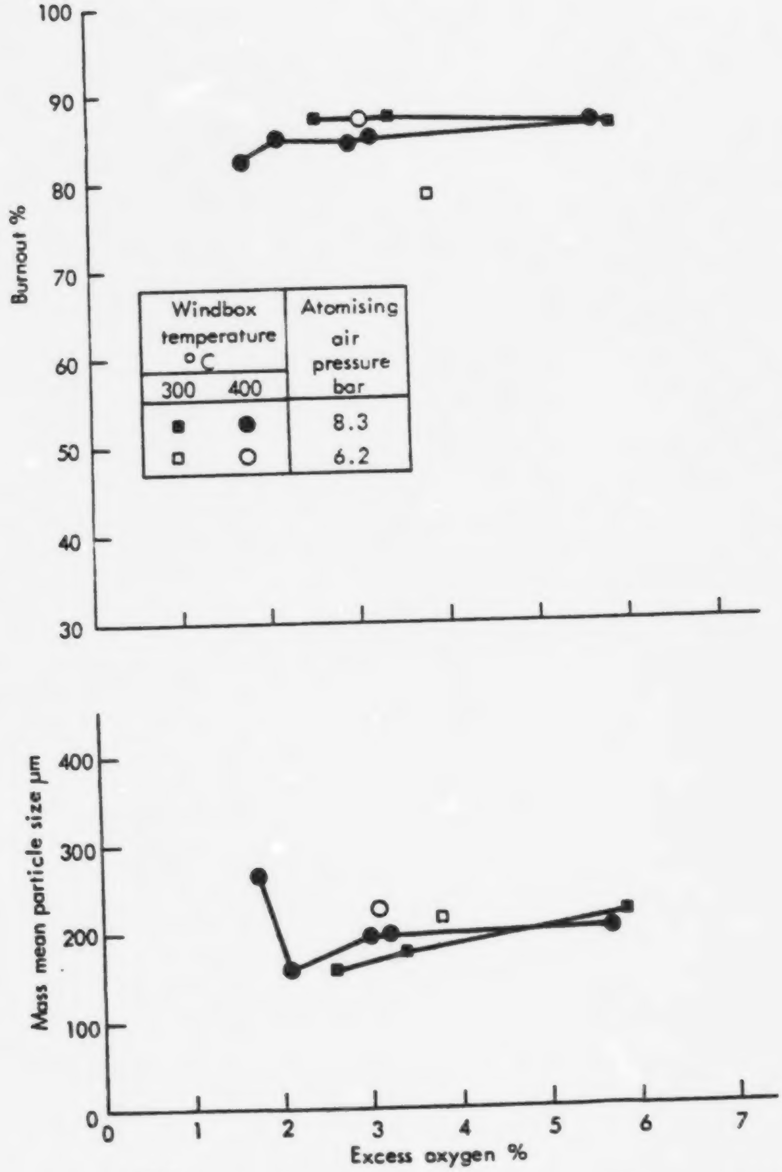

W·1

FIGURE 4. BURNOUT AND MEAN PARTICLE SIZE AFTER 2.5 SECONDS - SLURRY B

5·W·i

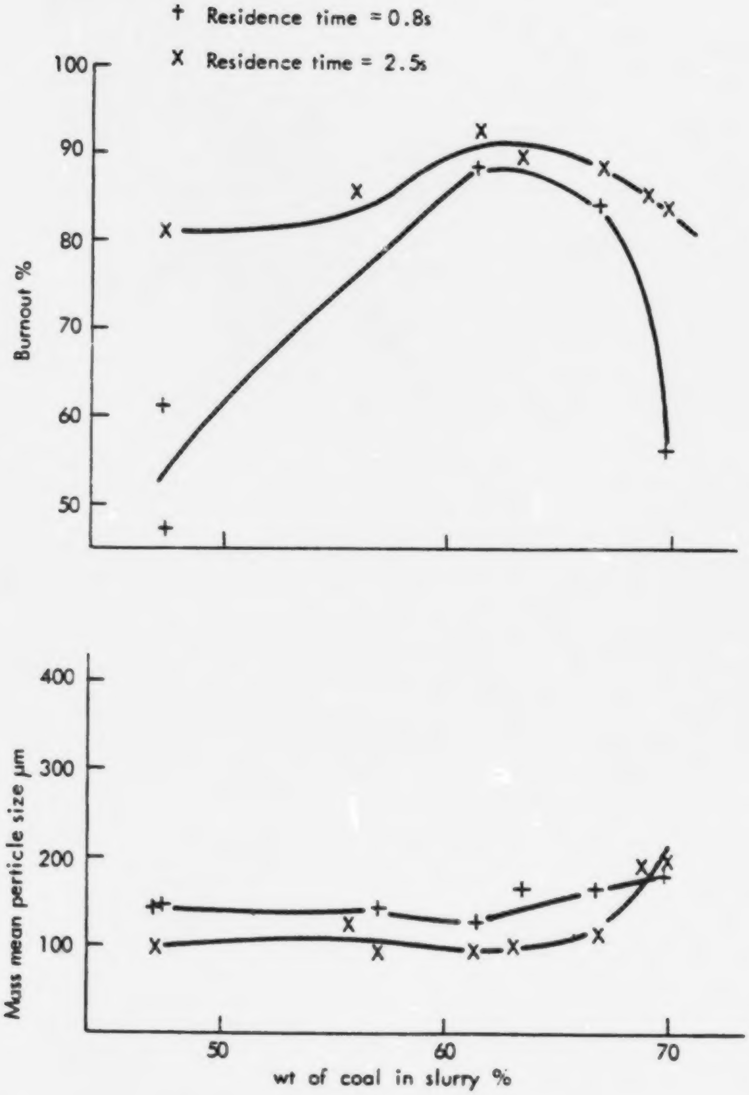

Windbox temp. = 400^{+23}_{-0} °C

Atomising air pressure = 8.3 bar

Excess oxygen = 3.2 ± 0.2 %

W·i

FIGURE 5. EFFECT OF COAL LOADING ON BURNOUT AND MEAN PARTICLE SIZE - SLURRY B

6.W.1

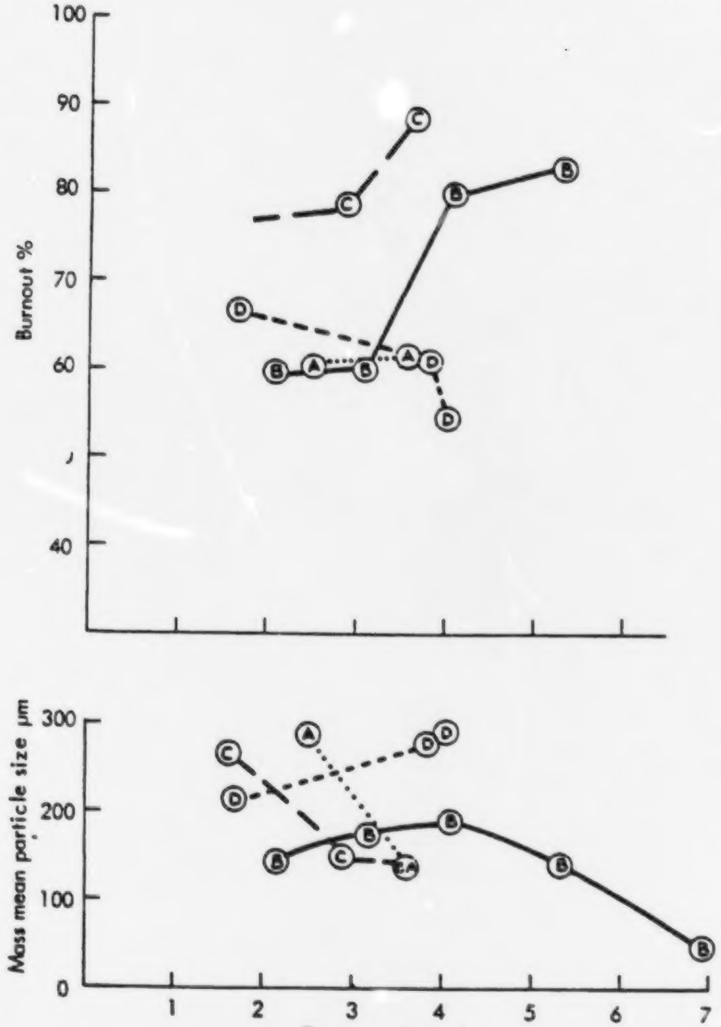

Residence time = 0.8s
Windbox temp = 400°C
Atomising air pressure = 8.3 bar

W.1

FIGURE 6. EFFECT OF SLURRY COMPOSITION ON BURNOUT AND MEAN PARTICLE SIZE

7·W·1

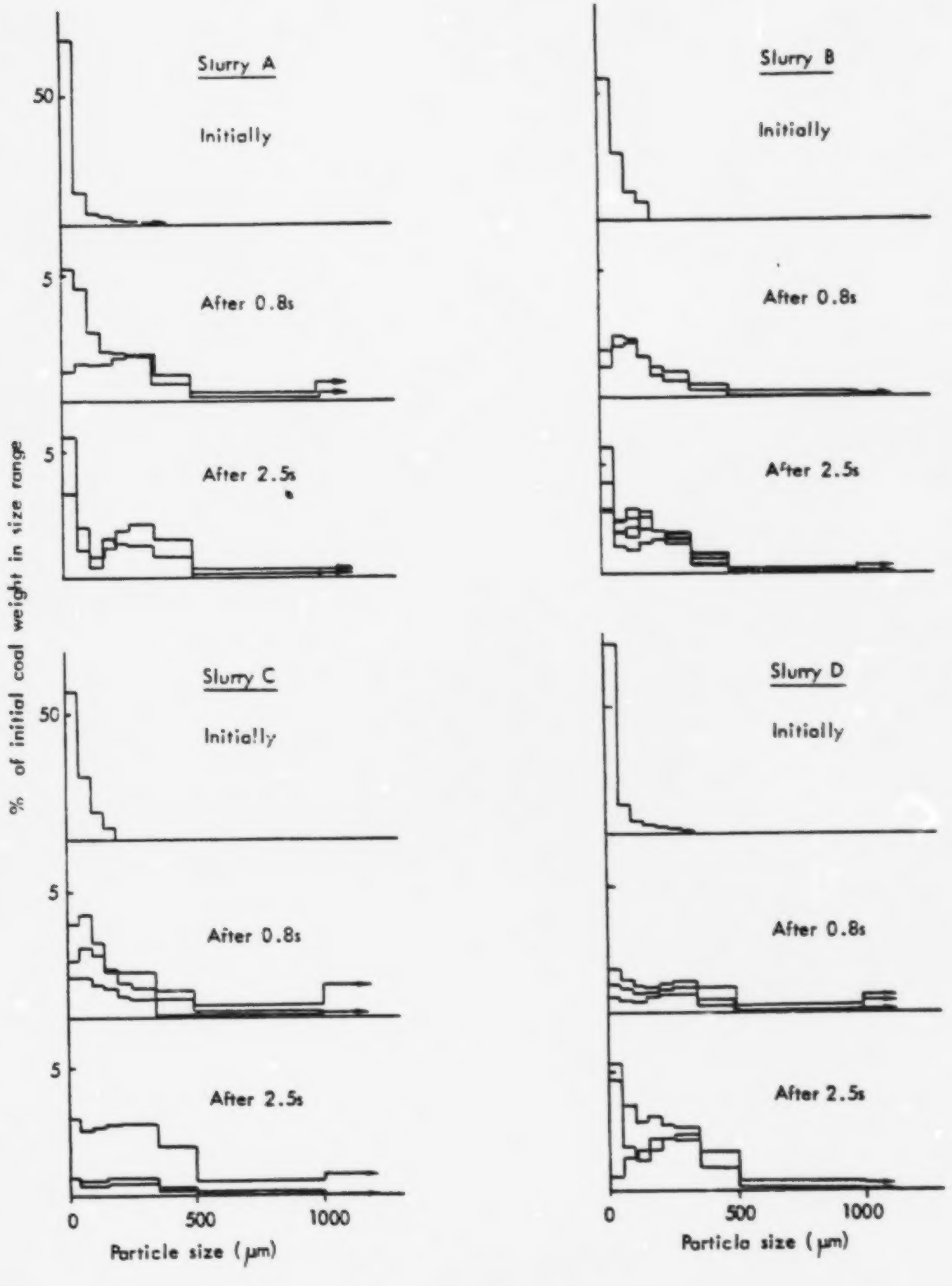

W1

FIGURE 7. PARTICLE SIZE VARIATION WITH TIME

9.W-1

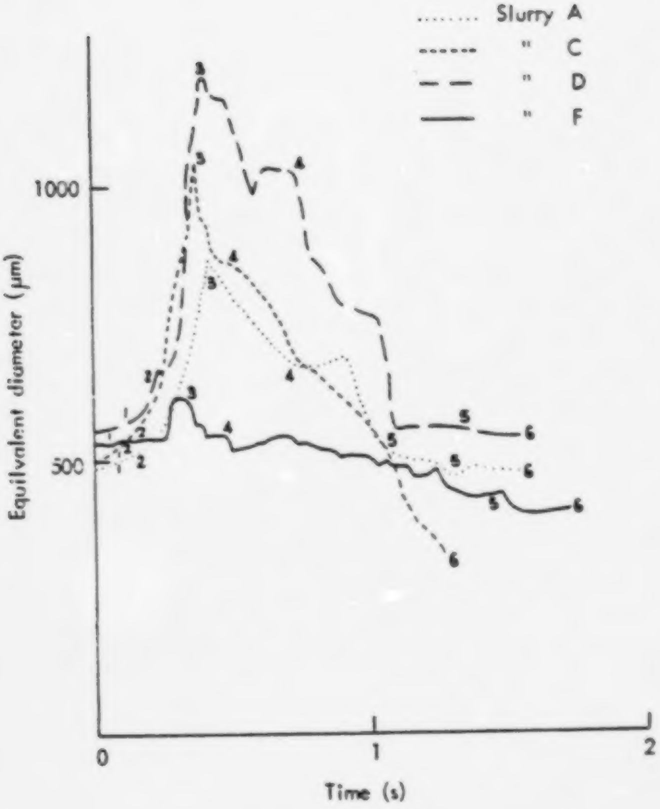

Code
1. Initial volatile release starts
2. Vigorous volatile release starts
3. Volatile release ends
4. First fragment leaves
5. Support fibre visible
6. Oxidation ends

FIGURE 9. W·1 TYPICAL DROP HISTORIES

5-6·W·2

TABLE 5 ·W·2

TYPICAL FPTF OPERATING CONDITIONS DURING LOWER KITTANNING TESTS

TEST	"STD" GRIND P.C LOW FIRING RATE	"STD" GRIND P.C HIGH FIRING RATE	"FINE" GRIND P.C HIGH FIRING RATE	CWM LOW FIRING RATE	CWM HIGH FIRING RATE
Total Heat Input (Btu/Hr)	4.18×10^6	4.63×10^6	4.47×10^6	3.73×10^6	5.00×10^6
Fuel Feed Rate (Lb/Hr)	250	282	275	350	459
Oxygen in Flue Gas (Mole %)	3.9	3.5	3.6	3.5	3.5
Combustion Air Temperature (°F)	1090	990	900	990	1000
Peak Furnace Temperature (°F)	2870	2960	2960	2770	2940
Furnace Residence Time (Seconds)	1.26	0.99	0.91	1.38	0.99
Furnace Outlet Temp. (°F)	2480	2610	2620	2340	2500
Convection Section Gas Temp					
Bank 1 (°F)	2330	2350	2450	2120	2280
Bank 2 (°F)	2160	2230	2290	1960	2130
Bank 3 (°F)	2050	2120	2140	1840	2000
Bank 4 (°F)	1860	1950	1960	1650	1780
Convection Section Gas Velocity					
Bank 1 (ft/sec)	67	74	75	59	82
Bank 2 (ft/sec)	63	71	71	55	78
Bank 3 (ft/sec)	60	68	68	52	74
Bank 4 (ft/sec)	56	63	63	48	67
Waterwall Metal Temp. (°F)	710	710	680	720	720
Convection Probe Temps. (°F)	1100	1100	1100	1100	1100
Erosion Probe Temp. (°F)	800	800	800	800	800

TABLE 6 W2

TYPICAL FPTF OPERATING CONDITIONS DURING SPLASH DAM TESTS

TEST	CWM#2 LOW FIRING RATE	CWM#2 HIGH FIRING RATE	CWM#3 HIGH FIRING RATE	CWM#4 HIGH FIRING RATE
Total Heat Input (Btu/Hr)	3.74×10^6	4.93×10^6	5.02×10^6	4.96×10^8
Fuel Feed Rate (Lb/Hr)	311	405	430	404
Oxygen in Flue Gas (Mole %)	5.0	4.1	3.8	3.1
Combustion Air Temperature (°F)	1010	960	1050	1030
Peak Furnace Temperature (°F)	2860	2980	2900	3030
Furnace Residence Time (Seconds)	1.27	0.93	0.98	0.99
Furnace Outlet Temp. (°F)	2410	2590	2500	2530
Convection Section Gas Temp.				
Bank 1 (°F)	2110	2350	2150	2290
Bank 2 (°F)	1980	2190	1990	2070
Bank 3 (°F)	1870	2020	1840	1880
Bank 4 (°F)	1680	1830	1650	1730
Convection Section Gas Velocity				
Bank 1 (ft/sec)	62	85	79	79
Bank 2 (ft/sec)	59	81	74	73
Bank 3 (ft/sec)	56	75	70	67
Bank 4 (ft/sec)	52	69	64	63
Waterwall Metal Temp. (°F)	670	660	700	780
Convection Probe Temps. (°F)	1100	1100	1100	1100
Erosion Probe Temp. (°F)	800	800	800	800

7·8·9-W·2

TABLE 7·W·2

FPTF TEST RESULTS

COAL, ATOMIZER DROPLET SIZE AND FLY ASH SIZE

TEST IDENTIFICATION	FIRING RATE	FLAME TEMP. (°F)	COAL MMD (μ)	SPRAY DROPLET MMD (μ)	FLY ASH COLLECTED HRS INTO TEST	FLY ASH MMD (μ)	CARBON IN FLY ASH (% WT)	CARBON CONVERSION (%)
P.C. "Std Grind"-L.Kittanning	Low	2870	45	-	(1)	8	1.7	99.9
P.C. "Std Grind"-L.Kittanning	High	2960	40	-	(1)	13	3.2	99.9
P.C. "Fine Grind"-L.Kittanning	High	2960	27	-	(1)	14	2.4	99.9
CWM#1-L. Kittanning	Low	2770	15	86	(1)	9	3.5	99.9
	High	2940	15	88	(1)	14	11.7	99.6
CWM #2 - Splash Dam	High	2920	50	76	5	12	3.5	99.9
	High	2950	50	76	42	15	10.6	99.6
	High	3040	50	76	68	21	18.8	99.3
CWM#3 - Splash Dam	High	2930	25	69	6	10	3.9	99.9
	High	2900	25	69	49	16	14.5	99.5
CWM#4 - Splash Dam	Low	2750	15	61	4(2)	13	5.5	99.9
	High	2800	15	106	4(2)	44	43.5	98.2
	High	2850	15	72	4(2)	27	29.2	98.9
	High	3020	15	72	6	12	9.6	99.7
	High	3150	15	72	74	19	16.6	99.3

(1) - Composite Sample
(2) - Short Term Test

TABLE 8·W·2

LOWER KITTANNING RELATIVE SLAGGING CHARACTERISTICS

TEST FUEL	FIRING RATE	AVERAGE PEAK FLAME TEMP. (°F)	WATERWALL PANEL COVERAGE	DEPOSIT THICKNESS (INCHES)	DEPOSIT PHYSICAL STATE	WW PANEL B HEAT FLUX (BTU/HR.FT^2) BEFORE SOOTBLOWING	AFTER SOOTBLOWING	SLAGGING PERFORMANCE
P.C.("STD")	Low	2870	50%	1/4-1/2	Lightly Sintered	82,820	--	Excellent
P.C.("STD")	High	2960	60%	1/2-3/4	Sintered	44,735	89,470	Very Good
P.C.("FNE")	High	2960	70%	1/2-3/4	Sintered	26,852	95,900	Very Good
CWM #1	Low	2770	10%	<1/8	Powdery	73,235	72,950	Excellent
CWM #1	High	2940	10%	<1/8	Powdery	94,963	94,960	Excellent

TABLE 9 -W·2

SPLASH DAM CWM TESTS

RELATIVE SLAGGING CHARACTERISTICS

TEST FUEL	FIRING RATE	AVERAGE PEAK FLAME TEMP. (°F)	WATERWALL PANEL COVERAGE	DEPOSIT THICKNESS (INCHES)	DEPOSIT PHYSICAL STATE	WW PANEL B HEAT FLUX (BTU/hr.ft^2) BEFORE* SOOTBLOWING	AFTER* SOOTBLOWING	SLAGGING PERFORMANCE
CWM #2	Low	2815	< 10%	< 1/8	Light Powder	68,000	68,000	Excellent
CWM #2	High	2975	30%	1/8 - 1/4	Lightly Sintered	60,000	99,000	Very Good
CWM #3	High	2905	< 10%	< 1/8	Light Powder	88,000	88,000	Excellent
CWM #4	High	3000	30%	< 1/8	Light Powder	84,000	92,000	Very Good
CWM #4	High	3100	60%	1/4 - 1/2	Sintered	-	-	-

*Sootblowing initiated after 40 hours into test

1-W-3

Slurries Used in Combustion Tests

The CWM used for the combustion tests were supplied by Atlantic Research Corporation (ARC) in Alexandria, Virginia. The CWM used in the characterization tests used a West Virginia bituminous coal with a particle size distribution of 87% through 200 mesh and contained about 70% solids including additives. Table 1 shows the coal analysis and selected mixture properties. A different CWM was used for the reactor profile tests. The second slurry was also based on a West Virginia bituminous coal with a particle size distribution of 87% through 200 mesh, and as-received, contained 73.5% solids (including additives). The coal analysis and mixture properties of this West Virginia coal are also shown in Table 1. This CWM was diluted with water to reduce the total solids loading to 70% solids before testing. Additive types used in both CWM are proprietary to ARC and were not given.

TABLE 1 W-3

COAL-WATER MIXTURES USED IN COMBUSTION CHARACTERIZATION AND MAPPING TESTS[1]

Coal Analysis	Mont [2] CWM	Moss-1 - CWM[3]
Proximate	wet basis	dry basis
Moisture	1.45	--
Ash	4.68	6.17
Volatile Matter	31.84	31.41
Fixed Carbon	62.03	62.43
Heating Value (kJ/kg)	33,888	33,677
Ultimate, % (dry basis)		
Carbon	83.57	82.37
Hydrogen	5.18	5.20
Nitrogen	3.87	1.38
Chlorine	0.14	0.06
Sulfur	0.90	0.76
Ash	4.75	6.17
Oxygen	3.59	4.06
Slurry Analysis		
Solids loading, %	70.4	73.5
Particle Size	87%-200 mesh	87%-200 mesh
Visocity (25°C)	1150 cp @ 88 sec $^{-1}$	2300 cp @ 100 sec $^{-1}$
Stabilizer/Additives	1%	1%

---

[1] CWM provided by Atlantic Research Corporation

[2] Slurry used for combustion characterization tests.

[3] Slurry used for combustion maps; diluted to 70% total solids before testing.

CWM Combustion Characterization Tests

Sixteen characterization tests, including four repeated tests to determine reproduceability, were conducted with stoichiometric ratios (SR) ranging from 0.8 to 1.4 and swirl numbers ranging from 0 to 3.0 to determine conditions of maximum burnout. The CWM and atomizing air feed rates were held fixed at 40 kg/hr and 46 kg/hr, respectively while the preheated secondary air flow was varied from about 220 to 430 kg/hr to achieve the range in SR values. Char samples were collected in the end section of the reactor about 2 meters from the nozzle tip, at a radial position halfway between the reactor centerline and wall, and analyzed for carbon conversion.

Test Results. Increasing stoichiometric ratio increased coal burnout for all swirl numbers, up to an SR of about 1.15. At SR's above 1.15, the coal burnout decreased, presumably due to the observed lower gas temperature, reduced stability of the CWM flame, and to reduced particle residence time. At an SR of 1.4 with no swirl, a stable CWM flame could not be sustained in the reactor.

Figure 7 shows the dramatic increase in coal burnout as the secondary stream swirl number (SN) was increased from 0 to 1.5. Swirl number was not significantly beneficial to coal burnout at swirl numbers above 1.5.

2·W·4

Table 2 · W·4

MIT Coal-Water Slurry Trials

Summary of Input and Operating Conditions of Selected Flames

CRF Run No.	89	97	306[3]	307	308	309	310A	310B
Fuel[1]	F1	F1	F2	F2	F2	F3	F2	F3
Fuel Firing Rate, MW_{th}	1	1	1	1	1	1	1	1
Flame Type, Unstaged or Staged	Unstaged	Unstaged	Unstaged	Staged	Staged	Unstaged	Unstaged	Unstaged
Burner Quarl, Angle of Divergence,	25°	25°	0° (Non Divergent)	0°	0°	0°	0°	0°
Burner Throat Diameter at Narrowest Point, mm	126	176	176	176	176	176	176	176
Atomizer Type	Peabody	Peabody	OR-KVB	OR-KVB	OR-KVB	OR-KVB	OR-KVB	OR-KVB
Combustion Air Swirl No., S	1.8	2.8	2.8	2.8	2.8	2.8	0.68, 1.2, 1.8, 2.8	2.8
Excess O_2, %	2	2	2	2	2	2	2	2
Combustion Chamber Heat Sink Configuration: No of 0.3 m Wide Furnace Sections:								
Water-Cooled Refractory Lined	14	11	14	14	14	14	14	14
Water-Cooled Bare Metal	-	3	-	-	-	-	-	-
Total	14	14	14	14	14	14	14	14
Secondary Air Injection Point, m from Burner Front Wall	-	-	-	2.9	2.9	-	-	-
Mode of Secondary Air Injection, T = tangential, R = radial	-	-	-	T	T	-	-	-
Primary Zone Fuel Equivalence Ratio, ϕ_P	-	-	-	1.2, 1.3, 1.5, 1.7	1.3	-	-	-
Effective Enrichment of Comb. Air, %	-	-	-	-	-	-	0, 1, 2, 3	2
Fuel Pressure, atm.	8.5-10.5	7.8-10.5	13.3-18.0	13.3-18.0	13.3-18.0	16.7-18.0	13.3-17.0	13.3-17.0
Atomizer Air Pressure, atm.	9.2	8.5	14.6	14.6	14.6	14.6	14.6	14.6
Fuel Temperature, °C	24	24	25	25	25	25	25	24
Air Temperature, °C	260	260	230	230	230	230	20, 230	230
Measurements - Level of Detail: M1, M2, M3[2]	M2	M2	M3	M1	M3	M3	M1	M2
Percentage Coal in Slurry	68	68	68	68	68	64	66	64

---

1. F1 = Occidental Research Corp. Bimodal Slurry, 83% < 75 μm
   F2 = OR Unimodal Slurry, 72% < 75 μm
   F3 = OR Fine Slurry, 95% < 45 μm, 98% < 75 μm

2. M1 = Scoping (Visual, Photographs, Cine Film, Exit Gas Composition
   M2 = Axial In-flame Measurements
   M3 = Detailed Map (Axial and Radial Measurements)

3. Run 306 A: swirl varied, S = .68 - 2.8
   Run 306 B: No. 2 fuel oil flame at same conditions as Run 306-306A

2.W.2

TABLE 2 ·W·2

LOWER KITTANNING FPTF TEST FUEL ANALYSES

TEST FUEL	PULVERIZED COAL			OIL	CMM #1	
	LOWER FIRING RATE "STD" As Received	HIGH FIRING RATE "STD" As Received	HIGH FIRING RATE "FINE" As Received	45% #6 55% #2	LOW FIRING RATE As Received	HIGH FIRING RATE As Received
Proximate, Wt. %						
Moisture (Total)	1.5	1.8	1.7	0.2	34.2	33.9
Volatile Matter	34.8	34.1	34.4	N/A	22.3	22.4
Fixed Carbon (Diff)	58.0	58.4	57.7	N/A	39.7	39.7
Ash	5.7	5.7	6.2	0.02	3.8	4.0
Total	100.0	100.0	100.0	--	100.0	100.0
HHV, Btu/lb	13705	13750	13650.	19025.	8850.	9000.
LB Ash/MM Btu	4.2	4.1	4.5		4.3	4.4
Ultimate, Wt. Percent						
Moisture (Total)	1.5	1.8	1.7	0.2	34.2	33.9
Hydrogen	4.9	4.9	4.9	11.	3.1	3.1
Carbon	77.9	77.3	77.2	85.9	50.3	50.7
Sulfur	0.7	0.7	.8	1.6	.7	.7
Nitrogen	1.4	1.4	1.4	0.3	1.2	1.0
Oxygen (Diff)	7.9	8.2	7.8	0.5	6.7	6.6
Ash	5.7	5.7	6.2	0.02	3.8	4.0
Total	100.0	100.0	100.0	100.0	100.0	100.0
Ash Fusibility, °F						
I.T.	2410.	2380.	2700.+	Carbon Residue	2320.	2240.
S.T.	2700.	2700.	2700.+	(Wt. Percent)	2700.+	2700.+
H.T.	2700.+	2700.+	2700.+	1.58	2700.+	2700.+
F.T.	2700.+	2700.+	2700.+		2700.+	2700.+
Ash Composition, Wt. %				Viscosity @ 77°F		
SIO2	62.2	63.1	64.3	91.0(SSU)	61.8	61.6
AL2O3	26.3	26.3	25.8		24.1	25.0
FE2O3	6.0	5.6	5.6	Specific Gravity	7.8	7.6
CAO	1.1	1.2	1.1	0.91	1.3	1.2
MGO	0.5	0.5	.5		.6	.5
NA2O	0.6	0.5	.4		.7	.6
K2O	1.0	1.0	1.1	Deg. Api	1.3	1.4
TIO2	1.1	1.3	1.2	24.0	1.8	1.7
SO3	0.9	1.1	.6		.6	.4
Total	100.4	100.1	100.6		100.0	100.0

TABLE 3 · W·2

SPLASH DAM FPTF TEST FUEL ANALYSES

Test Fuel	CWM #2		CWM #3	CWM #4
	LFR	HFR	HFR	HFR
	As Received		As Received	As Received
Proximate, WT. %				
Moisture (Total)	32.1	30.6	34.0	30.0
Volatile Matter	21.1	21.0	19.7	19.6
Fixed Carbon (Diff)	42.9	44.4	42.3	46.4
Ash	3.9	4.0	4.0	4.0
Total	100.0	100.0	100.0	100.0
HHV, Btu/lb	9,830.0	10,125.0	9,455.0	10,170.0
LB Ash/MM Btu	4.0	3.9	4.2	3.9
Ultimate, Wt. Percent				
Moisture (Total	32.1	30.6	34.0	30.0
Hydrogen	3.2	3.4	3.3	3.4
Carbon	55.3	56.8	53.2	57.1
Sulfur	0.5	0.5	0.6	0.6
Nitrogen	1.0	1.0	1.1	1.1
Oxygen (Diff)	4.0	3.7	3.8	3.8
Ash	3.9	4.0	4.0	4.0
Total	100.0	100.0	100.0	100.0
Ash Fusibility, °F				
I.T.	2,430	2,390	2,250	N/A
S.T.	2,700	2700+	2700+	N/A
H.T.	2700+	2700+	2700+	N/A
F.T.	2700+	2700+	2700+	N/A
Ash Composition, Wt. %				
SIO2	58.4	57.1	55.7	N/A
AL2O3	27.9	27.2	27.3	N/A
FE2O3	6.6	7.4	7.4	N/A
CAO	1.3	0.9	1.5	N/A
MGO	0.9	0.8	0.8	N/A
NA2O	0.9	0.8	1.1	N/A
K2O	2.3	2.1	2.2	N/A
TIO2	2.2	2.1	1.6	N/A
SO3	0.4	1.4	1.2	N/A
TOTAL	100.9	99.8	98.8	N/A

N/A Data Not available at time of printing.

S·W·2

TABLE 5 W·2

TYPICAL FPTF OPERATING CONDITIONS DURING LOWER KITTANNING TESTS

TEST	"STD" GRIND P.C LOW FIRING RATE	"STD" GRIND P.C HIGH FIRING RATE	"FINE" GRIND P.C HIGH FIRING RATE	CWM LOW FIRING RATE	CWM HIGH FIRING RATE
Total Heat Input (Btu/Hr)	4.18×10^6	4.63×10^6	4.42×10^6	3.73×10^6	5.00×10^6
Fuel Feed Rate (lb/Hr)	250	282	275	350	459
Oxygen in Flue Gas (Mole %)	3.9	3.5	3.6	3.5	3.5
Combustion Air Temperature (°F)	1090	990	900	990	1000
Peak Furnace Temperature (°F)	2870	2960	2960	2770	2940
Furnace Residence Time (Seconds)	1.26	0.99	0.91	1.38	0.99
Furnace Outlet Temp. (°F)	2480	2610	2620	2340	2500
Convection Section Gas Temp					
Bank 1 (°F)	2330	2350	2450	2120	2280
Bank 2 (°F)	2160	2230	2290	1960	2130
Bank 3 (°F)	2050	2120	2140	1840	2000
Bank 4 (°F)	1860	1950	1960	1650	1780
Convection Section Gas Velocity					
Bank 1 (ft/sec)	67	74	75	59	82
Bank 2 (ft/sec)	63	71	71	55	78
Bank 3 (ft/sec)	60	68	68	52	74
Bank 4 (ft/sec)	56	63	63	48	67
Waterwall Metal Temp. (°F)	710	710	680	720	720
Convection Probe Temps. (°F)	1100	1100	1100	1100	1100
Erosion Probe Temp. (°F)	800	800	800	800	800

TABLE 6 W·2

TYPICAL FPTF OPERATING CONDITIONS DURING SPLASH DAM TESTS

TEST	CWM#2 LOW FIRING RATE	CWM#2 HIGH FIRING RATE	CWM#3 HIGH FIRING RATE	CWM#4 HIGH FIRING RATE
Total Heat Input (Btu/Hr)	3.74×10^6	4.93×10^6	5.02×10^6	4.96×10^8
Fuel Feed Rate (Lb/Hr)	311	405	430	404
Oxygen in Flue Gas (Mole %)	5.0	4.1	3.8	3.1
Combustion Air Temperature (°F)	1010	960	1050	1030
Peak Furnace Temperature (°F)	2860	2980	2900	3030
Furnace Residence Time (Seconds)	1.27	0.93	0.98	0.99
Furnace Outlet Temp. (°F)	2410	2590	2500	2530
Convection Section Gas Temp.				
Bank 1 (°F)	2110	2350	2150	2290
Bank 2 (°F)	1980	2190	1990	2070
Bank 3 (°F)	1870	2020	1840	1880
Bank 4 (°F)	1680	1830	1650	1730
Convection Section Gas Velocity				
Bank 1 (ft/sec)	62	85	79	79
Bank 2 (ft/sec)	59	81	74	73
Bank 3 (ft/sec)	56	75	70	67
Bank 4 (ft/sec)	52	69	64	63
Waterwall Metal Temp. (°F)	670	660	700	780
Convection Probe Temps. (°F)	1100	1100	1100	1100
Erosion Probe Temp. (°F)	800	800	800	800

3·W·4

Table 3 ·W·4

Analytical Data on the Occidental Research Corp.
Experimental Coal-Water Slurry Fuels*

Characteristics of the Parent Coals

Moisture, wt % as received	1.01
Proximate Analysis wt %, dry	
Ash	4.88
Volatiles	33.72
Fixed Carbon	61.40
Sulfur	0.72
Heating Value Btu/lb, Dry	14,500
Ultimate Analysis wt %, dry	
Carbon	81.85
Hydrogen	5.27
Nitrogen	1.57
Chlorine	0.12
Sulfur	0.71
Ash	4.78
Oxygen (diff.)	6.15
Ash Mineral Composition wt %	
Silica	50.92
Alumina	32.78
Ferric Oxide	4.70
Titania	1.76
Lime	1.24
Magnesia	0.74
Sulfur Trioxide	0.58
Potassium Oxide	1.26
Sodium Oxide	0.77
Phos. Pentoxide	0.03
Undetermined	1.24
Grindability	NA
Ash Fusibility, °F	
I.D. 2700+	
Softening (H = W)	2700+
Softening (H = W/2)	2700+
Fluid	2700+

Characteristics of the CWS Fuels

	Bimodal Std. Particle Size Slurry	Unimodal Std. Particle Size Slurry	Fine Particle Size Slurry
% Solids	68.0	70.5	68.8
Coal Particle Size			
% < 75 µm	83	72	98
% < 45 µm	72	60	95
Mass median, µ	22	32	18
Apparent Viscosity cp, @ shear rate			
10 sec^{-1}	3570	6308	3062
110 sec^{-1}	1352	2905	2320
2500 sec^{-1}	-	719	2270
5000 sec^{-1}	-	600	1860
10000 sec^{-1}	-	588	1530

(Viscosity determined in 10 sec^{-1} shear rate range by Brookfield viscometer, "D" spindle, 30 rpm, in the 110 sec^{-1} shear range by Haake Rotovisco viscometer, and in the 3000+ sec^{-1} shear range by Burrell rheometer)

* Analyses of experimental fuels provided by Occidental Research Corp.

4.0 Mechanisms of NO Formation

The mechanistic pathways of nitrogen oxides formation in fossil fuel combustion are shown in Figure 5. 'Thermal' NO is formed from molecular nitrogen (N_2) in the combustion air via the Zeldovich mechanism, which involves a set of 3 elementary reactions (Table 4). Rates of formation of NO by this mechanism become noticeable at about 1540°C; thermal NO also increases with increasing oxygen concentration. The Zeldovich mechanism has been found to adequately model NO formation in non-hydrocarbon flames and also in fuel-lean and slightly fuel-rich (ϕ_b < 1.2) flames of nitrogen-free hydrocarbon fuels.

Fuel-derived NO is formed through a more complicated pathway. In the case of the homogeneous gas phase reactions (Fig. 5, Table 4), heterocyclic nitrogen compounds evolved from the fuel droplet rapidly decompose to cyanogens (HCN, CN). These in turn are oxidized to oxycyanogens (OCN, HNCO) which are then converted to the ammonia species or amines (N, NH, NH_2, NH_3). In the final steps of the bound nitrogen reaction sequence, the amines follow two competing parallel routes, one in which N_2 is formed by reaction with NO and the other in which they are oxidized by O or OH to NO. There are also a number of hydrocarbon-fragment/NO reactions (Table 4) which can result in the reduction of the latter to N_2.

In addition to the homogeneous gas phase reactions, a number of heterogeneous processes can take place which result in the conversion of the fuel-nitrogen to NO (oxidation of the fuel-nitrogen in the unburned residue) or to N_2 (reduction of NO in the gas phase by direct reaction with carbon in the residue or by various carbon-catalyzed gas phase reactions).

1·W·6,

concentrations can be achieved.

- Measurements on a series of sieved fractions of Pittsburgh Seam #8 suggest that the maximum achievable solids concentration decreases with decreasing median particle size. The cause of this unexpected result is unknown. However, as expected, increased particle size distribution width increases the maximum attainable solids concentration. T1

- The relative viscosity of coal slurries was found to be independent of temperature over the range 10° to 50°C. Similarly, changes in sedimentation rate between 10° and 60°C could be accounted for by changes in the density and viscosity of water.

([illegible]) ([illegible])

T2 From this summary of slurry behavior without additives it can be seen that among the possible functions of additives are the improvement of wetting, the modification of particle surface charge and therefore of slurry behavior, the creation of three-dimensional structure to prevent sedimentation in a slurry with a high surface charge, or the inducement of weak flocculation to increase median particle size and maximum solids concentration. The four additives used in this study provide illustrations of several of these possible effects.

Experimental

The four coals were obtained from the Pittsburgh Energy Technology Center of the Department of Energy ground nominally to 100% <100 mesh. Proximate and ultimate analyses of Pittsburgh Seam #8 were provided by the Pittsburgh Energy Technology Center. Proximate analyses of the other coals were performed by Conti Testing Laboratory. Median particle size was determined by sieve analysis and with a Coulter electronic particle counter. Some properties of the coal powders are shown in Table 1.

W·6

Table 1. Coal Analyses

	Pittsburgh Seam #8	Illinois #6	San Juan	Hiawatha
Proximate Analysis				
Moisture	1.7%	5.31%	10.09%	8.26%
Ash	10.9 %	9.74%	22.15%	7.51%
Fixed Carbon	50.5%	...	...	...
Sulphur	2.0%	3.80%	0.79%	0.80%
Volatiles	36.9 %	42.3 %	35.8%	43.7%
Heating Value, btu	12,802	11,822	8,976	11,596
Ultimate Analysis				
H	5.1%			
C	71.3%			
N	1.2%			
S	2.0%			
O	9.5%			
Ash	10.7 %			
Size Distribution	100% <100 mesh	95% <100 mesh	93% <100 mesh	95% <100 mesh
Median Diameter				
By Coulter counter	41 μm	57 μm	55 μm	56 μm
By Sieving	43 μm	57 μm	58 μm	65 μm

The analysis of soluble ions was performed on the supernatant liquid filtered from a 10%(wt) slurry of the particular coal which had been allowed to stand for four days with intermittent stirring. Cation analyses by atomic adsorption were performed by N.U.S. Corporation, Pittsburgh, PA, and the volumetric analysis for anions was done by the Water Chemistry Laboratory of the Civil Engineering Department of Carnegie-Mellon

2.W.6.

University. The pH of slurries was measured with a Corning meter. The critical surface tension for wetting was determined by a modified Walker wettability test(10) as described by Glanville and Wightman(11), using mixtures of methanol and water.

Slurries were mixed using a Sunbeam high-speed blender to combine weighed quantities of coal powder and fluid, either distilled water or surfactant solution. All slurries were mixed for four minutes in the blender, at the slowest speed for preparation of sedimentation samples, and at the highest speed for preparation of the usually more concentrated samples used for electrophoresis and rheology experiments. Measurements were made at room temperature.

Measurements of electrophoretic mobility of 50%(wt) slurries were made using a Mass Transport Analyzer (Micromeritics). Rheological measurements were made using a Brookfield digital viscometer, model HBTD, with a water-jacketed small sample adapter. Sedimentation rate and final settled volume were determined visually in 100-ml graduated cylinders using 20%(wt) slurries. This loading was used for sedimentation experiments because the precision is greatest in this concentration range. The 50% loading which was the concentration most suitable for the determination of electrophoretic mobility in concentrated slurries was also used for most rheological measurements. Surface tensions were obtained with a Cenco DuNouy ring tensiometer. Before surface tensions of slurry supernatants were measured, the samples were centrifuged to remove all solid particles.

The four surfactants, Triton X-100 (Rohm and Haas), CTAB (Fisher), SDS (manufactured by British Drug House and obtained from Gaillard and Schlesinger), and Aerosol OT (from American Cyanamid) were used without further purification.

Results

The results of analyses of slurry supernatant for inorganic ions dissolved from the coal surface are given in Table 2. The natural pH of slurries of each coal, which was independent of coal loading, and the critical surface tension for wetting determined with mixtures of methanol and water are given for each coal in Table 3.

.W.6

Table 2. Soluble Inorganic Ions in Slurry Supernatant

	Pittsburgh Seam #8	Illinois #6	San Juan	Hiawatha
Ion	mEquivalents/dm^3	mEquivalents/dm^3	mEquivalents/dm^3	mEquivalents/dm^3
Sodium	0.4	3.1	2.0	0.5
Potassium	0.1	0.1	0.1	0.1
Magnesium	6.2	0.4	1.0	1.1
Calcium	1.5	10.0	9.4	2.2
Iron, as Fe^{+3}	3.0	0.5	<0.001	0.01
Aluminum	0.5	<0.01	<0.01	<0.01
Silicon	0.6	0.2	0.3	0.7
Sulfate	7.0	11.0	10.0	2.9
Chloride	1.1	1.7	1.4	1.9
Nitrite and nitrate	<0.01	<0.01	<0.01	<0.01

Table 3. Natural pH and Critical Surface Tension for Wetting of the Coals

	Pittsburgh Seam #8	Illinois #6	San Juan	Hiawatha
Natural pH of slurry	3.0	4.1	6.3	5.2
Critical surface tension for wetting in methanol/water	mN/m	mN/m	mN/m	mN/m
As received	38.1	50.3	43.2	37.4
Washed	45.3	48.7	53.0	44.6

5.W6

W.6

Table 5. Surface Tension of Slurry Supernatants as a Function of Time

Surfactant	Coal	Surfactant Concentration (µmol/gm coal)	Initial pH	Time (days)	Surface Tension (mN/m)
Triton X-100	Pittsburgh #8	5.8	6.4	104	39
		6.9	2.8	0	32
		"	"	1	34
		"	"	7	36
		"	"	15	38
		11.5	2.8 and 6.4	0-104	31
	Illinois #6	12.9	3.5	53	70
		17.2	3.5	53	66
"		12.9	7.8	52	70
		17.2	7.6	52	65
	San Juan	4.3	6.1	56	71
		5.8	6.2	0	32
		"	"	7	37
		"	"	46	41
		11.6	"	0-45	31
CTAB	Pittsburgh #8	5.5	2.8	107	63
		11.9	"	0	37
		"	"	1	39
		"	"	14	42
		23.8	"	14	38
		47.6	"	0-14	36
		9.9	6.5	106	51
		19.8	8.3	106	43
		29.7	7.2	106	31
	Illinois #6	4.9	4.0	0	65
		"	"	1	71
		9.9	3.5	0	59
		"	"	1	70
		19.8	"	0	56
		"	"	1	65
		"	"	7	68
		29.6	3.3	61	67
		29.6	7.9	60	66
	San Juan	7.4-29.6	6.3	55	71

1·W·9

3. RESULTS AND DISCUSSION

3.1 Identification of Suspension Type

Figure 2 shows the Terminal Sediment Volumes for the three types of slurries at various solids concentrations expressed in percent weight. The black areas indicate the terminal sediment formed from settled coal particles, the white areas on top indicate clear liquid and the dotted areas dilute suspensions of non-settled coal particles.

The above clues lead to the following conclusions:

a) The slurries containing LIPAL 12A were aggregatively stable at all concentrations. This is deduced from the fact that the fines did not agglomerate and remained in suspension after the particles which are larger than 1 to 2 μm have settled.

b) On the other hand the slurries with no additives agglomerated at all concentrations. There were no fines to remain in suspension. They agglomerated.

c) The slurries containing AEROSOL OT were aggregatively stable up to concentrations of 55% solids. At higher concentrations, however, they agglomerated.

The above conclusions are confirmed by the TSV values. As is demonstrated in Fig. 1 stable suspensions give low TSV and the TSV increases as the agglomeration becomes more pronounced.

It can be concluded therefore that the three prepared slurries represent three typical suspension types: an aggregatively stable (LIPAL 12A), an agglomerating one (No additive) and an intermediate (AEROSOL OT).

3.2 Viscosity Data and Determination of ϕ_m

The relative viscosity values, obtained by the procedure described in section 2.2, for the three suspensions at various coal concentrations are presented in Table 1.

The data were plotted on a viscosity vs coal concentration graph and a smooth curve was drawn through the experimental points. A typical plot is shown in Fig. 3 for the case of slurries without an additive.

In order to determine the maximum coal concentration ϕ_m in each of the three cases a method employed originally by Frankel and Acrivos (1) was adopted. A plot $(\eta_r - 1)$ vs ϕ was made and the line was extrapolated to zero ordinate to give the value of ϕ_m. Data obtained from the smoothed out curve of Fig. 3 were plotted in this way in Fig. 4. Extrapolation gave a value of $\phi_m = 0.628$.

TABLE 1 ·W 9
Viscosities of Coal Water Slurries
(Pocahontas Coal)

Slurries With No Additives		Slurries With LIPAL 12A		Slurries With Aerosol OT	
Weight Concentration	Relative Viscosity cp	Weight Concentration	Relative Viscosity cp	% Weight Concentration	Relative Viscosity cp
35	109	45	19	45	30
40	233	50	43	50	56
45	407	55	69	55	805
50	1251	57.5	114	60	990
55	1697	60	180	61	1404
57.5	1752	61	405	63	1979
60	1975	62	1092	65	2500
63	2350	64	1140		
		65	2300		
		66	3792		
		68.5	4816		

In a recent publication (8) Heath and Tadros used successfully a different plotting method for obtaining ϕ_m values for their polystyrene latex dispersions. In their method $1/\eta^{1/2}$ was plotted against ϕ followed by an extrapolation to zero ordinate. The same data used in Fig. 4 when were replotted according to the Heath and Tadros method gave a value of $\phi_m = 0.725$ (Fig. 5)

Table 2 summarizes the ϕ_m values for the three slurries obtained by both the above methods. It can be seen there that although the two extrapolating methods gave different sets of values, the values within each set follow the expected trend. They increase as the aggregative stability of the suspension increases. In other words, the maximum packing is lower for the agglomerating slurry (without additives) and higher for the stable one (with LIPAL 12A). An intermediate value is found for the slurry with AEROSOL OT, which is stable, but to a lesser degree than the one with LIPAL.

2.W.9

TABLE 2 . W.9

Maximum Coal Volume Fraction, ϕ_m

Extrapolating Method	Slurry with no additives	Slurry with Aerosol OT	Slurry with LIPAL 12A
Frankel-Acrivos	.628	0.685	0.704
Heath-Tadros	.725	0.763	0.805

3.3 Testing of Previously Proposed Correlations

The above abtained values of ϕ_m were utilized in an attempt to correlate the viscosity date by Equations 4 and 5.

Equation 4 can be rearranged to give:

$$\frac{C'}{\mu_r - 1} = \left(\frac{\phi_m}{\phi}\right)^{1/3} - 1 \qquad (6)$$

This means that a plot of $(\mu_r - 1)^{-1}$ vs $(\phi_m/\phi)^{1/3}$ should give a straight line passing through $(\phi_m/\phi)^{1/3} = 1$.

A rearrangement of Equation 5, on the other hand, gives

$$\frac{0.75}{\mu_r^{1/2} - 1} = \frac{\phi_m}{\phi} - 1 \qquad (7)$$

Thus, a plot of $(\mu_r^{1/2} - 1)^{-1}$ vs ϕ_m/ϕ should give a straight line passing through $\phi_m/\phi = 1$ and having a slope of 1/0.75.

Four correlation plots were made according to the scheme in Table 3.

TABLE 3

Scheme for Correlation Testing

Correlation	Method for obtaining ϕ_m: Frankel-Acrivos	Method for obtaining ϕ_m: Heath-Tadros
Equ. 6	A	B
Equ. 7	C	D

The plots are presented in Fig. 6 according to the arrangement indicated by Table 3. An inspection of the plots indicates that in none of the four cases there is a universal correlation fitting the data from all three slurries. A promising clue, however, may be provided by case C. The data in C can be correlated by straight lines all converging towards $\phi_m/\phi = 1$ as expected from an equation of the form of Equ. 7. These lines, however, have slopes differing from the slope predicted by Equ. 7. (i.e. 1/0.75). Actually the slopes of possible straight lines drawn through the three sets of data points would vary from about 0.11 (for slurries with no additives) to 0.35 (for slurries with LIPAL 12A).

It can be concluded, therefore, that the apparent viscosity data of the coal water slurries tested could be correlated by the equation:

$$\mu_r = \left[1 + K\left(\frac{\phi/\phi_m}{1-\phi/\phi_m}\right)\right]^2 \qquad (8)$$

where K is different for each slurry. It can be also stated that K (which is the inverse of the slope of a line in Fig. 6C) decreases as the aggregative stability of the slurry increases.

1·W.10

No.C) were used. The results are given in Fig.1 and Table 1.

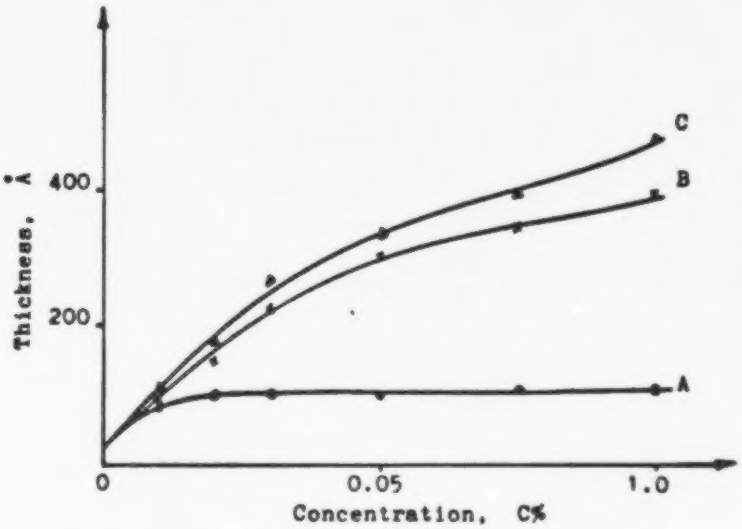

Fig.1 Relationship between the thicknesses of adsorption films and the additive concentrations(additives A,B,C) W.10

Table 1. The thicknesses of adsorption films formed on coal surface by different additives W 10

Additive No.	The thicknesses of adsorption films(at the equilibrium concentration of 0.05%)
A	100 Å
B	310 Å
C	340 Å

As can be seen from Fig.1, for additive No.A, the thicknesses of the adsorption films do not stop increaseing until the concentration of adsorbate reaches to a certain value, but for additives No.B and No.C, the thicknesses are still increasing continuously. And moreover, the adsorption film formed by additive No.C is thicker than that by additive No.B.

In order to reveal the relationship between the thickness of adsorption films and the adsorption abilities of additives, we have made the experiments of adsorption isotherms and FT-IR spectra as well to acquire a deeper understanding of the nature of the adsorption of additives on the solid surfaces. The results of experiments are shown in Fig.2

2·W·10

W·10

Table 2. Density of adsorption layer on coal surface

Additive	Γ (g/g)x10^3	l (Å)	ρ (g/c.c.)x10^3
A	1.25	100	23.3
B	1.25	310	7.71
C	0.80	340	4.38

As indicated by the results, a conclusion can be made that for additive A the adsorption force behaves the strongest, and the adsorption layer is the thinnest and closest; on the contrary, for additive C, the adsorption force behaves the weakest and the adsorption layer is the thickest and loosest. These additives could be arranged in series as following:

Adsorption strength	A > B > C
Thickness	C > B > A

Based upon the investigation mentioned above, experiments to measure rheological characteristics of CWS with these three additives have been carried out respectively. The results are shown in Fig.4 and Fig.5, the shear rate used in the experiment is $4.76 sec^{-1}$.

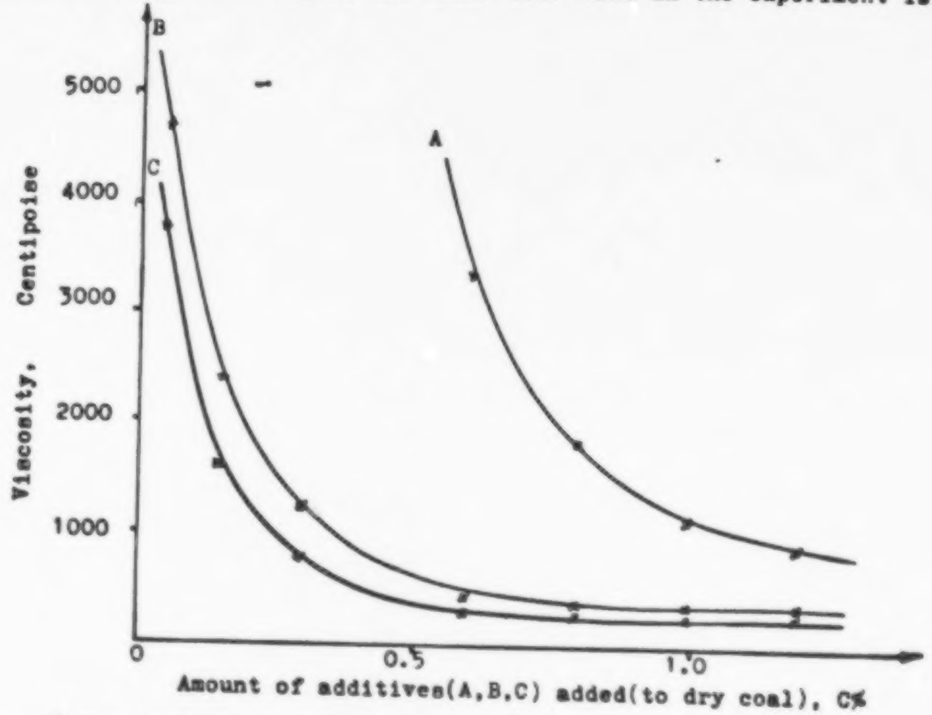

Fig.4 Effect of different additives on the viscosity of CWS at constant concentration of CWS (concentration of CWS is 65%)

W'10

1-2-W.12

Superheat and reheat steam temperature control may be maintained by a combination of gas recirculation and water attemperation through a load range of 66.6 to 100 percent.

·W·12

TABLE 1: FUEL ANALYSES

Ultimate Analysis (% Wt)	SRC-Water Slurry (66.6% solid)	No. 6 Fuel Oil
Carbon	57.65	82.20
Hydrogen	7.66	11.80
Nitrogen	1.20	0.22
Sulfur	0.65	0.64
Oxygen (by difference)	32.57	5.04
Ash	0.27*	0.10
Moisture (% Wt)	33.4	6.30
Higher Heating Value (Btu/lb)	10,630	17,490
Solid Particle Size (% minus 200 mesh)	88	
Fuel Viscosity	450 CP @ 200 sec^{-1}, 100 °F	14 CP @ 200 °F

---

* Includes 0.15% ash from Lomar D additive (sodium aryl sulfonate)

·W·12

TABLE 2: COMBUSTION TEST DATA

	SRC-Water Slurry	No. 6 Fuel Oil
Excess Air (%)	13.90	12.40
Secondary Air Temp. (°F)	557.00	610.00
Carbon Conversion Eff. (%)	98.80	99.98
Boiler Efficiency (%) (heat loss method)	81.60	82.90
CO (ppm)	28.00	23.00
SO_2 (lb/10^6Btu)	1.38	0.95
NOx (lb/10^6Btu)	0.49	0.27
Opacity	10.00	N/A

4 · W·10

W·10

Table 2. Density of adsorption layer on coal surface

Additive	Γ (g/g)x10^3	l (Å)	ρ (g/c.c.)x10^3
A	1.25	100	23.3
B	1.25	310	7.71
C	0.80	340	4.38

As indicated by the results, a conclusion can be made that for additive A the adsorption force behaves the strongest, and the adsorption layer is the thinnest and closest; on the contrary, for additive C, the adsorption force behaves the weakest and the adsorption layer is the thickest and loosest. These additives could be arranged in series as following:

Adsorption strength $A > B > C$
Thickness $C > B > A$

Based upon the investigation mentioned above, experiments to measure rheological characteristics of CWS with these three additives have been carried out respectively. The results are shown in Fig.4 and Fig.5, the shear rate used in the experiment is 4.76sec^{-1}.

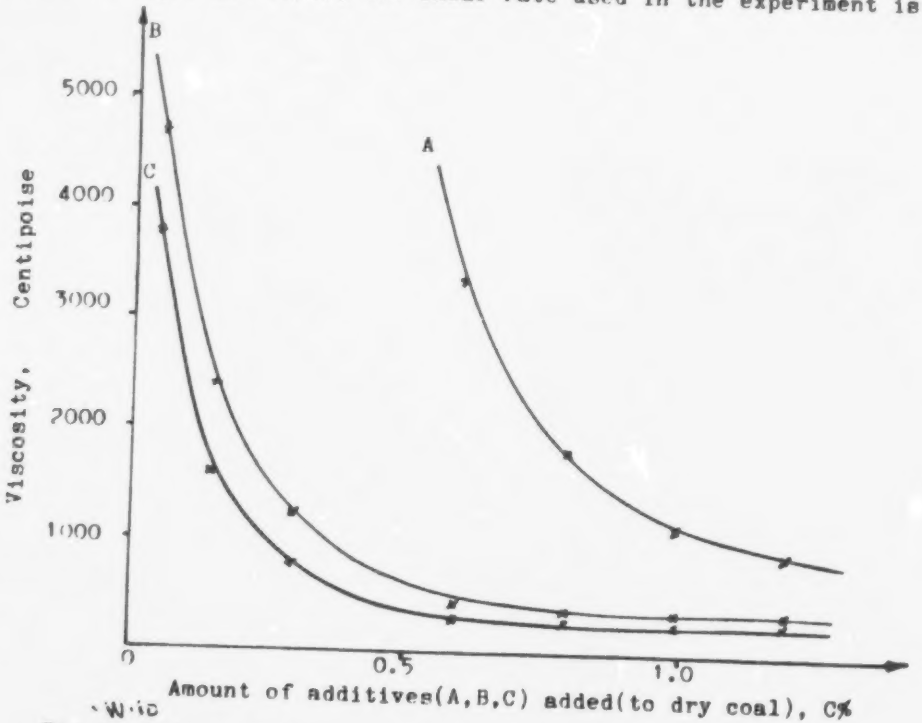

W·10

Fig.4 Effect of different additives on the viscosity of CWS at constant concentration of CWS (concentration of CWS is 65%)

1, A, W·13

TABLE I-A · W·13

RAW COAL ANALYSES

Description	Coal used to prepare ARC-Coal Montcoal		Coal used to prepare Co-Al Moss #1	
Basis	As Received	Dry	As Received	Dry
Total Moisture, %	3.8	--	3.8	--
Proximate Analysis, %				
Moisture	3.8	--	3.8	--
Volatile Matter	30.2	31.4	30.7	31.9
Fixed Carbon	61.7	64.1	58.8	61.1
Ash	4.3	4.5	6.7	7.0
Gross Heating Value Btu per lb	14180	14740	13940	14490
Btu per lb (M&A Free)	--	15430	--	15580
Ultimate Analysis, %				
Moisture	3.8	--	3.8	--
Carbon	79.9	83.1	78.6	81.7
Hydrogen	5.0	5.2	4.9	5.1
Nitrogen	1.36	1.41	1.19	1.24
Sulfur	0.71	0.74	0.56	0.58
Ash	4.3	4.5	6.7	7.0
Oxygen (Difference)	4.93	5.05	4.25	4.38
Total	100.00	100.00	100.00	100.00
Sulfur Forms, % as S				
Pyritic	0.03	0.03	0.06	0.06
Sulfate	0.04	0.04	Trace	Trace
Organic (Difference)	0.64	0.67	0.50	0.52
Total	0.71	0.74	0.56	0.58
Ash Analysis (Spectrographic), %				
Silicon as SiO_2	50.49		48.85	
Aluminum as Al_2O_3	33.01		29.22	
Iron as Fe_2O_3	6.02		7.80	
Titanium as TiO_2	1.56		1.19	
Calcium as CaO	1.35		2.43	
Magnesium as MgO	0.68		1.34	
Sodium as Na_2O*	0.81		0.81	
Potassium as K_2O*	1.81		2.10	
Sulfur as SO_3	1.31		2.85	
Phosphorus as P_2O_5	0.33		0.27	
Ash Fusion Temperatures, °F				
Atmosphere	Red.	Oxid.	Red.	Oxid.
A (I.D.)	2750+	2750+	2660	2740
B (S.T., Sp)	2750+	2750+	2750+	2750+
C (S.T., HSp)	2750+	2750+	2750+	2750+
D (F.T., 1/16")	2750+	2750+	2750+	2750+
E (F.T., Flat)	2750+	2750+	2750+	2750+

---

*By Flame Photometer

I·B·W·13

TABLE I-B-W-13

SLURRY ANALYSES(1)

Description	ARC-Coal -- from Atlantic Research		Composite Co-Al from Slurrytech	
Basis	As Received	Dry	As Received	Dry
Total Moisture, %	29.7	--	24.7	--
Solids, %	70.3	--	75.3	--
Proximate Analysis, %				
Moisture	29.7	--	24.7	--
Volatile Matter	23.1	32.9	23.2	30.8
Fixed Carbon	44.0	62.5	47.1	62.5
Ash	3.2	4.6	5.0	6.7
Gross Heating Value Btu per lb	10410	14810	11010	14620
Btu per lb (M&A Free)	-	15520	--	15670
Ultimate Analysis, %				
Moisture	29.7	--	24.7	--
Carbon	58.6	83.3	61.9	82.2
Hydrogen	3.6	5.1	3.8	5.1
Nitrogen	1.00	1.42	1.18	1.57
Sulfur	0.43	0.61	0.59	0.78
Ash	3.2	4.6	5.0	6.7
Oxygen (Difference)	3.47	4.97	2.83	3.65
Total	100.00	100.00	100.00	100.00
Sulfur Forms, % as S				
Pyritic	0.06	0.08	0.03	0.04
Sulfate	0.03	0.05	0.05	0.06
Organic (Difference)	0.34	0.48	0.51	0.68
Total	0.43	0.61	0.59	0.78
Ash Analysis (Spectrographic), %				
Silicon as SiO_2	50.80		44.60	
Aluminum as Al_2O_3	34.24		28.03	
Iron as Fe_2O_3	6.22		9.67	
Titanium as TiO_2	1.63		1.32	
Calcium as CaO	1.07		2.85	
Magnesium as MgO	0.57		1.31	
Sodium as Na_2O*	1.35		2.97	
Potassium as K_2O*	1.81		2.07	
Sulfur as SO_3	1.58		3.65	
Phosphorus as P_2O_5	0.11		0.28	
Ash Fusion Temperatures, °F				
Atmosphere	Red.	Oxid.	Red.	Oxid.
A (I.D.)	2750+	2750+	2270	2390
B (S.T., Sp)	2750+	2750+	2350	2590
C (S.T., HSp)	2750+	2750+	2450	2620
D (F.T., 1/16")	2750+	2750+	2540	2690
E (F.T., Flat)	2750+	2750+	2750+	2750+

---

(1) See Figure 10 for particle size distribution

*By Flame Photometer

11·B·W·13

TABLE II-B – W·3

ARC-COAL FIELD MEASUREMENTS (1)(2)

Sample Locations				Sample Date	Solids %	Viscosity - cps (5)		
Moyno Disch.	(3)			8/8/83	--	852	@	32°C
GATX		12375	Top	8/11/83	--	742	@	23
GATX		12375	Bot	8/11/83	--	6777	@	23.5
GATX		12378	Top	8/18/83	69.7	677	@	31
GATX			Mid	8/18/83	70.0	808	@	27.5
GATX			Bot	8/18/83	70.0	764	@	27.5
GATX		12382	Top	8/17/83	70.0	699	@	30.5
GATX			Mid	8/17/83	70.0	742	@	28
GATX			Bot	8/17/83	69.9	830	@	26.5
GATX		12375	Top	8/18/83	69.8	589	@	28
GATX			Mid	8/18/83	69.9	589	@	32
GATX			Bot	8/18/83	69.8	655	@	29.0
Moyno Disch.				8/18/83	70.1	852	@	30.5
Moyno Disch.				8/20/83	70.0	830	@	32
Moyno Disch.				8/20/83	70.2	742	@	37.0
Moyno Disch.				8/21/83	70.0	830	@	34.5
Moyno Disch.				8/25/83	69.8	742	@	36
Moyno Disch.				9/27/83		1020	@	28
GATX	(3)(4)	98925	Top	9/27/83	68.3	413	@	27.5
GATX			Mid	9/27/83	70.5	852	@	27.0
GATX			Bot	9/27/83	70.8	1040	@	25.0
GATX	(3)(4)	85456	Top	9/27/83	69.1	524	@	26
GATX			Mid	9/27/83	70.2	852	@	26
GATX			Bot	9/27/83	70.5	1000	@	24.5
Moyno Disch.	(3)			9/27/83	70.3	1150	@	24.5
Moyno Disch.				9/28/83	70.4	1150	@	27.5
Moyno Disch.	(3)			9/28/83	70.1	1090	@	26.0
GATX	(3)	85456	Outlet	9/28/83	70.5	983(?)	@	24.5

Notes:
(1) Sampling by ARC unless otherwise noted.
(2) Rail tank car sampling locations unless otherwise noted were: Top, 2' below surface; Mid, 5' below surface; Bot, 8' below surface.
(3) Sampling by B&W.
(4) Approximate rail tank car sampling locations: Top, at free surface; Mid, 5' below surface; Bot, 1' above bottom of car.
(5) Viscosity readings at 99.2 sec^{-1} by Brookfield Viscometer.

last slurry unloaded as readily as the first slurry 3-4 days earlier. There was a somewhat higher heel left in two of the cars because of the height of the snorkel tube above the car bottom. Long-term storage in these cars might be a problem if the normal sludge-type material in the bottom of the car built up to or over the snorkel tube opening. This trial was a success.

All the slurry was unloaded from the bottom of the railroad cars through 3" valves and hoses to a diaphragm pump which discharged to a 7,500-gallon stainless steel tank trailer. Approximately three hours were needed to fill the truck. The trailer was moved to the boiler where the slurry was unloaded into a 15,000-gallon day tank using duplicates of the loading equipment. Normal use was two trailers a day.

Conical screen-type strainers with 3/16" holes were used at the inlet to both diaphragm pumps. The screen ahead of the railcar unloading pump did accumulate soft material, probably from the small amount of sludge in the bottom of the cars, and was cleaned after each car. The screen near the day tank was cleaned infrequently.

cps (5)
32°F
23
23.5
31
27.5
27.5
30.5
28
26.5
28
32
29.0
30.5
32
37.0
34.5
36
28
27.5
27.0
25.0
26
26
24.5
24.5
27.5
26.0
.5

2' below

Mid, 5'

a some-
ube above
l sludge-
ng. This

lves and
trailer.
d to the
s of the

diaphragm
l, prob-
ter each

II-C W-13

TABLE II-C · W-13

CO-AL SAMPLING

Rail Car	Compartment	As Loaded % Solids(1)	As Loaded Viscosity(2)	% Solids(3)	Viscosity(4)	% S
256	A	75.2	869 cp	74.5		
	B	75.3	793	74.9		
257	A	75.4	855	74.7		
	B	75.2	920	75.0		
262	A	75.4	849	74.8		
	B	74.9	833	74.8		
266	A	75.2	887	75.3		
	B	75.0	850	75.2	876	
Average		75.2	857	74.9	876	

(1) Moisture Teller
(2) Brookfield Viscometer
(3) ASTM D-3173
(4) Haake Viscosity
(5) Hard Pack as vol % of tank car volume

The day tank was equipped with a 10 hp agitator. Blades were at two levels in
high tank, and each level consisted of three blades. Four vertical baffles were i
on the cylindrical sides to improve effectiveness. Speed was 45 rpm. The agit
considered successful in that no problems were recognized as caused by varyin
content of the slurry. An on-line, non-nuclear solids display instrument was to b
in the piping to indicate any differences in solids content with and without
operation. Unfortunately, there were problems in calibration, so the agitator
continuously as insurance.

Figure 3 shows an artist's concept of the plot plan. Slurry was fed by gravit
progressing cavity Moyno pump. A conical screen-type strainer at the pump inlet
moved to prevent pump cavitation caused by pressure drop across the strainer r
from solids buildup. Slurry feed was controlled by a variable speed drive on t
Initially, a variable frequency drive was used to control slurry feed rate thr
plant's digital control system. High torque requirements at low motor speed caus
lems which could have been corrected, but timeliness dictated a revision to a me
variable speed drive which worked satisfactorily. This meant that slurry control
automatic but was manually controlled by the operator from the control room.

The Moyno pump discharged to the piping system (see Figure 4) which contained
valve, a high pressure shutoff switch, a dual basket strainer, a master fuel tri
controlled by boiler interlocks, a Rosemount magnetic flowmeter with bypass, a
Motion flowmeter with bypass, individual burner shutoff valves controlled from th
safeguard system, tandem manual recirculation control valves, and a recirculati
back to the day tank.

Slurry was recirculated to the day tank to prevent solidification when no slurry wa
fired. It was also recirculated during one and two burner operation.

The basket strainers were cleaned each shift and frequently contained hardening
material with some apparently fibrous matter. These strainers had 3/16" holes.

Procedures for switching slurries from ARC-Coal to Co-Al had included washout of
tank and piping. The quantity of water required and its disposal problems brought
reconsideration. Laboratory mixing of slurry samples showed no ill effects, so pro
were modified to eliminate cleanout. Upon completion of the test with ARC-Coal, th
in the day tank was allowed to drop to about 2'. At this time, Co-Al slurry f

5-W-13

TABLE V - W-13

EPRI COAL-WATER SLURRY DEMONSTRATION BURN
TEST DATA SUMMARY AND BOILER EFFICIENCIES

DATE:	9/7/83	9/8/83	9/10/83	9/14/83	9/15/83	9/16/83	9/23/83
SLURRY BURNED	ARC	ARC	ARC	CO-AL	CO-AL	CO-AL	GAS ONLY
STEAM LOAD - MPPH	56.9	56.7	55.7	53.0	53.7	51.9	47.0
BOILER DRUM PRESSURE - PSIG	190	190	190	188	188	190	190
SLURRY FLOW:							
ROSEMOUNT - GPM	9.34	9.32	8.92	8.25	7.79	7.80	--
MICRO-MOTION - LB/MIN	98.45	98.15	96.30	88.96	86.77	85	--
CALCULATED - LB/MIN	98.08	97.98	95.5	88.67	84.29	81.50	--
DENSITY - LB/GAL	10.0	10.0	10.0	10.4	10.4	10.4	--
NATURAL GAS FLOW:							
ONE BURNER MCFH	5.69	5.35	5.60	2.44	5.51	4.9	58.0
AIR HEATER - MEASURED - MCFH	4.10	4.18	4.01	3.78	3.04	3.5	--
AIR HEATER CALCULATED MCFH	3.86	3.96	3.78	3.81	3.46	3.93	--
STEAM FLOW TO STEAM COIL - PPH	5313	5232	5179	5437	5185	4798	--
TEMPERATURES:							
AFTER HEATERS - °F	485	488.9	484.3	488	480	515	--
STACK GAS - °F	593	587.5	587.1	563	559	552	495
FEEDWATER - °F	265.3	265.8	266.4	265	265.3	--	--
PRESSURES:							
FD FAN STATIC - " W.C.	17.8	17.4	16.2	--	16.1	--	--
WINDBOX - " W.C.	13.2	12.65	11.1	11	12.7	--	--
FURNACE DRAFT - " W.C.	-0.15	-0.19	-0.35	-0.23	-0.25	--	--
STACK DRAFT " W.C.	1.1	-1.25	-1.4	-1.1	-1.05	--	--
SLURRY BURNERS AVG. - PSIG	181	177	187	174	154	--	--
ATOMIZING AIR TO BURNERS - PSIG	209	208	212	203	207	--	--
MISCELLANEOUS:							
BOILER EXIT O_2 - %	7.0	7.1	7.07	7.67	7.9	6.6	3.0
FLY ASH CONCENTRATION:							
LBS/1000 LBS GAS	2.39	2.35	2.22	0.96	2.33	2.64	--
GRAINS/SCF	1.31	1.28	1.21	0.52	1.27	1.44	--
SLURRY CONCENTRATION - % SOLIDS	70	70	70	75	74	74	--
SLURRY VISCOSITY - CP	800	800	800	860	500	500	--
CARBON IN FLY ASH - %	41.3	41.55	38.2	19.5	21.0	25.9	--
LOSSES:							
DRY GAS - %	14.754	14.623	14.732	16.073	14.384	13.967	9.062
HYDROGEN - %	4.973	4.925	4.963	4.648	4.977	4.967	11.493
MOISTURE - %	3.133	3.126	3.118	2.563	2.443	2.422	--
CARBON - %	2.713	2.750	2.380	1.441	1.507	1.977	--
RADIATION - %	0.7	0.7	0.7	0.7	0.7	0.7	0.7
TOTAL - %	26.273	26.124	25.893	25.425	24.011	24.033	21.255
BOILER EFFICIENCY - %	73.727	73.876	74.107	74.575	75.989	75.967	78.745
FURNACE FIRING RATE - MMBTU/HR	74.715	74.490	72.850	68.579	68.750	66.087	58.043
FURNACE HEAT RELEASE - MBTU/CU FT	28.015	27.930	27.315	25.714	25.778	24.780	21.763
GASEOUS EMISSIONS - ACUREX							
NOx - PPM	--	582(1)	--	--	676	--	102
SOx - PPM	--	512(1)	--	--	490	--	--
CO - PPM	--	447(1)	--	--	283	--	169
ORGANIC - PPM	--	2(1)	--	--	1	--	1
CO_2 - % (CORRECTED)	10.3(1)	10.2(1)	10.2(1)	9.4	10.1	10.2	10.1
O_2 - %	8.7(1)	9.8(1)	8.8(1)	9.3	8.8	8.5	3.0

(1) TYPICAL ANALYSES OR IMPUTED ANALYSES; NOT MEASURED BY ACUREX ON SPECIFIC DAY

3·W 13

TABLE III·W·13

BOILER PREDICTED PERFORMANCE BY BABCOCK & WILCOX

	Natural Gas	Slurry
Steam Flow, M lb/hr	60,000	60,000
Boiler Pressure, psig	175	175
Steam Condition	Saturated	Saturated
Feedwater, °F	250	265
Air Inlet, °F	100	100
Furnace Exit Gas, °F:		
- No Air Preheat		1720
- Air Preheat, 550°F		1970
Boiler Exit Gas, °F		550
Boiler Exit Excess Air, %	15	9
Heat Release, MBtu/cu ft	30,600	'
Blowdown, %	10	10
Heat Losses:		
- Dry Gas, %	18.9	
- H_2 in Fuel, %	11.9	
- Moisture in Air, %	0.2	
Radiation, %	0.9	
Unaccounted For	1.5	
Total Losses, %	23.4	
Efficiency, %	76.6	
Heat Release, MBtu/cu ft (1)	30,600	
Gas Velocities, fps:		
- Entering First Pass		25
- Around First Baffle		30
- Around Last Baffle		17
- Boiler Exit		20

(1) Furnace Volume 2667 cu ft

The front and side water walls were composed of 2-1/2" tubes on 5" centers, allowing exposed refractory between tubes. The front water wall extended along the roof down to the front water wall header which was located on top of the burner windbox, 7'2" above grade level. The side water walls ended 2'8" above grade level, just below the lower burner level centerline. The rear wall was formed of a refractory bridgewall 3'2" high where it meets tubes coming from the mud drum. The rear wall tubes were tangent construction up to about 12' above grade where they displaced to form screen tubes before going into the steam drum.

The furnace was 16'1-1/4" wide by 11'3" deep at the burner level with average height of 17'3". Furnace gases exited through the left hand third of the screen tubes while the other two thirds contained a refractory baffle.

The combustion air supply system required modifications based on the preliminary tests run in B&W's research unit. Windbox pressures of 9-12" were required for the existing burners to achieve the desired swirl and flame patterns. This required installation of a new temporary forced draft fan. High secondary air temperatures were provided by a steam coil heater (up to 305°F) and by a direct-fired natural gas heater (up to 600°F) as shown in Figure 6. While direct duct burning would reduce the oxygen content of the combustion air, the total effect was reduced by the use of steam preheating. The preliminary tests indicated this oxygen level would be acceptable.

1- W

TABLE I .W 14

Coal Water Mixture Properties

	A	B	C	D	E
H_2O%	29.3	26.9	29.1	29.9	36.1
* Viscosity Centistokes	1090 at 100^{-1} secs	1170 at 100^{-1} secs	323 at 10^{-1} secs	500 at 10^{-1} sec	
Coal particle size (% below 200 mesh 75 μ)	99.3	76.0	84.4	96.7	
Ash content	2.8	1.4	4.8	6.0	5.1
Coal volatile matter (% dry basis)	32.9	35.4	29.1	25.0	28.0
Calorific value of Mixture Btu/lb	10,393	10,260	9,982	9,715	7,866

*Viscosity measurements were made on a Contraves RM.15 viscometer at shear rates in the Newtonian region for the coal water mixture under investigation.

The work highlighted the individuality of the various coal water mixtures, not only due to the coal properties of the inherent coal but the overall physical properties of the mixtures. In order to achieve satisfactory combustion with the various mixtures, using the standard small scale atomiser as shown in Figure 3, alterations to the combustion air side of the burner system were required. The air swirler in the standard burner system is the full diameter of the air register with a 45° blade angle. This system was assigned a swirl number ratio of unity. Swirl numbers on vane type swirlers are calculated from the formula:- (1)

$$SN = \left\{ \frac{1 - \left(\frac{DH}{DS}\right)^3}{1 - \left(\frac{DH}{DS}\right)^2} \right\} \tan \theta$$

where

SN = Swirl Number
DH = Hub Diameter
DS = Swirler Diameter
θ = Blade Angle

For ready comparison purposes the swirl number of the standard swirler was equated to unity and a series of split swirlers was provided with blade angles ranging from 25 - 70° with swirl numbers as shown in Figure 6.

4·W·14

(3) FUNDAMENTAL WORK ON COAL WATER MIXTURE COMBUSTION

Basic coal water mixture combustion work has been carried out on a small test rig rated at 5 MW. This rig comprises a water cooled cylindrical combustion chamber 4 m (13 ft) long by 1.1 m (3.75 ft) diameter with a 5.2 m refractory lined stack equipped for temperature, gas analysis and particulate concentration measurements. Pre-heated combustion air is provided, from a gas oil fired heat exchanger, at temperatures up to 400°C. The general layout of the rig and its associated equipment for coal water mixture firing is shown in Figure 3.

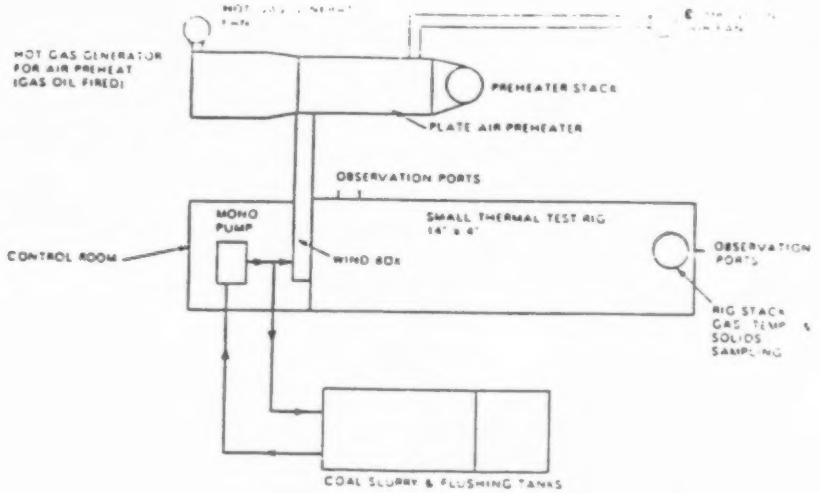
HOT GAS GENERATOR
FOR AIR PREHEAT
(GAS OIL FIRED)
PREHEATER STACK
PLATE AIR PREHEATER
OBSERVATION PORTS
MONO
PUMP
SMALL THERMAL TEST RIG
14' x 4'
CONTROL ROOM
WIND BOX
OBSERVATION
PORTS
RIG STACK
GAS TEMP &
SOLIDS
SAMPLING
COAL SLURRY & FLUSHING TANKS

FIGURE 3

GENERAL LAYOUT OF SMALL SCALE THERMAL TEST RIG

design ?

Early attempts at firing coal water mixtures highlighted both handling and atomiser design problems. The first atomisers used were scaled down versions of steam assisted nozzles used for firing coal oil slurries on the large test rigs. Problems arose due to burner blockage from two sources (1) heating of the coal water mixture via the steam in the burner gun causing breakdown of the slurry stabilising additive (2) the dilatancy of the coal water slurry created blockages in the atomiser on attempting to feed the slurry to the burner tip via a series of narrow slots and orifices of the scaled down version of the steam assisted atomiser. These problems were overcome by the use of air as the atomising medium and the developing of a special atomiser to avoid narrow orifices and sudden changes of direction in the slurry flow stream. The basic design principles of this small scale atomiser are shown in Figure 4.

?!

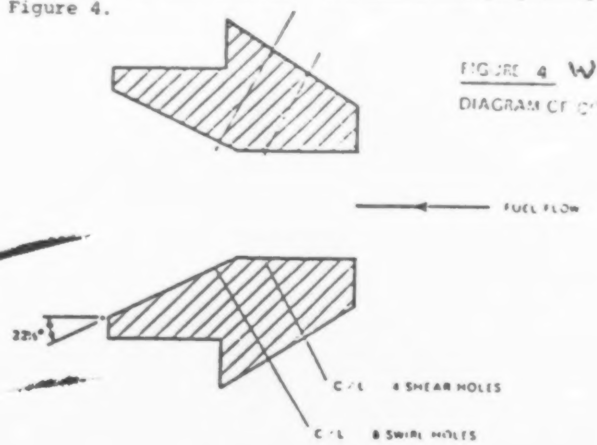
FUEL FLOW
22.5°
C/L 4 SHEAR HOLES
C/L 8 SWIRL HOLES

FIGURE 4 W·14

DIAGRAM OF COAL WATER MIXTURE [illegible]

1.W.15

TABLE 1.W.15

Co-AL Provided for EPRI-Sponsored Demonstration

	Parent Coal		Co-AL	
	As Received	Dry	As Received	Dry
Total Moisture, %	3.8	-	24.7	-
Solids, %	-	-	75.3	-
Viscosity, centipoise	-	-	860 (1)	-
Particle Size				
• % less than 50 mesh	-	-	99.4	-
• % less than 200 mesh	-	-	79.6	-
Proximate Analysis, %				
Moisture	3.8	-	24.7	-
Volatile Matter	30.7	31.9	23.2	30.8
Fixed Carbon	58.8	61.1	47.1	62.5
Ash	6.7	7.0	5.0	6.7
Gross Heating Value, Btu/lb	13940	14490	11010	14620
Ultimate Analysis, %				
Moisture	3.8	-	24.7	-
Carbon	78.6	81.7	61.9	82.2
Hydrogen	4.9	5.1	3.8	5.0
Nitrogen	1.19	1.24	1.18	1.57
Sulfur	0.56	0.58	0.59	0.78
Ash	6.7	7.0	5.0	6.7
Oxygen (difference)	4.25	4.38	2.83	3.75
Total	100.00	100.00	100.00	100.00
Sulfur Forms, % as S				
Pyritic	0.06	0.06	0.03	0.04
Sulfate	Trace	Trace	0.05	0.06
Organic (Diff.)	0.50	0.52	0.51	0.68
Total	0.56	0.58	0.59	0.78

---

(1) Measured by Brookfield RVT, #5 spindle at 100 rpm for one minute at 25°C.

4.W.15

TABLE 4 4.W.15

EPRI COAL-WATER SLURRY DEMONSTRATION BURN TEST DATA SUMMARY AND BOILER EFFICIENCIES[1]

DATE:	9/14/83	9/15/83	9/16/83	9/23/83
SLURRY BURNED	CO-AL	CO-AL	CO-AL	GAS ONLY
STEAM LOAD - MPPH	53.0	53.7	51.9	47.0
BOILER DRUM PRESSURE - PSIG	188	188	190	190
SLURRY FLOW:				
ROSEMOUNT - GPM	8.25	7.79	7.80	--
MICRO-MOTION - LB/MIN	88.96	86.77	85	--
CALCULATED - LB/MIN	88.67	84.29	81.50	--
DENSITY - LB/GAL	10.4	10.4	10.4	--
NATURAL GAS FLOW:				
ONE BURNER - MCFH	2.44	5.51	4.9	58.0
AIR HEATER - MEASURED - MCFH	3.78	3.04	3.5	--
AIR HEATER - CALCULATED - MCFH	3.81	3.46	3.93	--
STEAM FLOW TO STEAM COIL - PPH	5437	5185	4798	--
TEMPERATURES:				
AFTER HEATERS - °F	488	480	515	--
STACK GAS - °F	563	559	552	495
FEEDWATER - °F	265	265.3	--	--
PRESSURES:				
FD FAN STATIC - " W.C.	--	16.1	--	--
WINDBOX - " W.C.	11	12.7	--	--
FURNACE DRAFT - " W.C.	-0.23	-0.25	--	--
STACK DRAFT - " W.C.	-1.1	-1.05	--	--
SLURRY BURNERS AVG. - PSIG	174	154	--	--
ATOMIZING AIR TO BURNERS - PSIG	203	207	--	--
MISCELLANEOUS:				
BOILER EXIT O_2 - %	7.67	7.9	6.6	3.0
FLY ASH CONCENTRATION:				
LBS/1000 LBS GAS	0.96	2.33	2.64	--
GRAINS/SCF	0.52	1.27	1.44	--
SLURRY CONCENTRATION - % SOLIDS	75	74	74	--
SLURRY VISCOSITY - CP	860	500	500	--
CARBON IN FLY ASH - %	19.5	21.0	25.9	--
LOSSES:				
DRY GAS - %	16.073	14.384	13.967	9.062
HYDROGEN - %	4.648	4.977	4.967	11.493
MOISTURE - %	2.563	2.443	2.422	--
CARBON - %	1.441	1.507	1.977	--
RADIATION - %	0.7	0.7	0.7	0.7
TOTAL - %	25.425	24.011	24.033	21.255
BOILER EFFICIENCY - %	74.575	75.989	75.967	78.745
FURNACE FIRING RATE - MMBTU/HR	68.579	68.750	66.087	58.043
FURNACE HEAT RELEASE - MBTU/CU FT	25.714	25.778	24.780	21.763
GASEOUS EMISSIONS - ACUREX				
NOx - PPM	--	676	--	102
SOx - PPM	--	490	--	--
CO - PPM	-	283	--	169
ORGANIC - PPM	.	1	--	1
CO_2 - % (CORRECTED)	9.4	10.1	10.2	10.1
O_2 - %	9.3	8.8	8.5	3.0

---

1. Perkins, R.P. et al, "Coal-Water Slurry Test in an Industrial Boiler", American Power Conference, April 24 1984.

1-2-3 W·17

·W·17

TABLE 1. RESULTS OF SELECTIVE FLOCCULATION OF BITUMINOUS COAL FROM NATIONAL COAL BOARD (U.K.)

Inital Percent Ash	Ash Percent Removal	Final Ash Percent	Coal Recovery
32.4	82.5	10.2	74.3
18.9	53.8	10.3	93.4
16.7	57.1	8.8	94.7
45.5	78.4	19.9	71.1

·W·17

TABLE 2. RESULTS OF SELECTIVE FLOCCULATION OF SELECTED U. S. COALS

Coal	Rank	Initial Ash, percent	Ash Removal, percent	Final Ash, percent	Coal Recovery, percent
Upper Freeport (Pennsylvania)	Bituminous	9.2	81.8	2.7	67.9
Ohio 6A	Bituminous	12.0	72.0	5.0	72.6
Beulah (Texas)	Lignite	17.5	65.6	10.7	65.0

·W·17

TABLE 3. RESULTS OF SELECTIVE FLOCCULATION TESTS ON SELECTED COALS BY DAI-ICHI KOGYO SEIYAKU COMPANY, LTD, JAPAN(4)

Rank of Coal	Initial Ash, percent	Ash Removal, percent	Final Ash, percent	Coal Recovery, percent
Bituminous	24.3	81.0	6.0	93.5
Bituminous	8.5	87.8	1.2	93.2
Sub-bituminous	10.5	77.9	2.2	93.4

CWS	A	B	C	D	E	F	G
Manufacturer	1	1	2	1	3	2	4
Coal	Virg. 26 (mvb)	Beckley (lvb)	Virg. 31 (hvb)	Coal Mountain (hvb)	Nova Scotia (hvb)	Virg. 26 (mvb)	Cortonwood (hvb)
Volatiles % d.a.f.	26.2	18.7	30.7	35.9	37.5	28.1	33.4
Ash % d.b.	8.1	6.2	6.7	5.8	1.5	7.9	5.7
S % d.a.f.	1.1	1.1	0.9	1.0	0.8	1.1	1.35
CWS							
% Coal	70.4	70.4	70.0	69.6	71.7	70.4	67.3
$(100\ s^{-1})$ cP	780	940	nm	1830	1420	280	630

TABLE 2 - COAL WATER SLURRIES FOR THE NEOM/CANMET TRIALS

W20 (nm - not measured)

2-W.20

4.W.2c

Slurry	Coal type	Size distribution % 75 μm	Atomizing air required $\dot{m}_{atm}/\dot{m}_t$	Maximum turndown	Unsupported ingition with cold combustion air	Mean η_x %
A	mvb	90	17	3/1	yes	95
B	lvb	90	28	na	no	95
C	hvb	79	27	na	no	98
D	hvb	88	15	2/1	yes	98
E	hvb	73	14	3/1	yes	98
F	mvb	77	14-24	na	no	93
G	lvb	93	25	2/1	Borderline	95

W.2c

TABLE 4 - SUMMARY OF THE SLURRIES COMBUSTION PERFORMANCE
(na - not attempted)

NB No evident correlation between
[illegible]

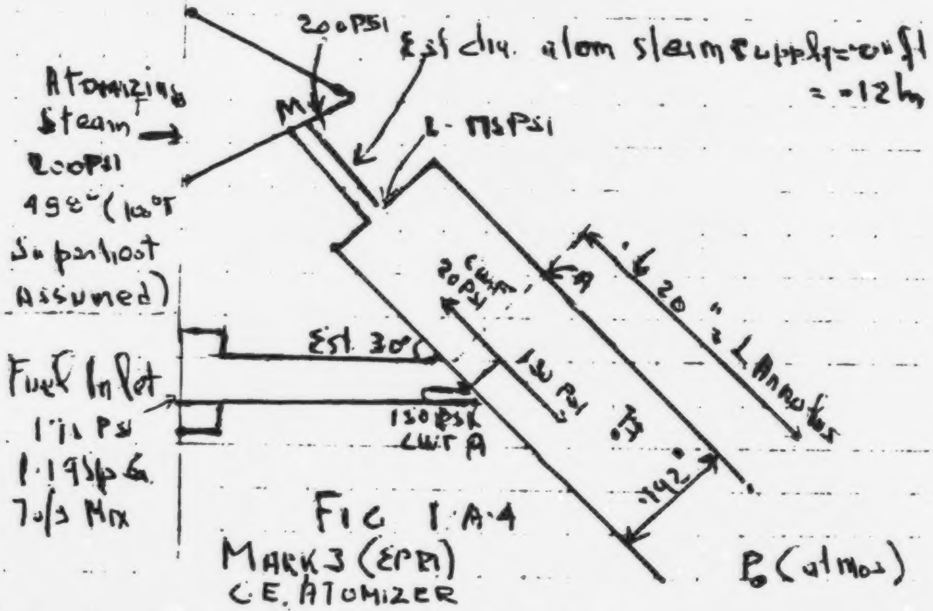
200PSI
Est dia. atom steam supply = .01 ft
= .12 in
Atomizing Steam →
200PSI
498° (100°F
Superheat
Assumed)
M
L - 175PSI
Cum. 20 PSI
A
.620 " = L Annulus
Est. 30°
Fuel Inlet
171 PSI
1.19 lb/G.
70/3 Mix
150 PSI
130 PSI
Unit A
.13
.042
P_o (atmos)

FIG 1·A·4
MARK 3 (EPRI)
C.E. ATOMIZER

1 A.4.1

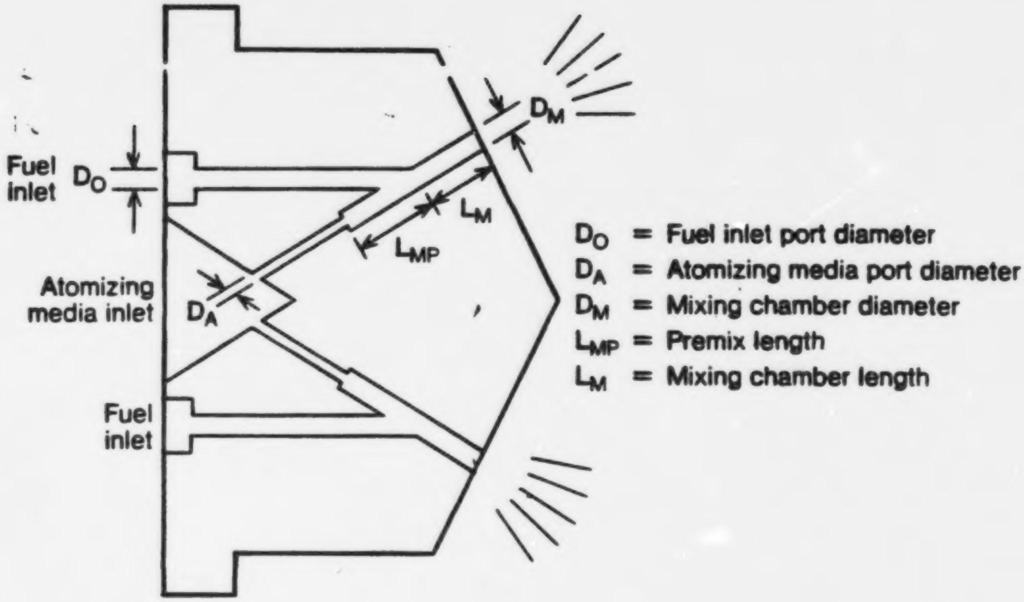
Fuel inlet
D_O
D_M
L_M
L_{MP}
Atomizing media inlet
D_A
Fuel inlet
D_O = Fuel inlet port diameter
D_A = Atomizing media port diameter
D_M = Mixing chamber diameter
L_{MP} = Premix length
L_M = Mixing chamber length

• A.4.1

Figure 3. Critical Dimensions "Y" Jet Atomizer Design, Cross-Sectional View

In addition to this test, EPRI has underway a number of other CWS projects (Figure 4):

- Development of standards/specifications for CWS purchase (RP1985-3). Eight slurries made with different coals are being subjected to bench and combustion tests. Test standards, as well as fuel specification guidelines, are being prepared.
- Prediction of long-term utility boilers effects and conversion costs (RP1895-4).
- Demonstration of pump effects (RP1895-10). The tests which are sponsored in cooperation with Long Island Lighting, ESEERCO, and NYSERDA are being performed at Adelphi Center for Energy Studies.
- An industrial boiler test (RP1895-7). A 30-day combustion test will be conducted in an industrial boiler to assess procedures for shipment, qualification, storage, handling, and combustion of larger CWS quantities. The test is planned for April 1983.

FIG 1.A.4.1

1.A.4.2

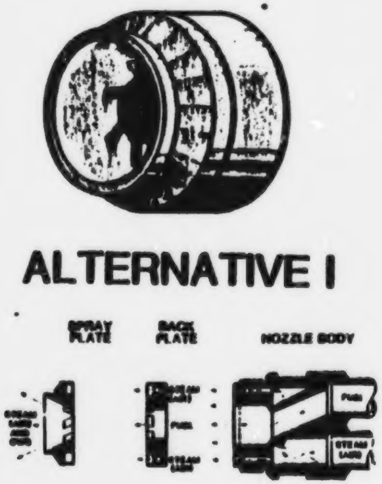
ALTERNATIVE I
SPRAY PLATE
BACK PLATE
NOZZLE BODY
STEAM (AIR) AND CWS
STEAM (AIR)
FUEL
STEAM (AIR)
FUEL
STEAM (AIR)

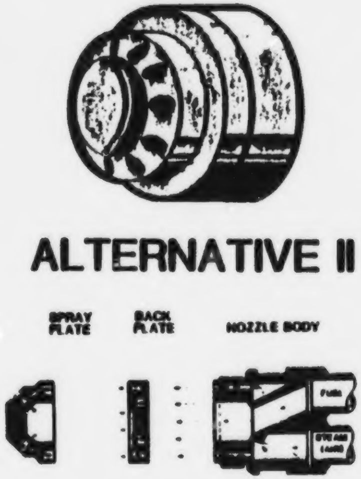
ALTERNATIVE II
SPRAY PLATE
BACK PLATE
NOZZLE BODY
FUEL
STEAM (AIR)

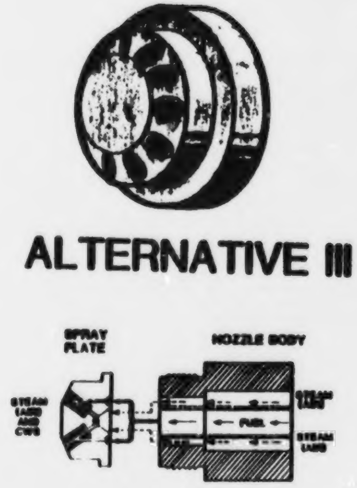
ALTERNATIVE III
SPRAY PLATE
NOZZLE BODY
STEAM (AIR) AND CWS
STEAM (AIR)
FUEL
STEAM (AIR)

1.A.4.2
Figure 4: Atomizer Alternatives

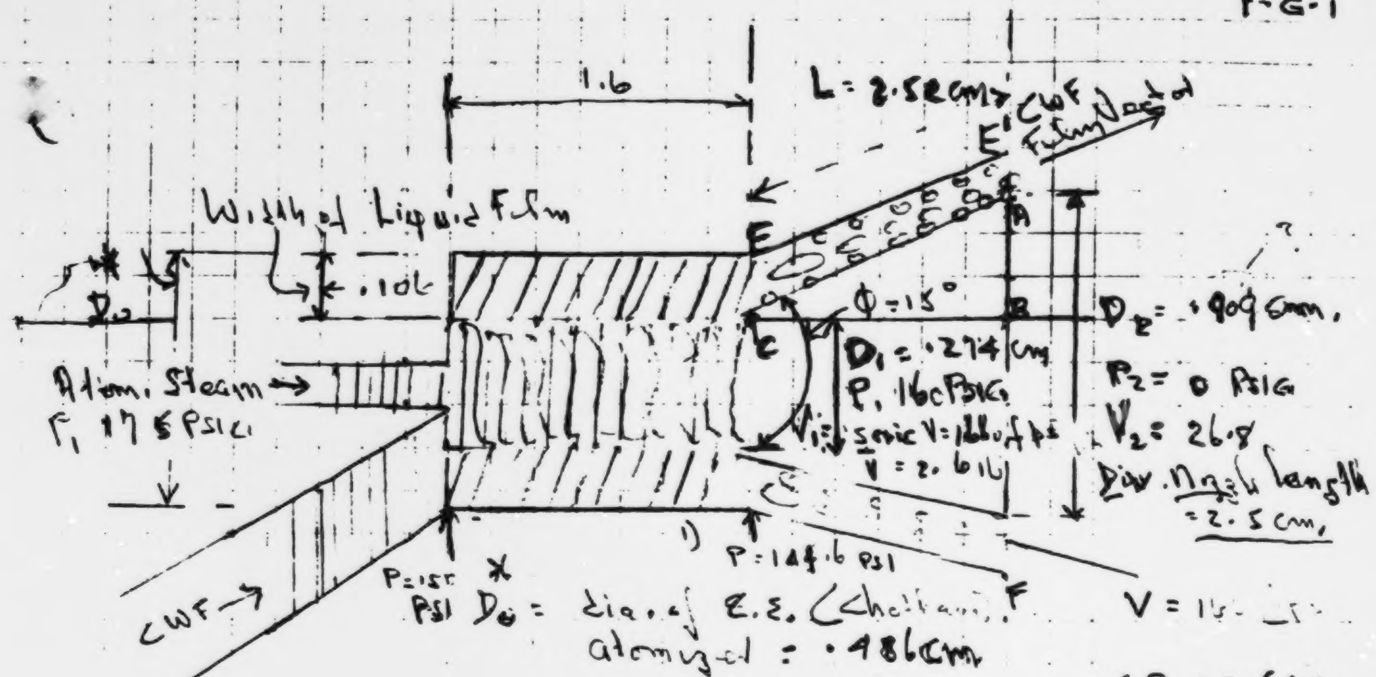
1.6
L = 2.52 cm
CWF Film ...
E'
E
A
B
C
F
Width of Liquid Film
.106
D0
Atom. Steam →
P1 175 PSIG
Φ = 15°
D1 = .274 cm
P1 160 PSIG
V1: sonic V = 1660 fps
V = 2.616
D2 = .909 cm
P2 = 0 PSIG
V2 = 26.8
Div. Angle length = 2.5 cm
P = 14.6 PSI
P = 15 PSI
CWF →
V = 15...
D0 = dia. of E.E. (Chellani) atomized = .486 cm

CB = 2.5 cm

FIG. G.1.1
Schematic of Y-Jet Atomizer

With added Diverging Angle

Dia. EF
= .909 + (2 x .106)
≈ 1.12 cm

Area (EF)
$= \pi \times \left(\frac{1.12}{2}\right)^2$
$= .985\ cm^2$

1) Stress in CWF due to friction

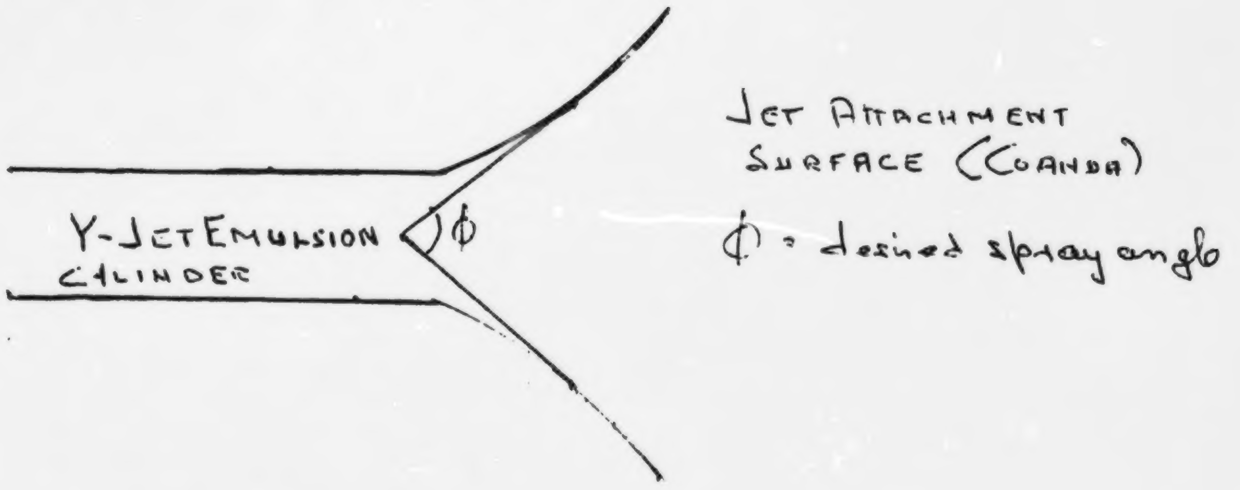
Y-JET EMULSION
CYLINDER
ϕ
JET ATTACHMENT
SURFACE (COANDA)
ϕ = desired spray angle

FIG. G·1·2
SCHEMATIC of the
ATTACHMENT of a COANDA SURFACE
to
A Y-JET ATOMIZER

FIG. G.1.2.F

SPRAY FORMATIONS
NOT TO SCALE
Ref. TABLES G.1.1 ; G.7.1 ; G.7.2
Figs. G.7.2 - G.7.3

AXIAL BURN-OUT DISTANCES

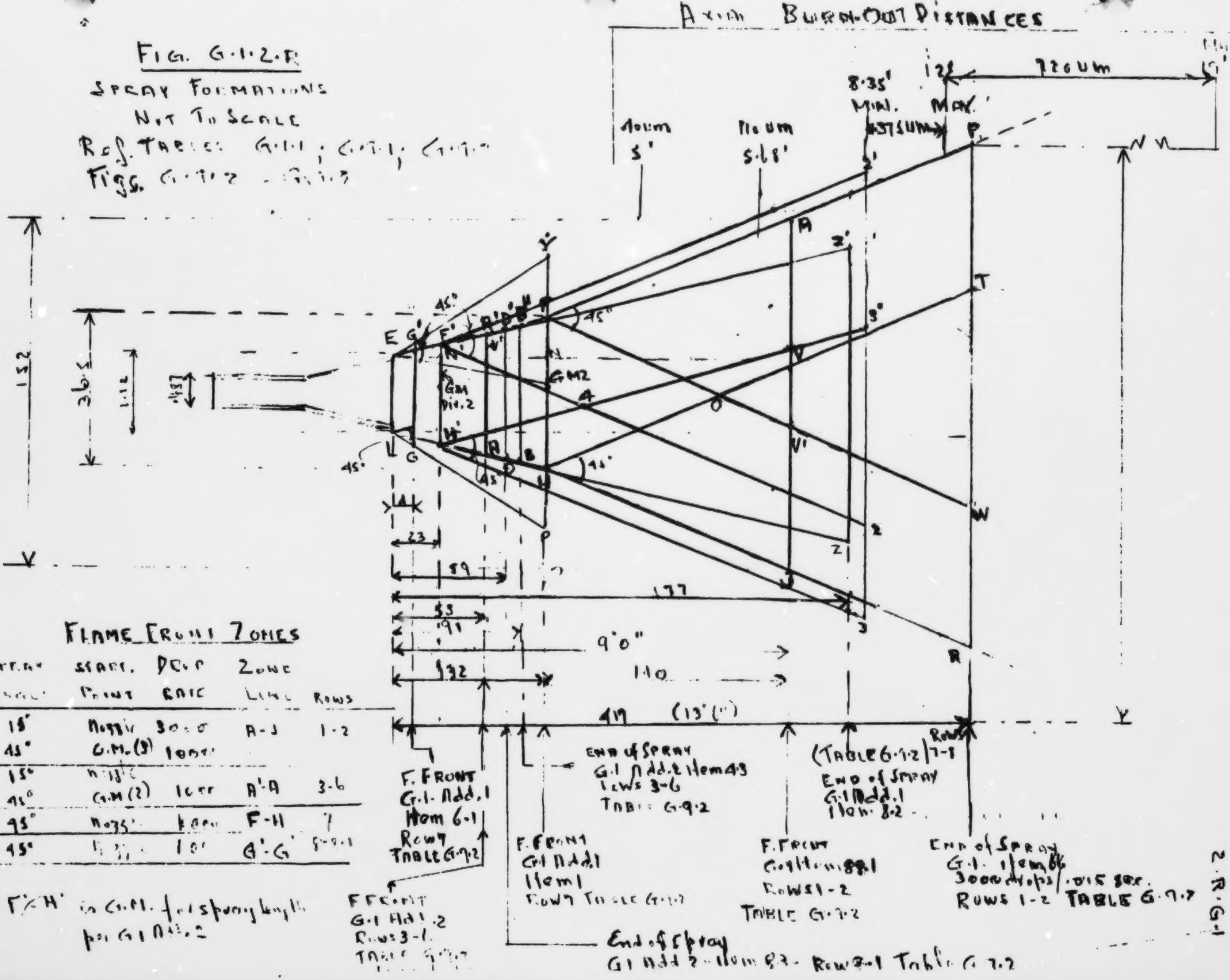

10 um
5'
110 um
5.68'
8.35'
MIN.
437.5 UM
12.2
MAX.
720 UM
P
P'
N
N
S'
A
Z'
T
3'
V
O
V'
W
2
Z
3
R
Y'
E
G'
F'
N'
A'
D
B'
H
GM
Div.2
GM2
4
H'
A
B
D
45°
45°
45°
45°
45°
L
G
P
Y
Y
152
36.5
11.1
1.8
14
23
59
53
91
132
177
9'0"
110
419
(13' 1")
F. FRONT G.1. Add.1 Item 6.1 Row 7 TABLE G.7.2
F FRONT G.1 Add.2 Rows 3-1 TABLE G.7.2
End of Spray G.1 Add.2 Item 4.3 Rows 3-6 TABLE G.9.2
F. FRONT G.1 Add.1 Item 1 Row 7 TABLE G.7.2
End of Spray G.1 Add.2 Item 8.3 Row 3-1 Table G.7.2
F. FRONT G.1 Item 8.1 Rows 1-2 TABLE G.7.2
(TABLE G.7.2) Rows 7-8
End of Spray G.1 Add.1 Item 8.2
End of Spray G.1 Item 6 3000 drops/.015 sec. ROWS 1-2 TABLE G.7.2

FLAME FRONT ZONES

Spray Angle	Start. Point	Drop Rate	Zone Line	Rows
15°	Nozzle	30000	A-J	1-2
45°	G.M.(3)	10000		
15°	Nozzle			
45°	G.M (2)	1000	A'-A	3-6
45°	Nozzle	1000	F-H	7
45°	[illegible]	10'	G'-G	8-9.1

N.B. F'/H' in G.M. for spray length per G.1 Add.2

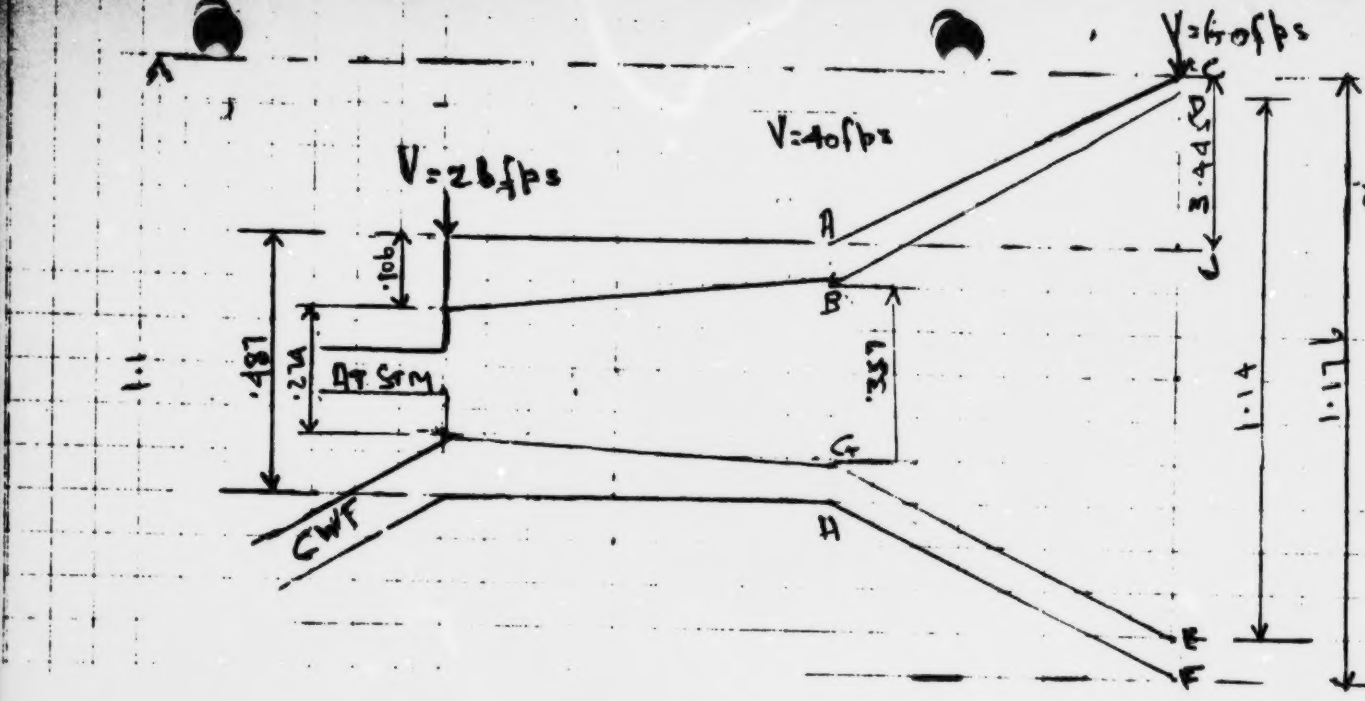
V=60fps
V=40fps
V=26fps
A
B
C
D
E
F
G
H
3.44
.106
.24
97.5μm
.487
.357
1.1
1.14
1.17
CWF

CD = .0156 cm
= 156 μm

20% biased value (.8 × .0156)
= .0125 cm

EF = CD = .0156 cm
biased value = .0184 cm

FIG. G.1.3 (N.T.S. - all dim. cm.)

C.E. ANNULUS WITH DIVERGENT NOZZLE
FLOW ASSUMED UNIFORM WITHIN OCE. OF
ANNULUS AND OF DIVERGENT NOZZLE

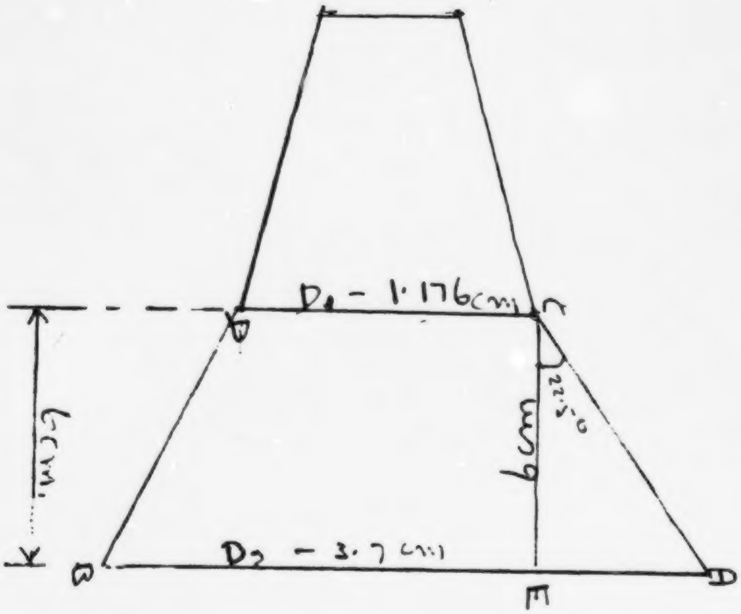
D₁ - 1.176cm
C
A
6cm
22.5°
6cm
B
D₂ - 3.7 cm
E
D

FIG. G. 1.4

DISTANCE TO ZONE WHERE VELOCITIES

REDUCED FROM 1660 fps to 166 fps

(NOTE: CD is Divergent Nozzle Exit)

Fig G.1.5.
Modes of Fluid Mixing

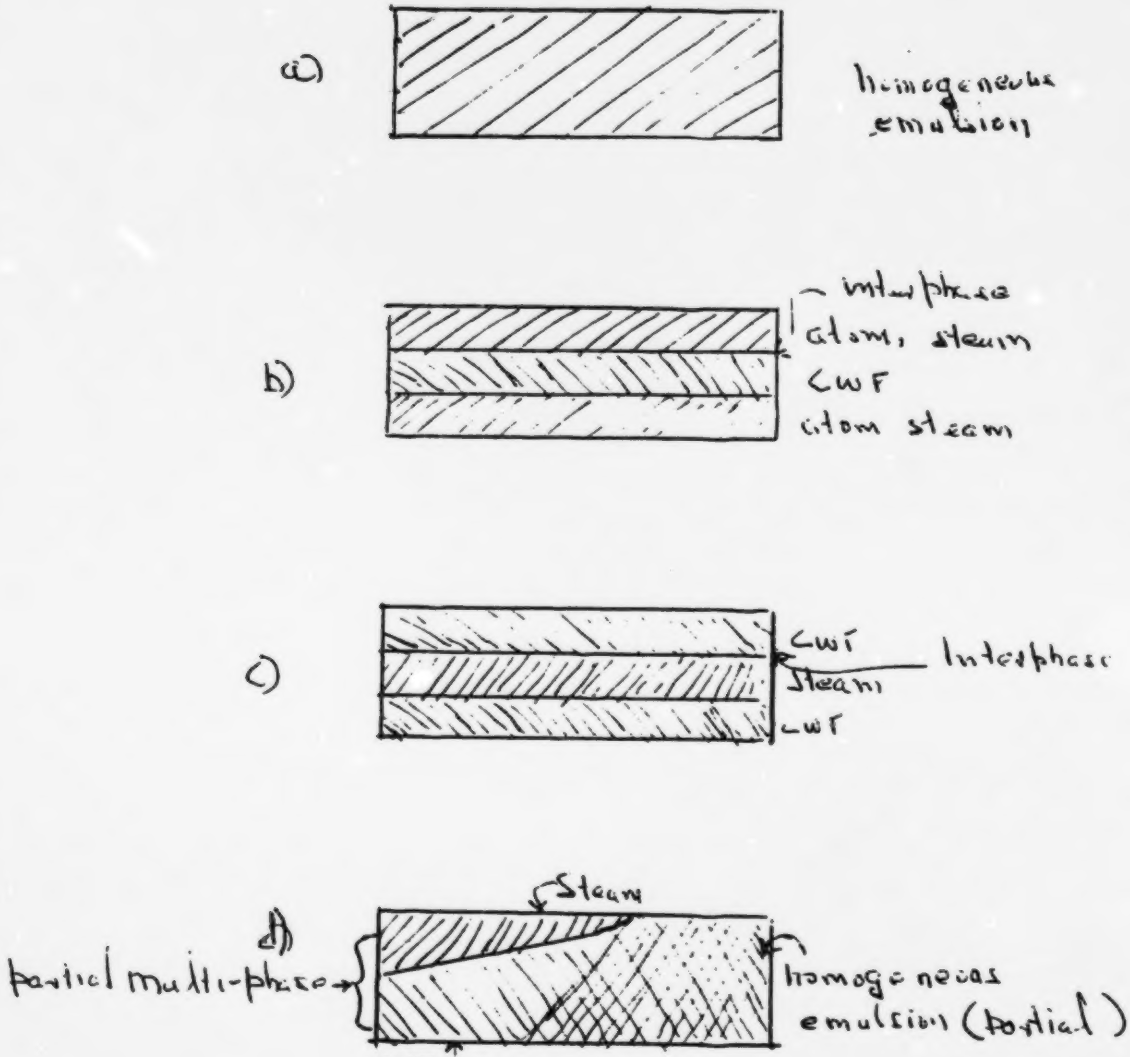
a)
homogeneous emulsion
b)
interphase
atom. steam
CWF
atom steam
c)
CWF
Interphase
Steam
CWF
d)
Steam
partial multi-phase
homogeneous emulsion (partial)
CWF

Determine Modes by:

1.- Use transparent annulus material

2.- Use Laser lighting plus electron microscope for modes a or b+c

3. Use Schlieren technique for mode d)

4·(10)G.1

FIG. 3 The disintegration of the fuel jet issuing from the atomizer (magnification 3.5 × full size).

(iii) the effect of axial and radial distance from the atomizer on the drop size distribution.

4.2.3. Pressure distribution within the atomizer

A second single jet atomizer was manufactured to the standard dimensions but with pressure tappings in the walls of the atomizing fluid port, fuel port and mixing chamber. The pressures within the atomizer were measured over the operating range of fuel and air flow rates.

4.2.4. The effect of atomizer geometry on the drop size distribution

Each geometrical dimension was changed independently and its effect on the drop size distribution measured under the same air/fuel mass ratio and fuel flow rate. In order to do this a series of atomizers had to be manufactured.

5. The experimental results

5.1. Fuel and air mixing and the disintegration of the liquid fuel

The disintegration of the liquid fuel remained fundamentally the same over the wide range (20:1) of fuel and air flow rates studied. A typical photograph of the break-up region is shown in Fig. 3. Increasing the air/fuel mass ratio reduced the break-up length. A similar break-up mechanism was observed in the jet issuing from the large-scale model. The break-up mechanism bears a similarity to that previously described for swirl spray pressure jet atomizers.[1] Fig. 4 shows an idealized model of the mixing between the atomizing air and the fuel with the subsequent disintegration of the fuel.

5.2. The effect of operational conditions on the performance of the atomizer

Fig. 5 shows that an increase in the air/fuel mass ratio

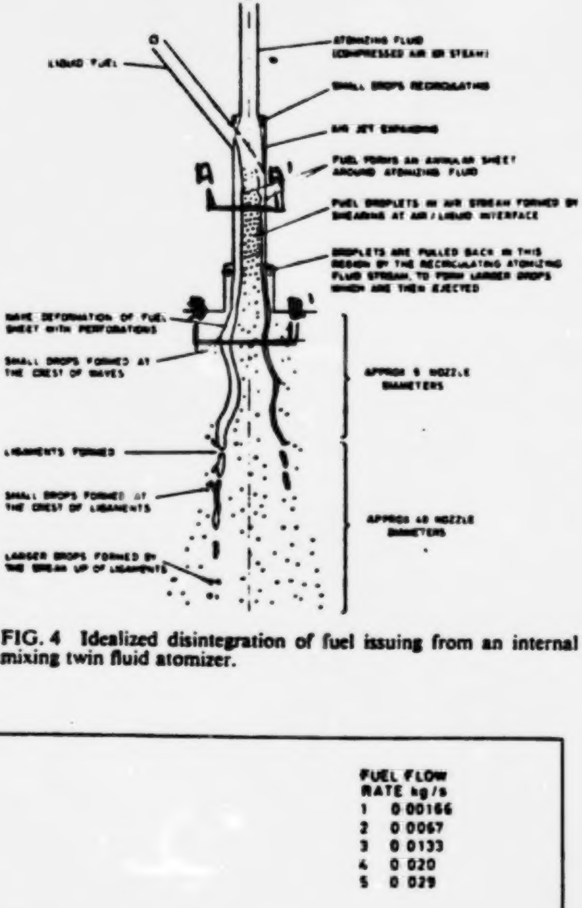
LIQUID FUEL
ATOMIZING FLUID (COMPRESSED AIR OR STEAM)
SMALL DROPS RECIRCULATING
AIR JET EXPANDING
A
A'
FUEL FORMS AN ANNULAR SHEET AROUND ATOMIZING FLUID
FUEL DROPLETS IN AIR STREAM FORMED BY SHEARING AT AIR / LIQUID INTERFACE
DROPLETS ARE PULLED BACK IN THIS REGION BY THE RECIRCULATING ATOMIZING FLUID STREAM, TO FORM LARGER DROPS WHICH ARE THEN EJECTED
B
B'
WAVE DEFORMATION OF FUEL SHEET WITH PERFORATIONS
SMALL DROPS FORMED AT THE CREST OF WAVES
APPROX 5 NOZZLE DIAMETERS
LIGAMENTS FORMED
SMALL DROPS FORMED AT THE CREST OF LIGAMENTS
APPROX 40 NOZZLE DIAMETERS
LARGER DROPS FORMED BY THE BREAK UP OF LIGAMENTS

FIG. 4 Idealized disintegration of fuel issuing from an internal mixing twin fluid atomizer.

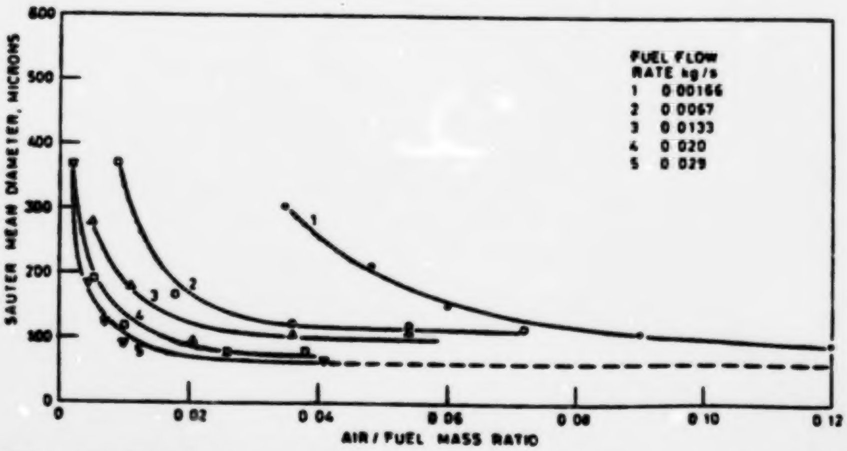

FIG. 5 The effect of air/fuel mass ratio on the Sauter mean diameter for various fuel flow rates.

Based on G.1 Addendum 2

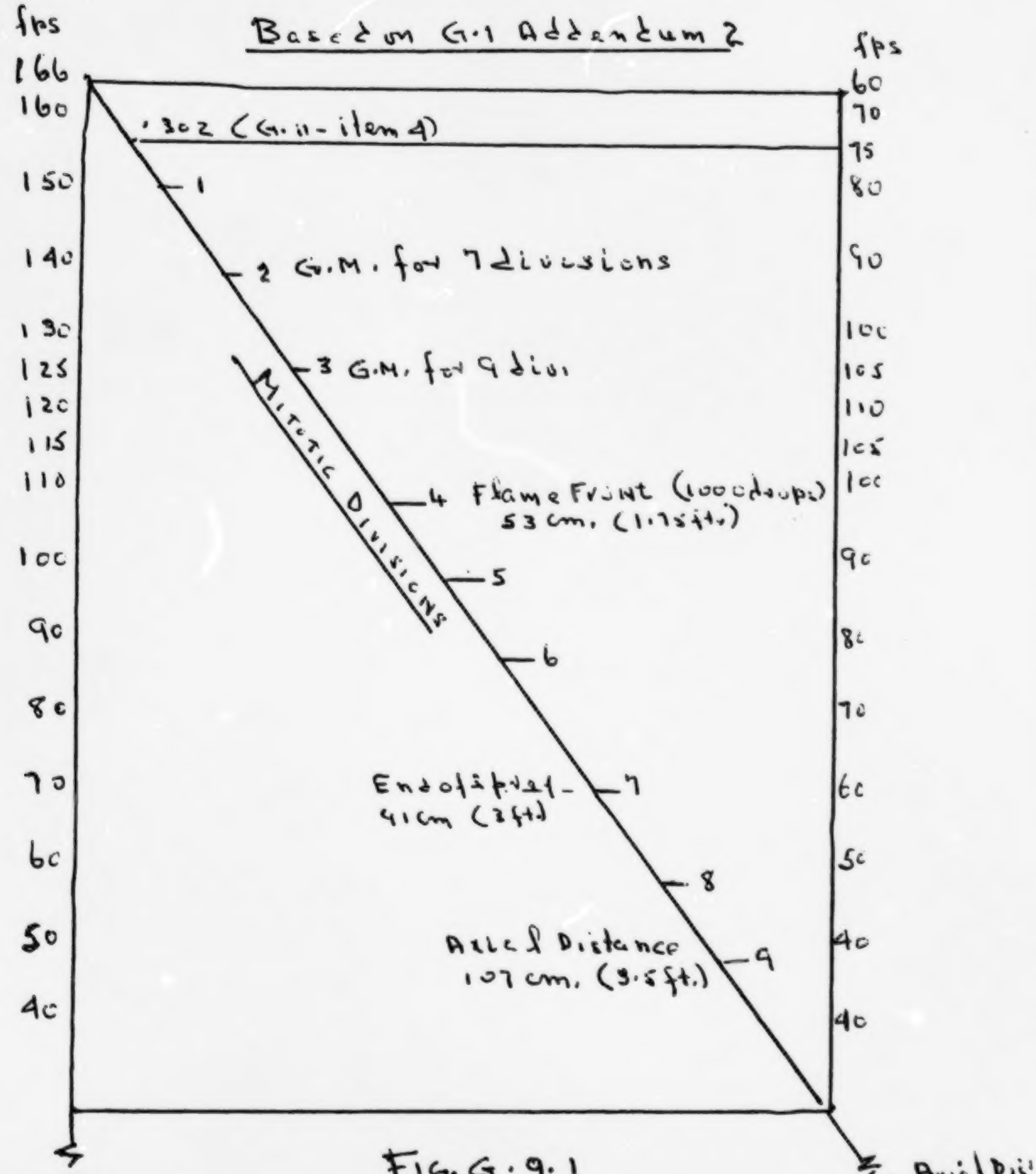

FIG. G.9.1

STEAM VELOCITIES – DECELERATIN from a POINT 3. cm. from NOZZLE (See G.1 Erratum Add. 1)

CWF DROP VELOCITIES – ACCELERATING – DECELERATING from NOZZLE EXIT (at 1000 drops/.005 sec.)

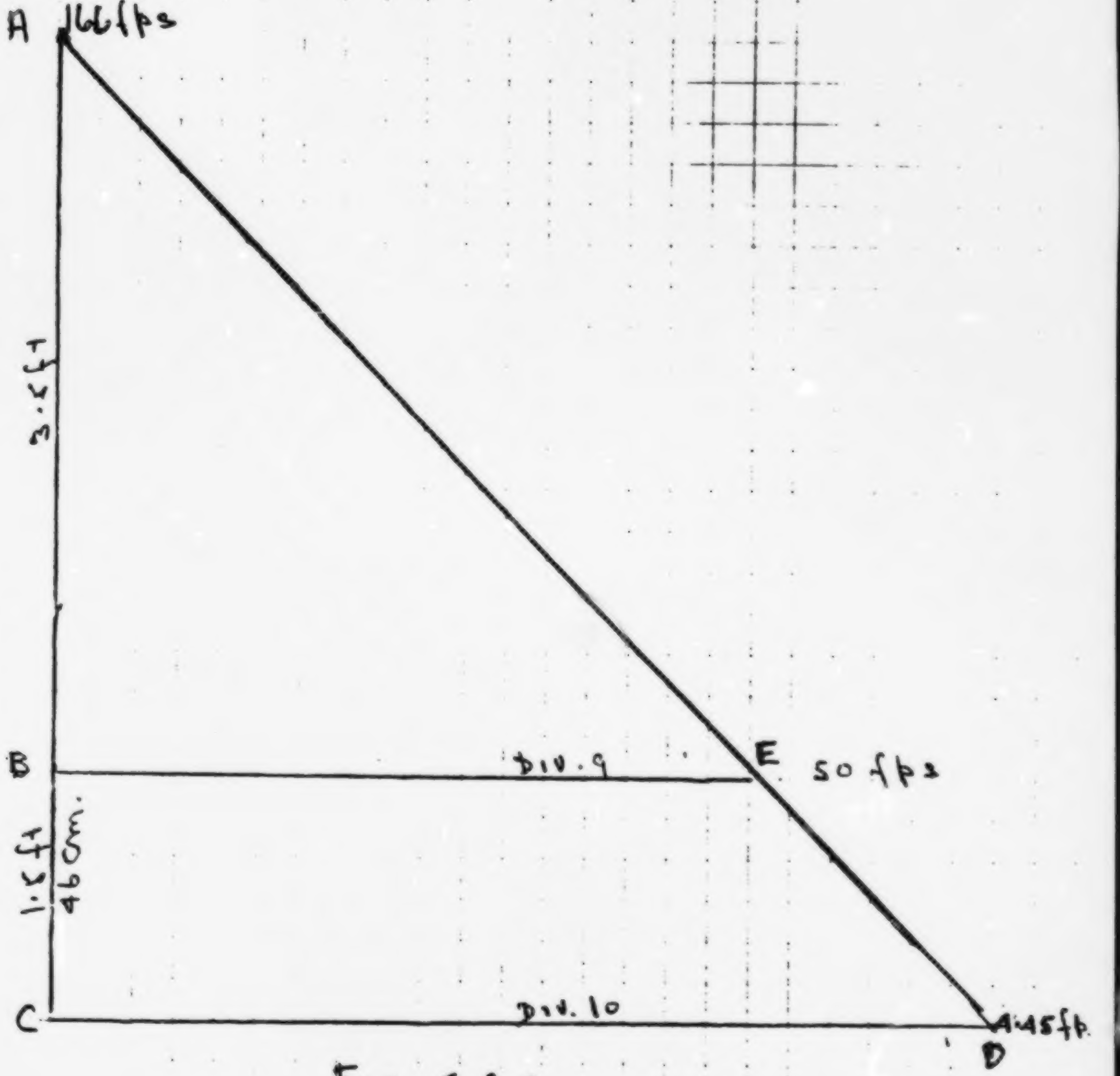
A 166 fps
3.5 ft
B
DIV. 9
E 50 fps
1.5 ft
46 cm.
C
DIV. 10
4.45 fp.
D

FIG. G.9.2

AXIAL DISTANCE from DIV. 9, FIG. G.9.1 to MIN. VELOCITY POINT of 4.45 fps.

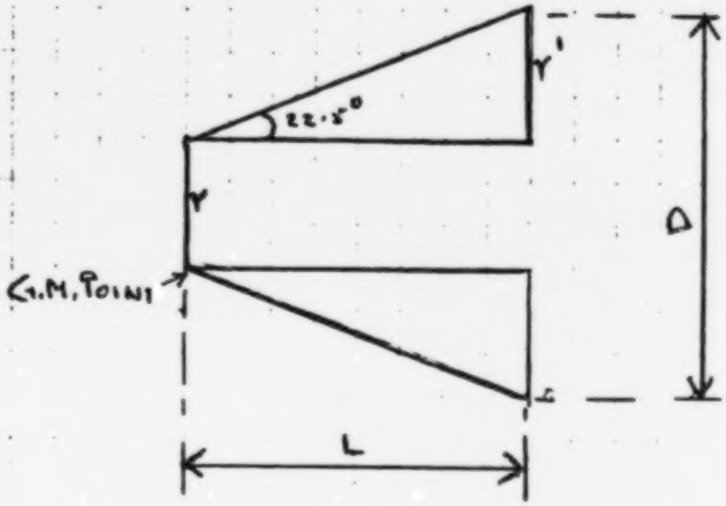

r'
22.5°
r
D
G.M. Point
L

FIG. G 10.1

Dimension Data for Eq. 1 - G.10

16.

SPRAY GEOMETRIES

Fig. G·11·1

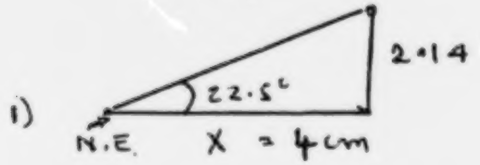
1)
N.E.
22·5°
X = 4cm
2·14

Area 14·4 cm²

See G.1 odh. 2 to G.11 Item 7

FIG. G·11·2

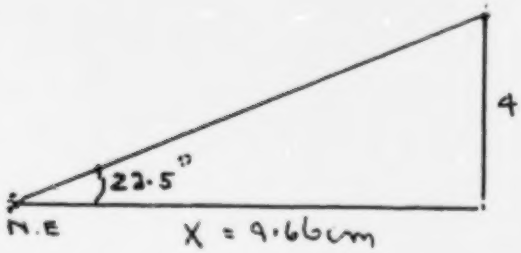
N.E
22·5°
X = 9·66cm
4

Area 50cm²

See G.11 Item 8·2

FIG. G·11·3

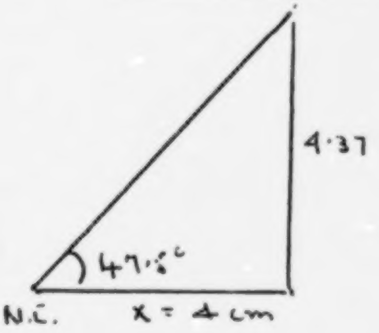
N.E.
47·5°
X = 4 cm
4·37

Area 60 cm²

See G.11. Items 11 & 11.1

---

1) N.E = nozzle exit

16 · Cont'd.

FIG. G·11·4

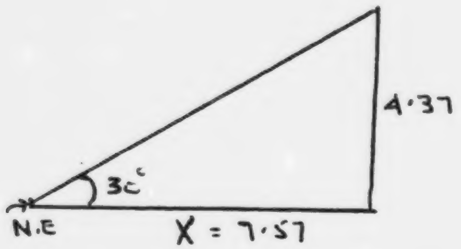
4·37 – Area 60 cm²
30°
N.E
X = 7·57

See G·11 Add.1
Item 5

FIG. G·11·5

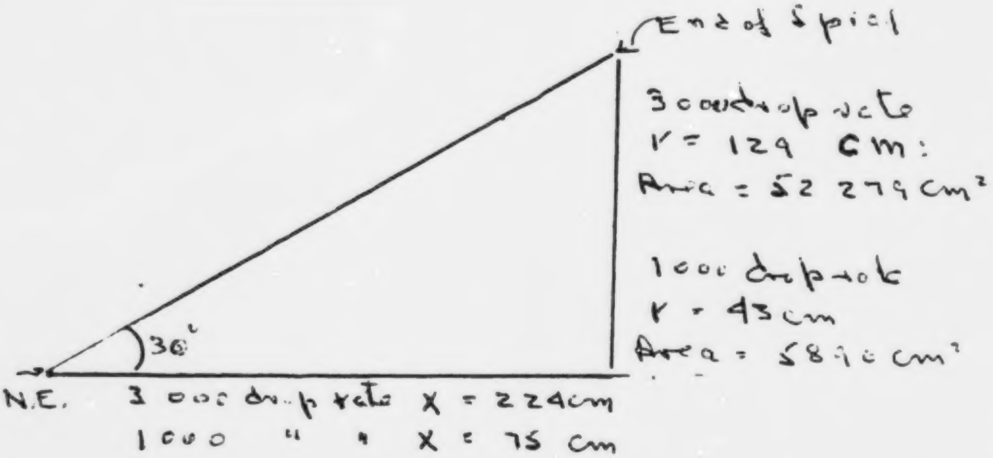
End of Spiral
3000 drop rate
Y = 129 cm:
Area = 52 279 cm²
1000 drip rate
Y = 43 cm
Area = 5890 cm²
30°
N.E.
3 000 drip rate X = 224 cm
1000 " " X = 75 cm

FIG. G·12·1

Spray Intersections

45° Spray Angle from G.M. Point 3

Initial Rate: 3000 Drops/.015 sec

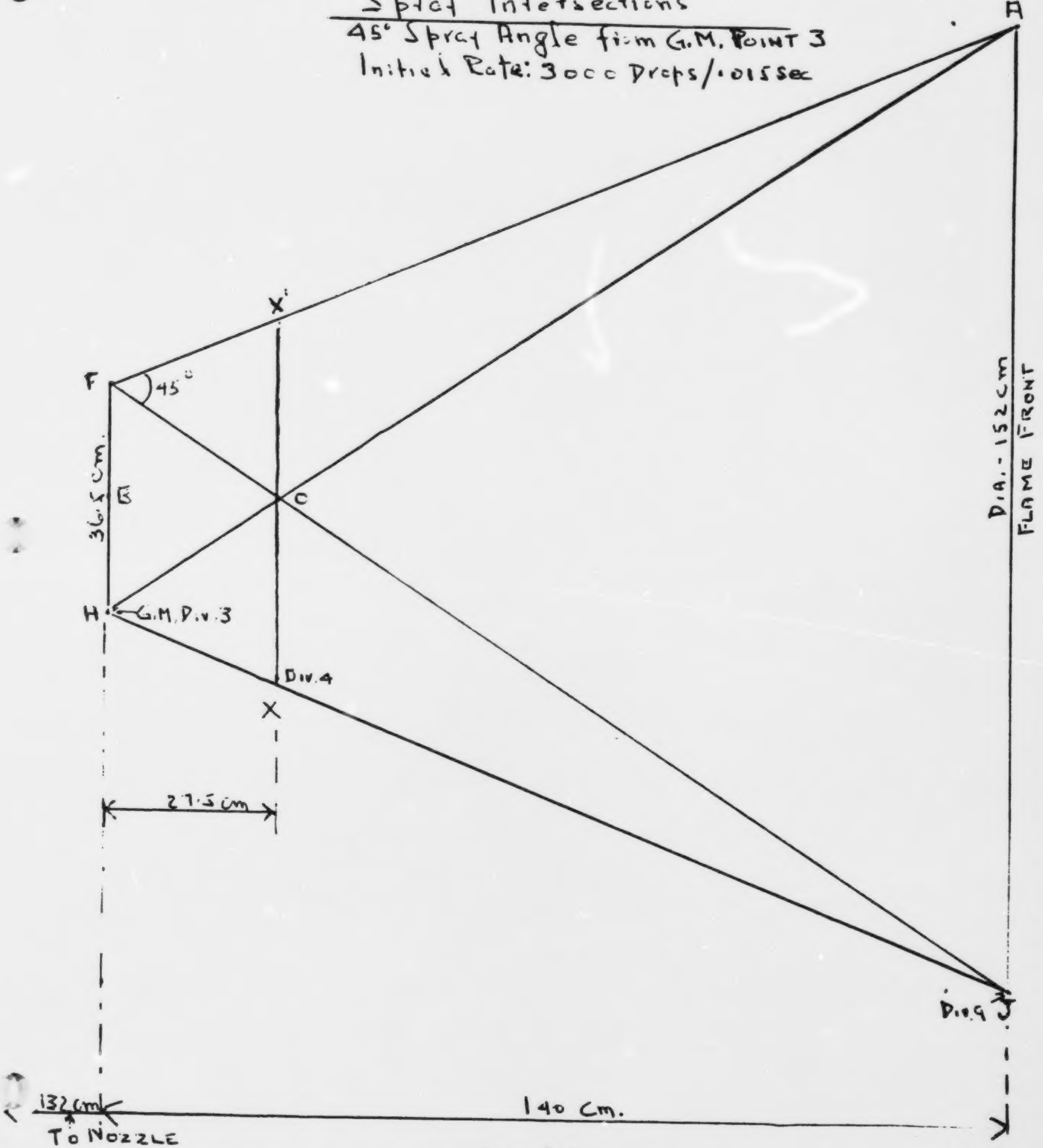
A
X'
F
45°
36.5 cm.
E
C
H
G.M. Div. 3
Div. 4
X
27.5 cm
DIA. - 152 cm
FLAME FRONT
Div. 9
J
132 cm
To Nozzle
140 cm.

Scale: $\frac{1}{4}$" = 5 cm.

FIG. G·12·2

Spray Intersections

45° Spray Angle from G.M. Point 2

Initial Rate: 1000 Drops/.005 sec.

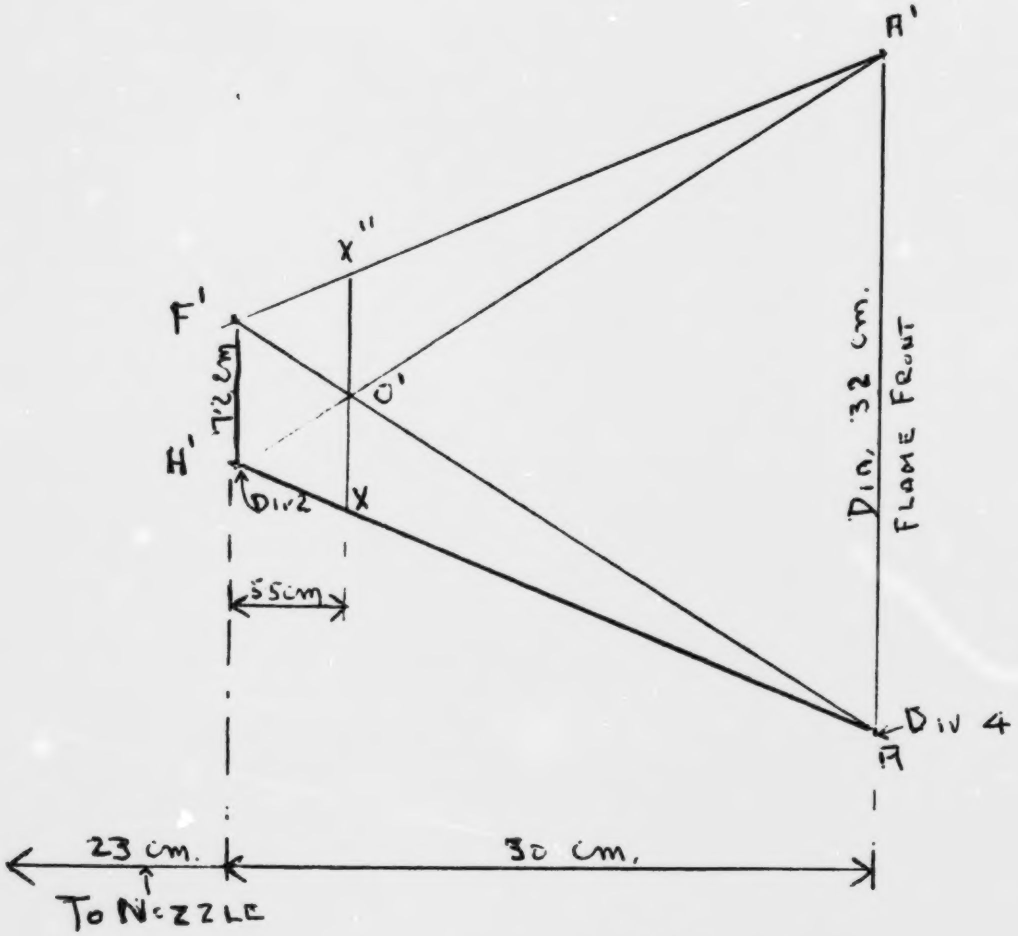
A'
X''
F'
7.2 cm
O'
H'
Div 2
X
5.5 cm
Dia. 32 cm.
FLAME FRONT
Div 4
A
23 cm.
To NOZZLE
30 cm.

Scale: $\frac{1}{4}$" = 2 cm.

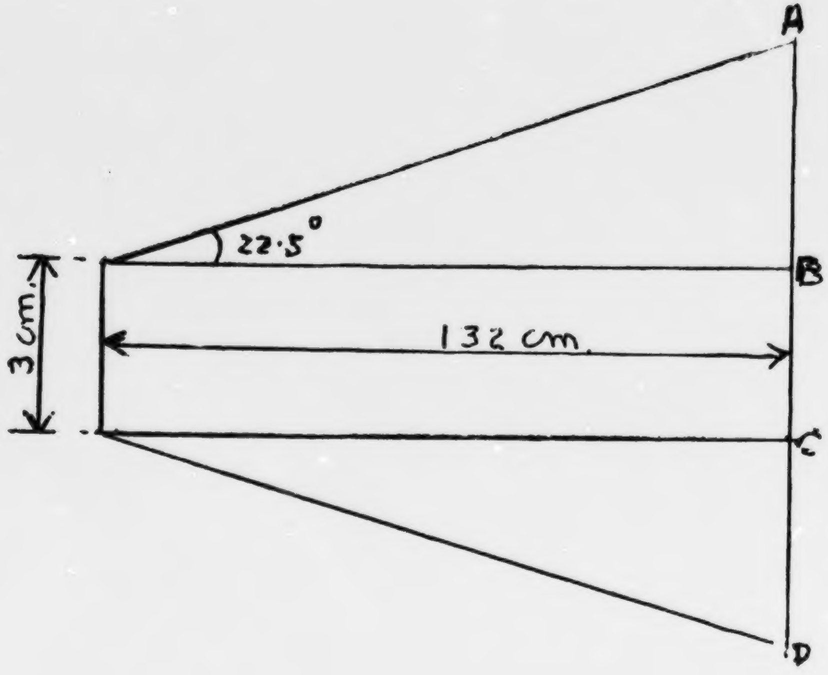

$$AB = 132 \tan 22.5^{\circ}$$
$$= 132 \times .414$$
$$= 54.5 \text{ cm.}$$

$$AD = 2\,AB + BC$$
$$= 109 + 3 = 112 \text{ cm.}$$

$$\text{Oce.} = \pi \times 115 = 351 \text{ cm.}$$

= G.M. Zone of total spray

FIG. G. 14.1

Determination of the G.M. Zone for a Spray Rate of 3000 drops/.015 sec.

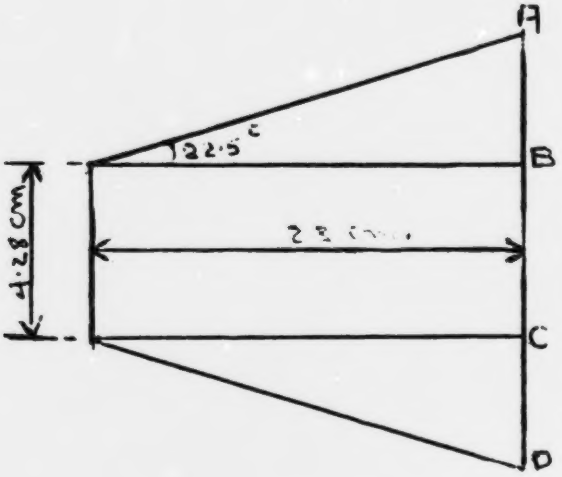
A
22.5°
B
4.28 cm
23 cm.
C
D

AB = 23 tan 22.5°

= 23 x .414

= 9.5

AD = 2 AB + BC

= 19 + 4.28 = 23.3 cm.

Oce = II x 23.3 = 73.2 cm.

= G.M. zone of total spray

FIG. G. 14.2

Determination of the G.M. Zone for a Spray Rate of 1000 Drops/.005 sec.

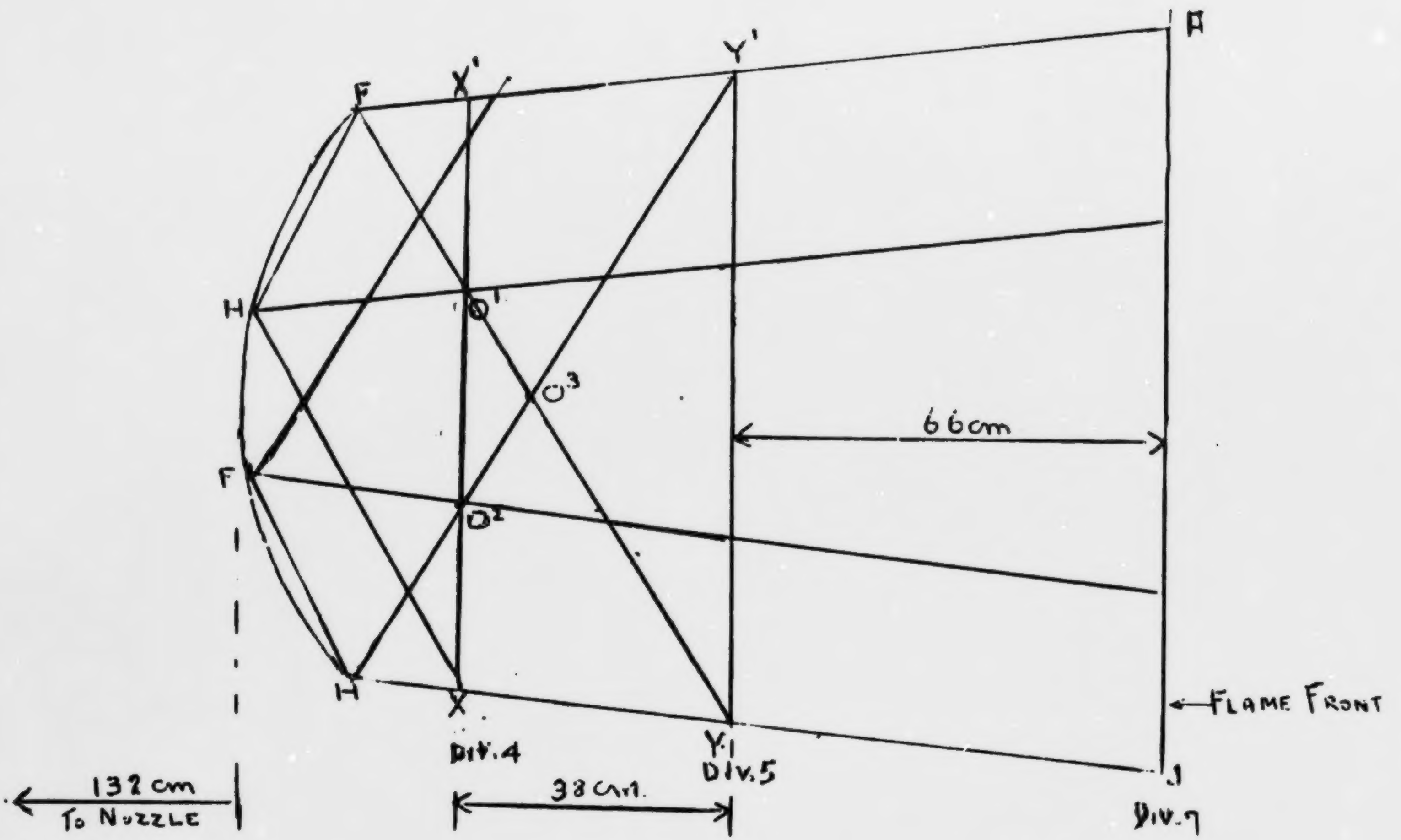
A
Y'
X'
F
H
O1
O3
66cm
F
O2
H
X
Y1
←FLAME FRONT
DIV.4
DIV.5
J
132 cm
To NOZZLE
38 cm.
DIV.7

FIG. G. 14.3

Intersections of Spray Flows from adjoining Annuli

CASE I I - 3000 drops/.013 Sec.
Scale: 1/4" - 6 cms.

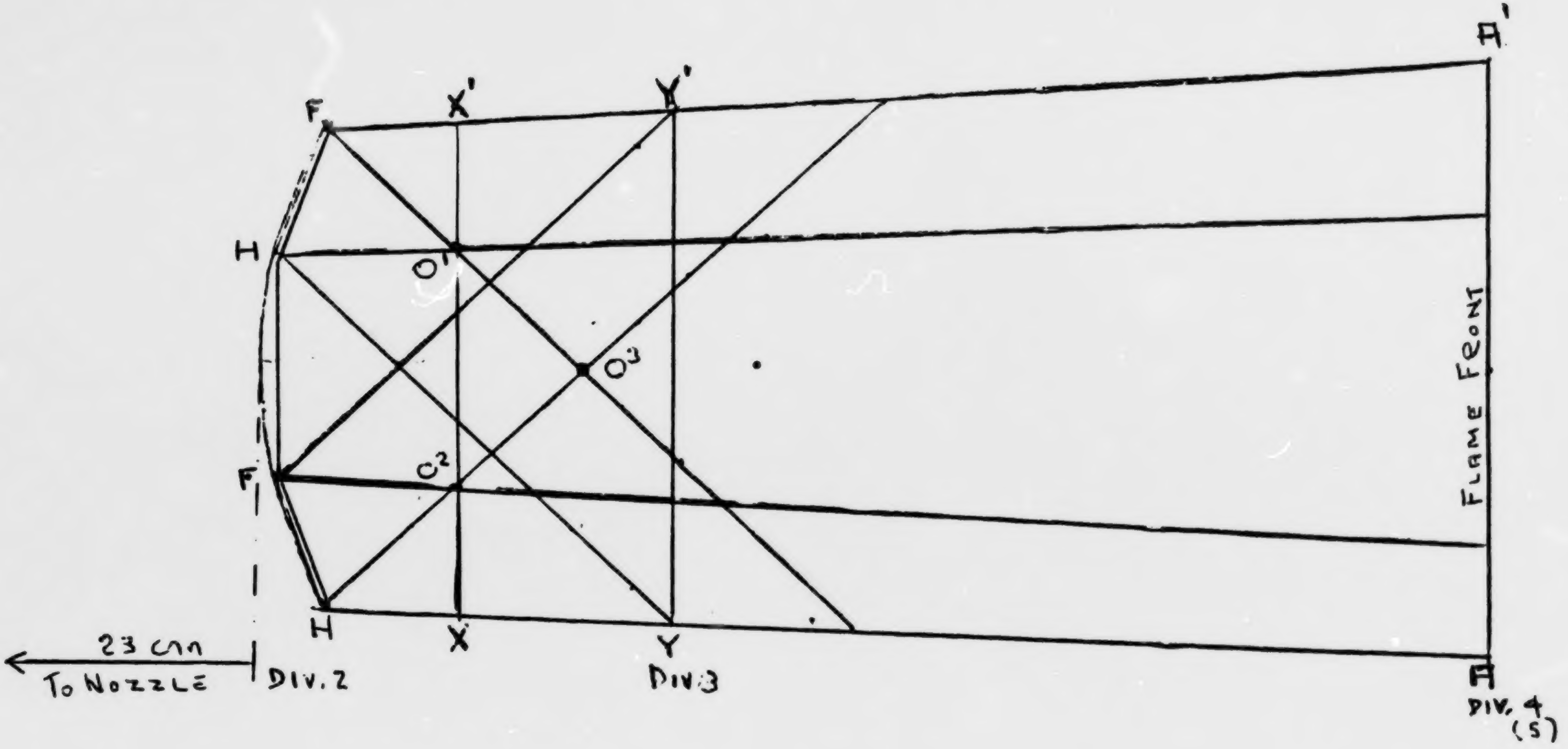

A'
F
X'
Y'
H
O'
O³
C²
F
FLAME FRONT
H
X
Y
23 cm
To NOZZLE
DIV.2
DIV.3
A
DIV. 4
(5)

FIG. G. 14.4

Intersections of Spray Flows from Adjoining Annuli

CASE II - 1000 drops/.005 sec.
SCALE: 1/4" = 1 cm.

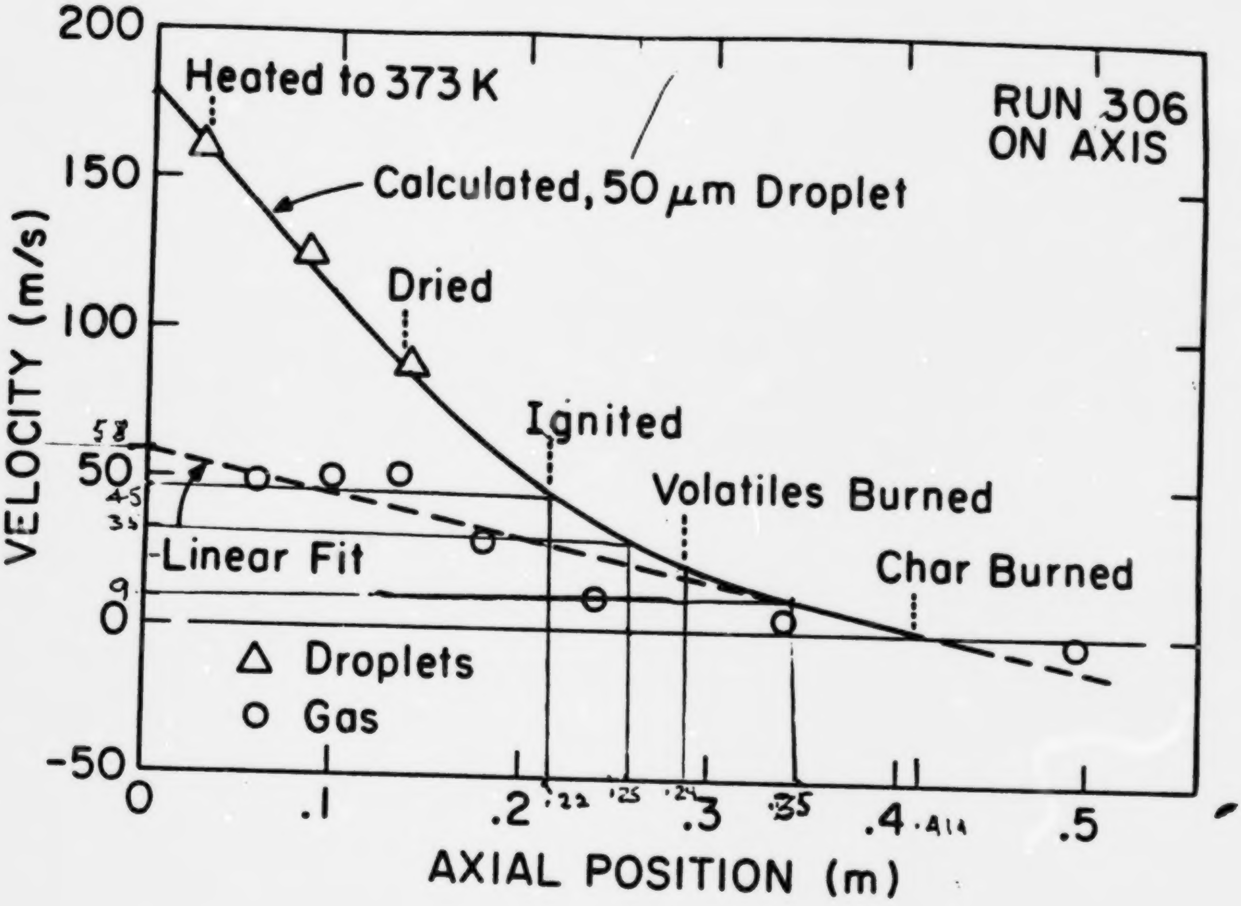

Figure 5. The dependence of droplet and gas velocities on distance from the burner along the axis. The gas velocity data were taken from Fig. 2; the droplet velocity data from high speed cine films (Monroe, 1983). The positions of the ignition and combustion processes and velocities for a 50 μm droplet were calculated as described in the text.

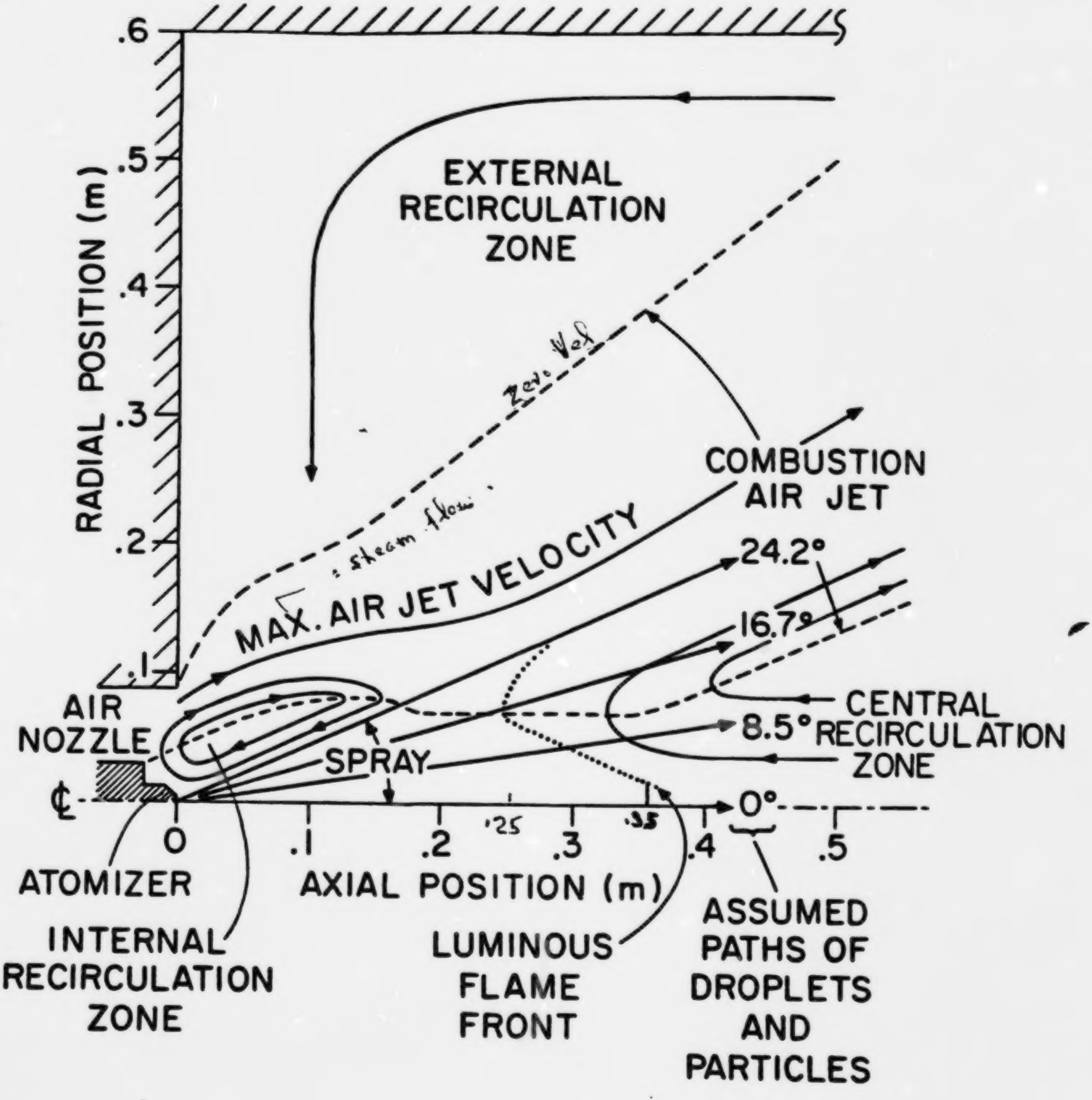
.6
.5
.4
.3
.2
.1
RADIAL POSITION (m)
EXTERNAL RECIRCULATION ZONE
Zero Vel
: steam flow
MAX. AIR JET VELOCITY
COMBUSTION AIR JET
24.2°
16.7°
8.5°
0°
CENTRAL RECIRCULATION ZONE
AIR NOZZLE
SPRAY
℄
0
.1
.2
.25
.3
.35
.4
.5
AXIAL POSITION (m)
ATOMIZER
INTERNAL RECIRCULATION ZONE
LUMINOUS FLAME FRONT
ASSUMED PATHS OF DROPLETS AND PARTICLES

G.15

Figure 3. Gas flow pattern in the region close to the burner.

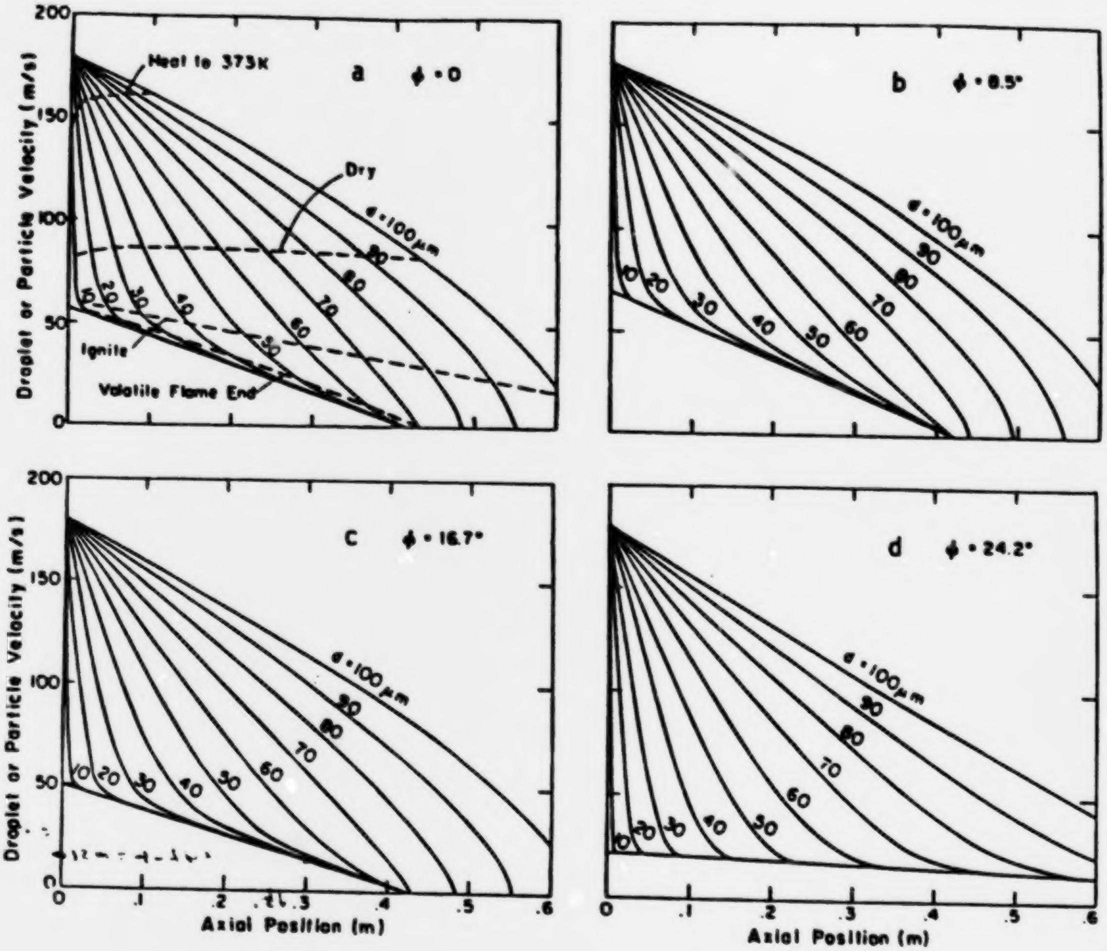

Figure 7. Calculated velocity decay for droplets/particles of 10 to 100 μm.

a. ϕ = 0
b. ϕ = 8.5°
c. ϕ = 16.7°
d. ϕ = 24.2°

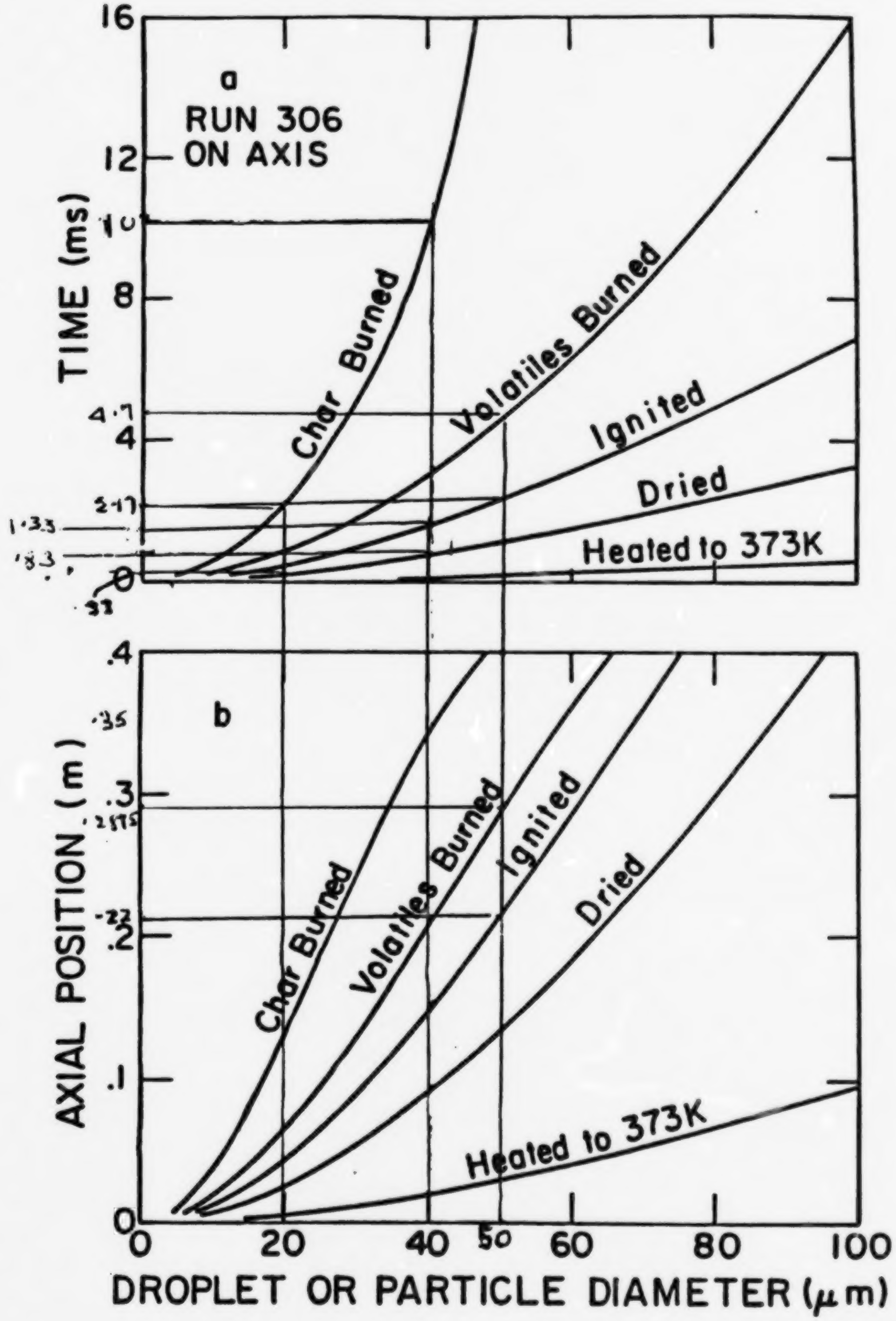

3.15

Figure 10. Dependence on droplet/particle size of: a. cumulative times, and b. Distances required for the ignition and combustion processes.

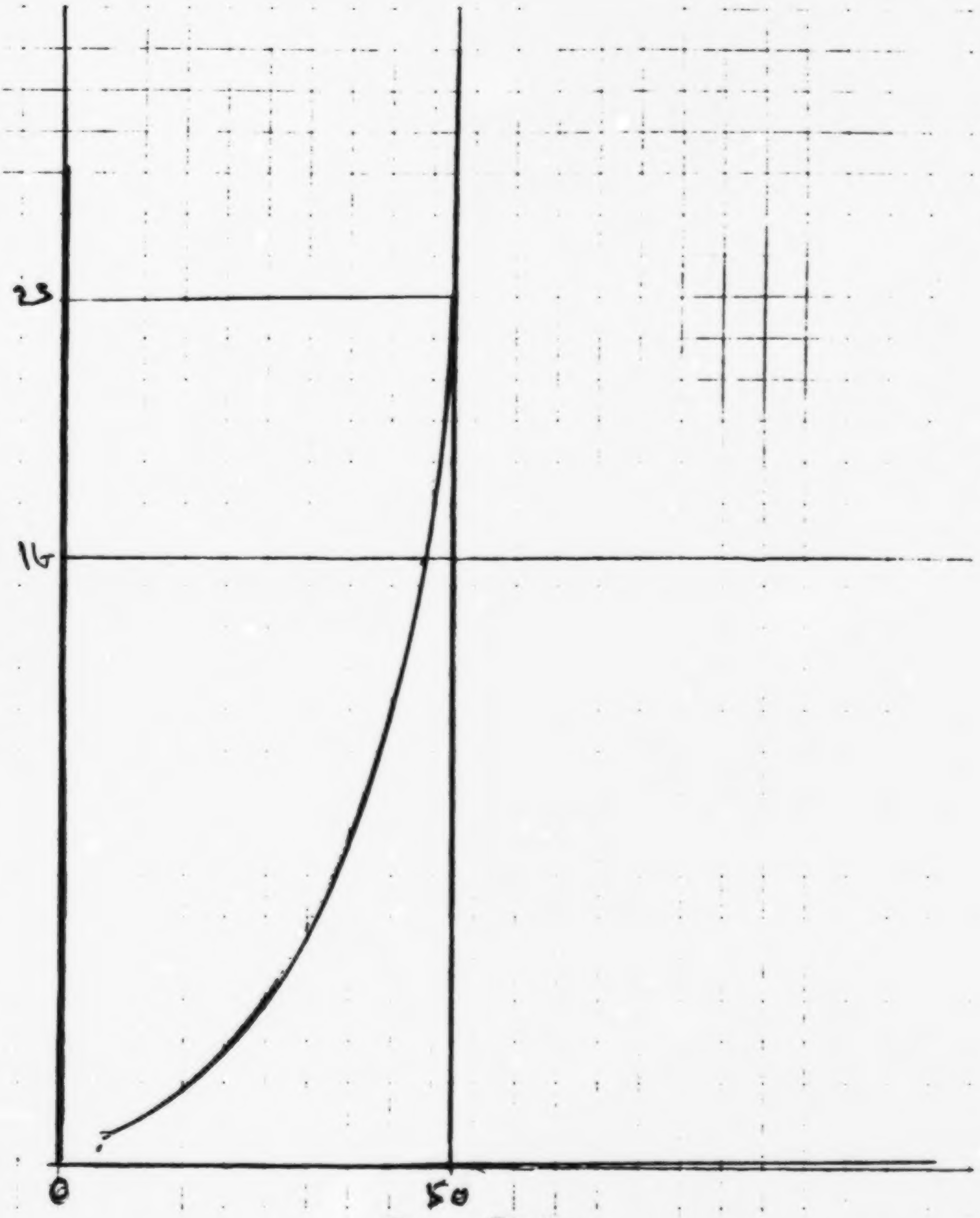

FIG G·15·11

EXTRAPOLATION of CHAR GRAPH
of
Fig. 11 (10)

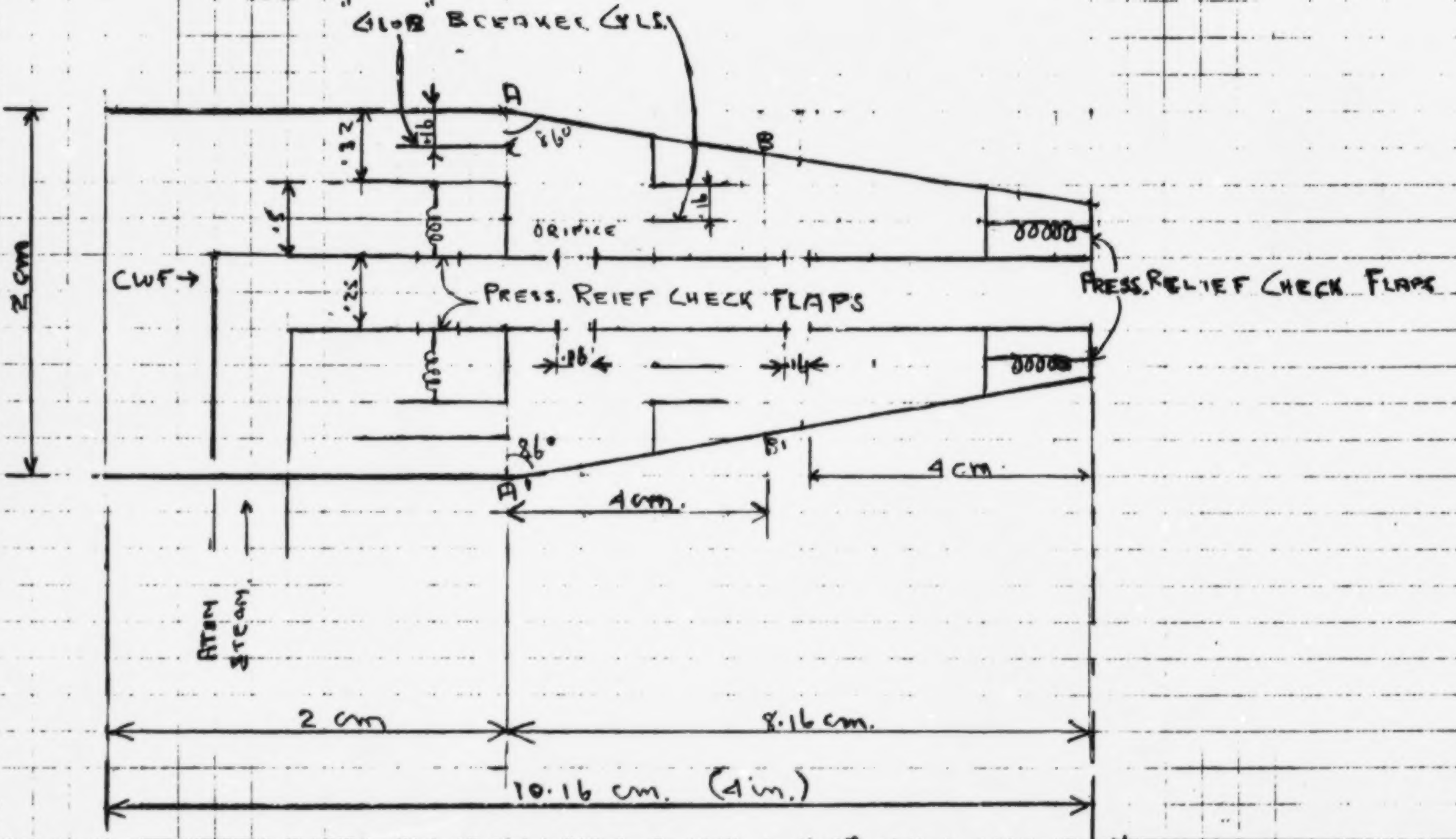
"GLOB" BREAKER CYLS.
A
.16
86°
B
.28
.16
.3
ORIFICE
CWF →
.32
PRESS. REIEF CHECK FLAPS
PRESS. RELIEF CHECK FLAPS
.16
.14
86°
B'
A'
4 cm.
4cm.
2 cm
ATOM STEAM
2 cm
8.16 cm.
10.16 cm. (4in.)

Fig. G.16.1 - Whaley-Grossman Homogenizer

Schematic of a CWF/steam Atomizer Annulu Designed for Optimum Homogeneity of Emulsion (for use per se or in Conjunction With a Divergent Nozzle or Mixing Chamber.

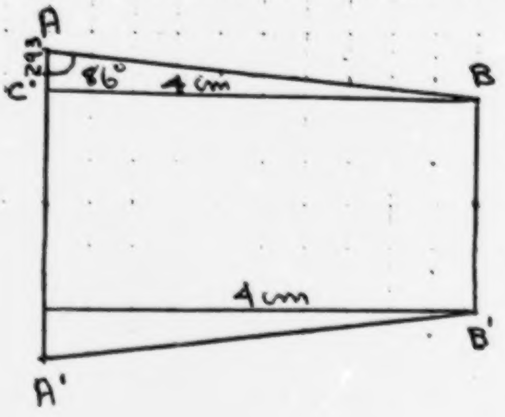

Fig. G.16.2 Division Point of 50% Flow.

Determine angle CAB given

$A\text{-}A^1$ = 2 cm.

BB^1 = 1.414 cm.

$$AC = \frac{AA^1 - BB^1}{2} \; \frac{2 - 1.414}{2} = .293 \text{ cm.}$$

CB = 4 cm.

$$\text{Then } \tan \; CAB = \frac{CB}{AC} = \tan^{-1} \frac{4}{.293}$$

$$= \tan^{-1} 13.65$$

$$= 86^{\circ}$$

The design and performance of internal mixing multijet twin fluid atomizers

by P. J. Mullinger & N. Chigier

An experimental investigation into the effects of operating conditions on the performance of internal mixing twin fluid atomizers has shown that: (1) the primary function of the atomizing fluid is to accelerate the fuel, (2) break up occurs outside the atomizer in a similar manner to a pressure jet and continues for up to 40 nozzle diameters under normal conditions, (3) increasing the atomizing air/fuel mass ratio and increasing the fuel flow rate both reduced the mean diameters of the spray and caused the experimental results to agree closely with the equation previously developed by Wigg, even at the much lower air/fuel mass ratios used in the present experiments and (4) the pressure distribution within the atomizer is dependent both on the fuel flow rate and the air/fuel mass ratio. Experiments concerned with the effects of the atomizer geometry on the spray showed that the geometry affected the performance in two ways: (1) some geometrical variables affected the atomizing fluid velocity and density and hence had an important effect on the drop size distribution, (2) other variables affected the distribution and the thickness of the fuel film in the mixing chamber and hence the drop size distribution. The remaining variables had little effect on the drop size distribution. On the basis of the experimental results guidance for atomizer designers is given and the preferred geometry for this type of atomizer shown.

1. Nomenclature

A = atomizing air flow rate, g/s
D_m = mass median diameter, microns
d_a = atomizing fluid port diameter, mm
d_c = protective counterbore diameter, mm
d_f = fuel port diameter, mm
d_m = mixing chamber diameter, mm
h = radius of mixing chamber, cm
l = premix length, mm
l_a = atomizing fluid port length, mm
l_f = fuel port length, mm
l_m = mixing length, mm
M = atomizing fluid/fuel mass ratio
P_a = atomizing fluid supply pressure, N/m^2
P_f = fuel supply pressure, N/m^2
P_m = pressure at mixing point, N/m^2
ΔP = pressure drop across fuel port, N/m^2
V = atomizing fluid velocity, m/s
W = fuel flow rate, g/s
θ = fuel port to mixing chamber entry angle
σ = surface tension of fuel, dynes/cm
ν = kinematic viscosity of fuel, centistokes
ρ_a = atomizing fluid density, g/cm^3

2. Introduction

In recent years the multijet internal mixing twin fluid atomizer has been increasingly used in oil burners designed for steam-raising applications. Twin fluid atomizers are particularly attractive for use in oil burners that are required to operate at high combustion efficiency with minimum excess air over a wide turn-down ratio. They are frequently used as an alternative to the duplex atomizer or the spill atomizer. The spray angle of the multijet internal mixing twin fluid atomizer does not vary with load, unlike that of the spill and duplex atomizers which exhibit considerable variations in spray angle at certain loads. This change of spray angle is one reason why it is difficult to achieve high combustion efficiencies with minimum excess air over a wide turn-down range with spill and duplex atomizers.

Unfortunately, however, the functioning and design of the multijet internal mixing twin fluid atomizer is not well understood and each atomizer has to be developed specially for each application. This is an expensive time-consuming operation and is therefore a major impediment to their widespread application. This paper describes the functioning of these atomizers and lays down some simple guide lines to assist the designer.

3. The atomizer

The atomizer consists essentially of a number of jets from a minimum of about six to a normal maximum of about 30 according to the duty for which the atomizer is required. The jets are arranged in a single block of metal to give a hollow conical spray. A cross-section through a single jet is shown in Fig. 1 where the geometrical variables of the atomizer are identified.

At the beginning of the present investigations it was known that these variables had an effect on the performance of the atomizer, but the significance of the effect of each variable was unknown. Furthermore, no information was available on the functioning of the atomizer or on the pressure-flow relationships of the two fluids passing through it.

4. Experimental apparatus and technique

Experiments were designed to investigate the functioning of the atomizer and the effect of operating conditions and atomizer geometry on its performance. For the experiments a single jet similar to that shown in Fig. 1 was used. To establish the validity of using the single jet, a two-jet atomizer was also manufactured. The geometry of these two atomizers was similar to that of the atomizer developed by the Admiralty Marine Engineering Establishment; the spacing between the jets on the two-jet atomizer was the same as the spacing on the Admiralty atomizer. These atomizers were tested at the same fuel port loading and air/fuel mass ratio. It was found that although intermixing occurred between the jets of the two-jet atomizer this had no effect on the drop size distribution produced, thus establishing the validity of the use of the single jet in the experiments.

4.1. Experimental apparatus

The apparatus is shown schematically in Fig. 2. A photographic technique was used to measure the drop size

---

*Formerly Department of Chemical Engineering and Fuel Technology, University of Sheffield; now an independent consultant.

†Department of Chemical Engineering and Fuel Technology, University of Sheffield.

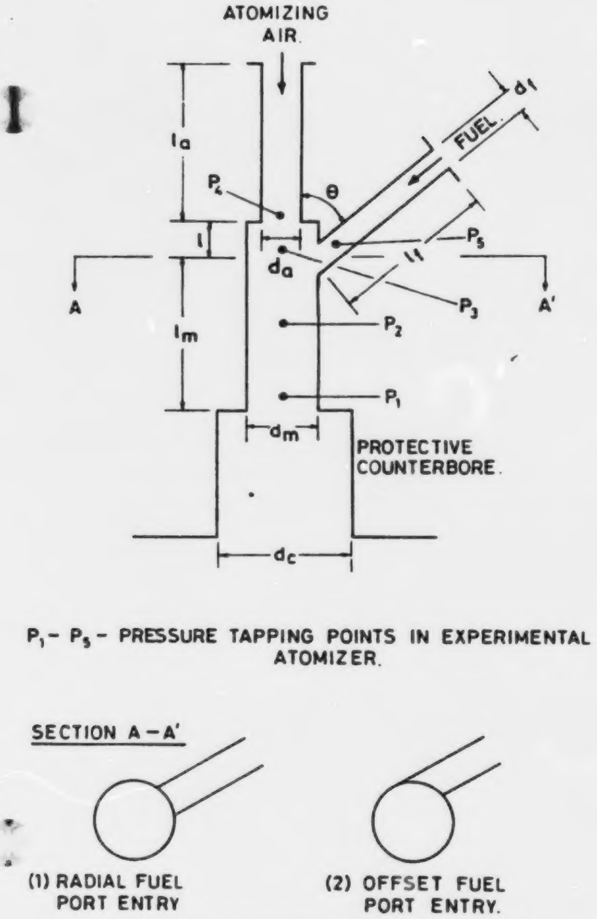
ATOMIZING AIR
FUEL
d_f
l_a
P_4
θ
P_5
l
d_a
l_f
P_3
A
A'
l_m
P_2
P_1
d_m
PROTECTIVE COUNTERBORE
d_c
$P_1 - P_5$ - PRESSURE TAPPING POINTS IN EXPERIMENTAL ATOMIZER.
SECTION A-A'
(1) RADIAL FUEL PORT ENTRY
(2) OFFSET FUEL PORT ENTRY

FIG. 1 Cross-section of internal mixing twin fluid atomizer.

distribution and investigate the break-up mechanism. The atomizer was arranged to spray vertically downwards into the spray separating chamber. A fan was used to maintain the air pressure in the chamber slightly below atmospheric to ensure that all the spray entered the chamber. Fuel was drawn from a reservoir at the bottom of the spray separating chamber by a gear pump via a 'rotameter', which measured the flow rate. The fuel passed from the pump to the atomizer via a needle valve, which controlled the flow rate. Atomizing air was taken from the service main via a rotameter, which measured the flow rate, and an adjustable pressure reducing valve to control the pressure at which the air was supplied to the atomizer.

An M.P.P. 5 in × 4 in technical camera fitted with a Xenotar 2.8 × 150 mm lens was used. Rear illumination was provided by a high voltage discharge spark, which was fired by an electronic delay unit triggered by the camera shutter. The optical system and the atomizer were mounted on simple screw traversing mechanisms to enable different *X*, *Y* positions in the spray to be photographed easily. The resultant negatives were back projected on to a translucent screen and the diameters of the drops were measured using a simple electronic data logging apparatus. The size distributions, etc., were then calculated using a computer.

4.2. The experimental investigations

In order to obtain a comprehensive understanding of the atomizer and its performance, four basic investigations were undertaken.

4.2.1. Fuel and atomizing air mixing and fuel break-up

The break-up of the fuel issuing from the single jet atomizer was studied photographically both with and without atomizing air. A wide range of air and fuel flow rates were used. The physical process of fuel and air mixing within the atomizer was studied photographically with the aid of a large-scale transparent perspex model passing air and water.

4.2.2. The effect of operating conditions on the drop size distribution

The single jet atomizer was used to study the effect of: (i) atomizing air/fuel mass ratio, (ii) fuel flow rate and

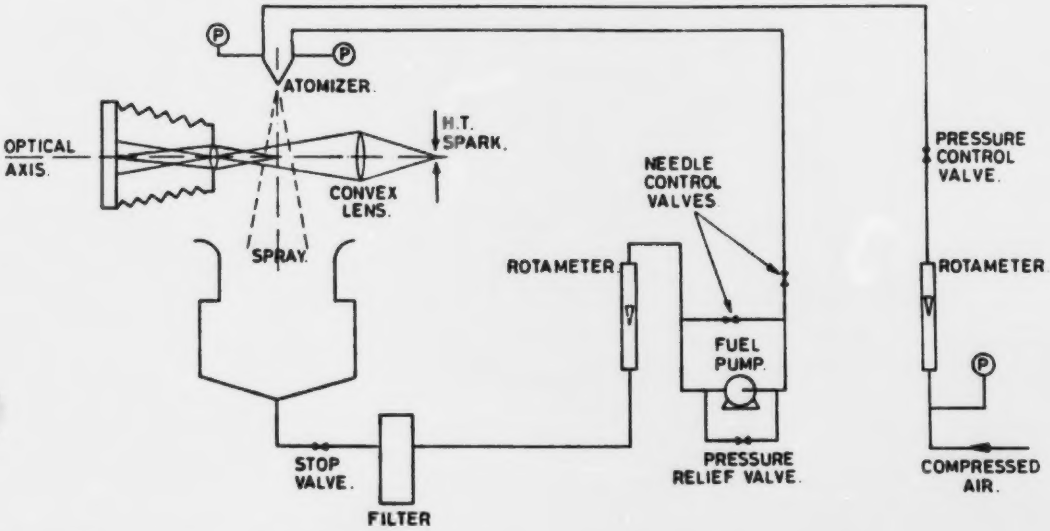
P
P
ATOMIZER.
OPTICAL AXIS.
H.T. SPARK.
CONVEX LENS.
SPRAY.
NEEDLE CONTROL VALVES
PRESSURE CONTROL VALVE.
ROTAMETER
ROTAMETER
FUEL PUMP
P
STOP VALVE.
FILTER
PRESSURE RELIEF VALVE.
COMPRESSED AIR.

FIG. 2 Schematic diagram of the experimental apparatus.

FIG. 3 The disintegration of the fuel jet issuing from the atomizer (magnification 3.5 × full size).

(iii) the effect of axial and radial distance from the atomizer on the drop size distribution.

4.2.3. Pressure distribution within the atomizer

A second single jet atomizer was manufactured to the standard dimensions but with pressure tappings in the walls of the atomizing fluid port, fuel port and mixing chamber. The pressures within the atomizer were measured over the operating range of fuel and air flow rates.

4.2.4. The effect of atomizer geometry on the drop size distribution

Each geometrical dimension was changed independently and its effect on the drop size distribution measured under the same air/fuel mass ratio and fuel flow rate. In order to do this a series of atomizers had to be manufactured.

5. The experimental results

5.1. Fuel and air mixing and the disintegration of the liquid fuel

The disintegration of the liquid fuel remained fundamentally the same over the wide range (20:1) of fuel and air flow rates studied. A typical photograph of the break-up region is shown in Fig. 3. Increasing the air/fuel mass ratio reduced the break-up length. A similar break-up mechanism was observed in the jet issuing from the large-scale model. The break-up mechanism bears a similarity to that previously described for swirl spray pressure jet atomizers.[1] Fig. 4 shows an idealized model of the mixing between the atomizing air and the fuel with the subsequent disintegration of the fuel.

5.2. The effect of operational conditions on the performance of the atomizer

Fig. 5 shows that an increase in the air/fuel mass ratio

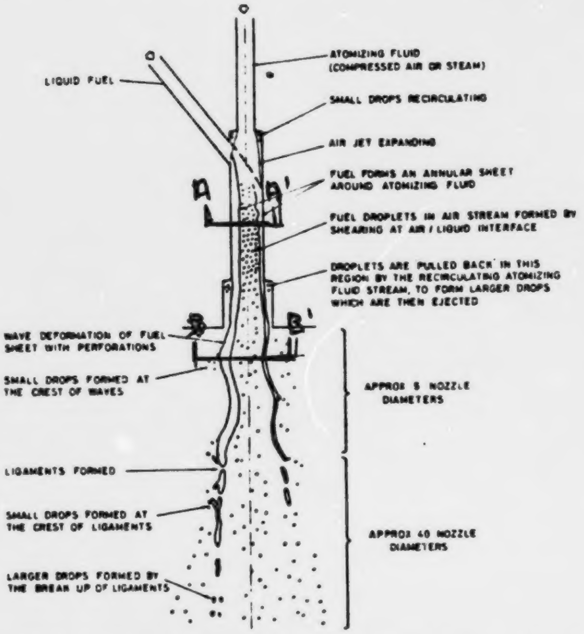
LIQUID FUEL
ATOMIZING FLUID (COMPRESSED AIR OR STEAM)
SMALL DROPS RECIRCULATING
AIR JET EXPANDING
FUEL FORMS AN ANNULAR SHEET AROUND ATOMIZING FLUID
A
A'
FUEL DROPLETS IN AIR STREAM FORMED BY SHEARING AT AIR / LIQUID INTERFACE
DROPLETS ARE PULLED BACK IN THIS REGION BY THE RECIRCULATING ATOMIZING FLUID STREAM, TO FORM LARGER DROPS WHICH ARE THEN EJECTED
B
B'
WAVE DEFORMATION OF FUEL SHEET WITH PERFORATIONS
SMALL DROPS FORMED AT THE CREST OF WAVES
APPROX 5 NOZZLE DIAMETERS
LIGAMENTS FORMED
SMALL DROPS FORMED AT THE CREST OF LIGAMENTS
APPROX 40 NOZZLE DIAMETERS
LARGER DROPS FORMED BY THE BREAK UP OF LIGAMENTS

FIG. 4 Idealized disintegration of fuel issuing from an internal mixing twin fluid atomizer.

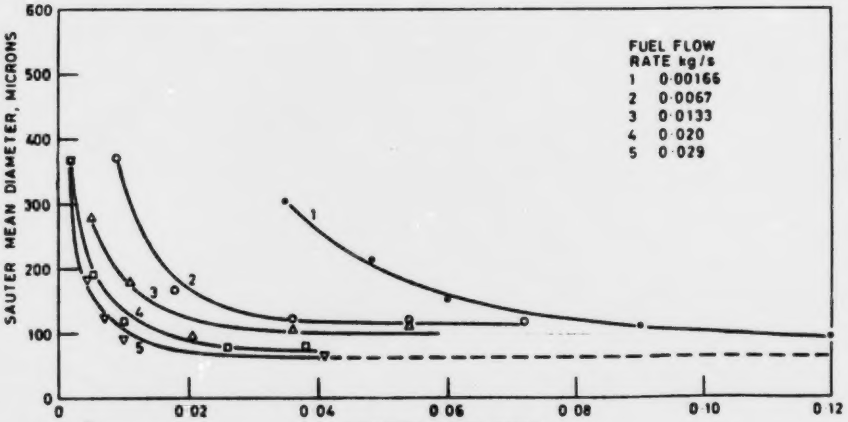

(10)

FIG. 5 The effect of air/fuel mass ratio on the Sauter mean diameter for various fuel flow rates.

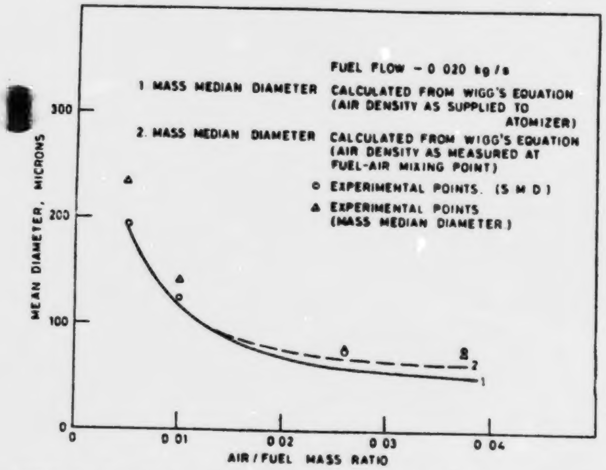

FIG. 6 Comparison between the effect of air/fuel mass ratio on the mass median diameter calculated from Wigg's equation and the experimental results.

causes a reduction in the Sautef mean diameter. Similarly an increase in the fuel flow rate causes a reduction in the Sauter mean diameter. Hence an atomizer required to produce a constant Sauter mean diameter over a wide operating range will require a larger air/fuel mass ratio at low load than at high load.

Wigg[2] produced an empirical formula for calculating the expected drop size from a twin fluid atomizer:

$$D_m = \frac{200\nu^{0.5}W^{0.1}\left(1+\dfrac{W}{A}\right)^{0.5}h^{0.1}\sigma^{0.2}}{\rho^{0.3}V} \quad . \quad (1)$$

Consideration of the terms in equation (1) shows that the air/fuel mass ratio, air density and relative velocity and viscosity have a considerable effect, but that the fuel flow rate and surface tension have less effect. The geometry of the atomizer is represented by the term h, which in the present case is the radius of the mixing chamber. This term does not in itself have a very great effect but frequently a change in the geometry has an effect on the atomizing fluid density or velocity, both of which themselves have an important effect on the drop size of the spray.

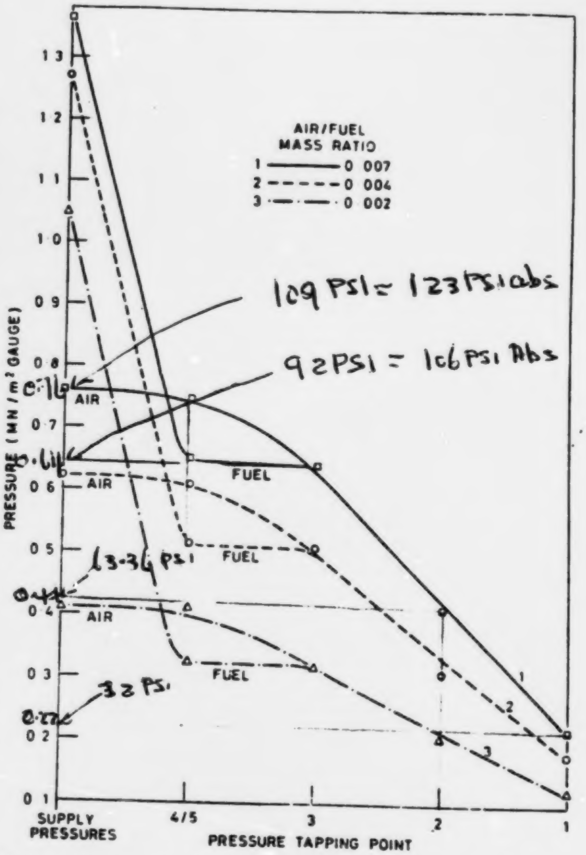

FIG. 8 Pressure distribution within atomizer for a fuel flow rate of 0.0294 kg/s and various air/fuel mass ratios.

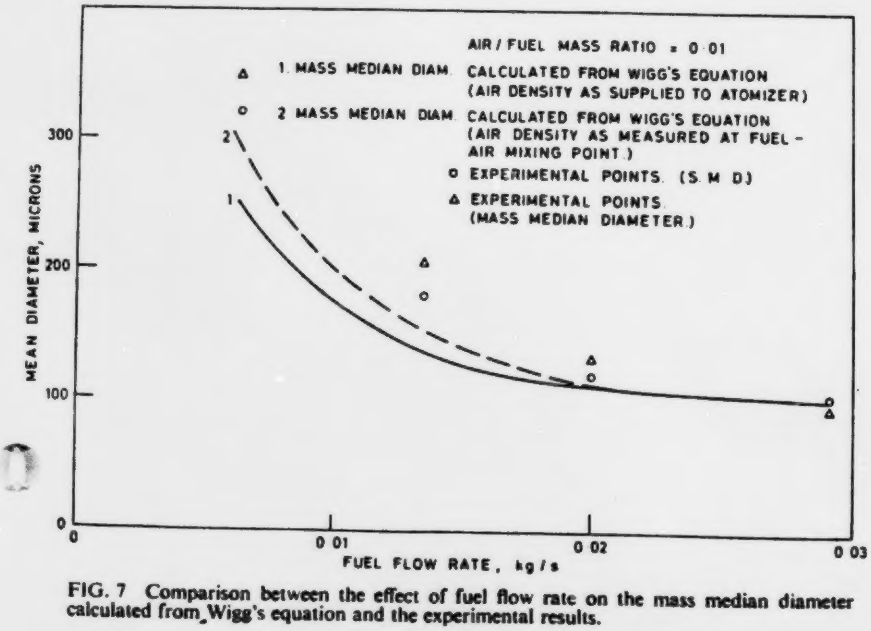

FIG. 7 Comparison between the effect of fuel flow rate on the mass median diameter calculated from Wigg's equation and the experimental results.

The correlation between the expected mass median diameter calculated from equation (1) and the experimental results is good and is shown in Fig. 6. The lowest air/fuel mass ratio shown is 0.005; this is a factor of 10 smaller than the lowest considered by Wigg. Good agreement occurs between the calculated and measured values well outside the range for which equation (1) was originally developed.

At first sight, from equation (1), an increase in the fuel flow rate would be expected to increase the mean diameter, whereas Fig. 5 shows the opposite to be the case. In practice an increase in the fuel flow rate results in an increase in the fuel and air supply pressures and hence an increase in the air density at the mixing point, resulting in equation (1) predicting a decrease in d_m as shown in Fig. 7.

5.3. Pressure distribution within the atomizer

The pressure-flow relationships of the atomizing fluid and fuel passing through the atomizer are difficult to predict owing to the interaction between the two fluids within the atomizer. Fig. 8 shows the pressure distribution within the atomizer at a fuel flow rate of 0.0294 kg/s for three air/fuel mass ratios. In this case the pressure drop of the fuel across the fuel port is high compared with that of the air across the atomizing fluid port. As expected, the pressure drop across the fuel port remains constant at constant fuel flow even for different air/fuel mass ratios. Increasing the air/fuel mass ratio increases the pressure drop across the atomizing fluid port as shown in Fig. 9. Increasing the fuel flow rate reduces the atomizing air mass flow rate at the same supply pressure as shown in Fig. 10, which compares the actual air flow with the flow theoretically predicted. If this blockage effect of the fuel is represented by the blockage coefficient C_B, then C_B is found to be inversely proportional to the fuel velocity as shown in Fig. 11. The effect of the atomizing air flow on the pressure drop of the fuel port is shown in Fig. 12. Without atomizing air the fuel flow follows closely that theoretically predicted. The blockage effect of the atomizing air is insignificant except at small fuel flow rates.

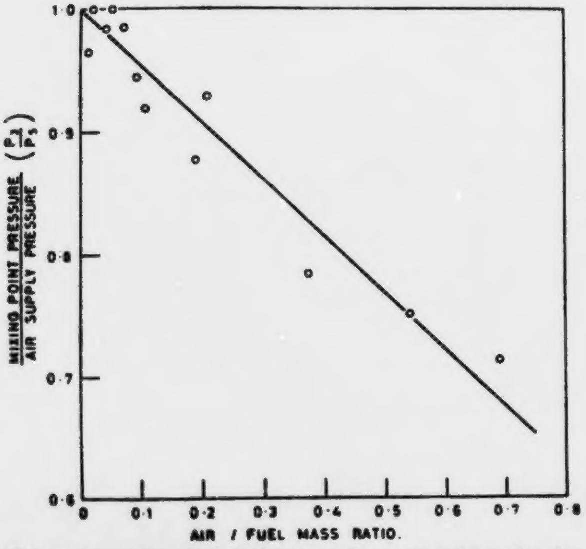

FIG. 9 The effect of air/fuel mass ratio on the mixing chamber pressure.

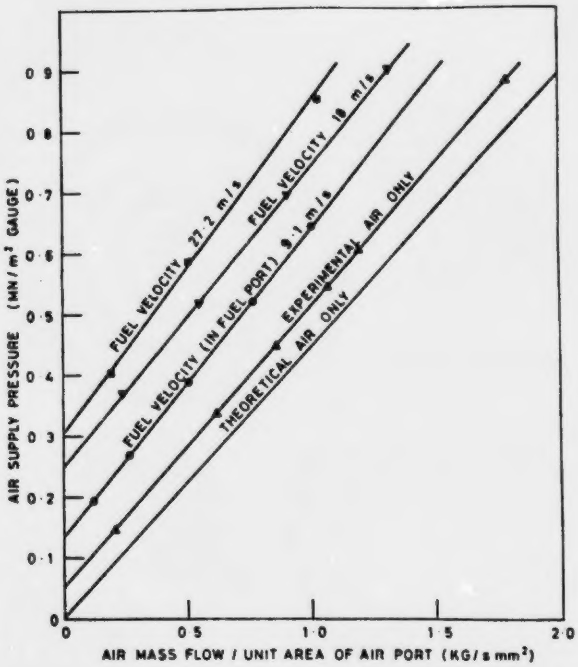

FIG. 10 The effect of air supply pressure on the air mass flow for various fuel flow rates.

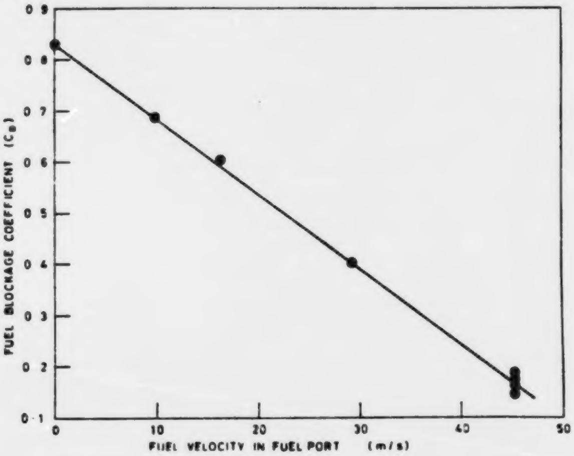

FIG. 11 The effect of fuel velocity on the blockage coefficient.

5.4. The effect of atomizer geometry

The effect of the atomizer's geometry on its performance is shown in Table 1. Three types of variables will be noted:

1. Those whose effect on the drop size distribution results from changes in the atomizing fluid velocity and density and as a result the effects can be calculated using equation (1), e.g. atomizing fluid port diameter.
2. Those which cause the coalescence of droplets or the maldistribution of fuel in the mixing chamber and result in a deterioration in the drop size distribution which cannot be calculated using equation (1), e.g. the protective counterbore.
3. Those which have no significant effect on the drop size distribution, e.g. the fuel port length.

TABLE 1 The effect of changes in the atomizer geometry on its performance

Variable	Measurement	Effect	Agreement between the experimental results and Wigg's equation	Remarks and design recommendations
1. Radial or offset fuel entry	Rosin Rammler size distribution	Radial entry gives finer spray	No. Wigg's equation predicts no effect on the spray	Radial entry should be used for all atomizer designs
2. θ	S.M.D.	Changing to 90° from 52° makes spray coarser for all d_f/d_o	No. Wigg's equation predicts no effect on the spray	Use $\theta \simeq 52°$
3. $\frac{d_m}{d_o}$	(*a*) S.M.D. (*b*) Pressure	Increasing d_m increases S.M.D. Increasing d_m reduces air and fuel supply pressures	Fair agreement. Wigg's equation predicts an increasing drop size with increasing d_m	Use smallest d_m consistent with available fuel and atomizing fluid supply pressures
4. $\frac{d_f}{d_o}$	(*a*) S.M.D. (*b*) Pressure	Little effect, S.M.D. a min for $1.0 < \frac{d_f}{d_o} < 1.6$ Increasing d_f causes fuel supply pressure to fall. Little effect on air pressure	No agreement. Wigg's equation predicts a slight fall in drop size as $\frac{d_f}{d_o}$ increases, but in practice a minimum occurs for $1.0 < \frac{d_f}{d_o} < 1.6$	Use $1 < \frac{d_f}{d_o} < 1.6$ according to fuel supply pressure available (also d_f must be less than d_m)
5. d/c	Rosin Rammler size distribution	Removal of protective counterbore gives finer spray	No agreement. Wigg's equation predicts no effects	Do not use protective counterbore unless atomizer is likely to receive rough handling
6. $\frac{d_o}{d_f}$ $\left(\text{at constant } \frac{d_m}{d_o}\right)$	S.M.D.	Increase in d_o causes a coarser spray owing to reduction in air density	Fairly good agreement	Use smallest d_o possible consistent with available supply pressure of atomizing fluid
7. $\frac{l}{d_o}$	S.M.D.	A minimum occurs at $\frac{l}{d_o} = 0.75$	No agreement. Wigg's equation predicts no effect	Use a value of $\frac{l}{d_o} \simeq 0.75$
8. $\frac{l_m}{d_m}$	(*a*) S.M.D. (*b*) Pressure	Increasing l_m reduces S.M.D. slightly, increasing l_m increases air and fuel supply pressures slightly	Fairly good agreement	Use a value of $\frac{l_m}{d_m} \simeq 4$
9. $\frac{l_o}{d_o}$	S.M.D.	Little effect for $2.0 < \frac{l_o}{d_o} < 10$	Good agreement. Wigg's equation predicts no effect	Chose a value of $\frac{l_o}{d_o}$ as convenient for the mechanical design of the atomizer
10. $\frac{l_f}{d_f}$	S.M.D.	Little effect for $2.0 < \frac{l_f}{d_f} < 10$	Good agreement. Wigg's equation predicts no effect	Chose a value of $\frac{l_f}{d_f}$ as convenient for the mechanical design of the atomizer

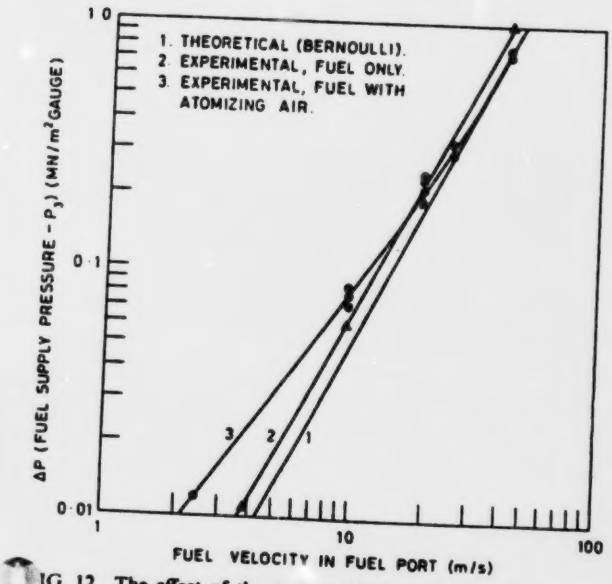

FIG. 12 The effect of the pressure drop across the fuel port on the fuel velocity in the port.

The effects on the performance of the atomizer of the more important variables are discussed below:

5.4.1. The effect on the spray of the fuel port entry to the mixing chamber

The Rosin Rammler drop size distributions for the radial and offset fuel port entries are shown in Fig. 13. The atomizer with the offset fuel port entry produces sprays considerably coarser than that with the radial fuel port entry to the mixing chamber. Although photographs of the break-up region showed little difference between the two atomizers, it is probable that the coarser spray was caused by the uneven distribution of the fuel in the mixing chamber.

5.4.2. The effect on the spray of the mixing chamber diameter

Fig. 14 shows the effect of the mixing chamber diameter on the Sauter mean diameter and Fig. 15 shows the effect on the fuel and air supply pressures. Increasing the mixing chamber diameter results in a marked increase in the Sauter mean diameter of the spray and a considerable reduction in the air and fuel supply pressures. This is generally in agreement with Wigg's equation which predicts an increase in the mass median diameter as the mixing chamber diameter is increased. This increase results largely from the decrease in the air density rather than from the increase in the term *h*, which has itself only a small effect.

5.4.3. The effect of change in atomizing fluid port diameter

The atomizing fluid port was increased keeping the expansion ratio d_m/d_a constant. This resulted in a small but significant increase in the coarseness of the spray. The Rosin Rammler distributions are shown in Fig. 16.

5.4.4. The effect of the fuel port diameter and entry angle on the Sauter mean diameter

Fig. 17 shows the effect of the fuel port diameter on the Sauter mean diameter for two entry angles 52° and 90°. Fig. 18 shows the effect of diameter on the fuel and air supply pressures. It was found that the angle had no significant effect on the pressure. As expected, an increase in the fuel port diameter causes the fuel supply pressure to fall, but owing to the interaction between the two fluids within the atomizer the air pressure rises slightly.

The slight increase in air density causes Wigg's equation to predict a slight fall in the mean diameter of the spray as the fuel port diameter is increased, which is not, in fact, the case. In practice the lower velocity, thicker fuel film which occurs with the larger fuel ports results in a coarser spray, although a minimum occurs for values of d_f/d_a between 1.0 and 1.4. Generally the 90° angled atomizer gives a coarser spray than the 52° angled atomizer. As a result of the fuel film having a lower axial velocity, an even thicker film will result than in the case of the 52° angled atomizer.

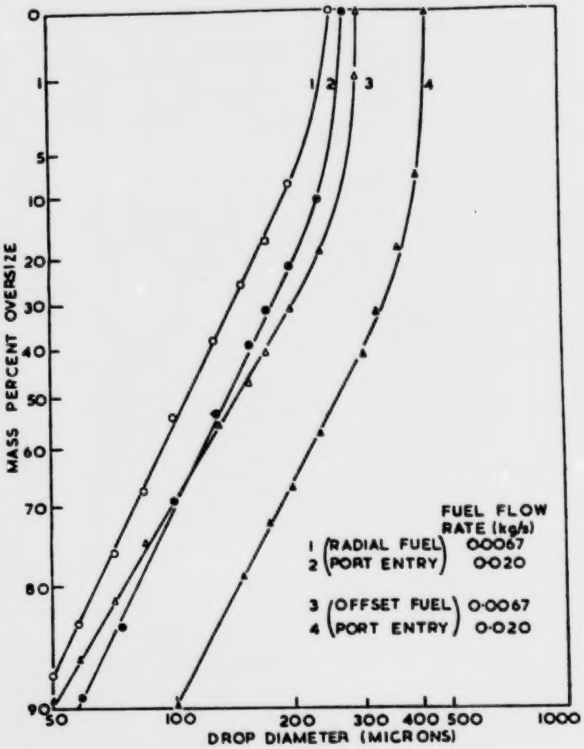

FIG. 13 The effect of having a radial or offset fuel port entry to the mixing chamber.

5.4.5. The effect of premix length on the Sauter mean diameter

It was found that the Sauter mean diameter produced by the atomizer was a minimum for a premix length of 0.7 which corresponds with the value of the standard atomizer. Examination of the photographs of the large-scale model show that the air jet becomes fully expanded to fill the mixing chamber in this region. Therefore the most efficient mixing occurs when the fuel is injected into the air stream just where it becomes fully expanded, see Fig. 19.

5.4.6. The effect of mixing length on the spray

Fig. 20 shows that the spray becomes finer as the mixing length is increased. The longer mixing length gives a greater time for momentum transfer between the atomizing air and the fuel, at the expense of increased

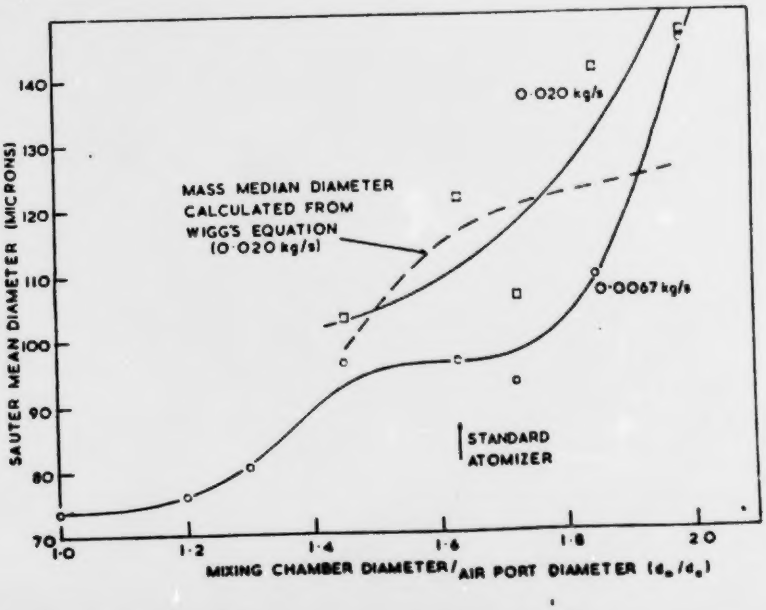

FIG. 14 The effect of mixing chamber diameter on the Sauter mean diameter.

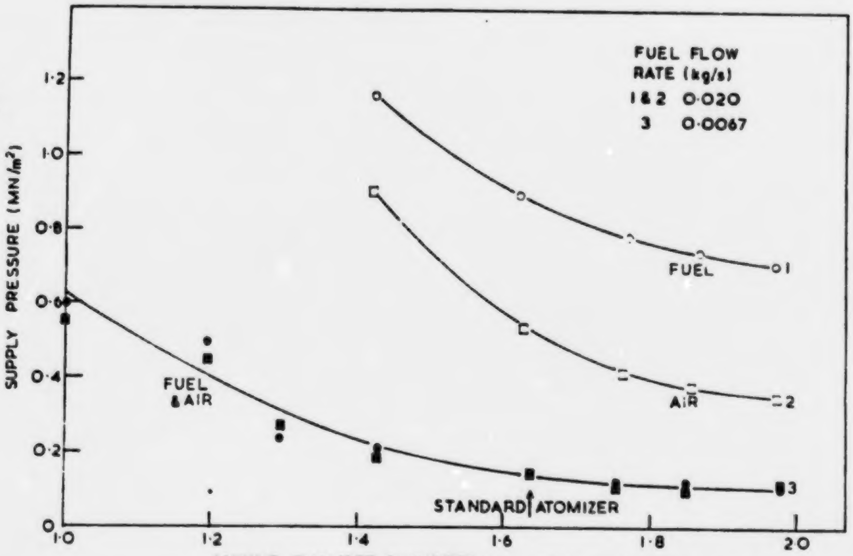

FIG. 15 The effect of mixing chamber diameter on the fuel and air supply pressures.

fuel and air supply pressures. This is in agreement with the findings of Gretzinger and Marshall.[5]

6. The design of multijet internal mixing twin fluid atomizers

The design procedure which follows has been developed from the experimental results[3] and from relevant previously published work.[2,4,5,6]

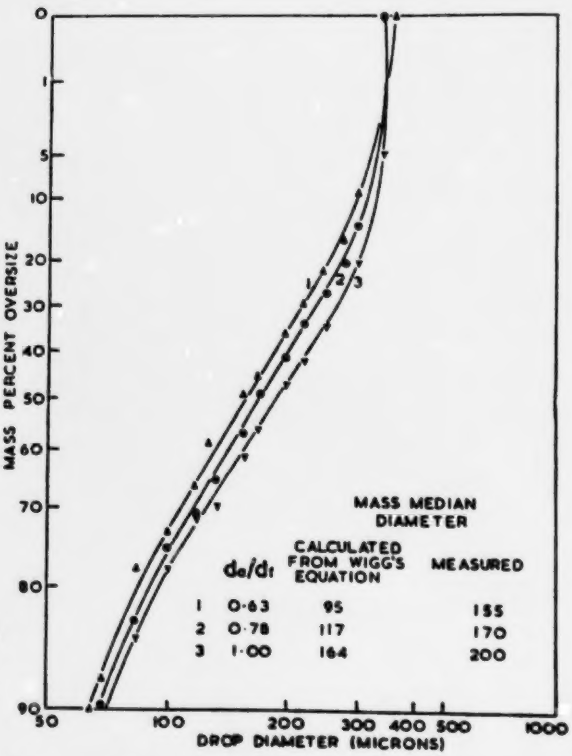

FIG. 16 The effect of changing the air port diameter on the spray (fuel flow rate 0.020 kg/s).

6.1. General requirements of a twin fluid atomizer design

1. The fuel should be supplied so as to form a thin continuous steady film in the mixing region.

2. The atomizing fluid should be supplied at the greatest possible velocity and density consistent with the available supply conditions. If steam is used it must be dry or preferably slightly superheated. This is because any water in the steam will also be atomized, thus reducing the amount of energy available in the steam for atomizing the fuel.

3. The atomizing fluid and the fuel should be provided with the greatest possible length in which to achieve controlled mixing.

4. The fuel and atomizing fluid ports should be sized to take full advantage of the supply pressures of fuel and atomizing fluid available especially if a large turndown ratio is required.

6.2. Preferred geometry for the multijet internal mixing twin fluid atomizer

From the analysis of the experimental results the following atomizer geometry is recommended and is shown in Table 2:

1. The atomizer should not have a protective counterbore unless it is absolutely essential to protect it from rough handling in which case the counterbore should be as short as possible.

2. The fuel port should make a radial intersection with the mixing chamber and the angle θ should be approximately 50°.

3. The ratio of the mixing chamber diameter/the atomizing fluid port diameter d_m/d_a should be within the range 1.4–1.8.

4. The premix length should be approximately three-quarters of the atomizing fluid port diameter, i.e. $l/d_a = 0.75$.

5. The mixing length should be approximately four times the mixing chamber diameter, $l_m/d_m = 4$.

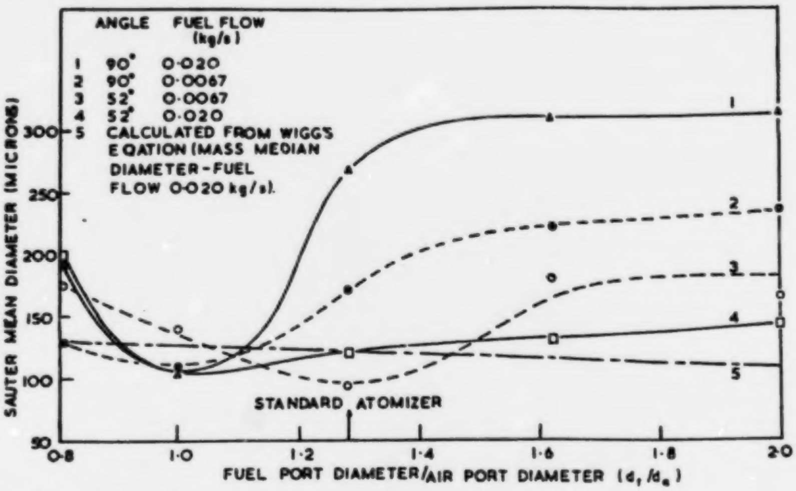

FIG. 17 The effect of fuel port diameter on the spray.

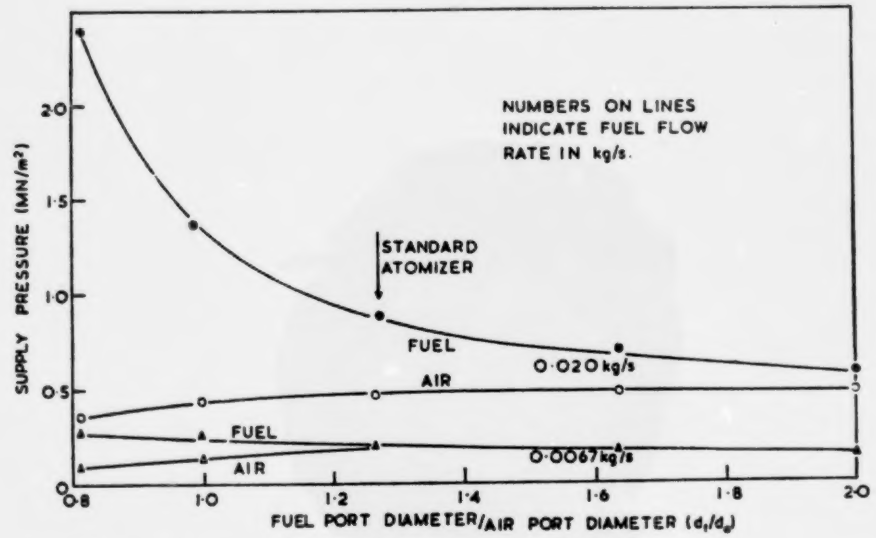

FIG. 18 The effect of fuel port diameter on the fuel and air supply pressures.

6. The lengths of the fuel port and the atomizing fluid port should be at least two diameters but may be longer as is convenient in the mechanical design of the atomizer, $l_a/d_a > 2$ and $l_f/d_f > 2$.

7. The mixing chamber diameter must be larger than the fuel port diameter, $d_m > d_f$.

8. The dimensions of d_a and d_f must be chosen to suit the operating conditions.

6.3. Procedure for the determination of suitable diameters for the fuel port and atomizing fluid port

6.3.1. Performance required from the atomizer

In order to proceed with the design it is first necessary to decide the required performance. This will depend on the application for which the atomizer is being designed. The various aspects of the performance which need to be specified are given below:

TABLE 2 Recommended geometry of twin fluid atomizer

1. Radial fuel port entry
2. $\theta = 52°$
3. $\frac{d_m}{d_a} \simeq 1.4\text{-}1.8$
4. $\frac{l}{d_a} \simeq 0.75$
5. $\frac{l_m}{d_m} = 4\text{-}5$
6. $d_m > d_f$
7. No counterbore used
8. $\frac{l_a}{d_a} > 2$ (as convenient)
9. $\frac{l_f}{d_f} > 2$ (as convenient)
10. d_a and d_f are chosen to suit the operating conditions

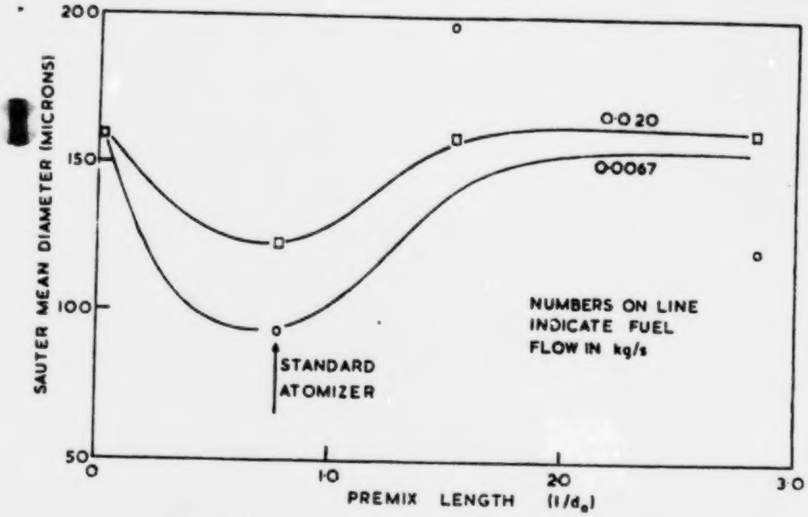

FIG. 19 The effect of premix length on the Sauter mean diameter.

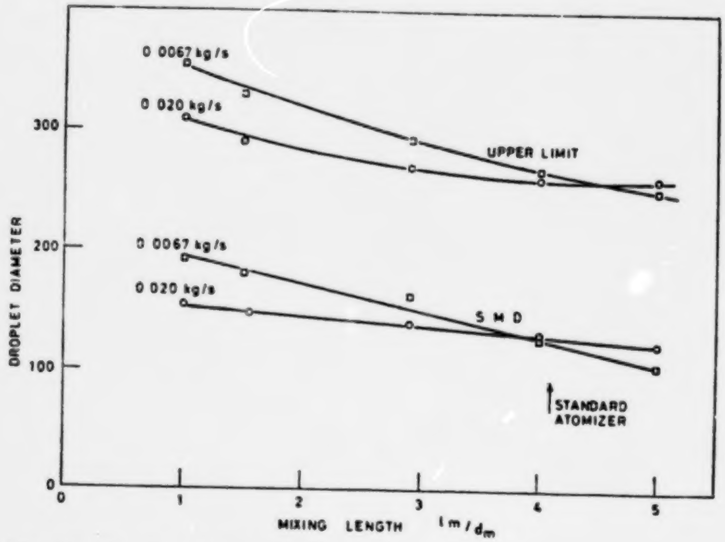

FIG. 20 The effect of mixing length on the spray.

1. Maximum fuel flow rate required from the atomizer.
2. Approximate turndown ratio required.
3. Maximum operating fuel supply pressure.
4. Maximum operating atomizing fluid supply pressure.
5. Required cone angle of spray.
6. Required mean diameter of spray.

Once these requirements are known, the design can proceed.

6.3.2. Design procedure

1. Choose the number of individual jets. The number of jets required is dependent on a number of factors. In general a minimum of six jets should be used for the lowest fuel flow rates and rather more at the highest fuel flow rates. The more jets there are the smaller they will be and the more difficult the atomizer will be to manufacture. However, if too few jets are used at the higher fuel flow rates their diameter will be so large that the atomizing fluid/fuel mixing will deteriorate. Ultimately, experience with the design of twin fluid atomizers will enable this choice to be readily made for different applications.

2. Use the highest atomizing fluid pressure available since increasing the atomizing fluid density reduces the Sauter mean diameter of the spray and results in economy of atomizing fluid. This does not necessarily apply where large quantities of atomizing fluid at low pressures are available cheaply, e.g. steam from waste heat boilers.

3. From equation (2) below, which is a rearrangement of Wigg's equation, calculate the approximate atomizing fluid/fuel mass ratio necessary to produce the required mass median diameter.

$$M = \frac{1}{\left(\dfrac{D_m \rho^{0.3} V}{200 \nu^{0.5} W^{0.1} h^{0.1} \sigma^{0.2}}\right)^2} - 1 \qquad (2)$$

V may normally be assumed to be the critical velocity of the atomizing fluid and ρ the atomizing fluid supply density.

4. Use this value of the atomizing fluid/fuel mass ratio, the atomizing fluid supply pressure and Fig. 9 to obtain the reduced pressure of the atomizing fluid in the mixing chamber. If this is significantly lower than the supply pressure, calculate the atomizing fluid density in the mixing chamber and use this value to obtain a more accurate value of the atomizing fluid/fuel mass ratio. Use Fig. 9 to obtain the new value of the pressure P_m in the mixing chamber for the corrected atomizing fluid/fuel mass ratio.

5. Decide the fuel supply pressure P_f for the maximum fuel flow rate. It is often advisable to use a pressure of 80% of that available to allow for occasional overload conditions, etc., then:

$$P = P_f - P_m$$

Use P and Fig. 12 to obtain the fuel velocity in the fuel port and hence the fuel port area and diameter required to pass the maximum fuel flow rate.

6. Use the fuel velocity V_f and Fig. 11 to estimate the fuel blockage coefficient C_B.

Then either:

(*a*) Calculate the theoretical flow of atomizing fluid through the atomizer and multiply by C_B to obtain the reduced atomizing fluid flow which will occur when fuel is also flowing.

Or:

(*b*) When using air as the atomizing fluid, Fig. 10 can be used to estimate the flow rate of atomizing air.

Hence calculate the required area and diameter of the atomizing fluid port.

7. Use the information contained in Section 6.2 to fix the remaining dimensions of the atomizer. If the mixing chamber diameter is not larger than the fuel port diameter, changes must be made to the fuel and/or atomizing fluid supply pressures and the ports must be re-sized using the above procedure.

8. Using drills of the nearest standard gauge, manufacture an atomizer to the design arrived at using the above procedure and conduct experiments to check that the atomizer gives a satisfactory performance.

7. Conclusions

As a result of extensive experimental work on twin fluid atomizers, the effect of the geometrical and operational variables on the performance of the internal mixing multijet type has been determined. A qualitative model of the operation of the atomizer has been presented. It was found that the main purpose of the atomizing fluid is to accelerate the fuel, which then breaks up outside the atomizer in a similar manner to a pressure jet atomizer.

Wigg's equation for the determination of mean drop size was found to agree closely with the experimental results, even at much lower values of atomizing air/fuel mass ratio than those for which it was originally developed. Furthermore, this agreement with Wigg's equation for a wide variety of different designs of twin fluid atomizer, both internal and external mixing, suggests that atomizer geometry has relatively little effect except for the way in which it affects atomizing fluid velocity and density, etc.

Internal mixing atomizers have the advantage that the atomizing fluid can generally be supplied to the mixing region at a higher pressure than with the external mixing type, and this results in a saving in the quantity of atomizing fluid required to produce the same mean diameter. However, because of the interaction between the fluids within the atomizer the prediction of the flow rates is more difficult.

A design procedure for multijet internal mixing twin fluid atomizers has been developed for the guidance of atomizer designers. This design procedure is not intended as a substitute for intelligent experimental work in the development of twin fluid atomizers, but should ease the present difficulties which result in much trial and error work when designing an internal mixing twin fluid atomizer for new operational conditions. These difficulties arise because there is no basis whatever on which to size the various ports of the atomizer.

8. Acknowledgment

The authors thank the Ministry of Defence (Navy) for financial support.

9. References

1. MELLOR, R. PhD thesis, University of Sheffield, 1969.
2. WIGG, L. D. *J. Inst. Fuel*, 1964 (Nov.), 37, 500–505.
3. MULLINGER, P. J. PhD thesis, University of Sheffield, 1973.
4. FRASER, R. P., EISENKLAM, P., and DOMBROWSKI, N. Liquid atomization in chemical engineering, Part 4: Twin fluid atomizers. *Brit. Chem. Eng.*, 1957 (Nov.), 2, 610–613.
5. GRETZINGER, F., and MARSHAL, W. R., Jn. *A.I.C.L.E. Jnl*, 1961, 7, 312–318.
6. LEFEBVRE, A. H., and NORSTER, E. R. A proposed 'double swirler' atomizer for gas turbine fuel injection, Cranfield Report SME No. 1, June 1972.

(*Paper received* 28 *August* 1973)

COANDA EFFECT

Theoretical and experimental investigation on attached-jet entrainment

By R. Medeot

Riello Bruciatori - Research Centre - Padova (Italy)

1. FOREWORD

In order to provide a simple recirculating device for a blueflame burner, a preliminary survey has been carried out on the available gas pumping methods.
Discarding "a priori" systems requiring moving components, we determined to investigate the so-called "attached-jet phenomenon", deeming it the most suitable for our application. This choice has been suggested also by an IITRI Report.

2. QUALITATIVE CONSIDERATIONS.

As it is well known, a gas jet stream skimming a solid convex surface attaches to it and the consequent deflection produces a pressure decrease which entrains ambient air.
This phenomenon, referred to as the Coanda effect, is a rather complicated one. A qualitative explanation may rise from the following considerations.
As it is known, a gas jet emerging from a slit or a hole carries with it some of the surrounding fluid which was originally at rest, because of the friction developed on its periphery. The resulting pattern of streamlines is shown in fig. 1.

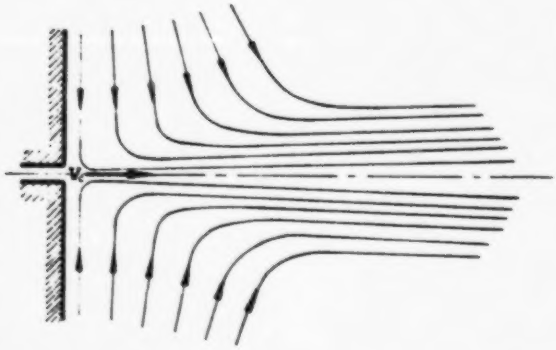

Fig. 1. - Streamline pattern for an emerging jet

The fluid acceleration causes a pressure gradient in radial direction. The radial symmetry will fail — and with it the radial equilibrium — if a surface is placed in the jet stream proximity; thrust by the pressure gradient, the jet tends to adhere to it. If the surface is convex, the jet will follow a curvilinear path and a further increase in the pressure gradient will occur as a consequence of the centrifugal forces (see fig. 2).

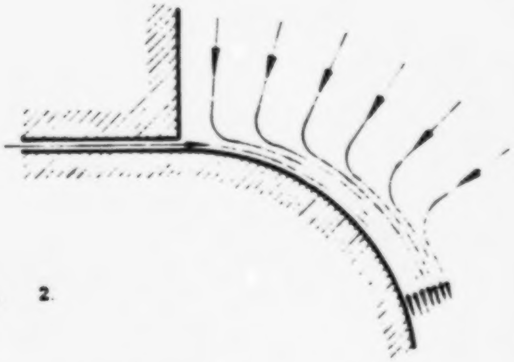

Fig. 2.

3. ANALYTICAL MODEL.

In order to calculate the variables involved in the phenomenon at issue, a model was considered bringing to a simple mathematical approach.
Referring to fig. 3, the inlet air (from now forward called "motive air") enters the system through the annular slit S and then attaches to and follows the surface of revolution C entraining the ambient gas of the room A. Then motive and entrained air blow off from annulus E.

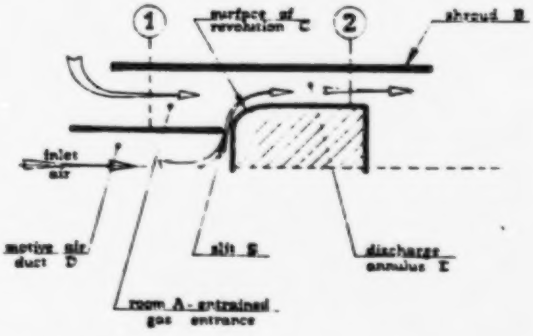

Fig. 3. - Model used in mathematical analysis of attached - jet device.

An exact analytical solution may be provided by the boundary-layer theory, the equation has been adapted by Boltze to the case of a viscous fluid flowing past a body of revolution when the stream is parallel to its axis.

In such a way it is possible to get an accurate description of velocity and pressure fields, but the involved mathematical developments are quite complicated.

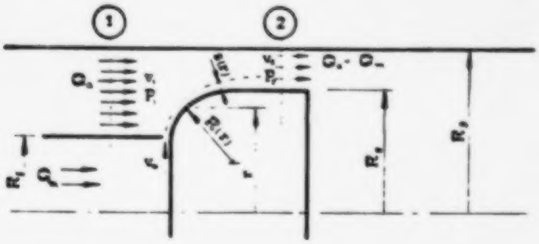

Fig 4.

Considering that average values of velocity and pressure are sufficient for our purpose, with reference to fig. 4 the following simplifying assumptions were made:

a. velocity and pressure profiles across planes 1 & 2 are uniform; b. jet momentum along the whole surface of revolution is constant and c. pressure gradient across the attached jet is essentially produced by centrifugal forces. Under the above mentioned assumptions an equation expressing the momentum conservation in axial direction is

$$(1)\quad A_1 p_1 + F_a - A_2 p_2 = \rho (Q_a + Q_m) v_2 - Q_a \rho v_1$$

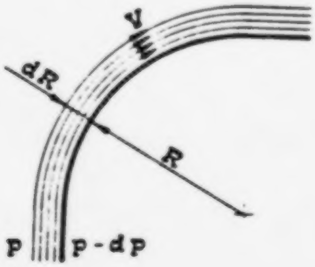

Fig. 5.

In a stream jet running along a curvilinear path (see fig 5) a radial pressure gradient originates which is expressed by:

$$(2)\quad \frac{dp}{dR} = \rho \frac{v^2}{R}$$

Integrating the expression [2] with respect to R under assumption c. in our case we obtain:

$$(3)\quad p_1 - p_s = \rho v(r)^2 \ln \left[1 + \frac{s(r)}{R(r)} \right]$$

When $s(r) << R(r)$ expression [3] becomes:

$$(4)\quad p_1 - p_s = \rho \frac{v(r)^2 s(r)}{R(r)}$$

which, integrated with respect to the area perpendicular to the x axis between the limits R_1 and R_2 gives

$$(5)\quad \int_A p_1 \, dA - \int_A p_s \, dA = 2\pi\rho \int_{R_1}^{R_2} \frac{v^2(r)\, s(r)\, r}{R(r)} \, dr$$

The term $\int_A p_s \, dA$ physically represents the force F_a and hence:

$$(6)\quad -F_a = 2\pi\rho \int_{R_1}^{R_2} \frac{v^2(r)\, s(r) r dr}{R(r)} - p_1 (A_1 - A_2)$$

The assumption b. about momentum conservation of the jet along the surface of revolution is expressed by equation:

$$(7)\quad \rho Q_m V_m = \rho Q(r) v(r)$$

Since $Q(r) = 2\pi r s(r) v(r)$ and $v_m = Q_m / 2\pi s R_1$ we obtain:

$$(8)\quad 2\pi\rho v(r)^2 s(r) = \rho Q_m^2 / 2\pi s R_1$$

Placing expression [8] in eq. [6], substituting this in eq. [1] and rearranging the terms yields:

$$(9)\quad (p_2 - p_1) + \rho\frac{V_2^2}{2} - \rho\frac{V_1^2}{2} = \rho\frac{Q_m^2}{2A_2^2}\left[\frac{A_2}{\pi s R_1}\int_{R_1}^{R_2}\frac{dr}{R(r)} - 1\right] +$$
$$- \rho\frac{Q_a^2}{2A_2^2}\left[\left(1 - \frac{A_2}{A_1}\right)^2 + \frac{2Q_m}{Q_a}\right]$$

The set of terms to the left of the equality sign represents the total head H of the systems, considered as a pumping device.

4. DISCUSSION OF THEORETICAL RESULTS

The characteristic curve total head-entrained flowrate for an attached jet pumping system is similar to those of a common blower. Fig. 6 shows an example of such a curve.

Later on the problem of optimization of the characteristic (H, Qa) will be discussed. We start with the analysis of the integral:

$$(10)\quad \int_{R_1}^{R_2} \frac{dr}{R(r)}$$

which summarizes the geometrical characteristics of the surface of revolution.

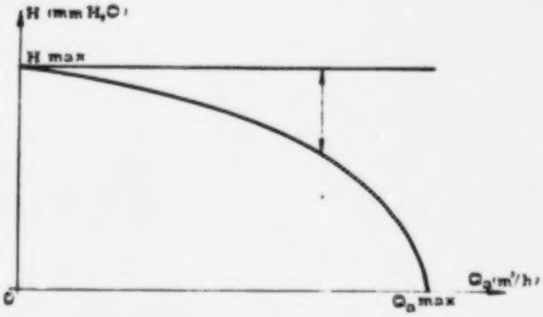

Fig 6

The discovery of the function f(x), whose curvature 1/R(x) maximizes the integral [10] is a typical functional problem. In our case we limited the analysis to a particular class of functions f(x), the elliptic ones, which are represented by the following expression.

$$(11)\quad \frac{x^2}{k^2}+y^2=R_0^2$$

Varying parameter k between 0 and ∞ we obtain all the possible ellipses and in particular for k = 1 we get a circumference of radius R_0, as shown in fig. 7.

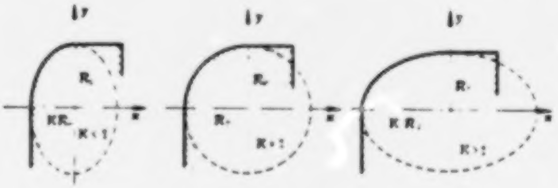

Fig 7

The curvature is represented by the expression:

$$(12)\quad \frac{1}{R(y)}=\frac{\frac{d^2y}{dx^2}}{\left[1+\left(\frac{dy}{dx}\right)^2\right]^{3/2}}=\frac{k\,R_0^2}{\left[y^2(k^2-1)+R_0^2\right]^{3/2}}$$

Thus we obtain:

$$(13)\quad \int_{R_1}^{R_2'}\frac{dr}{R(r)}=kR_0^2\int_0^{R_0}\frac{dy}{\left[(k^2-1)y^2+R_0^2\right]^{3/2}}=1$$

which allows to conclude that the efficiency of the pumping device is not affected by the shaping of the surface of revolution.

An optimization can also be performed with respect to the area A_2 of the discharging annulus.

Writing eq. 9 in the following form:

$$(14)\quad H=\frac{\rho}{2}\left\{\frac{1}{A_2}\left[\frac{Q_m^2}{\pi s R_1}+\frac{Q_a^2}{A_1}\right]-\frac{1}{A_2^2}(Q_a+Q_m)-\frac{Q_a^2}{A_1^2}\right.$$

and imposing the condition: $\dfrac{\partial H}{\partial A_2}=0$

we obtain, — Q_a, Q_m, A_1 and R_1 being constant, — that the total head H is maximum for:

$$(15)\quad A_2=A_1\,\frac{2(1+Q_a/Q_m)^2}{\left(\frac{Q_a}{Q_m}\right)^2+\frac{A_1}{\pi s R_1}}$$

The total head behaviour vs radius R_3 (i.e. area A_2) is shown in fig. 8 for different entrainment ratios $G = Q_a/Q_m$.

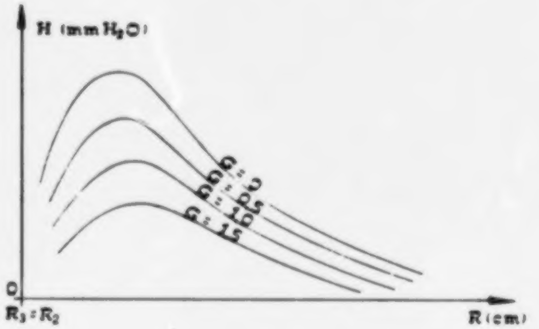

Fig 8

As concerns variables s and R_1 it is not possible to formulate a right criterion of optimization, while they are bound to the available pressure p_m of the moving air by equation:

$$(16)\quad p_m-p_1=\frac{\rho}{2}\left(\frac{Q_m}{2\pi R_1 s}\right)^2$$

which — Q_m being constant — is satisfied by infinite couples s, R_1.
Introducing expression (16) in eq. (9) we obtain:

$$(17)\quad H=\frac{1}{4\pi A_2}(p_m-p_1)\,s-f\,(Qa,\ Qm,\ A_1,\ A_2)$$

where f is a function independent of R_1 and s. From eq. (17) it seems it would be better to have large slit s than large radius R_1; this is correct, however, only if $s<(R_2-R_1)$. We must consider, besides, that the larger the slit, the smaller the radius R_1 of the inlet air duct, so that the pressure loss along this one increases and gets comparable with the pressure loss $p_m - p_1$ located across the slit.

5. EXPERIMENTAL INVESTIGATION.

In order to verify the validity and the limits of eq. (9) an experimental systematic investigation has been carried out, which covered all the range (flowrates, sizes and pressures) of interest in burner design.

5.1. Experimental Equipment.

Experimental data have been taken from the apparatus shown in schematic way in fig. 9. It is made prevalently of plastic material and consists of a cylindrical transparent frame (PERSPEX TUBE Ø 230/240) supported by two PVC plates. The left end of the frame bears the micrometric slit adjusting system while the right hand bears the entrained and motive air ducts.

Entrained air flowrate was measured by a calibrated orifice and regulated by a throttle, while motive air flowrate was measured by a rotameter and controlled by a flow regulating system.

In order to explore the total head dependence from radius R_3 (see fig. 4) inside the frame PERSPEX tubes were mounted of various sizes and provided with suitable centering blades.

The independence of the total head from the surface of revolution was verified using seven bodies machined from a PVC bar, which were different in size and shape. One of them is shown in fig. 10. Total head was measured by two velocity probes (Pitot tubes) placed up and downstream of the surface of revolution.

Motive and entrained air temperatures were taken by iron-constantan thermocouples.

Pressures and differential pressures were measured by 5 electrical dp-cells with 60 mm H_2O f.s.

5.2. Experimental Procedure.

In order to minimize the setting time for every run, an analysis has been conducted about the times required to perform each operation (i.e. components replacement or quantities adjusting). Afterwards the operations have been programmed in the inverse order with respect to their duration. The operations required for setting a run are:

a.	body of revolution replacement (R_2)	10 min.
b.	shroud replacement (R_3)	6 min.
c.	motive air flowrate adjustment (Q_n)	40 sec.
d.	entrained air flowrate adjustment (Q_a)	15 sec.
e.	slit width adjustment (s)	5 sec.

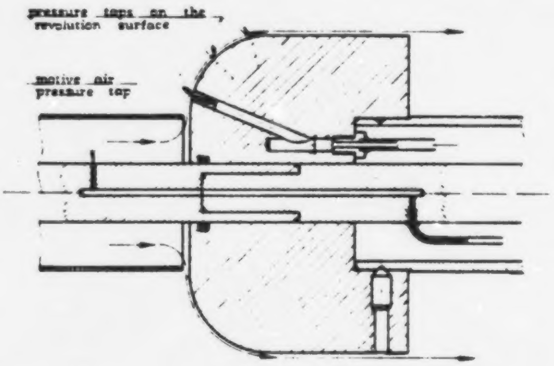
pressure taps on the revolution surface
motive air pressure tap

Fig 10

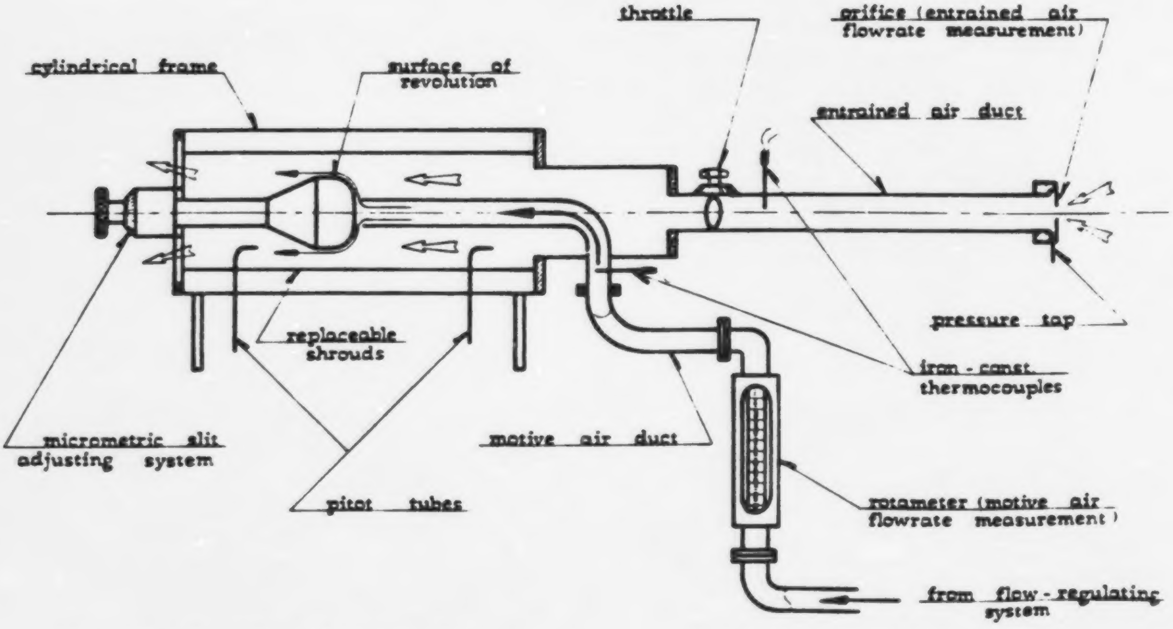
throttle
orifice (entrained air flowrate measurement)
cylindrical frame
surface of revolution
entrained air duct
pressure tap
replaceable shrouds
iron - const. thermocouples
micrometric slit adjusting system
motive air duct
pitot tubes
rotameter (motive air flowrate measurement)
from flow - regulating system

Fig. 9. - Experimental apparatus

Operation (e) precedes operations (c) and (d), because a variation of slit width involves a variation of motive and entrained air flowrate and then relative adjustment, so that to the initial time of 5 sec we have to add 55 sec required by the above mentioned operations.

The experimental procedure followed this scheme:

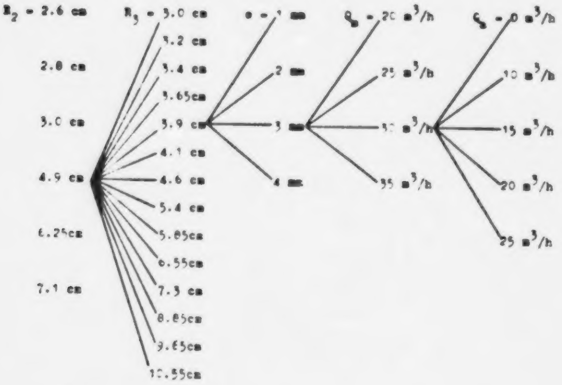

Including some preliminary trials, totally we carried out 2500 runs. The experimental data have been collected with the aid of a data logger and some of them are graphically presented at the end of this note.

5.3. Comparison with theoretical predictions.

In general we observed that experimental results fit quite well with theoretical predictions. Discrepancies increase when flowrates increase; this rises from the fact that we did not take in into account dissipative phenomena.

Then, writing eq. (9) in the form:

$$(18)\quad H = \frac{Q_m^2 \rho}{2\pi a R_1 A_2} - \rho\frac{(Q_a + Q_m)^2}{2 A_2^2} + \left(\frac{Q_a}{A_1}\right)^2 \left(\frac{A_1}{A_2} - 1\right)$$

we can observe that the first term to the right of the equality sign represents the pressure increase prodused by the motive force F_p, while the second can be interpreted as the pressure loss due to the passage of the total flowrate $Q_a + Q_m$ through the annular cross section of area A_2, discharge coefficient being equal to one.

In practice it results $\alpha \simeq 0{,}6 \div 0{,}8$.

Eq. (18) must be corrected as follows:

$$(19)\quad H = \frac{\rho Q_m^2}{2\pi a R_1 A_2} - \rho\frac{(Q_a + Q_m)^2}{2 A_2 \alpha^2} + \left(\frac{Q_a}{A_1}\right)^2 \left(\frac{A_1}{A_2} - 1\right)$$

Discrepancies can be observed also when we reduce the radius $R_u = R_2 — R_3$. In this case the hypothesis we formulated in par. 3 fails and the expression giving the force F_p exerted by the surface of revolution cannot be simplified as shown in expression [4].

At last we observe that eq. [9] fails when the phenomenon of boundary-layer separation occurs.

Increasing slits, decreasing radius R_u and flowrate Q_a facilitates the appearance of the phenomenon. The characteristics H, Q_a becomes similar to that shown in fig. 11.

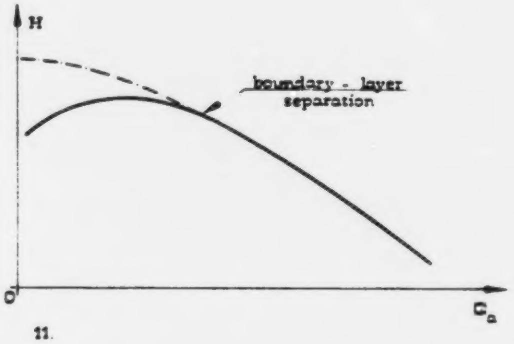

Fig. 11.

6. CONCLUSIONS.

Some supplementary trials have been carried out in order to describe in some detail the phenomenon of the attached jets.

In particular velocity maps have been traced in some interesting configurations, but the subject is beyond the aim of this note.

The conclusions we drew are the following:

— it is possible to predict with a good approximation the behaviour of a pumping device using the jet-attachment phenomenon.

— with pressure supplied by common blowers (~ 40 mm H_2O) it is possible to produce a sufficient amount of recirculation in order to get a blue-flame combustion.

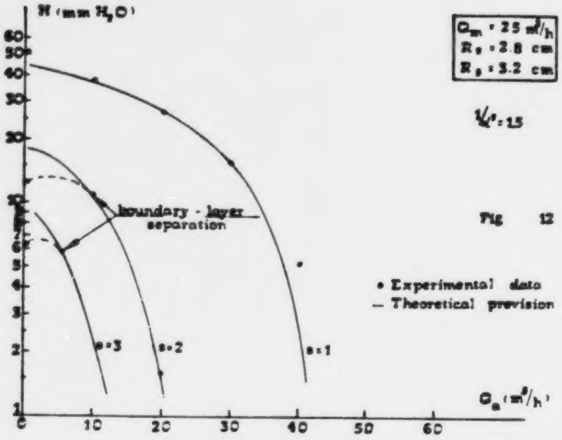

Fig 12

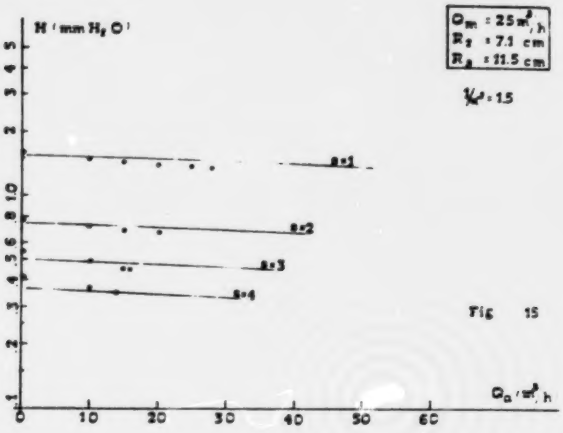

Fig 15

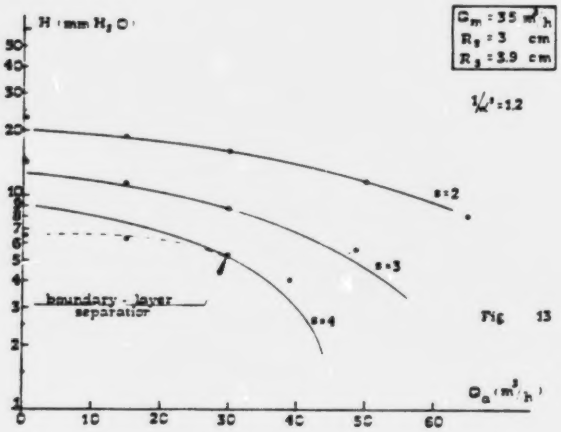

Fig 13

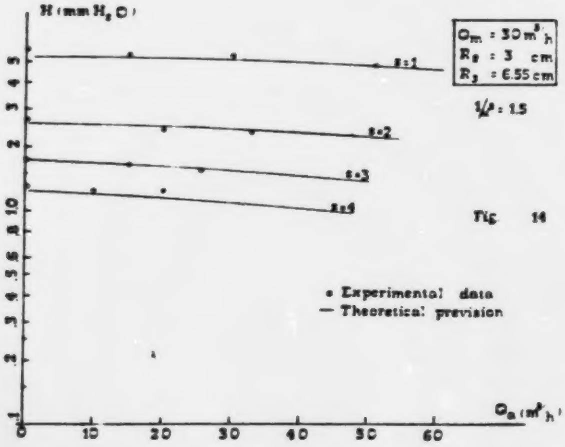

Fig 14

SYMBOL INDEX

A_1 A_2 = Annular areas of cross sections 1 & 2 respectively (m²)

F_s = Force exerted by surface of revolution (N)

G = Entrainment ratio (Qa/Qm)

H = Total head (N/m²)

P_1, P_2 = Pressures in sections 1 & 2 respectively (N/m²)

P_m = Pressure of the motive air (N/m²)

Q_a, Q_r = Entrained and motive air flowrate (n m³/sec)

Q(r) = Volumetric flowrate of the attached jet in the section distant from the x axis

V_1, V_2 = Air velocities in sections 1 & 2 respectively (m²)

α = Discharge coefficient

ρ = Air density (kg/m³)

APPLICATIONS OF THE COANDA EFFECT

When a liquid or gas flows along a solid surface, it tends to stick to the surface. This effect, named for a Romanian aircraft pioneer, has potential uses in such devices as burners and hovering vehicles

by Imants Reba

Everyone knows that it is not easy to pour a liquid smoothly out of a teapot spout or the mouth of a bottle. The liquid has an annoying tendency to flow around the lip and dribble down the curved surface of the spout or the side of the bottle. What causes the flow to bend and cling to the vessel's surface? Is it simply surface tension, as has usually been supposed? The answer is not quite so simple, and it has significant technological consequences.

In the year 1910 a young Romanian-born engineer named Henri Coanda tested a new flying machine he had built himself. He had been a student of Alexandre Gustave Eiffel, designer of the Eiffel Tower and one of the pioneers of modern aerodynamics, at the École Supérieure Aeronautique in Paris,

"TEAPOT EFFECT" is a low-speed form of the Coanda effect: water poured slowly from a glass tends to stick to the side of the glass in the same way that tea sticks to the spout of a teapot. High-speed fluids similarly adhere to a surface of suitable shape.

and the young engineer's approach to flying was both bold and imaginative. Coanda's machine was a kind of jet aircraft. It was equipped with an air compressor powered by a reciprocating engine; thrust was obtained by injecting fuel into the compressed air to provide a kind of afterburner. At the outset Coanda was confronted with the possibility that the flames from his two jet exhausts might set fire to the plane's fuselage, which was made of plywood. He therefore installed metal plates to deflect the exhaust flames away from the fuselage.

Coanda took his vehicle out for a test run on a field at Issy-les-Moulineaux, a Paris suburb. As he taxied across the field he saw with dismay that the deflecting plates, instead of diverting the exhaust away from the body of the plane, were actually sucking the flames toward it! Preoccupied with this surprising development and with handling the engine throttle, Coanda did not notice until the last moment that he was approaching the Paris city wall at high speed. He jerked back on the control stick, became airborne long enough to clear the wall, then crashed.

As far as is known, this was the first flight of a jet airplane. Reflecting on the incident, however, Coanda was less interested in the takeoff than in the strange phenomenon of the wrong-way bending of the jets by his deflector plates. At the first opportunity he discussed the event with Theodor von Kármán, the foremost theorist of aerodynamics, who was then working at the University of Göttingen. Von Kármán realized that the phenomenon was a new discovery and named it the Coanda effect.

Twenty-five years or more passed before any other investigator gave serious attention to the Coanda effect. Coanda himself went to work as chief engineer of the Bristol Aeroplane Company in Britain and became involved in various technical researches having nothing to do with this subject. In his spare time, however, he carried on experiments to examine the basic features of the effect and its possible uses.

Consider a sheet of fluid (gaseous or liquid) that is discharged through a slit onto an extended and rounded lip. As in the case of the teapot spout, the sheetlike stream will attach itself to the curved surface and follow its contour. Coanda found that by constructing a shoulder composed of a series of

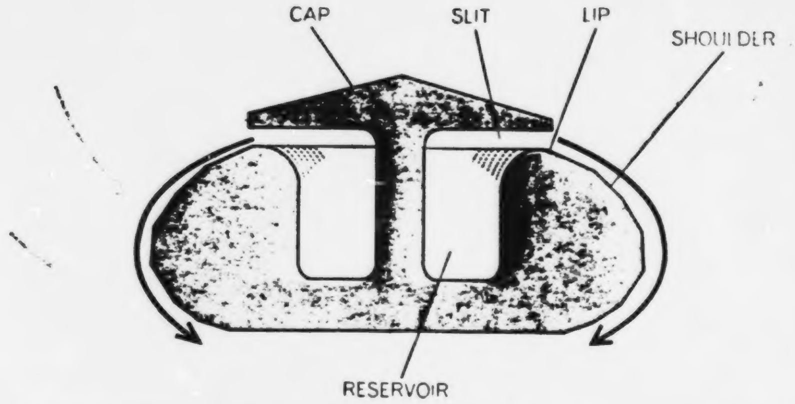

COANDA EFFECT was named for the tendency of a fluid, either gaseous or liquid, to cling to a surface that is near an orifice from which the fluid emerges. In this representation air from the reservoir emerges through the slit and, as shown by the dark color, closely follows the sides of the vessel. An important part of the effect is the tendency of the primary flow of air to entrain, or draw in, more air (*light color*) from the environment.

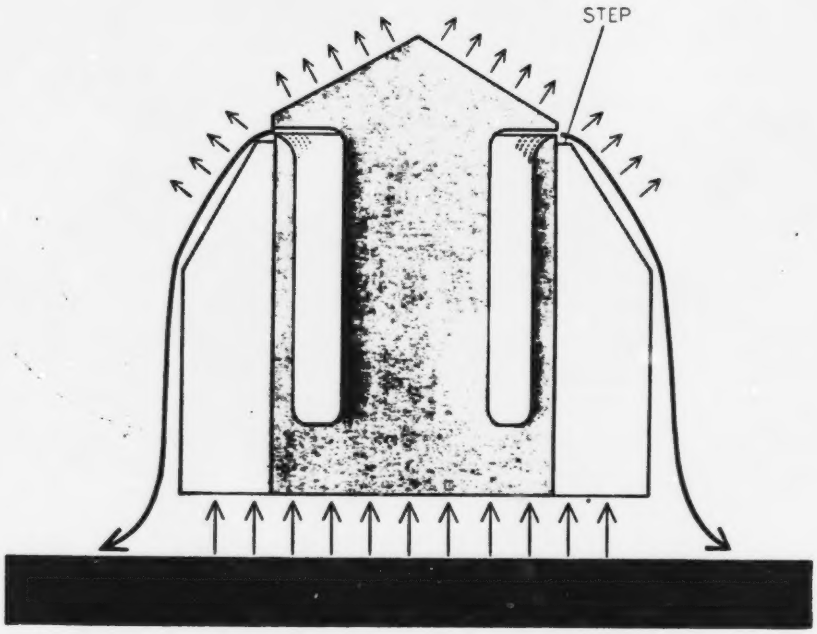

EXTERNAL NOZZLE was designed by the author in early tests of the Coanda effect as a means of generating lift. Pressure over the upper portion proved to be less than atmospheric; hence a vehicle with the shape of such a nozzle could be lifted by low pressure at top and higher pressure at bottom. Step near slit proved to be crucial in maintaining good lift.

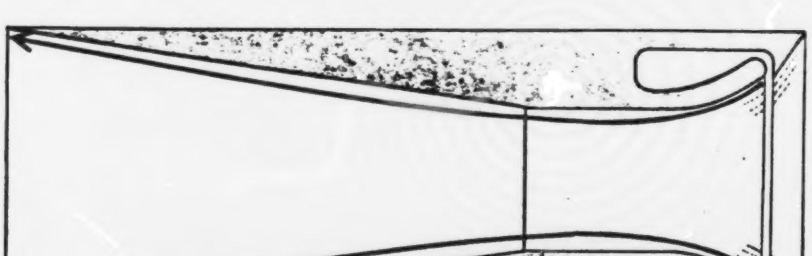

INTERNAL NOZZLE takes its name from the fact that the flow of air is through the inside of the nozzle. Otherwise the Coanda effect is the same as that in the external nozzle.

short, flat surfaces, each at a certain angle to the one before and each with a certain length, he could bend a jet stream around an arc of 180 degrees [*see top illustration on preceding page*]. Moreover, by experimenting with air blown through the slit he discovered that the deflected airstream sucked in air from the surroundings. As the jet flowed around the shoulder it entrained up to 20 times the amount of air in the original jet. Coanda measured the air pressure at various points along the surface over which the stream was flowing, and he established the significant fact that the pressure on the surface was less than atmospheric pressure: in other words, it represented a relative vacuum. Near the slit the existence of this vacuum accelerated the flow of the jet after it emerged from the slit.

From his experiments and calculations Coanda derived a remarkable conclusion. The Coanda effect, he argued, could lift and propel a vehicle by a process that was the reverse of that in conventional propulsion systems. Instead of applying force at the rear of the vehicle (such as a rocket or a boat) to propel it against the resistance of the air or water in front, one could use the Coanda effect to generate a vacuum at the front, so that the higher pressure at the rear would impel rather than propel it. Similarly, a Coanda-generated vacuum above the vehicle would provide lift. In conventional aircraft-propulsion systems the necessary vacuum above the wings is generated by driving the vehicle forward at high speed; the Coanda system would accomplish the same purpose without any forward motion or moving parts simply by blowing air over a rounded shoulder.

In aerodynamics the problem of propulsion is reduced to the problem of overcoming drag, a resistance whose components are high pressure at the nose of the vehicle and low pressure at the tail. Coanda's proposal, to put it briefly, consists of propelling the vehicle by means of "negative drag": low pressure at the nose and higher pressure at the rear. This suggestion is so completely contrary to ordinary concepts about the flow of a fluid around moving bodies that it has understandably met with great skepticism among aerodynamicists.

Undismayed by skeptics or by the general lack of interest in his ideas, Coanda proceeded to construct various nozzles embodying his effect and to design vehicles to be propelled by them. The fact that some of his designs took the shape of flying saucers has not helped matters. The Coanda effect might have been dismissed as an eccentric notion had it not attracted the attention of the team of Allied scientists that was assigned to investigate the German wartime research after the liberation of Paris in World War II. It was alleged that the Germans had conscripted Coanda into their jet-propulsion research. In any case, the Allied scientists examined Coanda's devices and suggested that the Coanda effect merited seri-

IMPORTANCE OF GEOMETRY in optimizing the Coanda effect is demonstrated by these shadow photographs. At left is the flow of an undeflected jet of air. With a curved surface outside the slit (*middle*) the air tends to follow the surface, but with distortions. A step at the exit of the slit (*right*) produced a better flow but not an ideal one because the air impinged on the surface.

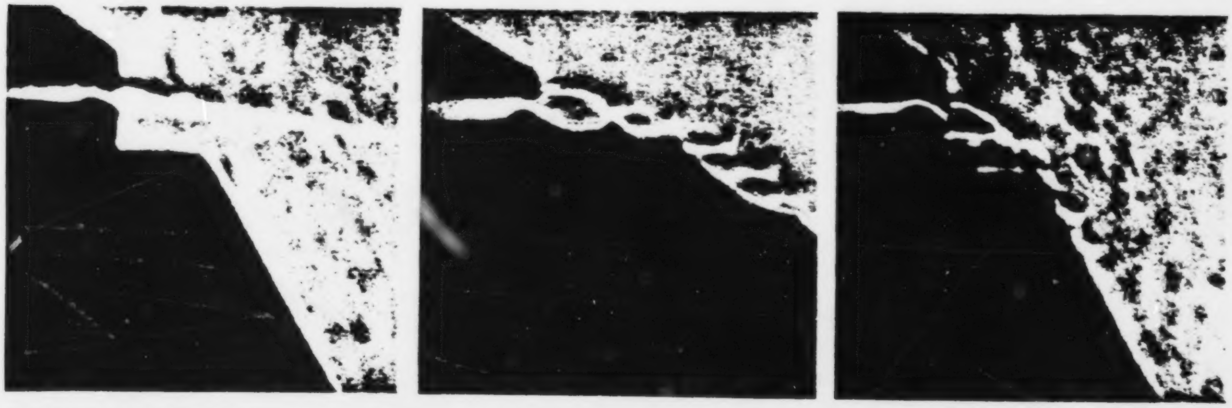

FURTHER MODIFICATIONS showed (*left*) that too high a step can cause the flow to separate from the surface. With a grooved surface (*middle*) the flow was undistorted. A well-balanced geometry (*right*) provided an ideal flow that was tangent to the surface.

ous study. A theoretical analysis by von Kármán in 1949 and experiments at the Cornell Aeronautical Laboratory in 1952 supported Coanda. Several other investigators, however, reported that his claims could not be confirmed, and this discouraged a thoroughgoing evaluation of his ideas.

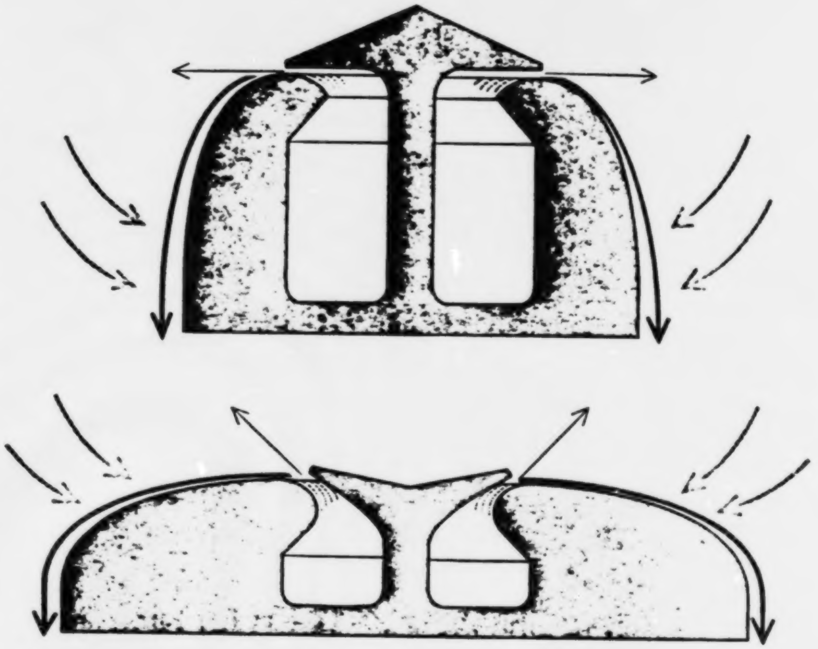

REORIENTATION OF SURFACES was necessary to progress from nozzle-like applications of the Coanda effect (*top*) to the wide-based shape (*bottom*) desirable for a ground-effect machine. The changes involved much experimentation with different configurations.

Happily unaware of the controversy among the experts, I was attracted to Coanda's concept by an article about him in a popular magazine in 1956. As a student at the Polytechnic Institute of Brooklyn, I was particularly interested in propulsion systems, and the unorthodox Coanda approach seemed exciting. When I went on to graduate studies at the institute, working as a research assistant in its newly established Rocket Propulsion Laboratory, I had the good fortune to obtain more technical information about the Coanda effect from T. Paul Torda, director of the laboratory, who had worked with von Kármán on the theoretical analysis.

I set out to test the effect with a nozzle of my own design. Coanda had experimented with both "external" and "internal" nozzles. In the former the deflecting shoulders were outside a tube; in the latter, inside [*see middle and bottom illustrations on page* 85]. My nozzle was of the external type: a roughly cone-shaped arrangement in which air blown outward through a slit circling the body would cascade over a shoulder angled 60 degrees from the slit. This form of the device was inspired by the thought that the Coanda effect might be applied to a "ground-effect machine," the type of vehicle that moves over the ground on a thin cushion of air. For such a machine one of the main problems is steering and related control, since it has no traction with the ground. It seemed that Coanda nozzles might provide such controls.

The first tests of the nozzle were successful. With a nozzle positioned upright in a model ground-effect machine, the Coanda phenomenon caused the model to take off and rise to a height of several inches when a fast stream of air was blown through the slit. Emerging from the slit at the speed of sound, the air accelerated to supersonic speed as soon as it began to flow over the shoulder.

In 1961, having joined the Armour Research Foundation, now the IIT Research Institute associated with the Illinois Institute of Technology, I was provided with funds for an investigation of the possible use of the Coanda effect for propulsion. Coanda had said that a Coanda nozzle, by increasing the momentum of the gas flow, could produce twice as much thrust as an ideal straight nozzle with the same input of energy. Experimenters testing his claim had failed to achieve any augmentation of thrust by means of the Coanda effect. Their test devices, however, were quite simple in design, whereas Coanda had developed rather sophisticated nozzles of complicated geometry. It therefore remained possible that with proper design a gain in thrust could be demonstrated.

As a start in our testing program I designed a one-piece nozzle six inches in diameter with a shoulder in the form of a series of successively angled flat surfaces, according to Coanda's original design. The results of its first test were most disappointing. The airstream from the slit did not flow around the shoulder contour; it promptly detached itself unless the slit opening was made very small or the flow was very gentle and undisturbed. I went home from the laboratory frustrated and discouraged. But my assistant, Edward Wohlthausen, stayed on and carefully went over every feature of the nozzle's construction. He discovered a seemingly trivial difference, which turned out to be crucial, between this model and the one I had built originally at Brooklyn Polytech. My first model had had a small step down from the mouth of the slit. This small step at the aperture, only about a thirty-second of an inch deep, made the difference between the airstream's clinging to the shoulder and separating from it. With such a step the new model also worked.

We then proceeded to extensive testing of some 30 different shoulder configurations. With the help of shadowgraph photography that showed details of the flow, we obtained several interesting insights into the Coanda effect [*see illustrations on opposite page*]. The small step at the very lip of the slit is important because it turns the flow from the slit into an eddy, or vortex, which in this device rings the entire nozzle and therefore forms what is called a ring vortex. It is the vortex–or rather the low pressure generated within it–that causes the stream from the slit to bend and thus follow the contour of the shoulder. The curving of the stream around the shoulder produces a force directed radially outward; this force, tending to pull air away from the shoulder surface, apparently accounts for the relative vacuum, or suction, next to the surface. To maintain the suction, which prevents separation of the stream from the surface and causes the flow to accelerate, the stream must hug the shoulder surface closely without actually impinging on it or adhering to it.

Our experiments showed clearly that the creation of a stable Coanda effect depends on the appropriate adjustment of many factors: the diameter of the slit, the strength of the jet, the depth of the step and various other details of the shoulder contour. Particularly crucial is the ratio of the slit diameter to the diameter of the nozzle as a whole. If the slit is too wide in relation to the shoulder breadth, the stream will tend to detach itself from the surface; if it is too narrow, the stream will tend to stick to the surface. Also important is the texture of the surface: a properly roughened surface helps to prevent distortion of the stream flow. In short, it takes a complex set of arrangements to produce a useful Coanda effect. It is no wonder that most investigators of the effect had found it to be an elusive phenomenon.

Obviously the effect depends primarily on the maintenance of a balance between the centrifugal force and the suction force as the stream flows around the shoulder and afterbody of the nozzle. We found by experiments that the efficiency of the effect could be enhanced by certain adjustments of the orientation of the slit and the slope of the shoulder; these controlled the distribution of pressure within the stream so that it did not separate from the surface.

Although we obtained high thrust efficiencies with such devices, we were not able to produce the gain in thrust (over the theoretical capabilities of conventional jet devices) that Coanda had said should be achievable. At this juncture, in the spring of 1963, Coanda himself visited my laboratory. (He was then 77 years old.) He examined the model with which I was working, bent over it and cupped his hands around the nozzle. The fluid in a manometer attached to the model promptly rose, showing an increase in the suction pressure. By simply forming a shroud around the nozzle with his hands Coanda had increased the device's production of thrust!

The shroud, Coanda explained, guides the streamlines of the entrained flow in a direction parallel to the surface of the model and thus enhances the suction pressure. Coanda went on to emphasize also the importance of proper design of the afterbody, or tail, beyond the shoulder. A suitably tapered afterbody, he said, would cause the flowing stream to exert a positive pressure on the rear of the body and thereby add to the propulsive thrust.

Not entirely convinced of this last argument, because it was so contrary to accepted ideas in aerodynamics, I nevertheless proceeded to build

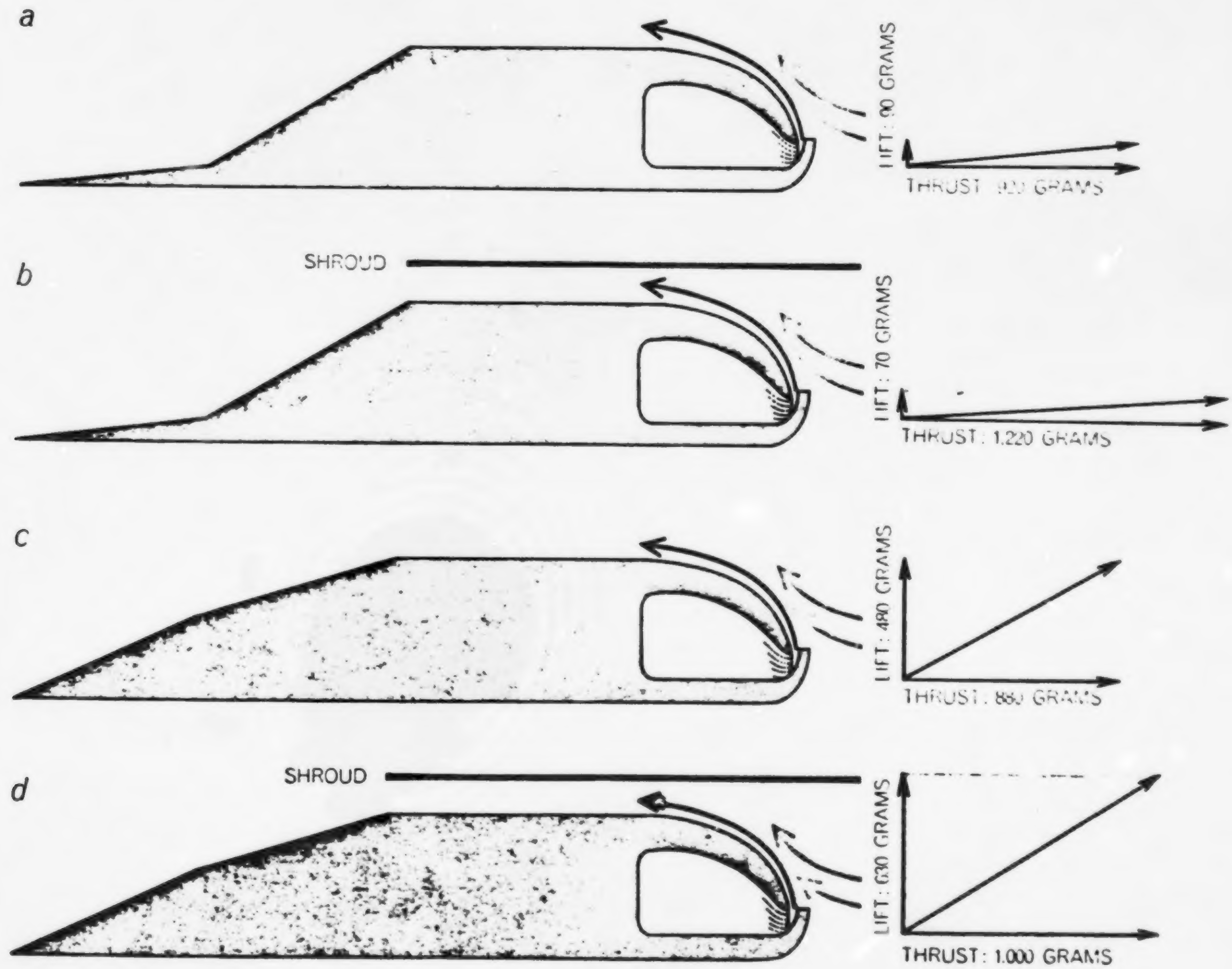

CONFIGURATION AND SHROUDING affect the performance of an airfoil. At *a* the Coanda effect over the airfoil at left produces the forces represented at right. At *b* the result of placing a shroud over the same airfoil is shown. An airfoil of different geometry appears unshrouded at *c* and shrouded at *d*. In each instance the data were obtained from an airfoil that was fixed rather than moving.

several models based on Coanda's recommendations. The shroud concept immediately proved its value in enhancing thrust. The afterbody theory, on the other hand, turned out to be harder to confirm. At length, after more than a year of experimenting with various afterbody configurations, we finally produced one that bore out Coanda's prediction [*see illustration on opposite page*]. This nozzle, with a shroud and a steeply tapered tail, produced a thrust 19 percent greater than that of an ideal jet lacking the augmentation of the Coanda effect.

Independent studies at the University of Toronto's Institute of Aerospace Science, at Pennsylvania State University and at the Research Center of the Huyck Corporation in Stamford, Conn., have also verified that Coanda nozzles are capable of augmenting thrust. Gains of up to 38 percent have been reported. Indeed, it can be said that Coanda's hypothesis of propulsion by negative drag has been confirmed.

This is not to say that the Coanda effect is fully understood. There is no doubt that the gain in thrust with the Coanda type of nozzle derives from the fact that a jet sheet flowing around a curved wall entrains more outside fluid than a straight jet stream does. But the mystery remains: Why does it do so? The answer probably lies in the turbulences set up within a curving jet sheet; presumably they promote vigorous mixing of portions of the fluid and so increase the rate of entrainment at the outer edge of the sheet. In any case, we now know from experiments that the Coanda effect does work to augment thrust, and we therefore have a sound basis for exploring possible useful applications of the phenomenon. Indeed, it has already shown its usefulness in another field, namely the device known as the fluid amplifier, whose functioning depends on the Coanda effect [see "Fluid Control Devices," by Stanley W. Angrist; SCIENTIFIC AMERICAN, December, 1964].

The first device we built to test the practical application of Coanda thrust was a small model called GEM (for ground-effect machine). This dome-shaped model, two feet in diameter, has a ring slit at the top, a shoulder configuration in the form of an ellipse with its major axis parallel to the ground and a short, collar-shaped shroud around the lower part [*see illustrations at right*]. The slit is inclined at an angle of 45 degrees from the horizontal, so that the jet is directed upward—contrary to all

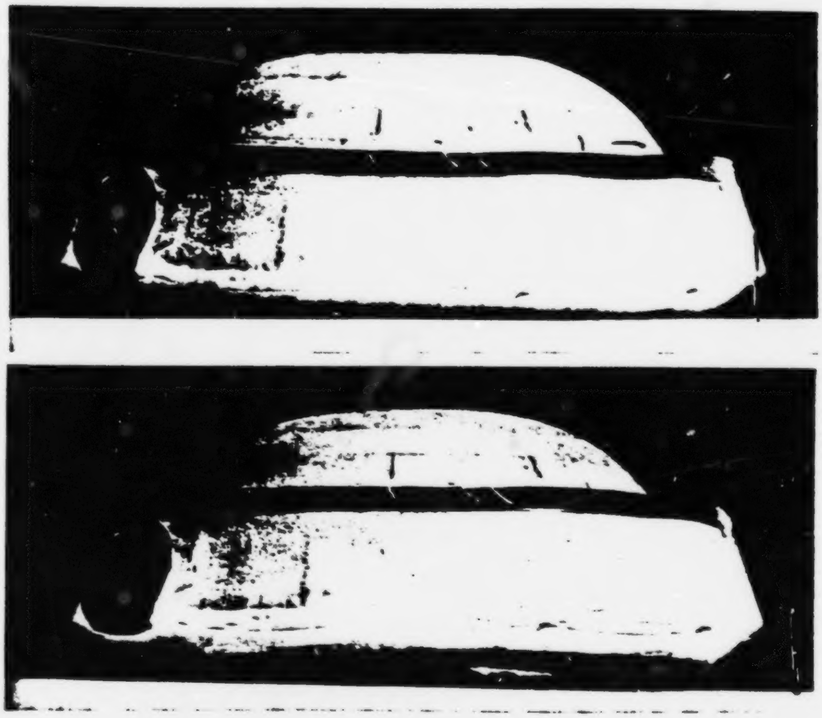

GROUND-EFFECT MACHINE, which is known by the acronym GEM, rests on a table at top and rises from the table at bottom. It achieves lift by means of air, but in an unusual way. Because of the Coanda effect the pressure at GEM's top is less than atmospheric. With this negative drag, or reduced resistance, over the upper portion of the surface, the higher pressure at the bottom lifts or drives the vehicle. The hole on the left side is the air intake.

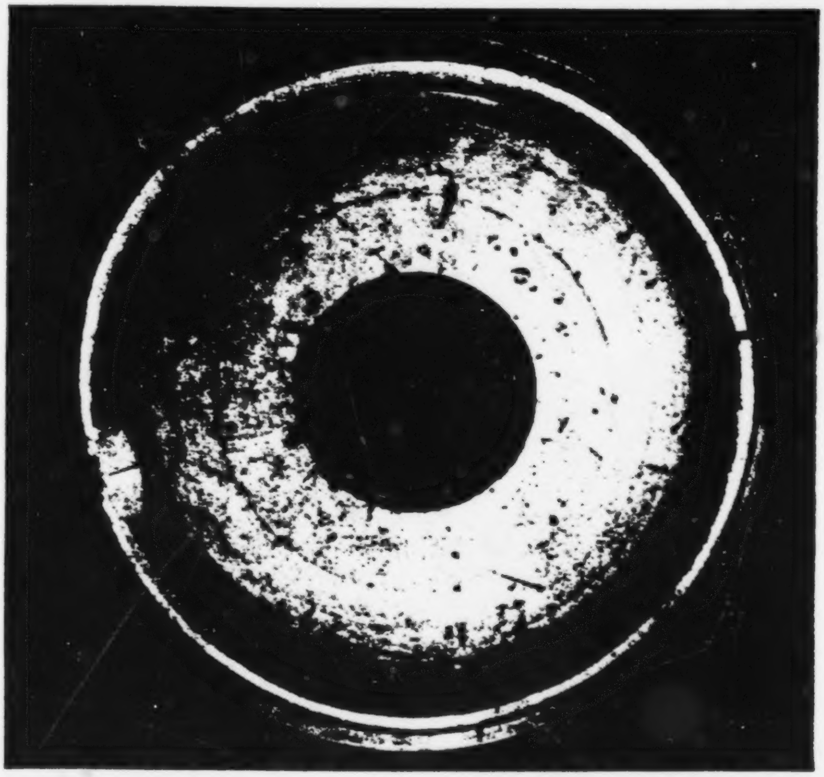

TOP VIEW of the GEM shows the slit from which the air emerges. The slit is the thin light circle near the outer edge of the dark central area. The dark circle just outside the slit is the step. This model, designed by the author, is approximately two feet in diameter.

conventional uses of jet thrust to generate lift. This vehicle is raised from the ground simply by the jet of air that produces a vacuum at the upper surface, flows around the shoulder and emerges at the bottom, thus producing the ground effect: pressure higher than that of the environment. The primary jet, generated by a small ducted fan, represents a comparatively modest application of power, the strength of the jet amounting to a pressure of four inches of water.

The cover hooding the slit at the top of the model can be tilted so that the slit is widened on one side and narrowed on the other; this maneuver, by skewing the distribution of force over the top surface, serves as a means of banking the vehicle in the air. By a simple modification of the vehicle's

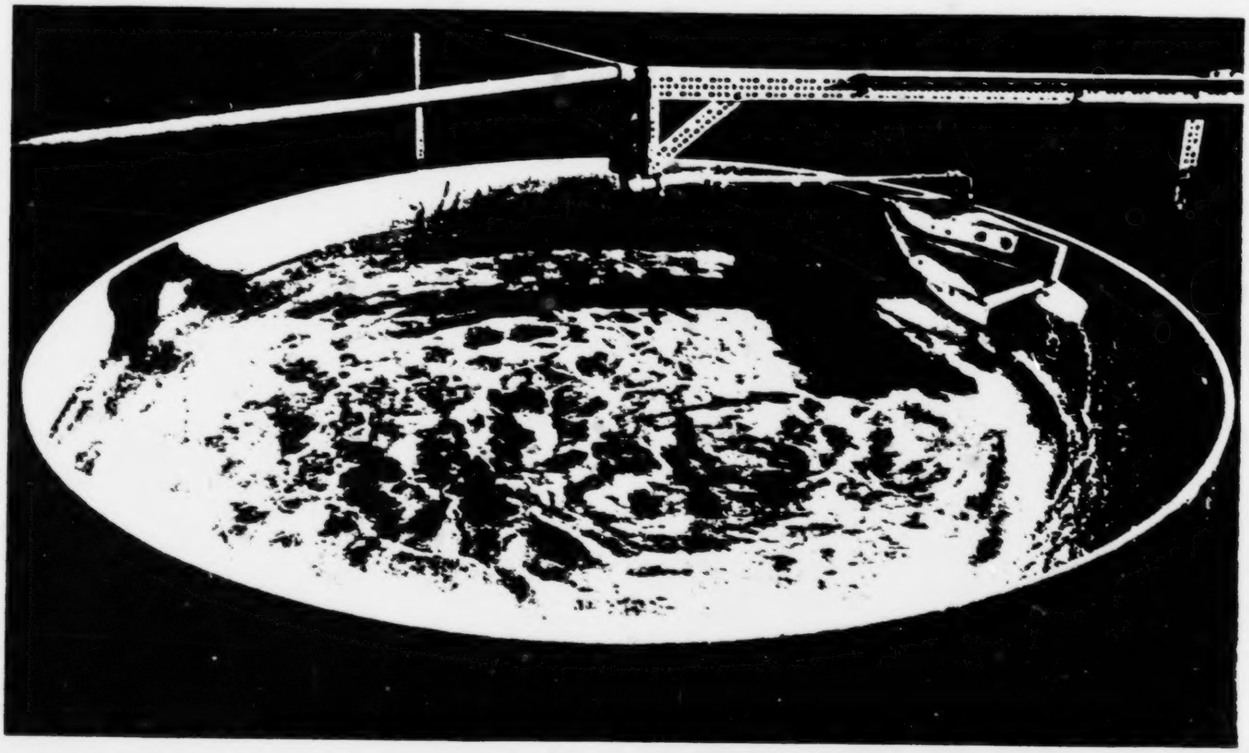

HYDROFOIL CRAFT using the Coanda effect has achieved speeds of more than 19 knots in this pool. The model is about four feet long. The wings on the hull are for stabilizing the craft and for generating a ground effect; propulsion is from an underwater foil.

KEY PART of the hydrofoil is this foil with several slits for achieving the Coanda effect. Water emerging from the slits (*right*) tends to curve around the foil because of the Coanda effect, thereby creating a negative drag similar to that in the airborne GEM.

form it has been endowed with forward propulsion. In this model the configuration of the body is asymmetrical, and the resulting asymmetrical distribution of forces in the jet sheet provides forward thrust to the vehicle.

The Coanda system offers several improvements over the present versions of ground-effect machines. It should reduce the amount of power needed for propulsion, reduce the weight of the machine, permit steering of the vehicle by banking and make it easier to mount slopes.

The estimated lift efficiency of the present rather crude model is about 25 pounds of lift per horsepower for a lift-off height of about a twentieth of the diameter of the vehicle. This performance is comparable to that of ground-effect vehicles operated by conventional means. It remains to be seen, however, if a vehicle of the Coanda type will retain comparable lift efficiency when it is scaled up to full size.

Another vehicle currently under development in our laboratory is a boat of the hydrofoil type, that is, a craft in which the foil lifts the hull out of the water. In this case, employing the Coanda effect, the hydrofoil is self-propelling: it provides not only the lift and controls but also the propulsion of the craft. Nozzles that emit jets of water are incorporated in the leading edges of the foil, the strut and water-intake pods. The craft has a hull with down-swept wings that I have designed to minimize drag, improve the craft's stability on the water and provide some additional lift by the ground effect [*see illustrations on opposite page*].

Our present model, four feet long and weighing 22 pounds, cruises at better than 20 miles per hour at the end of a tether in a circular pool 10 feet in diameter. It can lift its hull out of the water and ride on the hydrofoil at very low speed and without using any more power than is required for cruising. Control of the craft is accomplished by means of surfaces that do not protrude into the flow. Thanks to the large entrainment of fluid from the vicinity of the nozzles, the foil generates essentially no wake, very little spray and little noise. We believe the use of a "ventilating flow"—achieved by injection of small amounts of air—will minimize undesirable effects caused by cavitation (the formation and collapse of bubbles around the foil). If we are right, a full-scale version of the craft should be capable of speeds of more than 80 knots,

Several thousand scientists and engineers will see this message, but . . .

ONLY A FEW CAN QUALIFY

▪ Because of the nature of our work, not everyone can meet our exacting requirements. We are engaged primarily in analytical and theoretical studies dealing with questions of strategic and tactical warfare, economic development, and space systems — essentially *problem solving*—requiring disciplines in the physical sciences, engineering, mathematics, behavioral sciences and economics.

For those who meet our high standards and join our growing company, the rewards are extraordinary. Our professional staff is small. Each member has great creative freedom in the quiet of his own office. Each finds personal pride—and endless challenge—in his work. And there is tremendous professional satisfaction in contributing to the solution of problems of national and international import—problems that *must* be solved.

Moreover, you will be encouraged to continue your education or teach (our Research Center is less than a mile from the campus of the University of California at Santa Barbara). The working climate and personal benefits are among the most satisfying and progressive to be found anywhere.

During the next few months, we will add to our staff professionals capable of solving problems in these areas of activity:

SYSTEMS ANALYSIS
RADAR THEORY AND ANALYSIS
ELECTRONIC COUNTER MEASURES
OPTICAL SYSTEMS
BEHAVIORAL SCIENCES
ECONOMICS
PHYSICS
THEORETICAL AERODYNAMICS

If you possess intellectual curiosity and an outstanding record of academic and professional achievement, we'd like to hear from you—*whether or not you are presently considering a change of association.* We will send you a brief brochure which describes DRC in more detail and introduces present members of our professional staff. We'll also send you evidence of the delightful life available to those fortunate enough to live and work in world-famed Santa Barbara.

Please write in confidence to Mr. John S. Adams, Assistant to the President.

DRC

DEFENSE RESEARCH CORPORATION

. . . contributing to the solution of problems of national importance

POST OFFICE BOX 3587 · SANTA BARBARA, CALIFORNIA 93105

(Opportunities also exist in the Washington, D.C. area)
AN EQUAL OPPORTUNITY EMPLOYER

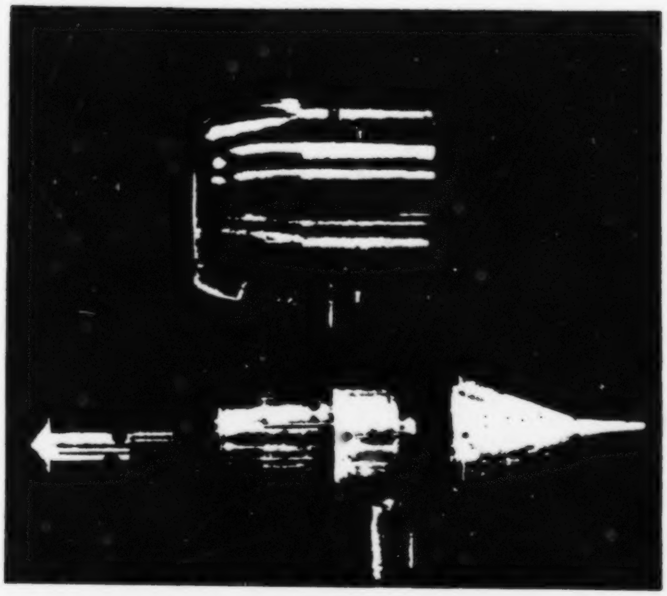

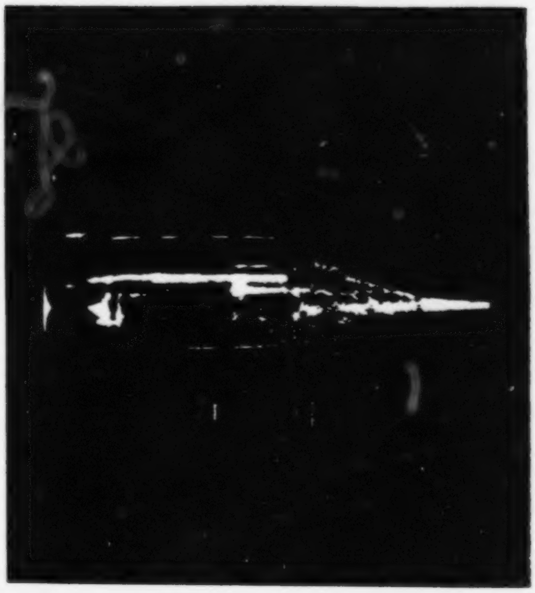

COANDA NOZZLE is shown disassembled at left and assembled at right. The plastic part is a shroud that enhances the Coanda effect. The conical part is the afterbody; pressure over it is slightly above atmospheric when the nozzle is operating to achieve thrust.

with a considerable saving of power over conventional high-speed hydrofoil boats.

Aside from the uses of the Coanda effect for propulsion systems, which are still in a highly experimental stage of development, there is another type of application in which the principle has already proved its value. Nozzles based on this principle are extraordinarily efficient as components of burners [*see illustration below*]. When properly shrouded, they produce an almost invisible flame with no smoke and essentially complete combustion of the fuel. In some applications most of the air for combustion is supplied by the nozzle's entrainment of air. In addition the nozzle can be used as a pump to recirculate unburned gases and thus produce blue-flame, smokeless combustion. To these advantages are added mechanical simplicity, compactness, comparatively low cost and the absence of moving parts. Attempts are now being made to adapt the Coanda nozzle to the burning of heavy fuel oils. Nozzles of this kind might also be employed in vehicle-propelling engines, and this possibility is now being considered.

It is in the field of propulsion, of course, that the prospects for employing the Coanda effect look most attractive. The promise of attaining a propulsion system that would produce its own dividend of power from the very nature of its design, that would have no moving parts such as propellers or fans, that could be blended into the contour of a vehicle without wasting space or significantly disturbing aerodynamic characteristics, that would be smaller, lighter and quieter than present engines—is indeed an incentive to further exploration of the Coanda effect.

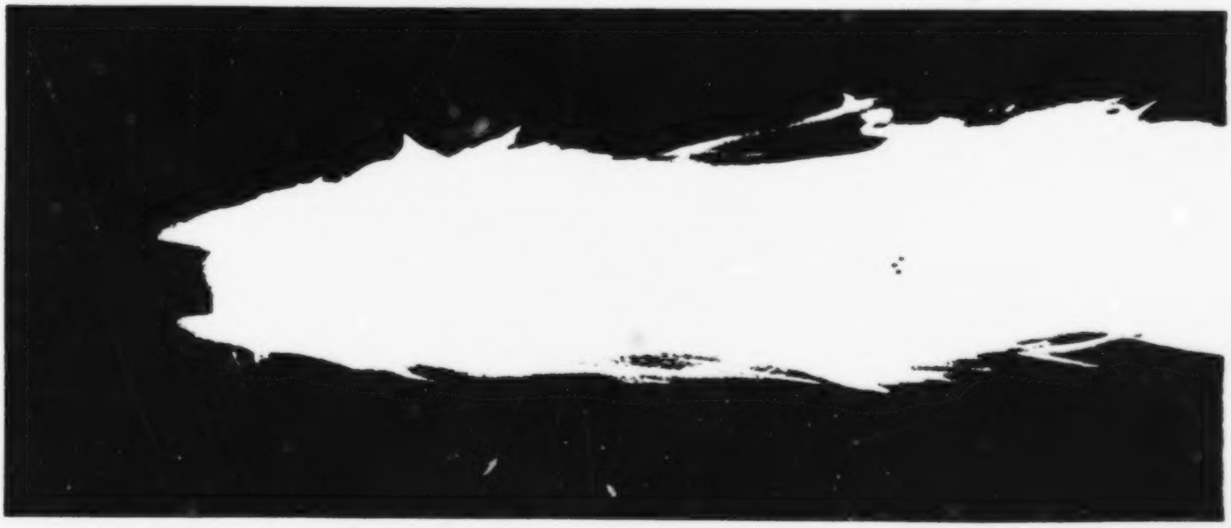

TYPICAL FLAME in a burner using a Coanda nozzle is blue, smokeless, quiet and well concentrated when the nozzle is properly shrouded. Almost total combustion of fuel is achieved. Much of air for combustion comes from entrainment of air by the Coanda effect.

B-1

CONTROL PARAMETERS FOR A 75 WT% COAL-WATER SLURRY: CO-AL

J. E. Funk Jr., D. R. Dinger, J. E. Funk Sr.
Alfred University Research Foundation
Alfred University, Alfred New York

Abstract

Co-Al is produced by the combination of a particle size distribution designed to yield interstitial porosity less than 8% and a specific surface area greater than 1.25 m^2/cc as measured by a computer algorithm and tested by pressure filtration, and an electrochemistry which effectively disperses the particles in the slurry. Yield stress required for stability and the viscosity versus shear rate behavior vary significantly with changes in these two parameters. Measurement techniques for particle size distribution, rheology and stability and data of each will be compared with the theoretical treatment.

Introduction

Work began at Alfred in 1976 to develop the procedures for preparation of a highly loaded coal/water mixture called Co-Al[1,2]. The fuel was prepared in pilot scale quantities in the summer of 1980 and was successfully burned unsupported by auxiliary fuel at the Babcock and Wilcox Company Alliance Research Center in October 1980[3]. Since a pilot demonstration plant is currently being designed for production of this new fuel, a major emphasis of the work at Alfred has been to define control parameters to be used for production of Co-Al.

In order to achieve the high loading and the low viscosities characteristic of Co-Al, the following control parameters have been defined:

(1) Particle size distribution that fits the following equation with n = 0.37:

$$\frac{CPFT}{100} = \frac{D^n - D_s^n}{D_L^n - D_s^n} \qquad (1)$$

where CPFT = cumulative percent finer than
D = any particle diameter in the distribution ①
D_L = largest particle diameter in the distribution ≃ 300 µm
D_s = smallest particle diameter in the distribution ≃ 0.1 µm
n = exponent the slope at D

(2) Electrochemistry of the slurry sufficient to effectively disperse all particles so that the system is in a state of deflocculation.

(3) A colloid content high enough to give a specific surface area >= 1.25 m^2/cc.

(4) Mv = 50

① CoAL - by Slurrytech

Particle Size Distribution

The size distribution of the particles must be one that allows the particles to be packed very close to the theoretical density of the particles or in other words to be packed with minimum porosity. This minimizes the amount of water in a slurry required to fill pores and maximizes the amount of water available for separating particles and imparting fluidity. Equation 1[2] is based on the work of Andreasen[4] and a number of computer models have been developed specifically for this problem.

Size analysis equipment used at Alfred to measure particle size analyses for comparison with Eq. 1 are a Micromeritics Sedigraph 5500L System and a Leeds & Northrup Microtrac Small Particle Analyzer. The Sedigraph 5500L has been used for the majority of the work. The Microtrac SPA has not yet been correlated with Sedigraph data. Size distributions from the Sedigraph are merged with sieve analyses data to give total size distributions from 4 mesh to < 1 Micron. Since these data are stored in the computer, various calculations can then be made.

An algorithm, based on Eq. 1 and Andreasen's[4] work, and the work of Westman & Hugill[5] has also been developed to calculate the minimum porosity to which a distribution of particles can be packed. It essentially shows the best fit of the actual distribution to the equation of the type shown in Eq. 1. This algorithm results in two parameters representative of the distribution: - the minimum porosity, and the specific surface area of equivalent spheres in the distribution.

Research designed to test the accuracy of this algorithm is currently in progress and a full description and explanation of the algorithm will be published elsewhere.

A filter press apparatus (Fig. 1) has been designed[2] specifically to test this algorithm and to measure the minimum porosities to which slurries can be packed. The press consists of a cylindrical steel cell, the top surface of which is a moveable piston and the bottom surface of which is a porous filter material. A known volume of slurry is poured into the cell, and the dilution fluid is pressed out. A load cell in the press measures pressure exerted by the piston, a second load cell measures the rate and volume of filtrate pressed out of the slurry, and a transducer (LVDT) measures the displacement of the piston. A given true volume of coal particles will pack to a minimum bulk volume if the packing efficiency is maximum (minimum porosity).

Preliminary results comparing the algorithm results with those measured using the filter press for an Upper Freeport slurry are presented in Table I.

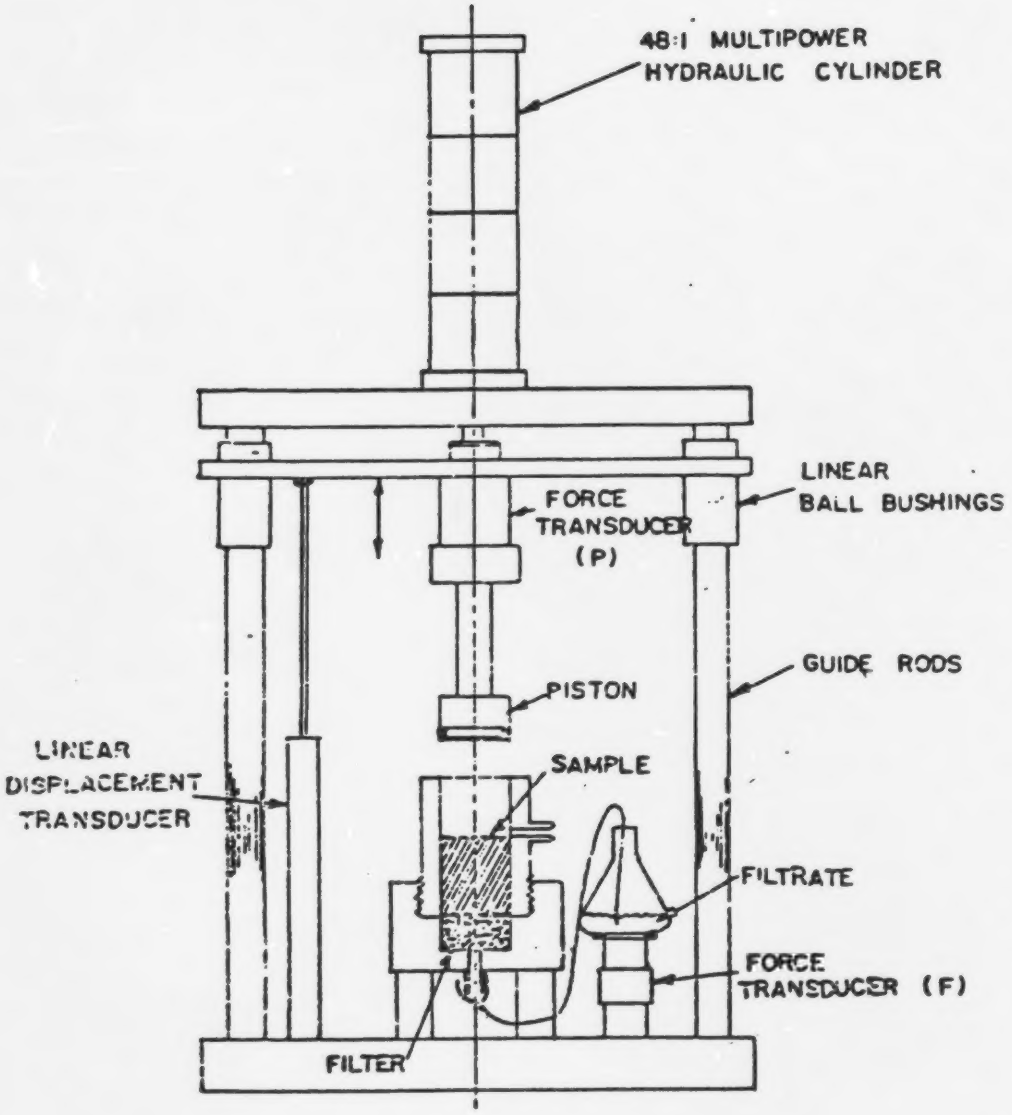
48:1 MULTIPOWER HYDRAULIC CYLINDER
LINEAR BALL BUSHINGS
FORCE TRANSDUCER (P)
GUIDE RODS
PISTON
SAMPLE
LINEAR DISPLACEMENT TRANSDUCER
FILTRATE
FORCE TRANSDUCER (F)
FILTER

Figure 1

Schematic Diagram Of The Pressure Filtration Apparatus

Table I

Comparison of Measured (Filter Press) And Calculated Minimum Porosities For Four Different Grinds Of Upper Freeport Co-Al

Sample	Filter Press	Computer Algorithm
75%	8.1%	7.4%
75% - Diluted to 65%	8.2%	7.4%
75%	8.6%	7.4%
75%	7.0%	6.2%

These preliminary results show very good agreement between the results calculated with the new algorithm and the results from the filter press.

Experience has shown that best slurries are produced when this calculated porosity is less than 8%.

Electrochemistry

An electrochemistry that effectively disperses the particles is also required in order to maximize the opportunity for each particle to occupy its position within the consist at minimum energy under shear. If the chemistry of this system is such that particles attract one another the system will flocculate, single particles are not free to move independently, and the viscosity will increase. On the other hand, when all particles repel each other, interparticle distance and fluidity will be maximized. This is determined by the ζ-potential developed upon the colloidal fraction of the consist and may be measured by any suitable electrophoretic or electrosmotic analyzer. A ζ-potential of approximately 50 mv should be suitable for most coal-water slurries.

Yield Stress and Stability

In order to produce a stable slurry a yield stress is required. In order to impart sufficient yield stress and, in general, to allow effectual working of the electrochemistry, the colloid fraction must be present in sufficient quantity.

Any measurement technique for obtaining surface area can be used although for this work, the surface area has been calculated by integrating particle size distribution of the slurry and assuming spheres for the consist. Curve fitting routines indicate D_s in the size distribution are from about 0.2 to 0.5 μm. Smaller particles are present in such small quantities as to have little effect upon the size distribution curve. This measurement requires a minimum surface area of 1.25 m^2/cc. Measurements by adsorption of gases which treats real particle shapes obviously give larger surface area than equivalent spheres.

Co-Al Slurries

The particle size distribution of an Upper Freeport Co-Al is shown in Fig. 2 compared with the matching Alfred distribution. The specific surface area of the slurry is about 1.7 m^2/cc, the calculated porosity is 6.2% and the ζ-potential is about 50 mv to effectively disperse the particles. The viscosity and yield stress behavior of this same slurry are shown in Figs. 3 and 4. If the size distribution is not correct, the viscosity will increase dramatically even in a system with identical chemistry to the slurry shown in Fig. 3. The same will happen if the chemistry of the sample shown in Fig. 3 is changed. As mentioned above, both size distribution and chemistry must be optimized to achieve the goal of a highly-loaded slurry at a low viscosity.

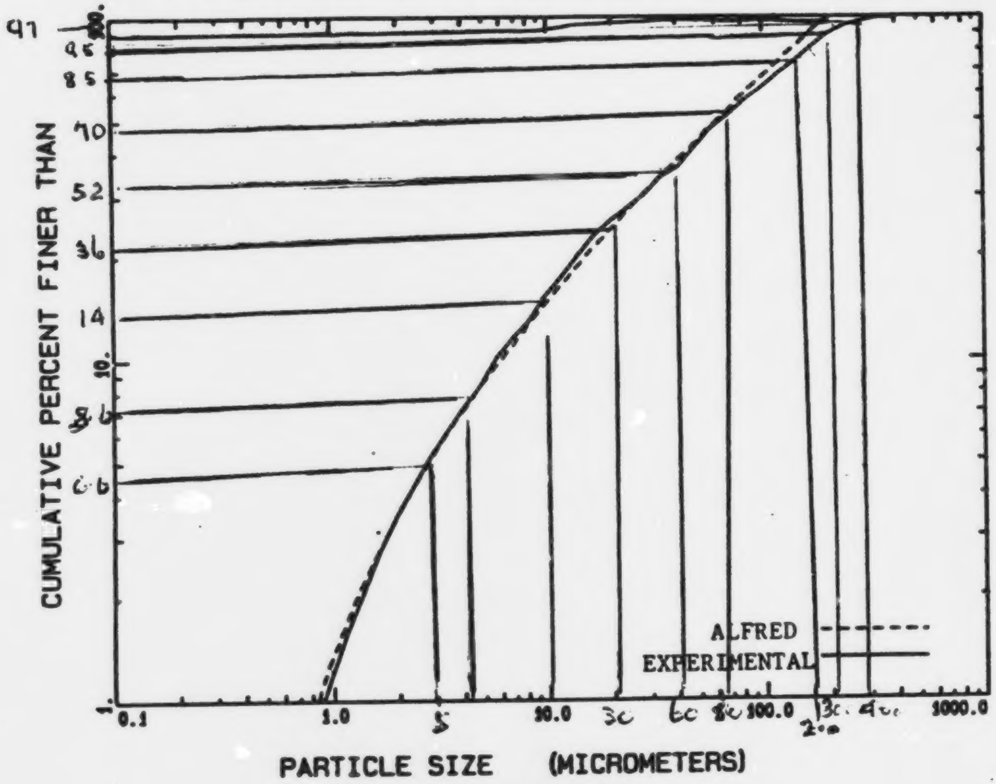

Figure 2

B·1

Upper Freeport Co-Al Size Distribution
And The Matching Alfred Distribution

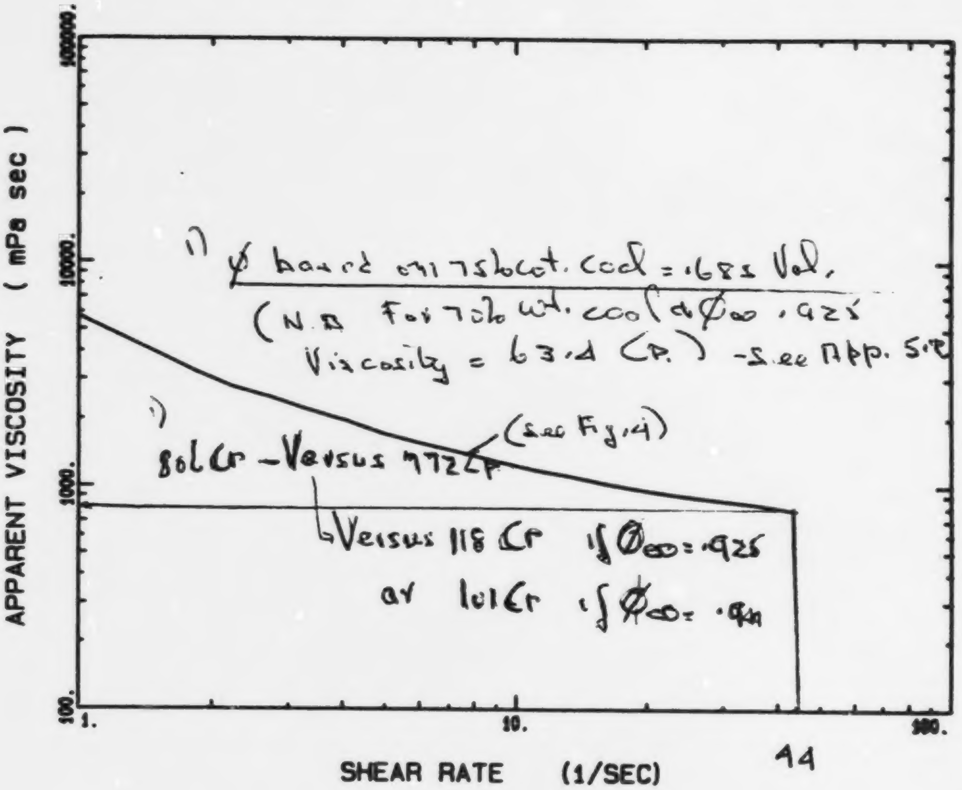

1) φ based on 75% wt. coal = .685 Vol.
(N.B. For 75% wt. coal φ∞ .925
Viscosity = 63.4 Cp.) - See App. 5.2

1) 801 Cp - Versus 772 Cp (see Fig. 4)
Versus 118 Cp if Ø∞ = .925
or 101 Cp if Ø∞ = .94

44

Figure 3
E-1
Apparent viscosity versus shear rate
plot for a 75 wt% Upper Freeport Co-Al

See App. 4.2

1) $\frac{\phi}{\phi_\infty}$ 2)

$\frac{.685}{.925} = .74$

$Vis = (1-.74)^{-3.54} = 118$ Cp

$\frac{.685}{.94} = .7287$

$(1-.7287)^{-3.54} = 101$ C

2) Values of ϕ_∞ from Table 1 based on Filter Press Testing (Fig. 1)

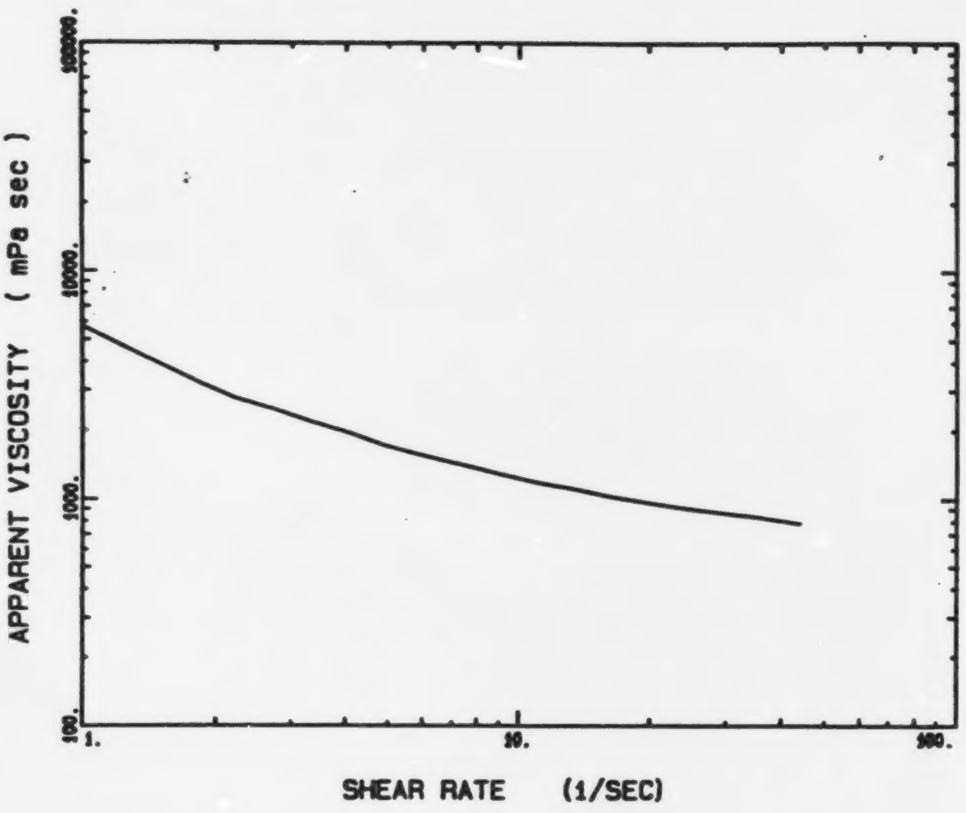

Figure 3
E-1
Apparent viscosity versus shear rate
plot for a 75 wt% Upper Freeport Co-Al

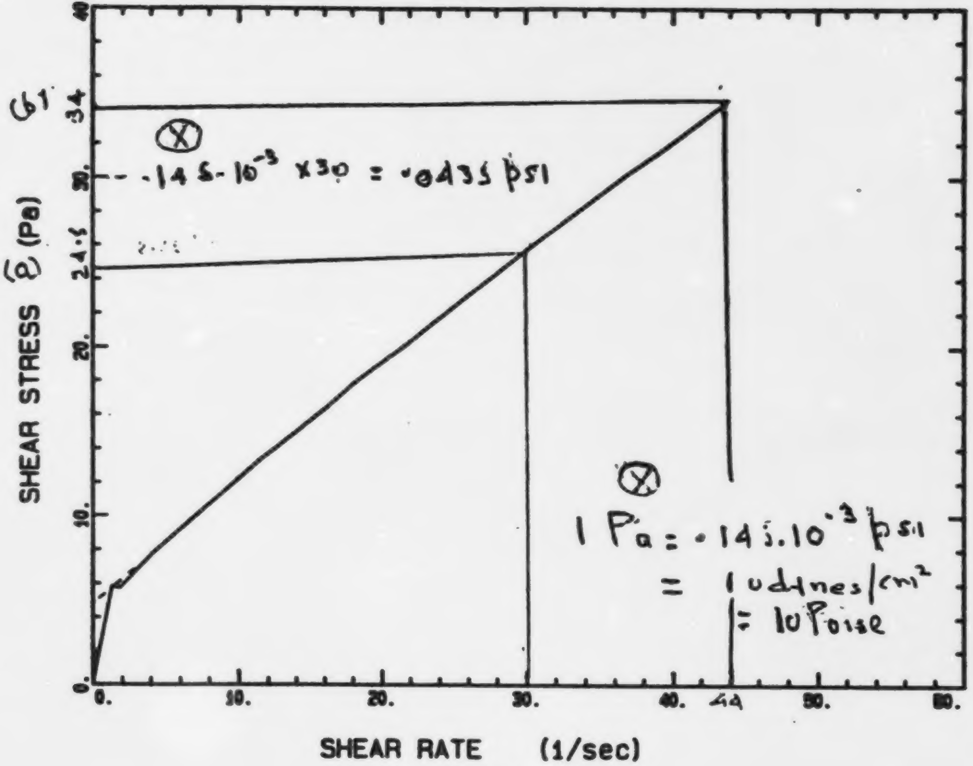

Figure 4

Shear stress versus shear rate plot
for a 75 wt% Upper Freeport Co-Al showing
a yield stress of about 6 Pa.

Vis. (a) = $\frac{24.5 \times 10}{30}$

= 8.17 Poise

Vis. (b) = $\frac{34 \times 10}{44}$

= 7.72

1) But SI ... graph = Newtonian Mode
(Co-ordinates ... Cartesian)

graph slope
under pseudo-
plastic mode

Summary

Control parameters for Co-Al slurries are:

(1) The particle size distribution be an Alfred distribution (Eq. 1) with a calculated minimum porosity of less than about 8% porosity.

(2) The electrokinetic potential must be sufficient to effectively disperse all particles.

(3) The colloidal fraction be present in sufficient quantity as to allow the proper working of the electrochemistry. Such quantity will be present when the specific surface area is greater than 1.25 m^2/cc.

These control parameters are all related such that the lack of any of them will produce a slurry with a high viscosity. It is only when all three are present and the values of each optimized that it is possible to have a highly loaded, low viscosity coal/water mixture.

References

1. J. E. Funk, D..R. Dinger, J. E. Funk Jr., D. F. Funk, "Preparation and Combustion of a High Solids Coal Water Fuel - Co-Al". DOE Workshop on Coal-Water Fuel Technology (March, 1981).

2. J. E. Funk, D. R. Dinger, J. E. Funk Jr. "Coal Grinding and Particle Size Distribution Studies for Coal Water Slurries at High Solids Content". Final Report Empire State Electric Energy Research Corporation (December 1980).

3. J. E. Funk, D. R. Dinger, J. E. Funk Jr., D. F. Funk, S. J. Vecci, G. A. Farthing Jr., and S. A. Johnson. "Combustion Tests of a High Solids Coal Water Fuel - Co-Al". Governor's Conference on Expanding the Use of Coal in New York State (May, 1981).

4. A. H. M. Andreasen and J. Anderson. "Uber die Beziehung zwischen Kornabstufung und Zwishenraum in Produkten aus losen Kornern". Kolloid Z., 50:217-218, (1930).

5. A. E. R. Westman and H. R. Hugill. "The Packing of Particles". Journ. of Amer. Ceram. Soc. 767-779 (1930).

9-8-81

Determine ϕ_∞ for 75% det. fraction = 68.5% volume fraction to yield a viscosity of 806 cP

$$(1+x)^{-3.54} = 806$$

$$-3.54 \log(1+x) = \overbrace{}^{\log 806} = 2.906$$

$$\log(1+x) = \frac{2.906}{-3.54} = -.821$$

$$= -1 + .179$$

antilog .179 = 1.51

$$\therefore \log(1+x) = -1\ (1.51) = \boxed{.151}$$

$$\left[\text{Proof } .151^{-3.54} = \underline{\underline{806}} \right]$$

Further proof $1+x = \boxed{.151}$

$x = .849$

i.e. $\frac{\phi}{\phi_\infty} = .849$

Log scale | log .151 = −.82 = .18

.18 × 63 = 11.34 (mm)

Vol ϕ_∞ for 75% det $= \frac{.685}{\phi_\infty} = .849$

$$\phi_\infty = \frac{.685}{.849} = \boxed{.807}$$

∴ (?) ϕ_∞ is not necessarily the value of (1 − % Porosity)?

C-E CANADA CWM NOZZLE DEVELOPMENT AND FIRING EXPERIENCE

D.A. Cook, J.D. Kearns
C-E CANADA
Combustion Engineering-Superheater Ltd.
OTTAWA, ONTARIO

D.A. Smith, M.J. Rini, R.C. LaFlesh
Combustion Engineering Inc.
Kreisinger Development Laboratory (KDL)
WINDSOR, CONN.

ABSTRACT

In September 1982 Combustion Engineering - Superheater Ltd. (C-E Canada) was awarded a contract to develop an atomizer/burner arrangement for firing coal-water-mixture (CWM) in a 20 MWe, tangentially fired utility unit at Chatham, New Brunswick. This contract was awarded under a tri-partite agreement between New Brunswick Electric Power Commission (NBEPC), the Cape Breton Development Corporation (CBDC) and the Department of Energy, Mines and Resources (EMR) of the Government of Canada. (Additional details of the overall scope covered under this tri-partite agreement were presented earlier in the Conference under "Demonstration Projects").

A four step procedure was followed in this development work. First, three promising atomizer designs were selected. These designs were then subjected to comparative cold flow atomization performance testing via laser diffraction methods, at the Combustion Engineering Kreisinger Development Laboratory (KDL) in Windsor, Conn.

This work resulted in the design of an atomizer which produced a high quality fuel spray at commercially acceptable atomizing air consumption rates. This atomizer was then incorporated into a specially designed coal-water-mixture burner register (installed in KDL's Full-Scale Burner Facility (FSBF)) and successfully combustion tested at a full-scale throughput of 70 x 10^6 Btu/hr. Carbon conversion efficiencies ranged from 94% to 98% and were found to be a strong function of atomizing media to fuel ratio. At optimum conditions the burner system exhibited a turn down of 3 to 1. This atomizer and its associated burner configuration were then installed in NBEPC's Unit #2 in Chatham, New Brunswick for further testing.

At this time,the test work at Chatham has not been completed. However, all required equipment modifications related to Unit #2 are complete and testing is scheduled to begin in July of this year.

INTRODUCTION

In order to develop domestic fuels and reduce the dependance upon imported heavy.oil, the Canadian Government has instituted an "Off-Oil Program". As part of this Program, a substitute fuel for electrical utilities (particularly in the Atlantic Provinces) and for major industrial users which presently burn oil, has had special emphasis. Since coal is a readily available fuel in Canada most interest has been directed toward it as the substitute fuel.

Of course, it is not an easy task to replace oil directly with coal. Coal varies in its composition from coal seam to coal seam. Its use as a substitute fuel may also result in boiler derating, unit modifications, and ash handling problems, which serve to complicate the conversion of any unit.

Much of the attention with regard to using coal has been directed toward producing coal slurry fuels, due to the preference of replacing oil with another liquid fuel. The early emphasis was directed toward coal-oil-mixtures (COM), which was typically a mixture of approximately 50% oil and 50% coal. However, the small cost differenial between COM and oil has resulted in the redirecting of emphasis toward coal-water-mixtures (CWM), which are most commonly produced as a combination of approximately 70% coal and 30% water. Due to the absence of oil in CWM the fuel is more cost effective than COM's, but there are problems associated with firing CWM that do not exist with a COM. The existence of 30% water adversely affects the burner stability, burn out time, ignitability, and volitility of the fuel. This coupled with the decreased Higher Heating Value (HHV) of CWM compared to both oil and COM means that a relative increase in throughput per burner is needed, thus increasing the potential for erosion within the nozzle.

A large number of small-scale (<20 x 10^6 Btu/hr) CWM combustion tests have been completed over the past few years, but 1981-82 saw the successful firing of CWM burners with throughputs as high as 80 x 10^6 Btu/hr. Atomizers in this size range are of interest to the electrical utility industry and therefore since 1982, interest has been generated and directed toward commercialization of CWM as a fuel for this use.

In order to commercialize this fuel, factors such as coal production, coal preparation, manufacturing of the CWM, distribution of the fuel, and finally utilization of the fuel will have to be addressed. The work covered in this report is mainly related to the latter aspect but also touches on some of the other factors.

Fuel Discussion

Since coal varies greatly in composition from seam to seam and CWM production methods also vary from supplier to supplier it is appropriate to begin any discussion on CWM firing with a delineation on the fuel. This section summarizes some of the important properties of CWM fuels and also presents the specifics of the fuel used in the work described in this paper.

The CWM was produced from metallurgical Cape Breton (Nova Scotia) coal. The slurry is approximately 72% solids and 28% liquid, with a small percentage of the liquid being a stabilizer, dispersant, and organic growth retardant.

The fuel used in the laboratory work at KDL, Windsor was manufactured in Sweden, but the fuel used in the demonstration project at Chatham, New Brunswick was manufactured in Sydney, Nova Scotia by CBDC using the same process. Table I provides an analysis of the fuel used in KDL test work.

In addition, to the fuel analysis one very important parameter that must be considered is viscosity. The viscosity of most liquid fuels can be grouped into the three main categories shown here in Figure 1. From an atomizer designer's point of view the pseudo plastic characteristic for a fuel is most desirable due to the fact that all atomizers subject the fuel to shear. Of course, the Newtonian characteristic is also acceptable due to the fact that its viscosity remains constant. But for an atomizer designer a dilatant fuel is undesirable for obvious reasons.

When preparing to fire any CWM it is very important to have the viscosity characteristics clearly identified as can be seen by the above discussion.

There are several other fuel properties such as: fuel agglomerating characteristics, grinds, char reactivity etc. that could be considered here, but their effect on CWM fuel is still under study and thus have not been included.

TABLE 1 - Fuel Analysis

			TYPICAL	
	CWM (AS REC'D)	CWM (DRY)	OIL	COM (50/50)
Proximate, wt %				
Moisture (total)	28.0		-	-
Volatile Water	26.6	37.0	-	-
Fixed Carbon	44.1	61.2	-	-
Ash	1.3	1.8	-	-
Total	100.0	100.00	-	-
HHV, Btu/lb	10900	15150	18500	15550
Kcal/Kg	6055	8420	10280	8640
Ultimate, wt. %				
Moisture (total)	28.0	-	0.1	1.
Hydrogen	4.1	5.7	10.6	8.
Carbon	60.2	83.6	84.8	83.5
Sulphur	.4	.5	3.5	2.5
Nitrogen	1.2	1.7	.6	1.
Oxygen (diff.)	4.8	6.7	.3	2.5
Ash	1.3	1.8	.1	1.5
Total	100.0	100.0	100.0	100.0
Viscosity (100 S^{-1} @ 25°C, Haake Method)	1800 mPA-S			

PROGRAM FOR DEVELOPMENT OF A BURNER SYSTEM FOR CHATHAM II

Once the CWM fuel was characterized, C-E began work on developing a burner configuration capable of satisfying the following requirements:

A) The ability to ignite CWM fuel with conventional ignition equipment as this capability would minimize unit modifications.

B) Stable operation of the burner over an acceptable range with the common standard of 4 to 1 being set as a goal.

C) Production of acceptable carbon conversion efficiencies over the operating range of the burner. This was considered a high priority item as it is a major factor in unit efficiency.

D) Operation of the burner with reasonable fuel and atomizing medium pressures and atomizing medium consumption. This was an attempt to limit the auxiliary energy costs in firing CWM.

E) The ability of the atomizer to withstand a minimum of 500 hours of continuous operation without deterioriation in spray quality caused by wear. The production of an atomizer capable of withstanding the highly erosive nature of the CWM has been a major factor limiting progress in firing CWM.

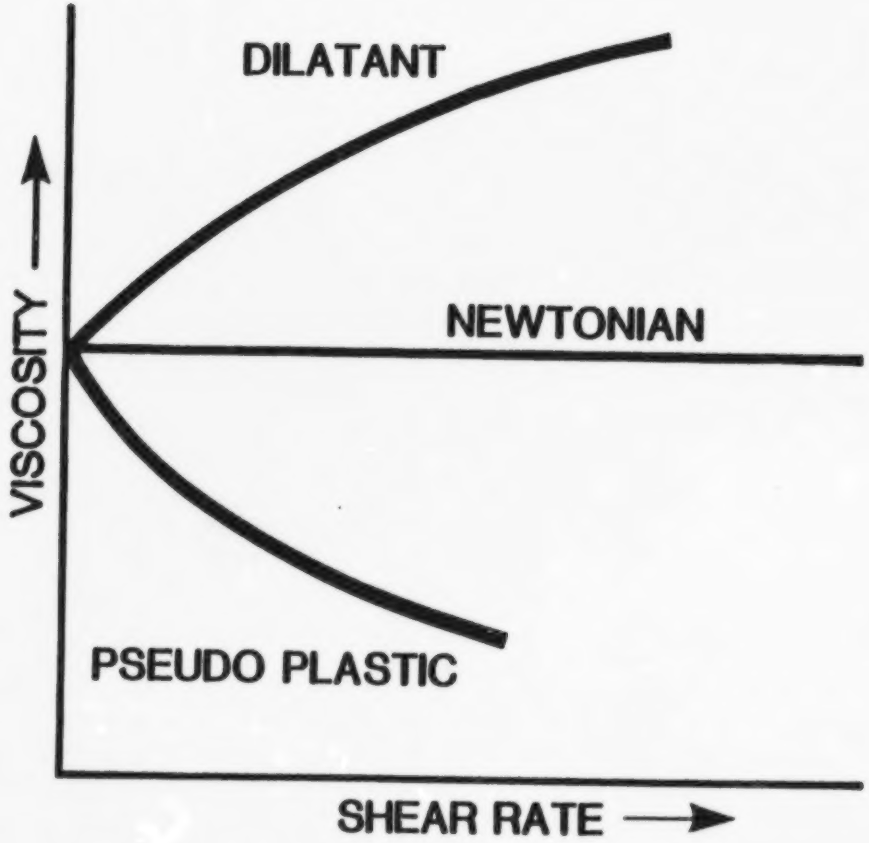

Figure 1: Viscosity Characteristics of Liquid Fuels

In order to satisfy these objectives a four step approach to the project was undertaken. The following is a step by step description of that approach.

1) A search of potential atomizer designs was initiated and three promising designs were selected.

2) These atomizer designs were then subjected to a series of atomization quality tests in KDL's Atomizer Test Facility (ATF). These tests compared the particle size distribution in the spray produced by each tip and resulted in the selection of the most promising tip of the three.

3) Based on C-E's experience with CWM and other slurry fuels a CWM burner register was designed and this atomizer/burner configuration was then combustion tested in KDL's Full Scale Burner Facility (FSBF). This work was performed in order to define the performance of the developed equipment and other operating parameters.

4) Then in order to carry out further full-scale testing this developed technology was then incorporated in Unit #2 at Chatham, New Brunswick by suitably modifying the unit.

FUEL SHIPPING, STORAGE AND HANDLING

Before discussing the step by step approach to the program it is useful to expound upon the fuel handling procedures followed during the course of the work.

The CWM fuel that was used for ATF and FSBF work at KDL was manufactured in Sweden (as mentioned earlier). It was loaded into pressurizable containers and shipped to the United States by container ship. The containers were then transported by truck to C-E's KDL site in Windsor, Conn. This mode of transportation worked very effectively.

At KDL the fuel was handled by the Alternate Fuels Handling Facility (AFHF) illustrated by the schematic shown in Figure 2. This facility is comprised of a 15,000 U.S. gallon storage tank, pumps, filters and associated equipment for unloading slurry type fuels. With the pressurizable containers the fuel could be unloaded into the AFHF by either directly pumping out the container or by pressurization of the container.

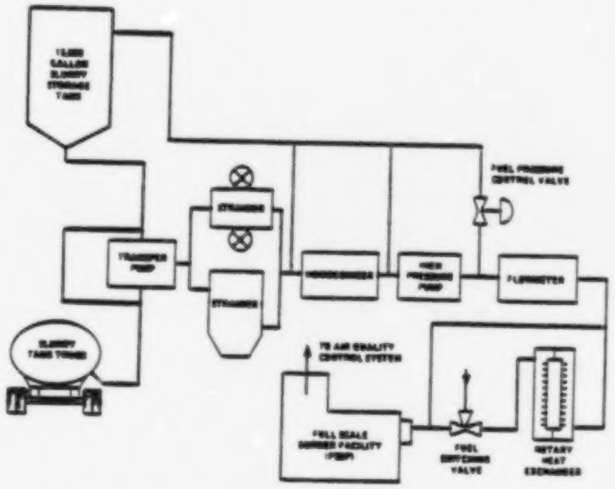
15,000 GALLON SLURRY STORAGE TANK
FUEL PRESSURE CONTROL VALVE
STRAINER
TRANSFER PUMP
STRAINER
HOMOGENIZER
HIGH PRESSURE PUMP
FLOWMETER
SLURRY TANK TRUCK
TO AIR QUALITY CONTROL SYSTEM
FULL SCALE BURNER FACILITY (FSBF)
FUEL SWITCHING VALVE
ROTARY HEAT EXCHANGER

Figure 2: Alternate Fuels Handling and Firing System

The fuel for the work at Chatham was transported via pressurizable rail car. It was then pumped directly into a 200 ton storage tank. Figure 3 is a schematic of the storage system and the remainder of the fuel piping at Chatham.

In handling this fuel the extremely close balance between moisture and solids came to light. It is necessary to pre-wet fuel lines and even the gun prior to firing the fuel. It is also necessary to purge all fuel lines with water after unit shut-down. Dead legs must also be avoided in fuel system design. If these procedures are not followed, fuel can quickly dry out and adhere to the walls of the pipe, eventually plugging the line.

1. SELECTION OF ATOMIZER DESIGNS

The first step in the program consisted of a search of atomizer literature and data, in accordance with C-E Canada's expertise, to define promising atomizer concepts. The following is a list of the various parameters that had to be considered in defining these potential designs:

1) Ability to withstand high erosion potential of fuel. If the atomizer was not inherently able to withstand high erosion a method of making it "erosion resistant" must be possible.

2) Ability to efficiently atomize the CWM fuel at reasonable pressures and atomizing medium consumption rates. It is necessary to create a fine fuel spray in order to separate the coal and water, yet this must be performed with a minimum consumption of energy.

3) Low pluggage potential was also necessary in order to ensure low plant maintenance.

With these factors in mind the three designs shown in Figure 4, were selected.

Alternative I was a design previously used to fire ammonia base spent sulfide (red) liquor as a fuel in pulp and paper facilities. Its ability to withstand the erosive and corrosive atmosphere of the red liquor led to its selection. Because of its single port fuel passage it possessed a very low pluggage potential along with an inherent "erosion resistance".

Alternative II was a design previously used on high viscosity fuel oils and due to its successful application there it was selected. However the tortuous paths that existed in the design produced a relatively high wear and pluggage potential.

Alternative III was a design previously used for firing CWM under the 1982 program undertaken at Combustion Engineering (Windsor, Conn.) in conjunction with the Electric Power Research Institute (EPRI). Its atomization performance had been proven and it had been previously made "erosion resistant" by the installation of tungsten carbide inserts.

All three atomizers were sized for a capacity of approximately 70 x 10^6 Btu/hr based on previously obtained performance data for these tips firing their original fuel and anticipated full load requirements for Chatham #2.

2. ATOMIZER TESTING AND SELECTION

Atomizer Test Facility

C-E's Atomizer Test Facility (ATF) is designed to quantitatively characterize the atomization quality of full scale (10 gpm) burner atomizers. The facility is uniquely configured to obtain droplet size distribution and droplet ballistics (velocity and trajectory) information from fuel sprays.

It operates in a cold flow (non-combustion) mode and has provisions for studying both conventional liquid and slurry fuels. Provisions for slurry fuels include a 700 gallon transportable fuel tank for storing and heating fuels prior to ATF testing. The tank is equipped with a mixer and recirculation system to minimize potential slurry solids stratification. A schematic of the Atomization Test Facility is shown in Figure 5.

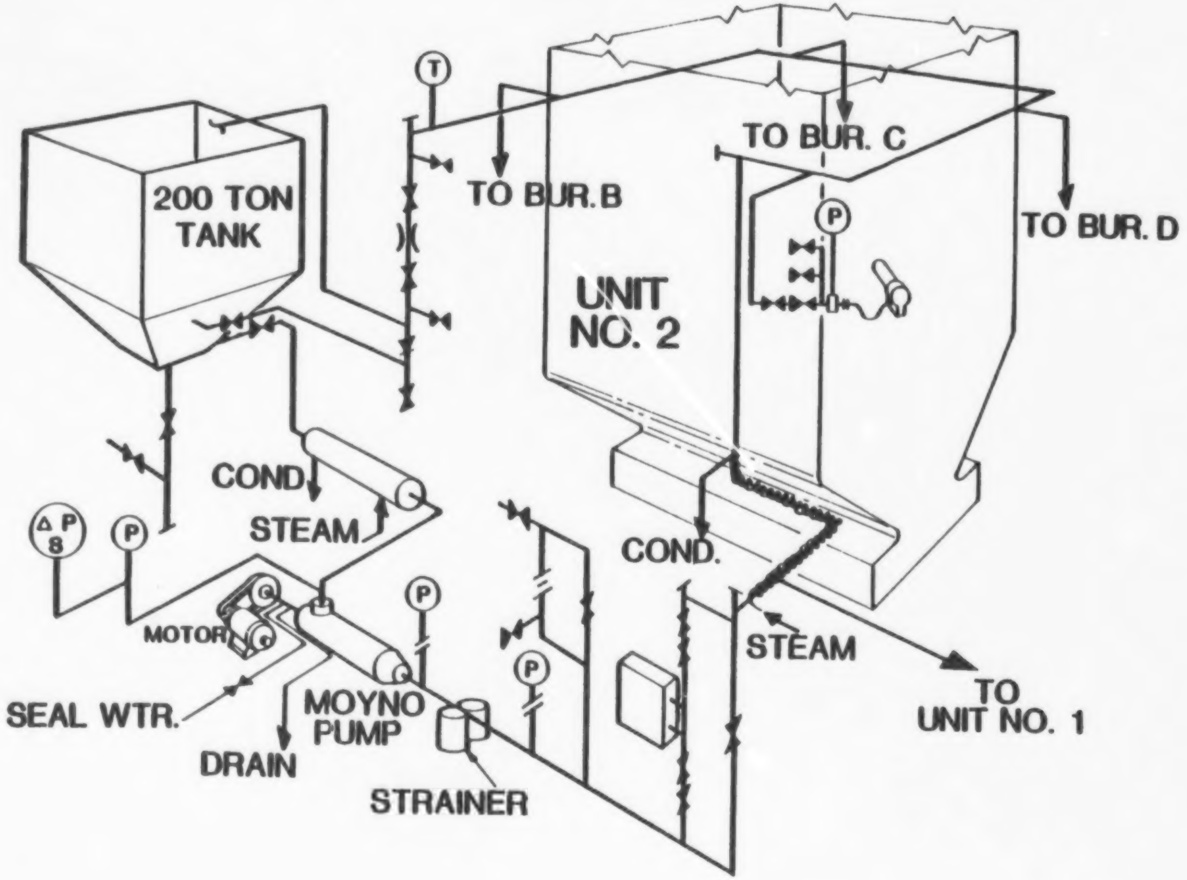
T
200 TON TANK
TO BUR.B
TO BUR. C
TO BUR. D
P
UNIT NO. 2
COND
STEAM
ΔP 8
P
P
P
MOTOR
SEAL WTR.
DRAIN
MOYNO PUMP
STRAINER
COND.
STEAM
TO UNIT NO. 1

Figure 3: Chatham #2 Fuel System

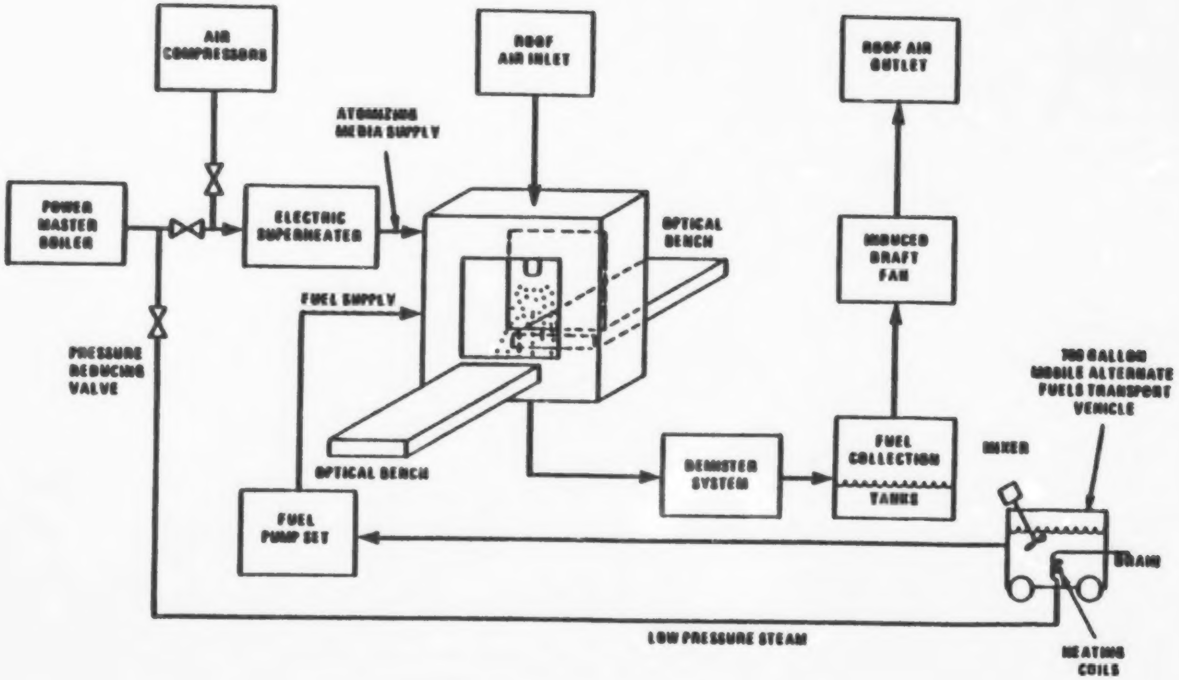
AIR COMPRESSORS
ROOF AIR INLET
ROOF AIR OUTLET
ATOMIZING MEDIA SUPPLY
POWER MASTER BOILER
ELECTRIC SUPERHEATER
OPTICAL BENCH
INDUCED DRAFT FAN
FUEL SUPPLY
PRESSURE REDUCING VALVE
700 GALLON MOBILE ALTERNATE FUELS TRANSPORT VEHICLE
OPTICAL BENCH
DEMISTER SYSTEM
FUEL COLLECTION
TANKS
MIXER
FUEL PUMP SET
DRAIN
LOW PRESSURE STEAM
HEATING COILS

Figure 5: Atomizer Test Facility

Test atomizers are centrally located in the spray chamber and spray vertically down, thus minimizing the effect of gravity in atomization droplet ballistics measurements. Also, a constant velocity profile (10ft/sec) airflow passes by the atomizer during testing to prevent potential droplet recirculation which would otherwise bias droplet trajectory information. Large windows in the spray chamber permit optical access across the atomized sprays. Optical spray diagnostic equipment is located on the two benches as shown. Once data is obtained from the spray, the fuel droplet laden air flow is demisted and exhausted from the facility. The collected fuel is then removed for reuse or disposal.

Optical Diagnostic Techniques

A laser diffraction technique was used by C-E in the ATF to determine the spray droplet size distribution.

The laser diffraction technique is based on the Fraunhofer diffraction of a parallel beam of monochromatic light by moving or stationary droplets (1). A Fourier Transform lens yields a stationary light pattern from the light diffracted by the particles. A multi-element photo-electric detector located at the focal plane of the Fourier Transform lens produces an electrical signal analogous to the diffracted light. A mini-computer compares this signal with the derived signal based on a Rosin-Rammler model which continuously modifies the mean diameter and exponent parameters until a best fit is obtained (1). Percentage weight fraction and percentage number fraction are then calculated from the best fit model.

Preliminary ATF Testing

Preliminary ATF testing was a comparative test to evaluate the performance of the three selected atomizer designs (geometries), outlined in Section 1. Each atomizer was tested at 100%, 50% and 30% fuel flow rates. The ATF laser diffraction system was utilized to record particle size distribution in each case. Air was used as the atomizing medium and the air to fuel ratio (A/F) was varied (0.06< A/F <0.87) at each load as the atomization quality was recorded. The CWM fuel and atomizing air were maintained at ambient temperature. It was found that the A/F had a significant effect on the performance of CWM atomizers.

The atomizers were compared on the basis of:

1) Atomizing media to fuel mass flow ratio (A/F). High A/F are not desirable from an economic standpoint, so A/F <0.2 were considered commercially acceptable in this evaluation.

2) Spray droplet mass median diameter (MMD). This is defined as the droplet diameter which divides the total mass of the spray into two equal parts. Previous work (2) has shown the stable combustion of CWM fuel with a MMD of 110-120 microns, so this was used as a reference value.

3) Spray droplet top size. The percentage of spray droplets above 320 microns was compared, as literature (3) suggests particles above 300 microns adversely affect carbon conversion.

4) Potential for atomizer wear

Using these four points for comparison Alternative I was eliminated from further testing. Although it possessed very low wear or pluggage potential its atomization performance was poor. At 100% fuel flow rate its MMD was in the 170-180 micron range which was considered marginal for stable combustion. It also required an A/F >.2 at this load which was considered to be beyond the commercial range.

At 100% fuel flow rate the atomization performance of Alternative III was superior to Alternative II at A/F <0.2. But their atomization performance was comparable at similar A/F for 50% and 30% fuel flow rates. When the percentage of spray droplets above 320 microns was compared for the atomizers at all three loads, Alternative III consistently produced a lower number than Alternative II.

These factors, coupled with the ability to more easily incorporate wear protection into Alternative III than II, were responsible for the selecting of the Y jet style as the atomizer to be used in combustion test work.

Final Atomizer Selection

An increase in specified fuel particle top size from 175 microns to 400 microns, coupled with the need to operate at a maximum fuel pressure of 150 psig and an air pressure of approximately 100 psig resulted in an iterative step in the Y jet design of Alternative III. In order to satisfy these criteria, the atomizer was extensively revised. The major change was the increasing of the minimum fuel nozzle orifice diameter. This tip (Figure 6) was ATF tested and its atomization efficiency surpassed that of the original Alternatives. This tip (Alternative IV) did produce a somewhat higher percentage of droplets in excess of 320 microns than the original Y jet design, but it still produced fewer than Alternative II.

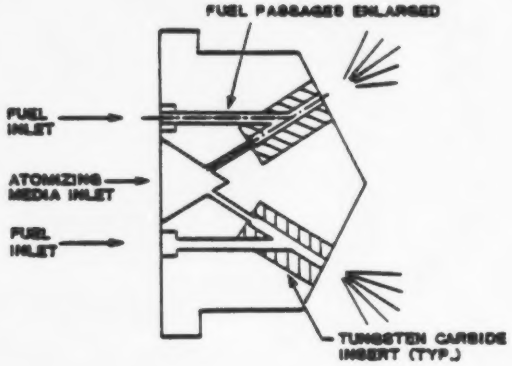

Figure 6: Y-Jet Design (Alternate IV)

3. COMBUSTION TEST WORK

The combustion test work was performed at KDL's Full-Scale Burner Facility (FSBF) in Windsor, Conn. The Alternative IV atomizer developed in the ATF was used in this stage of the work.

Test Facility

This large test furnace allows the development of firing systems of a size directly applicable to utility boilers, thus minimizing scale-up problems. The FSBF is capable of a maximum firing rate of 100 x 10^6 Btu/hr on coal and 300 x 10^6 Btu/hr on oil. All coals and liquid fuels ranging from No. 2 distillate to No. 6 residual oil, as well as coal-oil, coal-water and petroleum coke-oil slurries can be fired in the FSBF. Data collection includes fuel and air flow rates, radiative furnace heat measurements, and complete flue gas analysis. The flue gas is ducted into a wet scrubber where particulates and sulphur gases are removed prior to discharge to the atmosphere. The test furnace and major ancillary equipment are shown schematically in Figure 7.

The facility combustion chamber basically simulates a front wall, horizontal fired industrial type boiler. However, there are no pressure (steam or water) parts surrounding the combustion chamber. Instead, heat is absorbed by the atmospheric water jacket which surrounds the firing chamber. This simplified design allows easy modification of the facility to suit specific testing requirements. Further, the wall temperatures can be adjusted by the addition or removal of refractory panels to allow simulation of any desired temperature profile, or furnace outlet temperature. The heat release rate and furnace outlet temperature of the Chatham #2 unit were simulated by this method.

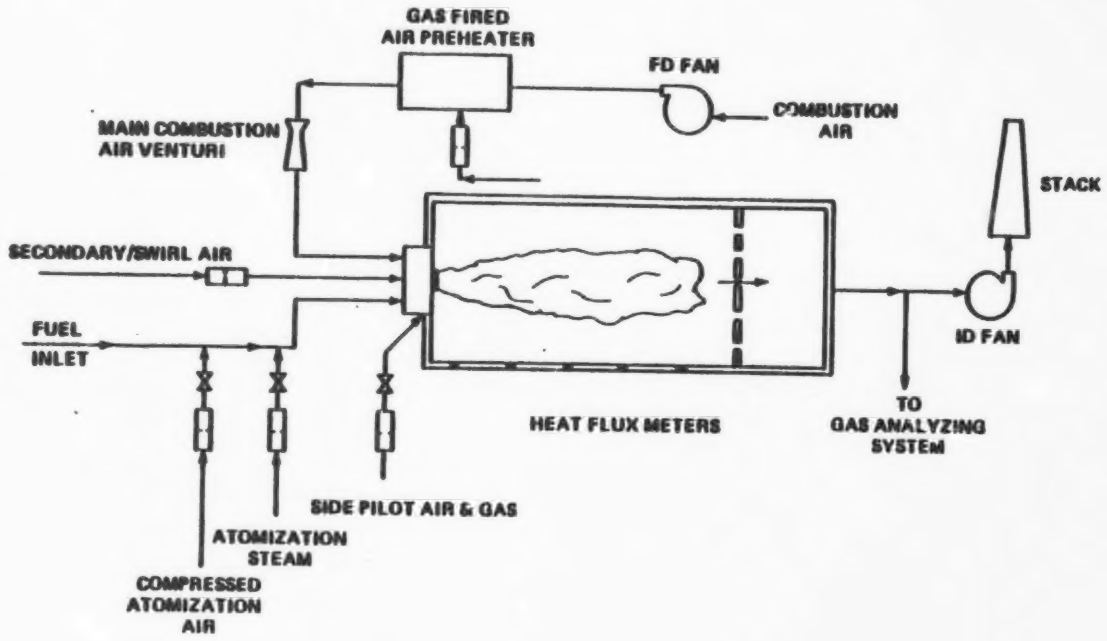
GAS FIRED
AIR PREHEATER
FD FAN
COMBUSTION
AIR
MAIN COMBUSTION
AIR VENTURI
STACK
SECONDARY/SWIRL AIR
FUEL
INLET
ID FAN
TO
GAS ANALYZING
SYSTEM
HEAT FLUX METERS
SIDE PILOT AIR & GAS
ATOMIZATION
STEAM
COMPRESSED
ATOMIZATION
AIR

Figure 7: KDL's Full-Scale Burner Facility

Burner Description

A full-scale model of the windbox arrangement (Figure 8) to be utilized in the actual field installation was installed in the FSBF. The bucket installed in the CWM compartment was based on the design used by C-E (Windsor) in their EPRI program (2). This bucket incorporated both a combustion air swirler and a refractory-lined divergent throat, two proven methods for inducing high amounts of recirculating gas flow. In an effort to increase the recirculation zone an area above and below the CWM bucket was also bricked off.

Approximately, 10-15% of the total combustion air was put through the CWM compartment with the balance of the combustion air being ducted through the auxiliary air compartments. Due to the very low windbox pressure that would be available at Chatham (2. - 2.5" wg) the auxiliary windbox compartments were not fitted with extension buckets in an attempt to reduce pressure drop. This low windbox pressure necessitated the boosting of the air pressure to the CWM compartment in order to provide adequate swirl.

Combustion Testing

Prior to conducting detailed combustion testing a period of shakedown testing was performed in order to define burner performance and the various operating parameters.

The burner's combustion performance was observed at firing rates ranging from 23 x 10^6 Btu/hr to 70 x 10^6 Btu/hr (33% - 100% boiler load). Operating parameters such as; combustion air temperature, atomizing medium temperature, CWM temperature and windbox pressure were held at relatively constant values, equivalent to those available in the field. Flame stability and appearance were very good over the range although some sparklers did appear at the lower loads. The flame remained "attached" to the burner above 50% load and nearly "attached" below 50%.

Detailed matrix testing was performed at two separate conditions; 100% fuel flow with air atomization and 100% fuel flow with steam atomization. Due to the current practice of using steam for atomization in utility boilers it was considered to be a very worthwhile test point.

The CWM was successfully ignited in the cold test furnace with the facility's standard 5 x 10^6 Btu/hr natural gas side pilot ignitor. One requirement for light-off was the aforementioned necessity of pre-wetting the fuel lines and also the gun prior to introducing the CWM. The actual light-off procedure was as follows: the 5 x 10^6 Btu/hr ignitor was lit first; a small flow of water to the gun and atomizer was started; next the atomizing medium flow was initiated. CWM was then started and simultaneously, the prewet water was shut off. A combustion air temperature of 550°F was used for this test work which is consistent with what was available in the field installation. It should be noted at this point, that because the furnace was lined with a thin layer of refractory to simulate the heat release rates of the field unit along with its furnace outlet temperature, the furnace wall temperature may have risen at a somehwat higher rate than would be seen in an actual cold furnace. Thus it might be necessary to leave the ignitor in operation for a longer period of time for the actual field installation than was necessary in the FSBF.

The testing with both air and steam atomization was considered successful. Additional discussion of the results are included in the "Conclusions" section of this report.

4. FIELD INSTALLATION AND TESTING

The technology and equipment developed in the ATF work and subsequent combustion test in the FSBF were transferred to a field installation.

Test Facility

The 20 Mwe, Unit #2 utility boiler located in Chatham, New Brunswick was designated as the field installation site. Unit #2 (Figure 9) was commissioned by New Brunswick Electric Power Commission (NBEPC) in 1956. It is a C-E Canada designed, tangentially fired, non reheat unit, supplying 210,000 lbs/hr of steam at 900°F and 875 psig. The unit was originally designed as a dual-fuel unit with pulverized coal being the main fuel and oil being an auxiliary fuel. Due to oil pricing and other factors, the unit has fired oil for the majority of its generating years. (1957-1977).

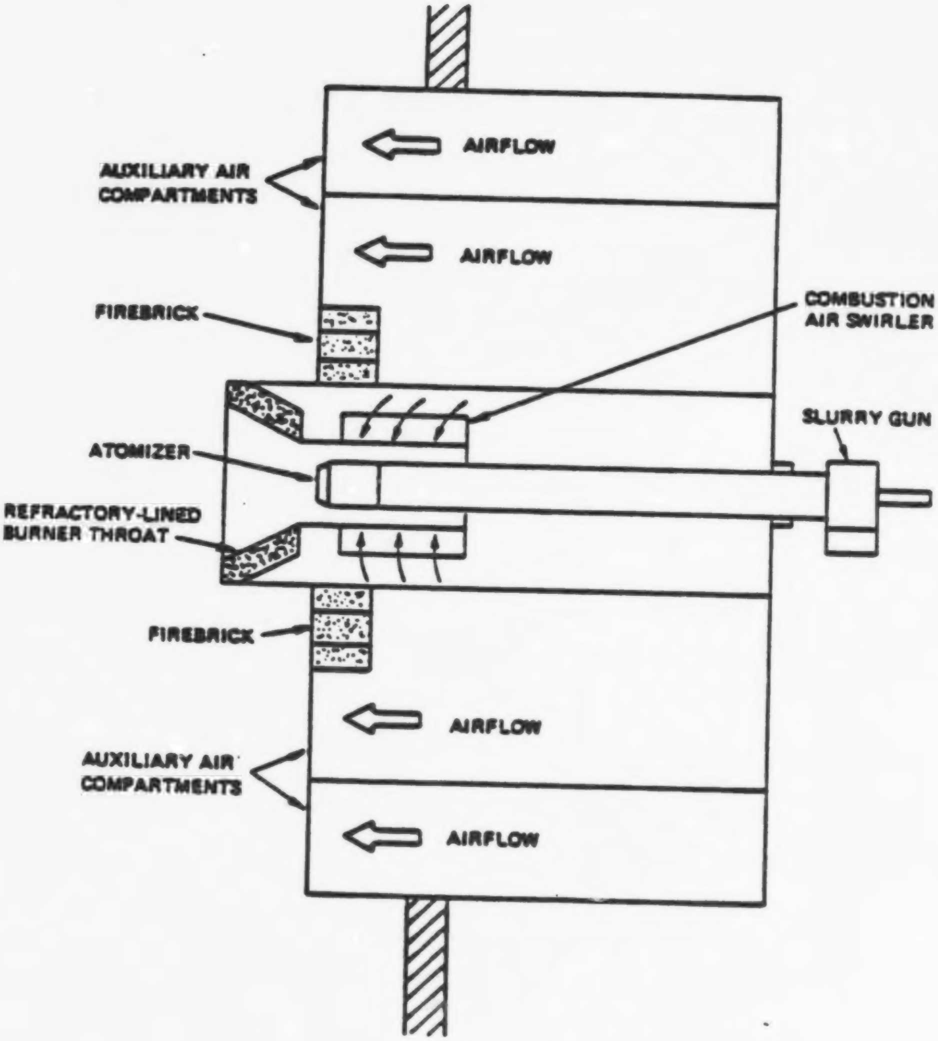
AIRFLOW
AUXILIARY AIR COMPARTMENTS
AIRFLOW
FIREBRICK
COMBUSTION AIR SWIRLER
SLURRY GUN
ATOMIZER
REFRACTORY-LINED BURNER THROAT
FIREBRICK
AIRFLOW
AUXILIARY AIR COMPARTMENTS
AIRFLOW

Figure 8: Windbox Configuration

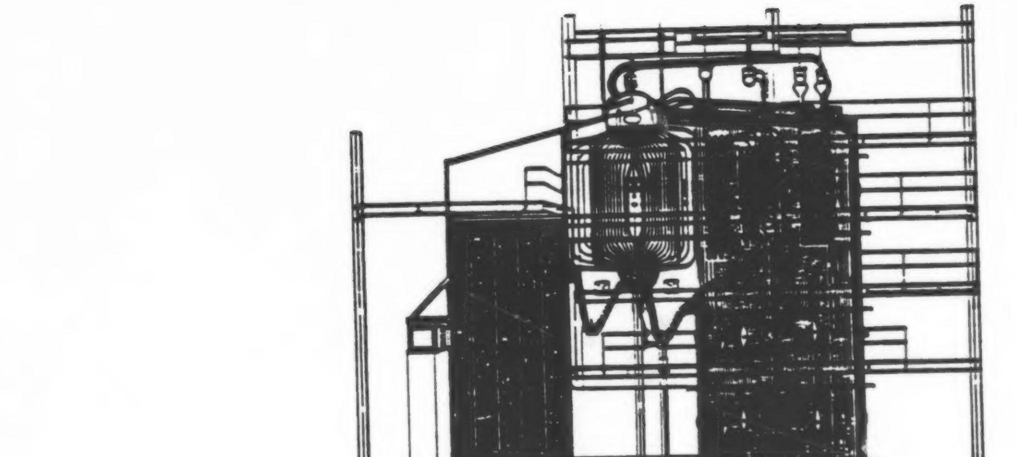

Figure 9: Chatham Unit #2

Test Program for Unit #2

The following overall objectives were identified for the test work at Chatham, Unit #2.

1) Determine the combustion characteristics of the fuel in utility boilers.

2) Evaluate the performance of coal-water mixture burner equipment as to reliability (resistance to wear) and efficiency.

3) Make measurements over a range of operating conditions in order to evaluate boiler performance and environmental implications of the fuel and compare it to oil.

4) Determine the technical feasibility of performing an on-line switch between oil and coal-water mixture.

5) Assess the performance of fuel handling equipment and instrumentation for coal-water mixture.

6) A comparison of steam vs. air atomization of CWM.

Unit #2 Modifications & Installations

Due to the extensive nature of the test program a great deal of effort was required on the part of NBEPC to fully equip the unit with adequate test points and equipment. The age of the unit also necessitated the addressing of many maintenance type items. As mentioned in the "Fuel Shipping ... Handling" section of this report a new fuel storage and supply system was also provided (Figure 3). The burner front was arranged with new lines for: pre-wet water, atomizing air, atomizing steam, and CWM.

The main work performed on the unit itself consisted of windbox modifications. Each windbox was stripped of its original coal, oil and top and bottom auxiliary air buckets first of all. Then the CWM refractory lined bucket was installed such that the same arrangement as was used at KDL resulted (Figure 8). Again the combustion air for the CWM compartment was supplied at a higher pressure than the remainder of the windbox via a booster fan.

This arrangement was subjected to preliminary CWM combustion testing in Oct. - Nov. 1983 (see section dealing with "Chatham Unit #2 Testing"). This work in Oct. - Nov. proved that it was necessary to make a few additional modifications to the windbox. These modifications consisted of three separate areas. The first being the CWM bucket itself. Due to physical limitations on the unit the original CWM bucket installed at Chatham was smaller in diameter than that tested at KDL. So new buckets were manufactured and installed to duplicate those tested at KDL.

Next it was decided to suffer an increased pressure loss and install auxiliary air buckets in each of the remaining windbox compartments (Figure 10).

Finally in order to evaluate the effect of furnace wall refractory in burning the high moisture CWM fuel, two opposing corners had refractory added to them as shown in Figure 11. From work performed with CWM by various organizations the key to stable CWM flames appears to lie in having high gas recirculation at the burner and/or having the heat radiating ability of refractory proximate to the burner to aid in the rapid vaporization of the water in the fuel. Both methods were incorporated in the Unit #2 design.

Fuel Problems

The fuel for use in the test work at Chatham was produced by CBDC in Cape Breton, Nova Scotia. The newness of the fuel manufacturing plant, coupled with the change from batch CWM production to continuous production resulted in the need for a fairly lengthy trial period before a consistant quality of fuel was obtained.

Equipment such as pumps and fuel control valves experienced high wear with the CWM and therefore had to be monitored closely. It also became evident that great care had to be taken to ensure that fuel lines were thoroughly flushed with water to remove all CWM during periods of shut-down. If fuel was permitted to lie in the lines it could plug them solid. As long as the operating parameters mentioned in this report were observed the fuel could be handled with little difficulty though.

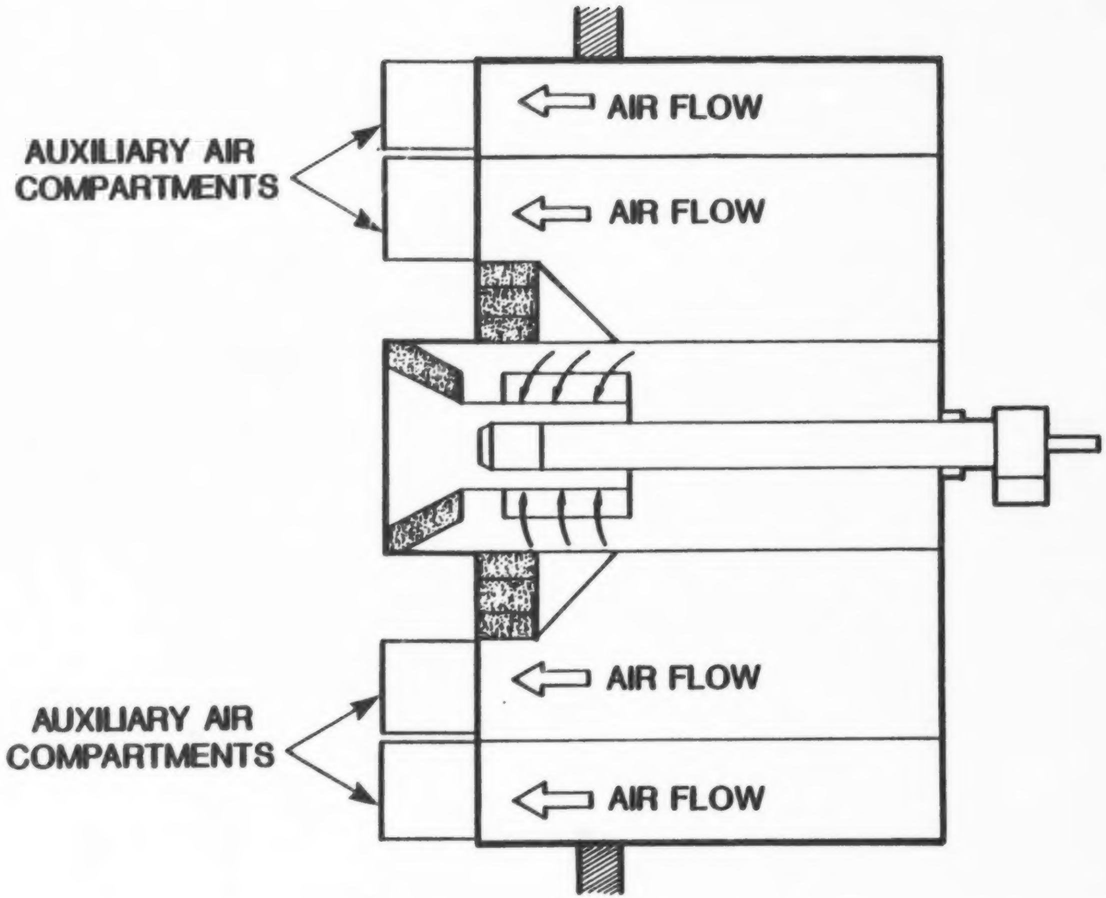
AIR FLOW
AIR FLOW
AIR FLOW
AIR FLOW
AUXILIARY AIR COMPARTMENTS
AUXILIARY AIR COMPARTMENTS

Figure 10: Chatham #2 Windbox with Aux. Air Buckets

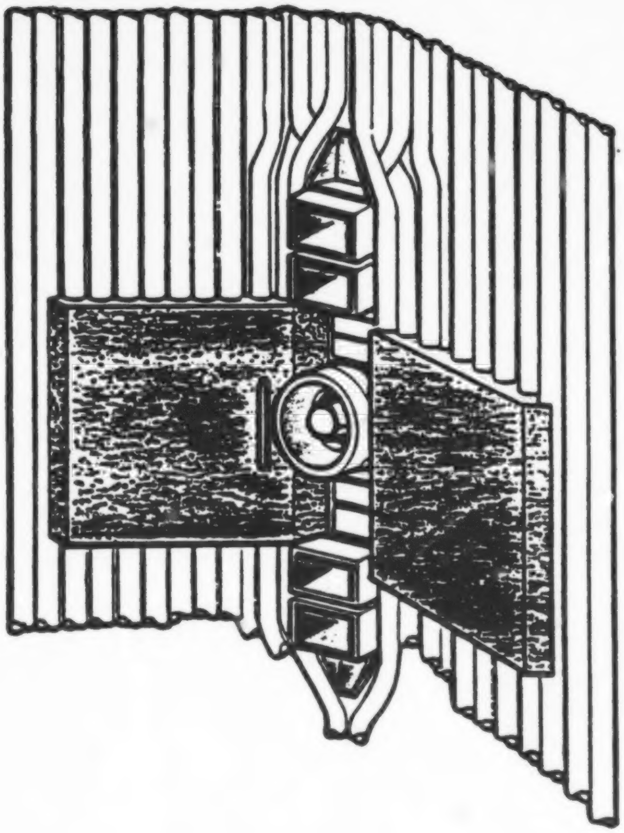

Figure 11: Refractory Application on Two Corners

Chatham Unit #2 Testing

In order to obtain comparison performance data for Unit #2, base line oil testing was performed on the modified unit in late October 1983. The oil was fired through the original oil guns which were inserted in through the CWM refractory bucket.

Actual preliminary testing on CWM proceeded in early November 1983 and approximately 500 tons of it was fired at that time. This testing proved inconclusive and brought about the modifications involving the replacing of the refractory lined bucket, addition of auxiliary air buckets and application of refractory to the unit walls. These modifications were completed in early February 84 and will be subjected to further testing in July 1984 upon receipt of CWM fuel.

CONCLUSIONS

Successful commercial scale laboratory development has provided the background information required to support a field demonstration of CWM technology at Chatham Unit 2.

During the laboratory work several atomizer designs were evaluated before a final design was selected. This atomizer produced mass median drop sizes in the range of 68-78 microns with air/fuel ratios of 0.15-0.12. It was also shown that this same atomizer could be successfully operated using superheated steam as the atomizing assist fluid in lieu of air. While erosion tests were not conducted as part of this program it would be realistic to expect that these atomizers will operate efficiently for 500 to 1000 hours, based on other previously obtained data on similar atomizers.

In parallel with the atomizer evaluation was the development of a burner register for CWM firing. Several iterative steps were required in this design before achieving the desired burner stability and turn down. This atomizer/burner combination was tested at 70 x 10^6 Btu/hr. Carbon conversion rates appear to be significantly affected by atomizing medium to fuel ratio (this having a direct effect on droplet fineness); additionally excess air, within certain ranges is expected to influence carbon conversion, although its effect may be more pronounced at lower loads. Due to the limited test work conducted at KDL it was not possible to quantitatively evaluate the effects of each of these parameters. But based on previous work by C-E and others, a strong relationship between droplet size distribution in the fuel spray and carbon conversion has been established. This appears to be born out by the fact that with air atomization at 100 psig an air/fuel ratio of <.1 was achieved with a resulting MMD of 107 microns and a carbon conversion of approximately 94%. While with 200 psig steam a steam/fuel ratio of <.15 was achieved resulting in a MMD of 51 microns and carbon conversion of 98%.

At the optimum conditions just reviewed the burner system exhibited a turndown ratio of 3 to 1.

Following the laboratory development effort at KDL the technology was transferred to NBEPC's Chatham Unit #2 for further testing.

Initial combustion trials at Chatham, conducted in November 1983, were inconclusive. Variations between burners installed at Chatham and the burner tested at KDL, coupled with variability in the fuel, resulted in an inability to properly evaluate burner performance. A second series of field trials will incorporate solutions which have been developed to address these key problem areas. The field trials are currently scheduled for July of this year. (1984)

References

1. Swithenbank, J. et.al., "Laser Diagnostic Technique for the Measurement of Droplet and Particle Size Distribution", University of Sheffield, Sheffield, England, Report # H18 245.

2. Manfred, R.K. et.al., "Development of a Coal-Water Slurry Burner", paper presented at Joint Power Generation Conference, Indianapolis, Indiana by Combustion Engineering Inc., Sept. 26-29, 1983. TIS-7409.

3. Pollock, W.H., Goetz, G.J. Park, E.D., "Advancing the Art of Boiler Design by Combining Operating Experience and Advanced Coal Evaluation Techniques", Chicago, Illinois, American Power Conference, April 18-20/1983.

TABLE G.9.2
DROP FORMATION AND COMPARISON OF AXIAL DISTANCES TO FLAME FRONT AND BURN-OUT (See Discussion G.10).

1	2	3	4	5	6	7	8	9		10		11		12		12.1		13		
										Diameter of Spray				Drop Concentration per cm^2 6)				Drop Velocity at Flame Front - cm./sec.		
Rows	Max. Drop Dia. at F. Front	Paper No.	Table No.	Initial Drop Generation Qty.	Time Period Secs.	Included Spray Angle	Point of Angle formation	Length of Spray		Flame Front		End of Spray		Flame Front		End of Spray		(G.1) CRL	(10) MIT	(11) Beer Chigier
								cm.	ft.	cm.	ft.	cm.	ft.	Qty.	Div 4)	Qty.	Div.			
1	720	G.1	G.1.2	3000	.015	15° 45°	Nozzle 3) G.M.	417	13.6	152	5	355	11.6	21	(D 7)	16	(D 9)	140		
2	375	G.1	G.1.2	3000	.015	15° 45°	Nozzle G.M.	417	13.6	152	5	355	11.6	21	(D 7)	16	(D 9)	140		
3	375	G.1 Add.2	G.9.1	1000	.005	15° 45°	Nozzle G.M.	91	3	32	1.05	63	2.06	20	(D 4)	41	(D.7)	140		
4	110.	G.1 Add.2	G.9.1	1000	.005	15° 45°	Nozzle G.M.	91	3	32	1.05	63	2.06	20	(D 4)	41	(D.7)	140		
5	2) 50	G.1 Add.2	G.9.1	1000	.005	15° 45°	Nozzle G.M.	91	3	32	1.05	63	2.06	20	(D 4)	41	(D.7)	140	8) 1 G.4500 Flame 900	
6	1) 40	G.1 Add.2	G.9.1	1000	.005	15° 45°	Nozzle G.M.	91	3	32	1.05	63	2.06	20	(D 4)	41	(D.7)	140		
7	5) 375	G.1 Add.1	G.1.1	3000	.015	45°	Nozzle	177	5.8	110	7.6	148	4.85	3	(D 3)	6	(D.5)	.2045		
8	4000	G.1 Add.1	G.1.1	3000	.015	45°	Nozzle	177	5.8	4.28	0 14	148	4.85	208 7)	(D<1)	6	(D.5)	140		
8.1	4000	G.1 Add.2	G.9.1	1000	.005	45°	Nozzle	59	1.93	4.28	0.14	50	1.64	70	(D<1)	17	(D.5)	140		
8.A	4000	G.1 Add 1	G.1.1	3000	.015	60°	Nozzle	177	5.8	8.75	0.23	224	6.7	7	<1	22	(D.7)	140		
8.1A	4000	G.1 Add.1	G.9.1	1000	.005	60°	Nozzle	59	1.93	8.75	0.23	86	2.23	7	<1	22	(D.7)	140		

	14	15	16	17	18	19	20	21	22		23		24	25	26	
	Axial Distance Nozzle to Flame Front - Ft. (cm.)				(Ref. Table G.9.1) Axial Distance Nozzle to Burn-out -- Feet)										(Total drops at Div.Pts. Table G.1.1 & G.9.1.)	
	G.1		(10)	(11)	(G.1.)CRL		(10)-MIT		Beer-Chigier				Areas cm^2			
Rows	CRL	Div. No.	MIT	Beer-Chigier	Min.	Max.	Min.	Max.	Min.	Max.	Min.	Max.	F.Front	End Spray	F.Front CLM 12	End Spray CLM 12.1
1	9' (272)	(7)			15.8'	23'				16'			18146	98980	384000	1,536,000
2	9' (272)	(7)			12.25'	16'				16'			18146	98980	384000	1,536,000
3	1.74'(53)	(4)	(35/25) 7)		8.35'	12'				16'			804	3117	16000	128000

														21	(D 7)	16	(D 9)	140	
3	375	G.1 Add.2	G.9.1	1000	.005	15° 45°	Nozzle G.M.	91	3	32	1.05	63	2.06	20	(D 4)	41	(D.7)	140	
4	110.	G.1 Add.2	G.9.1	1000	.005	15° 45°	Nozzle G.M.	91	3	32	1.05	63	2.06	20	(D 4)	41	(D.7)	140	
5	2)50	G.1 Add.2	G.9.1	1000	.005	15° 45°	Nozzle G.M.	91	3	32	1.05	63	2.06	20	(D 4)	41	(D.7)	140	
6	1)40	G.1 Add.2	G.9.1	1000	.005	15° 45°	Nozzle G.M.	91	3	32	1.05	63	2.06	20	(D 4)	41	(D.7)	140	1 G.4500 8) Flame 900
7	5)375	G.1 Add.1	G.1.1	3000	.015	45°	Nozzle	177	5.8	110	7.6	148	4.85	3	(D 3)	6	(D.5)	.2045	
8	4000	G.1 Add.1	G.1.1	3000	.015	45°	Nozzle	177	5.8	4.28	0.14	148	4.85	208 7)	(D <1)	6	(D.5)	140	
8.1	4000	G.1 Add.2	G.9.1	1000	.005	45°	Nozzle	59	1.93	4.28	0.14	50	1.64	70	(D <1)	17	(D.5)	140	
8.A	4000	G.1 Add 1	G.1.1	3000	.015	60°	Nozzle	177	5.8	8.75	0.23	224	6.7	7	< 1	22	(D.7)	140	
8.1A	4000	G.1 Add.1	G.9.1	1000	.005	60°	Nozzle	59	1.93	8.75	0.23	86	2.23	7	< 1	22	(D.7)	140	

	14	15	16	17	18	19	20	21	22		23		24	25	26	
	Axial Distance Nozzle to Flame Front - Ft. (cm.)				(Ref. Table G.9.1) Axial Distance Nozzle to Burn-out -- Feet)										(Total drops at Div.Pts. Table G.1.1 & G.9.1.)	
	G.1		(10)	(11)	(G.1.)CRL		(10)-MIT		Beer-Chigier				Areas cm^2			
Rows	CRL	Div. No.	MIT	Beer-Chigier	Min.	Max.	Min.	Max.	Min.	Max.	Min.	Max.	F.Front	End Spray	F.Front CLM 12	End Spray CLM 12 .1
1	9' (272)	(7)			15.8'	23'				16'			18146	98980	384000	1,536,000
2	9' (272)	(7)			12.25'	16'				16'			18146	98980	384000	1,536,000
3	1.74'(53)	(4)	(35/25) 7)		8.35'	12'				16'			804	3117	16000	128000
4	1.74'(53)	(4)	(35/25)		5.68'	6.8'							804	3117	16000	128,000
5	1.74'(53)	(4)	(35/25)		5.08'	5.58'		1.36' 9)					804	3117	16000	128,000
6	1.74'(53)	(4)	(35/25)		5.00'	5.38'		1.15' 10)					804	3117	16000	128,000
7	4.3'(132)	(3)											9503	17203	24000	96000
8	4' (122)	1	(35/25)										14.4	17203	3000	96000
8.1	4' (122)	1	(35/25)										14.4	1963	1000	32000
8.A	7.57 cm	1	(35/25)		8.5'	12'							60	39408	400	384000
8.1.A	7.57 cm	1	(35/25)		8.5'	12'							60	5808	400	128000